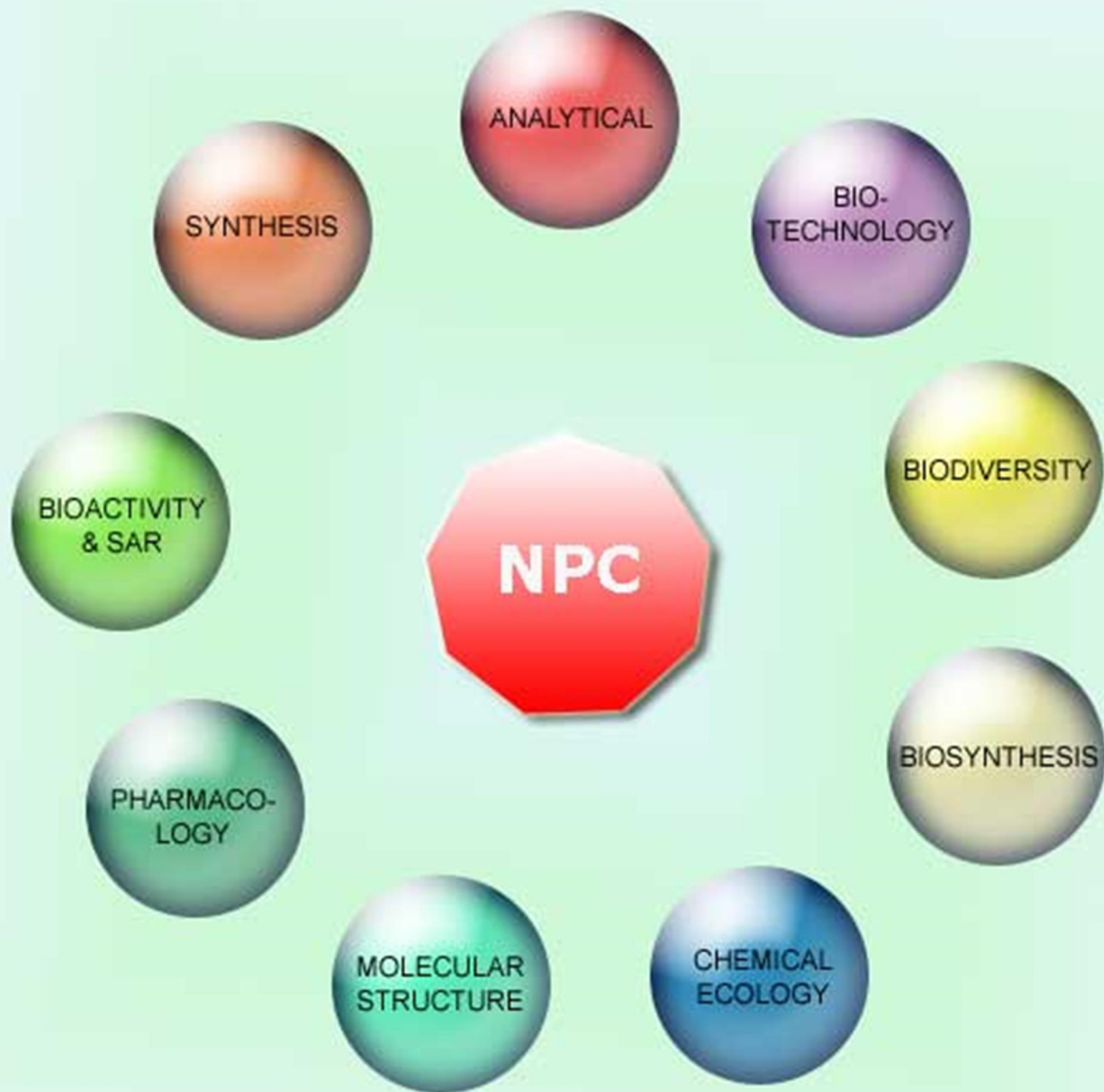


NATURAL PRODUCT COMMUNICATIONS

An International Journal for Communications and Reviews Covering all
Aspects of Natural Products Research



This Issue is Dedicated to
Professor Feng-Peng Wang
On the Occasion of his 70th Birthday

Volume 10, Issue 12, Pages 2019-2204, 2015
ISSN 1934-578X (printed); ISSN 1555-9475 (online)
www.naturalproduct.us

EDITOR-IN-CHIEF**DR. PAWAN K AGRAWAL**

*Natural Product Inc.
7963, Anderson Park Lane,
Westerville, Ohio 43081, USA
agrawal@naturalproduct.us*

EDITORS**PROFESSOR ALEJANDRO F. BARRERO**

*Department of Organic Chemistry,
University of Granada,
Campus de Fuente Nueva, s/n, 18071, Granada, Spain
ajbarre@ugr.es*

PROFESSOR ALESSANDRA BRACA

*Dipartimento di Chimica Bioorganicae Biofarmacia,
Università di Pisa,
via Bonanno 33, 56126 Pisa, Italy
braca@farm.unipi.it*

PROFESSOR DE-AN GUO

*State Key Laboratory of Natural and Biomimetic Drugs,
School of Pharmaceutical Sciences,
Peking University,
Beijing 100083, China
gda5958@163.com*

PROFESSOR YOSHIHIRO MIMAKI

*School of Pharmacy,
Tokyo University of Pharmacy and Life Sciences,
Horinouchi 1432-1, Hachioji, Tokyo 192-0392, Japan
mimakiy@ps.toyaku.ac.jp*

PROFESSOR STEPHEN G. PYNE

*Department of Chemistry
University of Wollongong
Wollongong, New South Wales, 2522, Australia
spyne@uow.edu.au*

PROFESSOR MANFRED G. REINECKE

*Department of Chemistry,
Texas Christian University,
Forts Worth, TX 76129, USA
m.reinecke@tcu.edu*

PROFESSOR WILLIAM N. SETZER

*Department of Chemistry
The University of Alabama in Huntsville
Huntsville, AL 35809, USA
wsetzer@chemistry.ua.edu*

PROFESSOR YASUHIRO TEZUKA

*Faculty of Pharmaceutical Sciences
Hokuriku University
Ho-3 Kanagawa-machi, Kanazawa 920-1181, Japan
y-tezuka@hokuriku-u.ac.jp*

PROFESSOR DAVID E. THURSTON

*Institute of Pharmaceutical Science
Faculty of Life Sciences & Medicine
King's College London, Britannia House
7 Trinity Street, London SE1 1DB, UK
david.thurston@kcl.ac.uk*

HONORARY EDITOR

PROFESSOR GERALD BLUNDEN
*The School of Pharmacy & Biomedical Sciences,
University of Portsmouth,
Portsmouth, PO1 2DT U.K.
axuf64@dsl.pipex.com*

ADVISORY BOARD

- | | |
|---|---|
| Prof. Viqar Uddin Ahmad
<i>Karachi, Pakistan</i> | Prof. Niel A. Koerbanally
<i>Durban, South Africa</i> |
| Prof. Giovanni Appendino
<i>Novara, Italy</i> | Prof. Chiaki Kuroda
<i>Tokyo, Japan</i> |
| Prof. Yoshinori Asakawa
<i>Tokushima, Japan</i> | Prof. Hartmut Laatsch
<i>Gottingen, Germany</i> |
| Prof. Roberto G. S. Berlinck
<i>São Carlos, Brazil</i> | Prof. Marie Lacaille-Dubois
<i>Dijon, France</i> |
| Prof. Anna R. Bilia
<i>Florence, Italy</i> | Prof. Shoei-Sheng Lee
<i>Taipei, Taiwan</i> |
| Prof. Maurizio Bruno
<i>Palermo, Italy</i> | Prof. Imre Mathe
<i>Szeged, Hungary</i> |
| Prof. César A. N. Catalán
<i>Tucumán, Argentina</i> | Prof. M. Soledade C. Pedras
<i>Saskatoon, Canada</i> |
| Prof. Josep Coll
<i>Barcelona, Spain</i> | Prof. Luc Pieters
<i>Antwerp, Belgium</i> |
| Prof. Geoffrey Cordell
<i>Chicago, IL, USA</i> | Prof. Peter Proksch
<i>Düsseldorf, Germany</i> |
| Prof. Fatih Demirci
<i>Eskişehir, Turkey</i> | Prof. Phila Raharivelomanana
<i>Tahiti, French Polynesia</i> |
| Prof. Ana Cristina Figueiredo
<i>Lisbon, Portugal</i> | Prof. Luca Rastrelli
<i>Fisciano, Italy</i> |
| Prof. Cristina Gracia-Viguera
<i>Murcia, Spain</i> | Prof. Stefano Serra
<i>Milano, Italy</i> |
| Dr. Christopher Gray
<i>Saint John, NB, Canada</i> | Prof. Monique Simmonds
<i>Richmond, UK</i> |
| Prof. Dominique Guillaume
<i>Reims, France</i> | Dr. Bikram Singh
<i>Palampur, India</i> |
| Prof. Duvvuru Gunasekar
<i>Tirupati, India</i> | Prof. John L. Sorensen
<i>Manitoba, Canada</i> |
| Prof. Hisahiro Hagiwara
<i>Niigata, Japan</i> | Prof. Johannes van Staden
<i>Scottsville, South Africa</i> |
| Prof. Tsukasa Iwashina
<i>Tsukuba, Japan</i> | Prof. Valentin Stonik
<i>Vladivostok, Russia</i> |
| Prof. Leopold Jirovetz
<i>Vienna, Austria</i> | Prof. Winston F. Tinto
<i>Barbados, West Indies</i> |
| Prof. Vladimir I Kalinin
<i>Vladivostok, Russia</i> | Prof. Sylvia Urban
<i>Melbourne, Australia</i> |
| Prof. Phan Van Kiem
<i>Hanoi, Vietnam</i> | Prof. Karen Valant-Vetschera
<i>Vienna, Austria</i> |

INFORMATION FOR AUTHORS

Full details of how to submit a manuscript for publication in Natural Product Communications are given in Information for Authors on our Web site <http://www.naturalproduct.us>.

Authors may reproduce/republish portions of their published contribution without seeking permission from NPC, provided that any such republication is accompanied by an acknowledgment (original citation)-Reproduced by permission of Natural Product Communications. Any unauthorized reproduction, transmission or storage may result in either civil or criminal liability.

The publication of each of the articles contained herein is protected by copyright. Except as allowed under national "fair use" laws, copying is not permitted by any means or for any purpose, such as for distribution to any third party (whether by sale, loan, gift, or otherwise); as agent (express or implied) of any third party; for purposes of advertising or promotion; or to create collective or derivative works. Such permission requests, or other inquiries, should be addressed to the Natural Product Inc. (NPI). A photocopy license is available from the NPI for institutional subscribers that need to make multiple copies of single articles for internal study or research purposes.

To Subscribe: Natural Product Communications is a journal published monthly. 2015 subscription price: US\$2,595 (Print, ISSN# 1934-578X); US\$2,595 (Web edition, ISSN# 1555-9475); US\$2,995 (Print + single site online); US\$595 (Personal online). Orders should be addressed to Subscription Department, Natural Product Communications, Natural Product Inc., 7963 Anderson Park Lane, Westerville, Ohio 43081, USA. Subscriptions are renewed on an annual basis. Claims for nonreceipt of issues will be honored if made within three months of publication of the issue. All issues are dispatched by airmail throughout the world, excluding the USA and Canada.



Professor Feng-Peng Wang

Editorial

It is my privilege and pleasure to introduce this issue, which is dedicated to Professor Feng-Peng Wang, West China School of Pharmacy, Sichuan University, China, on the occasion of his 70th birthday. The editors join me in paying tribute to Professor Wang for his outstanding contributions to natural products chemistry and diterpenoid alkaloids in particular.

He has published over 255 research papers, book chapters, reviews, and three books. He is on the Editorial Advisory Boards of several journals including *Journal of Asian Natural Products Research*, *Acta Pharmaceutica Sinica B*, the *Chinese Journal of Natural Medicines*, and *Natural Product Research and Development*.

I am extremely grateful for his contributions to *Natural Product Communications* from the very beginning. He has already published 16 articles in the journal, his first appearing in 2006 [Two new C₁₈-diterpenoid alkaloids from *Aconitum piepunense*. *Natural Product Communications*, **1**, 191-194.] and the most recent in 2015 [Recent advances in the synthesis of *Stemona* alkaloids. *Natural Product Communications*, **10**, 1093-1102]. I am also looking forward to his further publications in *NPC*, as well as his continued support.

It is a great pleasure to honor the outstanding achievements of Professor Wang on the occasion of his 70th birthday and to send him warm wishes from all his colleagues and friends. Special thanks to Professor Geoffrey A. Cordell (Natural Products Inc., Evanston, IL, USA) and Professor Qiao-Hong Chen (Department of Chemistry, California State University-Fresno, Fresno, CA, USA) for the preface. My thanks go to the authors and reviewers who have made this issue of *Natural Product Communications* possible.

We all express our appreciation for Prof. Wang's excellent contributions to natural products research and wish him all the best for his future.

Pawan K. Agrawal
Editor-in-Chief

Preface

It is a very great pleasure and honor to be invited to write a Preface to this issue of *Natural Product Communications* in recognition of the 70th birthday and the scientific achievements of my dear friend and illustrious colleague Professor Feng-Peng Wang of the West China College of Pharmacy at Sichuan University in Chengdu. He was born on May 11, 1945 in Changwu County, ShanXi Province. He received a B.S. degree in Pharmacy in 1969 from Sichuan Medical College, and was awarded a M.S. degree in 1981, and a Ph.D. degree in Medicinal Chemistry in 1984, from the Institute of Materia Medica, Peking Union Medical College & Chinese Academy of Medical Sciences. His M.S. supervisor was Dr. Qi-Cheng Fang and his Ph.D. supervisor was Academician Xiao-Tian Liang, himself a world-class natural product chemist and a pioneer in the field of natural products in China. In 1985, Professor Wang travelled to the United States and worked for two years as a postdoctoral research fellow in the laboratory of Professor S. William Pelletier at the Natural Products Institute in the University of Georgia. Professor Pelletier was a well-known alkaloid chemist with a substantial interest in the structure elucidation and chemistry of the diterpene alkaloids.

When he returned to China, Professor Wang resumed his lecturer position at the School of Pharmacy of West China University of the Medical Sciences where his talents, drive, and hard work led him through the academic and administrative ranks to become Professor and Dean of the School of Pharmacy, WCUMS, which in 2000 became assimilated with Sichuan University. He is presently a Professor of Medicinal and Natural Products Chemistry, and a highly regarded academic leader in Sichuan Province.

Professor Wang has been working in the field of natural products for over 50 years, and his research interests have consistently focused on the various groups of diterpenoid alkaloids, in particular, those which are derived from traditional Chinese medicines. His research involves the isolation, structure determination, chemistry, structural modifications, and synthesis of alkaloids, and in this process he has characterized 207 new natural products from a variety of plants. As a chemical transformation approach to the taxane diterpene system, he developed the process for the synthetic conversion of abundantly available diterpenoid alkaloids to taxane derivatives. These studies led to the development of numerous intriguing reactions, the formation of over 1000 diterpene alkaloid derivatives, and to his substantial reputation in the field of alkaloid chemistry.

He has also applied his talents in natural product chemistry to drug discovery and development, where he has made significant contributions, including four patents. Particularly, he was involved in the assessment of the effects of several traditional Chinese medicines, including *Fritillaria cirrhosa*, *Codonopsis tangshen*, and *Rhodiola rosea*. At the same time, he was responsible for the development of several standardized preparations of traditional Chinese medicines, including Huo Xiang Zheng Qi San, Wendan Decoction, Yupingsfengsan, and Ziziphi Spinosae Decoction. The first three preparations have already entered the Japanese market. In collaboration with a pharmaceutical company, he has also successfully developed the first, third-generation, multidrug resistance reversal agent (XiuTaiJun) in China. This drug was approved by the Chinese FDA to enter clinical trials, and a phase I study is almost completed.

Professor Wang has assumed responsibility for the development of 18 national and provincial research projects, and has supervised 64 Masters and Doctoral students and several postdoctoral research associates. Over the years, these results have been published in 223 peer-reviewed research articles and in 23 reviews. He is the author or co-author of 11 book chapters, and is an editor of three books. He has been a consistent and outstanding contributor to *The Alkaloids, Chemistry and Biology* series, with chapters on various aspects of the diterpene alkaloids in Volumes 42, 59, 67, and 69. These contributions established him as the world expert on diterpenoid alkaloids. Indeed, his last chapter on the C₁₉-diterpenoid alkaloids was a true “tour de force”, and constituted the whole volume of 578 pages! Two books which he has edited in Chinese, *The Chemistry of Alkaloids* and *Modern Chemistry of Natural Products*, are widely recognized by the natural product community in China as being essential texts.

As a result of his contributions to the chemistry of natural products, Professor Wang and his students have received a number of important awards. The doctoral dissertation of Qiao-Hong Chen, one of his graduate students, received an award as one of the Top 100 National Excellent Doctoral Dissertations in 2003. In 1991, Professor Wang received an Award for a Chinese Ph.D. with Outstanding Contributions from the Ministry of Education in China, the National Evaluation Institute of Degrees and Grade Education, and Peking Union Medical College & Chinese Academy of Medical Sciences. Since 1993, Professor Wang has received special government allocations from the State Council in China, and in 1995 he received the first prize of Wu JiePing Medical Research Award - Paul Janssen Phytochemistry Research Award. In 2002, and again in 2015, he achieved a First Place Natural Science Award from the Ministry of Education in China, and a first place Technology Invention Award from the Ministry of Education in 2004.

Professor Wang has also held a number of professional positions locally and nationally. He was the Chair of the Chengdu Pharmaceutical Association from 1995 to 2005, and the Associate Director of Medical Plant and Plant Medicine at the Botanical Society of China from 2003 to 2008. He has served as an editorial member for the *Journal of Asian Natural Products Research*, *Acta Pharmaceutica Sinica B*, the *Chinese Journal of Natural Medicines*, and *Natural Product Research and Development*. Professor Wang has dedicated his time to serve as a committee member for several key laboratories in China, including the Key Laboratory of Natural and Biomimetic Drugs at Peking University Health Science Center (1990-1996), the Key Laboratory of Phytochemistry and Sustainability of Western Plant Resources at the Kunming Institute of Botany, Chinese Academy of Sciences (1992-2007), at the Key Laboratory of Naturally Bioactive Chemicals and Their Functions, at the Institute of Materia Medica, Chinese Academy of Medical Sciences and Peking Union Medical College (2008-2012), at currently at the Key Laboratory of Basic Substance and Resource Utilization of Chinese Herbal Medicine, Institute of Materia Medica and Institute of Medicinal Plant Development, Chinese Academy of Medical Sciences and Peking Union Medical College (2012-present), and at

the Guangdong Higher Education Key Laboratory of Potential Chemical Components and Innovation of Traditional Chinese Medicines, College of Pharmacy, Jinan University (2010-present).

I have had the great pleasure of knowing Professor Wang for many years, indeed since he was with Professor Pelletier as a postdoctoral fellow, and worked with him on the chapters for *The Alkaloids* series, when I was the Editor. More personally though, I have been blessed to have had the great good fortune to have spent time in Chengdu with him on several occasions, and I have had the enormous pleasure to be the recipient of his tremendous generosity and hospitality. Together, we have traveled to many parts of Sichuan and Yunnan Provinces, as well as a highly memorable trip down the Yangtze River from Chongqing to Wuhan. We have visited many of the most spectacular sights in that part of China, including the giant panda sanctuaries in Wolong, the glorious Mt. Emei, one of the most revered mountains in Chinese Buddhism, the unparalleled scenery of Jiuzhaigou (twice!), several Tibetan autonomous areas, the ethnic communities in Lijiang and Shangri-la in Yunnan Province, and numerous wonderful temples and monasteries, as well as the remarkable water works of Dujiangyan. My life has been made significantly richer thanks to Professor Feng-Peng Wang, for which I am extremely grateful. So, at this time, it is truly and sincerely a very great pleasure to have the opportunity to honor him for his extensive contributions to natural products over the past 50 years, and to recognize the auspicious occasion of his 70th birthday.

Geoffrey A. Cordell,
Natural Products Inc.
Evanston, IL, USA

Preface

It is my great privilege and pleasure to be able to write a preface for this special issue of the *Natural Product Communications (NPC)* in honor of the seventieth birthday of Dr. Feng-Peng Wang, a professor of Medicinal and Natural Product Chemistry of Sichuan University in P. R. China. Professor Wang has dedicated his 45-year professional life to the advancement of natural products research and education in China.

Professor Feng-Peng Wang was born in a family of a remote village located in the northwest part of China. His illiterate parents lived on farming a small piece of land, but their vision statement was to highly inspire their children to pursue knowledge through reading books. Professor Wang earned a B.S. degree in pharmacy in 1969 from Sichuan Medical College; he then was awarded with a M.S. degree and a P.D. degree in Medicinal Chemistry in 1981 and 1984, respectively, from the Institute of Material Medica, Peking Union Medical College & Chinese Academy of Medical Sciences. His lifetime love of natural products (especially diterpenoid alkaloids) was initiated by his master thesis and Ph.D. dissertation, especially under the guidance of Professor Xiao-Tian Liang who was a founder and pioneer of Chinese natural products chemistry. After graduation he worked for two years at the University of Georgia, USA, with Professor S. W. Pelletier as a postdoctoral associate in the field of diterpenoid alkaloids. In 1987, he returned back to his Alma mater--the West China University of Medical Sciences, where he persisted in his work on isolation, structural determination, chemical reactions, synthesis, and biological evaluation of diterpenoid alkaloids from *Aconitum* and *Delphinium* species. Since 1990, his research interests were extended to the conventional syntheses of anticancer taxane analogs from diterpenoid alkaloids, development of multi-drug resistance reversal agents for the combination therapy of cancer, and development of diterpenoid alkaloids for the potential treatment of cardiovascular diseases.

His 45-year affiliation with Sichuan University can be concluded as an excellent researcher and educator with productivity and high quality in both publications and training graduate students. Professor Wang has made numerous outstanding contributions to the field of Natural Products featuring the one in the field of diterpenoid alkaloids, a class of the largest and most complicated group of terpenoid alkaloids with an intriguing chemistry and numerous bioactivities. Professor Wang has 'dug out' over 200 new diterpenoid alkaloids from various *Aconitum* and *Delphinium* plants and prepared over 1000 new diterpenoid alkaloids. One diterpenoid alkaloid (bulleyaconitine A) that was first isolated by Dr. Wang *et. al.* has been developed into clinical use as non-narcotic analgesic and anti-inflammatory drug in China. Some diterpenoid alkaloids with novel skeletons (e.g. atropurpuran) discovered by his research group have become attracting and challenging synthetic targets of many excellent research groups due to their intrinsic beauty and structural complexity. Very recently, one compound designated as "WF" isolated from "Fuzi" (a famous traditional Chinese medicine) has been established by Dr. Wang's research group as a promising candidate that significantly enhance the survival rate of mice with chronic heart failure and to appreciably improve the cardiac structure and functions in mice, as compared to cedilnid. He has successfully developed the first third-generation multi-drug resistance reversal agent (XiuTaiJun) in China, which has entered human phase I clinical studies in China. During his productive and distinguished career spanning over 45 years, Professor Wang has authored or coauthored over 240 peer-reviewed scientific publications and 11 book chapters, and is an editor for 3 books. As an expert on diterpenoid alkaloids, he has persistently committed to the series collections of "The Alkaloids" edited by Professor Geoffrey A. Cordell and has compiled four chapters for volumes 42, 59, 67, and 69. Two books entitled "The Chemistry of Alkaloids" and "Modern Chemistry of Natural Products" compiled by Dr. Wang have been widely recognized by and have indeed benefited to the natural product community in China.

In addition to the high quality of his own research work, he has successfully trained 40 Master's level and 26 doctoral students, and 3 postdoctoral associates. Most of his students have highly successful careers in academies or pharmaceutical industry. His contributions continue to inspire his students and young scientists. In addition to his formal presentations in the scientific literature, Professor Wang has been and still is very active in helping and inspiring young scientists by serving as an academic committee member in a variety of universities and research institutes throughout China.

Throughout his highly rewarding tenure, Professor Wang has achieved numerous awards, including the first prize of Wu Jieping Medical Research Award – Paul Janssen Phytochemistry Research Award in 1995, two Natural Science Awards and one Technology Invention Award from the Ministry of Education in China (First Place, 2002, 2004, and 2015). Additionally, one doctoral dissertation supervised by him has achieved an Award for Top 100 National Excellent Doctoral Dissertations in China in 2003.

The author was fortunate enough to be associated with Professor Wang in the late 1990s as one of his Ph.D. students which inspired the author to be interested in natural products and initiated an over 15-year productive collaboration. The author has benefited much from his guidance.

Qiao-Hong Chen
Department of Chemistry
California State University-Fresno
Fresno, CA 93740

Natural Product Communications

2015

Volume 10, Number 12

Contents

Original Paper

Petchienes A–E, Meroterpenoids from <i>Ganoderma petchii</i>	2019
Qin-Lei Gao, Ping-Xia Guo, Qi Luo, Hui Yan and Yong-Xian Cheng	
Megastigmane Glycosides from the Leaves of <i>Tripterygium wilfordii</i>	2023
Lin Ni, Xiao-mei Zhang, Xing Zhou, Jie Ma, Chuang-jun Li, Li Li, Tian-tai Zhang and Dong-Ming Zhang	
Cytochalasans and Sesquiterpenes from <i>Eutypella scoparia</i> 1–15	2027
Shuang Qi, Yue Wang, Zhonghui Zheng, Qingyan Xu and Xiamming Deng	
Concise Synthesis of Taiwaniaquinol B and 5- <i>epi</i> -Taiwaniaquinone G	2031
Yonggang Meng, Yizhen Liu, Zhigang Lv, Jinqian Wang, Yanyan Wang, Chuanjun Song and Junbiao Chang	
Effect of Enzyme Inhibitors on Terpene Trilactones Biosynthesis and Gene Expression Profiling in <i>Ginkgo biloba</i> Cultured Cells	2033
Lijia Chen, Hui Tong, Mingxuan Wang, Jianhua Zhu, Jiachen Zi, Liyan Song and Rongmin Yu	
Macrocyclic Diterpenoids from the Latex of <i>Euphorbia helioscopia</i>	2037
Juan Hua, Yan-Chun Liu, Shu-Xi Jing, Shi-Hong Luo and Sheng-Hong Li	
A New Triterpenoid from the Aerial Parts of <i>Agrimonia pilosa</i>	2041
Jiang-Hao Ma, Qing-Hua Jiang, Ying Chen, Xiu-Fang Nie, Tie Yao, Li-Qin Ding, Feng Zhao, Li-Xia Chen and Qiu Feng	
Two New 18-Norschiartane-type Schinortriterpenoids from <i>Schisandra lancifolia</i>	2045
Miao Liu, Yuan-Qing Luo, Wei-Guang Wang, Yi-Ming Shi, Hai-Yan Wu, Xue Du, Jian-Xin Pu and Han-Dong Sun	
Terpenoids and Steroids from <i>Euphorbia hypericifolia</i>	2049
Jin-Xin Zhao, Shan-Shan Shi, Li Sheng, Jia Li and Jian-Min Yue	
A Fragmentation Study of Six C ₂₁ Steroidal Aglycones by Electrospray Ionization Ion-Trap Time-of-Flight Tandem Mass Spectrometry	2053
Xing-Long Chen, Chang-An Geng and Ji-Jun Chen	
Three New Cytotoxic Withanolides from the Chinese Folk Medicine <i>Physalis angulata</i>	2059
Cai-Yun Gao, Ting Ma, Jun Luo and Ling-Yi Kong	
Diterpenoid Alkaloids from <i>Aconitum soongaricum</i> var. <i>pubescens</i>	2063
Lin Chen, Lianhai Shan, Jifa Zhang, Wenliang Xu, Mingyu Wu, Shuai Huang and Xianli Zhou	
Two New C ₁₈ -Diterpenoid Alkaloids from <i>Delphinium anthriscifolium</i>	2067
Lianhai Shan, Jifa Zhang, Lin Chen, Jiaxi Wang, Shuai Huang and Xianli Zhou	
Majusine D: A New C ₁₉ -diterpenoid Alkaloid from <i>Delphinium majus</i>	2069
Qi Zhao, Xiao-jun Gou, Wei Liu, Gang He, Li Liang and Feng-zheng Chen	
Epoxide Opening of a 7,17-Seco-7,8-Epoxy-C ₁₉ -Diterpenoid Alkaloid	2071
Hong Ji, Feng-Peng Wang and Qiao-Hong Chen	
Further Studies on Structure-Cardiac Activity Relationships of Diterpenoid Alkaloids	
Zhong-Tang Zhang, Xi-Xian Jian, Jia-Yu Ding, Hong-Ying Deng, Ruo-Bing Chao, Qiao-Hong Chen, Dong-Lin Chen and Feng-Peng Wang	2075
Monoterpene Indole Alkaloids from <i>Catharanthus roseus</i> Cultivated in Yunnan	2085
Bei Wang, Lu Liu, Ying-Ying Chen, Qiong Li, Dan Li, Ya-Ping Liu and Xiao-Dong Luo	
Two New Oxindole Alkaloid Glycosides from the Leaves of <i>Nauclea officinalis</i>	2087
Long Fan, Xiao-Jun Huang, Chun-Lin Fan, Guo-Qiang Li, Zhen-Long Wu, Shuo-Guo Li, Zhen-Dan He, Ying Wang and Wen-Cai Ye	
Lycopodium Alkaloids from <i>Diphasiastrum complanatum</i>	2091
Yu Tang, Juan Xiong and Jin-Feng Hu	
Effects of Adding Vindoline and MeJA on Production of Vincristine and Vinblastine, and Transcription of their Biosynthetic Genes in the Cultured CMCs of <i>Catharanthus roseus</i>	2095
Wenjin Zhang, Jiazeng Yang, Jiachen Zi, Jianhua Zhu, Liyan Song and Rongmin Yu	
Structures and Chemotaxonomic Significance of Stemona Alkaloids from <i>Stemona japonica</i>	2097
Min Yi, Xue Xia, Hoi-Yan Wu, Hai-Yan Tian, Chao Huang, Paul Pui-Hay But, Pang-Chui Shaw and Ren-Wang Jiang	
Chemical Constituents of <i>Euonymus glabra</i>	2101
Jie Ren, Yang-Guo Xie, Xing Wang, Shi-Kai Yan, Hui-Zi Jin and Wei-Dong Zhang	
Isoprenylated Flavonoids with PTP1B Inhibition from <i>Ficus tikoua</i>	2105
Lu-Qin Wu, Chun Lei, Li-Xin Gao, Hai-Bing Liao, Jing-Ya Li, Jia Li and Ai-Jun Hou	
Phenolic Derivatives from <i>Hypericum japonicum</i>	2109
Guoyong Luo, Min Zhou, Qi Ye, Jun Mi, Dongmei Fang, Guolin Zhang and Yinggang Luo	
Synthesis and Anti-Proliferative Effects of Quercetin Derivatives	2113
Sami M.R. Al-Jabban, Xiaojie Zhang, Guanglin Chen, Ermias Addo Mekuria, Liva Harinantenaina Rakotondraibe and Qiao-Hong Chen	

Continued Overleaf

Compounds with Antifouling Activities from the Roots of <i>Notopterygium franchetii</i> Chun Yu, Liqing Cheng, Zhongling Zhang, Yu Zhang, Chunmao Yuan, Weiwei Liu, Xiaojiang Hao, Weiguang Ma and Hongping He	2119
New Isochromane Derivatives from the Mangrove Fungus <i>Aspergillus ustus</i> 094102 Peipei Liu, Cong Wang, Zhenyu Lu, Tonghan Zhu, Kui Hong and Weiming Zhu	2123
Pericocins A–D, New Bioactive Compounds from <i>Periconia</i> sp. Yue-Hua Wu, Gao-Keng Xiao, Guo-Dong Chen, Chuan-Xi Wang, Dan Hu, Yun-Yang Lian, Feng Lin, Liang-Dong Guo, Xin-Sheng Yao and Hao Gao	2127
New Benzenoids from the Roots of <i>Lindera aggregata</i> Guo-Hao Ma, Che-Wei Lin, Hsin-Yi Hung, Sheng-Yang Wang, Po-Chuen Shieh and Tian-Shung Wu	2131
12-Membered Resorcylic Acid Lactones Isolated from <i>Saccharicola bicolor</i>, an Endophytic Fungi from <i>Bergenia purpurascens</i> Da-Le Guo, Min Zhao, Shi-Ji Xiao, Bing Xia, Bo Wan, Yu-Cheng Gu, Li-Sheng Ding and Yan Zhou	2135
Phenylpropanoid Glycosides from the Leaves of <i>Ananas comosus</i> Wen-Hao Chen, Xiao-Juan Huang, Huo-Ming Shu, Yang Hui, Fei-Yan Guo, Xiao-Ping Song, Ming-Hui Ji and Guang-Ying Chen	2137
Tannins and Antioxidant Activities of the Walnut (<i>Juglans regia</i>) Pellicle Tian-Peng Yin, Le Cai, Yang Chen, Ying Li, Ya-Rong Wang, Chuan-Shui Liu and Zhong-Tao Ding	2141
Chemical Constituents of <i>Cordyceps cicadae</i> Zhi-Bo Chu, Jun Chang, Ying Zhu and Xun Sun	2145
A New Bithiophene from the Root of <i>Echinops grijsii</i> Fang-Pin Chang, Chien-Chih Chen, Hui-Chi Huang, Sheng-Yang Wang, Jih-Jung Chen, Chang-Syun Yang, Chung-Yi Ou, Jin-Bin Wu, Guan-Jhong Huang and Yueh-Hsiung Kuo	2147
Cyclic Lipopeptides with Herbicidal and Insecticidal Activities Produced by <i>Bacillus clausii</i> DTM1 Da-Le Guo, Bo Wan, Shi-Ji Xiao, Sarah Allen, Yu-Cheng Gu, Li-Sheng Ding and Yan Zhou	2151
Synthesis of (6R,12R)-6,12-Dimethylpentadecan-2-one, the Female-Produced Sex Pheromone from Banded Cucumber Beetle <i>Diabrotica balteata</i>, Based on a Chiron Approach Wei Shen, Xiang Hao, Yong Shi and Wei-Sheng Tian	2155
A Rapid Study of Botanical Drug–Drug Interaction with Protein by Re-ligand Fishing using Human Serum Albumin–Functionalized Magnetic Nanoparticles Lin-Sen Qing, Ying Xue, Li-Sheng Ding, Yi-Ming Liu, Jian Liang and Xun Liao	2161
Serum Metabolomic Profiling of Rats by Intervention of <i>Aconitum soongaricum</i> Fan Zhang, Jiao Liu, Jun Lei, Wenjing He and Yun Sun	2165
Re-evaluation of ABTS⁺ Assay for Total Antioxidant Capacity of Natural Products Jian-Wei Dong, Le Cai, Yun Xing, Jing Yu and Zhong-Tao Ding	2169

Accounts/Reviews

Chemical Synthesis of the Echinopine Sesquiterpenoids Xiao-Yu Liu and Yong Qin	2173
Synergistic Effects of Dietary Natural Products as Anti-Prostate Cancer Agents Bao Vue, Sheng Zhang and Qiao-Hong Chen	2179
<i>Ligustrum lucidum</i> and its Constituents : A Mini-Review on the Anti-Osteoporosis Potential Chun-Tao Che and Man-Sau Wong	2189
Alice, Benzene, and Coffee: The ABCs of Ecopharmacognosy Geoffrey A. Cordell	2195

Additions/Corrections

Cytotoxic and Antimalarial Alkaloids from the Twigs of <i>Dasyaschalon obtusipetalum</i> Atchara Jaidee, Thanika Promchai, Kongkiat Trisuwant, Surat Laphookhieo, Roonglawan Rattanajak, Sumalee Kamchonwongpaisan, Stephen G. Pyne and Thunwadee Ritthiwigrom <i>Natural Product Communications</i> , 10 (7), 1175-1177 (2015)	2203
--	-------------

Manuscripts in Press

Cummulative Index

Contents	<i>i-xxi</i>
Author Index	<i>i-viii</i>
Keywords Index	<i>i-viii</i>

LIST OF AUTHORS

Al-Jabban, SMR	2113	He, H	2119	Luo, SH	2037	Wu, HY	2045,2097
Allen, S	2151	He, W	2165	Luo, XD	2085	Wu, JB	2147
But, PPH.....	2097	He, ZD	2087	Luo, Y	2109	Wu, LQ	2105
Cai, L	2141,2169	Hong, K	2123	Luo, YQ	2045	Wu, M	2063
Chang, FP	2147	Hou, AJ	2105	Lv, Z	2031	Wu, TS	2131
Chang, J	2145	Hu, D	2127	Ma, GH	2131	Wu, YH	2127
Chang, JU	2031	Hu, JF	2091	Ma, J	2023	Wu, ZLK	2087
Chao, RB	2075	Hua, J	2037	Ma, JH	2041	Xia, B	2135
Che, CT	2189	Huang, C	2097	Ma, T	2059	Xia, X	2097
Chen, JJ	2147	Huang, GJ	2147	Ma, W	2119	Xiao, GK	2127
Chen, L	2063	Huang, HC	2147	Mekuria, EA	2113	Xiao, SJ	2135,2151
Chen, CC	2147	Huang, S	2063,2067	Meng, Y	2031	Xie, YG	2101
Chen, DL	2075	Huang, XJ	2087,2137	Mi, J	2109	Xing, Y	2169
Chen, F	2069	Hui, Y	2137	Nie, XF	2041	Xiong, J	2091
Chen, G.....	2113	Hung, HY	2131	Ou, CY	2147	Xu, Q	2027
Chen, GD	2127	Ji, H	2071	Pu, JX	2045	Xu, W	2063
Chen, GY	2137	Ji, MH	2137	Qi, S	2027	Xue, Y	2161
Chen, JJ	2053	Jian, XX	2075	Qin, Y	2173	Yan, H	2019
Chen, L	2033,2067	Jiang, QH	2041	Qing, LS	2161	Yan, SK	2101
Chen, LX	2041,2071,2075	Jiang, RW	2097	Rakotondraibe, LH	2113	Yang, CS	2147
Chen, QH	2113,2179	Jin, HZ	2101	Ren, J	2101	Yang, J	2095
Chen, WH	2137	Jing, SX	2037	Shan, L	2063,2067	Yao, T	2041
Chen, XL	2053	Kong, LY	2059	Shaw, PC	2097	Yao, XS	2127
Chen, Y	2041,2141	Kuo, YH	2147	Shen, W	2155	Ye, Q	2109
Chen, YY	2085	Lei, C	2105	Sheng, L	2049	Ye, WC	2087
Cheng, L	2119	Lei, J	2165	Shi, SS	2049	Yi, M	2097
Cheng, YX	2019	Li, C	2023	Shi, Y	2155	Yin, TP	2141
Chu, ZB	2145	Li, D	2085	Shi, YM	2045	Yu, C	2119
Cordell, GA	2195	Li, GQ	2087	Shieh, PC	2131	Yu, J	2169
Deng, HY	2075	Li, J	2049,2105	Shu, HM	2137	Yu, R	2033,2095
Deng, X	2027	Li, JY	2105	Song, C	2031	Yuan, C	2119
Ding, JY	2075	Li, L	2023	Song, L	2033,2095	Yue, JM	2049
Ding, LQ	2041	Li, Q	2085	Song, XP	2137	Zhang, DM	2023
Ding, LS	2135,2161	Li, SG	2087	Sun, HD	2045	Zhang, F	2165
Ding, ZT	2141,2169	Li, SH	2037	Sun, X	2145	Zhang, G	2109
Ding,LS	2151	Li, Y	2141	Sun, Y	2165	Zhang, J	2063,2067
Dong, JW	2169	Lian, YY	2127	Tang, Y	2091	Zhang, S	2179
Du, X	2045	Liang, J	2161	Tian, HY	2097	Zhang, T	2023
Fan, CL	2087	Liang, L	2069	Tian, WS	2155	Zhang, W	2095
Fan, L	2087	Liao, HB	2105	Tong, H	2033	Zhang, WD	2101
Fang, D	2109	Liao, X	2161	Vue, B	2179	Zhang, X	2023,2113
Feng, Q	2041	Lin Ni, L	2023	Wan, B	2135,2151	Zhang, Y	2119
Gao, CY	2059	Lin, CW	2131	Wang, B	2085	Zhang, Z	2119
Gao, H	2127	Lin, F	2127	Wang, C	2123	Zhang, ZT	2075
Gao, LX	2105	Liu, CS	2141	Wang, CX	2127	Zhao, JX	2049
Gao, QL	2019	Liu, J	2165	Wang, FP	2071,2075	Zhao, F	2041
Geng, CA	2053	Liu, L	2085	Wang, J	2031,2067	Zhao, M	2135
Gou, X	2069	Liu, M	2045	Wang, M	2033	Zhao, Q	2069
Gu, YC	2135,2151	Liu, P	2123	Wang, SY	2131,2147	Zheng, Z	2027
Guo, DL	2135,2151	Liu, W	2069,2119	Wang, WG	2045	Zhou, M	2109
Guo, FY	2137	Liu, XY	2173	Wang, X	2101	Zhou, X	2023,2063,2067
Guo, LD	2127	Liu, Y	2031	Wang, Y	2027,2031,2087	Zhou, Y	2135,2151
Guo, PX	2019	Liu, YC	2037	Wang, YR	2141	Zhu, J	2033,2095
Hao, X	2119,2155	Liu, YM	2161	Wong, MS	2189	Zhu, T	2123
He, G	2069	Liu, YP	2085			Zhu, W	2123
		Lu, Z	2123			Zhu, Y	2145
		Luo, G	2109			Zi, J	2033,2095
		Luo, J	2059				
		Luo, Q	2019				

KEYWORDS INDEX

Absolute configuration.....	2045,2091	Jatrophane diterpenoid.....	2037	PTP1B inhibitor	2049
ABTS.....	2169	<i>Juglans regia</i>	2141	Quality control	2195
<i>Aconitum soongaricum</i> var. <i>pubescens</i>	2063	Latex.....	2037	Quantitative RT-PCR.....	2095
<i>Aconitum soongaricum</i>	2165	Lathyrane diterpenoid	2037	Quercetin.....	2113
<i>Agrimonia pilosa</i>	2041	Lauraceae	2131	Ranunculaceae	2165
Alice in Wonderland	2195	Ligustrum Lucidi Fructus	2189	Reaction time	2169
Amino acid	2145	<i>Diphasiastrum complanatum</i>	2091	Recommendation	2169
<i>Ananas comosus</i>	2137	Diterpenoid alkaloid...	2069,2071	Re-ligand fishing.....	2161
Anthriscifoline	2067	Diterpenoid alkaloid.....	2075	Resorcylic acid lactone	2135
Antibacterial activities	2137	Diterpenoid alkaloids	2063,2067	Rubiaceae	2087
Antifeedant activity.....	2063	DNA phylogenetics	2097	<i>Saccharicola bicolor</i>	2135
Antifouling	2119	Dopamine analogue.....	2145	Schinortriterpenoids	2045
Anti-inflammatory activity .	2037	Drug-drug interaction	2161	<i>Schisandra lancifolia</i>	2045
Anti-inflammatory.....	2041,2147	ECD	2091,2131	Scopararanes	2027
Antimicrobial activity	2127	Echinopine.....	2173	Scoparasins	2027
Anti-osteoporotic activity ...	2189	<i>Echinops grijsii</i>	2147	Sesquiterpenoid.....	2173
Antioxidant.....	214	Ecopharmacognosy	2195	Sex pheromone.....	2155
Anti-oxidation	2123	Endolichenic fungus	2127	Solvent	2169
Apocynaceae	2085	Enzyme inhibitors	2033	Spiro-compound.....	2019
<i>Aspergillus ustus</i>	2123	<i>Epi-taiwaniaquinone G</i>	2031	STAT1	2023
<i>Bacillus clausii</i>	2151	Epoxide-opening	2071	<i>Stemona</i> alkaloid	2097
Benzene	2195	ESI-IT-TOF-MS ⁿ	2053	<i>Stemona japonica</i>	2097
Benzenoids	2131	<i>Euonymus glabra</i>	2101	Steroid	2049
<i>Bergenia purpurascens</i>	2135	Euonyphenylpropane A	2101	Steroidal aglycones	2053
Bifuran derivative.....	2145	<i>Euphorbia helioscopia</i>	2037	Structure-activity relationships.....	2075
Biogenetic pathway	2041	<i>Euphorbia hypericifolia</i>	2049	Surfactin	2151
Biomarkers	2165	<i>Ficus tikoua</i>	2105	Synergy	2179
Biosynthesis	2033	Flavan	2101	Synthesis	2155
Bithiophene	2147	Fragmentation pathways	2053	Taiwaniaquinol B	2031
Bone health.....	2189	<i>Ganoderma petchii</i>	2019	Tandem reaction.....	2031
Bromeliaceae	2137	Ganodermataceae	2019	Tannin	2141
Butynyl-bithiophene.....	2147	Gene expression profiling	2095	Technology integration	2195
Cardioactive evatuation.....	2075	Gene expression	2033	Terpene trilactones	2033
<i>Catharanthus roseus</i> ..	2085,2095	<i>Ginkgo biloba</i>	2033	Tetrahydro-oxazine ring	2087
Cell proliferation	2113	Global health care	2195	TIAs	2095
Chemical constituent.....	2119	Glucosidase inhibition.....	2123	Total synthesis	2173
Chemical transformation.....	2091	Herbicidal	2151	Traditional medicines	2195
Chemotaxonomic significance.....	2097	Human serum albumin– functionalized magnetic nanoparticles	2161	<i>Tripterygium wilfordii</i>	2023
CMCs.....	2095	Insecticidal	2151	Triterpenoid.....	2049
Coffee	2195	Isochromane derivatives	2123	Umbelliferae	2119
Combination therapy	2179	Isoprenylated flavonoids	2105	Ursane 28-nortriterpene	2041
<i>Cordyceps cicadae</i>	2145	Pseudo-protodioscin	2161	Wilfordoninol	2023
Cytochalasan	2027	Protein tyrosine phosphatase		Wilfordoniside	2023
Cytotoxic activity	2027,2059	1B	2105	Withanolides	2059
Dehydrocoronaridine.....	2085				

Petchienes A–E, Meroterpenoids from *Ganoderma petchii*

Qin-Lei Gao^{a,c,1}, Ping-Xia Guo^{d,1}, Qi Luo^{a,c}, Hui Yan^a and Yong-Xian Cheng^{a,b,*}

^aState Key Laboratory of Phytochemistry and Plant Resources in West China, Kunming Institute of Botany, Chinese Academy of Sciences, Kunming 650204, People's Republic of China

^bCollege of Pharmacy, Chengdu University of Traditional Chinese Medicine, Chengdu 610075, People's Republic of China

^cUniversity of Chinese Academy of Sciences, Yuquan Road 19, Beijing 100049, People's Republic of China

^dShanxi University of Traditional Chinese Medicine, Taiyuan 030024, People's Republic of China

yxcheng@mail.kib.ac.cn

Received: September 23rd, 2015; Accepted: October 15th, 2015

Petchienes A–E (**1–5**), five new meroterpenoids, were isolated from the fruiting bodies of *Ganoderma petchii*. Their structures, including absolute configurations, were elucidated by means of spectroscopic and computational methods. Compound **4** was isolated as a racemic mixture, which was finally purified by chiral HPLC to yield individual (–) and (+)-enantiomers. Biological evaluation showed that compounds **2** and (–)-**4** could increase intracellular free calcium concentration at 10 µM in HEK-293 cells.

Keywords: *Ganoderma petchii*, Ganodermataceae, Meroterpenoids, Spiro-compound.

Meroterpenoids from the genus *Ganoderma* are characterized by a 1,4-dihydroxybenzene residue conjugated with a terpenoidal moiety. Since the discovery from *G. pfeifferi* of ganomycins A and B in this class of meroterpenoids [1], few other investigations associated with this compound class from *Ganoderma* species have been reported. We isolated a novel meroterpenoid termed lingzhiol from *G. lucidum* [2a], and since then, several structurally diverse meroterpenoids with renal or neural protective effects were characterized by us [2b–2e]. In our continuing efforts focused on the search of bioactive meroterpenoids from *Ganoderma*, *G. petchii* became our research target. This fungus is distributed in China, Sri Lanka, Malaysia, Singapore and Indonesia. In China, it is used as a healthcare mushroom and seen in several markets of Chinese medical materials. Our efforts on this fungus led to the isolation of five new meroterpenoids, and here we describe their isolation, structure characterization and biological evaluation.

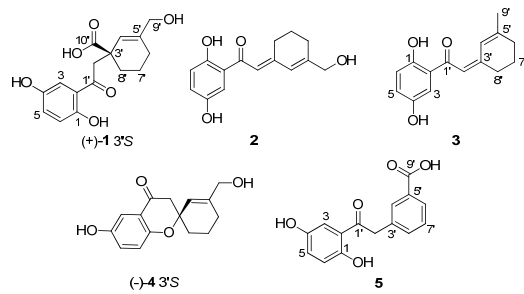


Figure 1: The chemical structures of compounds **1–5**.

Petchiene A (**1**) has the molecular formula C₁₆H₁₈O₆ derived from its HRESIMS, ¹³C NMR and DEPT spectra. The ¹H NMR spectrum (Table 1) of **1** contains a typical ABX spin system [δ_{H} 7.32 (1H, d, $J = 2.7$ Hz, H-3), 7.07 (1H, dd, $J = 8.9, 2.7$ Hz, H-5), 6.79 (1H, d, $J = 8.9$ Hz, H-6)], suggesting the presence of a 1,2,4-trisubstituted benzene ring, along with a resonance for an olefinic proton. The ¹³C NMR and DEPT spectra contain resonances for 16 carbons including five aliphatic methylenes (one oxygenated), four methines

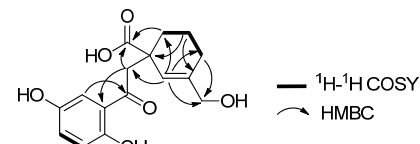


Figure 2: COSY and key HMBC correlations of **1**.

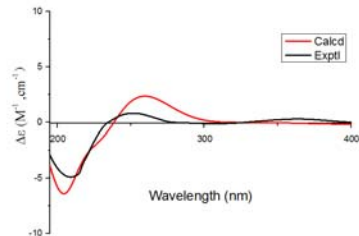


Figure 3: Calculated and experimental ECD spectra of (+)-**1** (red, at the B3LYP-SCRF (PCM)/6-311+G(2d,p)/B3LYP/6-311+G(2d,p) level in MeOH; black, experimentally observed in MeOH).

(all sp²), and seven quaternary carbons (one ketone, one carboxylic acid, four olefinic including two oxygenated). The ¹H-¹H COSY spectrum (Figure 2) showed correlations between H-5/H-6 and H-6'/H-7'/H-8'. In the HMBC spectrum, the correlation from H-3 to C-1' (δ_{C} 204.9) indicates that the phenyl unit is linked to C-1', and from H-2' (δ_{H} 3.49, 3.46) to C-2 (δ_{C} 120.1), C-1', C-3' (δ_{C} 44.8) indicate that C-2' is linked to C-1'. In addition, HMBC correlations between H-7'/C-3', C-5' and H-4'/C-6', C-8', in combination with COSY correlations of H-6'/H-7'/H-8' and degrees of unsaturation of **1**, indicate the presence of a six-membered ring. The positions of a carboxylic acid and a hydroxymethyl were assigned by the HMBC correlations between H-2', H-4'/C-10' and H-4', H-6'/C-9'. Hence, the planar structure of **1** was identified as shown. **1** was isolated as a non-racemic compound indicated by its optical rotation. The absolute configuration at the single chiral center of **1** was clarified by electronic circular dichroism (ECD) calculations. For this

purpose, DFT and TD-DFT calculations were carried out at 298 K in the gas phase with Gaussian 09 [3]. The ECD spectrum of (3'S)-**1**, correlates well with the experimental ECD spectrum of **1**, leading to the unambiguous assignment of the absolute configurations at the stereogenic centers in **1** as 3'S (Figure 3).

Petchiene B (**2**) was found to have the molecular formula C₁₅H₁₆O₄ (8 degrees of unsaturation) deduced from its HRESIMS, ¹³C NMR and DEPT spectra. The ¹H and ¹³C NMR spectra of **2** are similar to those of **1**. The only difference is that the Δ² double bond of **2** was formed by decarboxylation of **1** (Figure 4), which could be supported by HMBC correlations between H-2' (δ_H 6.77)/C-1', C-2, C-3' and H-7', H-8'/C-3' (δ_C 157.7). In addition, a ROESY correlation between H-2' (δ_H 6.77)/H-4' (δ_H 6.39) was observed, indicating a *trans* double bond between C-2' and C-3'.

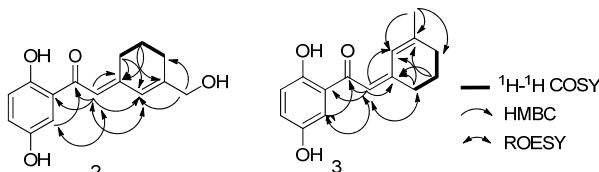


Figure 4: COSY and key HMBC correlations of **2** and **3**.

Table 1: ¹H NMR data of **1–3** (δ_H in ppm, J in Hz).

position	1 ^a	2 ^b	3 ^c
3	7.32 d (2.7)	7.26 d (2.8)	7.26 overlap, 7.25d (2.6) ^d
5	7.07 dd (8.9, 2.7)	6.97 dd (8.8, 2.8)	6.98 dd (8.8, 2.8)
6	6.79 d (8.9)	6.77overlap	6.86 d (8.8)
2'	a: 3.49 d (18.1) b: 3.46 d (18.1)	6.77 overlap	6.55s
4'	5.82 s	6.39 s	6.06 s
6'	2.00 t-like (5.9)	2.20 t (5.9)	2.18t (5.8)
7'	a: 1.82 m b: 1.72 m	1.79 m	1.76 m
8'	a: 2.20 m b: 1.66 m	3.02 t (6.0)	2.98 t (6.3) 2.48 t (5.9) ^d
9'	3.96 s	4.14 s	1.91 s

^a600 MHz in acetone-d₆. ^b600 MHz in methanol-d₄. ^c600 MHz in CDCl₃. ^din methanol-d₄.

Petchiene C (**3**), isolated as a yellow solid, has the molecular formula C₁₅H₁₆O₃ (8 degrees of unsaturation), based on its HRESIMS, ¹³C NMR and DEPT spectra. The NMR data of **3** closely resemble those of **2**, indicating that they are analogues. The only difference is that a hydroxymethyl group in **2** was replaced by a methyl in **3** evidenced from HMBC correlations between H₃-9' (δ_H 1.91)/C-4', C-5', C-6' (Figure 4). A ROESY correlation between H-2' (δ_H 6.56 in methanol-d₄)/H-8' (δ_H 2.48) was observed, indicating the configuration of the double bond.

The molecular formula of racemic petchiene D (**4**) was determined to be C₁₅H₁₆O₄ (8 degrees of unsaturation) by analysis of its HRESIMS, ¹³C NMR and DEPT spectra. Compound **4** could be generated from **2** via Michael addition reaction to construct a spiro compound. This conclusion is supported by the HMBC correlations between H-2'/C-1', C-2, C-3' (δ_C 79.1), C-4' and H-8'/C-2', C-3', C-4'. In addition, ROESY correlations between 4-OH (δ_H 9.43 in DMSO-d₆)/H-3, H-5 were observed, indicating the position of the free hydroxyl group in the benzene ring. Thus far, the planar structure of **4** was identified as shown. Chiral HPLC analysis indicated that **4** is racemic. Subsequent separation by chiral HPLC yielded (+)-and (-)-**4** in a ratio of 1.3:1; the absolute configuration at the stereogenic center was assigned to be 3'S for (-)-**4** by the same methods as those of **1** (Figure 6).

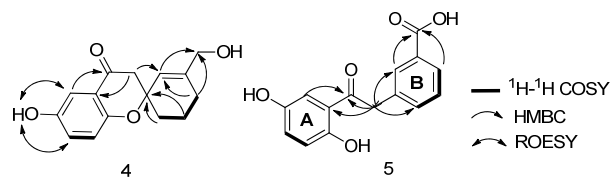


Figure 5: COSY and key HMBC correlations of **4** and **5**.

Table 2: ¹H NMR data of **4** and **5** (δ_H in ppm, J in Hz).

position	4 ^a	5 ^a
3	7.15 d (2.9)	7.36 d (2.9)
5	7.00 dd (8.9, 2.9)	7.10 dd (8.9, 2.9)
6	6.79 d (8.9)	6.80 d (8.9)
2'	a: 2.80d (16.5) b: 2.74 d (16.5)	4.39 s
4'	5.84 s	7.95brs
6'	a: 2.09overlap b: 1.99 m	7.92 d (7.7)
7'	a: 1.89 m b: 1.67 overlap	7.43t (7.6)
8'	a: 2.09overlap b: 1.67overlap	7.51 d (7.5)
9'	3.95s	

^a600 MHz in methanol-d₄.

Table 3: ¹³C NMR (150 MHz) data of **1–5** (δ_C in ppm).

No.	1 ^a	2 ^b	3 ^c	4 ^b	5 ^b
1	156.3	157.3	157.4	152.4	156.9
2	120.1	122.3	121.1	121.8	120.2
3	115.4	115.2	114.7	110.8	115.9
4	150.2	150.4	147.2	155.0	150.7
5	125.7	125.0	123.8	126.1	126.1
6	119.5	119.6	119.2	120.6	119.8
1'	204.9	197.1	195.5	194.7	204.8
2'	48.4	119.1	116.4	49.2	45.8
3'	44.8	157.7	157.7	79.1	136.4
4'	123.7	125.7	127.1	122.1	131.9
5'	141.4	154.3	151.6	145.6	132.4
6'	25.9	27.1	31.0	26.5	129.3
7'	19.9	23.2	22.3	19.4	129.7
8'	32.4	28.8	27.2	34.1	135.3
9'	66.6	66.1	24.9	66.1	170.0
10'	177.3				

^aIn acetone-d₆. ^b600 MHz in methanol-d₄. ^cIn CDCl₃.

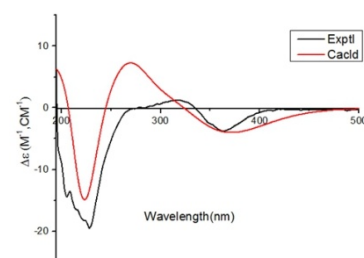


Figure 6: Calculated and experimental ECD spectra of (-)-**4** (red, at the B3LYP-SCRF (PCM)/6-311+G(2d,p)/B3LYP/6-311+G(2d,p) level in MeOH; black, experimentally observed in MeOH).

Petchiene E (**5**) was determined to have the molecular formula C₁₅H₁₂O₅ (10 degrees of unsaturation) on the basis of HRESIMS analysis. The ¹H NMR spectrum of **5** (Table 2) contains seven aromatic protons. The ¹³C NMR and DEPT spectra (Table 3) contain 15 signals ascribed to one sp³ methylene, seven methines (seven sp²), and seven quaternary carbon signals (one ketone, one carboxylic acid, and five sp²). The ¹H-¹H COSY spectrum shows the existence of fragments H-5/H-6, and H-6/H-7/H-8'. In the HMBC spectrum, correlations between H-3/C-1' and H-2'/C-2, C-1', C-3', C-4', C-8' indicate that the phenyl unit A is linked to C-1' and the phenyl unit B is linked to C-2' (Figure 5). The HMBC

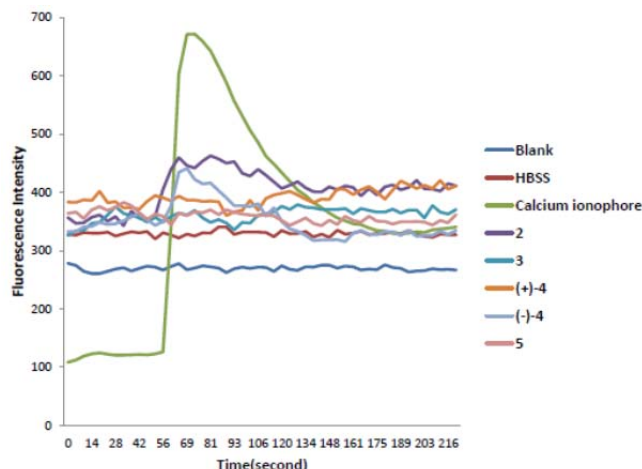


Figure 7: Effect of the isolates on intracellular Ca^{2+} concentration in HEK-293 cells.

correlations between H-4', H-6'/C-9' (δ_{C} 170.0) suggest that the carboxylic acid group is connected to C-5'. As a result, the structure of **5** was determined.

Biological evaluation: Calcium (Ca^{2+}) is a fundamental second messenger that is involved in a wide range of cellular processes and, therefore, is of potential interest in drug discovery [4]. The intracellular free Ca^{2+} concentration is regulated through multiple mechanisms in neurons, and abnormalities in Ca^{2+} signaling have been implicated in many neurological disorders [5]. Considering that many species of *Ganoderma* are used for the treatment of central nervous system associated diseases, the isolates were evaluated for their potential on the changes in Ca^{2+} in HEK-293 cells. The results showed that compounds **2** and $(-)$ -**4** could significantly elevate intracellular Ca^{2+} concentration at 10 μM (Figure 7). Whether these two compounds are beneficial for neurological disorders needs further investigation.

Experimental

General: Column chromatography (CC) was performed on silica gel (200–300 mesh; Qingdao Marine Chemical Inc., People's Republic of China), C-18 silica gel (40–60 μm ; Daiso Co., Japan), MCI gel CHP 20P (75–150 μm , Mitsubishi Chemical Industries, Tokyo, Japan) and Sephadex LH-20 (Amersham Pharmacia, Sweden). Optical rotations were recorded on a Horiba SEPA-300 polarimeter. UV spectra were recorded on a Shimadzu UV-2401PC spectrometer, IR spectra on a Brucker Tensor-27 spectrophotometer, and CD spectra on a Chirascan instrument. Semi-preparative HPLC was carried out using an Agilent 1200 liquid chromatography; the column used was a 250 mm \times 9.4 mm, i.d., 5 μm , Zorbax SB-C₁₈ and a 250 mm \times 10 mm, i.d., 5 μm , Daicel Chiralpak (IC), flow rate: 3 mL/min. NMR spectra were recorded on a Bruker AV-600 spectrometer, with TMS as an internal standard. EIMS and HREIMS were determined on an AutoSpec Premier P776 spectrometer. ESIMS and HRESIMS were measured on API QSTAR Pulsar 1 spectrometer.

Fungal material: The fruiting bodies of *G. petchii* (Lloyd) Steyaert were purchased from a market of Chinese medical materials located at Zhonghao-Luoshi-Wan of Kunming, People's Republic of China, in July 2014. A voucher specimen (CHYX-0588) was authorized by Prof. Zhu-Liang Yang at Kunming Institute of Botany and deposited at the State Key Laboratory of Phytochemistry and Plant Resources in West China, Kunming Institute of Botany, Chinese Academy of Sciences, People's Republic of China.

Extraction and isolation: The powdered fruiting bodies of *G. petchii* (60 kg) were extracted under reflux with 70% EtOH (150 L \times 2 h \times 3) to give a crude extract (3.39 kg), which was suspended in H₂O followed by extraction with EtOAc to afford an EtOAc soluble extract. Separation of this extract (2.09 kg) using a MCI gel CHP 20P column eluted with a gradient of aqueous MeOH (10%–100%) produced 8 portions (Fr.1–Fr.8). Among them, fr.5 (410 g) was further separated via MCI gel CHP 20P washed with a gradient of aqueous MeOH (20%–100%) to yield 7 fractions (Fr.5.1–Fr.5.7). Fr.5.4 (3.48 g) was submitted to a RP-18 column with a gradient of aqueous MeOH (30%–80%) to afford 8 sub-fractions (Fr.5.4.1–Fr.5.4.8). Fr.5.4.4 (233 mg) was purified by preparative TLC (2 drops of formic acid in CHCl₃/MeOH, 9:1) followed by semi-preparative HPLC (MeOH/H₂O, 43%) to yield compounds **1** (6.8 mg, $t_{\text{R}} = 23$ min), **2** (9.7 mg, $t_{\text{R}} = 18$ min) and **5** (1.0 mg, $t_{\text{R}} = 25$ min). Fr. 6 (50 g) was separated using MCI gel CHP 20P (MeOH/H₂O, 10:90, 30:70, 50:50, 70:30, 80:20) to yield 4 fractions (Fr.6.1–Fr.6.4). Fr. 6.3 (12 g) was subjected to gel filtration on Sephadex LH-20 (MeOH) followed by chromatography on a RP-18 column (MeOH/H₂O, 50%–70%) to yield **3** (5.3 mg, $t_{\text{R}} = 28$ min) and **4** (6.0 mg, $t_{\text{R}} = 26$ min). Racemic compound **4** was subjected to chiral HPLC to afford $(+)$ -**4** (2.2 mg) and $(-)$ -**4** (2.1 mg) (*n*-hexane/ethanol, 90:10).

Petchiene A (1)

Pale yellow solid.

$[\alpha]_D^{23,4}: +12.3$ (*c* 0.64, MeOH).

IR (KBr) ν_{max} : 3423, 2935, 2872, 1707, 1644, 1624, 1590, 1486, 1449, 1369, 1280, 1222, 1179, 998, 869, 831, 785 cm⁻¹.

UV (MeOH) λ_{max} ($\log \varepsilon$): 365 (3.57), 256 (3.87), 224 (4.17) nm.

CD (acetone): $\Delta\varepsilon_{209}-4.89$, $\Delta\varepsilon_{347}-0.80$.

¹H and ¹³C NMR: Tables 1 and 3.

ESIMS: *m/z* 305 [M–H]⁺.

HRESIMS: *m/z* 305.1043 [M–H]⁺ (calcd for C₁₆H₁₇O₆, 305.1031).

PetchieneB (2)

Yellow solid.

UV (MeOH) λ_{max} ($\log \varepsilon$): 380 (3.59), 320 (4.07), 220 (3.99), 202 (4.12) nm.

¹H and ¹³C NMR: Tables 1 and 3.

ESIMS: *m/z* 259 [M–H]⁺.

HRESIMS: *m/z* 259.0974 [M–H]⁺ (calcd for C₁₅H₁₅O₄, 259.0976).

Petchiene C (3)

Yellow solid.

UV (MeOH) λ_{max} ($\log \varepsilon$): 384 (1.50), 327 (3.66), 226 (3.99) nm.

¹H and ¹³C NMR: Tables 1 and 3.

ESIMS: *m/z* 243 [M–H]⁺.

HRESIMS *m/z* 243.1023 [M–H]⁺ (calcd for C₁₅H₁₅O₃, 243.1021).

(\pm)-Petchiene D (4)

Pale yellow solid.

{ $[\alpha]_D^{24}: +102.2$ (*c* 0.27, MeOH); $(+)$ -**4**} ; { $[\alpha]_D^{24}: -123.3$ (*c* 0.17, MeOH); $(-)$ -**4**} .

UV (MeOH) λ_{max} ($\log \varepsilon$): 362 (0.81), 255 (1.47), 228 (4.15) nm;

{CD (MeOH) $(+)$ -**4**: $\Delta\varepsilon_{230}+18.89$, $\Delta\varepsilon_{364}+2.99$; CD (MeOH) $(-)$ -**4**: $\Delta\varepsilon_{230}-18.89$, $\Delta\varepsilon_{364}-2.99$ }.

¹H and ¹³C NMR: Tables 2 and 3.

ESIMS: *m/z* 259 [M–H]⁺.

HRESIMS *m/z* 259.0974 [M–H]⁺ (calcd for C₁₅H₁₅O₄, 259.0970).

Petchiene E (5)

Pale yellow solid.

UV (MeOH) λ_{max} ($\log \varepsilon$): 368 (3.51), 256 (3.76), 223 (4.20), 202 (4.34) nm.

IR (KBr) ν_{max} : 3395, 3076, 2927, 1701, 1634, 1612, 1487, 1446, 1380, 1351, 1324, 1267, 1205, 1182, 784 cm^{-1} .

^1H and ^{13}C NMR: Tables 2 and 3.

ESIMS: m/z 271 [$\text{M}-\text{H}$] $^-$.

HRESIMS: m/z 271.0614 [$\text{M}-\text{H}$] $^-$ (calcd for $\text{C}_{15}\text{H}_{11}\text{O}_5$, 271.0612).

Calcium imaging assay: The calcium imaging assay was performed by an automated, cell-based fluorescence-imaging system (Array scan), as previously reported, with slight modification [6,7]. The HEK293 cells were seeded at a density of 2×10^4 cells/well in 96-well plate coated with poly-L-lysine and incubated for 12 h. Then, the HEK-293 cells were washed 3 times by HBSS (1.26 mM CaCl_2 , 0.493 mM MgCl_2 , 0.407 mM MgSO_4 , 5.33 mM KCl , 0.441 mM KH_2PO_4 , 4.17 mM NaHCO_3 , 137.93 mM NaCl , 0.338 mM NaHPO_4 , 5.56 mM D-Glucose, pH 7.2-7.4) and loaded finally with

2 μM Fluo-4 AM (DOJINDO) for 80 min at 37°C in HBSS. After incubation, the cells were washed mildly 3 times by HBSS. After the loading, calcium imaging was analyzed using Array scan VTI HCS Reader (Cellomics, The Thermo Scientific, Pittsburgh, PA). Fluorescence of Fluo-4 AM was excited at 488 nm, and emitted at 543 nm and recorded as times-series mode per 5 sec. The value of the changed fluorescence was expressed as the relative intensity compared with the initial value.

Acknowledgments - This work was financially supported by the National Natural Science Foundation of China (21472199), the Open Research Fund of State Key Laboratory Breeding Base of Systematic Research, Development and Utilization of Chinese Medicine Resources, NSFC-Joint Foundation of Yunnan Province (U1202222), the Young and Middle Aged Academic Leaders of Kunming and a project from Center of Cooperative Innovation for South China Medicine of Yunnan Province.

References

- [1] Luo Q, Tian L, Di L, Yan YM, Wei XY, Wang XF, Cheng YX. (2015) (\pm)-Sinensilactam A, a pair of rare hybrid metabolites with smad3 phosphorylation inhibition from *Ganoderma sinensis*. *Organic Letters*, **17**, 1565–1568.
- [2] (a) Yan YM, Ai J, Zhou LL, Chung ACK, Li R, Nie J, Fang P, Wang XL, Luo J, Hu Q, Hou FF, Cheng YX. (2013) Lingzhiols, unprecedented rotary door-shaped meroterpenoids as potent and selective inhibitors of p-smad 3 from *Ganoderma lucidum*. *Organic Letters*, **15**, 5488–5491; (b) Yan YM, Wang XL, Luo Q, Jiang LP, Yang CP, Hou B, Zuo ZL, Chen YB, Cheng YX. (2015) Metabolites from the mushroom *Ganoderma lingzhi* as stimulators of neural stem cell proliferation. *Phytochemistry*, **114**, 155–162; (c) Luo Q, Wang XL, Di L, Yan YM, Lu Q, Yang XH, Hu DB, Cheng YX. (2015) Isolation and identification of renoprotective substances from the mushroom *Ganoderma lucidum*. *Tetrahedron*, **71**, 840–845; (d) Luo Q, Di L, Dai WF, Lu Q, Yan YM, Yang ZL, Li RT, Cheng YX. (2015) Applanatumin A, a new dimericmeroterpenoid from *Ganoderma applanatum* that displays potent antifibrotic activity. *Organic Letters*, **17**, 1110–1113; (e) Zhou FJ, Nian Y, Yan YM, Gong Y, Luo Q, Zhang Y, Hou B, Zuo ZL, Wang SM, Jiang HH, Yang J, Cheng YX. (2015) Two new classes of T-type calcium channel inhibitors with new chemical scaffolds from *Ganoderma cochlear*. *Organic Letters*, **17**, 3082–3085.
- [3] Frisch MJ, Trucks GW, Schlegel HB, Scuseria GE, Robb MA, Cheeseman JR, Scalmani G, Barone V, Mennucci B, Petersson GA, Nakatsuji H, Caricato M, Li X, Hratchian HP, Izmaylov AF, Bloino J, Zheng G, Sonnenberg JL, Hada M, Ehara M, Toyota K, Fukuda R, Hasegawa J, Ishida M, Nakajima T, Honda Y, Kitao O, Nakai H, Vreven T, Montgomery Jr JA, Peralta JE, Ogliaro F, Bearpark M, Heyd JJ, Brothers E, Kudin KN, Staroverov VN, Keith T, Kobayashi R, Normand J, Raghavachari K, Rendell A, Burant JC, Iyengar SS, Tomasi J, Cossi M, Rega N, Millam JM, Klene M, Knox JE, Cross JB, Bakken V, Adamo C, Jaramillo J, Gomperts R, Stratmann RE, Yazev O, Austin AJ, Cammi R, Pomelli C, Ochterski JW, Martin RL, Morokuma K, Zakrzewski VG, Voth GA, Salvador P, Dannenberg JJ, Dapprich S, Daniels AD, Farkas O, Foresman JB, Ortiz JV, Cioslowski J, Fox DJ. (2010) *Gaussian 09, Revision C.01*, Gaussian, Inc., Wallingford CT.
- [4] Bonora M, Giorgi C, Pinton P. (2015) Novel frontiers in calcium signaling: A possible target for chemotherapy. *Pharmacological Research*, **99**, 82–85.
- [5] Burgoyne RD, Haynes LP. (2015) Sense and specificity in neuronal calcium signaling. *Biochimica et Biophysica Acta*, **1853**, 1921–1932.
- [6] Grynkiewicz G, Poenie M, Tsien RY. (1985) A new generation of Ca^{2+} indicators with greatly fluorescence properties. *Journal of Biological Chemistry*, **260**, 3440–3450.
- [7] Schlag BD, Lou Z, Fennell M, Dunlop J. (2004) Ligand dependency of 5-hydroxytryptamine 2C receptor internalization. *Journal of Pharmacology and Experimental Therapeutics*, **310**, 865–870.

Megastigmane Glycosides from the Leaves of *Tripterygium wilfordii*

Lin Ni^{a,b}, Xiao-mei Zhang^c, Xing Zhou^c, Jie Ma^a, Chuang-jun Li^a, Li Li^a, Tian-tai Zhang^a and Dong-Ming Zhang^{a,*}

^aState Key Laboratory of Bioactive Substance and Function of Natural Medicines, Institute of Materia Medica, Chinese Academy of Medical Sciences and Peking Union Medical College, Beijing 100050, China

^bCollege of Plant Protection, Fujian Agriculture and Forestry University, Fuzhou 350002, China

^cChongqing Academy of Chinese Materia Medica, Chongqing 400065, China

zhangdm@imm.ac.cn

Received: April 23rd, 2015; Accepted: November 15th, 2015

Two new megastigmane glycosides, named wilfordonisides A and B (**1** and **2**), and four known compounds (**3-6**) were isolated from the leaves of *Tripterygium wilfordii*, and one new aglycon, named wilfordoninol A (**2a**), was acquired by enzymatic hydrolysis of **2**. The absolute stereostructures of the compounds were determined by Mosher's method and by CD. At a concentration of 10 μM, compounds **1**, **3**, and **5** inhibited STAT1 translocation by 38.1 ± 0.9%, 55.8 ± 0.8%, and 53.9 ± 1.0%, respectively.

Keywords: *Tripterygium wilfordii*, Megastigmane glycosides, Wilfordonide, Wilfordoninol, STAT1.

Tripterygium wilfordii Hook. f., family Celastraceae, has been used in traditional Chinese medicine for the treatment of cancer, rheumatoid arthritis, and skin disorders for hundreds of years [1]. A number of studies have been focused in China on the chemistry and pharmacology of this species and hundreds of compounds have been reported [2], included triterpenoids [3], diterpenoids [4], lignins [5], and alkaloids [6]. In the course of chemical investigations of the leaves of *T. wilfordii*, we have isolated two new megastigmane glycosides, named wilfordonisides A and B (**1** and **2**), along with four known compounds (**3-6**) (Figure 1), and one new aglycon, named wilfordoninol A (**2a**), which was acquired by enzymatic hydrolysis of **2**. In this paper, we report the structure elucidation of the new compounds and their biological activities.

Wilfordonide A (**1**) was obtained as a colorless amorphous powder with a molecular formula of C₁₉H₃₄O₇, based on HRESIMS analysis (*m/z* 397.2207 [M + Na]⁺, calcd 397.2197). The molecular formula accounted for 3 degrees of hydrogen deficiency. The IR spectrum of **1** showed absorption bands at 3383 and 1666 cm⁻¹ ascribable to hydroxyl and double bond functions, respectively. The ¹H and ¹³C NMR (Tables 1 and 2) spectra of **1**, which were assigned by various NMR experiment, showed signals assignable to 1 β-glucose and 13 carbons of the aglycone moiety. The aglycone contained four methyls [δ_H 0.87, 0.90 (3H each, both s, H₃-11, 12; 1.24 (3H, d, J = 6.4 Hz, H₃-10), and 0.88 (3H, overlap, H₃-13)], and two methines [δ_H 3.90 (1H, m, H-3) and 4.25 (1H, m, H-9)] bearing an oxygen function and one *trans*-configuration double bond [δ_H 5.32 (1H, dd, J = 15.4 and 10.0 Hz, H-7) and 5.48 (1H, dd, J = 15.4 and 6.3 Hz, H-8)], together with two methylenes, two methines and a quaternary carbon. As shown in Figure 2, the ¹H-¹H COSY experiment on **1** indicated the presence of a partial structure, written in bold lines, and in the HMBC experiment, long range correlations were observed between the following: H₃-11 and C-1 (δ_c 36.1), C-12 (δ_c 32.2), C-6 (δ_c 58.9); H-8 and C-6, C-7 (δ_c 131.4), C-9 (δ_c 69.6), C-10 (δ_c 24.4); H₃-10 and C-8 (δ_c 138.8) and C-9; H₃-13 and C-4 (δ_c 44.2) and C-5 (δ_c 32.5). HMBC correlations from H-3(δ_H 3.90, m) to C-1' (δ_c 103.0); and from H-1' [δ_H 4.37 (1H, d, J = 7.8 Hz)] to C-3 (δ_c 76.0) suggested that the glucose was connected to C-3. The relative stereostructure of **1**, except for the 9-position, was

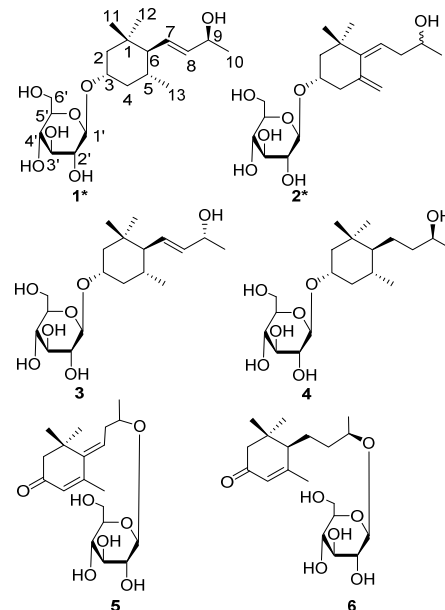


Figure 1 : Structures of compounds **1-6**.

characterized by the NOESY experiment, which showed NOE correlations between H-2β and H-3; H-3 and H-5; H-5 and H-4β; H-4α and H-6; and H-6 and H-2α, as shown in Figure 4.

Hydrolysis of **1** with snailase liberated its aglycon (**1a**), and glucose. The glucose was identified as D-(+)-glucose from its optical rotation {D-(+)-glucose had a positive optical rotation ($[\alpha]_D^{25}$ +45.7), and the optical rotation of glucose is $[\alpha]_D^{25}$ +39.8}. Finally, the absolute configuration of **1a** was characterized by application of the modified Mosher's method [7, 8].

Compound **1a** was treated with (*R*)- and (*S*)-α-methoxy-α-(trifluoromethyl)phenylacetyl chloride and gave the 3,9-di-(*S*)-MTPA ester (**1b**) and 3,9-di-(*R*)-MTPA (**1c**) ester, respectively. As

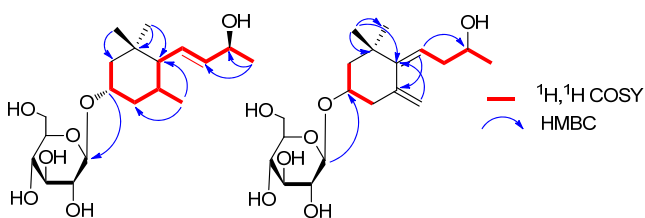
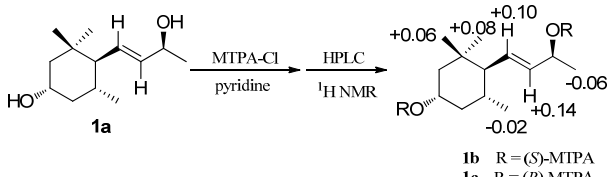
Figure 2: Key ^1H - ^1H COSY and HMBC correlations of 1 and 2.

Figure 3: Treatment of 1a by Mosher's method

shown in Figure 3, the signals due to protons attached to the 10- and 13-position in the 3,9-di-(S)-MTPA ester were observed at higher fields compared with those of the 3,9-di-(R)-MTPA ester [$\Delta\delta$: negative], while the signals due to protons of the 7-, 8-, 11- and 12-positions in the 3,9-di-(S)-MTPA ester were lower field compared with those of 3,9-di-(R)-MTPA ester [$\Delta\delta$: positive]. Thus, the absolute configurations at the 3 and 9-positions of **1a** were determined to be 3*S* and 9*R*. Accordingly, the absolute configuration of 3*S*, 5*R*, 6*R*, and 9*R* was established. Meanwhile, by comparison of spectroscopic data [8], compound **1a** had the same NMR data as sarmentol F.

Wilfordoniside B (**2**) was obtained as colorless oil with a molecular formula of $\text{C}_{19}\text{H}_{32}\text{O}_7$, based on HRESIMS analysis (m/z 395.2046 [$\text{M} + \text{Na}^+$, calcd 395.2040]). The molecular formula accounted for 4 indices of hydrogen deficiency. The IR spectrum of **2** showed absorption bands at 3395 and 1646 cm^{-1} ascribable to hydroxyl and double bond functions, respectively. The characteristic ^1H and ^{13}C NMR spectroscopic data (Tables 1 and 2) indicated that compound **2** was also a glycoside of a megastigmene derivative. As shown in Figure 2, the ^1H - ^1H COSY experiment on **2** indicated the presence of a partial structure, written in bold lines, and in the HMBC experiment, long range correlations were observed between the following: H₃-11 [δ_{H} 0.92 (3H, s)] and C-1 (δ_{C} 36.8), C-12 (δ_{C} 28.4), C-6 (δ_{C} 147.6); H-7 [δ_{H} 5.30 (1H, m)] and C-1, C-5 (δ_{C} 142.6), C-9 (δ_{C} 66.2); H-13 [δ_{H} 4.61 (1H, m) and 5.11 (1H, m)] and C-6. HMBC correlations from H-3 (δ_{H} 3.90, m) to C-1' (δ_{C} 100.8) suggested that the glucose was connected to C-3. The relative configuration of the C=C double bond between C-6 and C-7 was deduced as *Z* by NOE difference experiment showing strong enhancements of H₃-11 and H₃-12 on irradiation of H-7. Hydrolysis of **2** with snailase liberated its aglycon, a new norsesterpenoid, named wilfordoninol A (**2a**), and glucose. The glucose was also identified D-(+)-glucose by the similar and positive optical rotation. The absolute configuration of C-3 was determined by application of the CD helicity rule [9, 10]. Thus, since the CD spectrum of **2a** (Figure 5) showed a positive Cotton effect at 212 nm, the 3-position was determined to have the *S* configuration.

The known compounds were identified by comparison of spectroscopic data with those reported in the literature as crotonionoside H (**3**) [11], alangioside J (**4**) [12], (*E*)-4-[3'- β -D glucopyranosyloxy]butylidene]-3,5,5-trimethyl-2-cyclohexen-1-one (**5**) [13], and blumenol C glucoside (**6**) [14].

STAT1 (signal transducer and activator of transcription 1) plays a crucial role in signaling by interferons (IFNs), thereby regulating

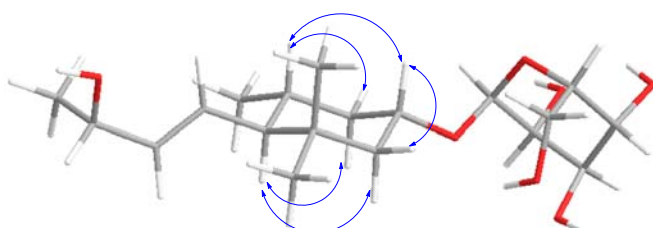


Figure 4: Key NOESY correlations of 1.

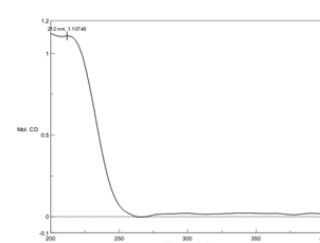


Figure 5: The CD curve of compound 2a.

Table 1: ^{13}C NMR spectral data of compounds 1-2 and 1a-2a

NO.	1^a	1a^b	2^c	2a^b
1	36.1	35.8	36.8	39.2
2	48.1	51.1	47.6	50.8
3	76.0	67.4	72.9	69.6
4	44.2	45.6	42.6	47.3
5	32.5	32.2	142.6	144.7
6	58.9	58.5	147.6	150.0
7	131.4	131.2	117.5	118.6
8	138.8	138.5	38.0	38.1
9	69.6	69.3	66.2	69.1
10	24.4	24.1	23.1	23.1
11	22.0	21.8	27.3	27.9
12	32.2	31.9	28.4	29.0
13	22.1	21.8	113.9	114.5
1'	103.0		100.8	
2'	75.4		73.4	
3'	78.4		76.7	
4'	72.0		70.0	
5'	78.1		76.7	
6'	63.1		61.0	

^a In MeOD-*d*₄ (125 MHz). ^b In MeOD-*d*₄ (150 MHz). ^c In DMSO-*d*₆ (125 MHz).

antiviral responses, cell proliferation, apoptosis, immune surveillance, and tumor suppression. The inhibitory effects of compounds **1** - **6** were evaluated *in vitro* for STAT1 translocation by immunofluorescence assay. Compounds **1**, **3**, and **5** inhibited STAT1 translocation by $38.1 \pm 0.9\%$, $55.8 \pm 0.8\%$, and $53.9 \pm 1.0\%$, respectively, at a concentration of 10 μM ; the other compounds showed weak activity.

Experimental

General experimental procedures: Optical rotations were measured on a JASCO P2000 automatic digital polarimeter, UV spectra on a JASCO V-650 spectrophotometer, and IR spectra on a Nicolet 5700 spectrometer using a FT-IR microscope transmission method. CD spectra were measured on a JASCO J-815 CD spectrometer. NMR spectra were acquired with an INOVA-500 spectrometer. HRESIMS were collected on an Agilent 1100 series LC/MSD ion trap mass spectrometer. Preparative HPLC was conducted using a Shimadzu LC-6AD instrument with a SPD-20A detector and a YMC-Pack ODS-A column (250×20 mm, 5 μm). Column chromatography (CC) was performed with silica gel (200-300 mesh, Qingdao Marine Chemical Inc., Qingdao, People's Republic of China), polyamide (60-100 mesh, Changfeng Chemical Inc., Jiangsu, People's Republic of China), D101 macroporous (Huangguang Chemical Inc., Tianjin, People's Republic of China),

Table 2: ^1H NMR spectral data of compounds **1-3** and **1a-3a**.

NO.	1^a	1a^b	2^c	2a^b
2 α	1.18, t, (12.4)	1.11, t (12.4)	1.31, m	1.28, m
2 β	1.87, br d (12.4)	1.69, br d (12.4)	1.83, m	1.95, m
3	3.90 (overlap)	3.73, m	3.89, m	3.88, m
4 α	1.05, q (12.4)	0.90, q (12.4)	1.83 (overlap)	1.80, m
4 β	2.13, br d (12.4)	1.98, br d (12.4)	2.75, dd (12.3, 3.4)	2.65, m
5	1.58, m	1.55, m		
6	1.33, t (10.0)	1.29, t (10.0)		
7	5.32, dd (15.4, 10.0)	5.30, dd (15.4, 10.0)	5.30, m	5.40, dd (8.0, 6.4)
8	5.48, dd (15.4, 6.3)	5.46, dd (15.4, 6.3)	2.13, m; 2.22, m	2.26, m; 2.38, m
9	4.25, m	4.23, m	3.60, dd (10.7, 5.9)	3.75, m
10	1.24, d (6.4)	1.23, d (6.5)	1.01, d (6.2)	1.15, d (6.2)
11	0.87, s	0.85, s	0.92, s	1.00, s
12	0.90, s	0.87, s	1.09, s	1.16, s
13	0.88 (overlap)	0.87 (overlap)	4.61, br s; 5.11, br s	4.68, d (2.2); 5.12, d (2.2)
1'	4.37, d (7.8)		4.25, d (7.8)	
2'	3.16, m		2.87, m	
3'	3.36, m		3.17, m	
4'	3.30, m		3.03, m	
5'	3.30, m		3.03, m	
6'	3.89, m; 3.68, m		3.65, m; 3.43, m	

^a In MeOD-*d*₄ (500 MHz). ^b In MeOD-*d*₄ (600 MHz). ^c In DMSO-*d*₆ (500 MHz).

and ODS (50 μm , YMC, Japan). TLC was carried out on glass precoated silica gel GF₂₅₄ plates. Compounds were visualized either under UV light or by spraying with 10% sulfuric acid in EtOH followed by heating.

Plant material: The leaves of *Tripterygium wilfordii* (TWHF) were collected in Taining, Fujian, China, in September 2009 and identified by Professor Lin Ma from the Institute of Materia Medica, Chinese Academy of Medical Sciences and Peking Union Medical College. A voucher specimen (No. 20090034) is deposited at the herbarium of the Institute of Material Medica, Chinese Academy of Medical Sciences and Peking Union Medical College, China.

Extraction and isolation: Air-dried leaves of TWHF (100 kg) were reduced to a coarse powder and refluxed with 80% EtOH (400 L \times 2h \times 3). After evaporation of ethanol *in vacuo*, the aqueous residue was diluted with water, and then partitioned with EtOAc (30L \times 3). The water layer was subjected to passage over polyamide by elution with water and 50% EtOH-water. The water extract was subjected to passage over D101 macroporous adsorption resin by elution with water and 30%, 60%, 95% EtOH-water in sequence to give fractions A1, A2 (651.0 g), A3 (338.5 g), and A4 (12.4g). Fraction A3, with an equal weight of diatomite, was successively refluxed with EtOAc, EtOH, MeOH to obtain fractions B1 (13.62 g), B2 (151.38 g) and B3 (68.87 g). Fraction B2 was subjected to CC on silica gel (200-300 mesh) with CHCl₃-MeOH (15: 1 – 1: 1) to afford 7 fractions (C1 - C7). Fraction C6 (8.625 g) was passed over an RP-18 column with MeOH-water (15%-75%), and finally purified by preparative HPLC (detected at 210 nm, 8 mL/min) to give **1** (43 mg), **2** (3 mg), **3** (8 mg), **4** (7 mg), **5** (5 mg), and **6** (14 mg).

Enzymatic hydrolysis of **1 and **2** with snailase:** A solution of **1** and **2** (8.0 and 3.0 mg, respectively) in H₂O (1.0 mL) was treated with snailase (10.0 and 5.0 mg, respectively). The solution was stirred at 37°C for 5 h; after cooling, the reaction mixture was extracted with EtOAc. The aqueous layer was subjected to CC on silica gel (200-300 mesh) with CH₃CN-H₂O (8:1) to afford glucose (1.8 mg). The EtOAc layer was purified by HPLC (25% CH₃CN-H₂O, detected at 210 nm, 8 mL/min) to furnish **1a** (2.3 mg) and **2a** (0.5 mg).

Wilfordoninol A (2a**)**
Colorless oil (MeOH).

^1H and ^{13}C NMR: Tables 1 and 2.

HRESIMS: *m/z* 233.1509 [M + Na]⁺ (calcd for C₁₃H₂₂NaO₂, 233.1522).

Preparation of (*R*)- and (*S*)-MTPA esters of **1a:** A solution of compound **1a** (1.0 mg) in dry CH₂Cl₂ (2.0 mL) was treated with (*R*)- α -methoxy- α -(trifluoromethyl)phenylacetyl chloride [(*R*)-MTPA-Cl, 10 mg] in the presence of anhydrous pyridine, and the mixture was stirred under reflux at 40°C for 6 h. After cooling, the reaction mixture was poured into ice-water and extracted with EtOAc. The EtOAc extract was washed successively with 5% HCl, NaHCO₃-saturated H₂O and brine, dried over Na₂SO₄ and filtered. Removal of the solvent from the filtrate under reduced pressure afforded a residue, which was purified by preparative HPLC (90% CH₃CN-H₂O, detected at 210 nm, 8 mL/min) to acquire the (*S*)-MTPA ester of **1a** (compound **1b**, 0.85 mg). Using a similar procedure, (*R*)-MTPA ester of **1a** (compound **1c**, 0.73 mg) was obtained from compound **1a** (1.0 mg) with (*S*)-MTPA-Cl (8 mg).

Compound **1b**

Colorless oil.

^1H NMR (600 MHz, CDCl₃) δ : 0.85, 0.91 (3H, each, both s, H₃-11, 12), 0.85 (3H, d, *J* = 6.0 Hz, H₃-13), 1.43 (3H, d, *J* = 6.0 Hz, H₃-10), 5.50 (1H, dd, *J* = 15.4, 10.0 Hz, H-7), 5.44 (1H, dd, *J* = 15.4, 7.8 Hz, H-8).

Compound **1c**

Colorless oil.

^1H NMR (600 MHz, CDCl₃) δ : 0.93, 0.97 (3H, each, both s, H₃-11, 12), 0.83 (3H, d, *J* = 6.0 Hz, H₃-13), 1.37 (3H, d, *J* = 6.0 Hz, H₃-10), 5.60 (1H, dd, *J* = 15.4, 10.0 Hz, H-7), 5.58 (1H, dd, *J* = 15.4, 7.8 Hz, H-8).

Biological activities: Recombinant U2OS cells (Thermo Scientific, Rockford IL, USA) that stably express human STAT1-EGFP fusion protein were cultured in DMEM supplemented with 10% FBS and G418 (0.5 mg/mL) in a 37°C incubator with 5% CO₂. Cells were plated in 96-well plates (2.5×10^3 cell mL⁻¹) and preincubated with samples for 30 min, followed by a further 1 h treatment with IFN- γ to evaluate the nuclear translocation of STAT1-EGFP. The capacity of translocation was detected with high content analysis by Cellomics ArrayScan VTM HCS Reader (Thermo Fisher Scientific Cellomics, Pittsburgh, PA, USA).

Wilfordoside A (1)

Colorless oil (MeOH).

 $[\alpha]_D^{25} = -52.3$ (*c* 0.1, MeOH).IR (microscope) ν_{max} : 3383, 2926, 1666, 1367, 1075, and 944 cm^{-1} . ^1H and ^{13}C NMR: Tables 1 and 2.HREIMS: m/z 397.2207 ($[\text{M} + \text{Na}]^+$, calc. $\text{C}_{19}\text{H}_{34}\text{NaO}_7$, 397.2197).**Wilfordoside B (2)**

Colorless oil (MeOH).

 $[\alpha]_D^{25} = -47.3$ (*c* 0.1 MeOH).IR (microscope) ν_{max} : 3395, 2921, 1646, 1468, 1419, and 1181 cm^{-1} . ^1H and ^{13}C NMR: Tables 1 and 2.HRESIMS: m/z 395.2046 ($[\text{M} + \text{Na}]^+$, calc. $\text{C}_{19}\text{H}_{32}\text{NaO}_7$, 395.2040).**Supplementary data:** NMR, IR, and CD data are available.

Acknowledgments - This work was supported by the National Key Technology R & D program of the Ministry of Science and Technology of China (No. 2011BAI01B05), the National Natural Science Foundation of China (NO. 21572275), and the National Mega-project for Innovative Drugs (No. 2012ZX09301002-002).

References

- [1] Brinker AM, Ma J, Lipsky PE, Raskin I. (2007) Medicinal chemistry and pharmacology of genus *Tripterygium* (Celastraceae). *Phytochemistry*, **68**, 732-766.
- [2] Zhou ZL, Yang YX, Ding J, Li YC, Miao ZH. (2012) Triptolide: structural modifications, structure-activity relationships, bioactivities, clinical development and mechanisms. *Natural Product Reports*, **29**, 457-475.
- [3] Duan H, Takaishi Y, Momota H, Ohmoto Y, Taki T, Jia Y, Li D. (2000) Triterpenoids from *Tripterygium wilfordii*. *Phytochemistry*, **53**, 805-810.
- [4] Ni L, Ma J, Li C J, Guo J M, Yuan SP, Hou Q, Guo Y, Zhang DM. (2015) Novel rearranged and highly oxygenated abietane diterpenoids from the leaves of *Tripterygium wilfordii*. *Tetrahedron Letters*, **56**, 1239-1243.
- [5] Cao X, Li C J, Yang JZ, Wei B X, Yuan SP, Luo Y M, Hou Q, Zhang DM. (2012) Four new neolignans from the leaves of *Tripterygium wilfordii*. *Fitoterapia*, **83**, 343-347.
- [6] Duan H, Tashihisa Y, Bando M, Kido M, Imakura Y, Lee KH. (1999) Novel sesquiterpene esters with alkaloid and monoterpane and related compounds from *Tripterygium hypoglaucum*: a new class of potent anti-HIV agents. *Tetrahedron Letters*, **40**, 2969-2972.
- [7] Ohtani I, Kusumi T, Kashman Y, Kakisawa H. (1991) High-field FT NMR application of Mosher's method. The absolute configurations of marine terpenoids. *Journal of the American Chemical Society*, **113**, 4092-4096.
- [8] Zhang Y, Nakamura S, Pongpiriyadacha Y, Matsuda H, Yoshikawa M. (2008) Absolute structures of new megastigmane glycosides, foloasalaciosides E₁, E₂, E₃, F, G, H, and I from the leaves of *Salacia chinensis*. *Chemical and Pharmaceutical Bulletin*, **56**, 547-553.
- [9] Oritani T, Yamashita K. (1972) Synthesis of optical active abscisic acid and its analogs. *Tetrahedron Letters*, **25**, 2521-2524.
- [10] Yoshikawa M, Shimada H, Saka M, Yoshizumi S, Yamahara J, Matsuda H. (1997) Medicinal foodstuffs. V. Moroherya. (1): Absolute stereostructures of corchoionosides A, B, and C, histamine release inhibitors from the leaves of Vietnamese *Corchorus olitorius* L. (Tiliaceae). *Chemical and Pharmaceutical Bulletin*, **45**, 464-469.
- [11] Kawakami S, Matsunami K, Otsuka H, Shinzato T, Takeda Y. (2011) Crotononionosides A-G: megastigmane glycosides from leaves of *Croton cascarilloides* Rauschel. *Phytochemistry*, **72**, 147-153.
- [12] Yoshikawa M, Morikawa T, Zhang Y, Nakamura S, Muraoka O, Matsuda H. (2007) Megastigmanes and their glucosides from the whole plant of *Sedum sarmentosum*. *Journal of Natural Products*, **70**, 575-583.
- [13] Khan SH, Mosihuzzaman M, Nahar N, Rashid MA, Rokeya B, Ali L, Khan A. (2003) Three megastigmane glycosides from the leaves of *Pterospermum semisagittatum*. *Pharmaceutical Biology*, **41**, 512-515.
- [14] Matsunami K, Otsuka H, Takeda Y. (2010) Structural revisions of blumenol C glucoside and byzantionoside B. *Chemical and Pharmaceutical Bulletin*, **58**, 438-441.

Cytochalasans and Sesquiterpenes from *Eutypella scoparia* 1-15Shuang Qi^{a,b}, Yue Wang^{a,b}, Zhonghui Zheng^{a,b}, Qingyan Xu^{a,b,*} and Xianming Deng^{a,b,*}^aState Key Laboratory of Cellular Stress Biology, Innovation Center for Cell Signaling Network, School of Life Sciences, Xiamen University, Xiamen, Fujian, 361102, China^bState-Province Joint Engineering Laboratory of Targeted Drugs from Natural Products, Xiamen University, Xiamen, Fujian, 361102, China

xuqingyan@xmu.edu.cn, xmdeng@xmu.edu.cn

Received: October 8th, 2015; Accepted: October 29th, 2015

Three new compounds, an open-chain cytochalasan scoparasin C (**1**), a pyrichalasan scoparasin D (**2**), and a β -eudesmol type sesquiterpene scopararane C (**5**), along with three known compounds (**3**, **4** and **6**), were isolated from the marine fungus *Eutypella scoparia* 1-15. Their structures were determined on the basis of comprehensive NMR and MS analysis. Compound **2** exhibited potent cytotoxicities with very low IC₅₀ values against several cancer cell lines, including A375, A549, HepG2 and MCF-7.

Keywords: Cytochalasan, Scoparasin, Scopararane, Cytotoxic activity.

Cytochalasans comprise a diverse group of fungal secondary metabolites with a characteristic tricyclic core structure in which an 11 to 14-membered macrocycle ring bearing either a carbocycle, a lactone or a cyclic carbonate, is fused to a highly substituted perhydroisoindol-1-one [1]. Based on the L-amino acids incorporated into the hydrogenated isoindolone, the canonical cytochalasans are divided into groups of cytochalasins (Phe), pyrichalasins (Tyr), chaetoglobosins (Trp), aspochalasins (Leu), and alachalasins (Ala) [2]. Cytochalasans exhibit a wide range of bioactivities, e.g., interfering with cellular mitosis, anti-parasite, inhibition of TNF- α and anticancer [3].

In our ongoing search for bioactive compounds from marine microbes, four cytochalasans (**1-4**) and two sesquiterpenes (**5-6**) were isolated from *Eutypella scoparia* 1-15, a fungal strain from mangrove rhizosphere soil of Jimei, Fujian Province, China. Compounds **1**, **2** and **5** were proved to be new natural products named scoparasin C, scoparasin D, and scopararane C, respectively.

Scoparasin C (**1**) was obtained as colorless oil. The molecular formula was established as C₃₂H₄₅NO₁₀ on the basis of HR-ESI-MS (*m/z* 626.2926 [M+Na]⁺, calcd. for C₃₂H₄₅NNaO₁₀⁺: 626.2936), with 11 degrees of unsaturation. A strong absorption band at 1716 cm⁻¹ in the IR spectrum indicated the presence of a ketone and/or a lactam carbonyl functional group, corresponding to the signal at δ 5.71 (1H, s, -NH-CO-) in the ¹H NMR (CDCl₃) spectrum. The ¹³C NMR and DEPT spectra showed 30 resolved peaks corresponding to 32 carbons, which were classified into eight methyls (four O-methyl, δ_c 55.3, 54.9, 53.9, and 54.4), three methylenes (δ_c 43.1, 42.0, and 36.0), eleven methines (four *sp*² methines, δ_c 131.9, 130.1, 127.3, and 114.5), eight quaternary carbons (two olefinic, with δ_c 129.4 and 158.8, two carbonyl with δ_c 171.0 and 218.1, and three *sp*³ carbon with δ_c 57.4, 77.7, and 84.9). The remaining quaternary carbon of δ_c 153.9 indicated a carbonate moiety. The ¹H spectrum indicated a *para*-methoxybenzene ring according to the presence of the characteristic proton resonances, δ 7.14 (d, *J* = 8.5 Hz, 2H), 6.90 (d, *J* = 8.6 Hz, 2H), and 3.82 (s, 3H). Apart from the eight degrees of unsaturation due to the benzene ring, three carbonyl groups, and one olefinic bond, the remaining three degrees of unsaturation indicated that **1** possessed a tricyclic framework. By extensive

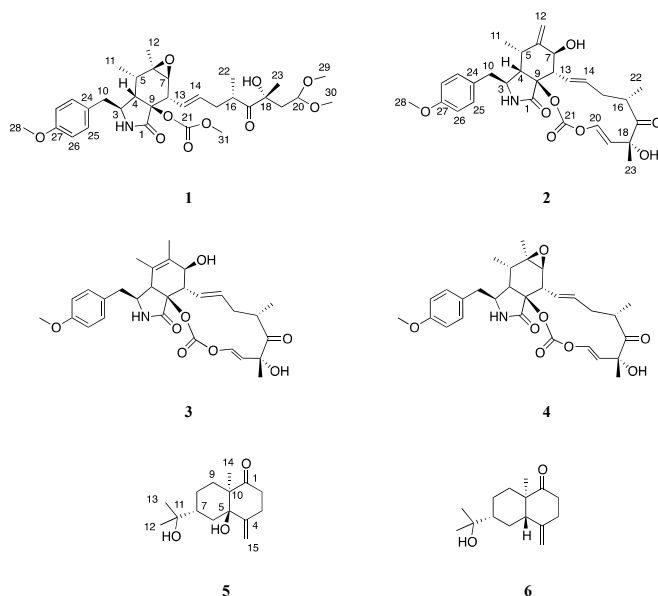


Figure 1: Structures of compounds **1-6** isolated from *Eutypella scoparia* 1-15.

analysis of the 2D NMR spectra (HMBC and ¹H-¹H COSY), the correlations from H-2 to C-3, C-4, and C-9, H-5 to C-3, C-4 and C-6, H-7 to C-8, C-9, and C-13, indicated the presence of a 10-phenyl-substituted perhydroisoindol-1-one skeleton, the structural feature of cytochalasans. Further analysis confirmed the epoxyp propane moiety, and the positions of the eight-carbon chain system and the methoxylcarbamate group at C-8 and C-9, respectively. Therefore, the structure of scoparasin C (**1**) was elucidated (Figure 1) as a new open-chain cytochalasan, a methoxyl derivative of cytochalasin Z₁₈ [4].

Scoparasin D (**2**) was obtained as white powder. The ¹H and ¹³C NMR spectra of **2** were similar to those of **1** with the exception of the absence of three methoxy groups (δ_c 53.9, 54.4, and 54.9) and the presence of two olefinic carbons (δ_c 120.3 and 142.2) (Table 1). The signal of H₃-12 (δ_H 1.34) in **1** was replaced with two signals of

Table 1: ^1H and ^{13}C NMR spectral data of compounds **1** and **2**.

Position	1			2			Position	1			2		
	δ_{H} (J in Hz)	δ_{C}	δ_{H} (J in Hz)	δ_{C}	δ_{H} (J in Hz)	δ_{C}		δ_{H} (J in Hz)	δ_{C}	δ_{H} (J in Hz)	δ_{C}		
1	/	171.0s	/	169.0s	17	/	218.1s	/	211.8s				
2-NH	5.71 (1H,s)		/ 4.49 (1H,bs)		18	/	77.7s		77.2s				
3	3.63 (1H, 4.1, 9.1)	54.3d	3.26 (1H,dd, 4.2, 9.4)	53.6d	19	2.24 (1H,dd, 5.7,14.5) 1.93 (1H,dd, 5.3,14.5)	42.0t	5.66 (1H,d, 11.8)	120.3d				
4	2.61 (1H,t, 4.4)	49.9d	2.96 (1H,m)	48.1d	20	4.47 (1H,t, 5.5)	102.9d	5.68 (1H,bs)	142.3d				
5	2.20 (1H)	35.5d	3.37 (1H,m)	32.1d	21	/	153.9s		149.6s				
6	/	57.4s	/	148.5s	22	1.10 (3H,d, 6.8)	17.1q	1.20 (3H,d)	20.2q				
7	2.81 (1H, d, 4.7)	60.1d	3.84 (1H,d, 11.3)	69.3d	23	1.32 (3H,s)	26.5q	1.54 (3H,s)	24.1q				
8	2.83 (1H,d, 5.3)	47.2d	2.97 (1H,m)	40.9d	24	/	129.4s		128.6s				
9	/	84.9s	/	86.2s	25	7.14 (2H, d, 8.7)	130.1d	7.06 (2H,d, 8.5)	130.3d				
10	2.93 (1H,dd, 9.7, 13.6) 2.85 (1H,dd, 4.5, 13.9)	43.1t	2.88 (1H,dd, 9.4, 13.6) 2.61 (1H,dd, 9.4, 13.7)	43.8t	26	6.90 (2H,d, 8.7)	114.5d	6.87 (2H,d, 8.5)	114.4d				
11	1.17 (3H,d, 7.4)	14.0q	1.18 (3H,d, 6.8)	14.6q	27	/	158.8s		158.9s				
12	1.34 (3H,s)	20.4q	5.42 (1H,bs) 5.20 (1H,bs)	114.5t	28	3.82 (3H,s)	55.3q	3.82 (3H, s)	55.3q				
13	5.99 (1H,dd, 7.9, 15.2)	127.3d	5.76 (1H,dd, 11.7, 15.1)	128.2d	29	3.32 (3H,s)	54.4q						
14	5.60 (1H,dd, 7.7, 15.2)	131.9d	5.39 (1H,m)	133.8d	30	3.34 (3H,s)	53.9q						
15	2.50 (1H,dd, 7.5, 14.0) 2.18 (1H,m)	36.0t	2.74 (1H,m)	38.8t	31	3.81 (3H, s)	54.9q						
16	3.19 (1H,dd, 5.8, 6.8)	39.6d	2.99 (1H,m)	40.9d									

Spectra were recorded at 600 MHz for ^1H using TMS as internal standard in CDCl_3 .

δ_{H} (5.20, bs, 1H) and δ_{H} (5.42, bs, 1H), characteristic of an exocyclic double bond. Further analysis of the COSY and HMBC spectra of **2** revealed the presence of a macrocyclic structure (Figure 1). This deduction was also confirmed by the molecule formula of **2**, $\text{C}_{29}\text{H}_{35}\text{NO}_8$, established on the basis of the HR-ESI-MS (m/z 548.2240 [$\text{M}+\text{Na}$] $^+$, calcd. for $\text{C}_{29}\text{H}_{35}\text{NNaO}_8^+$: 548.2255).

Compound **2** was previously obtained via semi-synthesis from phenochalasin B (**4**) [5], but it is the first time that it has been isolated from a natural source.

Previous isotope labeling experiments have proved that the skeletons of cytochalasans share the same stereochemistry, viz., *cis*-conjunction across the C-4/C-9, *trans*-conjunction across the C-8/C-9, and *S*-configuration at C-16. The cross-peaks at H-3/H-11 and H-5/H-8/H-10 in NOE correlations of compounds **1** and **2** suggested that both compounds had the same relative stereochemistry as previously isolated cytochalasans. The cross peak of H-16/H₃-23 indicated the *R*-configuration at C-18 in both compounds, which is consistent with known cytochalasans [6].

Scopararane C (**5**) had the molecular formula of $\text{C}_{15}\text{H}_{24}\text{O}_3$, deduced from HR-ESI-MS (m/z 253.1796 [$\text{M}+\text{H}$] $^+$, calcd. for $\text{C}_{15}\text{H}_{25}\text{O}_3^+$: 253.1798), which indicated four degrees of unsaturation in the molecule. The ^{13}C NMR and DEPT spectra (CDCl_3) displayed two sp^2 carbons (δ_{C} 148.4 and 110.8) and a carbonyl carbon (δ_{C} 214.2). The remaining two degrees of unsaturation were attributed to two rings. The ^{13}C NMR spectrum of **5** was similar to that of **6** except that δ_{C} 47.8 (d) in **6** was changed to δ_{C} 77.9 (s). Extensive analysis of ^1H NMR and HMBC spectra revealed that scopararane C (**5**) is a new β -eudesmol sesquiterpene.

Compound **3** and compound **4** had ^1H and ^{13}C NMR data that were identical to those of scoparasin A [7] and phenochalasin B [8], respectively. We further confirmed the structure of **3** by X-ray diffraction (Figure 2), which also demonstrated the absolute configurations of C-16 and C-18. Compound **6** was confirmed to be ent-4(15)-eudesmen-11-ol-1-one, a known β -eudesmol sesquiterpene.

All compounds were evaluated for their cytotoxic activities against A375, A549, HepG2 and MCF-7 cell lines by the MTT method [9].

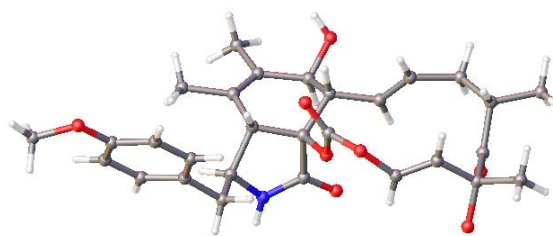


Figure 2: X-ray structure of **3**.

Table 2: IC₅₀ values of **2–4** against four cancer cell lines (μM).

Compsd	A375	A549	HepG2	MCF-7
2	1.08	2.25	3.51	3.40
3	5.74	10.85	9.44	>50
4	0.47	1.80	0.80	0.63

Compounds **1**, **5**, and **6** did not show any activity ($\text{IC}_{50} > 50 \mu\text{M}$), while compound **4** had potent inhibitory activities against all four cancer cell lines (Table 2). These results implied that the macrocycle might be essential for the bioactivity of cytochalasans.

Experimental

General experimental procedures: Infrared spectra (IR) were determined on a Thermo Nicolet iS5 FT-IR spectrometer, ultraviolet (UV) absorption spectra, in MeOH, on a Beckman Coulter DU 800 spectrophotometer, and optical rotations on a Perkin-Elmer 341 polarimeter. ^1H and ^{13}C NMR spectra were recorded in CDCl_3 on a 600 MHz Bruker Avance 600 spectrometer. HR-FT-MS were measured with a Bruker autoflex speed Maldi-ToF mass spectrometer. Silica GF₂₅₄ for thin layer chromatography (TLC) was produced by the Qingdao Marine Chemical Company, and Sephadex LH-20 by Pharmacia Biotech.

Fungal material: The fungal strain 1-15 was isolated from mangrove rhizosphere soil from Jimei, Fujian Province, China, in September, 2011. The fungus was identified as *Eutypella scoparia* by comparing the internal transcribed spaces (ITS) gene sequence with *Eutypella scoparia* PanM2024-1-P15 in the GenBank database, with 99% similarity (ITS1: 5'-TCGGTAGGTGAACCTGCGG -3', ITS4: 5'-TCCTCCGCTTATTGATATGC-3').

Fermentation: *Eutypella scoparia* 1-15 was cultured on potato dextrose agar (PDA) medium at 28°C for 35 days. A total of 20 L of fungal solid culture was prepared.

Extraction and isolation: The fermented material was diced and extracted 5 times with EtOAc/MeOH/AcOH (80:15:5, v/v/v) at room temperature. After removing the solvent under vacuum, the extract was partitioned between H₂O and EtOAc. Then the EtOAc layer was concentrated and resuspended in 95% methanol (70 mL), and washed with light petroleum (PE) 5 times. The MeOH layer was concentrated to afford the defatted extract (8 g). This was fractionated by medium-pressure liquid chromatography over an RP-18 column (170 g) eluting with 2 L each of H₂O-MeOH (100:0, 70:30, 50:50, 30:70, 0:100, v/v) to give fractions A-N. Compound **5** (6.0 mg) and **6** (9.5 mg) were obtained from fraction A (1.4 g) by silica gel CC (30 × 1.5 cm) eluting with EtOAc/PE (1:25, 1:20, 1:10, 1:6, v/v). Fraction E (1.8 g) was further purified by CC over silica gel (200–300 mesh) eluted with a CH₂Cl₂-MeOH gradient (from 200:1 to 0:100, v/v) to give compounds **1** (3 mg) and **4** (20 mg). Fraction I (2.0 g) was further purified over Sephadex LH-20 eluting with MeOH to give compounds **2** (2.3 mg) and **3** (5 mg).

Scoparasin C (1)

[α]_D²²: +20 (c 0.1, MeOH).

IR (KBr): 2967.5, 1747.2, 1716.3, 1513.2, 1263.9 cm⁻¹.

UV/Vis λ_{max} (MeOH) nm: 274, 225, 205.

MS (EI, 70 eV): m/z (%) = 626.44 [M+Na⁺] (100).

HRMS-FAB: m/z [M+Na⁺] calcd. for C₃₂H₄₅NNaO₁₀: 626.2936; found: 626.2926.

¹H and ¹³C NMR: Table 1.

Scoparasin D (2)

[α]_D²²: +88.0 (c 0.10, MeOH).

Rf: 0.58 (CHCl₃-MeOH, 10:1).

IR (KBr): 2967.5, 1767.5, 1716.0, 1512.7, 1248.3, 1032.9 cm⁻¹.

UV/Vis λ_{max} (MeOH) nm: 274, 225, 209.

MS (EI, 70 eV): m/z (%) = 548.26 [M+Na⁺] (100).

HRMS-FAB: m/z [M+Na⁺] calcd. for C₂₉H₃₅NO₈: 548.2255; found: 548.2240.

¹H and ¹³C NMR: Table 1.

Scoparasin A (3)

Rf: 0.58 (CHCl₃-MeOH, 10:1).

¹H NMR (600 MHz, CDCl₃): 1.21 (3H, s, Me-22), 1.53 (3H, s, Me-23), 1.55 (3H, s, Me-11), 1.70 (3H, s, Me-12), 2.17 (1H, m, Ha-15), 2.75 (1H, m, Hb-15), 2.78 (1H, m, Ha-10), 2.81 (1H, m, Hb-10), 2.85 (1H, m, H-8), 2.99 (1H, m, H-16), 3.44 (1H, t, J = 6.8 Hz, H-3), 3.81 (3H, s, Me-28), 3.90 (1H, m, H-7), 3.91 (1H, m, H-4), 5.41 (1H, ddd, J = 3.9 Hz, 10.6 Hz, 15.3 Hz, H-14), 5.69 (1H, d, J = 11.6 Hz, H-19), 5.76 (1H, s, NH), 6.24 (1H, dd, J = 11.3 Hz, 16.0 Hz, H-13), 6.70 (1H, d, J = 11.6 Hz, H-20), 6.89 (2H, d, J = 8.6 Hz, H-26), 7.10 (2H, d, J = 8.5 Hz, H-25).

¹³C NMR (150 MHz, CDCl₃): 14.0 (CH₃), 17.7 (CH₃), 20.3 (CH₃), 24.8 (CH₃), 39.0 (CH₂), 40.9 (CH₂), 43.2 (CH₂), 48.3 (CH), 50.0 (CH), 55.3 (CH₃), 59.2 (CH), 70.1 (CH), 76.6 (C), 86.2 (C), 114.3 (CH), 120.4 (CH), 128.6 (C), 129.4 (CH), 125.3 (C), 130.3 (CH), 131.7 (C), 133.5 (CH), 142.5 (CH), 149.0 (C), 158.7 (C), 169.9 (C), 211.5 (C).

MS (EI, 70 eV): m/z (%) = 548.36 [M+Na⁺] (100).

Crystallographic data of scoparasin A (**3**): White crystal obtained from MeOH-H₂O (1:1), orthorhombic, space group: P2₁2₁2₁, a = 11.6982(3) Å, b = 12.8520(5) Å, c = 17.2917(6) Å, V = 2599.73 (15) Å³, Z = 4, D_c = 1.343 g/cm³, μ (Cu K α) 0.805 mm⁻¹, $F(000)$ = 1120.0, crystal size 0.45×0.2×0.2 mm, 26153 reflections collected,

5356 independent reflections (R_{int} = 0.0769), final R 0.0417 [$>2\sigma(I)$] and wR_2 0.1234 (all data), Flack parameter 0.10 (17).

Phenochalasin B (4)

Rf: 0.57 (CHCl₃-MeOH, 10:1).

¹H NMR (600 MHz, CDCl₃): 1.19 (3H, s, Me-22), 1.53 (3H, s, Me-23), 1.13 (3H, d, J = 7.1 Hz, H-11), 1.26 (3H, s, Me-12), 2.17 (1H, m, Ha-15), 2.31 (1H, m, H-5), 2.68 (1H, m, Hb-15), 2.63 (1H, m, Ha-10), 2.84 (1H, m, Hb-10), 2.66 (1H, m, H-8), 2.96 (1H, m, H-16), 3.69 (1H, brs, H-3), 3.81 (3H, s, Me-28), 2.65 (1H, m, H-7), 3.01 (1H, m, H-4), 5.25 (1H, m, H-14), 5.63 (1H, d, J = 11.6 Hz, H-19), 6.14 (1H, s, NH), 5.91 (1H, dd, J = 9.3 Hz, 14.6 Hz, H-13), 6.53 (1H, d, J = 11.7 Hz, H-20), 6.89 (2H, d, J = 7.3 Hz, H-26), 7.08 (2H, d, J = 7.3 Hz, H-25).

¹³C NMR (150 MHz, CDCl₃): 13.2 (CH₃), 19.7 (CH₃), 20.3 (CH₃), 24.3 (CH₃), 35.8 (CH), 39.1 (CH₂), 44.1 (CH₂), 45.9 (CH), 60.4 (CH), 48.0 (CH), 53.7 (CH), 55.3 (CH₃), 57.3 (C), 76.7 (C), 87.0 (C), 114.3 (CH), 120.4 (CH), 127.9 (C), 128.4 (CH), 130.5 (CH), 131.6 (CH), 142.1 (CH), 149.4(C), 158.9 (C), 170.0 (C), 211.8 (C). MS (EI, 70 eV): m/z (%) = 548.26 [M+Na⁺] (100).

Scopararane C (5)

[α]_D²²: -35.5 (c 0.24, MeOH).

Rf: 0.58 (CHCl₃-MeOH, 10:1).

IR (KBr): 2924.8, 1699.9 cm⁻¹.

UV/Vis λ_{max} (MeOH) nm: 234, 220, 204.

¹H NMR (600 MHz, CDCl₃): 2.70 (1H, dd, J = 8.2 Hz, Ha-2), 2.42 (1H, dd, J = 1.7Hz, 8.2 Hz, Hb-2), 2.51 (1H, dd, J = 7.3 Hz, Ha-3), 3.02 (1H, dd, J = 2.0 Hz, 7.3 Hz, Hb-3), 1.81 (2H, m, H-6), 1.80 (1H, m, H-7), 1.77 (2H, m, H-8), 1.63 (2H, m, H-9), 1.27 (3H, s, H-12), 2.07 (3H, s, H-13), 1.08 (3H, s, H-14), 5.04 (1H, m, Ha-15), 5.11 (1H, dd, J = 0.8 Hz, 2.0 Hz, Hb-15).

¹³C NMR (150 MHz, CDCl₃): 20.1 (CH₃), 21.3 (CH₂), 26.7 (CH₃), 26.8 (CH₂), 28.1 (CH₃), 30.0 (CH₂), 30.9 (CH₂), 36.4 (CH₂), 42.9 (CH), 51.3 (C), 72.5 (C), 77.9 (C), 110.8 (CH₂), 148.4 (C), 214.2 (C).

MS (EI, 70 eV): m/z (%) = 253.18 [M+H⁺] (100).

HRMS-FAB: m/z [M + H⁺] calcd. for C₁₅H₂₅O₃⁺: 253.1798; found: 253.1796.

Ent-4(15)-eudesmen-11-ol-1-one (6)

Rf: 0.77 (CHCl₃-MeOH, 1:1).

¹H NMR (600 MHz, CDCl₃): 2.71 (1H, m, Ha-2), 2.39 (1H, dd, J = 2.0 Hz, 6.2 Hz, Hb-2), 2.45 (1H, m, Ha-3), 2.62 (1H, dd, J = 2.2 Hz, 7.6 Hz, Hb-3), 2.15 (1H, dd, J = 1.4 Hz, 11.5 Hz, H-5), 1.60 (1H, m, Ha-6), 1.85 (1H, m, Hb-7), 1.33 (1H, m, H-7), 1.24 (1H, m, Ha-8), 1.77 (1H, m, Hb-8), 1.37 (1H, m, Ha-9), 1.84 (1H, m, dd, J = 2.5 Hz, 5.6 Hz, Hb-9), 1.24 (3H, s, H-12), 1.25 (3H, s, H-13), 1.01 (3H, s, H-14), 4.80 (1H, d, J = 1.4 Hz, Ha-15), 5.11 (1H, d, J = 1.3 Hz, Hb-15).

¹³C NMR (150 MHz, CDCl₃): 16.6 (CH₃), 21.9 (CH₂), 26.9(CH₃), 24.4 (CH₂), 27.5 (CH₃), 32.1 (CH₂), 34.6 (CH₂), 38.1 (CH₂), 48.4 (CH), 47.8 (CH), 48.3 (C), 72.6 (C), 109.1 (CH₂), 146.5 (C), 215.1 (C).

MS (EI, 70 eV): m/z (%) = 237.40 [M+H⁺] (100).

Acknowledgments - This work was financially supported by the National High Technology Research and Development Program of China (No.2006AA09Z410), and the Fundamental Research Funds for the Central Universities (No.2011121037) to Q. Xu, and the National Natural Science Foundation of China (Nos. 81422045, U1405223 and 21272195), the Science and Technology Plan Project of Xiamen (No. 3502Z20133010), and the Fundamental Research Funds for the Central Universities of China (Nos. 2011121030 and 2013121032) to X. Deng.

References

- [1] Liu JT, Hu B, Gao Y, Zhang JP, Jiao BH, Lu XL, Liu XY. (2014) Bioactive tyrosine-derived cytochalansins form fungus *Eutypella* sp. D-1. *Chemistry and Biodiversity*, **11**, 800-806.
- [2] Scherlach K, Boettger D, Remme N, Christian H. (2010) The chemistry and biology of cytochalasans. *Natural Product Reports*, **27**, 869-886.
- [3] Liu JL, Hu ZY, Huang HY, Zheng ZH, Xu QY. (2012) Aspochalasin U, a moderated TNF- α inhibitor from *Aspergillus* sp. *Journal of Antibiotics*, **65**, 49-52.
- [4] Zhang Q, Xiao J, Sun QQ, Qin JC, Pescitelli G, Gao JM. (2014) Characterization of cytochalasins form the endophytic *Xylaria* sp. and their biological functions. *Journal of Agricultural and Food Chemistry*, **62**, 10962-10969.
- [5] Sharma SV, Oneyama C, Nakano H, Agatsuma T, Kanda Y, Tsumagari N, Ando K. From PCT Int. Appl. (2003), WO 2003006060 A1 20030123.
- [6] Feng YJ, Blunt JW, Cole ALJ, Munro MHG. (2002) Three novel cytochalasins X, Y, and Z from *Pseudeurotium zonatum*. *Journal of Natural Products*, **65**, 1274-1277.
- [7] Pongcharoen W, Rukachaisirikul V, Phongpaichit S, Rungindamai N, Sakayaroj J. (2006) Pimarane diterpene and cytochalasin derivatives from the endophytic fungus *Eutypella scoparia*PSU-D44. *Journal of Natural Products*, **69**, 856-858.
- [8] Tomoda H, Namatame I, Tabata N, Kawaguchi K, Si S, Omura S. (1999) Structure elucidation of fungal phenochalasins, novel inhibitors of lipid droplet formation in mouse macrophages. *Journal of Antibiotics*, **52**, 857-861.
- [9] Scudiero DA, Shoemaker RH, Paull KD, Monks A, Tierney S, Nofziger TH, Currens MJ, Seniff D, Boyd MR. (1998) Evaluation of a soluble tetrazolium/formazan assay for cell growth and drug sensitivity in culture using human and other tumor cell lines. *Cancer Research*, **48**, 4827-4833.

Concise Synthesis of Taiwaniaquinol B and 5-*epi*-Taiwaniaquinone G

Yonggang Meng,^{*} Yizhen Liu, Zhigang Lv, Jinqian Wang, Yanyan Wang, Chuanjun Song* and Junbiao Chang

College of Chemistry and Molecular Engineering, Zhengzhou University, 100 Science Avenue, Zhengzhou 450001, P. R. China

chjsong@zzu.edu.cn (C.S.) changjunbiao@zzu.edu.cn (J.C.)

Received: May 18th, 2015; Accepted: September 19th, 2015

The natural product taiwaniaquinol B and the unnatural 5-*epi*-taiwaniaquinone G were synthesized based on a highly efficient tandem acylation–Nazarov cyclization approach to build the tricyclic skeleton.

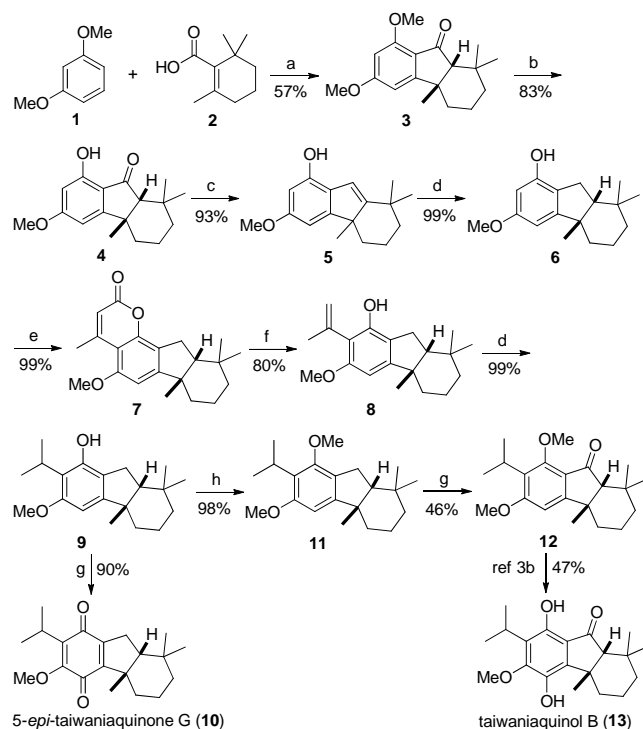
Keywords: Taiwaniaquinol B, 5-*Epi*-taiwaniaquinone G, Tandem reaction, Nazarov cyclization.

The taiwaniaquinoids are a family of tricyclic diterpenoids possessing a [6,5,6]-abeo-abietane skeleton isolated from *Taiwania cryptomerioides*, *Salvia dichroantha*, *Thuja standishii* and other related plants [1]. The unusual structural features and the promising biological activities [1d,2] of these compounds have attracted great interest for their chemical synthesis [3,4].

The tandem acylation–Nazarov cyclization approach for the construction of fused cyclopentenones by treatment of aromatics with α,β -unsaturated carboxylic acids in the presence of TFAA and a suitable Lewis acid catalyst [5] has been proved highly efficient in natural product synthesis [5b,6]. Herein, we report our synthetic route towards taiwaniaquinol B and the unnatural 5-*epi*-taiwaniaquinone G using this strategy as a key step.

As shown in Scheme 1, treatment of resorcinol dimethyl ether (**1**) with β -cyclogeranic acid (**2**) in the presence of TFAA and $ZnCl_2$ resulted in the formation of the desired acylation–Nazarov cyclization product **3** in 57% isolated yield [6b]. The relative stereochemistry of **3** was assigned as *cis* on the basis of NOE correlations which was the thermodynamically more stable product. Selective deprotection of the methoxy group adjacent to the carbonyl group in **3** by treatment with $BBBr_3$ gave **4**, which was converted into hexahydrofluorene derivative **6** in excellent yield via hydrogenation of the intermediate tetrahydrofluorene **5**. It needs to be indicated that all attempts to transform **4** directly into **6** via Wolff–Kishner or Clemmensen reduction failed to deliver the latter in any respectable yield. Next, the requisite isopropyl group was installed through a three-step sequence including Pechmann condensation of **6** with ethyl acetoacetate (EAA) to provide coumarin derivative **7**, hydrolysis and hydrogenation, which led to the formation of **9** in excellent combined yield. Oxidation of **9** with CrO_3 gave 5-*epi*-taiwaniaquinone G **10**, the spectroscopic data of which were identical to those previously reported in the literature [4c]. On the other hand, protection of the phenolic hydroxyl group in **9** gave **11**, which on treatment with CrO_3 was oxidized to tetrahydrofluorenone **12**. Finally, compound **12** could be converted into taiwaniaquinol B **13** following known literature procedures through selective demethylation, CAN oxidation, and sodium dithionite reduction [7].

In summary, we have developed a facile route to the synthesis of taiwaniaquinol B and the unnatural 5-*epi*-taiwaniaquinone G. The



Scheme 1: Reagents and conditions: (a) TFAA, $ZnCl_2$, toluene, reflux; (b) $BBBr_3$, DCM, $-60 - 0^\circ C$; (c) $LiAlH_4$, THF, $0^\circ C - rt$, then 6M HCl; (d) 10% Pd/C, H_2 , MeOH, $40^\circ C$; (e) MsOH, EAA, Al_2O_3 , rt; (f) KOH, DMSO/ H_2O , reflux; (g) CrO_3 , 3,5-dimethylpyrazole, DCM, $-15 - -10^\circ C$; (h) MeI, K_2CO_3 , acetone, reflux.

key steps involve a tandem acylation–Nazarov cyclization reaction to build the tricyclic skeleton and a Pechmann condensation strategy to install the isopropyl group onto the aromatic ring.

Experimental

General: MP, XT4A hot-stage apparatus; IR, IFS25 FT-IR spectrometer; NMR, Agilent 400 MHz spectrometer; MS, Q-TOF micro spectrometer. Flash column chromatography was performed over silica gel 200–300 mesh.

5,6,7,8,8a,9-Hexahydro-2-isopropyl-3-methoxy-4b,8,8-trimethyl-1H-fluorene-1,4(4bH)-dione (10) [4c]: A mixture of CrO_3 (238 mg,

2.38 mmol) and 3,5-dimethylpyrazole (229 mg, 2.38 mmol) in DCM (6 mL) was stirred at -15°C for 10 min. A solution of **9** (40 mg, 0.13 mmol) in DCM (6 mL) was added. The reaction mixture was allowed to warm to -10°C and stirred for a further 1 h before being quenched with H₂O (10 mL). The separated aqueous phase was extracted with DCM (3 x 10 mL). The combined organic extracts were dried over Na₂SO₄, then filtered and evaporated *in vacuo*. The residue was purified by column chromatography (CC) on silica gel (3% ethyl acetate in light petroleum) to give 5-*epi*-taiwaniaquinone G **10** (38 mg, 90%) as a yellow oil.

IR (neat): 1648, 1592, 1460 cm⁻¹.

¹H NMR (400 MHz, CDCl₃): 3.92 (s, 3H), 3.20 (sept, 1H, *J* = 7.0 Hz), 2.65 (dd, 1H, *J* = 18.0, 8.2 Hz), 2.36 (dd, 1H, *J* = 18.0, 11.4 Hz), 1.89 (m, 1H), 1.74 (dd, 1H, *J* = 11.4, 8.2 Hz), 1.52 (s, 3H), 1.46-1.40 (m, 2H), 1.30-1.28 (m, 3H), 1.21 (d, 3H, *J* = 7.0 Hz), 1.19 (d, 3H, *J* = 7.0 Hz), 1.08 (s, 3H), 0.93 (s, 3H).

¹³C NMR (100 MHz, CDCl₃): 187.5, 182.8, 156.7, 152.6, 146.3, 136.9, 61.2, 55.1, 48.1, 35.1, 34.4, 31.9, 31.2, 31.1, 29.6, 24.6, 24.4, 20.8, 20.7, 18.1.

HRMS-ESI: *m/z* [M + H⁺] calcd for C₂₀H₂₉O₃: 317.2117; found 317.2113.

2,3,4,4a,9,9a-Hexahydro-7-isopropyl-6,8-dimethoxy-1,1,4a-trimethyl-1*H*-fluoren-9*a*H-one (11): Methyl iodide (68 μL, 1.1 mmol) was added dropwise to a mixture of **9** (58 mg, 0.19 mmol) and K₂CO₃ (67 mg, 0.48 mmol) in acetone (3 mL). After addition, the mixture was heated at reflux for 3 h, then cooled and evaporated *in vacuo*. The residue was purified by CC on silica gel (3% ethyl acetate in light petroleum) to give **11** (60 mg, 98%) as a colorless solid.

MP: 115-116°C.

¹H NMR (400 MHz, CDCl₃): 6.42 (s, 1H), 3.79 (s, 3H), 3.75 (s, 3H), 3.48 (sept, 1H, *J* = 7.1 Hz), 2.82 (dd, 1H, *J* = 15.1, 7.8 Hz), 2.66 (dd, 1H, *J* = 15.1, 11.1 Hz), 1.83 (dd, 1H, *J* = 11.1, 7.8 Hz), 1.66-1.55 (m, 2H), 1.44-1.36 (m, 2H), 1.41 (s, 3H), 1.30 (d, 3H, *J* =

7.1 Hz), 1.29 (d, 3H, *J* = 7.1 Hz), 1.27-1.19 (m, 2H), 1.11 (s, 3H), 0.95 (s, 3H).

¹³C NMR (100 MHz, CDCl₃): 158.4, 155.0, 154.1, 126.4, 124.7, 101.1, 60.6, 57.6, 55.9, 45.6, 36.4, 35.3, 32.3, 31.2, 30.8, 29.6, 25.6, 25.1, 21.6, 21.5, 19.1.

HRMS-ESI: *m/z* [M + H⁺] calcd for C₂₁H₃₃O₂: 317.2481; found 317.2459.

2,3,4,4a-Tetrahydro-7-isopropyl-6,8-dimethoxy-1,1,4a-trimethyl-1*H*-fluoren-9*a*H-one (12): A mixture of CrO₃ (326 mg, 3.27 mmol) and 3,5-dimethylpyrazole (317 mg, 3.27 mmol) in DCM (7 mL) was stirred at -15°C for 10 min. A solution of **11** (58 mg, 0.18 mmol) in DCM (7 mL) was added. The reaction mixture was allowed to warm to -10°C and stirred for 10 h before being quenched with H₂O (15 mL). The separated aqueous phase was extracted with DCM (3 x 10 mL). The combined organic extracts were dried over Na₂SO₄, then filtered and evaporated *in vacuo*. The residue was purified by preparative TLC (3% ethyl acetate in light petroleum) to give **12** (21 mg, 46%, 71% based on recovered starting material) as a yellow oil, together with 20 mg of unreacted starting material recovered.

MP: 136-137°C.

¹H NMR (400 MHz, CDCl₃): 6.57 (s, 1H), 3.91 (s, 3H), 3.90 (s, 3H), 3.57 (sept, 1H, *J* = 7.1 Hz), 2.11 (s, 1H), 2.07 (m, 1H), 1.65-1.56 (m, 2H), 1.51-1.32 (m, 3H), 1.28 (d, 6H, *J* = 7.1 Hz), 1.25 (s, 3H), 1.23 (s, 3H), 0.70 (s, 3H).

¹³C NMR (100 MHz, CDCl₃): 204.5, 164.8, 164.0, 157.1, 128.1, 121.7, 99.8, 65.7, 62.1, 55.8, 41.4, 38.6, 34.5, 34.0, 33.4, 32.6, 24.7, 24.5, 21.2, 18.4.

Acknowledgments – We are grateful to Zhengzhou University (#1421316040) and the NSFC (#81330075; #21172202) for financial support.

References

- [1] (a) Lin WH, Fang JM, Cheng YS. (1995) Uncommon diterpenes with the skeleton of six-five-six fused-rings from *Taiwania cryptomerioides*. *Phytochemistry*, **40**, 871-873; (b) Kawazoe K, Yamamoto M, Takaishi Y, Honda, G, Fujita T, Sezik E, Yesilada E. (1999) Rearranged abietane-type diterpenes from *Salvia dichroantha*. *Phytochemistry*, **50**, 493-497; (c) Ohtsu H, Iwamoto M, Ohishi H, Matsunaga S, Tanaka R. (1999) Standishinal, a novel carbon skeletal diterpene from the bark of *Thuja standishii* (Gord.) Carr. *Tetrahedron Letters*, **40**, 6419-6422; (d) Chang CI, Chang JY, Kuo CC, Pan WY, Kuo YH. (2005) Four new 6-nor-5(6→7)abeo-abietane type diterpenoids and antitumor cytotoxic diterpene constituents from the bark of *Taiwania cryptomerioides*. *Planta Medica*, **71**, 72-76.
- [2] (a) Iwamoto M, Ohtsu H, Tokuda H, Nishino H, Matsunaga S, Tanaka R. (2001) Anti-tumor promoting diterpenes from the stem bark of *Thuja standishii* (Cupressaceae). *Bioorganic & Medicinal Chemistry*, **9**, 1911-1921; (b) Minami T, Iwamoto M, Ohtsu H, Ohishi H, Tanaka R, Yoshitake A. (2002) Aromatase inhibitory activities of standishinal and the diterpenoids from the bark of *Thuja standishii*. *Planta Medica*, **68**, 742-745.
- [3] Majetich G, Shimkus JM. (2010) The taiwaniaquinoids: A review. *Journal of Natural Products*, **73**, 284-298; and references therein.
- [4] (a) Alvarez-Manzaneda E, Chahboun R, Alvarez E, Tapia R, Alvarez-Manzaneda R. (2010) Enantioselective total synthesis of cytotoxic taiwaniaquinones A and F. *Chemical Communications*, **46**, 9244-9246; (b) Liao X, Stanley LM, Hartwig JF. (2011) Enantioselective total syntheses of (-)-taiwaniaquinone H and (-)-taiwaniaquinol B by iridium-catalyzed borylation and palladium-catalyzed asymmetric α-arylation. *Journal of the American Chemical Society*, **133**, 2088-2091; (c) Tapia R, Guardia JJ, Alvarez E, Haidour A, Ramos JM, Alvarez-Manzaneda R, Chahboun R, Alvarez-Manzaneda E. (2012) General access to taiwaniaquinoids based on a hypothetical abietane C7-C8 cleavage biogenetic pathway. *The Journal of Organic Chemistry*, **77**, 573-584; (d) Ozeki M, Satake M, Toizume T, Fukutome S, Arimitsu K, Hosoi S, Kajimoto T, Iwasaki H, Kojima N, Node M, Yamashita M. (2013) First asymmetric total synthesis of (+)-taiwaniaquinol D and (-)-taiwaniaquinone D by using intramolecular Heck reaction. *Tetrahedron*, **69**, 3841-3846; (e) Deng J, Li R, Luo Y, Li J, Zhou S, Li Y, Hu J, Li A. (2013) Divergent total synthesis of taiwaniaquinones A and F and taiwaniaquinols B and D. *Organic Letters*, **15**, 2022-2025; (f) Thommen C, Jana CK, Neuburger M, Gademann K. (2013) Syntheses of taiwaniaquinone F and taiwaniaquinol A via an unusual remote C-H functionalization. *Organic Letters*, **15**, 1390-1393.
- [5] (a) Song C, Knight, DW, Whatton MA. (2006) The first examples of Nazarov cyclizations leading to annulated pyrroles. *Organic Letters*, **8**, 163-166; (b) Li E, Li C, Wang J, Wang J, Dong L, Guo X, Song C, Chang J. (2014) Lewis acid-catalyzed tandem acylation-Nazarov cyclization for the syntheses of fused cyclopentenones. *Tetrahedron*, **70**, 874-879; (c) Huang C, Ding R, Song C, Lu J, Liu L, Han X, Wu J, Hou H, Fan Y. (2014) Template-induced diverse metal-organic materials as catalysts for the tandem acylation-Nazarov cyclization. *Chemistry-a European Journal*, **20**, 16156-16163.
- [6] (a) Song C, Liu H, Hong M, Liu Y, Jia F, Sun L, Pan Z, Chang J. (2012) Convergent formal synthesis of (±)-roseophilin. *The Journal of Organic Chemistry*, **77**, 704-706; (b) Wang J, Wang J, Li C, Meng Y, Wu J, Song C, Chang J. (2014) Synthesis of 5-*epi*-taiwaniaquinone G. *The Journal of Organic Chemistry*, **79**, 6354-6359.
- [7] Fillion E, Fishlock D. (2005) Total synthesis of (±)-taiwaniaquinol B via a domino intramolecular Friedel-Crafts acylation/carbonyl α-tert-alkylation reaction. *Journal of the American Chemical Society*, **127**, 13144-13145.

Effect of Enzyme Inhibitors on Terpene Trilactones Biosynthesis and Gene Expression Profiling in *Ginkgo biloba* Cultured Cells

Lijia Chen^{a*}, Hui Tong^{b*}, Mingxuan Wang^b, Jianhua Zhu^{a*}, Jiachen Zi^b, Liyan Song^{b,*} and Rongmin Yu^{a,b,*}

^aDepartment of Natural Products Chemistry, College of Pharmacy, Jinan University, Guangzhou 510632, China

^bBiotechnological Institute of Chinese Materia Medica, Jinan University, Guangzhou 510632, China

*These authors contribute equally to this work.

tzhujh@jnu.edu.cn; tsly@jnu.edu.cn; tyrm@jnu.edu.cn

Received: July 7th, 2015; Accepted: November 1st, 2015

The biosynthetic pathway of terpene trilactones of *Ginkgo biloba* is unclear. In this present study, suspension cultured cells of *G. biloba* were used to explore the regulation of the mevalonic acid (MVA) and methylerythritol 4-phosphate (MEP) pathways in response to specific enzyme inhibitors (lovastatin and clomazone). The results showed that the biosynthesis of bilobalide was more highly correlated with the MVA pathway, and the biosynthesis of ginkgolides was more highly correlated with the MEP pathway. Meanwhile, according to the results, it could be speculated that bilobalide might be a product of ginkgolide metabolism.

Keywords: *Ginkgo biloba*, Terpene trilactones, Biosynthesis, Enzyme inhibitors, Gene expression.

Ginkgo biloba L., a traditional herb in China, is one of the oldest living plants [1]. The leaf extract of ginkgo has been employed for treating cerebrovascular and cardiovascular diseases for centuries [2]. Modern pharmacological studies showed that *G. biloba* extract could be also used for the treatment of chronic schizophrenia and Alzheimer's disease, as well as possessing antitumor activity [3-5]. Terpene trilactones, which include ginkgolides and bilobalide, are surmised to be responsible for most of the pharmacological properties of *G. biloba* extracts.

Ginkgolides are commonly supposed to be acquired via the methylerythritol 4-phosphate (MEP) pathway [6], but several experiments indicated that mevalonic acid (MVA) pathway is dominant in undifferentiated *G. biloba* cells [7]. On the other hand, bilobalide (BB) is deemed to be synthesised through the MVA pathway [8], but some authors suggest that BB is a product of ginkgolides metabolism [9]. It has been reported that 1-deoxy-D-xylulose-5-phosphate synthase (DXS) and 1-deoxy-D-xylulose-5-phosphate reductoisomerase (DXR) are the rate-limiting enzymes for the MEP pathway. Similarly, HMG-CoA reductase (HMGR) catalyzes the major rate determining steps of the MVA pathway [10].

Inhibitors of key enzymes involved in the biosynthesis pathway have been used as an additional tool to study the regulation of secondary metabolite production in plants. Lovastatin (mevinolin) can induce a specific inhibition of HMGR in the MVA pathway [11]. Clomazone is a soil-applied herbicide, and is the precursor of 5-keto clomazone, an inhibitor of DXS in the MEP pathway [12]. In the present study, we investigated the yields of terpene trilactones and the expression of key biosynthetic genes in *G. biloba* cell cultures by feeding lovastatin and clomazone to gain a better understanding of the regulation of terpene trilactones biosynthesis.

Compared with control groups, the yields of ginkgolide A (GA), ginkgolide (GB) and ginkgolide (GC) in 20 μ M lovastatin-treated groups had a reduction of 12.6%, 11.4% and 16.4% at the 5th day, respectively, and that of BB had a reduction of 31.7% at the 9th day.

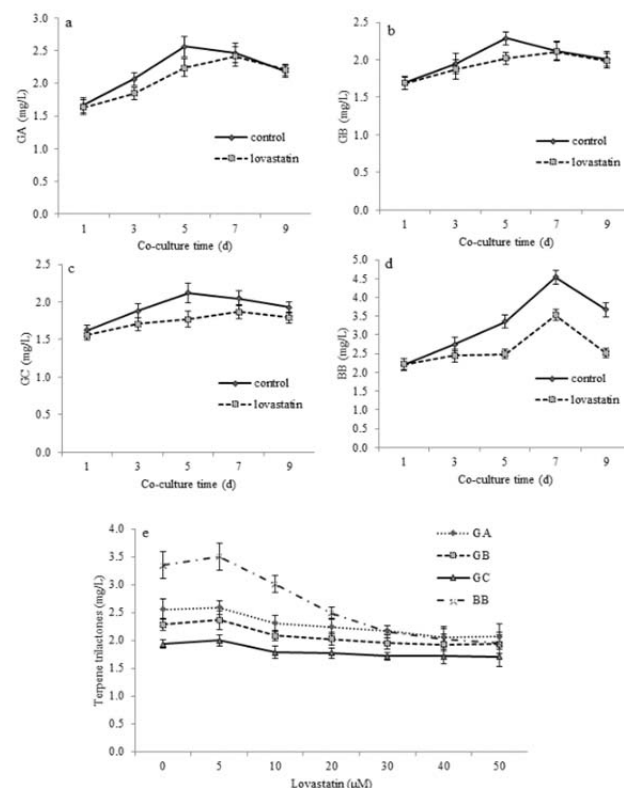


Figure 1: Effect of 20 μ M lovastatin on GA (a), GB (b), GC (c), and BB (d) production in *G. biloba* suspension cultured cells, and effect of lovastatin on terpene trilactones (e) production in *G. biloba* suspension cultured cells harvested at day 5 after treatment. Lovastatin was supplied to 14-day-old *G. biloba* suspension cultured cells.

Interestingly, the yields of GA, GB and GC in lovastatin-treated groups did not have an apparent reduction on the 9th day compared with those of control groups (Figure 1). In 50 μ M lovastatin-treated group, the yields of GA, GB, GC and BB had a reduction of 19.4%,

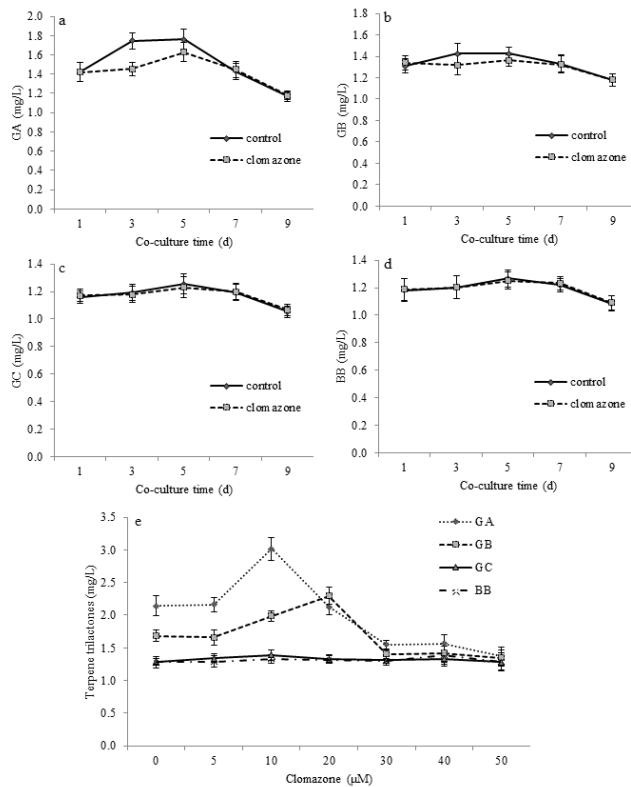


Figure 2: Effect of 40 μM clomazone on GA (a), GB (b), GC (c), and BB (d) production in *G. biloba* suspension cultured cells, and effect of clomazone on terpene trilactones (e) production in *G. biloba* suspension cultured cells harvested at day 5 after the treatment. Clomazone was supplied to 14-day-old *G. biloba* suspension cultured cells.

15.6%, 11.7% and 41.9% compared with the control group, respectively (Figure 1). These results indicated that BB was mainly synthesized from the MVA pathway, and parts of ginkgolides might be transformed into BB.

Compared with control groups, the yields of GA and GB in the 40 μM clomazone-treated groups had a reduction of 16.8% and 7.5% at the 3rd day, and that of GC and BB of 1.9% and 1.3% at the 5th day, respectively (Figure 2). In the 50 μM clomazone-treated group, the yields of GA and GB had a reduction of 36.3% and 20.0% (1.37 and 1.35 mg/L), while the yields of GC and BB were basically unchanged comparing with the control group (Figure 2). These results demonstrated that GA and GB were mainly obtained from the MEP pathway, and further indicated that the MVA pathway was the predominant one for BB.

After treatment with lovastatin (20 μM), the mRNA level of *HMGR* decreased significantly, and the transcript level of *DXS* decreased mildly. Conversely, the transcript level of *MECT* and *MVD* increased slightly. The trend in gene expressions was similar for the groups treated with different concentration of lovastatin (Figure 3). After treatment with 40 μM of clomazone, the mRNA level of *MECT* and *MVD* increased moderately. On the other hand, the *DXS* transcript level decreased slightly at the 1st day and then decreased rapidly with the increasing culture time, and *HMGR* remained stable. For the groups treated with different concentrations of clomazone, the results were similar (Figure 4). The qRT-PCR results of gene expression were consistent with the change in terpene trilactone concentrations in *G. biloba* cultured cells.

The present study provided a first attempt towards a better understanding of the regulation of the biosynthesis of terpene

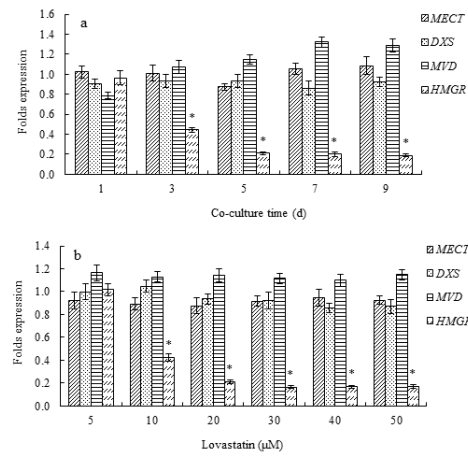


Figure 3: Effect of 20 μM lovastatin on the expression of terpene trilactones biosynthetic pathway genes (a) in *G. biloba* suspension cultured cells, and effect of lovastatin on the expression of terpene trilactones biosynthetic pathway genes (b) in *G. biloba* suspension cultured cells harvested at day 5 after the treatment. Lovastatin was supplied to 14-day-old *G. biloba* suspension cultured cells.

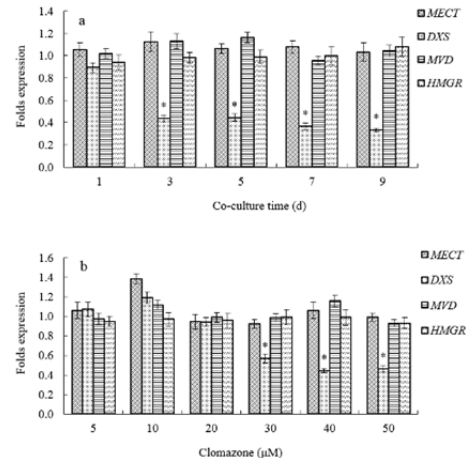


Figure 4: Effect of 40 μM clomazone on the expression of terpene trilactones biosynthetic pathway genes (a) in *G. biloba* suspension cultured cells, and effect of clomazone on the expression of terpene trilactones biosynthetic pathway genes (b) in *G. biloba* suspension cultured cells harvested at day 5 after the treatment. Clomazone was supplied to 14-day-old *G. biloba* suspension cultured cells.

trilactones in *G. biloba* cultured cells. The *in vivo* feeding experiments with two specific inhibitors, lovastatin and clomazone, showed that the biosynthesis of BB was more highly correlated with the MVA pathway, while the biosynthesis of ginkgolides was more highly correlated with the MEP pathway. Meanwhile, it could be speculated that BB might be a product of ginkgolides metabolism according to the results. This proposal requires further research by incorporation of labeled precursors and analyses of transgenic lines and mutants.

Experimental

Plant materials and methods: The cultured cells of *G. biloba* used in this research were established by our research group. Prior to the experiments, fresh 20-day-old cells (5.0 g) were transferred into 250 mL Erlenmeyer flasks and suspended in 100 mL of MS medium [13] supplemented with 30 g/L sucrose, 2.0 mg/L α -naphthalene acetic acid (NAA), 2.0 mg/L indolebutyric acid (IBA), and 5.0 mg/L ascorbic acid without agar, maintained in a rotary shaker (110 rpm) at 25°C in darkness.

Inhibitors treatment: After being filter-sterilized, the solutions of lovastatin and clomazone [14] were supplied individually to 14-day-

old suspension cultures to give final concentrations of 5, 10, 20, 30, 40 and 50 μM , respectively. Experiments for control group were made with corresponding blank solutions. 1, 3, 5, 7 and 9 days after the addition of the inhibitors, the cultured cells were harvested. The cultures were separated from liquid media by vacuum filtration, washed with distilled water, and dried at 50°C. The spent culture medium was used for analyzing terpene trilactones production. Elicitation experiments were made in triplicate.

Terpene trilactones extraction and determination: The cultured cells were separated from the culture medium by vacuum filtration and the spent medium was partitioned into ethyl acetate (v/v). The ethyl acetate extracts were combined and concentrated to dryness. The residue was dissolved in 1.0 mL of methanol and then analyzed by HPLC-ELSD. Dry cultured cells were extracted sonically with methanol 3 times. After concentration of the combined extract solutions under vacuum, the residue was dissolved in a mixture of water and ethyl acetate (1:1, v/v), and partitioning with ethyl acetate (v/v) 3 times. The ethyl acetate extracts were combined and concentrated to dryness. The residue was dissolved in 1.0 mL of methanol and then analyzed by HPLC-ELSD. For determination of ginkgolides and bilobalide, HPLC analysis was performed using a 1260 HPLC instrument (Agilent Technologies, US) equipped with an evaporative light-scattering detector (ELSD, Alltech Technologies, US). Chromatographic separations were performed

on an Agilent Hypersil C18 column (5 μm , 250 \times 4.0 mm) (Agilent Technologies, US) at 25°C with gradient elution consisting of methanol and water.

Monitoring gene expression by qPCR: The extraction of total RNA from cultured cells was performed using Trizol according to reference [15]. In the present study, transcript levels of GAPDH, the genes involved in the terpene trilactones biosynthesis pathway (*HMGR*, *MVD*, *DXS* and *MECT*), were monitored in cultured cells of *G. biloba* treated with either lovastatin or clomazone. The qPCR reference manuals of PrimeScriptTM reagent kit and SYBR® Premix Ex Taq™ were used.

Statistical analysis: All values are mean \pm SD. Statistical analyses were performed using an unpaired, two-tailed Student's t-test. All comparisons were made relative to untreated controls and significant difference is indicated as * $p < 0.05$.

Acknowledgments - This research was financially supported by the National Natural Science Foundation of China (No. 81274045 and 81573568), the Natural Science Foundation of Guangdong Province (No. 2014A030313385) and Pearl River Scientific and Technological New Star Program of Guangzhou (No. 2014J2200004).

References

- [1] Sabater-Jara AB, Souliman-Youssef S, Novo-Uzal E, Almagro L, Belchi-Navarro S, Pedreno MA. (2013) Biotechnological approaches to enhance the biosynthesis of ginkgolides and bilobalide in *Ginkgo biloba*. *Phytochemistry Reviews*, **12**, 191-205.
- [2] Zeng ZH, Zhu JH, Chen LL, Wen W, Yu RM. (2013) Biosynthesis pathways of ginkgolides. *Pharmacognosy Reviews*, **7**, 47-52.
- [3] Chen XC, Hong Y, Zheng PP. (2015) Efficacy and safety of extract of *Ginkgo biloba* as an adjunct therapy in chronic schizophrenia: A systematic review of randomized, double-blind, placebo-controlled studies with meta-analysis. *Psychiatry Research*, **228**, 121-127.
- [4] Liu X, Hao WL, Qin YR, Decker Y, Wang X, Burkart M, Schotz K, Menger MD, Fassbender K, Liu Y. (2015) Long-term treatment with *Ginkgo biloba* extract EGb 761 improves symptoms and pathology in a transgenic mouse model of Alzheimer's disease. *Brain Behavior and Immunity*, **46**, 121-131.
- [5] Liu SQ, Xu CY, Qin MB, Tan L, Zhuge CF, Mao YB, Lai MY, Huang JA. (2015) *Ginkgo biloba* extract enhances chemotherapy sensitivity and reverses chemoresistance through suppression of the KSR1-mediated ERK1/2 pathway in gastric cancer cells. *Oncology Reports*, **33**, 2871-2882.
- [6] Lange BM, Ghassemian M. (2003) Genome organization in *Arabidopsis thaliana*: a survey for genes involved in isoprenoid and chlorophyll metabolism. *Plant Molecular Biology*, **51**, 925-948.
- [7] Kang SM, Min JY, Kim YD, Park DJ, Jung HN, Karigar CS, Ha YL, Kim SW, Choi MS. (2006) Effect of supplementing terpenoid biosynthetic precursors on the accumulation of bilobalide and ginkgolides in *Ginkgo biloba* cell cultures. *Journal of Biotechnology*, **123**, 85-92.
- [8] Penuelas J, Munne-Bosch S. (2005) Isoprenoids: an evolutionary pool for photoprotection. *Trends in Plant Science*, **10**, 166-169.
- [9] Dewick PM. (2009) *Medicinal natural products: a biosynthetic approach*. Wiley, Chichester, England.
- [10] Shen G, Pang Y, Wu W, Liao Z, Zhao L, Sun X, Tang K. (2006) Cloning and characterization of a root-specific expressing gene encoding 3-hydroxy-3-methylglutaryl coenzyme A reductase from *Ginkgo biloba*. *Molecular Biology Reports*, **33**, 117-127.
- [11] Alberts AW, Chen J, Kuron G, Huff V, Hoffman C, Rothrock J, Lopez M, Joshua H, Harris E, Petchad A, Monagan R, Currie S, Stapley E, Albers-Schönberg G, Hensens O, Hirschfield J, Hoogsteen K, Liesch J, Springer J. (1980). Mevinolin: a highly potent competitive inhibitor of hydroxymethylglutaryl-coenzyme A reductase and a cholesterol-lowering agent. *Proceedings of the National Academy of Sciences*, **77**, 3957-3961.
- [12] Ferhatoglu Y, Barrett M. (2006) Studies of clomazone mode of action. *Pesticide Biochemistry and Physiology*, **85**, 7-14.
- [13] Murashige T, Skoog F. (1962) A revised medium for rapid growth and bioassays with tobacco tissue culture. *Physiologia Plantarum*, **15**, 473-497.
- [14] Rodriguez-Concepcion M, Grussem W. (1999) Arachidonic acid alters tomato HMG expression and fruit growth and induces 3-hydroxy-3-methylglutaryl coenzyme A reductase-independent lycopene accumulation. *Plant Physiology*, **119**, 41-48.
- [15] Liu JW, Zhu JH, Tang L, Wen W, Lv SS, Yu RM. (2013) Enhancement of vindoline and vinblastine production in suspension-cultured cells of *Catharanthus roseus* by artemisinic acid elicitation. *World Journal of Microbiology and Biotechnology*, **30**, 175-180.

Macrocyclic Diterpenoids from the Latex of *Euphorbia helioscopia*Juan Hua^{a,b}, Yan-Chun Liu^a, Shu-Xi Jing^a, Shi-Hong Luo^{a,*} and Sheng-Hong Li^{a,*}^aState Key Laboratory of Phytochemistry and Plant Resources in West China, Kunming Institute of Botany, Chinese Academy of Sciences, Kunming 650201, China^bUniversity of Chinese Academy of Sciences, Beijing 100049, China

shli@mail.kib.ac.cn and luoshihong@mail.kib.ac.cn

Received: September 25th, 2015; Accepted: October 15th, 2015

One new jatrophane diterpenoid, $7\alpha,9\beta,15\beta$ -triacetoxy- 3β -benzoyloxy- 14β -hydroxyjatrophane- $5E,11E$ -diene (**3**), together with four known macrocyclic diterpenoids, euphoheliosnoid A (**1**), epi euphoscopin B (**2**), euphohelioscopin A (**4**) and euphoscin C (**5**), were isolated from the stem latex of *Euphorbia helioscopia*. Their structures were established by spectroscopic analyses. In the anti-inflammatory assay, euphohelioscopin A (**4**) exhibited moderate inhibitory activity on the release of cytokine TNF- α ($IC_{50} = 23.7 \pm 1.7 \mu M$), IL-6 ($IC_{50} = 46.1 \pm 1.1 \mu M$) and chemokine MCP-1 ($IC_{50} = 33.7 \pm 3.8 \mu M$) in lipopolysaccharide (LPS) induced RAW 264.7 macrophages without notable cytotoxicity ($IC_{50} > 80 \mu M$).

Keywords: *Euphorbia helioscopia*, Latex, Jatrophane diterpenoid, Lathyrane diterpenoid, Anti-inflammatory activity.

Plant latex is a sticky emulsion stored in laticifers and usually released immediately from damaged tissue in over 20,000 species from about 40 families of flowering plants [1]. Besides various proteins, plant latex contains a wide range of secondary metabolites, including alkaloids, terpenoids, cardenolides and phenolics [1]. These metabolites have been widely accepted to play a significant defensive role against herbivores and pathogens [1, 2], and also possess significant pharmacological activities, such as anticancer, antiviral, and anti-inflammatory effects [3, 4].

Euphorbia is the largest genus in the family Euphorbiaceae that has been extensively distributed worldwide. All species of *Euphorbia* are characteristic for the production of a white latex that is rich in secondary metabolites especially terpenoids responsible for diverse biological activities [5, 6]. For example, tirucallol, a tetracyclic triterpenoid isolated from the latex of *E. lactea*, was reported to show anti-inflammatory activity *in vivo* [7]. Diterpenoid esters that were isolated from the latex of *E. poisonii* exhibited strong and selective cytotoxic effect against human kidney carcinoma (A-498) cell line [8].

E. helioscopia L., a biennial herb with milky latex widely distributed in most parts of China, has been used as a traditional Chinese medicine to treat malaria, osteomyelitis, and bacillary dysentery [9, 10]. Previous phytochemical investigations of *E. helioscopia*, mainly focused on the whole plant, have uncovered diverse secondary metabolites, including phenols, triterpenoids and a series of structurally interesting and potentially bioactive macrocyclic diterpenoids [11-15]. However, detailed investigation of the secondary metabolites in the latex is still lacking.

To characterize the lactic metabolites, the stem latex of *E. helioscopia* was suspended in methanol to remove the macromolecular proteins and polysaccharides, and was then analyzed by reversed-phase HPLC equipped with a diode array detector and recorded at 238 nm. Five major peaks with retention times of 6.90, 7.59, 7.99, 10.38 and 12.58 min, respectively, were detected in the chromatogram (Figure 1). Subsequently, using column chromatography and reversed-phase semi-preparative HPLC, the five compounds were isolated and identified as a new (**3**)

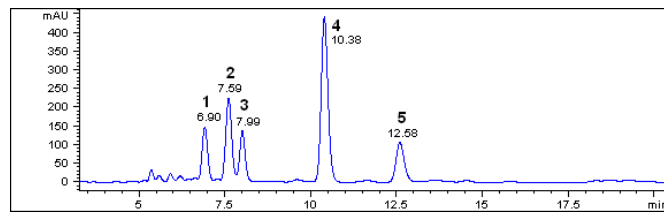


Figure 1: HPLC analysis of the secondary metabolites in stem latex of *Euphorbia helioscopia* (238 nm).

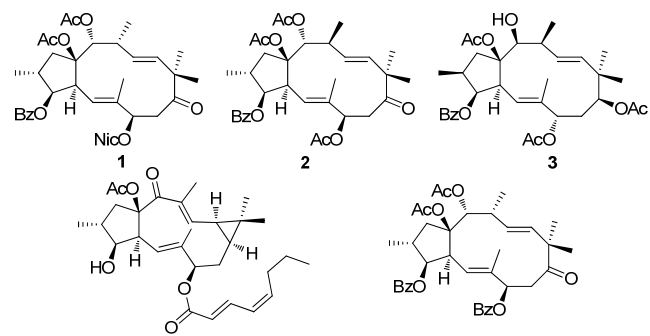


Figure 2: Chemical structures of compounds **1-5**.

and three known jatrophane diterpenoids (**1**, **2**, and **5**), and a known lathyrane diterpenoid (**4**) (Figure 2).

Compound **3** was obtained as a white solid. Its molecular formula was $C_{33}H_{44}O_9$ according to the ^{13}C NMR spectroscopic and HREIMS data ($[M^+]$, found: m/z 584.2977; calcd. for 584.2985). The 1H NMR spectrum showed the presence of eight methyl signals [δ_H 0.89, 0.91, 0.96, 1.05, 1.09, 1.76, 1.94, and 2.38 (each 3H)], and five aromatic protons [δ_H 8.05 (2H), 7.63 (1H) and 7.54 (2H)]. The ^{13}C NMR spectrum of **3** exhibited 33 carbon resonances. The carbonyl resonances (δ_C 169.1, 169.7, 174.6 and 165.6) together with the aforementioned proton signals revealed the presence of three acetoxy groups and a benzoyloxy group. Apart from the above 13 signals responsible for substituents, 20 carbons including five

Table 1: NMR spectral data of **3** in acetone-*d*₆.^a

Position	δ_{H} , (<i>J</i> [Hz])	δ_{C}	HMBC
1 α	2.86 (1H, dd, 13.4, 6.8)	45.1, t	C-2, 3, 4, 15, 16
1 β	2.19 (1H, t, 13.4)	37.9, d	C-1
2	2.29 (1H, m)	81.3, d	C-1, 15, -C=O (3-OBz)
3	5.39 (1H, t, 3.7)	81.3, d	
4	3.32 (1H, dd, 4.5, 10.2)	49.0, d	C-3, 5, 6
5	5.76 (1H, d, 10.2)	120.7, d	C-6, 7, 15, 17
6	-	133.8, s	-
7	4.89 (1H, d, 7.0)	73.8, d	C-5, 6, 8, 9, 17, -C=O (7-OAc)
8 α	2.11 (1H, dd, 3.3, 16.0)	33.1, t	C-7, 9, 10
8 β	1.83 (1H, ddd, 3.3, 7.0, 16.0)		
9	4.91 (1H, t, 3.2)	74.6, d	C-10, 18, -C=O (9-OAc)
10	-	40.1, s	-
11	5.09 (1H, d, 15.7)	136.1 d	C-9, 10, 18, 19
12	5.52 (1H, dd, 9.0, 15.7)	130.5, d	C-13, 14
13	2.54 (1H, m)	40.4, d	C-11, 12, 20
14	3.58 (1H, d, 5.6)	81.2, d	C-1, 12, 13, 15, 20
15	-	95.8, s	-
16	0.96 (3H, d, 6.6)	13.7, q	C-1, 2, 3
17	1.76 (3H, s)	15.9, q	C-4, 5, 6, 7
18	0.89 (3H, s)	20.4, q	C-9, 10, 11, 19
19	0.91 (3H, s)	22.9, q	C-9, 10, 11, 18
20	1.05 (3H, d, 7.0)	21.0, q	C-12, 13, 14
3-OBz			
C=O	-	165.6, s	-
1'	-	131.2, s	-
2'/6'	8.05 (2H, m)	130.3, d	C-2'/6', 4', -C=O (3-OBz)
3'/5'	7.54 (2H, t, 7.6)	129.4, d	C-1', 3'/5'
4'	7.63 (1H, t, 7.4)	133.8, d	C-2'/6'
7-OAc	1.09 (3H, s)	169.1, s	-
9-OAc	1.94 (3H, s)	21.1, q	-
15-OAc	2.38 (3H, s)	169.7, s	-
14-OH	4.86 (1H, d, 4.2)	22.4, q	-
		174.6, s	-

^a ¹H NMR was recorded at 600 MHz; ¹³C NMR was recorded at 150 MHz.

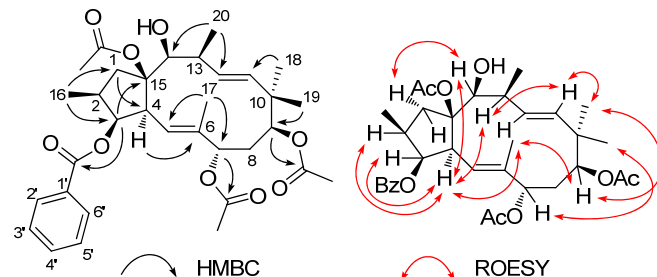


Figure 3: Key HMBC (black arrows, left), and ROESY (red arrows, right) correlations for the structure elucidation of **3**.

methyls, two methylenes, ten methines and three quaternary carbons were also observed in the ¹³C NMR spectrum, suggesting that **3** might be a jatrophane diterpenoid [9, 11]. The jatrophane skeleton was further confirmed by 2D NMR experiments, in which a disubstituted double bond ascribable to C-11 and C-12, and a trisubstituted double bond attributable to C-5 and C-6 were observed (Figure 3). The simultaneous HMBC correlations of the proton signals at δ_{H} 5.39 (H-3) and 8.05 (2H, H-2' and H-6') with the carbonyl carbon signal at δ_{C} 165.6 disclosed that the benzoyloxy group was attached to C-3. Similarly, the ¹H-¹³C long-range couplings from the proton signals at δ_{H} 4.89 (H-7) and 4.91 (H-9) with the carbonyl carbon signals at δ_{C} 169.1 and 169.7 demonstrated the presence of two acetoxy groups at C-7 and C-9, respectively. The last acetoxy group could be assigned to C-15 because no HMBC correlations were observed between the carbonyl carbon (δ_{C} 174.6) and any protons from the jatrophane skeleton, and further supported by the dramatically downfield

shifted C-15 (δ_{C} 95.8) compared with the chemical shift of the same carbon of similar jatrophane diterpenoids [9]. The ¹H-¹H COSY spectrum showed clear correlation between the proton at δ_{H} 3.58 (H-14) and the hydroxy resonance at δ_{H} 4.86, thus the hydroxy group was assignable to C-14.

The relative stereochemistry of **3** was established by analysis of the coupling constant pattern and ROESY spectrum. For the reported jatrophane diterpenoids, the angular proton H-4 is exclusively α -oriented and the C-15 acetoxy group β -oriented [5, 6]. The ROESY cross-peaks of H-4/H-3, H-4/H-13, H-4/H-14, H-1 α /H-2, H-1 α /H-14, and of Me-18/H-9 indicated α -orientation of these protons. The ROESY cross-peak of Me-19/H-7 revealed their β -orientation. Therefore, the structure of **3** was elucidated as 7 α ,9 β ,15 β -triacetoxy-3 β -benzoyloxy-14 β -hydroxyjatrophane-5*E*,11*E*-diene.

The four known compounds were identified as eupholiosnoid A (**1**) [13], epieuphoscin B (**2**) [14, 15], eupholioscin A (**4**) [15] and euphoscin C (**5**) [14] by comparison of their ¹H and ¹³C NMR data with those previously reported in the literatures.

The anti-inflammatory activity of eupholioscin A (**4**) was assayed as described previously [16]. The compound showed moderate inhibitory activity on the production of the pro-inflammatory cytokines TNF- α ($\text{IC}_{50} = 23.7 \pm 1.7 \mu\text{M}$), IL-6 ($\text{IC}_{50} = 46.1 \pm 1.1 \mu\text{M}$) and chemokine MCP-1 ($\text{IC}_{50} = 33.7 \pm 3.8 \mu\text{M}$) in lipopolysaccharide (LPS) stimulated RAW 264.7 macrophages, without notable cytotoxicity ($\text{IC}_{50} > 80 \mu\text{M}$).

Experimental

General: Column chromatography (CC) was performed on 200-300 mesh silica gel (Qingdao Marine Chemical Factory, China), Sephadex LH-20 (Amersham Pharmacia Biotech, Sweden) and MCI gel CHP-20P (75-150 μm , Mitsubishi Chemical Corp., Tokyo, Japan). Optical rotations were obtained on a Horiba-SEAP-300 spectropolarimeter, UV spectra were measured on a Shimadzu-210A double-beam spectrophotometer, and IR spectra in KBr discs were recorded on a Bruker-Tensor-27 spectrometer. NMR spectra were carried out on a Bruker Avance III 600 spectrometer (Bruker, Karlsruhe, Germany) with TMS as internal standard. MS were recorded on a VG-Auto-Spec-3000 spectrometer. Centrifugation was performed with an Eppendorf 5810R (Eppendorf, Hamburg, Germany). HPLC analysis was performed on an Agilent 1200 (Agilent, USA) series instrument equipped with a quaternary pump, a vacuum degasser, an autosampler, a thermostated column compartment and a diode array detector. Semi-preparative HPLC was also performed on the same system with a Zorbax SB-C₁₈, 9.4 \times 250 mm column at 30°C. TLC spots were visualized under UV light and by dipping into 5% H_2SO_4 in ethanol followed by heating.

Plant material: Latex of *E. helioscopia* was collected from plants growing in Kunming Botanical Garden in February 2014.

Metabolite analysis of latex by HPLC: One hundred μL stem latex of *E. helioscopia* was suspended in 200 μL methanol in an ultrasonic bath for 10 min and then centrifuged at 12,000 rpm for 5 min. After centrifugation, the supernatant was analyzed by HPLC. At a flow rate of 1 mL/min, 10 μL of the sample was injected into a Zorbax SB-C₁₈ column (5 μm , 4.6 \times 250 mm), and the column temperature was maintained at 30°C. A mobile phase composed of (A) water and (B) acetonitrile was used (0-20 min: isocratic 80% B, 20-25 min: linear gradient of 80-95% of B). The eluent was monitored at 200-400 nm.

Extraction and isolation: Ten mL stem latex was suspended in 50 mL methanol and centrifuged as described above. The supernatant was concentrated *in vacuo* to remove the organic solvent, and was then partitioned with EtOAc. The EtOAc fraction (205 mg) was chromatographed on a silica gel column, eluting successively with light petroleum/ethyl acetate (10: 0, 9: 1, 4: 1, 1: 1) and acetone to give 5 fractions (A-E). Fraction B was further subjected to MCI gel CC eluting with methanol/water (60-100%) to give 4 sub-fractions (2a-2d). Sub-fraction 2c (77 mg) (methanol/water, 80%) was purified by reversed-phase semi-preparative HPLC using 75% acetonitrile in water as eluent (flow rate: 3 mL/min; column: Zorbax SB-C₁₈, 5 μm, 9.4 × 250 mm; detection: UV 238 nm; retention times: *t* = 8.1, 9.4, 10.8, 12.1, 13.6, and 16.3 min) to yield **1** (3 mg), **2** (5 mg), **3** (4 mg), **4** (13 mg) and **5** (8 mg), respectively.

7α,9β,15β-Triacetoxy-3β-benzyloxy-14β-hydroxyjatropho-5E,11E-diene (3)

White solid.

[α]_D²⁰: -15.6 (*c* 0.06, MeOH).

UV λ_{max} (MeOH) nm ($\log \epsilon$): 201 (2.57), 228 (2.07), 271 (0.15).

IR (KBr) ν_{max} : 3423, 2926, 1738, 1628, 1246, 1026, 713 cm⁻¹.

¹H NMR (600 MHz, acetone-*d*₆) and ¹³C NMR (150 MHz, acetone-*d*₆): Table 1.

HR-EI-MS *m/z*: 584.2977 [M]⁺ (calcd for C₃₃H₄₄O₉, 584.2985).

References

- [1] Konno K. (2011) Plant latex and other exudates as plant defense systems: Roles of various defense chemicals and proteins contained therein. *Phytochemistry*, **72**, 1510-1530.
- [2] Agrawal AA, Konno K. (2009) Latex: a model for understanding mechanisms, ecology, and evolution of plant defense against herbivory. *Annual Review of Ecology and Systematics*, **40**, 311-331.
- [3] Wang HB, Wang XY, Liu LP, Qin GW, Kang TG. (2015) Tigiane diterpenoids from the Euphorbiaceae and Thymelaeaceae families. *Chemical Reviews*, **115**, 2975-3011.
- [4] Feng F, Liu WY, Chen YS, Guo QL, You QD. (2007) Five novel prenylated xanthones from *Resina Garcinia*. *Journal of Asian Natural Products Research*, **9**, 735-741.
- [5] Shi QW, Su XH, Kiyota H. (2008) Chemical and pharmacological research of the plants in genus *Euphorbia*. *Chemical Reviews*, **108**, 4295-4327.
- [6] Vasas A, Hohmann J. (2014) *Euphorbia* diterpenes: isolation, structure, biological activity, and synthesis (2008-2012). *Chemical Reviews*, **114**, 8579-8612.
- [7] Fernandez-Arche A, Saenz MT, Arroyo M, de la Puerta R, Garcia MD. (2010) Topical anti-inflammatory effect of tirucallol, a triterpene isolated from *Euphorbia lutea* latex. *Phytomedicine*, **17**, 146-148.
- [8] Fatope MO, Zeng L, Ohayaga JE, Shi G, McLaughlin JL. (1996) Selectively cytotoxic diterpenes from *Euphorbia poisonii*. *Journal of Medicinal Chemistry*, **39**, 1005-1008.
- [9] Chen HQ, Wang H, Yang B, Jin DQ, Yang SL, Wang MC, Xu J, Ohizumi Y, Guo YQ. (2014) Diterpenes inhibiting NO production from *Euphorbia helioscopia*. *Fitoterapia*, **95**, 133-138.
- [10] Cateni F, Zilic J, Altieri T, Zucchigna M, Procida G, Gaggeri R, Rossi D, Collina S. (2014) Lipid metabolites with free-radical scavenging activity from *Euphorbia helioscopia* L. *Chemistry and Physics of Lipids*, **181**, 90-98.
- [11] Lu ZQ, Guan SH, Li XN, Chen GT, Zhang JQ, Huang HL, Liu X, Guo DA. (2008) Cytotoxic diterpenoids from *Euphorbia helioscopia*. *Journal of Natural Products*, **71**, 873-876.
- [12] Zhang W, Guo YW. (2006) Chemical studies on the constituents of the Chinese medicinal herb *Euphorbia helioscopia* L. *Chemical & Pharmaceutical Bulletin*, **54**, 1037-1039.
- [13] Zhang W, Guo YW. (2005) Three new jatrophe-type diterpenoids from *Euphorbia helioscopia*. *Planta Medica*, **71**, 283-286.
- [14] Tao HW, Hao XJ, Liu PP, Zhu WM. (2008) Cytotoxic macrocyclic diterpenoids from *Euphorbia helioscopia*. *Archives of Pharmacal Research*, **31**, 1547-1551.
- [15] Yamamura S, Shizuri Y, Kosemura S, Ohtsuka J, Tayama T, Ohba S, Ito M, Saito Y, Terada Y. (1989) Diterpenes from *Euphorbia helioscopia*. *Phytochemistry*, **28**, 3421-3436.
- [16] Chen ZZ, Tong L, Feng YL, Wu JZ, Zhao XY, Ruan HL, Pi HF, Zhang P. (2015) Ursane-type nortriterpenes with a five-membered A-ring from *Rubus innominatus*. *Phytochemistry*, **116**, 329-336.

Anti-inflammatory assay: The murine macrophage RAW 264.7 cell line was cultured in DMEM medium supplemented with 10% heat-inactivated fetal bovine serum in a 37°C, 5% CO₂ incubator. Before anti-inflammatory assay, test compounds were assessed for their cytotoxicity against the RAW 264.7 cell line and were found to be non-toxic at the tested concentrations (80, 40, 20, 10, 5, and 0 μM). Anti-inflammatory activity was assessed by enzyme-linked immunosorbent assay (ELISA) using commercial tumor necrosis factor- α (TNF- α), interleukin-6 (IL-6), and monocyte chemoattractant protein 1 (MCP-1) detecting kits (BD Biosciences, Mountain View, CA, USA), as previously described [16].

Supplementary data: ¹H and ¹³C NMR, HSQC, HMBC, ROESY and ¹H-¹H COSY spectra of the new compound **3**.

Acknowledgments - This research was supported financially by the National Natural Science Foundation of China (31200263), the Youth Innovation Promotion association of Chinese Academy of Sciences (awarded to Shi-Hong Luo), the “Western Light” Program of Chinese Academy of Sciences (awarded to Shi-Hong Luo), and the “Hundred Talents Program” of the Chinese Academy of Sciences (awarded to Sheng-Hong Li).

A New Triterpenoid from the Aerial Parts of *Agrimonia pilosa*

Jiang-Hao Ma^{a,b,‡}, Qing-Hua Jiang^{c,‡}, Ying Chen^{a,b}, Xiu-Fang Nie^b, Tie Yao^b, Li-Qin Ding^a, Feng Zhao^d, Li-Xia Chen^{b,*} and Qiu Feng^{a,*}

^aSchool of Chinese Materia Medica and Tianjin State Key Laboratory of Modern Chinese Medicine, Tianjin University of Traditional Chinese Medicine, Tianjin 300193, China

^bDepartment of Natural Products Chemistry, School of Traditional Chinese Materia Medica, Key Laboratory of Structure-Based Drug Design & Discovery, Ministry of Education, Shenyang Pharmaceutical University, Shenyang 110016, China

^cDepartment of Pharmacy, Shengjing Hospital of China Medical University, Shenyang 110004, China

^dSchool of Pharmacy, Yantai University, Yantai 264005, China

fengqiu20070118@163.com; syzyclx@163.com

‡ These two authors contributed equally to this work.

Received: July 1st, 2015; Accepted: September 20th, 2015

(1S,3R,17R,18R,19R,20R,22R)-1,3,19,22-tetrahydroxy-28-norurs-12-en-2-one (**1**), along with 5 known triterpenoids (**2-6**), were isolated from the aerial parts of *Agrimonia pilosa* Ledeb. Their structures were established based on extensive spectroscopic and MS analysis. The absolute configuration of compound **1** was deduced by circular dichroism (CD). Compound **1** was the first example of a 28-norursene backbone isolated from the genus *Agrimonia*. Compounds **2-6** were tested for anti-inflammatory activities against RAW 264.7 macrophages. A plausible biosynthetic pathway for compound **1** in *A. pilosa* was also proposed.

Keywords: *Agrimonia pilosa*, Ursane 28-nortriterpene, Anti-inflammatory, Biogenetic pathway.

Agrimonia, family Rosaceae, includes about a dozen species, which are perennial herbaceous flowering plants, mainly distributed in the temperate regions of the Northern Hemisphere. Some species have been used in traditional medicine. *A. pilosa* Ledeb, common name Herba Agrimoniae, (*Xianhecao* in Chinese), is a traditional Chinese medicine (TCM), and is derived from the dried aerial parts of *A. pilosa* according to the Chinese Pharmacopoeia [1]. It is used for the treatment of abdominal pain, sore throat, headaches, bloody and mucoid dysentery and heat stroke. Pharmacological studies on the extracts prepared from the aerial parts of *A. pilosa* demonstrated broad biological properties, such as anti-inflammatory [2-3], anti-adipogenic [4], antioxidant [5] and antiviral [6] effects. Chemical studies on the aerial parts of *A. pilosa* showed the presence of flavonoids [7-9], 3,4-dihydroisocoumarins [2], and triterpenoids [10-11].

Recently, our research group has been examining the constituents of *A. pilosa* and has hitherto reported the isolation and identification of several flavonoids [12] and phenolic constituents [13]. Our continuous interest in bioactive constituents of this plant thus prompted us to investigate the other major chemical group in this plant - triterpenoids, and their inhibitory activities on NO and interleukin-6 (IL-6) production in RAW 264.7 macrophages induced by lipopolysaccharide (LPS). In this paper, we describe the isolation and structural elucidation of one new triterpenoid (**1**), together with five known ones (**2-6**) (Figure 1), and their *in vitro* anti-inflammatory evaluation on inhibitory activities in RAW 264.7 macrophages. The biogenetic pathway for compound **1** is also proposed (Scheme 1).

Compound **1** was obtained as a white amorphous powder. Its molecular formula was determined to be C₂₉H₄₆O₅, with seven degrees of unsaturation according to the positive-ion ESI-MS data

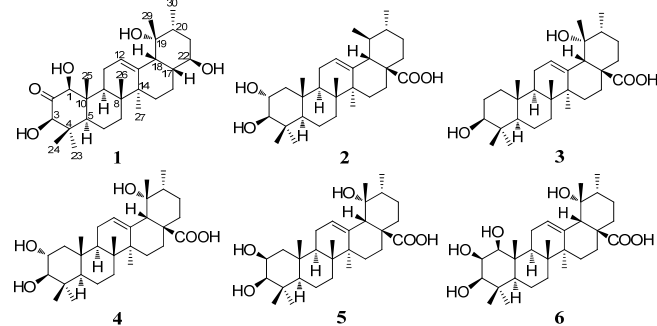


Figure 1: Structures of compounds **1-6** isolated from *Agrimonia pilosa*

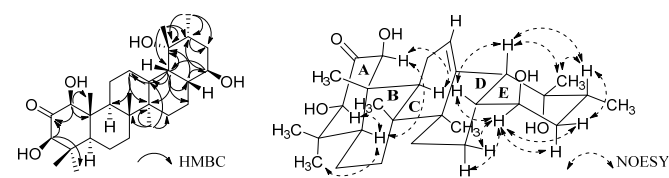
at m/z 497.4 [M+Na]⁺ and 473.2 [M-H]⁻, confirmed unambiguously from the pseudo-molecular ion peak at m/z 519.3340 [M+HCOO]⁻ obtained by high-resolution electrospray ionization mass spectrometry (HR-ESI-MS). The ¹H NMR spectrum (Table 1) of **1**, displayed the characteristic signals of six tertiary methyl groups at δ_H 1.21 (s, H-23), 0.69 (s, H-24), 0.80 (s, H-25), 0.86 (s, H-26), 1.31 (s, H-27) and 1.19 (s, H-29), one secondary methyl group at δ_H 0.92 (d, J = 5.8 Hz, H-30), three oxymethylene protons at δ_H 4.08 (s, H-1), 3.99 (d, J = 1.4 Hz, H-3) and 3.84 (like-dd, J = 2.0 Hz, H-22), and one tri-substituted olefinic proton at δ_H 5.35 (t, J = 3.6 Hz, H-12). In addition, the ¹³C NMR spectrum (Table 1) exhibited 29 carbon signals, including characteristic signals of seven methyls at δ_C 16.3 (C-23), 29.3 (C-24), 11.8 (C-25), 17.3 (C-26), 23.4 (C-27), 27.2 (C-29) and 15.6 (C-30), three oxygenated methines at δ_C 84.2 (C-1), δ_C 81.3 (C-3) and 72.3 (C-22), one quaternary oxygen-bearing carbon at δ_C 74.0 (C-19), two olefinic carbons at δ_C 128.7 (C-12) and 138.4 (C-13), and a ketone carbonyl carbon at δ_C 211.4 (C-2). The above NMR spectroscopic data were similar to those of 1β-hydroxy-2-oxopomolic acid [14], except for the appearance of a

Table 1: The ^1H and ^{13}C -NMR data^{a,b} of **1** in CDCl_3 .

No.	Carbon signals	Proton signals
1	84.2	4.08 (1H, s)
2	211.4	--
3	81.3	3.99 (1H, d, $J = 1.4$ Hz)
4	45.9	--
5	51.1	1.38 (1H, m)
6	18.2	1.75 (1H, d, $J = 10.1$ Hz) 1.58 (1H, m)
7	32.9	1.59 (1H, m)
8	40.5	1.44 (1H, m)
9	48.6	2.15 (1H, m)
10	49.7	--
11	26.3	2.48 (1H, ddd, $J = 21.0, 11.0, 3.6$ Hz) 2.16 (1H, m)
12	128.7	5.35 (1H, t, $J = 3.6$ Hz)
13	138.4	--
14	42.7	--
15	31.8	1.59 (1H, m) 1.23 (1H, m)
16	23.7	2.14 (1H, m) 1.23 (1H, m)
17	45.0	1.57 (1H, m)
18	47.9	2.38 (1H, d, $J = 5.6$ Hz)
19	74.0	--
20	34.3	1.93 (1H, m) 1.84 (1H, td, $J = 14.0, 2.4$ Hz)
21	33.9	1.40 (1H, m)
22	72.3	3.84 (1H, like-dd, $J = 2.0, 2.0$ Hz)
23	16.3	1.21 (3H, s)
24	29.3	0.69 (3H, s)
25	11.8	0.80 (3H, s)
26	17.3	0.86 (3H, s)
27	23.4	1.31 (3H, s)
29	27.2	1.19 (3H, s)
30	15.6	0.92 (3H, d, $J = 5.8$ Hz)

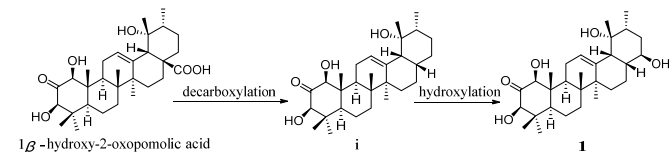
^a 600 MHz for ^1H NMR; the coupling constants (J) are in parentheses and reported in Hz; chemical shifts are given in ppm. ^b 100 MHz for ^{13}C NMR.

hydroxyl-carrying carbon and a methine instead of a methylene and a carboxyl group, which implied that compound **1** has a 28-norursene skeleton. This deduction was further supported by the HMBC correlations from δ_{H} 3.84 (H-22) to δ_{C} 47.9 (C-18) and 34.3 (C-20), and from δ_{H} 2.38 (H-18) to δ_{C} 128.7 (C-12), 138.4 (C-13), 42.7 (C-14), 23.7 (C-16), 45.0 (C-17) and 74.0 (C-19), and from δ_{H} 1.57 (H-17) to δ_{C} 72.3 (C-22) and 74.0 (C-19), and from δ_{H} 0.92 (Me-30) to δ_{C} 34.3 (C-20), 74.0 (C-19) and 33.9 (C-21), which established that a hydroxyl group was located at C-22 and a hydrogen atom instead of a carboxyl group located at C-17 of ring E (Figure 2). The location of the other functional groups and NMR data assignments of **1** were determined by HSQC and HMBC spectroscopic analysis. The strong NOESY correlations of δ_{H} 4.08 (H-1) with δ_{H} 1.38 (H-5) and 2.15 (H-9), δ_{H} 3.99 (H-3) with δ_{H} 1.38 (H-5) and 1.21 (Me-23) suggested that H-1 and H-3 were α -oriented on ring A, the same as for 1β -hydroxy-2-oxopomolic acid (Figure 2). Furthermore, the NOESY correlations of δ_{H} 2.38 (H-18) with δ_{H} 1.57 (H-17), 1.19 (Me-29) and 1.93 (H-20) suggested that ring D and E had a *cis*-configuration, and H-18 and H-20 were in the same orientation. The NOESY correlations of δ_{H} 1.93 (H-20) with δ_{H} 1.19 (Me-29) and 1.40 (H-21 β), and no correlations of H-20 with H-17 and H-22 indicated that ring E possessed a chair instead of a boat conformation [15]. H-21 α was axial-oriented, deduced by the triplet of doublets and vicinal coupling constant ($J = 14.0, 2.4$ Hz). The NOESY correlations of δ_{H} 3.84 (H-22) with δ_{H} 2.14 (H-16 α), 1.84 (H-21 α), 1.40 (H-21 β) and 1.23 (H-16 β) suggested that H-22 is equatorially-oriented (Figure 2). This is confirmed by the dd-like signal and vicinal coupling constant ($J = 2.0, 2.0$ Hz) that corresponds to a dihedral angle of ca. 60° from H-22 to H-17, H-21 α and H-21 β , respectively. The absolute configuration of **1** was established by the CD octant rule [16-17] due to the presence of a cyclohexone ring A moiety. In the CD spectrum of **1**, a positive Cotton effect at 284 nm ($\Delta\epsilon = +1.17$) due to the n- π^* electronic transition suggested 1S,3R,17R,18R,19R,20R,22R configurations of

**Figure 2:** Selected HMBC and NOESY correlations of compound **1**.

1. Therefore, compound **1** was established to be (1S,3R,17R,18R,19R,20R,22R)-1,3,19,22-tetrahydroxy-28-norurs-12-en-2-one.

The 28-norursene skeleton is unprecedented in the genus *Agrimonina* from the view point of chemotaxonomy. Compound **1** could be produced from 1β -hydroxy-2-oxopomolic acid, a key biosynthetic precursor isolated from *Rosa woodsii* (Rosaceae family), through decarboxylation [18] and hydroxylation reactions (Scheme 1).

**Scheme 1:** Plausible biogenetic pathway for compound **1**.

Five known triterpenoid derivatives were identified as corosolic acid (**2**) [19], pomolic acid (**3**) [20], tormentic acid (**4**) [19], *epi*-tormentic acid (**5**) [21], and $1\beta,2\beta,3\beta,19\alpha$ -tetrahydroxyurs-12-en-28-oic acid (**6**) [11], respectively, by analysis of their spectroscopic (NMR) and MS data with those reported in the literature.

Table 2: Inhibitory effects of compounds **2-6** on NO and IL-6 production induced by LPS in mouse monocyte-macrophage RAW 264.7 cells. (n=3).

Comp.	Anti-inflammatory activity (IC_{50} [μM])	
	NO	IL-6
2	33.2±2.8	42.5±3.2
3	25.6±1.9	42.2±2.7
4	52.6±4.8	76.7±5.5
5	55.6±4.2	85.1±6.9
6	59.1±4.0	>100
hydrocortisone ^a	56.5±4.6	63.1±5.2

^a Positive control

Compounds **2-6** were tested for their inhibitory activities on NO and IL-6 production in mouse monocyte-macrophage RAW 264.7 cells stimulated by LPS (Table 2). Compounds **2** and **3** showed mild inhibitory effects, while the activities of **4** and **5** were very weak. Compound **6** exhibited no significant inhibitory activity with an IC_{50} value higher than 100 μM concentration. The cytotoxic activities of compounds **2-6** against RAW 264.7 macrophages were also tested by the MTT assay, but none of the compounds exhibited significant cytotoxicity at their effective concentrations. The IC_{50} value of **1** was not acquired due to paucity of sample.

Experimental

Apparatus and reagents: Optical rotation was measured with a Perkin-Elmer 241 polarimeter. IR spectra were recorded on a Bruker IFS 55 spectrometer. The CD spectrum was determined with a Bio-Logic Science MOS-450 spectrometer. NMR experiments were performed on Bruker ARX-400 and AV-600 spectrometers. The chemical shifts are stated relative to TMS and expressed in δ values (ppm), with coupling constants are reported in Hz. The HRESIMS was obtained on an Agilent 6210 TOF mass spectrometer, and ESI-MS were recorded on an Agilent Series 1100 SL mass spectrometer. Silica gel GF254 prepared for TLC and

silica gel (200–300 mesh) for column chromatography (CC) were obtained from Qingdao Marine Chemical Factory (Qingdao, China). Sephadex LH-20 was a product of Pharmacia. Octadecyl silica gel was purchased from Merck Chemical Company Ltd. RP-HPLC separations were conducted using an LC-6AD liquid chromatograph with a YMC Pack ODS-A column ($250 \times 20\text{mm}$, $5 \mu\text{m}$, 120\AA) and SPD-10A VP UV/VIS detector. All reagents were either HPLC or analytical grade and were purchased from Tianjin Damao Chemical Company. Compounds were detected on TLC plates either under UV light or by heating after spraying with anisaldehyde- H_2SO_4 reagent.

Plant material: Dried aerial parts of *A. pilosa* were purchased from Shenyang Northeast Pharmacy, China, and identified by Professor Qishi Sun, Department of Pharmaceutical Botany, School of Traditional Chinese Materia Medica, Shenyang Pharmaceutical University. A voucher specimen (AP-20061010) has been deposited in the herbarium of the Department of Natural Products Chemistry, Shenyang Pharmaceutical University.

Extraction and isolation: The dried aerial parts of *A. pilosa* (10 kg) were cut into approximately 2 cm pieces and extracted with 70% EtOH ($100 \text{ L} \times 2 \text{ h} \times 2$). The resulting extract (1.0 kg) was concentrated *in vacuo*, suspended in H_2O (3 L), and partitioned successively with cyclohexane, EtOAc, and *n*-BuOH (3 L \times 3). The EtOAc extract (110 g) was subjected to silicagel CC ($10 \times 80 \text{ cm}$) and eluted with chloroform/MeOH (100:1, 30:1, 20:1, 10:1, 5:1, 2:1, 1:1 and 0:1 v/v) to obtain 7 fractions (EA-EG). Fraction EA (23 g) was subjected to a silica gel column ($6 \times 80 \text{ cm}$) and eluted with CH_2Cl_2 /EtOAc (from 40:1 to 0:1) to produce 7 fractions (EA1–EA7). Fraction EA4 (180 mg) was chromatographed over Sephadex LH-20 (CH_2Cl_2 /MeOH, 1:1; $1.5 \times 30 \text{ cm}$) to give compound **1** (3.5 mg). Fraction ED (20.6 g) was subjected to a silica gel column ($6 \times 80 \text{ cm}$) and eluted with CH_2Cl_2 /acetone (from 40:1 to 0:1) to yield ED1–ED6. Separation of ED4 (1.4 g) on a reversed-phase C_{18} silica gel column ($2.5 \times 30 \text{ cm}$) by elution with MeOH/ H_2O (30:70, 50:50, 70:30 and 100:0 v/v) yielded fractions ED4-1 to ED4-5. ED4-5 (380 mg) was purified by preparative TLC (CH_2Cl_2 /acetone, 3:1) to obtain **2** (11.5 mg) and **4** (22.3mg). ED5 (4.3 g) was subjected to RP- C_{18} silica gel CC ($2.5 \times 30 \text{ cm}$) and eluted with MeOH/ H_2O (1:9 to 8:2) to yield ED5-1 and ED5-2. ED5-1 (100 mg) was separated by HPLC (50%MeOH/ H_2O , 6mL/min) to afford compound **3** (56.2 mg, $t_{\text{R}} = 39 \text{ min}$) and compound **5** (28.8 mg, $t_{\text{R}} = 25 \text{ min}$). ED5-2 (120 mg) was purified by preparative TLC (CH_2Cl_2 /MeOH, 7:1) to obtain **6** (13.6 mg).

References

- [1] Chinese Pharmacopeia Committee (2010) *Pharmacopeia of the People's Republic of China*, Chinese Medicine Industry Press, Beijing, vol. I, pp. 94–95.
 - [2] Taira J, Nanbu H, Ueda K. (2009) Nitric oxide-scavenging compounds in *Agrimonia pilosa* Ledeb on LPS-induced RAW264.7 macrophages. *Food Chemistry*, **115**, 1221–1227.
 - [3] Taira J, Ohmine W, Ogi T, Nanbu H, Ueda K. (2012) Suppression of nitric oxide production on LPS/IFN- γ -stimulated RAW 264.7 macrophages by a novel catechin, pilosanol N, from *Agrimonia pilosa* Ledeb. *Bioorganic & Medicinal Chemistry Letters*, **22**, 1766–1769.
 - [4] Ahn EK, Lee JA, Seo DW, Hong SS, Oh JS. (2012) 1β -Hydroxy-2-oxopomolic acid isolated from *Agrimonia pilosa* extract inhibits adipogenesis in 3T3-L1 cells. *Biological & Pharmaceutical Bulletin*, **35**, 643–649.
 - [5] Zhu LC, Tan J, Wang BC, He R, Liu YP, Zheng C. (2009) Antioxidant activities of aqueous extract from *Agrimonia pilosa* Ledeb and its fractions. *Chemistry & Biodiversity*, **6**, 1716–1726.
 - [6] Shin WJ, Lee KH, Park MH, Seong BL. (2010) Broad-spectrum antiviral effect of *Agrimonia pilosa* extract on influenza viruses. *Microbiology and Immunology*, **54**, 11–19.
 - [7] Jung M, Park M. (2007) Acetylcholinesterase inhibition by flavonoids from *Agrimonia pilosa*. *Molecules*, **12**, 2130–2139.
 - [8] Kato H, Li W, Koike M, Wang YH, Koike K. (2010) Phenolic glycosides from *Agrimonia pilosa*. *Phytochemistry*, **71**, 1925–1929.
 - [9] Su G, Su S, Zhu T. (1984) Studies on bacteriostatic components from *Agrimonia pilosa* Ledeb. *Shenyang Yaoxue Xuebao*, **1**, 44–50.
 - [10] An R, Kim H, Jeong G, Oh S, Oh H, Kim Y. (2005) Constituents of the aerial parts of *Agrimonia pilosa*. *Natural Product Science*, **11**, 196–198.
 - [11] Kouno I, Baba N, Ohni Y, Kawano N. (1988) Triterpenoids from *Agrimonia pilosa*. *Phytochemistry*, **27**, 297–299.
 - [12] Pan Y, Liu HX, Zhuang YL, Ding LQ, Chen LX, Qiu F. (2008) Studies on isolation and identification of flavonoids in herbs of *Agrimonia pilosa*. *Zhongguo Zhongyao Zazhi*, **33**, 2925–2928.
- (1S,3R,17R,18R,19R,20R,22R)-1,3,19,22-tetrahydroxy-28-norurs-12-en-2-one (3)**
Amorphous white powder (MeOH).
 $[\alpha]_D^{25} : +46.0$ (c 0.10, MeOH).
CD (MeOH): 284 ($\Delta\epsilon = +1.17$) nm.
IR ν_{max} (KBr): 3448, 2928, 1715, 1618, 1459, 1384, 1021 cm^{-1} .
 $^1\text{H-NMR}$ (600 MHz, CDCl_3): Table 1.
 $^{13}\text{C-NMR}$ (100 MHz, CDCl_3): Table 1.
ESI-MS (m/z): 497.4 [$\text{M} + \text{Na}$]⁺, 473.2 [$\text{M} - \text{H}$].
HRESIMS (m/z): 519.3340 [$\text{M} + \text{HCOO}$][−] (calcd. for $\text{C}_{30}\text{H}_{47}\text{O}_7$: 519.3322).
- Inhibition of NO and IL-6 production bioassay:** The nitrite concentration in the medium was measured as an indicator of NO production according to the Griess reaction. Briefly, RAW 264.7 cells were seeded into 96-well tissue culture plates at a density of 1×10^5 cells/well, and stimulated with 1 $\mu\text{g}/\text{mL}$ of LPS in the presence or absence of test compounds. After incubation at 37°C for 24 h, 100 μL of cell-free supernatant was mixed with 100 μL of Griess reagent (mixture of equal volumes of reagent A and reagent B, A: 1%, w/v, sulfanilamide in 5%, w/v, phosphoric acid, B: 0.1%, w/v, of *N*-(1-naphthyl)ethylenediamine). The test groups, LPS groups, and control groups were treated in the same way as the experiment for NO analysis, respectively. Absorbance was measured in a microplate reader at 540 nm. Nitrite concentrations and the inhibitory rates were calculated by a calibration curve prepared with sodium nitrite standards. Cytotoxicity was determined by the mitochondria-dependent reduction of 3-(4,5-dimethylthiazol-2-yl)-2,5-diphenyl-2H-tetrazolium bromide (MTT) colorimetric assay, after 24 h incubation with test compound. The cells in the 96-well plates were cultured for 6 h, and the levels of IL-6 in the cell culture supernatant were detected by using a mouse IL-6 ELISA kit according to the manufacturer's recommendations [22]. Data are presented as the mean \pm standard deviation. Each experiment was performed at least 3 times.
- Supplementary data:** Spectral data relating to this article are available online.
- Acknowledgments** - This work was supported by the Program for Innovative Research Team of the Ministry of Education and Program for Liaoning Innovative Research Team in University. Finally, we are grateful to Dr Paul Owusu Donkor at Tianjin University of Traditional Chinese Medicine for linguistic corrections.

- [13] Liu HX, Liu ZX, Jiang QH, Ding LQ, Chen LX, Qiu F. (2010) Phenolic constituents of whole plant of *Agrimonia pilosa* Ledeb. *Zhongguo Zhongyao Zazhi*, **27**, 286-298.
- [14] Kashiwada Y, Wang HK, Nagao T, Kitanaka S, Yasuda I, Fujioka T, Yamagishi T, Cosentino M, Kozuka M, Okabe H, Ikeshiro Y, Hu CQ, Yeh E, Lee KH. (1998) Anti-AIDS agents. 30. Anti-HIV activity of oleanolic acid, pomolic acid, and structurally related triterpenoids. *Journal of Natural Products*, **61**, 1090-1095.
- [15] Konoshim T, Kozuka M. (1991) Constituenents of Leguminous plants, XIII. New triterpenoid saponins from *Wistaria brachybotrys*. *Journal of Natural Products*, **54**, 830-836.
- [16] Kirk DN. (1986) The chiroptical properties of carbonyl compounds. *Tetrahedron*, **42**, 777-818.
- [17] Djerassi C, Klyne W. (1962) Optical rotatory dispersion: application of the octant rule to some structural and stereochemical problems. *Journal of the Chemical Society*, 4929-4950.
- [18] Solomons TWG, Fryhle CB, Snyder SA. (2014) *Organic chemistry*, John Wiley & Sons, Inc. pp. 744-806.
- [19] Taniguchi S, Imayoshi Y, Kobayashi E, Takamatsu Y, Ito H, Hatano T, Sakagami H, Tokuda H, Nishino H, Sugita D, Shimura S, Yoshida T. (2002) Production of bioactive triterpenes by *Eriobotrya japonica* Calli. *Phytochemistry*, **59**, 315-323.
- [20] Ju JH, Zhou L, Lin G, Liu D, Wang LW, Yang JS. (2003) Studies on constituents of triterpene acids from *Eriobotrya japonica* and their anti-inflammatory and antitussive effects. *Zhongguo Zhongyao Zazhi*, **38**, 752-757.
- [21] Delgado G, Hernandez J. (1989) Triterpenoid acids from *Cunila lythrifolia*. *Phytochemistry*, **28**, 1483-1485.
- [22] Jiao WH, Gao H, Zhao F, He F, Zhou GX, Yao XS. (2011) A new neolignan and a new sesterterpenoid from the stems of *Picrasma quassoides* Bennet. *Chemistry & Biodiversity*, **8**, 1163-1169.

Two New 18-Norschiartane-type Schinortriterpenoids from *Schisandra lancifolia*

Miao Liu^{a,b}, Yuan-Qing Luo^{a,b}, Wei-Guang Wang^a, Yi-Ming Shi^{a,b}, Hai-Yan Wu^{a,b}, Xue Du^a, Jian-Xin Pu^{a,*} and Han-Dong Sun^{a,*}

^aState Key Laboratory of Phytochemistry and Plant Resources in West China, Kunming Institute of Botany, Chinese Academy of Sciences, Kunming 650201, People's Republic of China

^bUniversity of Chinese Academy of Sciences, Beijing 100049, People's Republic of China

pujianxin@mail.kib.ac.cn (J.-X. Pu), hdsun@mail.kib.ac.cn (H.-D. Sun).

Received: September 19th, 2015; Accepted: October 20th, 2015

Two new 18-norschiartane-type schinortriterpenoids, namely wuwezidilactones Q (**1**) and R (**2**) were isolated from the stems of *Schisandra lancifolia*. Their structures were determined on the basis of extensive spectroscopic analysis. The absolute configurations of the new compounds were further determined by ROESY and an empirical comparison of their experimental ECD spectra with literature.

Keywords: *Schisandra lancifolia*, Schinortriterpenoids, Absolute configuration.

Plants of Schisandraceae family, contains the genera *Schisandra* and *Kadsura*, represent an important group of plants. Some of these plants were important Traditional Chinese Medicines (TCMs), and used in Chinese folk for more than two thousand years. Chemical investigation on this family was mostly focused on lignans and triterpenoids since 1970's. In 2003, Sun and co-workers reported a novel highly oxygenated nortriterpenoid, micrandilactone A, from *Schisandra micrantha* [1]. This discovery revealed a new kind of natural triterpernoid, called as schinortriterpenoid (SNT). In the past decades, a series of SNTs with different novel skeletons were isolated and identified from this family [2,3], especially from *Schisandra* genus, attracting more and more attention from natural product chemists, as well as organic chemists.

Schisandra lancifolia (Rehd. et. Wils.) A. C. Smith, a species of *Schisandra* genus distributed in the southwest of China, was used to staunch, treat fractures, and eliminate stasis to reduce swelling [4]. Phytochemistry research of this species has led to the discovery of a series of SNTs with different new skeletons, such as 18-Norschiartanes [5], Norcloartanes [6], Schisanartanes [7], 1,2,3-trinorlancishiartanes [8], 2,3-dinorlancisciartanes [9], lancifoartanes [10], 12,22-cyclopreschisanartanes [11]. Our further investigation into this plant aimed at finding more SNTs with diverse skeletons led to the isolation of two new 18-norschiartane-type shinortriterpenoids. This article deals with the isolation, structure elucidation of the new compounds.

Wuwezidilactone Q (**1**) was obtained as a white amorphous powder. Its molecular formula $C_{28}H_{36}O_8$ was determined by HRESIMS at m/z 523.2298 [$M+Na$]⁺ (calcd for $C_{28}H_{36}O_8Na$ 523.2302) with 11 indices of hydrogen deficiency. ¹H, ¹³C NMR and DEPT spectra of **1** displayed three methyl singlets and one methyl doublet, six methylenes, four sp^3 methines, four oxygenated sp^3 methines, two trisubstituted double bonds, four sp^3 quaternary carbons and two ester groups. All of the above data of **1** suggested that **1** was a 18-norschiartane-type nortriterpenoid with 28 carbons. Comparison of NMR data of **1** with those of lancifodilactone A indicated that the acetoxy group at C-12 in lancifodilactone A was replaced by a hydroxyl group in **1** without causing significant chemical

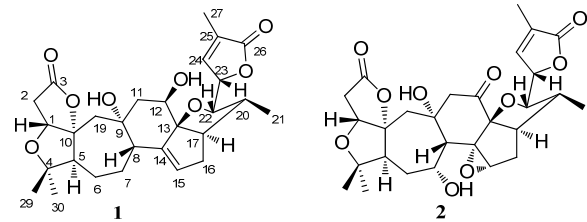


Figure 1: The structures of compounds **1** and **2**.

shifts at C-11, C-12, and C-13. This was confirmed by ¹H-¹H COSY correlation of H-11 with H-12 and HMBC correlations from H-12 to C-9, C-13, and C-14. Furthermore, compound **1** differed from lancifodilactone A at C-7 (δ_C 69.8) in ring C, the hydroxyl group at C-7 in lancifodilactone A was replaced by a methylene (δ_C 26.4) in **1**. In addition, a downfield shift of C-5 in **1** (δ_C 60.7) compared with that in lancifodilactone A (δ_C 52.3) could ascribe to the absence of γ -steric compression between the oxygen atom at C-7 and H-5 in **1** [5,12]. The change at C-7 was further proved by ¹H-¹H COSY correlations of H-7 with H-6, and H-8 and HMBC correlations from H-7 to C-5, C-8, C-9, and C-14. The relative configuration of **1** was deduced to be the same as that of lancifodilactone A from the similar carbon chemical shifts and ROESY correlations. The ROESY correlations of H-23 with Me-21, H-12 with H-17, and H-20 suggested that H-12 was α -oriented. The absolute configuration of C-23 could be determined by intense positive or negative cotton effects (CEs) around 210nm. The experimental ECD spectrum of **1** showed Negative CE at 212 nm, indicated that the absolute configuration of C-23 was "S" [12]. Thus, the absolute configuration of **1** was finally determined as shown in Figure 1 by an empirical comparison the experimental ECD with that of wuwezidilactones J-P.

Wuwezidilactone R (**2**) was obtained as a white amorphous powder. Its molecular formula $C_{28}H_{34}O_{10}$ was deduced by HRESIMS at m/z 553.2047 [$M+Na$]⁺ (calcd for $C_{28}H_{34}O_{10}Na$ 553.2044) with 12 indices of hydrogen deficiency. Careful Analysis of the ¹H, ¹³C NMR and DEPT spectra of **2** disclosed that **2** was also a 18-norschiartane-type nortriterpenoid. Structure of **2** was almost the

Table 1: ^1H and ^{13}C NMR data (acetone- d_6) of compounds **1** and **2**.

Position	1		2	
	δ_{H}	δ_{C}	δ_{H}	δ_{C}
1	4.29, d (4.8)	81.8 d	4.28, d (5.4)	82.1 d
2 α	2.44, d (18.0)	36.0 t	2.95, overlapped	35.6 t
2 β	2.92, overlapped		2.44, overlapped	
3		174.7 s		174.8 s
4		85.1 s		84.8 s
5	2.29, overlapped	60.7 d	2.76, dd (13.2, 4.8)	52.9 d
6 α	1.47, overlapped	27.6 t	2.03, overlapped	32.7 t
6 β	1.81, overlapped		1.76, overlapped	
7 α	1.81, overlapped	26.4 t		69.6 d
7 β	2.00, m		4.32, br t	
8	2.25, overlapped	49.3 d	2.73, br s	46.4 d
9		77.2 s		80.1 s
10		99.9 s		98.7 s
11 α	1.81, m	43.1 t	2.21, d (13.2)	54.0 t
11 β	1.91, dd (14.4, 2.4)		2.92, overlapped	
12	3.57, br d	72.9 d		202.4 s
13		97.8 s		93.7 s
14		143.4 s		74.3 s
15	5.58, m	128.0 d	3.96, br s	57.5 d
16 α	2.26, overlapped	31.9 t	2.09, overlapped	26.6 t
16 β	2.37, m		1.79, overlapped	
17	3.04, dt (9.0, 4.2)	45.7 d	2.59, m	41.6 d
19 α	2.09, overlapped	44.6 t	2.11, overlapped	45.2 t
19 β	2.18, d (15.6)		2.43, overlapped	
20	2.31, overlapped	37.9 d	2.51, m	38.2 d
21	1.01, d (6.6)	12.6 q	1.06, d (7.2)	11.9 q
22	3.52, dd (10.2, 3.6)	83.1 d	3.91, dd (9.6, 3.0)	85.3 d
23	5.01, m	81.0 d	4.88, m	81.0 d
24	7.28, m	147.8 d	7.23, m	147.2 d
25		130.3 s		130.9 s
26		174.4 s		174.0 s
27	1.84, br s	10.7 q	1.83, br s	10.8 q
29	1.14, s	22.4 q	1.14, s	22.3 q
30	1.29, s	29.2 q	1.27, s	28.7 q

δ_{H} were recorded at 600 MHz, δ_{C} were recorded at 150 MHz.

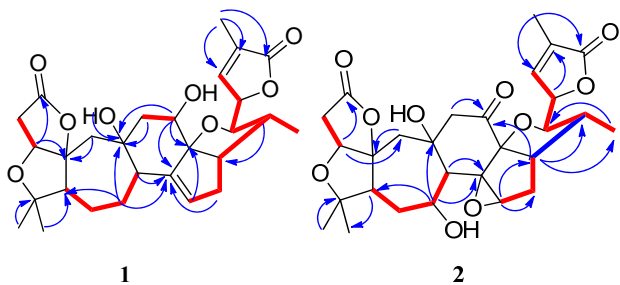


Figure 2: Selected HMBC (blue arrows $\text{H} \rightarrow \text{C}$) and ^1H - ^1H COSY (red lines) correlations of **1** and **2**.

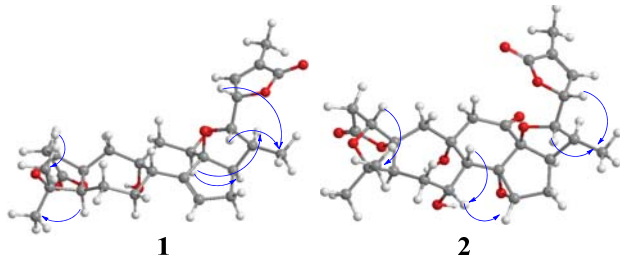


Figure 3: Key ROESY correlations (blue arrows) of **1** and **2**.

same as that of wuweizidilactone M except for a hydroxyl group at C-7 in **2** rather than an acetoxy group. This could be confirmed by the chemical shift at C-7 (δ_{C} 69.6), and the ^1H - ^1H COSY correlations of H-7 with H-6, and H-8 and HMBC correlations from H-5, H-6, and H-8 to C-7. The ROESY experiment of **2** was similar to wuweizidilactone M, revealed that they had a same relative configuration. The ROESY correlation of H-7 with H-15 suggested that H-7 was β -oriented. The absolute configuration of **23S** was proved by Negative CE at 209 nm in ECD spectrum. At last, the absolute configuration of **2** was finally determined as shown in Figure 1 by the same way as that of **1**.

Experimental

General: 1D and 2D NMR spectra were recorded on Bruker DRX 600 and DRX 500 spectrometers using TMS as the internal standard. Chemical shifts (δ) are expressed in ppm relative to the TMS signals. HRESIMS was performed on an API QSTAR Pulsar i spectrometer. UV spectra were obtained on a Shimadzu UV-2401PC spectrophotometer. IR spectra were obtained on a Bruker Tensor-27 FT-IR spectrometer using KBr pellets. Optical rotations were measured in MeOH with Horiba SEPA-300 and JASCO P-1020 polarimeters. Experimental ECD spectra were measured on a Chirascan instrument. Column chromatography (CC) was performed with silica gel (100~200 mesh; Qingdao Marine Chemical, Inc., Qingdao, People's Republic of China), MCI gel (CHP20P, 75~150 μm , Mitsubishi Chemical Corporation, Tokyo, Japan). Preparative HPLC was performed on an Agilent 1260 preparative liquid chromatograph with a Zorbax SB-C18 (21.2 mm \times 250 mm) column. Semipreparative HPLC was performed on an Agilent 1200 liquid chromatograph with a Zorbax SB-C18 (9.4 mm \times 250 mm) column. Fractions were monitored by thin layer chromatography, spots were visualized by UV light (254 nm and 365 nm) and by heating silica gel plates sprayed with 10% H_2SO_4 in EtOH. All solvents used in column chromatography were distilled including petroleum ether (60~90°C).

Plant Material: The stems of *S. lancifolia* were collected in Shangri-La of Yunnan Province, People's Republic of China, in October 2013 and identified by Prof. Xi-Wen Li at Kunming Institute of Botany. A voucher specimen has been deposited in the State Key Laboratory of Phytochemistry and Plant Resources in West China, Kunming Institute of Botany, Chinese Academy of Sciences.

Extraction and isolation: The air-dried and powdered stems of *S. lancifolia* (7.0 Kg) were extracted with aqueous acetone (4 \times 8L, 3 days each) at room temperature. The extracted solution was distilled under reduced pressure to remove acetone, and then was partitioned between EtOAc and H_2O to afford EtOAc part. The EtOAc extract (250 g) was eluted with $\text{CHCl}_3/\text{Me}_2\text{CO}$ (1:0, 9:1:8.2, 6:4, 1:1, 0:1) on silica gel column chromatography to give 6 fractions A-F. Fraction C (8:2) was decolorized on MCI gel with 90% MeOH/ H_2O and was separated on Rp-18 with MeOH/ H_2O (3:7, 4:6, 6:4, 7:3, 8:2, 1:0) to afford fractions C1-C6. Fraction C3 was separated on silica gel CC with petroleum ether/acetone (5:1, 3:1, 2:1, 1:1, 0:1) to obtain C31-C38. C33 was purified by Sephadex LH-20 CC, eluting with $\text{CHCl}_3/\text{MeOH}$ (1:1), and by preparative HPLC to afford **1** (1.9 mg).

Fraction D (6:4) was successfully separated on MCI gel with 90% MeOH/ H_2O to remove pigments and then on Rp-18 with MeOH/ H_2O (3:7, 4:6, 5:5, 6:4, 7:3, 8:2, 9:1, 1:0) to afford fractions D1-D8. D3 was separated over silica gel CC with petroleum ether/acetone (5:1, 3:1, 2:1, 1:1, 0:1) to afford D31-D36. D36 was purified by repeated Sephadex LH-20 CC, eluting with $\text{CHCl}_3/\text{MeOH}$ (1:1), and by Semipreparative HPLC to afford **2** (4 mg).

Wuweizidilactone Q (1)

$[\alpha]^{23}_{\text{D}}: +23$ (*c* 0.12, MeOH).

IR (KBr) ν_{max} : 3343, 2924, 1760, 1629, 1434, 1385, 1326, 1197, 1109, 1082, 1037.

UV (MeOH) λ_{max} nm ($\log \epsilon$): 204 (3.88).

ECD (*c* 0.05 MeOH) λ_{max} nm: 209, 251.

^1H NMR and ^{13}C NMR: Table 1.

HRESIMS: m/z 523.2298 [$\text{M}+\text{Na}$]⁺ (calcd for $\text{C}_{28}\text{H}_{36}\text{O}_8\text{Na}$, 523.2302).

Wuweizidilactone Q (2)

$[\alpha]^{23}_D: +34$ (*c* 0.24, MeOH).

IR (KBr) ν_{max} : 3442, 2925, 1762, 1629, 1384, 1221, 1175, 1106, 1067, 957 cm^{-1} .

UV (MeOH) λ_{max} nm (log ϵ): 208 (3.95), 275 (2.79).

ECD (*c* 0.07 MeOH) λ_{max} nm: 212, 302.

^1H NMR and ^{13}C NMR: Table 1.

HRESIMS: m/z 553.2047 [M+Na] $^+$ (calcd for $\text{C}_{28}\text{H}_{34}\text{O}_{10}\text{Na}$ 553.2044).

Supplementary data: 1D and 2D NMR, HRESIMS, UV, IR, and CD spectra of **1** and **2** are available.

Acknowledgments - This project was supported financially by the National Natural Science Foundation of China (81373290 and 21322204).

References

- Li RT, Zhao QS, Li SH, Han QB, Sun HD, Lu Y, Zhang LL, Zheng QT. (2003) Micrandilactone A: a Novel Triterpene from *Schisandra micrantha*. *Organic Letters*, **5**, 1023-1026.
- Xiao WL, Li RT, Huang SX, Pu JX, Sun HD. (2008) Triterpenoids from the Schisandraceae family. *Natural Product Reports*, **25**, 871-891.
- Shi YM, Xiao WL, Pu JX, Sun HD. (2015) Triterpenoids from the Schisandraceae family: an update. *Natural Product Reports*, **32**, 367-410.
- Wu ZY. (1988) *A Compendium of new China Herbal Medicine*; Shanghai Science and Technology Press: Shanghai; Vol. 1.
- Li RT, Li SH, Zhao QS, Lin ZW, Sun HD, Lu Y, Wang C, Zheng QT. (2003) Lancifodilactone A, a novel bisnortriterpenoid from *Schisandra lancifolia*. *Tetrahedron letters*, **44**, 3531-3534.
- Xiao WL, Li RT, Li SH, Li XL, Sun HD, Zheng YT, Wang RR, Lu Y, Wang C, Zheng QT. (2005) Lancifodilactone F: a novel nortriterpenoid possessing a unique skeleton from *Schisandra lancifolia* and its anti-HIV Activity. *Organic Letters*, **7**, 1263-1266.
- Xiao WL, Zhu HJ, Shen YH, Li RT, Li SH, Sun HD, Zheng YT, Wang RR, Lu Y, Wang C, Zheng QT. (2005) Lancifodilactone G: a unique nortriterpenoid isolated from *Schisandra lancifolia* and its anti-HIV activity. *Organic Letters*, **7**, 2145-2148.
- Luo X, Chang Y, Zhang XJ, Pu JX, Gao XM, Wu YL, Wang RR, Xiao WL, Zheng YT, Lu Y, Chen GQ, Zheng QT, Sun HD. (2009) Schilancidilactones A and B: two novel tetranortriterpenoids with an unprecedented skeleton from *Schisandra lancifolia*. *Tetrahedron Letters*, **50**, 5962-5964.
- Luo X, Shi YM, Luo RH, Luo SH, Li XN, Wang RR, Li SH, Zheng YT, Du X, Xiao WL, Pu JX, Sun HD. (2012) Schilancitrilactones A-C: three unique nortriterpenoids from *Schisandra lancifolia*. *Organic Letters*, **14**, 1286-1289.
- Shi YM, Wang XB, Li XN, Luo X, Shen ZY, Wang YP, Xiao WL, Sun HD. (2013) Lancolides, antiplatelet aggregation nortriterpenoids with tricyclo[6.3.0.0(2,11)]undecane-bridged system from *Schisandra lancifolia*. *Organic Letters*, **15**, 5068-5071.
- Shi YM, Yang J, Xu L, Li XN, Shang SZ, Cao P, Xiao WL, Sun HD. (2014) Structural characterization and antioxidative activity of lancifonins: unique nortriterpenoids from *Schisandra lancifolia*. *Organic Letters*, **16**, 1370-1373.
- Shi YM, Wang LY, Zou XS, Li XN, Shang SZ, Gao ZH, Liang CQ, Luo HR, Li HL, Xiao WL, Sun HD. (2014) Nortriterpenoids from *Schisandra chinensis* and their absolute configurational assignments by electronic circular dichroism study. *Tetrahedron*, **70**, 859-868.

Terpenoids and Steroids from *Euphorbia hypericifolia*

Jin-Xin Zhao, Shan-Shan Shi, Li Sheng, Jia Li and Jian-Min Yue*

State Key Laboratory of Drug Research, Shanghai Institute of Materia Medica, Chinese Academy of Sciences,
555 Zu Chong Zhi Road, Shanghai 201203, People's Republic of China

jmyue@simm.ac.cn

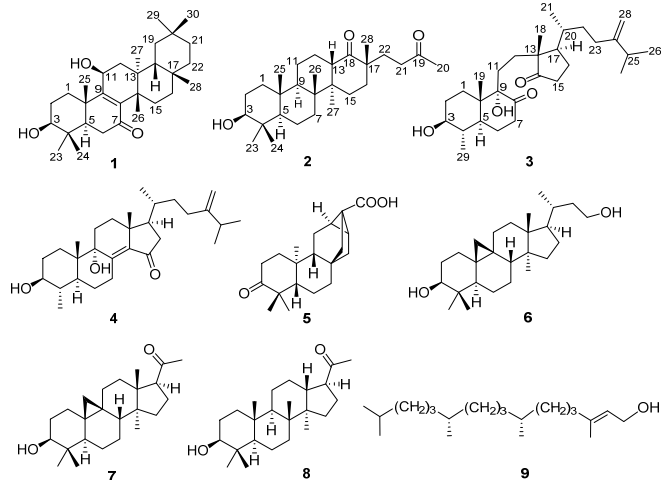
Received: September 28th, 2015; Accepted: October 30th, 2015

Two new triterpenoids and two new sterols, named euphyperins A–D (**1–4**), including an oleanane-type triterpenoid (**1**), a lupane-type nortriterpenoid (**2**), and two cholestanetype steroids (**3** and **4**), along with five known compounds (**5–9**) were isolated from the twigs and leaves of *Euphorbia hypericifolia*. Euphyperin B (**2**) represents a rare lupane-type nortriterpenoid, and euphyperin C (**3**) is a novel 8,14-secocholestane-type steroid. Euphyperin A (**1**) exhibited moderate PTP1B inhibitory activity with an $IC_{50} = 17.05 \pm 1.12 \mu\text{g/mL}$.

Keywords: *Euphorbia hypericifolia*, Triterpenoid, Steroid, PTP1B inhibitor.

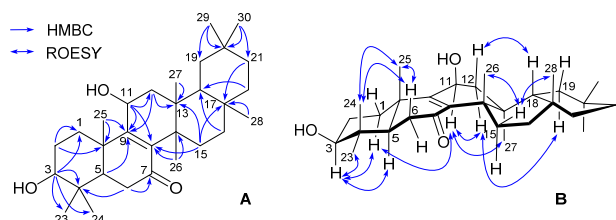
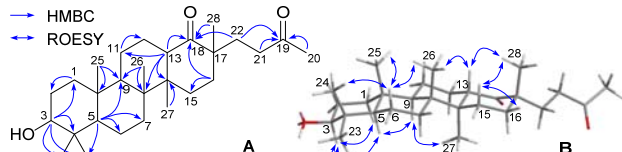
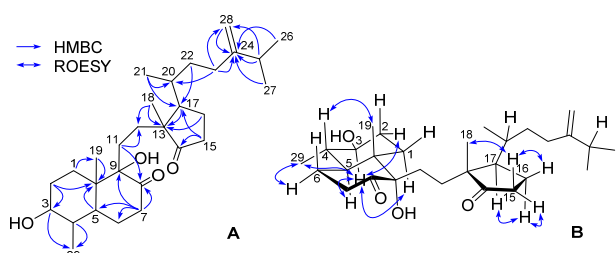
The genus *Euphorbia*, with more than 2000 species, is one of the largest genera of angiosperms [1]. Diterpenoids in this genus are the focus of natural product research, because of their wide range of potentially valuable bioactivities [2]. Our great interest in structural and biological diversities of this genus resulted in some exciting research findings, such as the first secolathyrane diterpenoid with an unprecedented skeleton [3], ingol-type diterpenoids with 11 β -HSD1 inhibitory activities [4], and abietane-type diterpenoids with anti-HIV activities [5]. *E. hypericifolia* Linn. (Euphorbiaceae) has long been used as a traditional herbal medicine in China for promoting lactation [6]. Previous chemical studies on this plant only afforded some flavonoids and ellagic acid [7]. In the continuing search for structurally diverse and bioactive compounds from the genus *Euphorbia*, four new compounds, named euphyperins A–D, including one oleanane-type triterpenoid, one degraded lupane-type triterpenoid, and two sterols, along with five known compounds were isolated from the twigs of *E. hypericifolia*. Among them, euphyperin B (**2**) represents a rare class of lupane-type nortriterpenoid [8], and euphyperin C (**3**) possesses a rare 8,14-secocholestane-type steroid skeleton, which has only been found previously in a marine sponge [9]. Euphyperin A (**1**) exhibited PTP1B inhibitory activity with an $IC_{50} = 17.05 \mu\text{g/mL}$. Herein we describe the isolation, structure characterization, and biological activities of these compounds.

Euphyperin A (**1**) was isolated as a white, amorphous powder, and its molecular formula was determined as $C_{30}H_{48}O_3$ (seven indices of hydrogen deficiency) based on an HR-EIMS ion at m/z 456.3606 [M^+] (calcd 456.3603), as well as comprehensive analysis of its ^1H and ^{13}C NMR spectra. The UV absorption band at 253 nm exhibited a conjugated unsaturated carbonyl system, consistent with the IR absorption (Supporting Information Figure S10) at 1649 cm^{-1} . The ^{13}C and DEPT spectra (Table 1) displayed 30 signals of carbons including eight methyls, nine methylenes, four methines (two oxygenated at δ_{C} 67.3 and 78.5) and nine quaternary. Three overlapped signals at δ_{C} 30.9 (C-17) and 39.9 (C-10 and C-14) were distinguished by HMBC correlations. The signals at δ_{C} 144.7, 158.8, and 201.1 confirmed the existence of the aforementioned enone system, which accounted for two indices of hydrogen deficiency, and the remaining five thus required **1** being pentacyclic. The above data with the aid of analysis of its 2D NMR spectra suggested that it was an oleanane-type triterpenoid bearing



an α,β -enone system and two hydroxyls. The attachments of these two hydroxyls were at C-3 and C-11, as determined by the chemical shifts of the relevant protons and carbons as well as the HMBC correlations (Figure 1A) from H-3 to C-1, C-4, C-23, and C-24, and from H-11 to C-8, C-9, and C-12. The tetrasubstituted Δ^8 double bond in the α,β -enone system was located by the multiple correlations from H-11, H₂-15, and H₃-26 to C-8 at δ_{C} 144.7, and from H-5, H-11, H₂-12, and H₃-25 to C-9 at δ_{C} 158.8, respectively. The location of the carbonyl group was assigned at C-7 as deduced from the HMBC correlations from H₂-6 to C-7 at δ_{C} 201.1. The above deduction unambiguously suggested that **1** was an analogue of 7-oxoisomultiflorenol [10], and the only difference was the presence of a hydroxy group at C-11 (δ_{C} 67.3).

The relative configuration of **1** was almost identical to that of 7-oxoisomultiflorenol by comparing their ^1H and ^{13}C NMR spectra, as well as analysis of the ROESY spectrum (Figure 1B) of **1**, in which the cross-peaks of H-1 α /H-3, H-3/H-5, and H-3/H₃-23 revealed that they were cofacial and assigned to be α -oriented randomly. In consequence, the ROESY cross-peaks of H-11/H-1 α , H-11/H-12 α , and H-11/H₃-27 suggested H-11 was also α -oriented. Thus, the structure of **1** was assigned.

Figure 1: Selected HMBC (A) and ROESY (B) correlations of **1**.Figure 2: Selected HMBC (A) and ROESY (B) correlations of **2**.Figure 3: Selected HMBC (A) and ROESY (B) correlations of **3**.

Euphyperin B (**2**), a white, amorphous powder, gave a molecular formula $C_{28}H_{46}O_3$ as determined by the ^{13}C NMR data and an HR-ESI(+)MS ion at m/z 453.3351 [$M + \text{Na}^+$] (calcd 453.3345), requiring six indices of hydrogen deficiency. The ^1H NMR spectrum (Table 1) of **2** showed signals of six singlet methyl groups (δ_H 0.76, 0.76, 0.86, 0.96, 1.11, and 1.14), one acetyl group (δ_H 2.15, s, H₃-20) and one oxygenated methine (δ_H 3.20, dd, $J = 11.3, 4.9$ Hz, H-3). The ^{13}C NMR and DEPT spectra (Table 1) displayed 28 carbon signals for seven methyls, ten methenes, four methines and seven quaternaries, including two carbonyls (δ_C 209.5 and 217.9). The two keto groups accounted for two indices of hydrogen deficiency, and the remaining four thus indicated **2** being tetracyclic. The aforementioned analysis obviously suggested that the structure of **2** resembled that of 29,30-dinor-3 β -acetoxy-18,19-dioxo-18,19-secolupane [8], and the only difference was the presence of a 3-OH in **2** replacing the 3-OAc in the latter as judged by the shielded H-3 ($\Delta\delta_H$ 1.25). This conclusion was confirmed by the HMBC correlations (Figure 2A) from H-3 to C-1, C-4, C-23, and C-24. The locations of the two keto groups at C-18 and C-19 were confirmed by the HMBC correlations from H-13, H₂-16, H₂-22, and H₃-28 to C-18 (δ_C 217.9), and from H₃-20, H₂-21, and H₂-22 to C-19 (δ_C 209.5).

The relative configuration of **2** was assigned in the same way as that of 29,30-dinor-3 β -acetoxy-18,19-dioxo-18,19-secolupane, mainly by comparing their NMR data, which were corroborated by the ROESY spectrum (Figure 2B), in which the α -axial orientation of H-3 was determined by the cross-peaks of H-3/H-1 α , H-5, and H₃-23. The correlations for H-6 β /H₃-24, H-6 β /H₃-25, H-6 β /H₃-26, H-13/H₃-26, H-13/H₃-28, H-15 β /H-16 β , and H-15 β /H₃-28 revealed that they were all β -oriented. The structure of **2** was therefore determined.

Euphyperin C (**3**) gave a molecular formula $C_{29}H_{48}O_4$ with six indices of hydrogen deficiency based on the ^{13}C NMR data and an HR-ESI(+)MS ion at m/z 483.3436 [$M + \text{Na}^+$] (calcd 483.3450).

Table 1: ^1H and ^{13}C NMR data of compounds **1** and **2** in CDCl_3 .

No.	δ_H (mult., J in Hz) ^a	δ_C ^b	δ_H (mult., J in Hz) ^a	δ_C ^b
1	α 1.58, m β 2.46, dd (13.2, 3.2)	33.8	α 0.95 td (12.4, 4.3) β 1.73 m	39.0
2	1.75, m (2H)	27.5	1.62 m (2H)	27.5
3	3.32, m	78.5	3.20 dd (11.3, 4.9)	78.9
4		39.1		39.0
5	1.64, dd (13.2, 5.9)	48.7	0.69 dd (11.4, 2.1)	55.6
6	α 2.41, dd (19.1, 5.9) β 2.45, dd (19.1, 13.2)	36.9	α 1.37 m β 1.55 m	18.4
7		201.1	1.31 m 1.48 m	34.2
8			144.7	41.1
9			158.8	51.0
10		39.9	3.20 dd (11.3, 4.9)	37.4
11	4.60, q (8.3)	67.3	1.20 m 1.56 m	20.1
12	β 1.39, m α 2.15, dd (12.7, 8.0)	42.5	1.30 m 1.64 m	22.3
13			39.7	2.70 dd (11.8, 3.6)
14			39.9	46.6
15	α 1.41, m β 2.29, dt (15.9, 9.0)	29.5	α 1.30 m β 2.04 td (13.4, 4.5)	27.0
16	1.35, m 1.52, m	35.6	β 1.52 m α 1.69 m	34.2
17			30.9	46.4
18	1.59, m		42.1	217.9
19	α 1.19, dd (13.9, 5.6) β 1.35, m	35.5		209.5
20			28.6	30.0
21	1.27, m 1.45, m	33.0	2.47 m (2H)	39.1
22	0.91, m 1.46, m	38.4	1.67 m (2H)	32.3
23	0.99, s		27.7	28.1
24	0.91, s		15.3	15.5
25	1.21, s		19.7	16.8
26	1.51, s		27.4	16.1
27	0.96, s		19.1	16.2
28	1.14, s		30.9	24.4
29	0.96, s		34.3	
30	0.98, s		32.0	

^{a,b} Data were measured at 400 and 125 MHz, respectively.

Interpretation of its ^1H NMR spectrum (Table 2) showed the presence of two methyl singlets (δ_H 0.74 and 0.86, each 3H), four methyl doublets (δ_H 1.00, 3H, d, $J = 6.6$ Hz; and three overlapped δ_H 1.03, each 3H, d, $J = 6.7$ Hz), one oxygenated methine (δ_H 3.16, 1H, td, $J = 10.4, 5.1$ Hz), and one terminal methine group (δ_H 4.68 and 4.74, each 1H, s). The ^{13}C NMR data (Table 2), with the aid of the HMBC spectrum (Figure 3A), displayed signals of 29 carbons, suggesting the existence of several characteristic functional groups including two keto groups (δ_C 215.4 and 224.5), one oxygenated methine (δ_C 75.9), one oxygenated quaternary carbon (δ_C 83.5), and one terminal methene group (δ_C 106.5 and 156.5). The above data indicated that **3** likely possessed a steroidal structure which was highly similar to that of (24R)-3 β -hydroxy-24-methyl-4-methylene-5 α -8,14-secocholestane-8,14-dione [9], except for the presence of a $\Delta^{24(28)}$ double bond and in the concomitant absence of a $\Delta^{4(29)}$ double bond. This deduction was further verified by the HMBC spectrum, in which the $\Delta^{24(28)}$ double bond was verified by the key correlations from H₂-23, H₂-25, H₃-26, H₃-27, and H₂-28 to C-24 at δ_C 156.5, and from H₂-23 and H₂-25 to C-28 at δ_C 106.5. In addition, CH₃-29 was located by the correlations from H-3 and H-4 to C-29 at δ_C 15.6.

The relative configuration of **3** was assigned by comparison of NMR data with those of (24R)-3 β -hydroxy-24-methyl-4-methylene-5 α -8,14-secocholestane-8,14-dione [9] and the ROESY experiment (Figure 3B). In particular, H-3 and CH₃-29 were assigned to be α -oriented on the basis of the ROESY cross-peaks of H-1/H-3, H-2 α /H-3, H-3/H-5, H-3/H₃-29, and H-6 α /H₃-29. The structure of **3** possessing a rare 8,14-secosteroid skeleton was thus elucidated as depicted.

Table 2: ^1H and ^{13}C NMR data of compounds **3** and **4** in CDCl_3 .

No.	δ_{H} (mult., J in Hz) ^a	$\delta_{\text{C}}^{\text{c}}$	δ_{H} (mult., J in Hz) ^b	$\delta_{\text{C}}^{\text{c}}$
1	α 1.27 m β 1.58 m	29.6	α 1.47 m β 1.75 m	29.7
2	β 1.51 m	30.4	β 1.47 m	30.7
	α 1.89 m		α 1.91 m	
3	3.16 td (10.4, 5.1)	75.9	3.16 m	75.9
4	1.35 m	40.2	1.28 m	40.0
5	1.51 m	44.1	1.69 m	41.8
6	β 1.39 m	26.4	β 1.12 m	25.0
	α 2.08 m		α 1.81 m	
7	2.48 m 2.52 m	36.8	α 1.96 m β 3.96 m	22.8
8		215.4		148.5
9		83.5		74.7
10		45.7		42.2
11	1.47 m 1.71 m	27.5	α 1.62 m β 1.96 m	28.0
12	1.14 td (13.3, 3.4) 1.51 m	30.2	α 1.51 m β 2.02 m	33.9
13		52.1		43.3
14		224.5		141.3
15	α 2.08 m	37.5		208.5
	β 2.40 dd (18.7, 8.7)			
16	β 1.51 m α 2.16 m	23.8	β 2.07 m α 2.43 dd (18.9, 7.5)	42.7
17	1.85 m	46.3	1.57 m	50.4
18	0.86 s	18.7	0.97 s	17.4
19	0.74 s	14.2	0.84 s	16.9
20	1.55 m	34.2	1.57 m	34.5
21	1.00 d (6.6)	18.3	1.04 d (6.6)	19.3
22	1.26 m 1.65 m	33.3	1.23 m 1.64 m	34.3
23	1.94 m 2.17 m	31.4	1.91 m 2.09 m	30.6
24		156.5		156.3
25	2.23 m	33.9	2.21 m	33.9
26	1.03 d (6.7)	22.0	1.02 d (6.7)	22.0
27	1.03 d (6.7)	22.1	1.02 d (6.7)	22.1
28	4.68 s 4.74 s	106.5	4.65 s 4.73 s	106.6
29	1.03 d (6.7)	15.6	1.02 d (6.7)	15.5

^{a-c} Data were measured at 400, 500, and 125 MHz, respectively.

Euphyperin D (**4**) was determined to possess a molecular formula $\text{C}_{29}\text{H}_{46}\text{O}_3$, as deduced from the ^{13}C NMR data and an HREIMS ion at m/z 442.3440 [M^+] (calcd 442.3447). The ^{13}C NMR spectrum (Table 2) showed the presence of two double bonds (δ_{C} 106.6, 141.3, 148.5, and 156.3) and two oxygenated carbons (δ_{C} 74.7 and 75.9), but no carbonyl groups. Further analysis of its ^1H and 2D NMR spectra indicated that **4** was a C29 steroid, structurally similar to **3** and 9 α -hydroxy-15-oxoconicasterol [11] and shared the same A ring and side chain from C-20 to C-28 with **3** and the same B, C, and D rings with 9 α -hydroxy-15-oxoconicasterol based on the similar NMR patterns of the involved protons and carbons, which were reaffirmed by the HMBC spectrum (Supporting Information Figure S30). The relative stereochemistry of **4** was established to be the same as that of **3** by NMR comparison and the biosynthetic reasoning that **4** undergoes reduction of the carbonyl at C-15 and subsequently oxidative cleavage of the $\Delta^{8(14)}$ double bond to form compound **3**. Accordingly, the structure of **4** was unequivocally characterized.

Five known compounds, 3-oxo-*ent*-trachyloban-17-oic acid (**5**) [12], 9,19-cyclo-24-nor-5 α ,9 β -cholane-3 β ,23-diol (**6**) [13], 9 β ,19-cyclo-4,4,14 α -trimethyl-3 β -hydroxy-5 α -pregnan-20-one (**7**) [14], 3 β -hydroxy-22,23,24,25,26,27-hexanordammarane-20-one (**8**) [15], and phytol (**9**) [16] were also isolated. Their structures were identified on the basis of the NMR and ESIMS data.

Protein tyrosine phosphatase 1B (PTP1B) plays a major role in metabolic signaling pathways, making it ideal as a therapeutic drug target for type 2 diabetes and obesity. In addition, triterpenoids as PTP1B inhibitors have recently been reported as potential agents for

the chemoprevention and therapy of breast cancer [17]. Euphyperins A (**1**) and B (**2**) were tested *in vitro* for their inhibitory effect on PTP1B activity [18], using oleanolic acid (purity > 97%; Sigma-Aldrich Co., St Louis, MO, USA) as the positive control (IC_{50} value: 1.05 $\mu\text{g}/\text{mL}$). Euphyperin A (**1**) displayed moderate PTP1B inhibitory activity with an IC_{50} value of $17.05 \pm 1.12 \mu\text{g}/\text{mL}$. Euphyperins A (**1**) and B (**2**) were also evaluated for their *in vitro* inhibition against XBP1 mRNA splicing, which is an important therapeutic target in cancer treatment, but neither was active.

Experimental

General experimental procedures: Optical rotations, Perkin-Elmer 341 polarimeter; UV, Shimadzu UV-2550 spectrophotometer; IR, Perkin Elmer 577 IR spectrometer; NMR, Bruker AM-400 or AM-500 NMR spectrometers; ESIMS and HR-ESIMS were performed on a Bruker Daltonics Esquire 3000 plus and a Waters-Micromass Q-TOF Ultima Global mass spectrometer, respectively. EIMS and HR-EIMS were obtained on a Finnigan MAT-95 mass spectrometer. Semi-preparative HPLC was carried out on a Waters 1525 binary pump system with a Waters 2489 UV detector and a YMC-Pack ODS-A column (250 \times 10 mm, S-5 μm). Silica gel (300 \times 400 mesh, Qingdao Marine Chemical Co. Ltd), C_{18} reversed-phase silica gel (150 \times 200 mesh, Merck), CHP20P MCI gel (75–150 μm , Mitsubishi Chemical Industries, Ltd.), D101-macroporous absorption resin (Sinopharm Chemical Reagent Co. Ltd, Shanghai, People's Republic of China), and Sephadex LH-20 gel (Amersham Biosciences) were used for column chromatography (CC), and precoated silica gel GF₂₅₄ plates (Qingdao Marine Chemical Co. Ltd) for TLC. All solvents used for CC were of analytical grade (Shanghai Chemical Reagents Co. Ltd), and all solvents used for HPLC were of HPLC grade (J&K Scientific Ltd.).

Plant material: The twigs and leaves of *Euphorbia hypericifolia* were collected in September 2011 from Guangxi Province, People's Republic of China, and were authenticated by Professor Shao-Qing Tang of Guangxi Normal University. A voucher specimen (accession number: EuH-2011-1Y) has been deposited in Shanghai Institute of Materia Medica, Chinese Academy of Sciences.

Extraction and isolation: Air-dried powder of *E. hypericifolia* (5 kg) was extracted with 95% EtOH, 3 times, and the resulting residue was suspended in H_2O and partitioned between H_2O and EtOAc to give a crude extract (630 g). This was subjected to CC (D101-macroporous absorption resin, eluted with 30%, 80%, and 90% EtOH in H_2O) to obtain the major part (240 g) as monitored by TLC. This part was subjected to an MCI gel column (MeOH/ H_2O , 50 to 100%) to give 5 major fractions, A–E. Fraction D was subjected to silica gel CC eluted with light petroleum/acetone (20:1 to 1:1, v/v) to afford 8 fractions (D1–D8). Fraction D4 (10:1 to 8:1) was separated over a column of C_{18} reversed-phase silica gel (MeOH/ H_2O , 60% to 85%) to give 5 sub-fractions (D4a–D4e). Fraction D4e was purified over a silica gel column eluted with light petroleum/ethyl acetate (5:1 to 3:1) to give 2 fractions D4e1 and D4e2, each of which was further purified on a column of Sephadex LH-20 eluted with ethanol to produce compounds **2** (10 mg) and **3** (3 mg). In similar procedures, fraction D4b yielded compound **5** (3 mg). Of fraction D5 (8:1 to 5:1), sub-fraction D5c2 was purified over a column of Sephadex LH-20 to yield compound **4** (4 mg), and sub-fraction D5c3 by semi-preparative HPLC with a mobile phase of 80% CH_3CN in H_2O to yield compound **1** (5 mg). Fraction D2 (16:1 to 12:1) was chromatographed on a column of C_{18} reversed-phase silica gel (MeOH/ H_2O , 65% to 85%) to give 3 major fractions, each of which was separated by semi-preparative HPLC

(75% CH₃CN in H₂O) to produce compounds **6** (12 mg), **7** (5 mg), and **8** (4 mg). Fraction E was purified over a column of silica gel (light petroleum/ethyl acetate, 100:1 to 20:1) to afford the major compound **9** (4.2 g).

Euphyperin A (1)

White amorphous powder.

$[\alpha]^{27}_D: +1.5$ (*c* 0.14, MeOH).

IR (KBr) ν_{max} : 3423, 2952, 2925, 2866, 1649, 1458, 1381, 1308, 1269, 1038 cm⁻¹.

UV (MeOH) λ_{max} (log ε): 253 (3.74) nm.

¹H and ¹³C NMR: Table 1.

ESI(+)MS *m/z*: 457.5 [M + H]⁺, 936.1 [2M + Na]⁺; ESI(-)MS *m/z* 501.8 [M + HCO₂]⁻; EIMS *m/z*: 456 [M]⁺ (52), 438 (28), 423 (44), 302 (30), 387 (37), 252 (93), 191 (100), 95 (30).

HR-EIMS *m/z*: 456.3606 [M]⁺ (calcd for C₃₀H₄₈O₃, 456.3603).

Euphyperin B (2)

White amorphous powder.

$[\alpha]^{27}_D: +24.9$ (*c* 0.33, MeOH).

IR (KBr) ν_{max} : 3500, 2937, 2864, 1701, 1448, 1381, 1362, 1286, 1047, 1003 cm⁻¹.

UV (MeOH) λ_{max} (log ε): 208 (4.10) nm.

¹H and ¹³C NMR: Table 1.

ESI(+)MS *m/z*: 431.2 [M + H]⁺, 883.5 [2M + Na]⁺.

HR-ESI(+)MS *m/z*: 453.3351 [M + Na]⁺ (calcd for C₂₈H₄₆O₃Na, 453.3345).

Euphyperin C (3)

White amorphous powder.

$[\alpha]^{27}_D: -6.8$ (*c* 0.18, MeOH).

References

- [1] Ma JS. (1997) In *Zhongguo Zhiwu Zhi*. Science Press, Beijing, China, **44**, p. 26.
- [2] Vasas A, Hohmann J. (2014) *Euphorbia* diterpenes: Isolation, structure, biological activity, and synthesis (2008–2012). *Chemical Reviews*, **114**, 8579–8612.
- [3] Liao SG, Zhan ZJ, Yang SP, Yue JM. (2005) Lathyranoic acid A: First secolathyrane diterpenoid in nature from *Euphorbia lathyris*. *Organic Letters*, **7**, 1379–1382.
- [4] Qi WY, Zhang WY, Shen Y, Leng Y, Gao K, Yue JM. (2014) Ingol-type diterpenes from *Euphorbia antiquorum* with mouse 11 β -hydroxysteroid dehydrogenase type 1 inhibition activity. *Journal of Natural Products*, **77**, 1452–1458.
- [5] Zhao JX, Liu CP, Qi WY, Han ML, Han YS, Wainberg MA, Yue JM. (2014) Eurifoloids A–R, structurally diverse diterpenoids from *Euphorbia nerifolia*. *Journal of Natural Products*, **77**, 2224–2233.
- [6] Ma JS. (1997) In *Zhongguo Zhiwu Zhi*. Science Press, Beijing, China, **44**, p. 41.
- [7] Rizk AM, Rimpler H, Ismail SI. (1977) Flavonoids and ellagic acid from *Euphorbia hypericifolia* L. (= *E. indica* Lam.). *Fitoterapia*, **48**, 99–100.
- [8] Chiang YM, Kuo YH. (2002) Novel triterpenoids from the aerial roots of *Ficus microcarpa*. *The Journal of Organic Chemistry*, **67**, 7656–7661.
- [9] Umeyama A, Shoji N, Enoki M, Arihara S. (1997) Swinhosterols A–C, 4-methylene seco steroids from the marine sponge *Theonella swinhonis*. *Journal of Natural Products*, **60**, 296–298.
- [10] Akihisa T, Yasukawa K, Kimura Y, Takido M, Kokke WCMC, Tamura T. (1994) Five D:C-friedo-oleanane triterpenes from the seeds of *Trichosanthes kirilowii* Maxim. and their anti-inflammatory effects. *Chemical & Pharmaceutical Bulletin*, **42**, 1101–1105.
- [11] Zhang HJ, Yi YH, Lin HW. (2010) Oxygenated 4-methylidene sterols from the South China sea sponge *Theonella swinhonis*. *Helvetica Chimica Acta*, **93**, 1120–1126.
- [12] Pan L, Zhou P, Zhang X, Peng S, Ding L, Qiu SX. (2006) Skeleton-rearranged pentacyclic diterpenoids possessing a cyclobutane ring from *Euphorbia wallichii*. *Organic Letters*, **8**, 2775–2778.
- [13] Corsano S, Piancatelli G. (1967) Correlation of acetylacteol with cycloartenol. *Ricerca Scientifica*, **37**, 360–365.
- [14] Rodriguez-Hahn H, Romo de Vivar A, Ortega A, Aguilar M, Romo J. (1970) Structure of argentatines A, B, and C from *Parthenium argentatum*. *Revista Latinoamericana de Química*, **1**, 24–38.
- [15] Crabbe P, Ourisson G, Takahashi T. (1958) Preparation of 8,14-dimethyl-18-nortestosterone. *Tetrahedron*, **3**, 279–302.
- [16] Gellerman JL, Anderson WH, Schlenk H. (1975) Synthesis and analysis of phytol and phytienoyl wax esters. *Lipids*, **10**, 656–661.
- [17] Uddin MN, Sharma G, Yang JL, Choi HS, Lim SI, Kang KW, Oh WK. (2014) Oleanane triterpenes as protein tyrosine phosphatase 1B (PTP1B) inhibitors from *Camellia japonica*. *Phytochemistry*, **103**, 99–106.
- [18] Zhang W, Hong D, Zhou Y, Zhang Y, Shen Q, Li J, Hu L, Li J. (2006) Ursolic acid and its derivative inhibit protein tyrosine phosphatase 1B, enhancing insulin receptor phosphorylation and stimulating glucose uptake. *Biochimica et Biophysica Acta-General Subjects*, **1760**, 1505–1512.
- [19] Zhang H, Zhang CR, Zhu KK, Gao AH, Luo C, Li J, Yue JM. (2013) Fluegirosines A–C: A biogenesis inspired example in the discovery of new bioactive scaffolds from *Flueggea virosa*. *Organic Letters*, **15**, 120–123.

A Fragmentation Study of Six C₂₁ Steroidal Aglycones by Electrospray Ionization Ion-Trap Time-of-Flight Tandem Mass Spectrometry

Xing-Long Chen^{a,b}, Chang-An Geng^a and Ji-Jun Chen^{a,*}

^aKunming Institute of Botany, Chinese Academy of Sciences, Kunming 650201, PR China

^bUniversity of Chinese Academy of Sciences, Beijing 100049, PR China

chenjj@mail.kib.ac.cn

Received: September 1st, 2015; Accepted: November 23rd, 2015

The fragmentation patterns of six C₂₁ steroidal aglycones, metaplexigenin (**1**), caudatin (**2**), qingyangshengenin (**3**), penupogenin (**4**), 20-cinnamoylsarcostin (**5**), and gagamine (**6**), were analyzed by high-resolution electrospray ionization ion-trap time-of-flight tandem mass spectrometry (HR-ESI-IT-TOF-MSⁿ). The [M-H]⁻ ions of steroids **1-3** that contain a carbonyl functional group at C-20 (Type I) and [M+H]⁺ ions of steroids **5-6** that possess a hydroxyl group at C-20 (Type II) were readily observed in MS analyses. The fragmentation pathways and diagnostic fragment ions for these six steroidal aglycones were proposed on the basis of their MSⁿ analyses. The common fragmentation pathways for type I steroidal aglycones include the neutral loss of the ester group at C-12 and the hydroxyl moieties on the steroid skeleton, as well as the cleavage of ring D. Their diagnostic fragment ions were identified as *m/z* 361(**B**), 343 (**C**), 325 (**D**), 307 (**F**), 283 (**G**), 259 (**E**), and 243 (**H**). The fragmentation behavior of penupogenin (**4**) in type II was similar to those of type I, with *m/z* 363 (**B'**), 345 (**C'**), 327 (**D'**), 309 (**F'**), 283 (**G'**), and 243 (**H'**) as its diagnostic fragment ions. The ester group at C-20 was difficult to cleave in the MSⁿ analyses of 20-cinnamoylsarcostin (**5**) and gagamine (**6**) so that the loss of this ester group was slower than that at C-12 and hydroxyl groups; the key ions at *m/z* 329 (**I**), 311 (**J**), 293 (**K**), and 275 (**L**) were characteristic for **5** and **6**. The base ion peaks were derived from the loss of the substituent group at either C-12 or C-17 for both type I and type II steroidal aglycones.

Keywords: ESI-IT-TOF-MSⁿ, Fragmentation pathways, Diagnostic ions, C₂₁ Steroidal aglycones.

C₂₁ steroids, the major chemical components of the family Asclepiadaceae, have been proved to possess prolific bioactivities, such as antitumor [1], immunosuppressive [2], appetite-suppressant [3], and anti-hepatitis B virus [4,5]. Attention has been paid to the rapid detection and capture of C₂₁ steroids for bioactivity screening and new drug development. Nevertheless, the isolation and identification of C₂₁ steroids from natural materials are difficult due to their thermal instability and low abundance in natural materials. It is thus imperative to establish highly sensitive and accurate methods to analyze C₂₁ steroids.

Recently, electrospray ionization (ESI) techniques linked with multi-stage tandem mass spectrometry (MSⁿ) have been extensively applied to analyze natural products including alkaloids [6], steroidal saponins [7], and triterpenoid saponins [8]. ESI-MSⁿ techniques make it possible to determine the relationship between a precursor and its fragment ions, by which the fragmentation patterns can be sorted out and natural products in plants may be precisely analyzed [9,10].

Since most naturally-occurring C₂₁ steroids exist as glycosides, the MSⁿ techniques have mainly been used to test the presence of C₂₁ steroidal glycosides in plants and to establish online methods to analyze the glycoside structures [11-16]. However, no systematic study of the ESI-MSⁿ fragmentation of C₂₁ steroidal aglycones has been reported so far. Additionally, some limitations may arise from the low resolution of mass spectrometers utilized in previous molecular formula predictions [7, 13-16]. In this study, the fragmentation of six C₂₁ steroidal aglycones was explored using a LC/MS-IT-TOF mass spectrometer equipped with an electrospray ionization source and ion-trap and time-of-flight mass analyzers (ESI-IT-TOF). This mass spectrometer enables fast acquisition of multistage tandem spectra (MS¹⁻¹⁰) with high accuracy and

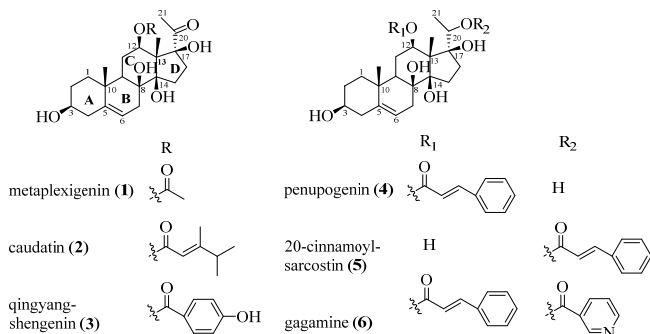


Figure 1: Structures of compounds **1-6**

resolution. The six steroidal aglycones, metaplexigenin (**1**), caudatin (**2**), qingyangshengenin (**3**), penupogenin (**4**), 20-cinnamoylsarcostin (**5**), and gagamine (**6**) (as shown in Figure 1), are classified into type I that contain a carbonyl group at C-20 (steroids **1-3**) and type II that possess a hydroxyl group at C-20 (steroids **4-6**). A high resolution mass technique was first applied to investigate the fragmentation patterns of C₂₁ steroidal aglycones that may be used for the characterization of other structure-related steroids.

Prior to the MSⁿ analyses, the full-scan mass spectra of steroids **1-6** in both positive and negative ion modes were acquired in automatic pattern. The [M-H]⁻ ions for metaplexigenin (**1**), caudatin (**2**), qingyangshengenin (**3**), and penupogenin (**4**) were easily obtained. In contrast, only [M+H]⁺ ions for 20-cinnamoylsarcostin (**5**) and gagamine (**6**) were observed. Therefore, the MSⁿ investigations for steroids **1-4** in negative mode and for steroids **5-6** in positive mode were chosen, as shown in Tables 1-6. The mass spectra of steroids **1-6** are shown as Figures S1-S6 in the supporting information.

Table 1: Data for accurate masses and elemental composition of steroid **1** observed from tandem mass spectra in negative mode

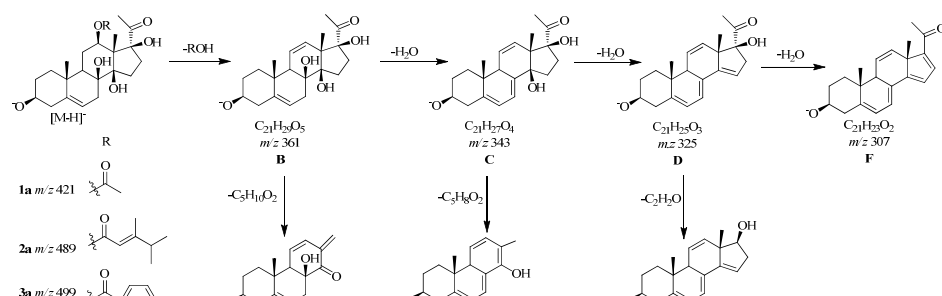
MS ⁿ	Precursor ion (<i>m/z</i>)	Product ion (<i>m/z</i>)	Elemental composition	Measured (<i>m/z</i>)	Calculated (<i>m/z</i>)	Error (mDa)	Intensity (%)	Ion name	Assignment	
(-)MS	422	421	C ₂₃ H ₃₃ O ₇	421.2214	421.2232	-1.8	100	1a	[M-H] ⁻	
	421	361	C ₂₁ H ₂₉ O ₅	361.2008	361.2020	-1.2	100	B	1a -C ₂ H ₄ O ₂	
		343	C ₂₁ H ₂₇ O ₄	343.1890	343.1915	-2.5	43	C	B-H ₂ O	
		325	C ₂₁ H ₂₅ O ₃	325.1775	325.1809	-3.4	32	D	C-H ₂ O	
	361	343	C ₂₁ H ₂₇ O ₄	343.1891	343.1915	-2.4	100	C	B-H ₂ O	
		325	C ₂₁ H ₂₅ O ₃	325.1787	325.1809	-2.2	83	D	C-H ₂ O	
		259	C ₁₆ H ₁₉ O ₃	259.1323	259.1340	-1.7	21	E	B-C ₅ H ₁₀ O ₂	
		325	C ₂₁ H ₂₅ O ₃	325.1787	325.1809	-2.2	100	D	C-H ₂ O	
		307	C ₂₁ H ₂₃ O ₂	307.1670	307.1704	-3.4	16	F	D-H ₂ O	
		283	C ₁₉ H ₂₃ O ₂	283.1676	283.1704	-2.8	23	G	D-C ₂ H ₂ O	
MS ³		243	C ₁₆ H ₁₉ O ₂	243.1371	243.1391	-2.0	44	H	C-C ₃ H ₈ O ₂	
		325	307	C ₂₁ H ₂₃ O ₂	307.1672	307.1704	-3.2	45	F	D-H ₂ O
		283	C ₁₉ H ₂₃ O ₂	283.1686	283.1704	-1.8	100	G	D-C ₂ H ₂ O	
		291	C ₂₀ H ₁₉ O ₂	291.1373	291.1391	-1.8	100	I	F-CH ₄	
MS ⁴		265	C ₁₉ H ₂₁ O	265.1582	265.1598	-1.6	56	II	F-C ₂ H ₂ O	
		283	C ₁₉ H ₂₁ O	265.1574	265.1598	-2.4	100	II	G-H ₂ O	
		265	C ₁₉ H ₂₁ O	265.1598	265.1598	0.0	100			

Table 2: Data for accurate masses and elemental composition of steroid **2** observed from tandem mass spectra in negative mode

MS ⁿ	Precursor ion (<i>m/z</i>)	Product ion (<i>m/z</i>)	Elemental composition	Measured (<i>m/z</i>)	Calculated (<i>m/z</i>)	Error (mDa)	Intensity (%)	Ion name	Assignment	
(-)MS	490	489	C ₂₈ H ₄₁ O ₇	489.2853	489.2858	-0.5	100	2a	[M-H] ⁻	
	489	361	C ₂₁ H ₂₉ O ₅	361.1993	361.2020	-2.7	100	B	2a -C ₂ H ₁₂ O ₂	
		343	C ₂₁ H ₂₇ O ₄	343.1878	345.1915	-3.7	32	C	B-H ₂ O	
		325	C ₂₁ H ₂₅ O ₃	325.1771	325.1809	-3.8	23	D	C-H ₂ O	
	361	343	C ₂₁ H ₂₇ O ₄	343.1882	345.1915	-3.3	100	C	B-H ₂ O	
		325	C ₂₁ H ₂₅ O ₃	325.1776	325.1809	-3.3	93	D	C-H ₂ O	
		259	C ₁₆ H ₁₉ O ₃	259.1318	259.1340	-2.2	20	E	B-C ₅ H ₁₀ O ₂	
		325	C ₂₁ H ₂₅ O ₃	325.1778	325.1809	-3.1	100	D	C-H ₂ O	
		307	C ₂₁ H ₂₃ O ₂	307.1664	307.1704	-4.0	12	F	D-H ₂ O	
		283	C ₁₉ H ₂₃ O ₂	283.1678	283.1704	-2.6	29	G	D-C ₂ H ₂ O	
MS ³		243	C ₁₆ H ₁₉ O ₂	243.1360	243.1391	-3.1	33	H	C-C ₃ H ₈ O ₂	
		325	307	C ₂₁ H ₂₃ O ₂	307.1664	307.1704	-4.0	66	F	D-H ₂ O
		283	C ₁₉ H ₂₃ O ₂	283.1669	283.1704	-3.5	100	G	D-C ₂ H ₂ O	
		291	C ₂₀ H ₁₉ O ₂	291.1415	291.1391	+2.4	100	I	F-CH ₄	
MS ⁴		265	C ₁₉ H ₂₁ O	265.1580	265.1598	-1.8	56	J	F-C ₂ H ₂ O	
		283	C ₁₉ H ₂₁ O	265.1515	265.1598	-8.3	88	J	G-H ₂ O	
		265	C ₁₉ H ₂₁ O	265.1598	265.1598	0.0	100			

Table 3: Data for accurate masses and elemental composition of steroid **3** observed from tandem mass spectra in negative mode

MS ⁿ	Precursor ion (<i>m/z</i>)	Product ion (<i>m/z</i>)	Elemental composition	Measured (<i>m/z</i>)	Calculated (<i>m/z</i>)	Error (mDa)	Intensity (%)	Ion name	Assignment	
(-)MS	500	499	C ₂₈ H ₃₅ O ₈	499.2344	499.2337	+0.7	100	3a	[M-H] ⁻	
	499	361	C ₂₁ H ₂₉ O ₅	361.2005	361.2020	-1.5	26	B	3a -C ₂ H ₄ O ₃	
		343	C ₂₁ H ₂₇ O ₄	343.1885	345.1915	-3.0	85	C	B-H ₂ O	
		325	C ₂₁ H ₂₅ O ₃	325.1781	325.1809	-2.8	100	D	C-H ₂ O	
	361	343	C ₂₁ H ₂₇ O ₄	343.1887	345.1915	-2.8	100	C	B-H ₂ O	
		325	C ₂₁ H ₂₅ O ₃	325.1777	325.1809	-3.2	52	D	C-H ₂ O	
		259	C ₁₆ H ₁₉ O ₃	259.1324	259.1340	-1.6	61	E	B-C ₅ H ₁₀ O ₂	
		325	C ₂₁ H ₂₅ O ₃	325.1786	325.1809	-2.3	100	D	C-H ₂ O	
		307	C ₂₁ H ₂₃ O ₂	307.1675	307.1704	-2.9	14	F	D-H ₂ O	
		283	C ₁₉ H ₂₃ O ₂	283.1683	283.1704	-2.1	40	G	D-C ₂ H ₂ O	
MS ³		243	C ₁₆ H ₁₉ O ₂	243.1371	243.1391	-2.0	45	H	C-C ₃ H ₈ O ₂	
		325	307	C ₂₁ H ₂₃ O ₂	307.1675	307.1704	-2.9	100	F	D-H ₂ O
		283	C ₁₉ H ₂₃ O ₂	283.1684	283.1704	-2.0	31	G	D-C ₂ H ₂ O	
		281	C ₁₉ H ₂₁ O ₂	281.1534	281.1547	-1.3	10	I	D-C ₂ H ₂ O	
		265	C ₁₉ H ₂₁ O	265.1558	265.1598	-4.0	50	J	G-H ₂ O	
MS ⁴	283	265	C ₁₈ H ₁₇ O ₂	265.1233	265.1234	-0.1	100	J'	3i-CH ₄	
		259	231	C ₁₅ H ₁₉ O ₂	231.1363	231.1391	-2.8	100	K	E-CO

**Figure 2:** Proposed common fragmentation pathways for steroids **1-3**.

Common fragmentation pathways for type I steroids: In the single-stage mass spectra, the $[\text{M}-\text{H}]^-$ ions for type I C_{21} steroidal aglycones **1-3** were observed at m/z 421.2214 (**1a**), 489.2853 (**2a**), and 499.2344 (**3a**), corresponding to the molecular formulas of $\text{C}_{23}\text{H}_{33}\text{O}_7$, $\text{C}_{28}\text{H}_{41}\text{O}_7$ and $\text{C}_{28}\text{H}_{35}\text{O}_8$, respectively. These three

$[\text{M}-\text{H}]^-$ ions were selected as precursor ions to perform MS² experiments, from which the common ion at m/z 361 (**B**) was acquired as the base ion peak due to the loss of ROH (R= acetyl, tigloyl and *p*-hydroxybenzoyl) at C_{12} . Additionally, fragment ions **C** (m/z 343) and **D** (m/z 325) were also detected, which may be

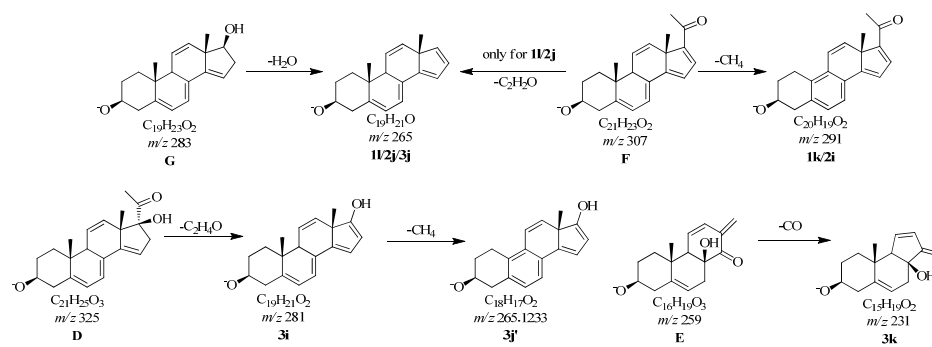


Figure 3: Other fragmentation pathways of compounds 1-3.

Table 4: Data for accurate masses and elemental composition of steroid 4 observed from tandem mass spectra in negative mode

MS ⁿ	Precursor ion (<i>m/z</i>)	Product ion (<i>m/z</i>)	Elemental composition	Measured (<i>m/z</i>)	Calculated (<i>m/z</i>)	Error (mDa)	Intensity (%)	Ion name	Assignment
(-)MS	512	511	C ₃₀ H ₃₉ O ₇	511.2663	511.2701	-3.8	100	4a	[M-H] ⁻
MS ²	511	363	C ₂₁ H ₃₁ O ₅	363.2148	363.2177	-2.9	100	B'	4a-C ₉ H ₈ O ₂
MS ³	363	345	C ₂₁ H ₂₉ O ₄	345.1960	345.2071	-11.1	17	C'	B'-H ₂ O
	327	C ₂₁ H ₂₇ O ₃	327.1895	327.1966	-7.1	29	D'	C'-H ₂ O	
	309	C ₂₁ H ₂₅ O ₂	309.1812	309.1860	-4.8	29	F'	D'-H ₂ O	
	299	C ₁₉ H ₂₃ O ₃	299.1630	299.1653	-2.3	100	4i	B'-C ₂ H ₆ O ₂	
	283	C ₁₉ H ₂₃ O ₂	283.1670	283.1704	-3.4	54	G	D'-C ₂ H ₄ O ₂	
	243	C ₁₆ H ₁₉ O ₂	243.1316	243.1391	-7.5	17	H	C'-C ₅ H ₁₀ O ₂	
MS ⁴	299	281	C ₁₉ H ₂₁ O ₃	281.1519	281.1547	-2.8	100	4j	4i-H ₂ O

ascribed to the sequential elimination of 8-OH and 14-OH from **B**. To investigate further the fragmentation patterns of ions **B**, **C** and **D**, they were chosen as precursor ions in MS³ analyses to generate ions **C** to **H**. Ions **B-H** were identified as the key fragment ions for steroids 1-3, of which ion **E** at *m/z* 259 was derived from ion **B** through ring D cleavage of the C₂₁ skeleton as C₅H₁₀O₂ segment. Ion **F** at *m/z* 307 was generated from ion **D** via the removal of one molecule of H₂O from 17-OH and 16-H. Ion **G** also originated from ion **D** through the elimination of 17-OAc as a C₂H₂O segment and ion **H** could be generated by the cleavage of ring D as a C₅H₈O₂ segment in precursor ion **C** (Figure 2).

Other fragmentation pathways for steroids 1-3: The other fragmentation pathways of steroids 1-3 were mainly involved in methyl group loss on the C₂₁ steroid skeleton. Ions at *m/z* 291 (**1k/2i**) and *m/z* 265 (**1l/2j**) were both obtained in MS⁴ experiments of precursor ions **F** and **G** for metaplexigenin (1) and caudatin (2). The 10-Me and 17-OAc in ion **F** were eliminated as CH₄ and C₂H₂O segments to produce **1k/2i** at *m/z* 291 and **1l/2j** at *m/z* 265, respectively. The latter ion can also be generated from ion **G** by losing 17-OH. The ion **3j** at *m/z* 265 for qingyangshengenin (3) was also generated from ion **G** in the MS⁴ analysis. It was also found that precursor ion **D** can give rise to a peculiar ion at *m/z* 281 (**3i**) corresponding to the departure of 17-OAc as a C₂H₄O segment in MS³ investigation. Removal of the methyl group at C-10 in ion **3i** as a CH₄ segment yielded a fragment at *m/z* 265.1233 (**3j'**'), ascribed with the molecular formula C₁₈H₁₇O₂, which was different from the ion **3j** (*m/z* 265.1558, C₁₉H₂₁O). Precursor ion **E** lost one molecule of CO to afford ion **3k** at *m/z* 231 in MS⁴ experiment, and such a fragmentation pattern demonstrated the mechanism that ring D cleavage in ion **B** generated ion **E** by forming a carbonyl on ring C (Figure 3).

Fragmentation pathways for steroid 4: The fragmentation pathways for penupogenin (4) were similar to that of type I C₂₁ steroid aglycones. Its single-stage MS analysis led to the detection of a [M-H]⁻ ion at *m/z* 511.2663 (**4a**) as the base ion peak in negative mode with the chemical composition of C₃₀H₃₉O₇. Ion **4a** lost the cinnamoyl group at C-12 as one molecule of cinnamic acid to afford ion **B'** at *m/z* 363 in MS² analysis. The mass of fragment **B'** was 2 Da more than that of ion **B** owing to the presence of a

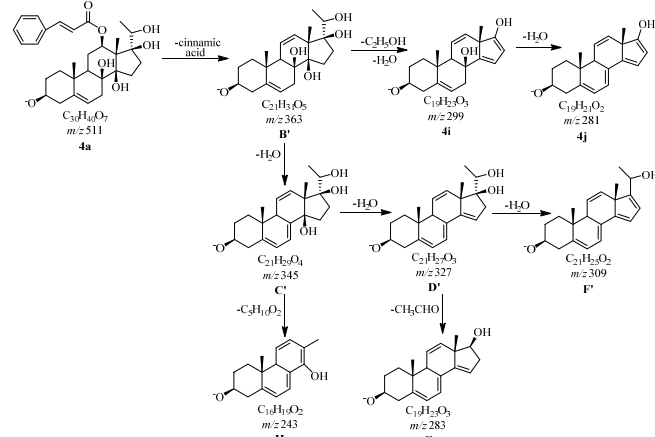


Figure 4: Proposed fragmentation pathways for compound 4.

hydroxyl group at C-20, and so the product ions of **B'** were ions **C'** at *m/z* 345, **D'** at *m/z* 327, and **F'** at *m/z* 309 in MS³ experiment, which could be interpreted by the same fragmentation routes as ions **C** (*m/z* 343), **D** (*m/z* 325) and **F** (*m/z* 307). Furthermore, ions **G** at *m/z* 283 and **H** at *m/z* 243 were also found whose molecular formula and fragmentation pathways were similar to the above explanations, as described in Figure 2. In addition to ions **C'**, **D'**, **F'**, **G**, and **H**, ion **4i** at *m/z* 299 was obtained as well due to the loss of the substituent group at C-17 as CH₃CH₂OH and of the hydroxyl group at C-14 as H₂O. Ultimately, **4i** eliminated 8-OH to produce ion **4j** at *m/z* 281 in the MS⁴ experiment (Figure 4).

Fragmentation pathways of steroids 5-6: Fragmentation of 20-cinnamoylsarcostin (5) and gagamine (6) gave rise to [M+H]⁺ ions **5a** at *m/z* 513.2789 (C₃₀H₄₁O₇) and **6a** at *m/z* 618.3006 (C₃₆H₄₄NO₈), in the first-stage mass spectrum. Due to the lack of an ester group at C-12, **5a** departed 8-OH to yield ion **5b** at *m/z* 495 in MS² investigation. Additionally, ions **5c** at *m/z* 477, **5d** at *m/z* 459, **I** at *m/z* 329, **J** at *m/z* 311, and **K** at *m/z* 293 were also detected. **5c** was generated from **5b** because of the loss of 7-OH, while **5d** was yielded from **5c** due to the loss of one molecule of H₂O at C-14 and C-15. The loss of the cinnamoyl substituent at C-20 as cinnamic acid in **5c** and **5d** led to the generation of ions **I** and **J**, respectively.

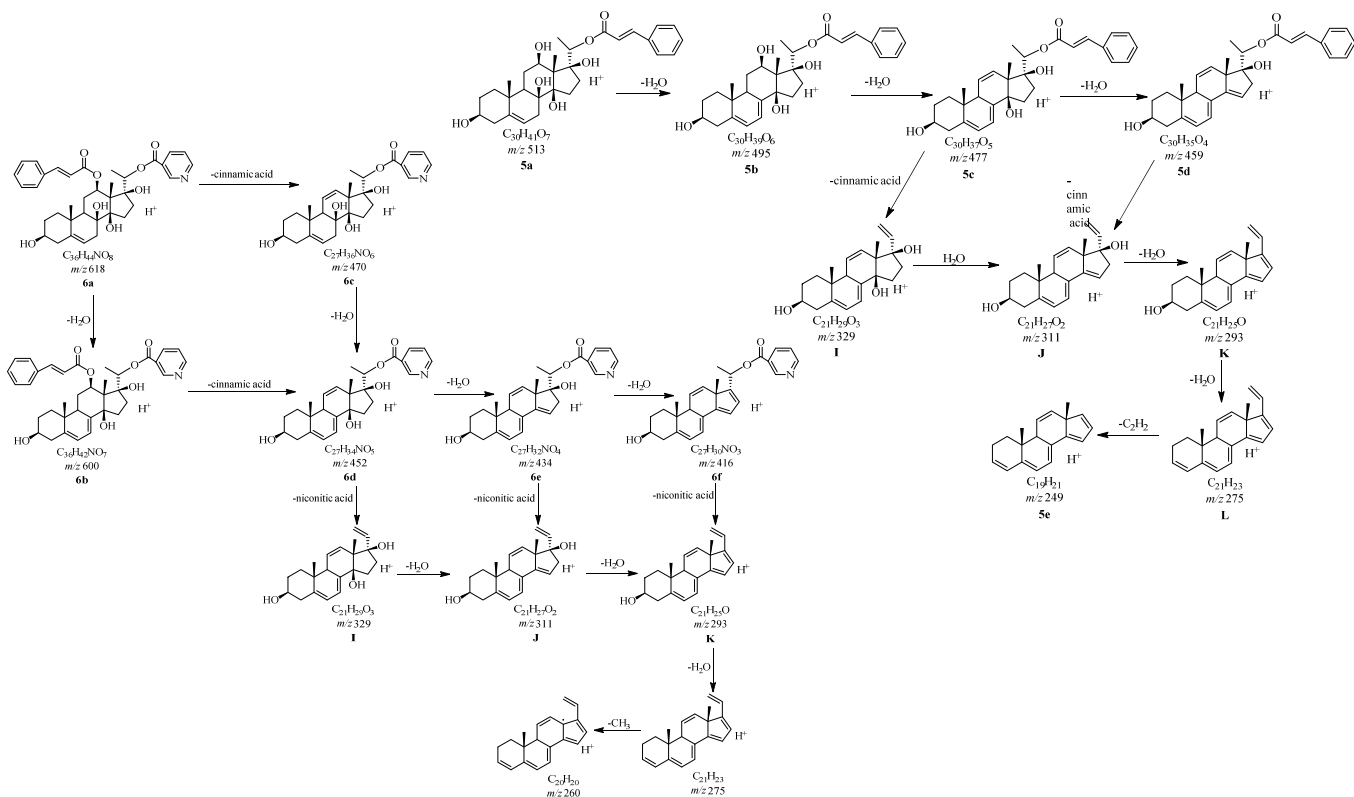


Figure 5: Proposed fragmentation pathways of ss 5–6

Table 5: Data for accurate masses and elemental composition of steroid 5 observed from tandem mass spectra in positive mode

MS ⁿ	Precursor ion (<i>m/z</i>)	Product ion (<i>m/z</i>)	Elemental composition	Measured (<i>m/z</i>)	Calculated (<i>m/z</i>)	Error (mDa)	Intensity (%)	Ion name	Assignment
(+)-MS	512	513	C ₃₀ H ₄₁ O ₇	513.2798	513.2847	-4.9	100	5a	[M+H] ⁺
MS ²	513	495	C ₃₀ H ₃₉ O ₆	495.2675	495.2741	-6.6	43	5a-H ₂ O	
		477	C ₃₀ H ₃₇ O ₅	477.2572	477.2636	-6.4	43	5b	5a-H ₂ O
		459	C ₃₀ H ₃₅ O ₄	459.2476	459.2530	-5.4	17	5d	5c-H ₂ O
		329	C ₂₁ H ₂₉ O ₃	329.2074	329.2111	-3.7	100	I	5c- cinnamic acid
		311	C ₂₁ H ₂₇ O ₂	311.1981	311.2006	-2.5	83	J	I-H ₂ O or 5d- cinnamic acid
MS ³	477	293	C ₂₁ H ₂₅ O	293.1867	293.1900	-3.3	26	K	J-H ₂ O
		459	C ₃₀ H ₃₃ O ₄	459.2454	459.2530	-7.6	28	5d	5c- H ₂ O
		329	C ₂₁ H ₂₉ O ₃	329.2074	329.2111	-3.7	100	I	5c- CINN
		311	C ₂₁ H ₂₇ O ₂	311.1970	311.2006	-3.6	100	J	I-H ₂ O or 5d- cinnamic acid
	459	293	C ₂₁ H ₂₅ O	293.1872	293.1900	-2.8	45	K	J-H ₂ O
		311	C ₂₁ H ₂₇ O ₂	311.1987	311.2006	-1.9	100	J	5d- cinnamic acid
	329	293	C ₂₁ H ₂₅ O	293.1885	293.1900	-1.5	80	K	J-H ₂ O
MS ⁴	311	311	C ₂₁ H ₂₇ O ₂	311.2000	311.2006	-0.6	100	J	I-H ₂ O
	293	293	C ₂₁ H ₂₅ O	293.1864	293.1900	-3.6	54	K	J-H ₂ O
	275	275	C ₂₁ H ₂₃	275.1821	275.1794	+2.7	44	L	K-H ₂ O
	249	249	C ₁₉ H ₂₁	249.1547	249.1638	-9.1	43	5e	L-C ₂ H ₂

The ion **J** might also be originated from ion **I** through the elimination of one molecule of H₂O at C-14 and C-15. The ion **K** at *m/z* 293 could be interpreted by the hydroxyl group departure at C-17 in ion **J**. Similarly, ions **5d** and **I-K** were all observed in MS³ analyses of **5c** (*m/z* 477), **5d** (*m/z* 459), and **J** (*m/z* 329). Finally, the MS⁴ experiment of ion **J** (*m/z* 311) afforded ions **K** at *m/z* 293, **L** at *m/z* 275, and **5e** at *m/z* 249. Among them, fragment **L** arose from ion **K** because of the departure of 3-OH, and ion **5e** was generated by the elimination of the ethylene moiety at C-17 in ion **L** as a C₂H₂ segment.

Two dissociation pathways were observed from ion **6a** (*m/z* 618) in MS² investigation, leading to the fragments at *m/z* 600 (**6b**) and *m/z* 470 (**6c**) due to the loss of H₂O and cinnamic acid segments. Further elimination of 20-cinnamoyl and 8-OH in **6b** and **6c** yielded ion **6d**

at *m/z* 452. Elimination of 14-OH in **6d** led to the generation of ion **6e** at *m/z* 434, and the subsequent departure of 17-OH in **6e** produced ion **6f** at *m/z* 416 with a more stable conjugated structure. The above dissociation routes were confirmed by MS³ experiments of precursor ions **6b**, **6c** and **6d**, in which ions **6d-6f** were all obtained. Apart from ions **6e** and **6f**, two non-nitrogen ions **I** at *m/z* 329 (C₂₁H₂₉O₃) and **J** (C₂₁H₂₇O₂) at *m/z* 311 were also found from precursor ion **6d**. In addition, the MS³ analyses of ion **6f** provided ions **K** at *m/z* 293 and **L** at *m/z* 275. Ions **I** to **L** were the common product ions for 20-cinnamoylsarcostin (**5**) and gagamine (**6**), which could be regarded as the diagnostic ions for C₂₁ steroid aglycones with the same skeleton, and 14-OH, 17-OH, and 3-OH were eliminated one by one from ions **I** to **L**, resulting in a more stable conjugated system. In MS⁴ investigations, precursor ions **6e** and **K** gave rise to versatile fragments, **6f**, **J-L**, and **6g** at *m/z* 260,

Table 6: Data for accurate masses and elemental composition of steroid **6** observed from tandem mass spectra in positive mode

MS ⁿ	Precursor ion (<i>m/z</i>)	Product ion (<i>m/z</i>)	Elemental composition	Measured (<i>m/z</i>)	Calculated (<i>m/z</i>)	Error (mDa)	Intensity (%)	Ion name	Assignment
(+)-MS MS ²	617	618	C ₃₆ H ₄₄ NO ₈	618.3006	618.3061	-5.5	100	6a	[M+H] ⁺
		600	C ₃₆ H ₄₂ NO ₇	600.2879	600.2956	-7.7	8	6b	6a -H ₂ O
		470	C ₂₇ H ₄₄ NO ₆	470.2472	470.2537	-6.5	16	6c	6a -cinnamic acid
		452	C ₂₇ H ₃₄ NO ₅	452.2359	452.2431	-7.2	74	6d	6c -H ₂ O or 6b -cinnamic acid
MS ³	600	434	C ₂₇ H ₃₂ NO ₄	434.2269	434.2326	-5.7	85	6e	6d -H ₂ O
		416	C ₂₇ H ₃₀ NO ₃	416.2189	416.2220	-3.1	31	6f	6e -H ₂ O
		452	C ₂₇ H ₃₄ NO ₅	452.2359	452.2431	-7.2	24	6d	6b -cinnamic acid
		434	C ₂₇ H ₃₂ NO ₄	434.2287	434.2326	-3.9	24	6e	6d -H ₂ O
	470	416	C ₂₇ H ₃₀ NO ₃	416.2121	416.2220	-9.9	16	6f	6e -H ₂ O
		452	C ₂₇ H ₃₄ NO ₅	452.2387	452.2431	-4.4	100	6d	6c -H ₂ O
		434	C ₂₇ H ₃₂ NO ₄	434.2295	434.2326	-3.1	67	6e	6d -H ₂ O
		416	C ₂₇ H ₃₀ NO ₃	416.2165	416.2220	-5.5	13	6f	6e -H ₂ O
	452	434	C ₂₇ H ₃₂ NO ₄	434.2274	434.2326	-5.2	65	6e	6d -H ₂ O
		416	C ₂₇ H ₃₀ NO ₃	416.2181	416.2220	-3.9	20	6f	6e -H ₂ O
		329	C ₂₁ H ₂₉ O ₃	329.2072	329.2111	-3.9	6	I	6c -niconitic acid
		311	C ₂₁ H ₂₇ O ₂	311.1979	311.2009	-3.0	69	J	I -H ₂ O or 6e -niconitic acid
MS ⁴	416	293	C ₂₁ H ₂₅ O	293.1867	293.1900	-3.3	100	K	6f -niconitic acid
		275	C ₂₁ H ₂₃	275.1768	275.1794	-2.6	43	L	K-H ₂ O
		434	C ₂₇ H ₃₀ NO ₃	416.2221	416.2220	+0.1	14	6f	6e -H ₂ O
		416	C ₂₁ H ₂₇ O ₂	311.1982	311.2009	-2.7	36	J	6e -niconitic acid
		311	C ₂₁ H ₂₅ O	293.1869	293.1900	-2.1	100	K	J-H ₂ O or 6f -niconitic acid
	293	275	C ₂₁ H ₂₃	275.1768	275.1794	-2.6	8	L	K-H ₂ O
		260	C ₂₀ H ₂₀	260.1538	260.1560	-2.2	100	6g	L-CH ₃

among which **6f** and **J** to **L** have been clarified in the MS³ experiments and the ion **6g** could be explained by the loss of 13-Me as a CH₃ segment (Figure 5).

In conclusion, high resolution MSⁿ fragmentation studies of C₂₁ steroidal aglycones showed characteristic fragmentation patterns different from those of C₂₁ steroidal glycosides. [M-H]⁻ ions for metaplexigenin (**1**), caudatin (**2**), qingyangshengenin (**3**) and penupogenin (**4**), and [M+H]⁺ ions for 20-cinnamoylsarcostin (**5**) and gagamine (**6**) were obtained in their single-stage mass spectra. The loss of ROH (R= acetyl, tigloyl, *p*-hydroxylbenzoyl, cinnamoyl and nicotinoyl), H₂O, C₂H₄O, C₂H₂O and CH₄ was the characteristic fragmentation from the precursor ions due to the presence of ester groups, hydroxyl, 1-*O*-ethyl and methyl groups. In particular, the most active 12-ester group was always first eliminated to give rise to the ion at [M-H-ROH]⁻ as the base ion peak for compounds **1-4**. Ions at *m/z* 361 (**B**), 343 (**C**), 325 (**D**), 307 (**F**), 283 (**G**), 259 (**E**), and 243 (**H**) were the common product ions for steroids **1-3**. Steroid **4** displayed similar fragmentation pathways as steroids **1-3** to yield ions at *m/z* 363 (**B'**), 345 (**C'**), 327 (**D'**), 309 (**F'**), 283 (**G**), and 243 (**H**). All these ions could be recognized as the diagnostic ions for structural characterization. The substituent group at C-12 in compounds **5-6** was also the active group, leading to the departure of either a H₂O or cinnamic acid segment, with the key fragments being *m/z* 329 (**I**), 311(**J**), 293 (**K**), and 275 (**L**). Besides, the substituent group loss at either C-12 or C-17 gave rise to high abundance ions, even as the base ion peak for all six steroids. These findings demonstrate the possible online analytical ability of ESI-IT-TOF tandem mass spectrometry for establishing an effective method to analyze C₂₁ steroidal aglycones.

Experimental

General: Acetonitrile, HPLC grade, was purchased from Merck Co. Ltd., Germany. Deionized water was purified using a MingCheTM-

D 24UV Merck Millipore system (Merck Millipore, Shanghai, China).

Steroids **1-6** were isolated in our laboratory from *Cynanchum auriculatum* Royle ex Wight., *Gymnema yunnanense* Tsiang, and *Marsdenia incisa* P. T. Li et Y. P. Li. Their structures were confirmed by the analysis of their spectroscopic data. Sample solutions with a final concentration of 0.25 mg·mL⁻¹ were prepared by dissolving each sample in 80% CH₃CN in H₂O. The samples were loaded onto the spectrometer via a syringe pump at the flow rate of 5 μL·min⁻¹.

Apparatus and analytical conditions: MSⁿ analyses were conducted on a LCMS-IT-TOF mass spectrometer (Shimadzu, Kyoto, Japan). Precise mass was corrected by calibration using the sodium trifluoroacetate clusters. The mass resolution was about 10 000 full width at half maximum (FWHM). The Shimadzu Composition Formula Predictor was used to speculate the molecular formula. MS experiments were achieved in automatic pattern, and MS2-5 experiments were performed in manual mode. The ESI-MS analytical conditions were as follows: drying gas pressure, 100.0 kPa; nebulizing gas (N₂) flow, 0.5 L min⁻¹; spray voltage, +4.50/-3.50 kV; detector voltage, 1.60 kV; equipment temperature, 40.0°C; heat block temperature, 200.0°C; curved desolvation line (CDL) temperature, 200.0°C; collision energy, 50%; collision gas (Ar), 50%; precursor ion selected width, *m/z* ±3.0 Da, and selected time, 20 ms; collision induced dissociation (CID) collision time, 30 ms; ion accumulation time, 10 ms; and q = 0.251; scan range, *m/z* 100–1000 for MS.

Acknowledgments - This work was supported by the National Natural Science Foundation of China for Distinguished Young Scholars (No. 81025023) and the Youth Innovation Promotion Association, CAS.

Reference

- [1] Shan L, Zhang WD, Zhang C, Liu RH, Su J, Zhou Y. (2005) Antitumor activity of crude extract and fractions from root tuber of *Cynanchum auriculatum* Royle ex Wight. *Phytotherapy Research*, **19**, 259-261.
- [2] Li XY, Sun HX, Ye YP, Chen FY, Pan YJ. (2006) C-21 steroidal glycosides from the roots of *Cynanchum chekiangense* and their immunosuppressive activities. *Steroids*, **71**, 61-66.
- [3] Heeren FR, Horak RM, Maharaj VJ, Vleggaar R, Senabe JV, Gunning PJ. (2007) An appetite suppressant from *Hoodia* species. *Phytochemistry*, **68**, 2545-2553.

- [4] Wang LJ, Geng CA, Ma YB, Huang XY, Luo J, Chen H, Guo RH, Zhang XM, Chen JJ. (2012) Synthesis, structure–activity relationships and biological evaluation of caudatin derivatives as novel anti-hepatitis B virus agents. *Bioorganic & Medicinal Chemistry*, **20**, 2877-2888.
- [5] Wang LJ, Geng CA, Ma YB, Luo J, Huang XY, Chen H, Zhou NJ, Zhang XM, Chen JJ. (2012) Design, synthesis, and molecular hybrids of caudatin and cinnamic acids as novel anti-hepatitis B virus agents. *European Journal of Medicinal Chemistry*, **54**, 352-365.
- [6] Wang Y, Song FR, Xu QX, Liu ZQ, Liu SY. (2003) Characterization of aconitine-type alkaloids in the flowers of *Aconitum kusnezoffii* by electrospray ionization tandem mass spectrometry. *Journal of Mass Spectrometry*, **38**, 962-970.
- [7] Piaz FD, Leo MD, Braca A, Simon FD, Morelli I, Tommasi ND. (2005) Electrospray ionization mass spectrometry for identification and structural characterization of pregnane glycosides. *Rapid Communications in Mass Spectrometry*, **19**, 1041-1052.
- [8] Han LF, Pan GX, Wang YF, Song XB, Gao XM, Ma BP, Kang LP. (2011) Rapid profiling and identification of triterpenoid saponins in crude extracts from *Albizia julibrissin* Durazz. by ultra high-performance liquid chromatography coupled with electrospray ionization quadrupole time-of-flight tandem mass spectrometry. *Journal of Pharmaceutical and Biomedical Analysis*, **55**, 996-1009.
- [9] Geng CA, Ma YB, Zhang XM, Yao SY, Xue DQ, Zhang RP, Chen JJ. (2012) Mulberrofuran G and isomulberrofuran G from *Morus alba* L.: antihepatitis B virus activity and mass spectrometric fragmentation. *Journal of Agricultural and Food Chemistry*, **60**, 8197-8202.
- [10] Geng CA, Chen H, Chen XL, Zhang XM, Lei LG, Chen JJ. (2014) Rapid characterization of chemical constituents in *Saniculiphyllum guangxiense* by ultra fast liquid chromatography with diode array detection and electrospray ionization tandem mass spectrometry. *International Journal of Mass Spectrometry*, **361**, 9-22.
- [11] Liu YB, Su EN, Li JB, Zhang JL, Yu SS, Qu J, Liu J, Li Y. (2009) Steroidal glycosides from *Dregea sinensis* var. *corrugata* screened by liquid chromatography-electrospray ionization tandem mass spectrometry. *Journal of Natural Products*, **72**, 299-237.
- [12] Avula B, Wang YH, Pawar RS, Shukla YJ, Smillie TJ, Khan IA. (2008) Identification and structural characterization of steroidal glycosides in *Hoodia gordoni* by ion-trap tandem mass spectrometry and liquid chromatography coupled with electrospray ionization time-of-flight mass spectrometry. *Rapid Communications in Mass Spectrometry*, **22**, 2587-2596.
- [13] Zheng ZG, Zhang WD, Kong LY, Liang MJ, Li HL, Lin M, Liu RH, Zhang C. (2007) Rapid identification of C₂₁ steroidal saponins in *Cynanchum versicolor* Bunge by electrospray ionization multi-stage tandem mass spectrometry and liquid chromatography/tandem mass spectrometry. *Rapid Communications in Mass Spectrometry*, **21**, 279-285.
- [14] Liang MJ, Zheng ZG, Yuan Y, Kong LY, Shen YH, Liu RH, Zhang C, Zhang WD. (2007) Identification and quantification of C₂₁ steroidal saponins from radix *Cynanchi atrati* by high-performance liquid chromatography with evaporative light scattering detection and electrospray mass spectrometric detection. *Phytochemical Analysis*, **18**, 428-435.
- [15] Tai YP, Cao XJ, Li XY, Pan YJ. (2006) Identification of C-21 steroidal glycosides from the roots of *Cynanchum chekiangense* by high-performance liquid chromatography/tandem mass spectrometry. *Analytical Chimica Acta*, **572**, 230-236.
- [16] Cao XJ, Tai YP, Li XY, Ye YP, Pan YJ. (2006) Screening for pregnane glycosides with immunological activities from the stems of *Stephanotis mucronata* by high-performance liquid chromatography/tandem mass spectrometry. *Rapid Communications in Mass Spectrometry*, **20**, 403-411.

Three New Cytotoxic Withanolides from the Chinese Folk Medicine *Physalis angulata*

Cai-Yun Gao, Ting Ma, Jun Luo* and Ling-Yi Kong*

State Key Laboratory of Natural Medicines, Department of Natural Medicinal Chemistry, China Pharmaceutical University, 24 Tong Jia Xiang, Nanjing, 210009, People's Republic of China

cpu_lykong@126.com (L.Y. Kong), luojun1981ly@163.com (J. Luo)

Received: September 16th, 2015; Accepted: October 29th, 2015

Physagulides M-O, three new withanolides (**1-3**), were isolated from the aerial parts of *Physalis angulata* L. Their structures were elucidated through extensive spectroscopic techniques, including 1D and 2D NMR, and HRESIMS. The absolute configurations (22-R) of these new compounds were determined by CD analysis. Compounds **1** and **3** showed significant selective cytotoxic activities on the MG-63 cell line, with IC₅₀ values of 4.28 and 5.44 μM, respectively.

Keywords: *Physalis angulata*, Withanolides, Cytotoxic activity.

Withanolides are a group of C₂₈ ergostane-type steroids with a δ-lactone oxidized at C-22 and C-26, distributed mainly in plants belonging to the genera *Physalis*, *Withania*, *Datura*, *Hyoscyamus*, *Jaborosa*, *Nicandra* and *Tubocapsicum* of the family Solanaceae [1]. In recent years, withanolides have gained significant scientific interest due to their various structures and notable biological properties [2], including immunosuppression [3], quinine reductase induction [4], antiproliferative [5], anti-inflammation [6], and antitumor activities [7a, b]. *Physalis angulata* L., a widely distributed species throughout the east and southwest regions of China [8], is commonly used as a traditional Chinese medicine for antipyretic, anti-inflammatory and diuretic purposes [9]. Phytochemical research has indicated that withanolides, with diverse structures and significant antitumor activities, are the main constituents of this plant [10]. As a part of our research program on bioactive constituents from Chinese folk medicines, three new withanolides (**1-3**) were isolated from the aerial parts of the title plant. Their structures were elucidated through extensive spectroscopic techniques, including 1D and 2D NMR, and HRESIMS. The absolute configuration (22-R) of these new compounds was determined by CD analysis. An antiproliferative activities screen indicated that compounds **1** and **3** had selective significant cytotoxic activity on the MG-63 cell line with IC₅₀ values of 4.28 and 5.44 μM, respectively [11]. Herein, we report the isolation, structure elucidation and cytotoxic activity of these new compounds.

Physagulide M (**1**) was obtained as a white amorphous solid, and its HRESIMS showed a [M+NH₄]⁺ peak at *m/z* 578.3326 (calcd 578.3324) corresponding to a molecular formula of C₃₁H₄₄O₉. The strong IR absorptions at 3444 and 1707 cm⁻¹ indicated the presence of hydroxy groups and an α, β-unsaturated ketone [12], which was supported by an UV absorption at 227 nm [13]. The whole features of the ¹H and ¹³C NMR (Table 1) data of **1**, especially the five methyl signals at δ_H 1.08, 1.30, 1.01, 1.86, and 1.93, and a set of carbon signals of an α, β-unsaturated ketone (δ_C 166.5, 122.2 and 149.1), indicated that compound **1** was a withanolide derivative, such as physagulin N [9]. Two characteristic olefinic protons of the α, β-unsaturated ketone in ring A seen in the ¹H NMR spectra of many normal withanolides [14] were absent in the spectrum of **1** (Table 1); instead of methylene protons at δ_H 3.08 (dd, *J*=15.1, 5.3

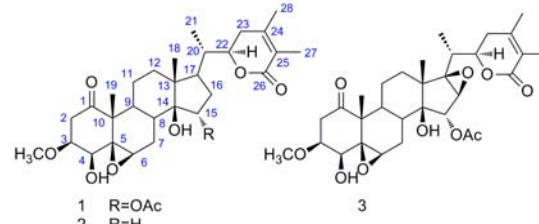


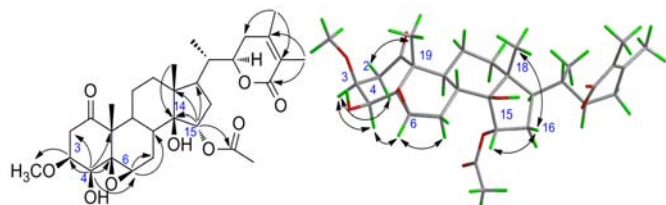
Figure 1: The structures of compounds **1-3**.

Hz, H-2β), and δ_H 2.57 (dd, *J*=15.2, 3.7 Hz, H-2α), one more oxymethine proton at δ_H 3.73 (ddd, *J*=5.3, 3.7, 3.4 Hz, H-3), and an additional methoxyl signal (δ_H 3.32, s, 3H) were observed. Moreover, an HMBC correlation between a methoxyl signal at δ_H 3.32 (s, 3H) and C-3 (δ_C 77.3) was observed. The aforementioned evidence suggested that the typical Δ^{2,3} of normal withanolides was absent and a methoxyl group was located at C-3. The signal at δ_H 3.51 (d, *J*=3.4 Hz, H-4) and HMBC correlations between H-4 and C-2 (δ_C 39.1), C-3 (δ_C 77.3), C-5 (δ_C 64.3), and C-10 (δ_C 50.7) suggested that a hydroxyl group was located at C-4. Signals at δ_H 3.29 (s, H-6), δ_C 64.3 (C-5) and 61.8 (C-6) could be assigned for an epoxy group linked at C-5/6 [15], which was proved by the HMBC correlations from H-4 to C-5 and C-6, from H-6 to C-7 (δ_C 24.5) and C-8 (δ_C 35.1) (Figure 2). Two olefinic methyl signals at δ_H 1.86 (3H, s, Me-27) and δ_H 1.93 (3H, s, Me-28) and a doublet at δ_H 4.32 (ddd, *J*=13, 4.6, 3.5 Hz, H-22) indicated the presence of a typical α, β-unsaturated-δ-lactone in the side chain, which was confirmed by the HMBC correlations shown in Figure 2 [16]. HMBC correlations between H-15 (δ_H 4.99) and C-14 (δ_C 84.5), C-13 (δ_C 46.3), C-17 (δ_C 52.5) and the carbonyl group (δ_C 169.8) suggested that an acetoxy group was located at C-15 (δ_C 80.6) (Figure 2). The remaining hydroxy group was placed at C-14 (δ_C 84.5) by the key HMBC correlations from Me-18 and H-15 to C-14 (Figure 2). Thus, the planar structure of **1** was elucidated as shown in Figure 1.

The relative stereochemistry of **1** was established by analysis of the ROESY spectrum [17]. Correlations of H-3 with H-4 and H-2α, of H-4 with H-6, and of H-2β with Me-19 indicated the α-orientations of H-3, H-4 and H-6. The β-orientation of H-15 was supported by the ROESY correlations between H-15, Me-18 and H-16β (Figure 2).

Table 1: ^1H (500MHz) and ^{13}C NMR (125 MHz) data for compounds **1–3** in CDCl_3 (δ in ppm, J in Hz).

Position	1		2		3	
	δ_{H}	δ_{C}	δ_{H}	δ_{C}	δ_{H}	δ_{C}
1		209.9			210.2	210.2
2	3.08, dd (15.1, 5.3) 2.57, dd (15.2, 3.7)	39.1	3.12, dd (14.6, 4.8) 2.57, dd (14.6, 4.1)	38.9	3.12, dd (15.0, 4.7) 2.57, dd (15.0, 3.8)	38.9
3	3.73, ddd (5.3, 3.7, 3.4)	77.3	3.75, ddd (4.8, 4.1, 3.3)	77.7	3.74, ddd (4.7, 3.8, 3.5)	77.3
4	3.51, d (3.4)	75.0	3.50, d (3.3)	75.2	3.51, d (3.5)	75.0
5		64.3			64.6	64.1
6	3.29, br s	61.8	3.32, br s	62.7	3.27, s	62.1
7	2.51, m 1.49, m	25.9	2.48, m 1.58, m	27.1	2.56, m 1.40, m	25.6
8	1.60, m	36.3	1.58, m	35.3	1.58, m	34.4
9	1.82, m	38.5	1.50, m	39.0	1.90, m	37.3
10		50.7			51.0	50.4
11	1.93, m 1.43, m	21.4	1.50, m 1.41, m	21.7	1.59, m 1.20, m	20.6
12	1.81, m 1.59, m	41.2	1.44, m 1.31, m	41.5	1.60, m 1.59, m	31.6
13		46.3			46.9	46.6
14		84.5			84.8	81.4
15	4.99, d (4.5)	80.6	1.70, m 1.54, m	32.8	5.03, s	77.6
16	2.01, m 1.67, m	33.6	1.26, m 1.25, m	29.8	3.48, s	59.0
17	1.70, m	52.5	1.51, m	53.1		76.3
18	1.08, s	17.1	1.04, s	16.4	1.12, s	15.6
19	1.30, s	16.0	1.35, s	16.6	1.30, s	16.3
20	2.09, m	37.5	2.10, m	37.9	2.56, m	33.7
21	1.01, d (6.6)	16.1	0.99, d (6.6)	15.8	1.00, d (7.1)	13.4
22	4.32, ddd (13.0, 4.6, 3.5)	78.3	4.48, ddd (13.0, 4.3, 3.5)	78.5	4.50, dt (12.5, 4.0)	76.8
23	2.47, m 1.96, m	31.6	2.46, m 2.03, m	31.5	2.38, m 2.13, m	32.5
24		149.1			149.2	149.2
25		122.2			122.1	122.2
26		166.5			166.8	166.3
27	1.86, s	12.5	1.87, s	12.6	1.87, s	12.6
28	1.93, s	20.6	1.93, s	20.6	1.93, s	20.7
OAc	2.05, s	169.8			2.10, s	169.6
		21.8				21.0
OMe	3.32, s	56.8	3.35, s	56.8	3.32, s	56.7

**Figure 2:** The key HMBC and ROESY correlations of compound **1**.

The obvious positive Cotton effect at 249 nm in the ECD spectrum of **1** indicated that the absolute configuration of C-22 was assigned as *R* [18]. On the basis of all the above evidence, the structure of **1** was established as (20*S*, 22*R*)-15*α*-acetoxy-5*β*, 6*β*-epoxy-4*β*, 14*β*-dydroxy-3*β*-methoxy-1-oxowitha-24-en-26, 22-olide, and named physagulide M.

The spectral characteristics of physagulide N (**2**) were very similar to those of **1**, with the major difference being the absence of signals corresponding to the acetoxy group in **1**, consistent with the 58.0061 mass units less than **1** in the HRESIMS. The upfield shifts of the C-15 from δ_{C} 80.6 in **1** to 32.8 suggested that there was no acetoxy group linked at C-15. The similar ROESY and ECD spectra indicated that the relative and absolute configuration of **2** were the same as those of **1**. Thus, compound **2** was established as (20*S*, 22*R*)-5*β*, 6*β*-epoxy-4*β*, 14*β*-dydroxy-3*β*-methoxy-1-oxowitha-24-en-26, 22-olide, and named as physagulide N.

Physagulide O (**3**) gave a molecular formula of $\text{C}_{31}\text{H}_{42}\text{O}_{10}$ by HRESIMS (m/z 592.3117 [$\text{M}+\text{NH}_4$] $^+$, calcd. for 592.3116). Comparison of the NMR data of **3** and **1** indicated that they have

identical A-C rings and side chains. The key difference was the substitution pattern in ring D. A secondary epoxy group linked at C-16/17 was proposed by the NMR signals at δ_{H} 3.48 (br s, H-16), δ_{C} 59.0 (C-16) and δ_{C} 76.3 (s, C-17). This was consolidated by the HMBC spectral analysis, in which H-15 (δ_{H} 5.03) was correlated to C-14 (δ_{C} 81.4), C-13 (δ_{C} 46.6) and C-17 (δ_{C} 76.3), and H-16 (δ_{H} 3.48) to C-15 (δ_{C} 77.6). The orientation of the epoxy group was deduced to be β based on the ROESY cross-peaks for H-16 (δ_{H} 3.48) with Me-21 (δ_{H} 1.00). The absolute configuration of C-22 was established as *R* through the same ECD Cotton effects of **3** compared with **1** [18]. Thus, the structure of **3** was established as (20*S*, 22*R*)-15*α*-acetoxy-5*β*, 6*β*:16*β*, 17*β*-diepoxy-4*β*, 14*β*-dyhydroxy-3*β*-methoxy-1-oxowitha-24-en-26, 22-olide, and named as physagulide O.

Cytotoxic activities of all compounds were examined against three human cancer cell lines (MG-63, HepG-2, and MDA-MB-231); doxorubicin was used as the positive control with IC_{50} values of 0.46, 3.72, and 3.70 μM , respectively. Compounds **1** and **3** demonstrated significant selective cytotoxic activity on MG-63 with IC_{50} values of 4.28 and 5.44 μM , respectively (Table 2). From the results of this cytotoxicity evaluation, these compounds may be valuable for cancer therapy.

Table 2: Cytotoxicity of compounds **1–3** against three human cancer cell lines.

Compound	IC_{50} (μM)		
	MG-63	HepG-2	MDA-MB-231
1	4.28	>20	>20
2	>20	>20	>20
3	5.44	>20	>20
Doxorubicin ^a	0.46	3.72	3.70

^aDoxorubicin was used as a positive control.

Experimental

General: Optical rotations were measured with a JASCO P-1020 polarimeter. IR data were obtained on a Bruker Tensor 27 spectrometer, UV spectra on a Shimadzu UV-2501 PC spectrophotometer, and 1D and 2D NMR spectra, using CDCl₃ as solvent, on a Bruker Avance III NMR spectrometer at 500 MHz (¹H) and 125 MHz (¹³C). HRESI mass spectra were collected with an Agilent 6520B UPLC-Q-TOF mass spectrometer. Circular dichroism(CD) spectra were recorded on a JASCO 810 spectropolarimeter. HPLC analysis was run on an Agilent 1200 instrument equipped with a multiple wavelength diode array detector (DAD). Preparative HPLC was performed on a Shimadzu instrument equipped with a Shim-pack RP-C₁₈ column (20×200 mm², 10 μm), and a flow rate of 10.0 mL/min. Column chromatography (CC) was carried out using macroporous resin D-101 (pore size B 13-14 nm, 26-60 mesh, Qingdao Marine Chemical Co. Ltd., Qingdao, China), Silica gel (100-200 mesh and 200-300 mesh, Qingdao Marine Chemical Co. Ltd., Qingdao, China) and ODS RP-C₁₈ (40-63μm, FuJi, Japan).

Plant material: Whole plants of *Physalis angulata* were collected in August 2014, in Lin Yi, Shan Dong Province, China, and were identified by Professor Zhang Mian of the Research Department of Pharmacognosy, China Pharmaceutical University. A voucher specimen (No.PA-201407-LY) is deposited in the department of Natural Medicinal Chemistry, China Pharmaceutical University.

Extraction and isolation: The air-dried aerial parts of *P. angulata* (1 kg) were powdered and extracted with CH₂Cl₂-MeOH (1:1) at room temperature, 3 times. After removing the solvent under vacuum, the residue (70 g) was subjected to column chromatography (CC) on D-101 macroporous resin and eluted with a step gradient of EtOH-H₂O (20:80, 40:60, 60:40, 80:20, 95:5, v/v) to yield 5 fractions: Fr. A-E. Fr. C (7g) was then chromatographed over silica gel with increasing polarities of CH₂Cl₂-MeOH (40:1, 20:1, 10:1, 0:100 v/v) to obtain 4 sub-fractions (Fr. C1-C4). Fr. C3 was applied to ODS MPLC eluted with isocratic MeOH-H₂O (50:50 v/v) to afford 8 sub-fractions (Fr.C3A-H). Fr.C3C was chromatographed over ODS with acetonitrile-H₂O (35:65, v/v) to give 2 sub-fractions (Fr.C3C 1-2). Fr.C3C1 was applied to preparative HPLC with MeOH-H₂O (55:45 v/v) to yield **1** (6.2 mg) and **3** (14.7 mg). Fr.C3H was chromatographed over Sephadex LH-20 with MeOH to yield 2 sub-fractions (Fr.C3H 1-2). Fr.C3H1 was subjected to preparative HPLC with MeOH-H₂O (60:40, v/v) to yield **2** (1.6 mg).

References

- [1] Chen LX, He H, Qiu F. (2011) Natural withanolides: an overview. *Natural Product Reports*, **28**, 705-740.
- [2] Ye Y, Li XQ, Tang CP. (2010) Natural products chemistry research 2008's progress in China. *Chinese Journal of Natural Medicines*, **41**, 68-80.
- [3] Sun LJ, Liu JW, Liu P, Yu YJ, Ma L, Hu LH. (2005) Immunosuppression effect of withangulatin A from *Physalis angulata* via heme oxygenase 1-dependent pathways. *Process Biochemistry*, **46**, 482-488.
- [4] Ding H, Hu ZJ, Yu LY, Ma ZJ, Ma XQ, Chen Z, Wang D, Zhao XF. (2014) Induction of quinone reductase (QR) by withanolides isolated from *Physalis angulata* L. var. *villosa* Bonati (Solanaceae). *Steroids*, **86**, 32-38.
- [5] Zhang HP, Bazzill J, Gallagher RJ, Subramanian C, Grogan PT, Day VW, Kindscher K, Cohen MS, Timmermann BN. (2013) Antiproliferative withanolides from *Datura wrightii*. *Journal of Natural Products*, **76**, 445-449.
- [6] Kaileh M, Berghe WV, Heyerick A, Horion J, Piette J, Libert C, Keukeleire DD, Essawi T, Haegeman G. (2007) Withaferin A strongly elicits IκB kinase β hyperphosphorylation concomitant with potent inhibition of its kinase activity. *Journal of Biological Chemistry*, **282**, 4253-4264.
- [7] (a) He QP, Ma L, Luo GY, Hu LH. (2007) Cytotoxic withanolides from *Physalis angulata* L. *Chemistry & Biodiversity*, **4**, 443-449; (b) Alali FQ, Amrine CSM, El-Elimat T, Alkofahi A, Tawaha K, Gharaibah M, Swanson SM, Falkinham III JO, Cabeza M, Sánchez A, Figueroa M, Oberlies NH. (2014) Bioactive withanolides from *Withania obtusifolia*. *Phytochemistry Letters*, **9**, 96-101.
- [8] Yang YJ, Chen MG, Hu L, Zhu DN. (2013) Chemical constituents of whole plant of *Physalis angulata*L.. *Chinese Pharmaceutical Journal*, **48**, 1715-1718.

PhysagulideM (1)

White amorphous solid.

[α]_D²⁰+10.5 (c 0.42, MeOH).

CD: Δε₂₅₀ +4.92 (c 0.3, MeCN).

IR (KBr): 3444, 2925, 1707, 1383, 1256, 1095 cm⁻¹.

UV/Vis λ_{max} (MeOH) nm (log ε): 227 (3.95), 206 (3.93).

¹H and ¹³C NMR data: see Table 1.

HRESIMS: m/z 578.3326 [M+NH₄]⁺ (calcd for C₃₁H₄₈NO₉, 578.3324).

Physagulide N (2)

White amorphous solid.

[α]_D²⁰-1.5 (c 0.18, MeOH).

CD: Δε₂₅₀ +5.30 (c 0.3, MeCN).

IR (KBr): 3449, 2932, 1702, 1383, 1137 cm⁻¹.

UV/Vis λ_{max} (MeOH) nm (log ε): 227 (4.21), 207 (4.20).

¹H and ¹³C NMR data: see Table 1.

HRESIMS: m/z 520.3265 [M+NH₄]⁺ (calcd for C₂₉H₄₆NO₇, 520.3269).

Physagulide O (3)

White amorphous solid.

[α]_D²⁰+21.6 (c 0.13, MeOH).

CD: Δε₂₅₀ +4.84 (c 0.3, MeCN).

IR (KBr): 3489, 2929, 1707, 1381, 1225, 1097 cm⁻¹.

UV/Vis λ_{max} (MeOH) nm (log ε): 227(4.58).

¹H and ¹³C NMR data: see Table 1.

HRESIMS:m/z 592.3117 [M+NH₄]⁺ (calcd for C₃₁H₄₆NO₁₀, 592.3116).

Cytotoxicity assay: The cytotoxicity bioassay of all new compounds against human cancer cells (MG-63, HepG-2, MDA-MB-231) was determined *in vitro* with the MTT assay, as described previously [19]. Doxorubicin was used as the positive control [20]. All experiments were carried out in triplicate.

Supplementary data: NMR spectra (¹H and ¹³C NMR, HSQC, HMBC and ROESY), HRESIMS and CD spectra for the new compounds (**1-3**).

Acknowledgments - This research was supported in part by the National Natural Science Foundation of China (81430092), the Program for New Century Excellent Talents in University (NCET-2013-1035), the Priority Academic Program Development of Jiangsu Higher Education Institutions (PAPD) and by the Program for Changjiang Scholars and Innovative Research Team in University (IRT1193).

- [9] Abe F, Nagafuji S, Okawa M, Kinjo J. (2006) Trypanocidal constituents in plants 6. Minor withanolides from the aerial parts of *Physalis angulata*. *Chemical & Pharmaceutical Bulletin*, **54**, 1226-1228.
- [10] Schirmer Pigatto AG, Mentz LA, Gonçalves Soares GL. (2014) Chemotaxonomic characterization and chemical similarity of tribes/genera of the Solanoideae subfamily (Solanaceae) based on occurrence of withanolides. *Biochemical Systematics and Ecology*, **54**, 40-47.
- [11] Cordero CP, Morantes SJ, Páez A, Rincón J, Aristizábal FA. (2009) Cytotoxicity of withanolides isolated from *Acnistus arborescens*. *Fitoterapia*, **80**, 364-368.
- [12] Zhang HP, Samadi AK, Gallagher RJ, Araya JJ, Tong X, Day VW, Cohen MS, Kindscher K, Gollapudi R, Timmermann BN. (2011) Cytotoxic withanolide constituents of *Physalis longifolia*. *Journal of Natural Products*, **74**, 2532-2544.
- [13] Kim KH, Choi SU, Choi SZ, Son MW, Lee KR. (2011) Withanolides from the rhizomes of *Dioscorea japonica* and their cytotoxicity. *Journal of Agricultural and Food Chemistry*, **59**, 6980-6984.
- [14] Hsieh PW, Huang ZY, Chen JH, Chang FR, Wu CC, Yang YL, Chiang MY, Yen MH, Chen SL, Yen HF, Lübken T, Hung WC, Wu YC. (2007) Cytotoxic withanolides from *Tubocapsicum anomalum*. *Journal of Natural Products*, **70**, 747-753.
- [15] Fang ST, Liu JK, Li B. (2012) Ten new withanolides from *Physalis peruviana*. *Steroids*, **77**, 36-44.
- [16] Guan YZ, Shan SM, Zhang W, Luo JG, Kong LY. (2014) Withanolides from *Physalis minima* and their inhibitory effects on nitric oxide production. *Steroids*, **82**, 38-43.
- [17] Nagafuji S, Okabe H, Akahane H, Abe F. (2004) Trypanocidal constituents in plants. 4. Withanolides from the aerial parts of *Physalis angulata*. *Biological & Pharmaceutical Bulletin*, **27**, 193-197.
- [18] Shingu K, Yahara S, Nohara T, Okabe H. (1992) Three new withanolides, physagulins A, B and D from *Physalis angulata* L.. *Chemical & Pharmaceutical Bulletin*, **40**, 2088-2091.
- [19] Mosmann T. (1983) Rapid colorimetric assay for cellular growth and survival: application to proliferation and cytotoxicity assays. *Journal of Immunological Methods*, **65**, 55-63.
- [20] Choudhary MI, Hussain S, Yousuf S, Dar A, Mudassar, Atta ur R. (2010) Chlorinated and diepoxywithanolides from *Withania somnifera* and their cytotoxic effects against human lung cancer cell line. *Phytochemistry*, **71**, 2205-2209.

Diterpenoid Alkaloids from *Aconitum soongaricum* var. *pubescens*Lin Chen^{a,b,c}, Lianhai Shan^a, Jifa Zhang^a, Wenliang Xu^a, Mingyu Wu^a, Shuai Huang^{a*} and Xianli Zhou^{a,b*}^aSchool of Life Science and Engineering, Southwest Jiaotong University, Chengdu, 610031 China^bKey Laboratory of Advanced Technologies of Materials, Ministry of Education, School of Material Science and Engineering, Southwest Jiaotong University, Chengdu, 610031 China^cSchool of Chemistry and Chemical Engineering, China West Normal University, Nanchong, 637002 China

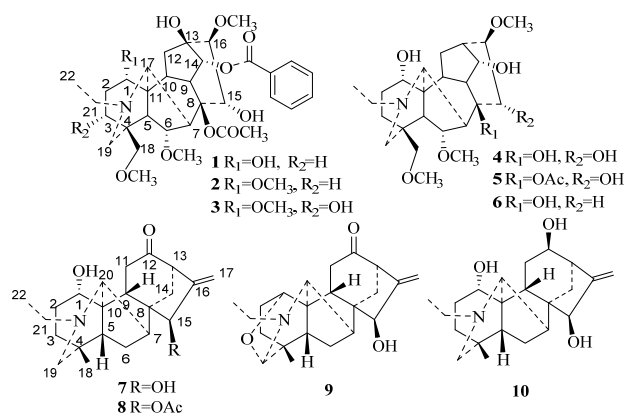
shuaih@home.swjtu.edu.cn; xxbiochem@163.com

Received: October 8th, 2015; Accepted: October 20th, 2015

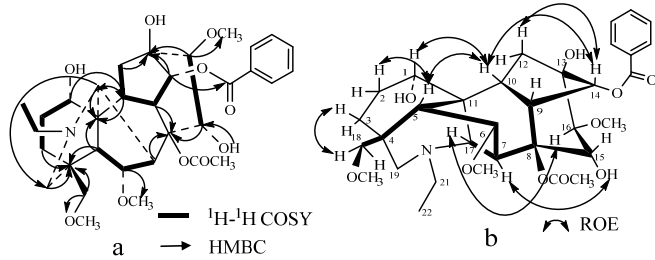
One new diterpenoid alkaloid, pubescensine (**1**), along with nine known diterpenoid alkaloids (**2–10**) were isolated from the roots of *Aconitum soongaricum* var. *pubescens*. Their structures were elucidated by spectroscopic analyses and comparison with previously reported data. All the compounds were evaluated for their antifeedant activities. The aconitine-type diterpenoid alkaloids (**1–6**) showed considerably potent antifeedant activity ($EC_{50} < 1 \text{ mg/cm}^2$), while the activities of napelline-type diterpenoid alkaloids (compds. **7, 9** and **10**) were not significant ($EC_{50} > 50 \text{ mg/cm}^2$).

Keywords: *Aconitum soongaricum* var. *pubescens*, Diterpenoid alkaloids, Antifeedant activity.

Much attention has been paid to diterpenoid alkaloids not only for their complex structures, but also for their biological activities such as anti-inflammatory, analgesic, anti-arrhythmia, antifungal, and cytotoxic properties [1–3], as well as insecticidal and antifeedant activities [4–6]. Recently, in the course of our investigation of new bioactive diterpenoid alkaloids from plants of the genera *Aconitum* and *Delphinium*, we discovered that the crude alkaloid extract from *A. soongaricum* var. *pubescens* roots possesses significant feeding deterrent activity against *Pieris rapae* Linne. Chemical investigation of the active extract led to the isolation of ten diterpenoid alkaloids: pubescensine (**1**), 3-deoxyaconitine (**2**), aconitine (**3**), 15- α -hydroxyneoline (**4**), taurenine (**5**), bullatine B (**6**), songorine (**7**), 15-acetylsongorine (**8**), songoramine (**9**) and 12-*epi*-napelline (**10**) (Figure 1). Among these compounds, **1** is a new diterpenoid alkaloid. In this paper, we report the isolation, structure elucidation and antifeedant activities of these alkaloids.

Figure 1: Structures of compounds **1–10**.

Pubescensine (**1**) was obtained as a white amorphous powder. Its molecular formula was determined to be $C_{33}H_{45}NO_{10}$ from the $[M+H]^+$ peak at m/z 616.3123 (calcd. for $C_{33}H_{46}NO_{10}$ 616.3122) in the HR-ESI-MS. The IR spectrum indicated that **1** possesses hydroxyl (3485 cm^{-1}) and carbonyl (1723 cm^{-1}) groups. The ^{13}C -NMR and DEPT spectra of **1** (Table 1) exhibited the presence of five methylenes (δ_C 29.5, 30.0, 36.3, 56.2, 79.8), ten methines

Figure 2: Key ^1H - ^1H COSY, HMBC (a) and ROESY (b) correlations of **1**.

(δ_C 39.6, 43.3, 43.6, 44.0, 62.9, 71.9, 78.7, 79.1, 83.7, 89.8), and four quaternary carbons (δ_C 38.1, 49.2, 74.0, 91.9). In addition, three methoxyl groups [δ_H 3.17(s), 3.31(s), 3.77(s)], an acetyl group [δ_H 1.42 (s)], a benzoyl group [δ_H 7.46 (t), 7.58 (t), 8.02 (d)] and a *N*-ethyl group [δ_H 1.15 (t), 2.44 (m), 2.82 (overlapped)] were present in the structure according to the ^1H NMR spectrum. The above-mentioned data revealed that compound **1** is an aconitine-type diterpenoid alkaloid [7].

Comparison of the 1D-NMR data of **1** with those of the known alkaloid 3-deoxyaconitine (**2**) [8] indicated that there was a hydroxyl group at C(1) in **1** instead of the methoxyl group in **2**, which was also confirmed by the difference of 14 mass units between the two compounds. The hydroxyl group at C(1) was assigned an α -orientation based on the signal of H-1 at δ_H 3.67 (broad singlet) and the resonance of C-1 at δ_C 71.9 in the NMR spectra [7], which was further supported by the cross-peaks between H-C(1) with H-C(10) and H-C(10) with H-C(14) in the ROESY spectrum. Their chemical shifts and multiplicity (Table 1) suggested that ring A possesses a boat conformation [7]. The complete planar structure of **1** was further verified by the analyses of the HMBC and ^1H - ^1H COSY spectra (Figure 2). The configuration of **1** could be assigned as H_β -C(1), H_β -C(6), H_β -C(10), H_β -C(14), H_β -C(15) and H_α -C(16) based on the observation of the related cross-peaks in its ROESY spectrum (Figure 2). Thus, the structure of pubescensine was assigned to be **1**. The structures of compounds **2–10** were identified by comparison of their spectral data with those described in the literature [8–16].

Table 1: ^1H and ^{13}C NMR data for compound **1**.

Position	δ_{C}	δ_{H} (mult., J = Hz)	Position	δ_{C}	δ_{H} (mult., J = Hz)
1	71.9 d	3.67 br s	18	79.8 t	a 3.11 ABq (8.4)
2	30.0 t	α 1.62 m β 1.52 m	19	56.2 t	b 3.55 ABq (8.4) a 2.30 d (10.8)
3	29.5 t	α 1.26 m β 1.90 m	21	48.7 t	b 2.61 d (10.8) a 2.44 m b 2.82 ^a
4	38.1 s	-	22	13.0 q	1.15 t (7.2)
5	44.0 d	2.26 d (6.4)	6-OCH ₃	58.1 q	3.17 s
6	83.7 d	3.98 d (6.4)	16-OCH ₃	61.5 q	3.77 s
7	43.6 d	2.82 ^a	18-OCH ₃	59.1 q	3.31 s
8	91.9 s	-	8-OAc	21.4 q	1.42 s
9	43.3 d	2.82 ^a		172.4 s	-
10	39.6 d	2.16 m		165.9 s	-
11	49.2 s	-	14-OBz	129.7 s	-
12	36.3 t	α 2.20 ^a β 2.27 ^a	1'	129.6 d	8.02 d (7.2)
13	74.0 s	-	2', 6'	128.7 d	7.46 t (7.2)
14	79.1 d	4.89 d (4.8)	3', 5'	133.3 d	7.58 t (7.2)
15	78.7 d	4.49 dd (2.7, 5.4)	13-OH	-	3.94 ^b s
16	89.8 d	3.41 d (5.4)	15-OH	-	4.45 ^b d (2.7)
17	62.9 d	2.91 s			

^aOverlapped signals. ^bThe signal disappeared after exchange with D₂O

The antifeedant activities of the isolated compounds **1–10** were evaluated against *Pieris rapae* Linne (Table 2). The most antifeedant activity was found for compounds **3**, **1** and **2** (EC₅₀ < 0.05 mg/cm²), respectively, followed by **6**, **4** and **5** (EC₅₀ < 1 mg/cm²). The antifeedant activities of napelline-type diterpenoid alkaloids (**7**, **9** and **10**) were not significant (EC₅₀ > 50 mg/cm²). When the antifeedant activities of the compounds were compared for different classes, the napelline-type diterpenoid alkaloids were less active than the aconitine-type diterpenoid alkaloids.

Table 2: Antifeedant activities of the compounds isolated from *A. soongaricum* var. *pubescens* against *Pieris rapae* (n=3).

Compds.	EC ₅₀ (mg/cm ²) (95% confidence limits)	Compds.	EC ₅₀ (mg/cm ²) (95% confidence limits)
1	0.03 (0.01, 0.11)	6	0.41 (0.09, 2.10)
2	0.05 (0.01, 0.34)	7	>50
3	0.02 (0.01, 0.11)	8	nt
4	0.47 (0.33, 0.70)	9	>50
5	0.66 (0.32, 1.38)	10	>50

nt: not test (insufficient compound available)

Experimental

General: Optical rotations, Perkin-Elmer 341 polarimeter; NMR, Bruker AV600; IR, Thermo Fisher Nicolet 6700; HR-ESI-MS, Waters ACQUITY UPLC/Xevo G2-S QTOF mass spectrometer.

Plant material: The roots of *A. soongaricum* Stapf var. *pubescens* were collected in Houxia, Xinjiang Uygur Autonomous Region of China, in August 2014, and were identified (voucher specimen: C. Ren & L. Wang 705) by Prof. Qing-Er Yang of the Institute of Botany, Chinese Academy of Sciences.

Extraction and isolation: Dried and powdered roots of *A. soongaricum* var. *pubescens* (5.3 kg) were extracted with 95% EtOH 3 times at rt, for 3 days each time. After removal of the solvent, the extract (2000 g) was suspended in water (3 L) and adjusted to pH 2 with hydrochloric acid solution, and then successively extracted with light petroleum (4×1 L) and ethyl acetate (4×1 L). Then, 28% aq. NH₄OH soln. (2 L) was added to the aq. soln. to bring it to pH 10. The solutions were extracted with CH₂Cl₂ (4×1 L). The CH₂Cl₂ extracts were concentrated to produce the crude alkaloid extract (20 g). Column chromatography (CC) of the crude alkaloid extract over silica gel, using a CH₂Cl₂/MeOH

(60:1, v/v) mixture with increasing polarity afforded fractions A–E based on TLC analysis. Fraction A was separated by silica gel CC (light petroleum/Me₂CO/Et₂NH, 8:1:0.1, v/v/v) to obtain **2** (3-deoxyaconitine, 23 mg) and **9** (songoramine, 15 mg). CC (silica gel, light petroleum /Me₂CO/Et₂NH, 6:1:0.1, v/v/v) of fraction B afforded **7** (songorine, 1.5 g) and **8** (15-acetylsongorine, 2 mg). Fraction C was chromatographed on a silica gel column and eluted with light petroleum/Me₂CO/Et₂NH (3:1:0.1-0:1:0.1, v/v/v) to afford **1** (pubescensine, 14 mg), **5** (taurenine, 25 mg) and **3** (aconitine, 300 mg). Fr. D was subjected to CC on silica gel and eluted with light petroleum/CH₂Cl₂ (1:1- 0:1, v/v) to give **6** (bullatine B, 460 mg). Fr. E was subjected to CC on silica gel and eluted with CH₂Cl₂/MeOH (10:1-1:1, v/v) to give **10** (12-epinapelline, 200 mg) and **4** (15- α -hydroxyneoline, 120 mg).

Pubescensine

White amorphous powder.

[α]_D²⁰: -0.7 (c 0.3, CH₂Cl₂).

HR-ESI-MS *m/z* [M+H]⁺: 616.3123 (calcd. for C₃₃H₄₆NO₁₀ 616.3122).

¹H (CDCl₃, 600 MHz) and ¹³C NMR (CDCl₃, 150 MHz): Table 1.

IR (KBr) ν_{max} : 3485, 2927, 2823, 2584, 1723, 1602, 1452, 1382, 1315, 1279, 1240, 1180, 1108, 1027, 984, 960, 919, 897, 710 cm⁻¹.

Antifeedant bioassays: A *Pieris rapae* colony was reared on cabbage foliage and maintained at 24 ± 1°C, > 70% relative humidity with a photoperiod of 16:8 h (L:D) in a growth chamber.

The antifeedant properties of the test compounds were evaluated using the choice leaf-disc method described by González-Coloma *et al.* [17, 18]. Choice experiments were conducted with newly-emerged third-instar larvae of *P. rapae*. Fresh cabbage leaves were cut into leaf discs (2 cm diameter) and then treated on the upper surface with 15 μ L of either the test substance emulsions or deionized water containing acetone and Tween-20 (10: 0.012, v/v) for control. After air drying for 1 h, 2 treated leaves and 2 control leaves were arranged alternatively on 2% agar beds (2-3 mm) in 15 cm diameter Petri dishes. Four healthy and starved 3 h instars were placed in each dish and allowed to feed in a growth chamber (environmental conditions as described above). Three replicates were prepared for each treatment. Feeding was terminated after consumption of 50–70% of the control disks, and then the area of leaves consumed was examined with a LI-3000 portable area meter (American Lincoln Co. Ltd). Percent feeding reduction (%FR) was determined for each arena by the equation:

$$\% \text{FR} = (CK - T) / CK \times 100$$

Where CK and T are control leaf disc areas eaten and treated leaf disc areas eaten, respectively.

Compounds with a FR > 50% were tested in a dose-response experiment to calculate their relative potency (EC₅₀ values, the effective dose for 50% feeding reduction), which was determined from linear regression analysis (%FR on log dose).

Supplementary data: NMR, IR and HR-ESI-MS for compound **1**.

Acknowledgments - This work was financially supported by the National Natural Science Foundation of China (31171695), the Science and Technology Support Programs of Sichuan Province (2013SZ0083), the Research Foundation for Educational Commission of Sichuan Province (15TD0048 and 15ZB0140) and the Fundamental Research Funds for Central Universities (2682014RC15).

References

- [1] Dzhakhangirov FN, Sultankhodzhaev MN, Tashkhodzhaev B, Salimov BT. (1997) Diterpenoid alkaloids as a new class of antiarrhythmic agents. Structure-activity relationship. *Chemistry of Natural Compounds*, **33**, 190–202.
- [2] Ameri A. (1998) The effects of aconitum alkaloids on the central nervous system. *Progress in Neurobiology*, **56**, 211–235.
- [3] Panter KE, Manners GD, Stegelmeier BL, Lee S, Gardner DR, Ralphs MH, Pfister JA, James LF. (2002) Larkspur poisoning: toxicology and alkaloid structure-activity relationships. *Biochemical Systematics and Ecology*, **30**, 113–128.
- [4] Ulubelen A, Mericli AH, Mericli F, Kilincer N, Ferizli AG, Emekci M, Pelletier SW. (2001) Insect repellent activity of diterpenoid alkaloids. *Phytotherapy Research*, **15**, 170–171.
- [5] Liu ZL, Cao J, Zhang HM, Lin LL, Liu HJ, Du SS, Zhou LG, Deng ZW. (2011) Feeding deterrents from *Aconitum episcopale* roots against the red flour beetle, *Tribolium castaneum*. *Journal of Agricultural and Food Chemistry*, **59**, 3701–3706.
- [6] Reina M, González-Coloma A. (2007) Structural diversity and defensive properties of diterpenoid alkaloids. *Phytochemistry Reviews*, **6**, 81–95.
- [7] Pelletier SW, Mody NV, Joshi BS, Schramm LC. (1984) *Alkaloids: Chemical and Biological Perspectives*, Vol. 2, Pelletier SW. (Ed.). Wiley, New York, 205–210.
- [8] Pelletier W, Mody NV, Katsui N. (1977) The structures of sachaconitine and isodelphinine from *Aconitum miyabei* Nakai. *Tetrahedron Letters*, **46**, 4027–4030.
- [9] Hanuman JB, Katz A. (1993) Isolation and identification of four norditerpenoid alkaloids from processed and unprocessed root tubers of *Aconitum ferox*. *Journal of Natural Products*, **56**, 801–809.
- [10] Takayama H, Hasegawa S, Sakai S, Haginiwa J, Okamoto T. (1981) Structure elucidation of a new aconite alkaloid, 15- α -hydroxyneolin. *Chemical & Pharmaceutical Bulletin*, **29**, 3078–3080.
- [11] Tel'nov VA, Vaisov ZM, Yunusov MS, Gorelova AP. (1992) Alkaloids of the cultivated species *Aconitum tauricum*. *Chemistry of Natural Compounds*, **28**, 91–94.
- [12] Shim SH, Kim JS, Kang SS, Son KH, Bae KH. (2003) Alkaloidal constituents from *Aconitum jaluense*. *Archives of Pharmacal Research*, **26**, 709–715.
- [13] Wiesner K., Itô S, Valenta Z. (1958) The structure of napelline and songorine. *Experientia*, **14**, 167–169.
- [14] Fan ZC, Zhang ZQ. (2008) Molecular and crystal structure of 15-acetylsongorine and songoramine isolated from *Aconitum szechenyianum* Gay. *Structural Chemistry*, **19**, 413–419.
- [15] Csupor D, Forgo P, Csedó K, Hohmann J. (2006) C₁₉ and C₂₀ Diterpene alkaloids from *Aconitum toxicum* R_{CHB}. *Helvetica Chimica Acta*, **89**, 2981–2986.
- [16] Zhapova Ts, Semenov AA. (1993) 12-*epi*-Napelline and its N-oxide from *Aconitum baicalense*. *Chemistry of Natural Compounds*, **29**, 791–794.
- [17] González-Coloma A, Reina M, Cabrera R, Castanera P, Gutierrez C. (1995) Antifeedant and toxic effects of sesquiterpenes from *Senecio palmensis* to Colorado potato beetle. *Journal of Chemical Ecology*, **21**, 1255–1270.
- [18] González-Coloma A, Terrero D, Perales A, Escoubas P, Fraga BM. (1996) Insect antifeedant ryanodane diterpenes from *Persea indica*. *Journal of Agricultural and Food Chemistry*, **44**, 296–300.

Two New C₁₈-Diterpenoid Alkaloids from *Delphinium anthriscifolium*Lianhai Shan^{a,b}, Jifa Zhang^a, Lin Chen^c, Jiaxi Wang^a, Shuai Huang^{a*} and Xianli Zhou^{a,b*}^aSchool of Life Science and Engineering, Southwest Jiaotong University, Chengdu, 610031 China^bKey Laboratory of Advanced Technologies of Materials, Ministry of Education, School of Material Science and Engineering, Southwest Jiaotong University, Chengdu, 610031 China^cSchool of Chemistry and Chemical Engineering, China West Normal University, Nanchong, 637002 China

shuah@home.swjtu.edu.cn; xxbiochem@163.com

Received: September 17th, 2015; Accepted: October 6th, 2015

Two new C₁₈-diterpenoid alkaloids, anthriscifoltine A (**1**) and anthriscifoltine B (**2**), along with three known diterpenoid alkaloids, deoxydelcorine (**3**), anthriscifolcine A (**4**) and anthriscifolcine G (**5**), were isolated from the whole herbs of *Delphinium anthriscifolium* var. *majus*. Their structures were elucidated by spectroscopic methods, including 1D, 2D NMR, and HR-ESI-MS.

Keywords: *Delphinium anthriscifolium* var. *majus*, Diterpenoid alkaloids, Anthriscifoltine, NMR.

Delphinium anthriscifolium var. *majus* is an herbaceous plant belonging to the family Ranunculaceae. It is widely distributed in Guizhou, Sichuan, Hubei and Shanxi provinces in China, but currently is also cultivated in other regions. It contains many diterpenoid alkaloids having biological activities such as anti-inflammatory, analgesic, anti-arrhythmia, antifungal, and cytotoxic properties [1,2]. As a part of our efforts to study the chemical composition of *D. anthriscifolium*, we have now isolated and identified two C₁₈-diterpenoid alkaloids, anthriscifoltine A (**1**) and anthriscifoltine B (**2**), along with three known compounds, deoxydelcorine (**3**), anthriscifolcine A (**4**) and anthriscifolcine G (**5**). In this paper, we report the extraction, isolation, and structure elucidation of these alkaloids.

The molecular formula of anthriscifoltine A (**1**), was determined as C₃₀H₄₅NO₉ from the HR-ESI-MS ion at m/z 564.3185 [M+H]⁺ (calcd. for C₃₀H₄₆NO₉, 564.3173). The IR spectrum indicated that **1** possesses hydroxyl (3462 cm⁻¹) and carbonyl (1736 cm⁻¹) groups. The ¹H NMR and ¹³C NMR data (Table 1) of **1** indicated the presence of the signals of a 2-methylbutanoyloxy group (MbO) at [δ_H 2.38 (1H, m), 1.47 (2H, m), 0.91 (3H, t, *J* = 7.2 Hz), 1.14 (3H, d, *J* = 6.6 Hz) and δ_C 177.0 (s), 41.2 (d), 26.6 (t), 11.6 (q), 16.5 (q)] [3], an *N*-ethyl group [δ_H 1.07 (3H, t, *J* = 7.2 Hz), 2.75 (2H, m), δ_C 14.0 (q) and 50.8 (t)], two methoxyl groups [δ_H 3.27 (3H, s) and 3.28 (3H, s), δ_C 55.8 (q) and 55.9 (q)], an acetyl group [δ_H 2.04 (3H, s), δ_C 21.8 (q) and 170.5 (s)] and a methylenedioxy group [4.89 (1H, br s) and 4.94 (1H, br s), δ_C 94.0 (t)]. The remaining 18 carbons were assigned based on 1D- and 2D-NMR data. The presence of only one non-oxygenated quaternary carbon signal (δ_C 55.5 s) indicates that compound **1** is a C₁₈-diterpenoid alkaloid [4a,b]. The locations of the acetoxy group at C-6 and the 2-methylbutanoyloxy group at C-14 were determined by the correlations in the HMBC experiment. Besides the two ester groups, the two methoxyl groups were attributed to C-1 and C-16, respectively, and the methylenedioxy group was assigned to be at C-7 and C-8 as revealed by the long-range HMBC correlations. The existence of seven oxygenated carbons deduced from its ¹³C NMR spectrum suggests that **1** has one hydroxyl group, in addition to two methoxy groups, two ester groups, and a methylenedioxy group. The location of the hydroxyl group at C-10 was further confirmed by the HMBC correlations.

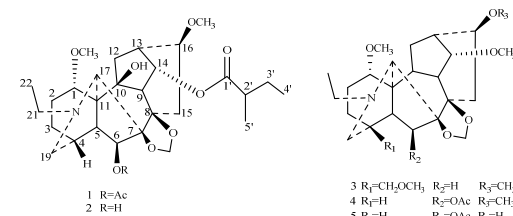
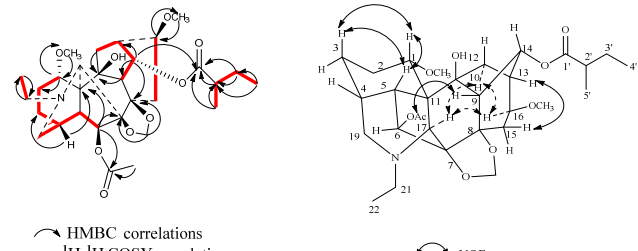


Figure 1: Structures of compounds 1–5.

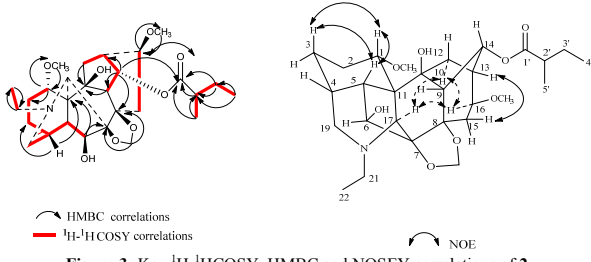
Figure 2: Key ¹H-¹H COSY, HMBC and NOSEY correlations of **1**.

The relative configuration of anthriscifoltine A was deduced from the vicinal coupling constants (Table 1) and a NOESY experiment. In the NOESY spectrum of **1**, the cross-peak between H-17 and H-16 proved that 16-OCH₃ has a β-position. The acetoxy group at C-6 was determined to have a β-orientation as well based on the multiplicity of H-6 (singlet) in the ¹H NMR spectrum [5a]. The coupling constants of H-1 at δ_H 3.55 (1H, t, *J* = 8.4 Hz) and H-14 at δ_H 5.28 (1H, t, *J* = 4.8 Hz) confirmed the β-position of axial H-1 [5b] and the α-position of H-14, respectively [5c]. Therefore, the structure of anthriscifoltine A (**1**) was determined as shown in Figure 1. The full assignment of anthriscifoltine A (**1**) was based on the 1D- and 2D NMR spectral data (Table 1, Figure 2).

The molecular formula of anthriscifoltine B (**2**) was determined to be C₂₈H₄₃NO₈ from the [M+H]⁺ peak at m/z 522.3084 (calcd. for C₂₈H₄₄NO₈, 522.3067) in the HR-ESI-MS. The IR absorption spectrum indicated that **2** possesses hydroxyl (3445 cm⁻¹) and carbonyl (1731 cm⁻¹) groups. The ¹³C NMR data of anthriscifoltine B (**2**) were very similar to those of **1** except for lacking a signal for an acetyl group. The proton signal of H-6 at δ_H 5.27 in compound **1** was shifted upfield to δ_H 4.27 in compound **2** suggesting that 6-OAc

Table 1: ^1H and ^{13}C NMR data for compounds **1** and **2**.

Position	1	δ_{H} (mult., J (Hz))	2	δ_{H} (mult., J (Hz))
1	77.4 d	3.55 t(8.4)	77.5 d	3.62 t(9.0)
2	26.4 t	2.06 α m, 2.12 β m	26.5 t	2.06 α m, 2.12 β m
3	28.9 t	1.43 β m, 1.80 α m	29.8 t	1.40 β m, 1.73 α m
4	34.1 d	2.09 m	34.7 d	2.08 m
5	44.8 d	1.87 m	46.1 d	1.81 m
6	81.3 d	5.27 s	82.4 d	4.27 s
7	91.9 s	-	92.8 s	-
8	81.7 s	-	82.6 s	-
9	50.4 d	3.49 d(5.4)	51.0 d	3.55 d(5.4)
10	83.4 s	-	83.0 s	-
11	55.5 s	-	55.8 s	-
12	35.5 t	1.71 α m, 2.56 β m	34.9 t	1.74 α m, 2.57 β m
13	37.5 d	2.80 m	36.6 d	2.74 m
14	74.3 d	5.28 t(4.8)	74.3 d	5.28 t(4.8)
15	39.1 t	1.84 β dd(7.8, 16.2)	38.5 t	1.83 β dd(7.8, 16.2)
		3.13 α d(16.2)		3.01 α d(16.2)
16	81.7 d	3.23 d(8.4)	81.3 d	3.21 d(8.4)
17	64.8 d	3.08 d(1.8)	64.4 d	3.03 d(1.8)
19	50.7 t	2.83 m	51.0 t	2.75 m
21	50.6 t	2.75 m	50.8 t	2.68 m
22	14.0 q	1.07 t(7.2)	14.0 q	1.06 t(7.2)
1-OCH ₃	55.8 q	3.27 s	55.8 q	3.25 s
16-OCH ₃	55.9 q	3.28 s	55.9 q	3.26 s
O-CH ₂ -O	94.0 t	4.89 br s	93.5 t	5.05 br s
		4.94 br s		5.13 br s
6-OAc	170.5 s	-	-	-
	21.8 q	2.04 s	-	-
14-MbO 1'	177.0 s	-	176.8 s	-
2'	41.2 d	2.38 m	41.2 d	2.35 m
3'	26.6 t	1.47 m	26.5 t	1.47 m
4'	11.6 q	0.91 t(7.2)	11.7 q	0.90 t(7.2)
5'	16.5 q	1.14 d(6.6)	16.4 q	1.14 d(7.2)

**Figure 3:** Key ^1H - ^1H COSY, HMBC and NOSEY correlations of **2**.

in **1** was substituted by a hydroxyl group, which was confirmed by the difference of 42 mass units between those two compounds. Thus, the structure of anthriscifoltine B was determined as compound **2**. The full assignment of anthriscifoltine B (**2**) was based on the 1D- and 2D-NMR spectral data (Table 1, Figure 3). The structures of compounds **3–5** were identified by comparison of their spectral data with those described in the literature [5a,b,d].

Experimental

General: Optical rotations, Perkin-Elmer 341 polarimeter; NMR, Bruker AV600; IR, Thermo Fisher Nicolet 6700; HR-ESI-MS, Waters ACQUITY UPLC/Xevo G2-S QTOF mass spectrometer.

References

- [1] (a) Dzhakhanirov FN, Sultankhodzhaev MN, Tashkhodzhaev B, Salimos BT. (1997) Diterpenoid alkaloids as a new class of antiarrhythmic agents. Structure-activity relationship. *Chemistry of Natural Compound*, **33**, 190–202; (b) Ulubelen A, Mericli A, Kilincer N, Ferizli AG, Emecki M, Pelletier SW. (2001) Insect repellent activity of diterpenoid alkaloids. *Phytotherapy Research*, **15**, 170–171.
- [2] Ameri A. (1998) The effects of aconitum alkaloids on the central nervous system. *Progress in Neurobiology*, **56**, 211–235.
- [3] Pelletier SW, Oliver D, Dailey Jr., Mody NV. (1981) Isolation and structure elucidation of the alkaloids of *Delphinium glaucescens* Rybd. *The Journal of Organic Chemistry*, **46**, 3284–3293.
- [4] (a) Pelletier SW, Mody NV, Joshi BS, Schramm LC. (1984) *Alkaloids: Chemical and Biological Perspectives*, Vol. 2, Pelletier SW. (Ed). John Wiley, New York, 205–213; (b) Wang FP. (1982) ^{13}C Nuclear magnetic resonance of diterpenoid alkaloids. *Organic Chemistry*, **3**, 161–169.
- [5] (a) Song L, Liang XX, Chen DL, Wang FP. (2007) New C₁₈-diterpenoid alkaloids from *Delphinium anthriscifolium* var. *savatieri*. *Chemical & Pharmaceutical Bulletin*, **55**, 918–921; (b) Song L, Liu XY, Chen QH, Wang FP. (2009) New C₁₉- and C₁₈-diterpenoid alkaloids from *Delphinium anthriscifolium* var. *savatieri*. *Chemical & Pharmaceutical Bulletin*, **57**, 158–161; (c) Diaz JG, Ruiz JG, Herz W. (2005) Norditerpene and diterpene alkaloids from *Aconitum variegatum*. *Phytochemistry*, **66**, 837–846; (d) Salimov BT, Yunusov MS, Abdullaev ND, Vaisov ZM. (1985) Corumdephine-a new alkaloid from *Delphinium corumbosum*. *Khimiya Prirodykh Soedinenii*, **1**, 91–94.

Plant material: The whole herbs of *D. anthriscifolium* var. *majus* were collected in Longshanwa, Zhuxi county, Hubei province of China, in April 2015, and were identified (voucher specimen: L H. Shan & J X. Wang 801) by Prof. Qing-Er Yang of the Institute of Botany, Chinese Academy of Sciences.

Extraction and isolation: Dried and powdered whole herbs of *D. anthriscifolium* (21.5 kg) were extracted with 95% EtOH, 4 times at room temperature, for a week each time. After removal of the solvent, the extract (2000 g) was suspended in water (3 L) and adjusted to pH 2 with HCl, and then successively extracted with light petroleum (4×1 L) and ethyl acetate (4×1 L). The pH value of the aqueous layer was adjusted to 10 with aqueous ammonium hydroxide solution and the subsequent mixture was extracted with CH₂Cl₂ (4×1 L). The CH₂Cl₂ extracts were concentrated to produce the crude alkaloid extract (28.5 g). Column chromatography of the crude alkaloid extract over silica gel, using a CH₂Cl₂:MeOH (80:1, v/v) mixture with increasing polarity afforded fractions A–G based on TLC analysis. Fraction A was separated by silica gel CC (light petroleum /Me₂CO/Et₂N 50: 1: 0.1, v/v/v) to obtain compounds **1** (25 mg), **2** (30 mg), **3** (8 mg), **4** (16 mg) and **5** (20 mg).

Anthriscifoltine A (**1**)

White amorphous powder.

$[\alpha]_D^{20} : -15.3$ (c 0.56, CHCl₃).

IR (KBr) ν_{max} : 3462, 2958, 2924, 2873, 2854, 2821, 1736, 1670, 1461, 1368, 1242, 1199, 1156, 1130, 1091, 1057, 962 cm⁻¹.

^1H (CDCl₃, 600 MHz) and ^{13}C NMR (CDCl₃, 150 MHz): Table 1.

HR-ESI-MS m/z : [M+H]⁺ 564.3185 (calcd. for C₃₀H₄₆NO₉ 564.3173).

Anthriscifoltine B (**2**)

White amorphous powder.

$[\alpha]_D^{20} : -4.9$ (c 0.56, CHCl₃).

IR (KBr) ν_{max} : 3445, 2956, 2924, 2854, 2823, 1731, 1668, 1463, 1379, 1239, 1199, 1156, 1128, 1091, 1058, 964 cm⁻¹.

^1H (CDCl₃, 600 MHz) and ^{13}C NMR (CDCl₃, 150 MHz): Table 1.

HR-ESI-MS m/z : [M+H]⁺ 522.3084 (calcd. for C₂₈H₄₄NO₈ 522.3067).

Supplementary data: NMR, IR and HR-ESI-MS for compounds **1** and **2**.

Acknowledgments - This work was financially supported by the National Natural Science Foundation of China (31171695), the Science and Technology Support Programs of Sichuan Province (2013SZ0083), Innovation Team Fund of Sichuan Province Education Department (15TD0048), Applied Basic Research of Sichuan Province (2014JY0125) and the Fundamental Research Funds for Central Universities (2682013CX033, 2682014RC15).

Majusine D: A New C₁₉-diterpenoid Alkaloid from *Delphinium majus*

Qi Zhao, Xiao-jun Gou, Wei Liu, Gang He, Li Liang and Feng-zheng Chen*

Key Laboratory of Medicinal and Edible Plant Resources Development of Sichuan Education Department,
Chengdu University, Chengdu 610106, P.R. China

fzchen7200@163.com

Received: August 30th, 2015; Accepted: October 31st, 2015

A new C₁₉-diterpenoid alkaloid, designated as majusine D (**1**), has been isolated from *Delphinium majus* W. T. Wang. The structure was elucidated by detailed NMR-spectroscopic studies.

Keywords: *Delphinium majus*, C₁₉-diterpenoid alkaloid, Majusine D.

Diterpenoid alkaloids are believed to be the major bioactive components of the genus *Delphinium* [1–4], a large genus within the Ranunculaceae family. *D. majus* W. T. Wang is distributed mainly in southwest Sichuan and northwest Yunnan of mainland China, especially around the Jinsha River basin [5]. In our previous papers, three new C₁₉-diterpenoid alkaloids and six new C₂₀-diterpenoid alkaloid have been reported [6]. Continuing investigations seeking new bioactive compounds of *D. majus* have now led to the isolation of one other new C₁₉-diterpenoid alkaloid, majusine D (**1**). This paper deals with the separation and structural elucidation of this new alkaloid.

Compound **1** was obtained as an amorphous powder. Its positive-ion HRESI-MS showed a quasi-molecular ion peak at *m/z* 466.2812, corresponding to the molecular formula, C₂₅H₃₉NO₇. Its NMR spectra exhibited the presence of an *N*-ethyl group [δ_H 1.03 (3H, t, *J* 7.6 Hz); δ_C 13.7 q, 50.3 t], four methoxyl groups [δ_H 3.33, 3.35, 3.36, 3.42 (each 3H, s); δ_C 56.3 q, 59.3 q, 59.2 q, 51.3 q], two unsaturated methines [δ_H 5.39, 5.66 (each 1H); δ_C 131.5d, 125.0 d]. Its ¹³C NMR spectrum displayed seven oxygenated carbon signals (δ_C 72.2d, 74.7 d, 78.5d, 81.0 s, 82.2 d, 90.5 d, 91.2s), suggesting that **1** possessed three hydroxyl groups in addition to four methoxyl groups. All of the available evidence revealed that **1** was a lycocotonine-type C₁₉-diterpenoid alkaloid [2]. A triplet signal at δ_H 3.95 (*J* = 5.6 Hz) was attributed to H-14 β , implying the presence of an oxygen substituted group at the C-14 position. Comparison of the NMR data of **1** (Table 1) with those of deltatsine (**2**) [7] revealed that they were similar (Figure 1). The major difference between them was that methylenes at C-2 and C-3 in deltatsine (**2**) were replaced by two unsaturated methines in **1**. Correlations between OCH₃-6 and C-6, OCH₃-8 and C-8, OCH₃-16 and C-16, OCH₃-18 and C-18 in the HMBC spectrum (Figure 2) suggested that the methoxyl groups could be assigned to C-6, and C-8, and C-16, and C-18, respectively. The occurrence of a $\Delta^{2(3)}$ double bond was corroborated by the correlations from H-2 to C-4 and from H-19 to C-3 in the HMBC spectrum (Figure 2). The secondary hydroxyl group was located at C-1 on the basis of the correlation with H-2 in the COSY spectrum, while the α -orientation of OH-1 was confirmed in the NOEDS spectrum by the coupling between H-1 β (3.62 d) and H-10 β (2.27 m). The molecular framework of majusine D is elucidated as Figure 1. Moreover, the ¹³C NMR spectrum showed that the compound contain an ester carbonyl (δ_C 172.4s), three oxygenated carbon signals (δ_C 74.1 d, 71.4 d, 64.5 t),

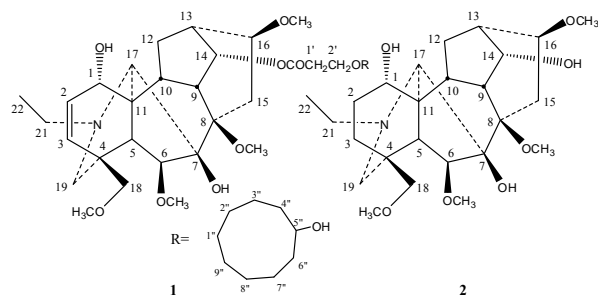


Figure 1: The structures of compounds **1** and **2**.

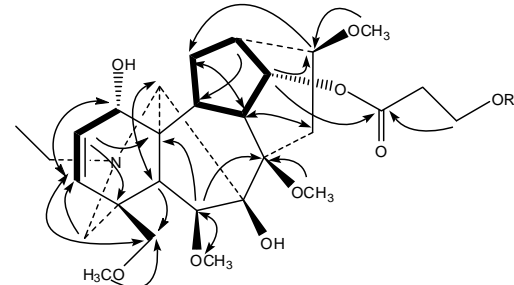


Figure 2: Key ¹H-¹H COSY (—) and HMBC (→) correlations of **1**.

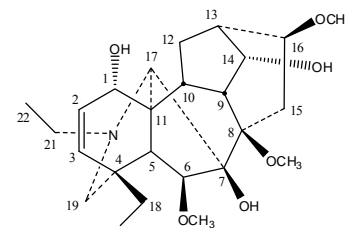


Figure 3: The hydrolysis product of the C₁₄-ester group from **1**.

eight secondary carbons (δ_C 33.9, 32.4, 29.1, 28.3, 27.0, 26.8, 25.5, 20.2). In the HMBC spectrum, there are connections of H-14 β , H-1' (δ_H 2.43 2H), and H-2' (δ_H 4.20, 2H, t, *J* = 5.2 Hz) to ester carbonyl (δ_C 172.4). In the IR spectrum, a peak at 726 cm⁻¹ displayed that the compound contained a series of four connected secondary carbons. Therefore, the structure of majusine D may be deduced as **1** (Figure 1). Compound **1** is a new C₁₉-diterpenoid alkaloid, and the hydrolysis product of the C₁₄-ester group (Figure 3) from compound **1** is also a new alkaloid.

Table 1: ^1H and ^{13}C NMR spectroscopic data for compounds **1** and **2**.

Position		1	2
	δ_{H}	δ_{C}	δ_{C}
1	3.62 d (4.4)	72.2 d	72.2 d
2	5.66 dd (9.2, 4.4)	125.0 d	27.0 t
3	5.39 d (9.2)	131.5 d	29.2 t
4	-	37.0 s	37.1 s
5	1.65 br s	48.7 d	48.8 d
6	3.79 br s	90.5 d	90.6 d
7	-	91.2 s	91.2 s
8	-	81.0 s	81.1 s
9	2.01 m	45.0 d	45.1 d
10	2.27 m	39.7 d	39.8 d
11	-	48.4 s	48.5 s
12	1.61 m, 1.41 m	28.5 t	28.4 t
13	2.26 m	39.7 d	39.8 d
14	3.95 t (5.6)	74.7 d	74.6 d
15	2.58 m, 1.78 m	31.2 t	30.9 t
16	3.38 (hidden)	82.2 d	82.2 d
17	2.82 br s	66.4 d	66.4 d
18	3.11, 3.27 ABq, (8.8)	78.5 t	78.6 t
19	2.37, 2.39 ABq, (7.6)	57.2 t	57.2 t
21	2.77 m, 2.91 m	50.3 t	50.2 t
22	1.03 t (7.6)	13.7 q	13.7 q
6-OCH ₃	3.36 s	59.2 q	59.2 q
8-OCH ₃	3.42 s	51.3 q	51.3 q
16-OCH ₃	3.33 s	56.3 q	56.2 q
18-OCH ₃	3.35 s	59.3 q	59.1 q
CO	-	174.2 s	
1'	2.43 (hidden)	33.9 t	
2'	4.20 t (5.2)	64.5 t	

(400 MHz for ^1H NMR, 50 MHz for ^{13}C NMR, CDCl₃, δ in ppm, J in Hz)

Experimental

General: Optical rotation was measured on a Autopol Automatic Polarimeter. IR spectra were obtained on a Perkin-Elmer FT-IR Spectrum Two. ^1H and ^{13}C NMR spectra were taken on a Varian Unity INOVA 400/45 NMR spectrometer in CDCl₃ with TMS as the internal standard. The ESIMS and HRESIMS were recorded on either a VG Auto Spec 3000 or a Finnigan-MAT 90 instrument. Silica gel H (Qingdao Sea Chemical Factory, Qingdao, People's Republic of China) was used for column chromatography. Zones on TLC (silica gel G) were detected using modified Dragendorff's reagent.

References

- [1] Wang, FP, Liang XT. (1992) Chemistry of the diterpenoid alkaloids. In *The Alkaloids: Chemistry and Physiology*, Vol. **42**, Cordell GA (Ed.), Academic Press, New York, 151–247.
- [2] Wang FP, Chen QH, Liang XT. (2009) The C19-diterpenoid alkaloids. In *The Alkaloids: Chemistry and Biology*, Vol. **67**, Cordell GA (Ed.), Elsevier Science, New York, 101-298.
- [3] Wang FP, Chen QH. (2010) The C19-diterpenoid alkaloids. In *The Alkaloids: Chemistry and Biology*, Vol. **69**, Cordell GA (Ed.), Elsevier Science, New York, 1-577.
- [4] Wang FP, Chen QH, Liu XY. (2010) Diterpenoid alkaloids. *Natural Product Reports*, **27**, 529-570.
- [5] Chinese Academy of Science China Flora Editorial board. (1979) *Flora Republicae Popularis Sinicae*, Vol. **27**. Beijing, Science Press, 442.
- [6] Chen FZ, Chen DL, Chen QH, Wang FP. (2009) Diterpenoid Alkaloids from *Delphinium majus*. *Journal of Natural Products*, **72**, 18-23.
- [7] Joshi BS, Glinski JA, Chokshi HP. (1984) Deltatsine, a new C19-diterpenoid alkaloid from *Delphinium tatsienense* Franch. *Heterocycles*, **22**, 2037-2042.

Plant material: *Delphinium majus* was collected in Yanbian County, Sichuan Province, People's Republic of China, in June 2012. The plant was authenticated by associate professor Qi Zhao of the Key Laboratory of Medicinal and Edible Plant Resources, Development of Sichuan Education Department, Chengdu University, where a voucher specimen (201201) has been deposited.

Extraction and isolation: Air-dried and powdered whole herbs of *Delphinium majus* (2.0 kg) were percolated with 0.1 M HCl (7 L). The obtained acid aqueous solution was basified with 10% aqueous NH₄OH to pH 9-10 and then extracted with ethyl acetate (4 L × 3). Removal of the solvent under reduced pressure afforded the total crude alkaloids (8.2 g) as a yellowish amorphous powder, which was chromatographed over a silica gel column, eluting with cyclohexane-acetone (8:1→1:1) gradient system, to give fractions A (105 mg), B (2.3 g), C (1.8 g), and D (2.9 g). Fraction D was separated over a silica gel H column, eluting with CHCl₃-CH₃OH (40:1 → 10:1), to yield majusine D (**1**) (11 mg).

Majusine D (**1**)

White amorphous powder.

$[\alpha]_D^{20} : +22.6 (c \ 1.0, \text{CHCl}_3)$.

IR (KBr): 3478, 2939, 1636, 1233, 726 cm⁻¹.

^1H NMR: Table 1.

^{13}C NMR: Table 1.

ESI-MS *m/z* (%): 466 (100), 678[M+H]⁺ (1).

HR-ESI-MS *m/z*: found 466.2812 (100), calcd. for C₂₅H₃₉NO₇, 466.2804; 678.4166 (1.2)[M+H]⁺, calcd. for C₃₇H₆₀NO₁₀, 678.4139.

Acknowledgments - This work was financially supported by Chengdu Science and Technology Bureau (No. 12DXYB155JH-002) and the Science and Technology Department of Sichuan Province (No.2014JY0144).

Epoxide Opening of a 7,17-Seco-7,8-Epoxy-C₁₉-Diterpenoid AlkaloidHong Ji^a, Feng-Peng Wang^{b*} and Qiao-Hong Chen^{c*}^aPharmaceutical Research Center, School of Pharmaceutical Science, Guangzhou Medical University, Guangzhou, Guangdong 511436, China^bDepartment of Chemistry of Medicinal Natural Products, West China College of Pharmacy, Sichuan University, Chengdu, Sichuan 610041, China^cDepartment of Chemistry, California State University, Fresno, 2555 E. San Ramon Ave. M/S SB70, Fresno, California USA 93740

wfp@scu.edu.cn, qchen@csufresno.edu

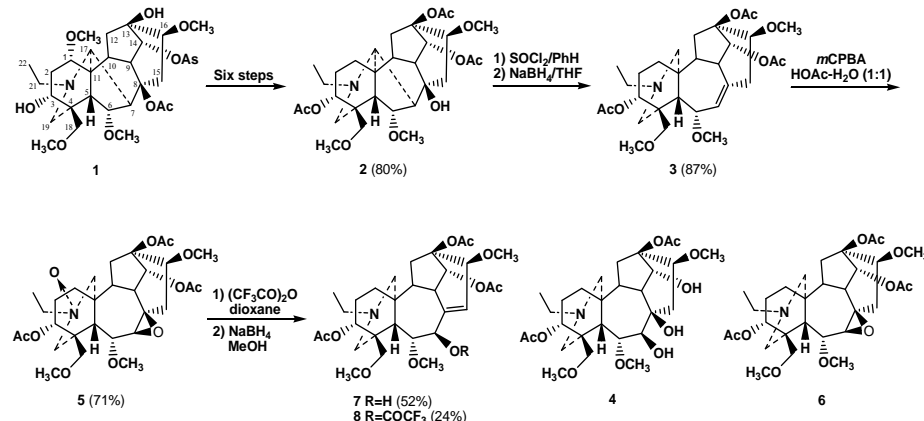
Received: September 23rd, 2015; Accepted: October 28th, 2015

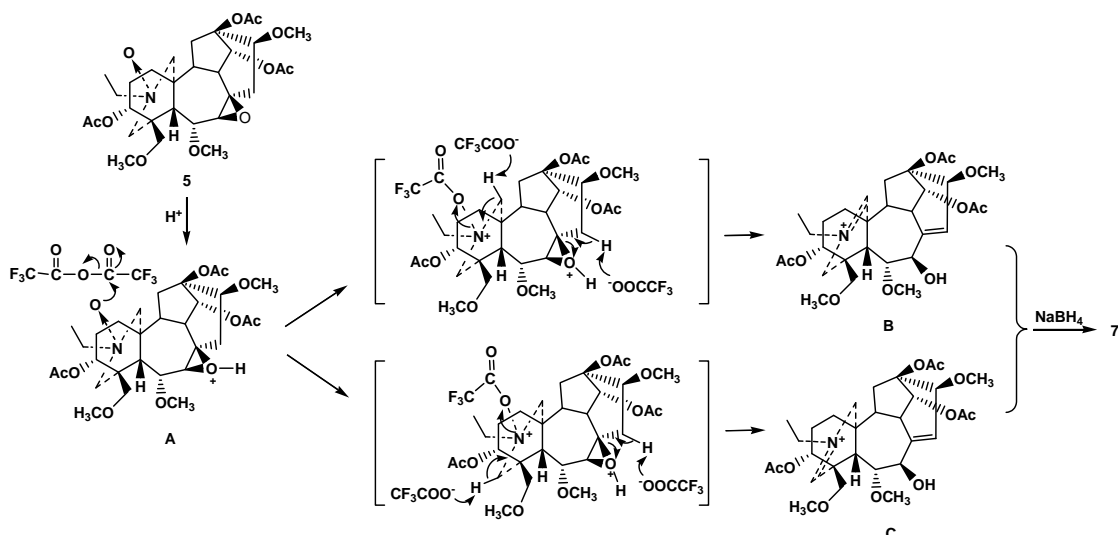
A new and effective approach toward epoxide opening of a 7,17-seco-7,8-epoxy-C₁₉-diterpenoid alkaloid is herein described. The starting epoxide was prepared from naturally occurring yunnaconitine via a nine-step transformation. Treatment of this epoxide with trifluoroacetic anhydride in dioxane at 110°C followed by reduction with sodium boron hydride generated two epoxide opening compounds **7** and **8**. Each of their structures is characteristic of a $\Delta^{8,15}$ bridgehead double bond and a 7 β -oxygen-substituted group.

Keywords: C₁₉-diterpenoid alkaloid, Epoxide-opening.

Numerous C₁₉-diterpenoid alkaloids have been isolated from a variety of *Aconitum* and *Delphinium* (Ranunculaceae). Certain species have long been used as traditional Chinese medicines for the treatment of various diseases [1-2]. It has been demonstrated that C₁₉-diterpenoid alkaloids exhibited a plethora of biological activities [3-4]. We started to develop conversional synthesis of taxoids starting from C₁₉-diterpenoid alkaloids since early 1990s. During the course, several novel approaches to the taxane ABC ring system and numerous intriguing reactions of C₁₉-diterpenoid alkaloids have been reported [5-13]. We have found that modifications of ring B, including cleavage of C7-C17, enlargement of ring B, functionalization of C-7 and C-8 for assembly of the $\Delta^{8,15}$ bridgehead double bond, and introduction of functional groups with specific configurations, were part of the critical steps to our successful conversions from aconitine-type C₁₉-diterpenoid alkaloids [5-7] to the core structure of taxoids. During the B-ring modifications of yunnacotinine [11], an efficient and convenient approach to the 7,8-epoxide opening was found. We herein describe this epoxide-opening reaction, together with the structure characterization of the novel C₁₉-diterpenoid alkaloid derivatives resulted from this reaction.

Naturally occurring yunnaconitine (**1**) was readily converted to its derivative **2** through a six-step procedure in 80% overall yield according to the procedure as previously described by us [7]. In hope to facilitate the functionalization of C-7 and C-8, the C7-C17 bond in alkaloid **2** was cleaved by reacting with thionyl chloride in benzene followed by reducing with NaBH₄ to furnish compound **3** (Figure 1) [7]. The oxygenated groups at C-7 and C-8 was desired for the construction of the $\Delta^{8,15}$ bridgehead double bond in taxoid ABC ring system. Several attempts to introduce oxygenated groups at C-7 and C-8 were unfortunately failed. For example, addition of the $\Delta^{7,8}$ double bond in **3** through oxymercurcation reaction did not occur. The attempted addition with HOBr or Br₂ was also not successful probably due to the participation of the nitrogen atom. Dihydroxylation of 7,17-seco-diterpenoid alkaloid **3** produced expected 7,8-oxygenated alkaloid **4**. As compared with **3**, the NMR spectra of **4** showed the absence of the $\Delta^{7,8}$ double bond as well as an acetyl group, and the presence of two additional oxygenated carbons (δ_H 3.75 d and δ_C 71.3 d for a tertiary carbon; δ_C 76.0 s for a quaternary carbon), indicating the structure of compound **4** as described in Figure 1. However, we had to give up this synthetic method due to the extremely low yield of **4**.





Scheme 1: A Plausible Mechanism from 5 to Compounds 7 and 8

Table 1: NMR spectral data of compound 7 in CDCl_3 (400 MHz for ^1H , 100 MHz for ^{13}C).

No.	δ_{C}	δ_{H} mult. (J in Hz)	HMBC ($\text{H} \rightarrow \text{C}$)
1	27.7 t	1.59 m 1.77 m	C-2, C-3, C-5, C-11 C-2, C-3, C-5, C-11
2	34.9 t	1.37 m 1.82 m	C-1, C-4, C-11 C-1, C-3, C-4, C-11
3	72.5 d	5.02 dd (10.8, 6.8)	C-2, C-4, C-18, C-19
4	42.5 s	—	—
5	39.4 d	1.71 brs	C-3, C-4, C-6, C-11, C-18
6	81.0 d	3.60 d (5.2)	C-4, C-5, C-7, C-8, C-11, 6-OCH ₃
7	74.1 d	3.97 d (5.2)	C-6, C-8, C-9
8	137.1 s	—	—
9	47.5 d	2.62 m	C-7, C-8, C-11, C-12, C-15
10	38.5 d	2.47 m	C-8, C-9, C-11, C-12, C-14
11	37.4 s	—	—
12	45.5 t	1.23 m 1.94 m	C-10, C-14 C-9, C-11, C-13, C-14
13	85.1 s	—	—
14	74.8 d	5.47 d (3.6)	C-8, C-10, C-13
15	122.3 d	5.78 d (5.2)	C-8, C-9, C-13, C-16
16	80.9 d	4.45 d (5.2)	C-8, C-12, C-14, 16-OCH ₃
17	52.2 t	2.12 m 2.38 m	C-5, C-10, C-11 C-5, C-11
18	73.2 t	3.37 ABq (9.2) 3.52 ABq (9.2)	C-3, C-4, C-5, C-19, 18-OCH ₃ C-3, C-4, C-5, C-19, 18-OCH ₃
19	57.3 t	2.32 m 2.50 m	C-3, C-5, C-18 C-3, C-4, C-5, C-18
21	50.9 t	2.42 q (6.8)	C-22
22	12.1 q	0.98 t (6.8)	C-21
6-OCH ₃	56.1 q	3.26 s	C-6
16-OCH ₃	58.8 q	3.46 s	C-16
18-OCH ₃	59.2 q	3.33 s	C-18
3-OAc	171.0 s	—	—
13-OAc	21.1 q	2.03 s	3-OCO
170.9 s	—	—	—
13-OAc	21.9 q	2.07 s	13-OCO
170.3 s	—	—	—
14-OAc	21.2 q	2.06 s	14-OCO

In order to avoid the possible oxidation of nitrogen and subsequently to improve the yield, acidic conditions were selected for the epoxidation of alkaloid 3. Exposure of compound 3 to 30% H_2O_2 in formic acid for 2 h generated epoxides 5 (59%) and 6 (10%). The molecular formulas of compounds 5 and 6 ($\text{C}_{30}\text{H}_{45}\text{NO}_{11}$ and $\text{C}_{30}\text{H}_{45}\text{NO}_{10}$) were determined by their HR-MS data. In the NMR spectra of 6, the signals for the $\Delta^{7,8}$ double bond disappeared while the characteristic signals at $\delta_{\text{H}} 3.75$ (1H, d, $J = 8.8$ Hz), and $\delta_{\text{C}} 65.6$ d and 60.4 s were observed. Compound 5 possesses the same unsaturated degree as 6, but with 16 more mass units as compared with 6 as determined by their mass spectra, indicating that epoxide 5 is the *N*-oxidation derivative of 6. The NMR spectra of 5 exhibited characteristic signals at $\delta_{\text{H}} 1.61$ (3H, t, $J = 6.8$ Hz) and $\delta_{\text{C}} 12.1$ q for an *N*-ethyl group [14].

The comparison of the ^{13}C -NMR spectra of 5 and 6 showed different δ values at C-1, C-2, and C-3, especially at C-17, C-19, C-21, and C-22, due to the *N*-oxidation effect [14]. This led to the determination of the structure for epoxide 5. Treatment of 3 with an excess *m*CPBA in $\text{HOAc-H}_2\text{O}$ (1:1) under refluxing conditions also afforded compound 5 in 71% yield. Considering that the nitrogen oxidation was inevitable and that attempt to reduce 5 into 6 failed, epoxide 5 was directly used as a substrate for the subsequent epoxide ring-opening reaction. We attempted to treat 5 with acid activated silica gel or various kinds of acids (98% formic acid, 20% H_2SO_4 and trifluoroacetic acid *etc.*) respectively, but no reactions occurred in such cases. An acetic anhydride instead of acids was used in the reaction, resulting in an unidentified product. We then tried to use trifluoroacetic anhydride which yielded two inseparable, highly polar products. The ^1H NMR spectrum of the crude product suggested that they are the corresponding iminium salts containing the $\Delta^{8,15}$ double bond. Without further purification, the crude product was directly reduced with NaBH_4 in MeOH , leading to two expected 7-oxygenated-7,17-*seco*-diterpenoid alkaloids 7 and 8. The molecular formulas for these two desired products are $\text{C}_{30}\text{H}_{45}\text{NO}_{10}$ and $\text{C}_{32}\text{H}_{44}\text{F}_3\text{NO}_{11}$, respectively, as determined by their HR-MS data. The NMR spectra of 7 displayed the absence of the signals for the epoxide moiety but the presence of characteristic signals at $\delta_{\text{H}} 5.78$ (1H, d, $J = 5.2$ Hz), and $\delta_{\text{C}} 137.1$ s and 122.3 d for a trisubstituted double bond. This double bond was attributed to C-8 and C-15 due to the multi-bond $^1\text{H}-^{13}\text{C}$ correlations of H-15 with C-8, C-9, C-13 and C-16 in its HMBC spectrum. In the NMR spectra of 7, in addition to the distinctive upfield shifts of C-17, C-19, and C-21, the chemical shifts for *N*-ethyl group at $\delta_{\text{H}} 0.98$ (3H, t, $J = 6.8$ Hz) and $\delta_{\text{C}} 12.1$ q were also greatly changed as compared with those of 5, suggesting that the *N*-oxide in 5 has been reduced back to tertiary amine. The structure of 7 was confirmed by its 2D NMR data, as shown in Table 1. The NMR spectra of 8 are very similar to those of 7, except for the existence of signals for an additional trifluoroacetyl group. The structure of 8 was thus determined as illustrated in Figure 1. The plausible mechanism for the formation of 7-oxygenated compounds 7 and 8 was proposed. As shown in Scheme 1, in the presence of trifluoroacetic anhydride and a trace amount of H_2O in dioxane, protonation of epoxide oxygen in 5, followed by ring opening and elimination resulted in the formation of the $\Delta^{8,15}$ double bond. Additionally, esterification of *N*-oxide in 5 with trifluoroacetic anhydride and subsequent

Polonovski-like process can produce a pair of regiosomeric immonium salts **B** and **C**. Reduction of immonium salts may yield compound **7** while reduction of the immonium salts followed by acylation may generate compound **8**.

Table 2: ¹³C NMR spectral data of compounds **4–6** and **8** (50 MHz, CDCl₃).

No.	4	5	6	8
1	27.9 t	23.2 t	26.4 t	26.8 t
2	32.5 t	36.7 t	38.0 t	34.3 t
3	74.4 d	72.5 d	74.5 d	71.9 d
4	42.7 s	41.6 s	42.5 s	41.0 s
5	44.2 d	45.0 d	45.3 d	37.7 d
6	81.8 d	79.9 d	79.6 d	77.7 d
7	71.3 d	65.6 d	65.6 d	76.1 d
8	76.0 s	60.4 s	60.5 s	137.6 s
9	42.6 d	54.2 d	53.8 d	47.9 d
10	39.1 d	38.8 d	39.3 d	42.2 d
11	37.4 s	38.5 s	37.4 s	37.4 s
12	34.5 t	37.7 t	37.4 t	43.8 t
13	84.3 s	84.2 s	83.8 s	85.0 s
14	80.9 d	78.9 d	79.2 d	74.5 d
15	46.4 t	46.1 t	46.7 t	121.9 d
16	81.3 d	81.2 d	80.9 d	79.3 d
17	58.4 t	69.6 t	54.7 t	51.6 t
18	73.5 t	72.4 t	72.0 t	70.0 t
19	52.3 t	65.2 t	48.1 t	57.7 t
21	50.8 t	62.4 t	51.5 t	50.5 t
22	12.1 q	8.7 q	13.3 q	12.2 q
6-OCH ₃	56.3 q	56.2 q	55.8 q	56.1 q
16-OCH ₃	58.1 q	57.3 q	57.6 q	58.6 q
18-OCH ₃	59.2 q	59.1 q	58.9 q	59.1 q
3-OAc	170.8 s	170.7 s	170.6 s	170.7 s
	21.2 q	21.2 q	21.1 q	21.1 q
13-OAc	170.2 s	170.5 s	170.4 s	170.9 s
	21.7 q	21.6 q	21.4 q	21.5 q
14-OAc	—	170.1 s	170.1 s	170.3 s
	—	21.4 q	21.2 q	21.3 q
7-OCOCF ₃	—	—	—	159.3 s
	—	—	—	114.7 s

In conclusion, a convenient and effective epoxide-opening method of 7,17-seco-7,8-epoxy-C₁₉-diterpenoid alkaloid was found. The products **7** and **8** achieved from this study serve as critical intermediates for the assembly of a taxoid ring system bearing a $\Delta^{8,15}$ bridgehead double bond and an oxygenated group at 7 β position. Higher reactivity of trifluoroacetic anhydride and the rigid structure of the C₁₉-diterpenoid alkaloid derivatives may be the main reasons for the formation of products **7** and **8** with the $\Delta^{8,15}$ bridgehead double bond and with the hydroxyl group at the 7 β position.

Experimental

General: Melting points were determined on a Kofler block (uncorrected); IR spectra were recorded on a Nicolet FT-IR 200 SXV spectrometer; Optical rotations were measured in a 1.0-dm cell by a PE-314 polarimeter at 20 \pm 1 °C; ¹H- and ¹³C-NMR spectra were acquired on a Varian INOVA 400/54 or a Bruker AC-E 200 spectrometer in CDCl₃ with TMS as internal standard; MS spectra were obtained on Finnigan LCQ and Micromass Auto Spec Ultima-Tof spectrometer; Silica gel GF₂₅₄ and H (10–40 μ m, Qingdao Sea Chemical Factory, China) were used for TLC, Chromatotron, and CC.

Compound 4: A solution of KMnO₄ (131 mg, 0.83 mmol) in H₂O (13 mL) was added dropwise to a solution of compound **3** (235 mg, 0.41 mmol) and NaCO₃ (470 mg, 5.66 mmol) in dioxane-H₂O (1:1, 20 mL). The mixture was stirred at room temperature for 20 min. The precipitate was removed by vacuum filtration and washed with dioxane. The filtrate and washings were combined, and the solvent was removed under reduced pressure. This residue was suspended in H₂O (20 mL) and extracted with ethyl acetate (20 mL \times 3), the combined organic extracts were dried with anhydrous NaSO₄, and the solvent was removed under reduced pressure. Chromatography

of the residue (200 mg) on silica gel (6 g) using cyclohexane-acetone (4:1) as eluent afforded compound **4** (white amorphous powder, 30 mg, 13%).

MP: 166–168 °C.

[α]_D²⁰: -32.5 (*c* 1.20, CHCl₃).

IR (KBr): 3462, 1742, 1451, 1253 cm⁻¹.

¹H NMR (400 MHz, CDCl₃): 0.99 (3H, t, *J* = 7.2 Hz, NCH₂CH₃), 2.04, 2.10 (each 3H, s, 2 \times OAc), 3.26, 3.37, 3.38 (each 3H, s, 3 \times OMe), 3.75 (1H, d, *J* = 5.2 Hz, H-7 α), 3.89 (1H, d, *J* = 5.2 Hz, H-14 β), 4.31 (1H, t, *J* = 4.8 Hz, H-16 α), 4.35 (1H, d, *J* = 6.0 Hz, H-6 β), 4.99 (1H, dd, *J*₁ = 11.2 Hz, *J*₂ = 7.2 Hz, H-3 β), 5.56 (1H, d, *J* = 4.8 Hz, OH-7).

¹³C NMR: Table 2.

ESI-MS: *m/z* (%) = 556 [M + H⁺] (100).

HRMS-ESI: *m/z* [M + H⁺] calcd for C₂₈H₄₆NO₁₀: 556.2998; found: 556.2989.

Compound 5 and 6: A solution of compound **3** (135 mg, 0.24 mmol) in HCOOH (3 mL) was cooled in an ice-water bath, and 30% H₂O₂ (2 mL) was added dropwise. After stirring for 10 min, the mixture was allowed to warm to room temperature and stirred for 2 h. After pouring into ice water (5 mL), the solution was basified with conc. NH₄OH to pH 10. The aqueous layer was extracted with CHCl₃ (8 mL \times 3). The combined extracts were dried (Na₂SO₄) and concentrated. The residue (153 mg) was subjected to column chromatography (silica gel H, 3 g), eluted with CHCl₃–MeOH (18:1) to afford **5** (white amorphous powder, 84 mg, 59%) and **6** (white amorphous powder, 14 mg, 10%).

Compound 5

MP: 116–118 °C.

[α]_D²⁰: +18.6 (*c* 2.30, CHCl₃).

IR (KBr): 1738, 1261, 892, 811 cm⁻¹.

¹H NMR (200 MHz, CDCl₃): 1.61 (3H, t, *J* = 7.0 Hz, NCH₂CH₃), 2.08, 2.11, 2.13 (each 3H, s, 3 \times OAc), 3.25, 3.35, 3.44 (each 3H, s, 3 \times OMe), 3.91 (1H, t, *J* = 8.0 Hz, H-16 α), 4.49 (1H, d, *J* = 6.2 Hz, H-6 β), 4.67 (1H, brs, H-7), 4.84 (1H, d, *J* = 5.0 Hz, H-14 β), 5.18 (1H, dd, *J*₁ = 10.8 Hz, *J*₂ = 7.2 Hz, H-3 β).

¹³C NMR: Table 2.

ESI-MS: *m/z* (%) = 596 [M + H⁺] (100).

HRMS-ESI: *m/z* [M + H⁺] calcd for C₃₀H₄₆NO₁₁: 596.3075; found: 596.3087.

Compound 6

MP: 132–134 °C.

[α]_D²⁰: -27.3 (*c* 0.68, CHCl₃).

IR (KBr): 1738, 1245, 1193, 936, 797 cm⁻¹.

¹H NMR (400 MHz, CDCl₃): 1.10 (3H, t, *J* = 7.2 Hz, NCH₂CH₃), 2.04, 2.06, 2.09 (each 3H, s, 3 \times OAc), 3.21, 3.25, 3.32 (each 3H, s, 3 \times OMe), 3.75 (1H, d, *J* = 8.8 Hz, H-7), 3.82 (1H, t, *J* = 8.0 Hz, H-16 α), 4.01 (1H, d, *J* = 6.4 Hz, H-6 β), 4.89 (1H, d, *J* = 5.2 Hz, H-14 β), 4.93 (1H, dd, *J*₁ = 12.4 Hz, *J*₂ = 5.6 Hz, H-3 β).

¹³C NMR: Table 2.

ESI-MS: *m/z* (%) = 580 [M + H⁺] (100).

HRMS-ESI: *m/z* [M + H⁺] calcd for C₃₀H₄₆NO₁₀: 580.2995; found: 580.2982.

Compound 5: To a solution of compound **3** (135 g, 0.24 mmol) in HOAc-H₂O (1:1, 5 mL) was added *m*CPBA (165 mg, 0.96 mmol). The mixture was refluxed for 2 h and cooled prior to being poured into ice water (5 mL). The solution was basified with conc. NH₄OH solution to pH 10 and extracted with CHCl₃ (8 mL \times 3). The extracts were dried (Na₂SO₄) and concentrated. Column chromatography

(silica gel H, 3 g) of the residue (148 mg) using CHCl₃-MeOH (18:1) as eluent afforded **5** as a white amorphous powder (102 mg, 71%).

Compound 7 and 8: To a solution of compound **5** (142 mg, 0.24 mmol) in dioxane (10 mL) was added trifluoroacetic anhydride (1 mL). The mixture was refluxed for 3 h and then concentrated under reduced pressure. The residue was diluted with H₂O (10 mL), basified with conc. NH₄OH solution to pH 10, and extracted with CHCl₃ (8 mL×3). The extracts were dried (Na₂SO₄) and concentrated to give a crude. The crude was dissolved in MeOH (5 mL), to which was added NaBH₄ (36 mg, 0.96 mmol). The solution was stirred at room temperature for 4 h. After removal of the solvent, the residue was diluted with water (5 mL). The subsequent mixture was extracted with ethyl acetate (4 mL×3), the extracts were dried (Na₂SO₄), and the organic solvent was removed *in vacuo*. Chromatography of the residue (138 mg) on silica gel (4 g) using cyclohexane-acetone (6:1) as eluent afforded **7** (a white amorphous powder, 71 mg, 52%) and **8** (a white amorphous powder, 39 mg, 24%).

Compound 7

MP: 123-124°C.

[α]_D²⁰: +23.3 (*c* 0.82, CHCl₃).

References

- [1] Amiya T, Bando H. (1988) *The Alkaloids*. Vol. **34**, Brossi A. (Ed). Academic Press, San Diego, 95-179.
- [2] Wink M. (1998) *Alkaloids: Biochemistry, Ecology, and Medicinal Applications*. Roberts MF, Wink M. (Ed). Plenum Press, New York. 11-44.
- [3] Wang FP, Chen QH. (2010) The C₁₉-diterpenoid alkaloids. In *The Alkaloids, Chemistry and Biology*. Vol. **69**, Cordell, GA. (Ed). Elsevier, London UK. 1-577.
- [4] Wang FP, Chen QH, Liu XY. (2010) Diterpenoid alkaloids. *Natural Product Reports*, **27**, 529-570.
- [5] Wang FP, Xu L. (2005) To seek an approach toward the chemical conversion of C₁₉-diterpenoid alkaloids to taxoids. *Tetrahedron*, **61**, 2149-2167.
- [6] Zou CL, Cai L, Ji H, Xie GB, Wang FP. (2008) A novel approach to the taxane ABC ring system through chemical conversion from C₁₉-diterpenoid alkaloid deltaline. *Tetrahedron*, **64**, 7594-7604.
- [7] Ji H, Chen QH, Zhu M, Wang FP. (2010) Conversational studies towards taxoids from C₁₉-diterpenoid alkaloids by the BAC sequence. *Journal of Asian Natural Product Research*, **12**, 968-977.
- [8] Cheng H, Xu L, Chen DL, Chen QH, Wang FP. (2012) Construction of functionalized B/C/D-ring system of C₁₉-diterpenoid alkaloids via intramolecular Diels-Alder reaction followed by Wagner-Meerwein rearrangement. *Tetrahedron*, **68**, 1171-1176.
- [9] Liang XX, Tang P, Chen QH, Wang FP. (2012) Synthesis of taxane ABC tricyclic skeleton from lycocotonine. *Natural Product Communications*, **7**, 697-703.
- [10] Liu ZG, Xu L, Chen QH, Wang FP. (2012) Construction of A/E/F ring systems of C₁₉-diterpenoid alkaloids with both C-1 and C-6 oxygen functions. *Tetrahedron*, **68**, 159-165.
- [11] Ji H, Chen QH, Wang FP. (2009) A novel conversion of C₁₉-diterpenoid alkaloids into aconane-type diterpenes with eight-membered ring system *via* skeletal rearrangement of corresponding diazonium derivatives. *Chemical and Pharmaceutical Bulletin*, **57**, 233-239.
- [12] Wang FP, Chen QH. (2003) Further studies on the synthesis of 7,17-seco norditerpenoid alkaloids. *Journal of Asian Natural Products Research*, **5**, 43-48.
- [13] Wang L, Chen QH, Wang FP. (2012) Unusual reactions of a 7,17-seco-type C₁₉-diterpenoid alkaloid derived from deltaline. *Natural Product Communications*, **7**, 721-724.
- [14] Bai YL, Desai HK, Pelletier SW. (1995) N-oxides of some norditerpenoid alkaloids. *Journal of Natural Products*, **58**, 929-933.

IR (KBr): 3468, 1740, 1452, 1366, 1092 cm⁻¹.

¹H NMR (400 MHz) and ¹³C NMR (100 MHz, CDCl₃): Table 1.

ESI-MS: *m/z* (%) = 580 [M + H⁺] (100).

HRMS-ESI: *m/z* [M + H⁺] calcd for C₃₀H₄₆NO₁₀: 580.2995; found: 580.2981.

Compound 8

MP: 137-139°C.

[α]_D²⁰: +10.5 (*c* 0.24, CHCl₃).

IR (KBr): 1788, 1525, 1374, 1078 cm⁻¹.

¹H NMR (400 MHz, CDCl₃): 0.98 (3H, t, *J* = 6.8 Hz, NCH₂CH₃), 2.02, 2.04, 2.08 (each 3H, s, 3×OAc), 3.10, 3.41, 3.47 (each 3H, s, 3×OMe), 3.85 (1H, d, *J* = 5.2 Hz, H-6 β), 4.04 (1H, d, *J* = 4.8Hz, H-16 α), 4.94 (1H, dd, *J*₁ = 11.2 Hz, *J*₂ = 7.2 Hz, H-3 β), 5.47 (1H, d, *J* = 3.6 Hz, H-14 β), 5.57 (1H, d, *J* = 4.8 Hz, H-7), 5.96 (1H, d, *J* = 5.2 Hz, H-15).

¹³C NMR: Table 2.

ESI-MS: *m/z* (%) = 698 [M + Na⁺] (100).

HRMS-ESI: *m/z* [M + Na⁺] calcd for C₃₂H₄₄F₃NO₁₁Na: 698.2259; found: 698.2272.

Acknowledgments - Financial support for this research was provided by the National Natural Science Foundation of China (No. 30873147).

Further Studies on Structure-Cardiac Activity Relationships of Diterpenoid Alkaloids

Zhong-Tang Zhang^a, Xi-Xian Jian^a, Jia-Yu Ding^b, Hong-Ying Deng^a, Ruo-Bing Chao^{b*}, Qiao-Hong Chen^{c*}, Dong-Lin Chen^a and Feng-Peng Wang^{a,*}

^aDepartment of Chemistry of Medicinal Natural Products and ^bDepartment of Chemistry of Medicinal Analysis, West China College of Pharmacy, Sichuan University, Chengdu 610041, PR. China

^cDepartment of Chemistry, California State University, Fresno, 2555E. San Ramon Ave. M/S SB 70 Fresno, California 93740, USA

wfp@scu.edu.cn; rbchao@scu.edu.cn; qchen@csufresno.edu

Received: July 12th, 2015; Accepted: August 14th, 2015

The cardiac effect of thirty-eight diterpenoid alkaloids was evaluated on the isolated bullfrog heart model. Among them, twelve compounds exhibited appreciable cardiac activity, with compounds **3** and **35** being more active than the reference drug lanatoside. The structure-cardiac activity relationships of the diterpenoid alkaloids were summarized based on our present and previous studies [2]: i) 1 α -OMe or 1 α -OH, 8-OH, 14-OH, and NH (or NMe) are key structural features important for the cardiac effect of the aconitine-type C₁₉-diterpenoid alkaloids without any esters. C₁₈-diterpenoid alkaloids, lycocotonine-type C₁₉-diterpenoid alkaloids, and the veatchine- and denudatine-type C₂₀-diterpenoid alkaloids did not show any cardiac activity; ii) the presence of 3 α -OH is beneficial to the cardiac activity; iii) the effect on the cardiac action of 6 α -OMe, 13-OH, 15 α -OH, and 16-demethoxy or a double bond between C-15 and C-16 depends on the substituent pattern on the nitrogen atom.

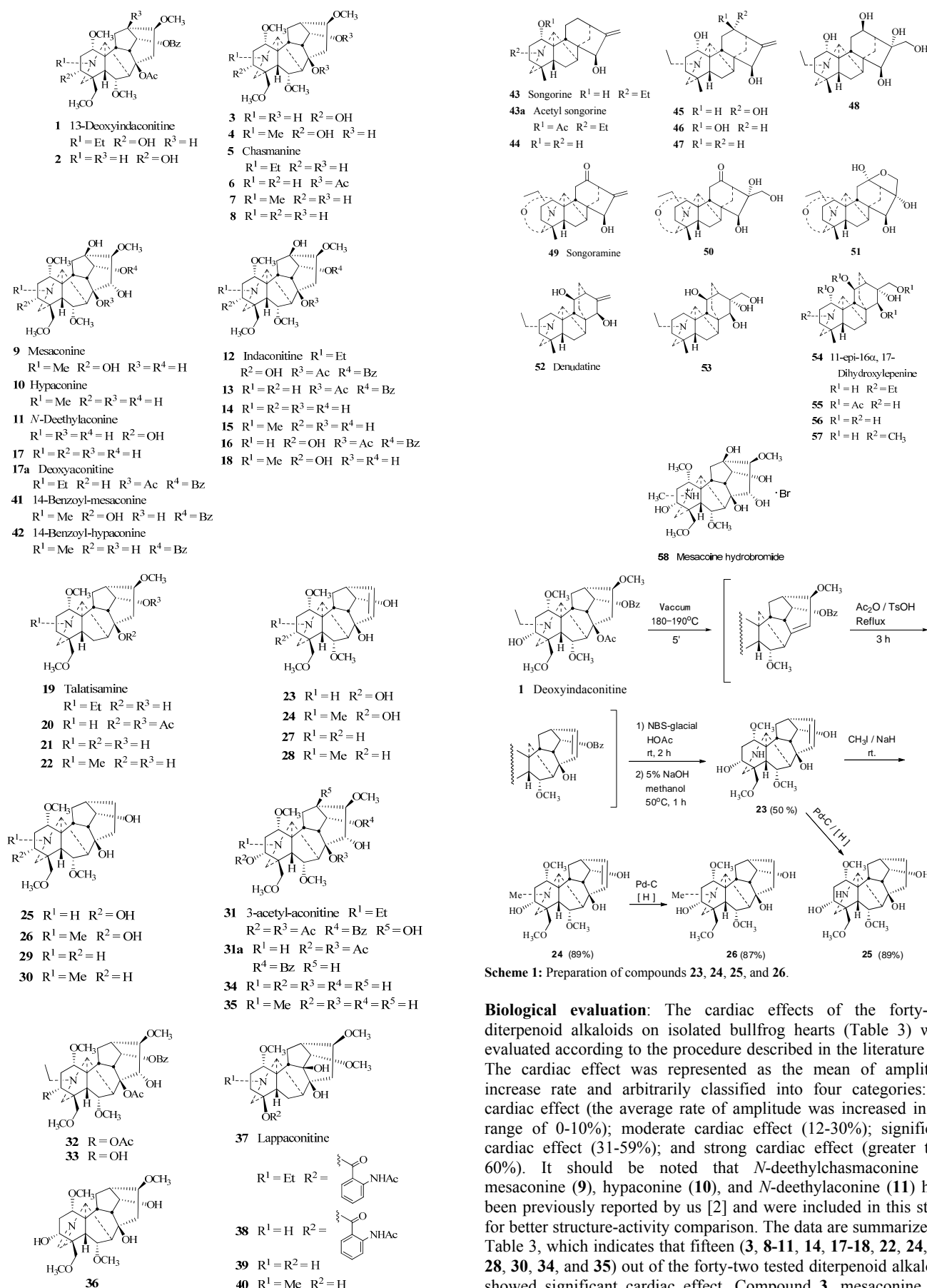
Keywords: Diterpenoid alkaloid, Cardioactive evatuation, Structure-activity relationships.

“Fuzi” (*Aconitum carmichaeli*) is a profound folk medicine throughout China, Japan, and Korea, as well as other regions in Southeast Asia. In search of diterpenoid alkaloids with considerable cardiac effect, we have previously isolated C₁₉-diterpenoid alkaloids as its chemical components with cardiac activity [1] and initiated the associated structure-activity relationships [2]. For further in-depth structure-activity studies and search for possible candidates for clinical development, thirty-eight C₁₈, C₁₉, and C₂₀-diterpenoid alkaloids were designed and synthesized using either mesaconine and hypaconine or lappaconitine, songorine, acetylsongorine, denudatine, and 11-epi-16 α ,17-dihydroxylepenine as the starting materials. Their cardiac effect was assessed on the isolated bullfrog heart model. The preparation, biological evaluation, and systematic structure-activity relationships of these alkaloids are presented herein.

The known and naturally occurring diterpenoid alkaloids, 13-deoxyindaconitine, chasmanine, 14-benzoylmesaconine, 14-benzoylmesaconine, indaconitine, deoxyaconitine, talatisamine, 3-acetylaconitine, lappaconitine, songorine, acetylsongorine, songoramine, denudatine, 11-epi-16 α ,17-dihydroxylepenine, and mesaconine hydrobromide, were extracted from either *Aconitum* or *Delphinium* spp. by one of our laboratories.

All N-deethylation of diterpenoid alkaloids in this paper was achieved according to the method reported by us [3, 4]; all N-methylation was accomplished by reacting with methyl iodide in the presence of sodium hydride. Compound **3** was prepared by N-deethylation of 13-deoxyindaconitine (**1**) followed by hydrolysis. Compound **4** was prepared by methylation of **2** followed by hydrolysis. Compound **6** was made by acylation of chasmanine (**5**), followed by N-deethylation. Compounds **7** and **8** were obtained by methylation of **6** followed by hydrolysis. Compound **13** was prepared by treatment of indaconitine (**12**) with thionyl chloride, followed by hydrogenation (H₂/Pd). Compounds **14** and **15** were

made from **13** using a similar procedure as that illustrated for the preparation of compounds **3** and **4**, respectively. Similarly, compounds **17** and **18** were prepared from **17a** and **12**, respectively. Compounds **21** and **22** were produced from talatisamine (**19**) via a three-step procedure including acetylation, N-deethylation, and hydrogenation. Compounds **23**, **24**, **25**, and **26** were prepared from 13-deoxyindaconitine (**1**) through a reaction sequence as shown in Scheme 1, including pyrolysis, isopyro rearrangement, N-deethylation, N-methylation or Pd/C-catalyzed hydrogenation. Similarly, compounds **27**, **28**, **29**, and **30** were obtained from chasmanine (**5**) through diacetylchasmanine (**6**). Compound **34** was prepared from 3-acetylaconitine (**31**) by a three-step reaction sequence including Barton's oxygenation [5], N-deethylation, and hydrolysis. Methylation of **31a** (prepared from **31**) with CH₃I/NaH, followed by hydrolysis, gave compound **35**. Compound **36** was prepared from 13-deoxyindaconitine (**1**) by N-deethylation and hydrolysis. Compound **38** was produced by N-deethylation of lappaconitine (**37**). Compounds **39** and **40** were prepared from compound **38** via hydrolysis, and methylation and hydrolysis, respectively. Compound **44** was prepared from songorine (**43**) according to the procedure described in the literature [3, 4]. Reduction of songorine (**43**) with NaBH₄ resulted in compounds **45** and **46**, while reduction of songorine (**43**) using the Huang-Minlon method with modification led to compound **47**. Oxidation of compound **46**, songoramine (**49**), and denudatine (**52**) with H₂O₂-MeOH produced compounds **48**, **50** and **51**, as well as **53**, respectively. Treatment of **55** [prepared from 11-epi-16 α -17-dihydroxylepenine (**54**)] with 5% NaOH solution in methanol followed by CH₃I-NaH gave compounds **56** and **57**. Their structures were established by comparison of their ¹H (¹³C) NMR data with those reported in the literature [6], as well as the high resolution mass data. The ¹³C NMR spectral data for all compounds (Tables 1, 2) were assigned based on comparing them with those of analogues.



Biological evaluation: The cardiac effects of the forty-two diterpenoid alkaloids on isolated bullfrog hearts (Table 3) were evaluated according to the procedure described in the literature [7]. The cardiac effect was represented as the mean of amplitude increase rate and arbitrarily classified into four categories: no cardiac effect (the average rate of amplitude was increased in the range of 0-10%); moderate cardiac effect (12-30%); significant cardiac effect (31-59%); and strong cardiac effect (greater than 60%). It should be noted that *N*-deethylchasmaconine (**8**) mesaconine (**9**), hypaconine (**10**), and *N*-deethylaconine (**11**) have been previously reported by us [2] and were included in this study for better structure-activity comparison. The data are summarized in Table 3, which indicates that fifteen (**3**, **8-11**, **14**, **17-18**, **22**, **24**, **25**, **28**, **30**, **34**, and **35**) out of the forty-two tested diterpenoid alkaloids showed significant cardiac effect. Compound **3**, mesaconine (**9**),

hypaconine (**10**), and compound **35** exhibit better cardiac effect than the reference drug lanatoside C.

A broad range (potent-to-inactive) of cardiac effects has been observed for the forty-two diterpenoid alkaloids with the following structure-activity relationships:

- 1) C_{18} -diterpenoid alkaloids (e.g. **39**, **40**) or the aconitine-type alkaloids containing a monoester [e.g. 14-benzoylmesaconine (**41**) and 14-benzoylhypaconine (**42**)], the veatchine-type C_{20} -diterpenid alkaloids (e.g. **43-48**, **50**, and **51**), and the denudatine-type C_{20} -diterpenoid alkaloids (e.g. **53**, **56** and **57**) did not exhibit any apparent cardiac effect. Additionally, no considerable effect was observed for the aconitine-type alkaloids that contain an imine moiety (e.g. **36**).
- 2) Consistent with the results that we previously reported [2], the aminoalcohol group of aconitine-type C_{19} -diterpenoid alkaloids bearing both hydroxyl groups at C-8 and C-14 are most essential structure features for the cardiac activity. The substituent pattern on the nitrogen atom (NH, NMe, or NEt), the hydroxyl group at C-3, C-15, and C-13, and the methoxyl group at C-6 can appreciably contribute to or abolish the activity. These can be specified as below: i) the alkaloids with a 3 α -OH (e.g. **3**, **4** and **18**) are more potent than those without it (e.g. **8**, **7**, and **15**), suggesting the presence of a 3 α -OH is beneficial to the cardiac effect, which is consistent with the conclusions in our previous paper [2]; ii) in addition to alkaloids **15** and **28**, the alkaloids that possess a methyl group on the nitrogen atom [e.g. mesaconine (**9**), **22**, **28**, and **35**] are more active than the corresponding compounds containing a hydrogen instead [e.g. *N*-deethylamine (**11**), **21**, **27**, and **34**]. The similar effect of the NMe on the cardiac activity can also be concluded by comparing the activity of **24/23**, **22/21**, and **30/29**. However, alkaloids that contain a NH moiety but no 13, 15 α -OH (e.g. **3**, **8**, and **29**) have greater activity than those with a NMe moiety (e.g. **4**, **7**, and **30**); iii) except for compound **7**, an alkaloid possessing a 16 α -OMe (e.g. **4**) is more active than the corresponding one without it (e.g. **26**) and the one with a double bond between C-15 and C-16 (e.g. **24**); iv) the alkaloids **7** and **8** that contain a 13-OH have significantly improved activity compared with their

corresponding alkaloids **15** and **14** that lack the 13-OH, suggesting that this group is also a determining factor for the cardiac action. V) the effect of 6 α -OMe on the cardiac activity depends on the substituent pattern on the nitrogen atom. Both NMe-containing compounds **7** and **22** did not show any cardiac activity, no matter with either the presence or absence of a 6 α -OMe. However, introduction of 6 α -OMe into the NH-containing compound **21** led to compound **8** with enhanced cardiac effect.

In conclusion, the structure-cardiac activity relationships of diterpenoid alkaloids are summarized as below based on our previous and current studies: i) 1 α -OMe or 1 β -OH, 8-OH, 14-OH, and NH (or NMe) are critical structural features necessary for the cardiac effect of the aconitine-type C_{19} -diterpenoid alkaloids without any esters. C_{18} -diterpenoid alkaloids, lycocytidine-type C_{19} -diterpenoid alkaloids, and the veatchine- and denudatine-type C_{20} -diterpenoid alkaloids did not possess any significant cardiac activity; ii) the existence of 3 α -OH can significantly improve the cardiac activity; iii) the effects on the cardiac activity of 6 α -OMe, 13-OH, 15 α -OH, and 16-demethoxy or a double bond between C-15 and C-16 heavily depend upon the substituent pattern on the nitrogen atom; iv) interestingly, mesaconine hydrobromide (**58**) without showing any *in vitro* cardiac activity exhibited significant and quick *in vivo* efficacy that is comparable with the free base mesaconine (**9**) [8].

Experimental

General methods: Melting points were determined on a Kofler block (uncorrected). IR spectra were obtained on a Nicolet FT-IR 200 SXV spectrophotometer. 1 H and 13 C NMR spectra were taken on a Varian Unity INOVA 400/54 NMR spectrometer in CDCl₃ with TMS as the internal standard. The ESIMS and HRESIMS were recorded on either a VG Auto Spec 3000 or a Finnigan-MAT 90 instrument. Silica gel H (Qingdao Marine Chemical Factory, Qingdao, China) was used for column chromatography (CC). Zones on TLC (silica gel G) plates were detected with modified Dragendorff's reagent.

Table 1: 13 C NMR spectral data of compounds **2-4**, **6**, **7**, **13-15**, **17**, **18**, and **20-25** (100 MHz, CDCl₃).

No.	2 ^a	3	4	6	7	13 ^b	14	15	17	18	20 ^c	21	22	23	24	25
1	83.2	75.2	83.1	83.7	82.1	83.1	83.0	85.7	83.4	84.1	83.1	84.6	86.2	81.8	82.7	82.3
2	37.5	34.7	33.9	28.9	34.7	35.1	29.3	34.8	28.4	35.3	28.0	30.5	32.5	35.3	34.0	34.3
3	71.4	71.5	72.3	23.3	25.8	23.4	23.6	25.8	22.8	72.3	24.9	26.1	25.8	71.6	71.8	71.5
4	43.6	43.6	43.5	38.9	39.4	39.0	39.1	39.4	38.6	43.4	37.8	38.3	38.2	43.8	43.5	43.7
5	47.5	47.9	48.4	43.8	48.5	44.0	49.2	50.4	51.5	50.1	44.3	38.5	37.5	54.9	47.9	57.0
6	81.3	82.1	81.9	82.4	82.1	82.5	82.6	82.1	82.2	82.8	24.6	27.0	24.6	81.3	81.5	81.3
7	55.5	56.3	51.2	53.4	51.4	43.6	57.3	51.1	47.4	50.8	47.4	52.7	45.1	47.5	47.5	48.2
8	85.5	81.7	71.9	85.8	72.4	85.6	74.3	72.8	76.1	72.3	85.9	73.2	72.7	73.8	73.8	75.1
9	42.6	47.7	48.0	43.8	49.2	43.6	44.8	49.1	42.7	47.8	42.4	46.3	46.8	46.6	47.1	47.2
10	39.5	38.5	37.8	39.0	37.8	40.2	41.1	42.3	41.0	41.6	38.8	44.0	44.7	38.5	38.5	34.8
11	49.7	49.4	50.1	50.4	50.2	50.3	48.9	50.0	48.8	49.9	37.8	48.2	48.6	49.2	49.8	50.1
12	27.5	27.2	27.8	28.5	28.0	29.0	35.9	35.6	36.7	33.7	28.5	24.9	27.4	31.4	32.6	30.5
13	44.6	45.2	45.1	43.4	45.4	74.5	76.3	76.7	78.2	76.5	41.1	45.6	45.6	45.6	45.2	45.3
14	75.5	72.6	75.3	75.4	75.4	78.9	78.9	79.4	78.4	79.2	75.3	75.4	75.4	74.0	74.1	74.7
17	56.6	58.4	63.2	57.0	63.5	57.7	59.1	63.4	61.8	63.1	56.4	55.8	63.7	57.6	64.4	59.0
18	77.5	77.7	77.1	79.8	80.4	79.9	80.1	80.4	79.8	77.0	78.8	79.1	79.2	77.8	77.1	78.1
19	40.8	40.7	49.7	*	56.3	*	50.0	56.1	50.1	49.5	49.0	47.2	*	66.9	49.8	48.9
NCH ₃	-	-	42.1	-	42.3	-	-	42.1	-	42.0	-	-	42.5	-	42.2	-
1-OMe	55.1	55.7	56.3	55.2	56.3	55.3	55.3	56.5	55.3	56.3	55.6	56.3	56.4	55.7	56.3	55.6
6-OMe	56.3	56.3	57.2	56.4	56.4	57.5	57.4	57.2	56.2	57.0	-	-	-	57.5	57.4	57.3
16-OMe	57.5	57.2	56.3	57.9	57.3	58.8	57.6	57.6	58.0	57.5	56.9	57.0	56.5	-	-	-
18-OMe	59.1	59.1	59.1	59.0	59.1	59.0	58.0	59.1	59.0	59.0	59.3	59.3	59.4	59.2	59.1	59.2
15	34.6	38.9	38.8	37.5	38.8	39.7	42.6	39.6	80.7	39.5	37.5	39.0	38.5	129.6	129.6	30.1
16	82.3	81.7	81.8	82.2	81.8	83.0	82.4	84.3	91.0	81.8	82.4	82.0	82.1	131.4	131.5	23.8

a: OAc: 169.5 s, 21.5 q; OBz: 166.1 s (COO), 130.1 s (1"), 129.5 d (2", 6"), 128.4 d (3", 5"), 133.0 d (4"); *b*: OAc: 169.5 s, 21.3 q; OBz: 166.0 s, (COO), 129.8 s (1"), 129.5 d (2", 6"), 128.4 d (3", 5"); *c*: OAc \times 2: 170.8 s, 169.3 s, 22.2 q, 21.2 q.

Table 2: ^{13}C NMR spectral data of compounds **27-30**, **34-36**, and **38-40** (100 MHz, CDCl_3)

NO	26	27	28	29	30	34	35	36	38^a	39	40
1	82.7	83.1	85.4	82.6	85.8	82.2	83.1	82.7	82.4	82.5	82.7
2	34.0	24.1	26.2	25.6	25.8	30.4	31.0	33.3	29.5	34.1	36.8
3	71.8	29.8	34.8	31.8	30.6	70.6	70.5	72.3	26.2	25.7	26.8
4	43.5	39.3	39.4	38.8	39.5	44.8	44.7	49.5	77.3	70.4	70.8
5	47.9	53.9	48.5	57.4	52.4	53.3	50.2	57.0	36.7	52.1	49.6
6	81.5	82.0	81.7	82.4	82.4	85.2	84.7	81.8	23.6	23.4	26.1
7	47.5	44.8	48.1	44.7	49.8	45.6	45.7	45.7	52.3	36.4	35.8
8	73.7	74.4	73.9	76.3	75.1	79.4	79.3	71.2	83.5	75.5	75.4
9	47.1	46.8	47.8	47.4	47.9	49.4	49.0	47.7	76.0	77.9	78.5
10	38.5	38.3	38.7	34.6	34.9	42.0	41.7	37.3	49.1	49.4	46.4
11	49.5	49.9	49.8	50.2	50.7	50.8	51.4	51.4	52.7	52.7	50.7
12	32.6	31.5	32.9	32.3	34.9	33.9	34.0	26.9	24.4	25.6	23.4
13	45.2	44.8	45.6	44.8	45.4	46.5	46.5	44.1	44.2	47.5	49.5
14	74.1	74.1	74.2	75.4	74.8	76.3	76.1	75.2	90.0	89.9	89.9
15	129.6	128.3	129.7	29.0	30.4	79.9	79.9	37.1	44.0	43.6	44.4
16	131.5	132.8	131.6	23.3	22.9	91.9	92.2	81.5	82.2	82.5	84.8
17	64.4	58.7	64.4	58.3	63.8	57.5	65.3	62.0	57.1	57.7	62.9
18	77.1	80.3	80.5	80.0	80.6	77.3	76.1	78.8	-	-	-
19	49.8	49.3	56.2	49.0	56.2	41.6	42.5	166.3	50.8	52.0	60.1
NCH ₃	42.2	-	42.4	-	42.4	-	49.6	-	-	-	42.2
1-OMe	56.3	55.4	56.4	55.3	56.5	55.5	55.9	55.8	55.8	55.6	55.9
6-OMe	57.4	57.6	57.5	57.7	57.3	57.3	57.1	57.0	-	-	-
14-OMe	-	-	-	-	-	-	-	-	56.0	56.3	57.7
16-OMe	-	-	-	-	-	59.3	59.2	56.5	57.8	55.8	56.7
18-OMe	59.1	59.1	59.1	59.1	59.2	58.3	58.3	59.3	-	-	-

a: NHAc: 171.3 s (NCO), 25.4 (25.2) q (CH_3CON); 169.0 (167.2) s (COO), 141.5 (140) s (2''), 134.3 (133.1) d (4''), 130.9 (127.3) d (6''), 122.4 (122.2) d (5''), 121.3 (120.1) (3''), 115.5 s (1'').

Table 3: ^{13}C NMR spectral data of compounds **44-48**, **50**, **51**, **53**, **56** and **57** (100 MHz, CDCl_3)

NO	44	45	46	47	48^a	50	51^a	53^a	56^b	57^a
1	67.3	69.8	69.6	69.6	69.2	67.8	67.8	26.3	68.4	69.1
2	29.6	29.8	30.6	20.4	27.9	29.8	28.9	19.7	31.1	29.8
3	30.6	31.1	31.4	31.5	28.9	24.1	23.2	39.3	38.0	36.7
4	33.5	33.6	33.5	34.6	35.9	37.7	36.9	33.4	34.4	34.4
5	46.4	48.1	47.9	49.6	48.9	48.7	49.0	50.6	51.3	49.7
6	21.8	23.3	19.1	22.3	22.7	23.9	22.9	21.8	24.2	23.0
7	45.6	43.3	44.0	44.1	45.8	45.7	45.5	41.9	45.8	44.5
8	48.2	50.5	50.7	47.6	49.8	50.7	49.5	41.9	44.5	42.7
9	36.0	37.0	36.2	35.3	39.1	30.4	31.6	52.3	52.8	51.8
10	51.0	52.4	52.9	48.9	53.3	51.5	50.0	44.6	51.9	52.1
11	36.0	32.3	23.4	37.2	31.2	29.6	28.4	71.0	71.4	69.8
12	210.3	67.3	31.9	210.2	79.7	213.0	107.7	38.8	46.7	44.9
13	53.0	43.7	40.6	53.1	47.3	53.8	53.4	20.0	21.2	20.0
14	36.8	35.5	35.3	40.1	37.2	37.4	32.3	25.2	28.1	27.3
15	77.5	76.8	77.6	77.0	82.3	75.4	81.1	75.3	85.2	83.8
16	148.4	153.8	164.8	150.2	88.4	78.8	86.9	77.5	80.2	79.3
17	111.3	111.9	106.1	114.4	71.4	68.1	68.6	65.3	68.8	67.8
18	24.4	26.3	26.6	26.2	25.6	18.8	17.7	25.4	25.7	25.1
19	46.1	58.2	58.6	57.4	57.9	92.8	92.5	56.7	47.7	58.1
20	57.7	66.3	66.3	69.3	66.2	65.6	65.6	71.2	61.3	67.5
21	-	50.9	50.7	51.1	54.6	48.2	47.7	50.3	-	42.5
22	-	13.2	13.4	13.5	13.7	14.1	13.0	12.1	-	-

a: $\text{CDCl}_3+\text{CD}_3\text{OD}$, b: CD_3OD .

Table 4: Cardiac effects of 42 diterpenoid alkaloids and lanatoside on isolated bullfrog hearts

Compound	Rate of amplitude increase (%)	Result ^a	Compound	Rate of amplitude increase (%)	Result ^a
control ^b	0	0	30	17.0	(+)
3	85.0	(+++)	34	31.5	(++)
4	31.0	(++)	35	176.7	(++++)
7	-57.0	(-)	36	-42.0	(-)
8	23.9	(+)	38	-50.0	(-)
9	82.0 [2]	(+++)	39	-27.0	(-)
10	118.0 [2]	(+++)	40	-53.0	(-)
11	28.0 [2]	(+)	41	-27.0	(-)
14	45.0	(++)	42	-18.0	(-)
15	0	(-)	43	-55	(-)
17	36.0	(++)	44	-29	(-)
18	23.6	(+)	45	-34	(-)
18a	0 [2]	(-)	46	(-)	(-)
21	0	(-)	47	-56	(-)
22	19.0	(+)	48	(-)	(-)
23	8.0	(-)	50	-5	(-)
24	25.0	(+)	51	-30	(-)
25	20.0	(+)	53	-40	(-)
26	-48.0	(-)	56	-26	(-)
27	8.0	(-)	57	-43%	(-)
28	31.0	(++)	58	0	(-)
29	-29.0	(-)	Lanatoside C	73.3	(+++)

a: The results were judged based on the average rate of amplitude increase: (-): 0-10%, (+): 12-30%, (++) 31-59%, (+++) 60-120%; b: distilled water; c: the cardioactive duration of alkaloids can reach 30'; the concentration of the tested compounds: 0.01 mol/mL ; 0.0002 mol/mL for lanatoside C.

Preparation of compound 2: To a solution of 13-deoxyindoconitine (**1**, 680 mg, 1.10 mmol) in glacial acetic acid (20 mL) was added NBS (600 mg, 3.4 mmol), and the mixture was kept stirred at room temperature for 3 h prior to being basified to pH 10 with conc. ammonium hydroxide. The mixture was extracted with chloroform; the combined extracts were dried and concentrated. The residue was purified by CC on silica gel, eluting with light petroleum: acetone (3:1, saturated with conc. ammonium hydroxide) to give compound **2** (476 mg, 74%).

Compound 2

^1H NMR (400 MHz, CDCl_3): 8.05 (2H, d, $J = 7.2$ Hz, H-2'', 6''), 7.55 (1H, t, $J = 7.6$ Hz, H-4''), 7.49 (2H, t, $J = 7.6$ Hz, H-3'', 5''), 5.07 (1H, t, $J = 4.8$ Hz, H-14 β), 4.13 (1H, d, $J = 6.8$ Hz, H-6), 3.82 (1H, dd, $J = 10.0, 5.6$ Hz, H-3), 3.85, 3.32, 3.29, 3.19 (each 3H, s, OMe \times 4), 1.33 (3H, s, OAc-8).

^{13}C NMR (100 MHz, CDCl_3): Table 1.

ESIMS: m/z 586 [M+H] $^+$.

HRMS-ESI: m/z [M+H] $^+$ calcd for $\text{C}_{32}\text{H}_{44}\text{NO}_9$: 586.3016, found: 586.3016

Preparation of compound 3: Compound **2** (320 mg, 0.55 mmol) was dissolved in a solution of sodium hydroxide in methanol (5%, 10 mL), and the reaction solution was stirred at 60°C for 1 h. After concentration *in vacuo*, the residue was subjected to CC on silica gel eluting with CHCl_3 : MeOH: diethylamine (97:7:1) to yield compound **3** (242 mg, 77%).

Compound 3

^1H NMR (400 MHz, CDCl_3): 3.17 (1H, d, $J = 6.4$ Hz, H-1), 1.97, 2.51 (each 1H, m, H-2), 3.71 (1H, t, $J = 5.6$ Hz, H-3), 1.95 (1H, t, $J = 6.8$ Hz, H-5), 4.25 (1H, d, $J = 6.8$ Hz, H-6), 3.17 (1H, hidden, H-7), 2.13 (1H, t, $J = 5.2$ Hz, H-9), 1.64 (1H, m, H-10), 1.65, 1.97 (each 1H, m, H-12), 2.29 (1H, m, H-13), 4.10 (1H, t, $J = 4.8$ Hz, H-14 β), 1.78, 2.39 (each 1H, m, H-15), 3.38 (1H, hidden, H-16), 1.88 (1H, s, H-17), 3.69, 3.81 (each 1H, ABq, $J = 9.2$ Hz, H-18), 2.93, 3.38 (each 1H, ABq, $J = 13.2$ Hz, H-19), 3.31 (3H, s, OCH₃-1), 3.32 (3H, s, OCH₃-6), 3.24 (3H, s, OCH₃-16), 3.29 (3H, s, OCH₃-18).

^{13}C NMR (100 MHz, CDCl_3): Table 1.

HRMS-ESI: m/z [M+H] $^+$ calcd for $\text{C}_{23}\text{H}_{38}\text{NO}_7$: 440.2648, found: 440.2650.

Preparation of compound 4: To a solution of compound **2** (150 mg, 0.26 mmol) in anhydrous THF (5 mL) was added sodium hydride (80%, 7 mg, 0.23 mmol), and the mixture was stirred at room temperature before the addition of methyl iodide (18 μL). The reaction was allowed to proceed with stirring for 2 h. Removal of the solvent afforded a residue, to which was added a solution of sodium hydroxide in methanol (5%, 6 mL). A general work-up afforded a crude product, which was purified by CC (silica gel, CHCl_3 -MeOH, 9:1) to give compound **4** (100 mg, 85%).

Compound 4

^1H NMR (400 MHz, CDCl_3): 4.57 (1H, brs, OH), 3.02 (1H, dd, $J = 10.0, 6.8$ Hz, H-1), 4.23 (1H, d, $J = 6.8$ Hz, H-6), 4.07 (1H, t, $J = 4.8$ Hz, H-14 β), 3.66 (1H, dd, $J = 11.6, 6.0$ Hz, H-3 β), 3.33, 3.24 (each 3H, s, OMe \times 2), 3.31 (6H, s, OCH₃ \times 2), 2.30 (3H, s, NCH₃).

^{13}C NMR (100 MHz, CDCl_3): Table 1.

HR-ESI: m/z [M+H] $^+$ calcd for $\text{C}_{24}\text{H}_{40}\text{NO}_7$: 454.2805; found: 454.2800.

Preparation of compound 6: To a solution of chasmanine (**5**, 400 mg, 0.88 mmol) in acetic anhydride (6 mL) was added TsOH (400 mg), and the reaction was allowed to proceed with stirring at room

temperature for 16 h. A general work-up provided a white solid, to which was added glacial acetic acid (20 mL) and NBS (710 mg). The subsequent reaction mixture was stirred at room temperature for 3 h before being concentrated. The white residue was subjected to CC on silica gel eluting with light petroleum: acetone:diethylamine (80:20:1) to furnish compound **6** (250 mg, 65%).

Compound 6

^1H NMR (400 MHz, CDCl_3): 4.81 (1H, t, $J = 4.8$ Hz, H-14 β), 4.06 (1H, d, $J = 5.6$ Hz, H-6), 3.01, 3.58 (each 1H, ABq, $J = 8.4$ Hz, H-18), 3.32, 3.31, 3.26, 3.22 (each 3H, s, OMe \times 4), 2.04, 1.97 (each 3H, s, OAc \times 2).

^{13}C NMR (100 MHz, CDCl_3): Table 1.

HR-ESI: m/z [M+H] $^+$ calcd for $\text{C}_{24}\text{H}_{40}\text{NO}_6$: 438.2856; found: 438.2859.

Preparation of compound 7: To a solution of compound **6** (114 mg, 0.26 mmol) in anhydrous THF (20 mL) was added sodium hydride (80%, 6 mg, 0.2 mmol), and the mixture was stirred at room temperature for 15 min before the addition of methyl iodide (14 μL). The reaction was allowed to proceed for 2 h at room temperature. A general work-up procedure gave a residue, to which was added a solution of sodium hydroxide in methanol (5%, 3 mL). The subsequent reaction mixture was stirred at 60°C for 1 h and the solvent was removed *in vacuo*. The white foam was purified by CC eluting with CHCl_3 : MeOH: diethylamine (97:3:1) to yield compound **7** (83 mg, 74%).

Compound 7

^1H NMR (400 MHz, CDCl_3): 4.60 (1H, brs, OH), 4.20 (1H, d, $J = 6.8$ Hz, H-6), 4.13 (1H, t, $J = 4.5$ Hz, H-14 β), 3.60, 3.70 (each 1H, ABq, $J = 8.0$ Hz, H-18), 3.40 (1H, d, $J = 9.2$ Hz, H-16), 3.34, 3.31, 3.30, 3.25 (each 3H, s, OMe \times 4), 2.31 (3H, s, NCH₃).

^{13}C NMR (100 MHz, CDCl_3): Table 1.

HRMS-ESI: m/z [M+H] $^+$ calcd for $\text{C}_{24}\text{H}_{40}\text{NO}_6$: 428.2856; found: 438.2859.

Preparation of compound 8: To a solution of chasmanine (**5**, 600 mg, 1.32 mmol) in acetic anhydride (60 mL) was added TsOH (40 mg) and the reaction was allowed to proceed for 16 h. After a general work-up, the white residue was dissolved in glacial acetic acid (20 mL). To this solution was added NBS (713 mg, 4.00 mmol), and the subsequent reaction solution was stirred at room temperature for an additional 3 h. After the second standard work-up, the crude product was purified by CC (silica gel, light petroleum: acetone, 4:1 with 1% diethylamine) to give compound **8** (440 mg, 65 %).

Compound 8

^1H NMR (400 MHz, CDCl_3): 3.23, 3.31, 3.33, 3.35 (each 3H, s, OMe \times 4), 3.65 (1H, ABq, $J = 8.4$ Hz, H-18), 4.18 (1H, t, $J = 5.2$ Hz, H-14 β), 4.23 (1H, t, $J = 6.8$ Hz, H-6).

^{13}C NMR (100 MHz, CDCl_3): 81.7 (C-1), 23.2 (C-2), 28.6 (C-3), 38.7 (C-4), 44.7 (C-5), 82.3 (C-6), 40.1 (C-7), 73.9 (C-8), 47.6 (C-9), 44.4 (C-10), 48.9 (C-11), 28.9 (C-12), 57.1 (C-13), 75.3 (C-14), 41.4 (C-15), 82.4 (C-16), 57.4 (C-17), 79.8 (C-18), 49.9 (C-19), 55.2 (C-1'), 56.1 (C-6'), 57.6 (C-16'), 59.0 (C-18').

HRMS-ESI: m/z [M+H] $^+$ calcd for $\text{C}_{23}\text{H}_{38}\text{NO}_6$: 424.2699; found: 424.2705.

Preparation of compound 13: To a solution of indoconitine (**12**, 4 g, 6.4 mmol) in THF (12 mL) was added thionyl chloride (6 mL), and the reaction mixture was stirred at 40°C for 2 h. Removal of volatile solvent gave a white solid, which was dissolved in ethanol

(95%, 10 mL) and glacial acetic acid (2 mL). To the mixture was added 10% Pd-C and the reaction was allowed to proceed in the presence of hydrogen. A general work-up gave white foam, which was dissolved in glacial acetic acid (9 mL). To the subsequent mixture was added NBS (260 mg), and the reaction mixture was stirred at room temperature for 3 h. After a general work-up, the crude residue was purified by CC eluting with cyclohexane: acetone: diethylamine (75:25:1) to yield compound **13** (2.73 g, 71%).

Compound 13

¹H NMR (400 MHz, CDCl₃): 8.05 (1H, d, *J* = 7.2 Hz, H-2", 6"), 7.56 (1H, t, *J* = 7.6 Hz, H-4"), 7.43 (2H, t, *J* = 7.6 Hz, H-3", 5"), 4.93 (1H, d, *J* = 5.2 Hz, H-14β), 4.03 (1H, brs, NH), 4.00 (1H, d, *J* = 6.8 Hz, H-6), 3.55, 3.28, 3.24, 3.18 (each 3H, s, OMe × 4), 1.31 (3H, s, OAc-8).

¹³C NMR (100 MHz, CDCl₃): Table 1.

HRMS-ESI: *m/z* [M+H]⁺ calcd for C₂₃H₄₄NO₉: 586.3016; found: 586.3021

Preparation of compound 14: Compound **13** (95 mg, 0.16 mmol) was dissolved in a solution of sodium hydroxide in methanol (1%, 3 mL). The reaction mixture was stirred at 60°C for 1 h before removal of solvent. The crude residue was purified by CC on silica gel eluting with CHCl₃: MeOH: diethylamine (95:5:1) to provide compound **14** (51 mg, 73%).

Compound 14

¹H NMR (400 MHz, CDCl₃): 4.13 (1H, d, *J* = 6.4 Hz, H-6), 3.99 (1H, d, *J* = 4.8 Hz, H-14β), 3.81 (1H, brs, OH), 3.64 (1H, ABq, *J* = 8.4 Hz, H-18), 3.42, 3.34, 3.31, 3.21 (each 3H, s, OCH₃ × 4).

¹³C NMR (100 MHz, CDCl₃): Table 1.

HRMS-ESI: *m/z* [M+H]⁺ calcd for C₂₃H₃₈NO₇: 440.2648; found: 440.2649.

Preparation of compound 15: To a solution of compound **13** (95 mg, 0.16 mmol) in anhydrous THF (5 mL) was added sodium hydride (80%, 5 mg), and the mixture was stirred for 15 min before the addition of methyl iodide (11 μL). The reaction was allowed to proceed for an additional 2 h. A standard work-up provided a white solid, to which was added a solution of sodium hydroxide in methanol (5%, 5 mL). The subsequent reaction mixture was stirred at 60°C for 1 h prior to another standard work-up. The crude residue was purified by CC eluting with CHCl₃: MeOH: diethylamine (97:3:1) to give compound **15** (24 mg, 71%).

Compound 15

¹H NMR (400 MHz, CDCl₃): 4.11 (1H, d, *J* = 7.2 Hz, H-6), 4.02 (1H, brs, OH), 3.97 (1H, t, *J* = 4.8 Hz, H-14β), 3.69, 3.33 (each 1H, ABq, *J* = 8.4 Hz, H-18), 3.42, 3.30, 3.30, 3.25 (each 3H, s, OCH₃ × 4), 2.99 (1H, dd, *J* = 10.8, 6.8 Hz, H-1), 2.31 (3H, s, NCH₃).

¹³C NMR (100 MHz, CDCl₃): Table 1.

HRMS-ESI: *m/z* [M+H]⁺ calcd for C₂₄H₄₀NO₇: 454.2805; found: 454.2806.

Preparation of compound 17: To a solution of dexoyaconitine (**17a**, 315 mg, 0.50 mmol) in glacial acetic acid (10 mL) was added NBS (267 mg, 1.5 mmol), and the reaction mixture was kept stirred at room temperature for 3 h. A standard work-up procedure gave a crude residue, which was subjected to CC eluting with light petroleum: acetone: diethylamine (66:33:1) to furnish *N*-deethyl-deoxyaconitine (24 mg, 80%). This compound was dissolved in a solution of sodium hydroxide in methanol (5%, 10 mL) and refluxed for 30 sec. After removing the solvent, the residue was dissolved in CHCl₃: MeOH (9:3, 10 mL) and filtered. The filtrate

was concentrated and subjected to CC eluting with CHCl₃: MeOH (95:5, saturated with conc. NH₄OH) to yield compound **17** (115 mg, 76%).

Compound 17

¹H NMR (400 MHz, CDCl₃): 4.61 (1H, d, *J* = 6.8 Hz, H-15), 4.20 (1H, brs, OH), 3.85 (1H, d, *J* = 6.4 Hz, H-14β), 4.14 (1H, d, *J* = 6.4 Hz, H-6), 3.70, 3.35, 3.32, 3.19 (each 3H, s, OCH₃ × 4), 3.07, 3.60 (each 1H, ABq, *J* = 8.4 Hz, H₂-18).

¹³C NMR (100 MHz, CDCl₃): Table 1.

HRMS-ESI: *m/z* [M+H]⁺ calcd for C₂₃H₃₈NO₈: 456.2597; found: 456.2599

Preparation of compound 18: To a solution of indaconitine (**12**, 440 mg, 0.7 mmol) in glacial acetic acid (12 mL) was added NBS (375 mg, 2.1 mmol), and the reaction was allowed to proceed at room temperature for 4 h prior to being basified with conc. ammonium hydroxide to pH 10. The subsequent mixture was extracted with CHCl₃ (20 mL × 3); the combined extracts were dried over anhydrous sodium sulfate and concentrated under reduced pressure. The crude residue was purified by CC eluting with light petroleum: acetone: diethylamine (75:25:1) to yield *N*-deethylindaconitine (329 mg, 78%). To the solution of this compound (300 mg, 0.5 mmol) in THF (10 mL) was added sodium hydride (80%, 15 mg, 0.5 mmol) followed by methyl iodide (35 μL, 0.6 mmol) under argon. The subsequent reaction was allowed to proceed for 2 h before the solvent was removed. To the residue was added a solution of sodium hydroxide in methanol (15 mL), and the reaction was allowed to proceed with refluxing for an additional 1 h. The reaction mixture was first acidified with conc. HCl to pH 2 then basified with conc ammonium hydroxide to pH 10. The mixture was extracted with chloroform, and the combined extracts were dried over anhydrous sodium sulfate and concentrated. The crude residue was purified by CC eluting with CHCl₃: MeOH (95:5, saturated with conc. ammonium hydroxide) to give compound **18** (185 mg, 78%).

Compound 18

¹H NMR (400 MHz, CDCl₃): 4.15 (1H, d, *J* = 6.8 Hz, H-6), 3.66 (1H, dd, *J* = 11.2, 6.8 Hz, H-3β), 3.41, 3.32, 3.31, 3.25 (each 3H, s, OCH₃ × 4), 2.32 (3H, s, NCH₃).

¹³C NMR (100 MHz, CDCl₃): Table 1.

HRMS-ESI: *m/z* [M+H]⁺ calcd for C₂₄H₄₀NO₈: 470.2754; found: 470.2750.

Preparation of compound 20: To a solution of talasamine (**19**, 1.1 g, 2.61 mmol) in acetic anhydride (6 mL) was added TsOH (600 mg), and the reaction was allowed to proceed at room temperature for 16 h. After a standard work-up, the white residue was dissolved again in glacial acetic acid (40 mL). To this solution was added 7 equivalents of NBS, and the reaction was continued with stirring at room temperature for 4 h. After the second standard work-up, the white foam was subjected to CC eluting with cyclohexane: acetone: diethylamine to furnish an imine (230 mg). Hydrogenolysis of this imine catalyzed by Pt₂O at 60°C for 24 h yielded a white residue, which was purified by CC eluting with CHCl₃: MeOH: diethylamine (90:10:1) to furnish compound **20** (250 mg, 20%).

Compound 20

¹H NMR (400 MHz, CDCl₃): 4.80 (1H, t, *J* = 4.8 Hz, H-14β), 3.31, 3.28, 3.27 (each 3H, s, OCH₃ × 3), 2.03, 1.94 (each 3H, s, OAc).

¹³C NMR (100 MHz, CDCl₃): Table 1.

HRMS-ESI: *m/z* [M+H]⁺ calcd for C₂₆H₄₀NO₇: 478.2805; found: 478.2804.

Preparation of compound 21: Compound **20** (100 mg, 0.20 mmol) was dissolved in a solution of sodium hydroxide in methanol (5%, 10 mL), and the reaction mixture was stirred at 60°C for 1 h. After a general work-up procedure, the white residue was purified by CC eluting with CHCl₃: MeOH: diethylamine (90:10:1) to generate compound **21** (24 mg, 30%).

Compound 21

¹H NMR (400 MHz, CDCl₃): 4.56 (1H, brs, OH), 4.18 (1H, d, *J* = 4.5 Hz, H-14β), 3.34, 3.29, 3.27 (each 3H, s, OMe × 3), 3.95, 3.09 (each 1H, ABq, *J* = 8.8 Hz, H₂-18).

¹³C NMR (100 MHz, CDCl₃): Table 1.

HRMS-ESI: *m/z* [M+H]⁺ calcd for C₂₂H₃₆NO₅: 394.2593; found: 394.2591.

Preparation of compound 22: To a solution of compound **20** (105 mg, 0.22 mmol) in THF (5 mL) was added sodium hydride (80%, 7 mg, 0.22 mmol), and the mixture was stirred for 15 min before the addition of methyl iodide (15 μL). The reaction was allowed to proceed with stirring at room temperature for 2 h. A general work-up gave a white solid, to which was added a solution of sodium hydroxide in methanol (5%, 3 mL). The subsequent reaction mixture was stirred at 60°C for an additional 1 h and then concentrated under reduced pressure. The crude residue was purified by CC on silica gel eluting with CHCl₃: MeOH (97:3) to yield compound **22** (59 mg, 65%).

Compound 22

¹H NMR (400 MHz, CDCl₃): 4.81 (1H, brs, disappeared with D₂O, OH), 4.13 (1H, t, *J* = 4.8 Hz, H-14β), 3.34, 3.29, 3.27 (each 3H, s, OMe × 3), 2.26 (3H, s, NCH₃).

¹³C NMR (100 MHz, CDCl₃): Table 1.

HRMS-ESI: *m/z* [M+H]⁺ calcd for C₃₃H₃₈NO₅: 408.2750; found: 408.2755.

Preparation of compounds 23, 24, 25 and 26: Pyrolysis of 13-deoxyindaconitine (**1**, 1.2 g, 1.95 mmol) at 180–190°C under vacuum for 5 min followed by CC (light petroleum: acetone: diethylamine, 80:16:1) provided a white powder (650 mg, 62%). This was dissolved in acetic anhydride (25 mL), to which was added TsOH (200 mg). The subsequent solution was refluxed for 3 h prior to being cooled to 0°C. The mixture was basified with conc. NH₄OH to pH > 10, and extracted with chloroform 3 times. The combined extracts were dried over anhydrous sodium sulfate and concentrated *in vacuo*. The crude residue was subjected to CC eluting with light petroleum: acetone (5:1) to give a rearranged product (white amorphous powder, 590 mg, 80%). To a solution of this product in glacial acetic acid (10 mL) was added NBS (450 mg, 3 eq), and the reaction mixture was stirred at room temperature for 2 h. The mixture was cooled to 0°C and basified with conc ammonium hydride to pH > 10, which was extracted with chloroform 3 times. The combined extracts were dried over anhydrous sodium sulfate and concentrated. The crude residue (520 mg) was dissolved in a solution of sodium hydroxide in methanol (5%) and stirred at 50°C for 1 h. After removal of solvent, the residue was partitioned between water and ethyl acetate. The organic layers were dried over anhydrous sodium sulfate and concentrated *in vacuo*. The residue was purified by CC eluting with light petroleum: acetone: diethylamine (60:30:1) to yield compound **23** (white amorphous powder, 400 mg, 50%). To a solution of compound **23** (200 mg, 0.24 mmol) in THF was added sodium hydride (8.0 mg) and methyl iodide (20 μL), and the reaction was allowed to proceed at room temperature for 2 h. After removal of solvent, the residue was purified by CC eluting with chloroform: methanol (50:1) to give compound **24** (white amorphous

powder, 180 mg, 89%). To a solution of compound **23** (100 mg, 0.23 mmol) in 95% ethanol (3 mL) was added 2 drops of glacial acetic acid and Pt₂O (10 mg). The reaction was allowed to proceed in the presence of hydrogen under 30 MPa for 20 h. The mixture was basified with conc. ammonium hydroxide to pH > 10. A standard work-up procedure followed by CC [chloroform: methanol (50:1)] yielded compound **25** (white amorphous powder, 90 mg, 89%). According to a similar procedure, hydrogenation of **24** (100 mg, 0.23 mmol), followed by CC (silica gel, CHCl₃: MeOH = 100:1) gave compound **26** (87 mg, 87%).

Compound 23

¹H NMR (400 MHz, CDCl₃): 5.89 (1H, d, *J* = 9.6 Hz, H-16), 5.72 (1H, d, *J* = 9.6 Hz, H-15), 4.34 (1H, d, *J* = 6.8 Hz, H-6), 4.01 (1H, t, *J* = 4.8 Hz, H-14β), 3.36, 3.31, 3.24 (each 3H, s, OCH₃ × 3).

¹³C NMR (100 MHz, CDCl₃): Table 1.

HRMS-ESI: *m/z* [M+H]⁺ calcd for C₂₂H₃₄NO₆: 408.2386; found: 408.2381.

Compound 24

¹H NMR (400 MHz, CDCl₃): 5.87 (1H, d, *J* = 9.6 Hz, H-16), 5.63 (1H, d, *J* = 9.6 Hz, H-15), 4.30 (1H, d, *J* = 6.8 Hz, H-6), 4.03 (1H, t, *J* = 4.8 Hz, H-14β), 3.34, 3.32, 3.23 (each 3H, s, OMe × 3), 2.26 (3H, s, NCH₃).

¹³C NMR (100 MHz, CDCl₃): Table 1.

HRMS-ESI: *m/z* [M+H]⁺ calcd for C₂₃H₃₆NO₆: 422.2543 ; found: 422.2540

Compound 25

¹H NMR (400 MHz, CDCl₃): 4.27 (1H, d, *J* = 6.4 Hz, H-6), 4.02 (1H, t, *J* = 4.8 Hz, H-14β), 3.34, 3.31, 3.29 (each 3H, s, OCH₃ × 3).

¹³C NMR (100 MHz, CDCl₃): Table 1.

HRMS-ESI: *m/z* [M+H]⁺ calcd for C₂₂H₃₆NO₆: 410.2543; found: 410.2560.

Compound 26

¹H NMR (400 MHz, CDCl₃): 4.23 (1H, d, *J* = 6.8 Hz, H-6), 4.03 (1H, t, *J* = 4.8 Hz, H-14β), 3.32, 3.31, 3.27 (each 3H, s, OCH₃ × 3), 3.01 (1H, dd, *J* = 9.2, 6.0 Hz, H-1), 2.36 (3H, s, NCH₃). 2.90, 2.59 (each 1H, ABq, *J* = 11.2 Hz, H₂-19).

¹³C NMR (100 MHz, CDCl₃): Table 2.

HRMS-ESI: *m/z* [M+H]⁺ calcd for C₂₃H₃₈NO₆: 424.2699; found: 424.2700.

Preparation of compounds 27, 28, 29 and 30: These 4 compounds were prepared from chasmanine (**5**, 2.0 g, 4.45 mmol) using the same procedure described for the preparation of compounds **23–26**.

Compound 27

White amorphous powder, 300 mg, 17% yield.

¹H NMR (400 MHz, CDCl₃): 5.84 (1H, m, H-16), 5.76 (1H, d, *J* = 9.6 Hz, H-15), 4.30 (1H, d, *J* = 6.8 Hz, H-6), 3.97 (1H, t, *J* = 5.2 Hz, H-14β), 3.33, 3.29, 3.16 (each 3H, s, OCH₃ × 3).

¹³C NMR (100 MHz, CDCl₃): Table 2.

HRMS-ESI: *m/z* [M+H]⁺ calcd for C₂₂H₃₄NO₅: 392.2437; found: 392.2435.

Compound 28

White amorphous powder, 140 mg, 93% yield.

¹H NMR (400 MHz, CDCl₃): 5.89 (1H, m, H-16), 5.64 (1H, d, *J* = 9.6 Hz, H-15), 4.25 (1H, d, *J* = 6.8 Hz, H-6), 4.04 (1H, t, *J* = 4.4 Hz, H-14β), 3.33, 3.31, 3.23 (each 3H, s, OCH₃ × 3), 3.01 (1H, dd, *J* = 10.0, 6.8 Hz, H-1), 2.26 (3H, s, NCH₃).

¹³C NMR (100 MHz, CDCl₃): Table 2.

HRMS-ESI: m/z [M+H]⁺ calcd for C₂₃H₃₆NO₅: 406.2593; found: 406.2591.

Compound 29

White amorphous powder, 65 mg, 91% yield.

¹H NMR (400 MHz, CDCl₃): 4.22 (1H, d, J = 6.4 Hz, H-6), 4.06 (1H, t, J = 4.8 Hz, H-14 β), 3.35, 3.31, 3.22 (each 3H, s, OCH₃ × 3).

¹³C NMR (100 MHz, CDCl₃): Table 2.

HRMS-ESI: m/z [M+H]⁺ calcd for C₂₂H₃₆NO₅: 394.2593; found: 394.2599.

Compound 30

White amorphous powder, 63 mg, 91% yield.

¹H NMR (400 MHz, CDCl₃): 4.18 (1H, d, J = 6.8 Hz, H-6), 4.04 (1H, t, J = 4.8 Hz, H-14 β), 3.31, 3.30, 3.28 (each 3H, s, OCH₃ × 3), 3.01 (1H, dd, J = 10.4, 6.4 Hz, H-1), 2.72, 2.41 (each 1H, ABq, J = 10.4 Hz, H₂-19), 2.31 (3H, s, H₃-21).

¹³C NMR (100 MHz, CDCl₃): Table 2.

HRMS-ESI: m/z [M+H]⁺ calcd for C₂₃H₃₈NO₇: 408.2648 ; found: 408.2642.

Preparation of compound 31a: To a solution of 3-acetylaconitine (**31**, 600 mg, 0.87 mmol) in THF (72 mL) was added imidazole (8 mg), NaH (696 mg), CS₂ (7.2 mL) and CH₃I (5.4 mL, 0.08 mmol), and the reaction was allowed to proceed at room temperature for 3 h. A general work-up yielded a residue (400 mg), to which was added benzene (20 mL) and *n*-Bu₃SnH (0.24 mg), and the reaction mixture was refluxed for 1 h. After removal of solvent, a general work-up gave a residue (300 mg). To a solution of this residue (180 mg) in glacial acetic acid (5.5 mL) was added NBS (144 mg, 0.81 mmol), and the reaction mixture was stirred at room temperature for 1.5 h. After removal of the solvent, the residue was diluted with water (15 mL), basified with ammonium hydroxide to pH > 10, and extracted with CHCl₃ (10 mL × 3). The combined extracts were dried over anhydrous sodium sulfate and concentrated under reduced pressure. The residue was purified by CC eluting with light petroleum: acetone: diethylamine (75:15:1) to produce compound **31a** (150 mg, 26 %).

Compound 31a

¹H NMR (400 MHz, CDCl₃): 8.02 (2H, d, J = 7.6 Hz), 7.56 (1H, t, J = 7.2 Hz), 7.44 (2H, t, J = 7.6 Hz), 5.20 (1H, t, H-3), 5.06 (1H, t, J = 4.4 Hz, H-14 β), 4.38 (1H, d, J = 5.2 Hz, H-15), 4.18 (1H, d, J = 6.4 Hz, H-6), 3.73 (1H, d, J = 8.8 Hz, H-18), 3.53, 3.28, 3.26, 3.21 (each 3H, s, OCH₃ × 4), 2.06 (3H, s, OAc-3), 1.42 (3H, s, OAc-8). HRMS-ESI: m/z [M+H]⁺ calcd for C₃₄H₄₆NO₁₁: 644.3071; found: 644.3123.

Preparation of compound 34: Compound **31a** (70 mg, 0.11 mmol) was dissolved in a solution of sodium hydroxide (5%, 2 mL), and the reaction was allowed to proceed at room temperature overnight. A general work-up gave a residue, which was subjected to CC on silica gel eluting with CHCl₃: MeOH (10:1, saturated with conc. NH₄OH) to yield compound **34** (40 mg, 81%).

Compound 34

¹H NMR (400 MHz, CDCl₃): 8.02 (2H, d, J = 7.2 Hz), 7.56 (1H, t, J = 7.2 Hz), 7.44 (2H, t, J = 7.6 Hz), 5.04 (1H, t, J = 4.4 Hz, H-14 β), 4.91 (1H, dd, J = 12.0, 6.0 Hz, H-3), 4.40 (1H, d, J = 2.4 Hz, OH-15), 4.34 (1H, dd, J = 6.0, 2.4 Hz, H-15), 4.13 (1H, d, J = 6.4 Hz, H-6), 3.82 (1H, d, J = 8.8 Hz, H-18), 3.53, 3.29, 3.22, 3.20 (each 3H, s, OCH₃ × 4), 2.34 (3H, s, NCH₃), 2.06 (3H, s, OAc-3), 1.44 (3H, s, OAc-8); ¹³C NMR (100 MHz, CDCl₃): Table 2.

HRMS-ESI: m/z [M+H]⁺ calcd for C₂₃H₃₈NO₇: 440.2648 ; found: 440.2650.

Preparation of compound 35: To a solution of compound **31a** (110 mg, 0.17 mmol) in THF (5.5 mL) was added sodium hydride (4.1 mg, 0.17 mmol) and methyl iodide (10.7 uL, 0.17 mmol), and the reaction mixture was stirred at room temperature for 2 h. A general work-up gave a crude residue, to which was added a solution of sodium hydroxide in methanol (5%, 2 mL). The subsequent reaction mixture was stirred overnight and concentrated under reduced pressure. The crude residue was subjected to CC on silica gel eluting with CHCl₃: MeOH (20:1) to yield compound **35** (34 mg, 84.1%).

Compound 35

¹H NMR (400 MHz, CDCl₃): 3.82 (1H, br.s, H-3), 4.27 (1H, d, J = 6.4 Hz, H-6), 4.04 (1H, d, J = 4.8 Hz, H-14 β), 3.45, 3.77 (each 1H, ABq, J = 8.4 Hz, H₂-18), 3.32, 3.31, 3.37, 3.39 (each 3H, s, OMe × 4).

¹³C NMR (100 MHz, CDCl₃): Table 2.

HRMS-ESI: m/z [M+H]⁺ calcd for C₂₄H₄₀NO₈: 470.2754; found: 470.2750.

Preparation of compound 36: To a solution of 13-deoxyindaconitine (**1**, 200 mg, 0.28 mmol) in glacial acetic acid (10 mL) was added NBS (310 mg, 1.22 mmol), and the reaction was allowed to proceed at 130°C for 10 h. A general work-up provided a residue, to which was added a solution of sodium hydroxide in methanol (5%, 10 mL). The subsequent reaction mixture was stirred at 50°C for 1 h before removing the methanol. The crude residue was purified by CC eluting with CHCl₃: MeOH (40:1) to give compound **36** (115 mg, 70%).

Compound 36

¹H NMR (400 MHz, CDCl₃): 7.47 (1H, s, H-19), 3.67 (1H, dd, J = 10.4, 6.4 Hz, H-1), 3.38, 3.36, 3.25, 3.20 (each 3H, s, OCH₃ × 4).

¹³C NMR (100 MHz, CDCl₃): Table 2.

HRMS-ESI: m/z [M+H]⁺ calcd for C₂₃H₃₆NO₇: 438.2492; found: 438.2496.

Preparation of compound 38: To a solution of lappaconitine (**37**, 2.336 g, 4 mmol) in glacial acetic acid (70 mL) was added NBS (2.136 g, 12 mmol), and the reaction was allowed to proceed at room temperature for 2 h. The reaction was quenched by pouring the reaction mixture into ice water, which was basified with conc ammonium hydroxide to pH 10 and extracted with chloroform (20 mL × 3). The combined extracts were dried over anhydrous sodium sulfate and concentrated. The residue (2.3 g) was purified by CC on silica gel eluting with light petroleum: acetone: diethylamine (75:25:1) to give *N*-deethyllappaconitine (**38**, 1.87 g, 84%).

Compound 38

¹H NMR (400 MHz, CDCl₃): 8.63 (8.56) (1H, d, J = 8.4 Hz, H-6"), 7.90 (1H, d, J = 8.0 Hz, H-3"), 7.50 (7.44) (1H, t, J = 8.0 Hz, H-4"), 7.01 (6.99) (1H, t, J = 8.0 Hz, H-5"), 6.51 (6.66) (each 1H, brs, NH), 3.37 (3H, s, OCH₃), 3.27, 3.26 (each 3H, s, OCH₃ × 2), 2.91 (3H, s, NCOCH₃).

¹³C NMR (100 MHz, CDCl₃): Table 2.

HRMS-ESI: m/z [M+H]⁺ calcd for C₃₀H₄₁N₂O₈: 557.2863; found: 557.2959

Preparation of compound 39: Compound **38** (300 mg, 0.54 mmol) was dissolved in a solution of sodium hydroxide in methanol (10%), and the mixture was stirred at 60°C for 1 h and then basified with conc. NH₄OH to pH 11. After removing the solvents, the residue was purified by CC eluting with CHCl₃: MeOH (95:5 - 9:1, saturated with conc. ammonium hydroxide) to furnish compound **39** (168 mg, 79%).

Compound 39

¹H NMR (400 MHz, CDCl₃): 3.43 (1H, ABq, *J* = 8.4 Hz, H-18), 3.41, 3.30, 3.28 (each 3H, s, OCH₃ × 3).
¹³C NMR (100 MHz, CDCl₃): Table 2.
HRMS-ESI: *m/z* [M+H]⁺ calcd for C₂₁H₃₄NO₆: 396.2386; found: 396.2388.

Preparation of compound 40: To a solution of compound **38** (420 mg, 0.755 mmol) in THF (10 mL) was added sodium hydride (18 mg, 0.755 mmol) under argon, and the mixture was stirred for 15 min before the addition of methyl iodide (50 μ L, 0.801 mmol). The reaction was allowed to proceed with stirring at room temperature for 2 h, and the solvent was removed under reduced pressure. To the residue was added a solution of sodium hydroxide in methanol (5%, 15 mL), and the subsequent mixture was stirred at 60°C for 1 h prior to being basified with conc. ammonium hydroxide to pH 11. The solvent was removed *in vacuo*, and the residue was subjected to CC on silica gel eluting with chloroform: methanol (95:5, saturated with conc. ammonium hydroxide) to yield compound **40** (263 mg, 85%).

Compound 40

¹H NMR (400 MHz, CDCl₃): 3.40, 3.30, 3.29 (each 3H, s, OCH₃ × 3), 2.29 (3H, s, NCH₃).
¹³C NMR (100 MHz, CDCl₃): Table 2.
HRMS-ESI: *m/z* [M+H]⁺ calcd for C₂₂H₃₆NO₆: 410.2543 ; found: 410.2541.

Preparation of compound 44: To a solution of acetylsongorine (**43a**, 600 mg, 1.38 mmol) in isopropanol (15 mL) was added NBS (740 mg, 4.17 mmol), and the reaction mixture was stirred at 30°C for 2 h. After being basified with conc. ammonium hydroxide to pH > 10, the mixture was extracted with chloroform: methanol (10:1, 30 mL × 3). The combined extracts were dried over anhydrous sodium sulfate and concentrated. The crude residue was subjected to CC eluting with CHCl₃: MeOH (20:1) to provide a white amorphous powder (280 mg). This was dissolved in a solution of sodium hydroxide in methanol (5%, 10 mL) and the consequent mixture was stirred at 50°C for 2 h. After removal of solvent, the residue was subjected to CC on silica gel eluting with CHCl₃: MeOH (20:1) to yield compound **44** (150 mg, 25%).

Compound 44

¹H NMR (400 MHz, CDCl₃): 5.19, 5.14 (each 1H, s, H₂-17), 4.28 (1H, s, H-15), 3.57 (1H, s, H-20), 0.67 (3H, s, H₃-18).
¹³C NMR (100 MHz, CDCl₃): Table 3.
HRMS-ESI: *m/z* [M+H]⁺ calcd for C₂₀H₂₈NO₃: 330.2069; found: 330.2072.

Preparation of compounds 45 and 46: To a solution of songorine (**43**, 420 mg, 1.18 mmol) in methanol (30 mL) was added NaBH₄ (100 mg, 2.63 mmol), and the reaction mixture was stirred at room temperature for 35 min. The mixture was basified with conc. ammonium hydroxide to pH 10 and extracted with chloroform (20 mL × 3). The combined extracts were dried over anhydrous sodium sulfate and concentrated *in vacuo*. The crude residue was purified by CC on silica gel eluting with CHCl₃: MeOH (30:1) to yield compounds **45** (160 mg, 40%) and **46** (250 mg, 60%).

Compound 45

¹H NMR (400 MHz, CDCl₃): 5.16, 5.14 (each 1H, s, H₂-17), 4.17 (1H, s, H-15), 3.93 (1H, dd, *J* = 7.6, 6.4 Hz, H-12), 3.52 (1H, dd, *J* = 9.6, 6.8 Hz, H-1), 3.36 (1H, s, H-20), 1.06 (3H, t, *J* = 7.2 Hz, H₃-22), 0.77 (3H, s, H₃-18).
¹³C NMR (100 MHz, CDCl₃): Table 3.
HRMS-ESI: *m/z* [M+H]⁺ calcd for C₂₂H₃₄NO₃: 360.2539; found: 360.2538.

Compound 46

¹H NMR (400 MHz, CDCl₃): 5.33, 5.12 (each 1H, s, H₂-17), 4.21 (1H, s, H-15), 4.18 (1H, dd, *J* = 9.2, 5.6 Hz, H-12), 3.87 (1H, dd, *J* = 8.8, 6.4 Hz, H-1), 3.47 (1H, s, H-20), 1.14 (3H, t, *J* = 7.2 Hz, H₃-22), 0.80 (3H, s, H₃-18).
¹³C NMR (100 MHz, CDCl₃): Table 3.
HRMS-ESI: *m/z* [M+H]⁺ calcd for C₂₂H₃₄NO₃: 360.2539; found: 360.2540.

Preparation of compound 47: To a solution of songorine (**43**, 50 mg, 0.14 mmol) in 2 ml TEG was added NH₂NH₂ H₂O (0.4 mL, 7 mmol) and KOH (40 mg, 0.7 mmol), and the reaction was allowed to proceed under reflux at 160°C for 1 h. After removal of water and hydrazine, the reaction was allowed to proceed at 180°C for an additional 1 h. After cooling to room temperature, the reaction mixture was diluted with water and extracted with ethyl acetate (20 mL × 3). The combined extracts were dried over anhydrous sodium sulfate and concentrated under reduced pressure. The crude residue was purified by CC eluting with light petroleum: ethyl acetate: diethylamine (75:25:1) to furnish compound **47** (40 mg, 82%).

Compound 47

¹H NMR (400 MHz, CDCl₃): 5.01 (2H, s, H₂-17), 4.19 (1H, d, *J* = 8.4 Hz, H-15), 3.97 (1H, t, *J* = 6.0 Hz, H-1), 3.34 (1H, s, H-20), 1.06 (3H, t, *J* = 7.2 Hz, H₃-22), 0.78 (3H, s, H₃-18).
¹³C NMR (100 MHz, CDCl₃): Table 3.
HRMS-ESI: *m/z* [M+H]⁺ calcd for C₂₂H₃₄NO₂: 344.2590; found: 344.2585.

Preparation of compound 48: To a solution of compound **46** (90 mg, 0.25 mmol) in formic acid (85%, 10 mL) was added hydrogen peroxide (30%, 0.4-5 mL), and the reaction was allowed to proceed at room temperature for 5 h. The reaction mixture was basified with conc. ammonium hydroxide to pH > 10 and extracted with chloroform: methanol (5:1, 10 mL × 3). The combined extracts were dried over anhydrous sodium sulfate and concentrated under reduced pressure. The crude residue was purified by CC eluting with CHCl₃: MeOH (20:1, saturated with conc.NH₄OH) to give compound **48** (30 mg, 35%).

Compound 48

¹H NMR (400 MHz, CDCl₃): 4.41 (1H, d, *J* = 13.2 Hz, H-12), 3.97, 3.36 (each 1H, ABq, *J* = 8.4 Hz, H₂-17), 3.73 (1H, s, H-15), 0.74 (3H, s, H₃-18).
¹³C NMR (100 MHz, CDCl₃): Table 3.
HRMS-ESI: *m/z* [M+H]⁺ calcd for C₂₂H₃₆NO₅: 394. 2593; found: 374.2585.

Preparation of compounds 50 and 51: To a solution of songoramine (**49**, 100 mg, 0.28 mmol) in formic acid (85%, 10 mL) was added hydrogen peroxide (30%, 0.5 mL), and the reaction was allowed to proceed at room temperature for 20 h prior to being basified with 25% ammonium hydroxide to pH > 10. The subsequent mixture was extracted with ethyl acetate (20 mL × 3). The combined extracts were dried over anhydrous sodium sulfate and concentrated *in vacuo*. CC of the crude residue on silica gel eluting with CHCl₃: MeOH (30:1) furnished compounds **50** (60 mg, 85%) and **51** (35 mg, 32%).

Compound 50

¹H NMR (400 MHz, CDCl₃): 4.10, 3.70 (each 1H, ABq, *J* = 8.0 Hz, H₂-17), 4.03 (1H, d, *J* = 5.2 Hz, H-1), 3.83 (1H, s, H-19), 3.70 (1H, s, H-15), 1.03 (3H, t, *J* = 7.2 Hz, H₃-22), 0.82 (3H, s, H₃-18).
¹³C NMR (100 MHz, CDCl₃): Table 3.
HRMS-ESI: *m/z* [M+H]⁺ calcd for C₂₂H₃₂NO₅: 390.2280; found: 390.2279.

Compound 51

¹H NMR (400 MHz, CDCl₃): 3.97 (1H, d, *J* = 5.2 Hz, H-1), 3.70 (1H, s, H-15), 3.55, 3.50 (each 1H, ABq, *J* = 7.6 Hz, H₂-17), 1.02 (3H, t, *J* = 7.2 Hz, H₃-22), 0.84 (3H, s, H₃-18).

¹³C NMR (100 MHz, CDCl₃): Table 3.

HRMS-ESI: *m/z* [M+H]⁺ calcd for C₂₂H₃₂NO₅: 390.2280; found: 390.2279.

Preparation of compound 53: To a solution of denudatine (**52**, 20 mg, 0.06 mmol) in methanol (1 mL) was added hydrogen peroxide (0.1 mL), and the reaction was allowed to proceed at 60°C for 20 h prior to being quenched with 25% ammonium hydroxide to pH > 10. The mixture was extracted with chloroform: methanol (5:1, 10 mL × 3). The combined extracts were dried over anhydrous sodium sulfate and concentrated under reduced pressure. The crude residue was purified by CC on silica gel, using CHCl₃: MeOH (50:1) as eluent, to provide compound **53** (13 mg, 60%).

Compound 53

¹H NMR (400 MHz, CDCl₃): 3.82 (1H, d, *J* = 9.2 Hz, H-11), 3.38, 3.43 (each 1H, ABq, *J* = 12.0 Hz, H₂-17), 3.26 (1H, s, H-15), 1.06 (3H, t, *J* = 7.2 Hz, H₃-22), 0.73 (3H, s, H₃-18).

¹³C NMR (100 MHz, CDCl₃): Table 3.

HRMS-ESI: *m/z* [M+H]⁺ calcd for C₂₂H₃₆NO₄: 378.2644; found: 378.2648.

Preparation of compound 55: To a solution of compound **54** (70 mg, 0.12 mmol) in CH₂Cl₂ (2 mL) was added *m*CPBA (70 mg, 0.39 mmol), and the reaction mixture was kept stirred at room temperature for 30 min prior to being concentrated. To the residue was added Fe₂SO₄·7H₂O (130 mg, 0.46 mmol) and the subsequent mixture was stirred at room temperature for 3 h. After general workup, the crude product was purified by CC over silica gel eluting with CHCl₃: MeOH (100:1) to furnish compound **55** (23 mg, 35%).

Compound 55

¹H NMR (400 MHz, CDCl₃): 5.16 (1H, s, H-15), 5.12 (1H, m, H-1), 5.00 (1H, m, H-11), 3.91 (1H, m, H-20), 2.05, 2.05, 1.98, 1.99 (each 3H, s, OAc × 4), 1.03 (3H, t, *J* = 7.2 Hz, H₃-22), 0.72 (3H, s, H₃-18).

¹³C NMR (100 MHz, CDCl₃): Table 3.

References

- [1] Liu XX, Jiang XX, Cai, XF, Chao RB, Chen, QH, Chen DL, Wang XL, Wang FP. (2012) Cardioactive C₁₉-diterpenoid alkaloids from the lateral roots of *Aconitum carmichaeli* "FuZi". *Chemical & Pharmaceutical Bulletin*, **60**, 144-149.
- [2] Jiang XX, Tang P, Liu XX, Chao RB, Chen, QH, She XK, Chen DL, Wang XL, Wang FP. (2012) Structure-cardiac activity relationship of C₁₉-diterpenoid alkaloids. *Natural Product Communications*, **7**, 713-720.
- [3] Wang FP, Li ZB, Yang JS, Li BG. (1999) Modification of norditerpenoid alkaloids: II. A simple and convenient preparation of the imine derivatives of norditerpenoid alkaloids. *Chinese Chemical Letters*, **10**, 453-456.
- [4] Wang FP, Xu L. (2005) To seek an approach toward the chemical conversion of C₁₉-diterpenoid alkaloids to taxoids. *Tetrahedron*, **61**, 2149-2167.
- [5] Barton DHB, McCombie SW. (1975) New method for the deoxygenation of secondary alcohols, *Journal of the Chemical Society, Perkin Transactions I*, 1574-1585
- [6] Pelletier SW, Mody NV. (1984) In *Alkaloids: Chemical and Biological Perspective*, Pelletier SW. (Ed), Vol. 2, John Wiley & Sons, Chichester, 205-462.
- [7] Ding H. (2008) In *Experiential Pharmacology*, Ding H. (Ed), Science Press, Beijing, China. 504-506.
- [8] Wang FP. Unpublished data.

HRMS-ESI: *m/z* [M+H]⁺.calcd for C₂₈H₄₀NO₉ : 534.2703; found: 534.2740.

Preparation of compound 56: Compound **55** (30 mg, 0.06 mmol) was dissolved in a solution of sodium hydroxide in methanol (5%, 10 mL), and the subsequent reaction solution was stirred at 60°C for 2 h. The reaction mixture was concentrated *in vacuo*, and the residue was purified by CC over silica gel, eluting with CHCl₃: MeOH (20:1, saturated with 25% ammonium hydroxide) to furnish compound **56** (7 mg, 35%).

Compound 56

¹H NMR (400 MHz, CDCl₃): 4.55 (1H, d, *J* = 9.2 Hz, H-11), 4.21 (1H, dd, *J* = 10.4, 6.8 Hz, H-1), 4.16 (1H, s, H-15), 3.80, 3.77 (each 1H, ABq, *J* = 12.0 Hz, H₂-17), 3.86 (1H, s, H-20), 0.83 (3H, s, H₃-18).

¹³C NMR (100 MHz, CDCl₃+CD₃OD): Table 3.

HRMS-ESI: *m/z* [M+H]⁺ calcd for C₂₀H₃₂NO₅: 366.2280; found: 366.2276.

Preparation of compound 57: To a solution of compound **55** (58 mg, 0.10 mmol) in THF (2 mL) was added sodium hydride (3.0 mg, 0.13 mmol), followed by methyl iodide (7 μL, 0.10 mmol). The reaction mixture was stirred at room temperature for 3 h prior to removing THF *in vacuo*. To the residue was added a solution of sodium hydroxide (5%) in methanol (10 mL), and the subsequent reaction mixture was stirred at 60°C for 2 h. After removing methanol, the residue was subjected to CC, eluting with CHCl₃: MeOH (50:1, v/v, saturated with 25% ammonium hydroxide) to yield compound **57** (35 mg, 92 %).

Compound 57

¹H NMR (400 MHz, CDCl₃): 4.38 (1H, d, *J* = 9.2 Hz, H-11), 4.06 (1H, dd, *J* = 10.4, 6.8 Hz, H-1), 2.25 (3H, s, H₃-21), 0.65 (3H, s, H₃-18).

¹³C NMR (100 MHz, CD₃OD): Table 3.

HRMS-ESI: *m/z* [M+H]⁺ calcd for C₂₁H₃₂NO₅: 378.2280; found: 378.2271.

Acknowledgments - This research was financially supported by the National Natural Science Foundation of China (No. 81072550).

Monoterpene Indole Alkaloids from *Catharanthus roseus* Cultivated in Yunnan

Bei Wang^{a,b}, Lu Liu^{a,b}, Ying-Ying Chen^{a,b}, Qiong Li^{a,b}, Dan Li^{a,b}, Ya-Ping Liu^{a,*} and Xiao-Dong Luo^{a,*}

^aState Key Laboratory of Phytochemistry and Plant Resources in West China, Kunming Institute of Botany, Chinese Academy of Sciences, Kunming 650201, People's Republic of China

^bUniversity of Chinese Academy of Sciences, Beijing 100049, People's Republic of China

xdluo@mail.kib.ac.cn; liuyaping@mail.kib.ac.cn

Received: July 14th, 2015; Accepted: July 27th, 2015

A new monoterpene indole alkaloid, 15,20-dehydro-3 α -(2-oxopropyl) coronaridine (**1**), along with sixteen analogues (**2–17**) were isolated from the leaves of *Catharanthus roseus* cultivated in Yunnan. The new alkaloid was elucidated on the basis of extensive spectroscopic analysis, and the known alkaloids were identified by comparison with the reported spectroscopic data. Among them, alkaloid **16** was isolated from *Catharanthus* for the first time.

Keywords: *Catharanthus roseus*, Apocynaceae, Monoterpene indole alkaloids, 15,20-Dehydro-3 α -(2-oxopropyl) coronaridine.

Catharanthus roseus (L.) G. Don. (Apocynaceae), a perennial evergreen herb with medicinal and ornamental values, is widely distributed in continental Africa, America, Asia, Australia, Europe, and in some islands of the Pacific Ocean [1]. *C. roseus* has been studied widely in view of its remarkable anticancer properties, especially the bisindole alkaloids, vinblastine and vincristine [1]. In previous investigations, we found that plant secondary metabolites would be influenced significantly by the ecological environments [2]. *C. roseus* has also been cultivated widely in China as an outside ornamental, which inspired us to search for structurally diverse indole alkaloids from the same plant in different ecological environments. Phytochemical investigation of the alkaloids of *C. roseus* cultivated in Xishuangbanna, a tropical rainforest zone, afforded a new alkaloid 15,20-dehydro-3 α -(2-oxopropyl) coronaridine (**1**), along with sixteen analogues (**2–17**), coronaridine (**2**) [3], tetrahydroalstonine (**3**) [4], ajmalicine (**4**) [4], ajmalicinine (**5**) [5], serpentine (**6**) [6], 19-*epi*-alstonine (**7**) [7], yohimbine (**8**) [8], 19,20-dehydro-16-*epi*-yohimbine (**9**) [9], 16*R*-sitsirikine (**10**) [10], isositsirikine (**11**) [10], 16*R*-dihydrositsirikine (**12**) [11], pericyclivine (**13**) [12], akuammidine (**14**) [12], 17-acetyllochnerine (**15**) [13], 21-carbonylnormavacurine (**16**) [14], and 19*S*-*epi*-misiline (**17**) [15]. Among them, alkaloid (**16**) was isolated from this plant for the first time.

Alkaloid **1** was isolated as a white amorphous powder. Its molecular formula was deduced as C₂₄H₂₈N₂O₃ based on ¹³C NMR and HRESIMS data. The ¹H NMR spectrum of **1** showed characteristic signals of an unsubstituted indole alkaloid moiety at δ_{H} 7.47 (1H, d, 7.8 Hz, H-9), 7.08 (1H, td, 7.2 Hz, H-10), 7.14 (1H, td, 7.2 Hz, H-11), and 7.23 (1H, d, 7.8 Hz, H-12). Additionally, the ¹H spectrum displayed signals for an ethyl side chain at δ_{H} 2.25/2.10 (2H, m, H-19) and 1.07 (3H, t, Me-18), a bridgehead proton adjacent to a nitrogen at δ_{H} 4.15 (1H, br s, H-21), a methoxy group at δ_{H} 3.71 (3H, s), a -COCH₃ group (δ_{H} 2.13, 3H, s), and an olefinic proton at δ_{H} 5.77 (1H, d, 6.0 Hz, H-15). The ¹H-¹H COSY spectrum suggested two main spin systems: δ_{H} 2.76/1.85 (dd/dd, H₂-17)/ δ_{H} 2.66 (m, H-14) [δ_{H} 3.36 (m, H-3/N)]/ δ_{H} 2.48/2.33 (dd/dd, H₂-22)/H-15 and H₂-19/Me-18. The HMBC correlations from H-3 to δ_{C} 51.5 (t, C-5) and δ_{C} 62.1 (d, C-21) revealed that C-3, C-21, and C-5 originated from carbons attached to N-4. Likewise, the HMBC cross-peaks of H-21/C-2, δ_{C} 54.8 (s, C-16), δ_{C} 38.7 (t, C-17) and

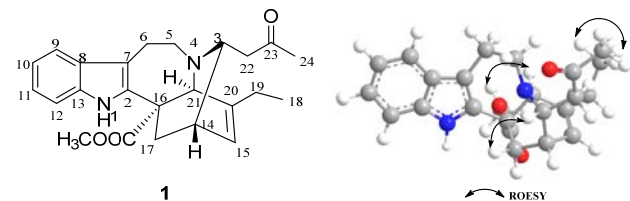


Figure 1: Structure and ROESY correlations of compound **1**.

Table 1: ¹H and ¹³C NMR data for **1** (CDCl₃, 600 and 150 MHz, respectively).

position	δ_{H} , mult. (<i>J</i> in Hz)	δ_{C} , type	HMBC
1	7.62, br s		7, 8
2		136.2, s	
3	3.36, m	55.9, d	5, 21
5	3.44, m; 3.32, m	51.5, t	7, 21
6	3.26, m; 2.90, m	21.5, t	
7		110.7, s	
8		128.9, s	
9	7.47, br d (7.8)	118.2, d	
10	7.08, td (7.2)	119.5, d	
11	7.14, td (7.2)	121.9, d	
12	7.23, br d (7.8)	110.4, d	
13		134.9, s	
14	2.66, m	34.7, d	16, 20
15	5.77, d (6.0)	121.7, d	3, 21
16		54.8, s	
17	2.76, dd (13.2, 3.6) 1.85, dd (13.2, 2.4)	38.7, t	
18	1.07, t (7.2)	11.2, q	
19	2.25, m; 2.10, m	26.3, t	15
20		150.1, s	
21	4.15, br s	62.1, d	
22	2.48, dd (16.2, 4.8) 2.33, dd (16.2, 7.8)	49.3, t	14
23		209.1, s	
24	2.13, s	31.1, q	
-COOCH ₃		174.0, s	
-COOCH ₃	3.71, s	52.3, q	

H-17/C-2, C-16, C-21, δ_{C} 174.0 (s, -COOCH₃) implied that CH-21, CH₂-17 and the methoxycarbonyl group were connected via C-16, H-14/ δ_{C} 49.3 (t, C-22), C-16, δ_{C} 150.1 (s, C-20) and H-15/ δ_{C} 26.3 (t, C-19), δ_{C} 55.9 (d, C-3); C-21 showed a double bond located at C-15/C-20 and a 3 α -(2-oxopropyl). These observations suggested that **1** possessed an ibogan-type monoterpene indole alkaloid carbon skeleton, similar to that of 3-(2-oxopropyl) coronaridine [3]. The differences between them were that a methylene and a methine in 3-(2-oxopropyl) coronaridine [3] were replaced by a double bond (δ_{C} 150.1, s, C-20; 127.1, d, C-15) in **1**. In its ROESY spectrum, the

NOE correlations between H-21/ δ_H 3.71 (-COOCH₃), placed H-21 and COOCH₃ on the same face. Biogenetically, they were assigned with an α -orientation, and H-14 with a β -orientation of coronaridine derivatives isolated from Apocynaceae [16]. Moreover, NOE correlations between H-14 and H-3 suggested that H-14 and H-3 were on the same face, whereas the correlations between Me-18 and Me-24 positioned them on the opposite side (Figure 1). The specific rotation of **1** $[\alpha]_D^{21} -11$ (c 0.13, CHCl₃) was also similar to that observed for ervatamine G $[\alpha]_D^{20} -23$ (c 0.3, CHCl₃) [16]. Based on the above evidence, the structure of **1** was elucidated as shown.

Experimental

General experimental procedures: Optical rotation, JASCO P-1020 digital polarimeter; UV, Shimadzu UV-2401 PC spectrophotometer; IR, Bruker Tensor-27 infrared spectrophotometer; 1D and 2D NMR, Bruker AM-400 and DRX-600 spectrometers; ESIMS, Bruker HTC/Esquire spectrometer; HREIMS, Waters AutoSpec Premier P776 spectrometer; Semipreparative HPLC was performed on an Agilent 1260 HPLC with a ZORBAX SB-C18 (9.4 \times 250 mm). TLC were visualized by Dragendorff's reagent and 10% H₂SO₄ in ethanol.

Plant material: Air-dried stems and branches of *C. roseus* were collected in November 2012 from Xishuangbanna, Yunnan province, P. R. China. The plant was identified by Mr Hai-Chuan Tai. A voucher specimen (No. Tai2012110503) has been deposited in KIB, CAS.

Extraction and isolation: The air-dried and powdered stems and branches of *C. roseus* (9.0 kg) were extracted with MeOH under reflux conditions, and the solvent was evaporated *in vacuo*. The residue was dissolved in 0.37% HCl (pH 2-3) and the solution was subsequently basified using 10% ammonia to pH 9-10. The basic solution was partitioned with EtOAc, affording a two-phase mixture. The EtOAc fraction (190 g) was subjected to CC over silica gel (Fr. A-F). Fr. A (6.5 g) was subjected to silica gel CC

(light petroleum/acetone, 9:1:0:1, v/v) and recrystallization to yield **3** (700 mg), and **4** (26.5 mg). Fr. B (9.8 g) was eluted *via* silica gel CC under isocratic conditions (light petroleum/acetone, 7:1, v/v) to afford **1** (1.8 mg), **2** (5.6 mg), **8** (1.5 mg), **10** (4.7 mg), and **17** (10.0 mg). Compounds **14** (6.3 mg), **5** (10.3 mg), **9** (4.5 mg), and **11** (3.0 mg) were obtained from Fr. C (11.2 g) by silica gel CC with isocratic elution using light petroleum/acetone, 5:1. Fr. D (35.5 g) was subjected to silica gel CC (CHCl₃/MeOH, 20:1:0:1) and further resolved by semi-HPLC to yield compounds **15** (2.4 mg), **12** (1.7 mg), **13** (159.6 mg), and **16** (30.7 mg). Fr. E (95.3 g) was chromatographed on a RP-18 column with MeOH/H₂O (20:1:1:0, v/v) gradient system to give fractions E1-E8. Fractions E3 (6.3 g) and E5 (9.6 g) were separated on a Sephadex LH-20 column eluting with CHCl₃/MeOH (1:1, v/v) and further by PTLC to yield **6** (10.8 mg), and **7** (4.8 mg).

15, 20-Dehydro-3 α -(2-oxopropyl) coronaridine (**1**)

White amorphous powder.

$[\alpha]_D^{21} -11$ (c 0.13, CHCl₃).

Rf: 0.5 (light petroleum-ethyl acetate, 10:1).

IR (KBr): 3425, 2962, 2925, 1714, 1632, 1461, 1383, 1262, 1095, 1028, 804 cm⁻¹.

UV/Vis λ_{max} (MeOH) nm (log ε): 240 (3.70), 284 (3.59).

¹H and ¹³C NMR (CDCl₃): Table 1.

ESIMS : *m/z* (%) = 393 [M + H]⁺ (100).

HRESIMS : found *m/z* 393.2181 (Calcd. for 393.2178).

Supplementary data: NMR and mass spectra of the new compound **1**, and ¹³C NMR data of compounds **2-17**.

Acknowledgments - The authors are grateful to the Natural Science Foundation of China (81225024, 31170334), and the Ministry of Science and Technology of P. R. China (2013BAI11B02) for partial financial support, and to the analytical group of KIB for spectral measurement.

References

- [1] Mujib A, Ilah A, Aslam J, Fatima S, Siddiqui ZH, Maqsood M. (2012) *Catharanthus roseus* alkaloids: application of biotechnology for improving yield. *Plant Growth Regulation*, **68**, 111-127.
- [2] Liu YP, Lai R, Yao YG, Zhang ZK, Pu ET, Cai XH, Luo XD. (2013) Induced furoeudesmanes: a defense mechanism against stress in *Laggera pterodonta*, a Chinese herbal plant. *Organic Letters*, **15**, 4940-4943.
- [3] Okuyama E, Gao LH, Yamazaki M. (1992) Analgesic components from Bornean medicinal plants, *Tabernaemontana pauciflora* Blume and *Tabernaemontana pandacaqui* Poir. *Chemical & Pharmaceutical Bulletin*, **40**, 2075-2079.
- [4] Wenkert E, Chang CJ, Chawla HPS, Cochran DW, Hagaman EW, King JC, Orito K. (1976) General methods of synthesis of indole alkaloids. 14. Short routes of construction of yohimboid and ajmalicinoid alkaloid systems and their carbon-13 nuclear magnetic resonance spectral analysis. *Journal of the American Chemical Society*, **98**, 3645-3655.
- [5] Madinaveitia A, Reina M, Fuente Gdl, Gonzalez AG. (1996) Obovamine, a new indole alkaloid from *Stemmadenia obovata*. *Journal of Natural Products*, **59**, 185-189.
- [6] Wachsmuth O, Matusch R. (2002) Anhydronium bases from *Rauvolfia serpentina*. *Phytochemistry*, **61**, 705-709.
- [7] Dinda B, De UC. (2002) 19-Epialstonine from *Amphicome emodi* roots. *Indian Journal of Chemistry, Section B: Organic Chemistry Including Medicinal Chemistry*, **41B**, 2698-2700.
- [8] Itoh A, Kumashiro T, Yamaguchi M, Nagakura N, Mizushima Y, Nishi T, Tanahashi T. (2005) Indole alkaloids and other constituents of *Rauvolfia serpentina*. *Journal of Natural Products*, **68**, 848-852.
- [9] Dos Santos Torres ZE, Silveira ER, Rocha e Silva LF, Lima ES, Carvalho de Vasconcellos M, Uchoa DEdA, Braz Filho R, Pohl AM. (2013) Chemical composition of *Aspidosperma ulei* Markgr. and antiplasmodial activity of selected indole alkaloids. *Molecules*, **18**, 6281-6297.
- [10] Zhang BJ, Yan JM, Wu ZK, Liu YP, Bao MF, Cheng GG, Luo XD, Cai XH, Li Y. (2013) Alkaloids from *Ochrosia borbonica*. *Helvetica Chimica Acta*, **96**, 2288-2298.
- [11] Robert GMT, Ahond A, Poupat C, Potier P, Jolles C, Jousselin A, Jacquemin H. (1983) *Aspidosperma* from Guiana: alkaloids from *Aspidosperma marcgravianum*. *Journal of Natural Products*, **46**, 694-707.
- [12] Farnsworth NR, Loub WN, Blomster RN, Gorman M. (1964) Pericyclivine, a new *Catharanthus* alkaloid. *Journal of Pharmaceutical Sciences*, **53**, 1558.
- [13] Kam TS, Iek IH, Choo YM. (1999) Alkaloids from the stem-bark of *Alstonia macrophylla*. *Phytochemistry*, **51**, 839-844.
- [14] Liu L, Chen YY, Qin XJ, Wang B, Jin Q, Liu YP, Luo XD. (2015) Antibacterial monoterpenoid indole alkaloids from *Alstonia scholaris* cultivated in temperate zone, *Fitoterapia*, **105**, 160-164.
- [15] Atta ur Rahman, Silva WSJ, Alvi KA, De Silva KT. (1987) Isolation and structural studies on the alkaloids of *Petchia ceylanica*. *Phytochemistry*, **26**, 543-545.
- [16] Zhang DB, Yu DG, Sun M, Zhu XX, Yao XJ, Zhou SY, Chen JJ, Gao K. (2015) Ervatamines A-I, anti-inflammatory monoterpenoid indole alkaloids with diverse skeletons from *Ervatamia hainanensis*. *Journal of Natural Products*, **78**, 1253-1261.

Two New Oxindole Alkaloid Glycosides from the Leaves of *Nauclea officinalis*

Long Fan^{a,b,c}, Xiao-Jun Huang^{a,b}, Chun-Lin Fan^a, Guo-Qiang Li^a, Zhen-Long Wu^{a,b}, Shuo-Guo Li^{a,b}, Zhen-Dan He^c, Ying Wang^{a,b,*} and Wen-Cai Ye^{a,b,*}

^aInstitute of Traditional Chinese Medicine & Natural Products, College of Pharmacy, Jinan University, Guangzhou 510632, P. R. China

^bJNU-HKUST Joint Laboratory for Neuroscience & Innovative Drug Research, Jinan University, Guangzhou 510632, P. R. China

^cDepartment of Pharmacy, School of Medicine, Shenzhen University, Shenzhen 518060, P. R. China

chyewc@gmail.com; wangying_cpy@163.com

Received: July 18th, 2015; Accepted: August 6th, 2015

Two new oxindole alkaloid glycosides, nauclealomide A and (3S,7R)-javaniside, were isolated from the leaves of *Nauclea officinalis*. Their structures and absolute configurations were elucidated by means of NMR, HRESIMS, X-ray diffraction, acid hydrolysis and quantum chemical CD calculation. Nauclealomide A is a novel monoterpenoid oxindole alkaloid possessing a rare tetrahydro-2H-1,3-oxazine ring.

Keywords: *Nauclea officinalis*, Rubiaceae, Oxindole alkaloid, Tetrahydro-2H-1,3-oxazine ring.

The genus *Nauclea* (Rubiaceae) comprises thirty-five species which are mainly distributed in Africa and tropical regions of Asia and Australia [1]. The plants of this genus are rich in indole alkaloids, which exhibit antimalarial, antiproliferative and renin-inhibitory activities [2-5]. To date, phytochemical investigations have led to the isolation of more than 70 indole alkaloids from the genus. The bark and twigs of *Nauclea officinalis* Pierre ex Pitard is used as a traditional medicine in China for treatment of colds, swelling of the throat, pink eye and other ailments [1]. During the course of an ongoing search for new alkaloids from medicinal plants in China [6-12], the EtOH extract of the leaves of *N. officinalis* was further investigated, which led to the isolation of two new oxindole alkaloid glycosides, nauclealomide A (**1**) and (3S,7R)-javaniside (**2**) (Figure 1). The structures of indole alkaloids **1** and **2** were elucidated by NMR, HRESIMS, X-ray diffraction, acid hydrolysis, as well as CD analysis. Herein, the isolation and structural elucidation of the new indole alkaloids are described.

Nauclealomide A (**1**) showed a molecular formula of C₂₆H₃₀N₂O₁₀ based on the HRESIMS (*m/z* 553.1791 [M + Na]⁺; calculated for C₂₆H₃₀N₂O₁₀Na: *m/z* 553.1793). The UV spectrum of **1** showed absorption maxima at 211 and 242 nm. The IR spectrum exhibited absorptions at 3394 and 1648 cm⁻¹, which suggested the presence of amino and α,β-unsaturated carbonyl functional groups. The ¹H and ¹³C NMR spectra of **1** displayed signals due to two carbonyl groups (δ_C 180.1 and 166.1), a trisubstituted double bond [δ_H 7.44 (1H, d, *J* = 2.4 Hz); δ_C 149.7 and 109.0], a terminal vinyl group [δ_H 5.56 (1H, dt, *J* = 17.0, 10.1 Hz), 5.29 (1H, dd, *J* = 17.0, 1.8 Hz) and 5.24 (1H, dd, *J* = 10.1, 1.8 Hz); δ_C 134.1 and 120.7] and an *ortho*-substituted benzene ring [δ_H 7.25 (1H, br d, *J* = 7.5 Hz), 7.25 (1H, br t, *J* = 7.5 Hz), 7.02 (1H, br t, *J* = 7.5 Hz) and 6.84 (1H, br d, *J* = 7.5 Hz); δ_C 142.3, 131.4, 131.1, 125.4, 123.9 and 111.0]. In addition, the NMR spectra of **1** displayed signals due to a sugar unit [δ_H 4.69 (1H, d, *J* = 7.9 Hz), 3.87 (1H, dd, *J* = 11.8, 1.7 Hz), 3.66 (1H, dd, *J* = 11.8, 5.3 Hz), and 3.37-3.20 (4H, overlapped); δ_C 100.4, 78.3, 78.2, 74.7, 71.5 and 62.6]. Acid hydrolysis of **1** afforded D-glucose, which was identified by HPLC analysis using authentic samples as references.

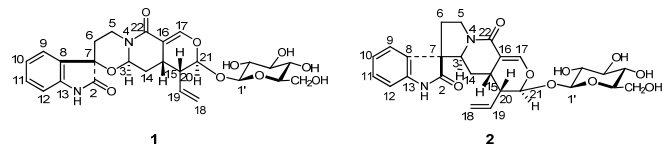


Figure 1: Structures of **1** and **2**.

In addition, the β-configuration for D-glucose was further determined based on the large ³J_{H1,H2} coupling constant (*J* = 7.9 Hz) of the anomeric proton. Taken together, these spectral data suggested that **1** was a monoterpenoid oxindole alkaloid with a β-D-glucose unit [13-15].

With the aid of ¹H-¹H COSY, HSQC, HMBC, and ROESY experiments, all of the ¹H and ¹³C NMR signals of **1** were assigned as shown in Table 1. The ¹H-¹H COSY spectrum of **1** revealed the presence of three spin coupling systems (C-9 to C-12, C-5 to C-6, and C-3 to C-21/C-18, Figure 2). In the HMBC spectrum, the correlations between H-17 and C-15/C-16/C-21/C-22, and between H-3 and C-22 revealed the presence of ring E, which was fused to ring D. In addition, the HMBC correlation between H-21 and C-1' indicated that the glucose was located at C-21. Moreover, HMBC correlations between Ha-5 and C-3/C-7/C-22, as well as between Ha-6 and C-2/C-7/C-8 were also observed (Figure 2).

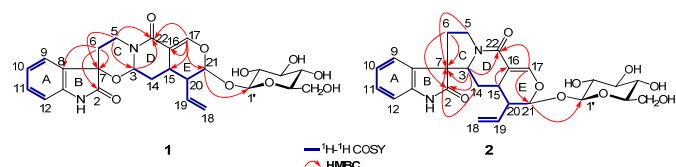
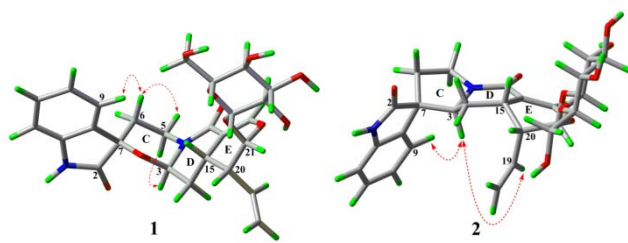


Figure 2: ¹H-¹H COSY and selected HMBC correlations of **1** and **2**.

Comparison of the NMR data of **1** with those of javaniside [13,14] indicated that they were very similar, except for the obvious down-field shift of H-3 (from δ_H 4.09 to 6.28), C-3 (from δ_C 65.5 to 80.0) and C-7 (from δ_C 58.0 to 77.6). Furthermore, according to the

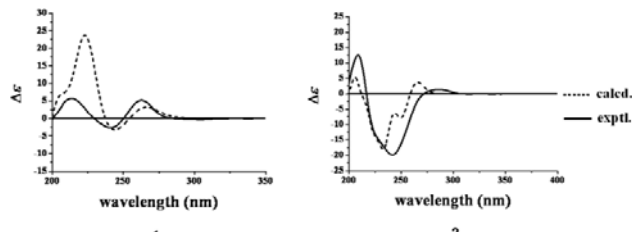
Table 1: NMR spectroscopic data for **1** and **2** in CD₃OD (400 MHz for ¹H, 100 MHz for ¹³C, δ in ppm, J in Hz).

Position		1		2	
	δ_{C}	δ_{H}	δ_{C}	δ_{H}	δ_{H}
2	180.1	-	181.5	-	-
3	80.0	6.28 t (2.8)	63.8	3.95 m	a 3.93 m
5	39.3	a 4.60 ddd (13.0, 4.9, 1.8) b 3.75 dd (13.0, 3.0)	44.9	b 3.83 m	b 2.36 dt (13.0, 9.8)
6	32.4	a 2.11 td (14.1, 5.4) b 1.77 m	34.3	b 2.21 ddd (13.0, 7.5, 1.6)	a 2.21 ddd (13.0, 7.5, 1.6)
7	77.6	-	57.7	-	-
8	131.4	-	129.8	-	-
9	125.4	7.25 br d (7.5)	124.0	7.25 br d (7.5)	7.25 br d (7.5)
10	123.9	7.02 br t (7.5)	123.7	7.05 td (7.5, 1.0)	7.24 td (7.5, 1.0)
11	131.1	7.25 br t (7.5)	130.0	7.24 td (7.5, 1.0)	6.91 dt (7.5, 1.0)
12	111.0	6.84 br d (7.5)	111.0	-	-
13	142.3	-	143.4	-	-
14	29.7	1.76 m	24.7	a 1.77 dt (13.7, 9.4) b 1.51 dt (13.7, 4.5)	a 1.77 dt (13.7, 9.4) b 1.51 dt (13.7, 4.5)
15	23.4	3.27 m	24.9	3.18 m	3.18 m
16	109.0	-	109.9	-	-
17	149.7	7.44 d (2.4)	147.5	7.14 d (2.6)	a 5.11 dd (10.1, 1.9) b 5.06 dd (17.0, 1.9)
18	120.7	a 5.29 dd (17.0, 1.8) b 5.24 dd (10.1, 1.8)	120.6	b 5.06 dd (17.0, 1.9)	5.59 dt (17.0, 10.1)
19	134.1	5.56 dt (17.0, 10.1)	133.8	2.41 ddd (10.1, 5.3, 1.6)	2.41 ddd (10.1, 5.3, 1.6)
20	44.3	2.61 ddd (10.1, 5.8, 1.7)	45.7	5.37 d (1.6)	5.37 d (1.6)
21	98.1	5.46 d (1.7)	97.4	-	-
22	166.1	-	167.7	-	-
1'	100.4	4.69 d (7.9)	99.9	4.65 d (7.9)	4.65 d (7.9)
2'	74.7	3.20 m	74.6	3.15 dd (9.0, 7.9)	3.15 dd (9.0, 7.9)
3'	78.2	3.37 m	77.8	3.35 t (9.0)	3.35 t (9.0)
4'	71.5	3.30 m	71.5	3.25 t (9.0)	3.25 t (9.0)
5'	78.3	3.31 m	78.3	3.28 dd (5.7, 2.0)	3.28 dd (5.7, 2.0)
6'	62.6	a 3.87 dd (11.8, 1.7) b 3.66 dd (11.8, 5.3)	62.6	a 3.84 dd (12.0, 2.0) b 3.62 dd (12.0, 5.7)	a 3.84 dd (12.0, 2.0) b 3.62 dd (12.0, 5.7)

**Figure 3:** Selected ROESY correlations of **1** and **2**.

molecular formula and the degree of unsaturation, the remaining oxygen atom could be assigned as a bridge between C-3 and C-7 to form a tetrahydro-2*H*-1,3-oxazine ring (Figure 2).

The relative configuration of **1** was deduced from coupling constants and ROESY data. The coupling constants of ³J_{20,21} (*J* = 1.7 Hz) and ³J_{20,15} (*J* = 5.8 Hz) suggested the presence of β/β/α orientation for H-15, H-20 and H-21 [13-15], while the coupling constant of ³J_{3,14} (*J* = 2.8 Hz) indicated the presence of α configuration of H-3. In the ROESY spectrum, the correlations between H-3 and Hb-5, as well as between Ha-6 and H-9/Ha-5 indicated the presence of β/α/β configuration of Ha-5, Hb-5 and Ha-6 (Figure 3). The absolute configuration of C-15 in these indole alkaloids was determined as *S* biosynthetically based on secologanin [16]. Thus, the absolute configuration of **1** was elucidated as 3*R*,7*R*,15*S*,20*R*,21*S*, which was consistent with the results obtained by the following quantum chemical CD calculation experiment (Figure 4).

**Figure 4:** Calculated and experimental CD spectra of **1** and **2**.

The molecular formula of (3*S*,7*R*)-javanside (**2**) was established as C₂₆H₃₀N₂O₉ (*m/z* 537.1823 [M + Na]⁺; calculated for C₂₆H₃₀N₂O₉Na: *m/z* 537.1844) by HRESIMS. Acid hydrolysis of **2** also afforded D-glucose. Similar to **1**, the NMR spectra of **2** revealed the presence of two carbonyl groups (δ_{C} 181.5 and 167.7), a trisubstituted double bond [δ_{H} 7.14 (1H, d, *J* = 2.6 Hz); δ_{C} 147.5 and 109.9], a terminal vinyl group [δ_{H} 5.59 (1H, dt, *J* = 17.0, 10.1 Hz), 5.11 (1H, dd, *J* = 10.1, 1.9 Hz) and 5.06 (1H, dd, *J* = 17.0, 1.9 Hz); δ_{C} 133.8 and 120.6], and an *ortho*-substituted benzene ring, which suggested that **2** was also a monoterpenoid oxindole alkaloid with a glucose moiety [13-15].

With the aid of 1D and 2D NMR experiments, all of the ¹H and ¹³C NMR signals of **2** were assigned (Table 1). The ¹H-¹H COSY spectrum of **2** revealed the presence of three spin coupling systems in bold (Figure 2). In the HMBC spectrum, the correlations between H-17 and C-21/C-22, between H-15 and C-16, as well as between H-3 and C-22 revealed the presence of ring E, which was fused to ring D. Moreover, the HMBC correlations between H₂-6/H-5b/H-3/H₂-14 and C-7, and between H-3/H₂-6 and C-2 were observed, which indicated that ring C was fused to ring D and then linked to ring B via the spiro-carbon (C-7). In addition, the HMBC correlation between H-21 and C-1' indicated that the glucose was located at C-21.

The relative configuration of **2** could be established by a ROESY experiment. In the ROESY spectrum, the correlation between H-3 and H-19 indicated the α orientation of H-3. In addition, the ROESY correlation between H-9 and H-3 suggested that the carbonyl group at C-2 was above the C/D/E plane (Figure 3). Considering the biogenetic pathway of these indole alkaloids, the absolute configuration of C-15 was determined as *S* [16]. Thus, the absolute configuration of **2** was elucidated as 3*S*,7*R*,15*S*,20*R*,21*S*, which was consistent with the results obtained by the single crystal X-ray diffraction experiment (Figure 5) and the quantum chemical CD calculation experiment (Figure 4).

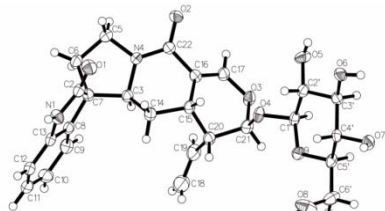


Figure 5: Perspective view of the crystal structure of **2**.

Experimental

General experimental procedures: Optical rotations were measured on a JASCO P-1020 polarimeter, UV spectra on a JASCO V-550 UV/VIS spectrophotometer with a 1 cm length cell, and IR spectra on a JASCO FT/IR-480 plus FT-IR spectrometer. ^1H , ^{13}C , and 2D NMR spectra were recorded on a Bruker AV-400 spectrometer and HRESIMS on an Agilent 6210 ESI/TOF mass spectrometer. CD spectra were obtained using a JASCO J-810 circular dichroism spectrometer. For column chromatography, silica gel (300–400 mesh; Qingdao Marine Chemical Group Corporation) and Sephadex LH-20 (Pharmacia) were used. TLC analyses were carried out using precoated silica gel GF₂₅₄ plates (Yantai Chemical Industry Research Institute). Analytical high-performance liquid chromatography (HPLC) was performed on an Agilent chromatograph equipped with a G1311C pump and a G1315D diode-array detector (DAD) with a Cosmosil 5C₁₈-MS-II column (4.6 × 250 mm, 5 μm). Preparative HPLC was carried out on an Agilent instrument equipped with a G1310B pump and a G1365D detector with a Cosmosil 5C₁₈-MS-II Waters column (10 × 250 mm, 5 μm). X-ray crystallographic analysis was carried out on an Agilent Gemini S Ultra diffractometer with Cu K α radiation ($\lambda = 1.5418 \text{ \AA}$).

Plant material: The leaves of *N. officinalis* were collected in Sanya city, Hainan province of P. R. China, in July of 2008, and authenticated by Professor Wei-ping Chen (Hainan Branch Institute of Medicinal Plants, Chinese Academy of Medical Science). A voucher specimen (No. 20090223) was deposited in the Institute of Traditional Chinese Medicine and Natural Products, Jinan University, Guangzhou, P. R. China.

Extraction and isolation: Air-dried and powdered leaves of *N. officinalis* (4.8 kg) were extracted with 95% EtOH (50 L × 3, 3 days each) at room temperature. The EtOH solution was evaporated under reduced pressure to afford a residue (250.0 g), which was suspended in water and partitioned successively with light petroleum and EtOAc. The basic solution was then partitioned with *n*-BuOH to afford *n*-BuOH and emulsion fractions. The emulsion fraction (5.0 g) was subjected to silica gel CC, eluting with CHCl₃ - MeOH (100:0 → 80:20) to give 9 fractions (Fr. 1–9). Fr. 7 (669.0 mg) were further purified on a Sephadex LH-20 column using MeOH as eluent, then nauclealomide A (**1**, 10.0 mg) and (*3S,7R*)-javaniside (**2**, 15.0 mg) were finally obtained by preparative HPLC using MeOH-H₂O (43:57, 3 mL/min) as the mobile phase.

References

- [1] Editorial Committee of Chinese Herbs. (1999) *Chinese Herbs*, Vol. **6**. Shanghai Science and Technology Press, Shanghai, China. 456.
- [2] He ZD, Ma CY, Zhang HJ, Tan GT, Tamez P, Sydara K, Bouamanivong S, Southavong B, Soejarto DD, Pezzuto JM, Fong HHS. (2005) Antimalarial constituents from *Nauclea orientalis* (L.) L. *Chemistry & Biodiversity*, **2**, 1378–1386.
- [3] Sun JY, Lou HX, Dai SJ, Xu H, Zhao F, Liu K. (2008) Indole alkaloids from *Nauclea officinalis* with weak antimalarial activity. *Phytochemistry*, **69**, 1405–1410.
- [4] Erdelmeier CAJ, Regenass U, Rali T, Sticher O. (1992) Indole alkaloids with *in vitro* antiproliferative activity from the ammoniacal extract of *Nauclea orientalis*. *Planta Medica*, **58**, 43–48.

Nauclealomide A (**1**)

yellowish amorphous solid.

$[\alpha]_D^{27} = -55$ (*c* 0.17, MeOH).

IR (KBr): ν_{max} 3394, 1707, 1648, 1482, 1072 cm^{-1} .

UV (MeOH) λ_{max} (log ϵ): 211 (4.32), 242 (4.10) nm.

^1H and ^{13}C NMR data (CD₃OD, 400 and 100 MHz): Table 1.

HRESIMS *m/z*: 553.1791 [M + Na]⁺ (calcd for C₂₆H₃₀N₂O₁₀Na: 553.1793).

(*3S,7R*)-Javaniside (**2**)

colourless plates.

$[\alpha]_D^{27} = -212$ (*c* 0.25, MeOH).

IR (KBr): ν_{max} 3394, 1703, 1652, 1587, 1470, 1072, 1015 cm^{-1} .

UV (MeOH) λ_{max} (log ϵ): 211 (4.50), 244 (4.33) nm.

^1H and ^{13}C NMR data (CD₃OD, 400 and 100 MHz): Table 1.

HRESIMS *m/z*: 537.1823 [M + Na]⁺ (calcd for C₂₆H₃₀N₂O₉Na: 537.1844).

Crystal data of (*3S,7R*)-javaniside (2**):** The X-ray data of indole alkaloid **2** were collected using a Sapphire CCD with a graphite monochromated Cu K α radiation, $\lambda = 1.54184 \text{ \AA}$ at 173.00(10) K. The structure was solved by direct methods using the SHELXS-97 program, and refined by the SHELXL-97 program and full-matrix least-squares calculations [17]. C₂₆H₃₂N₂O₁₀, $M_r = 532.54$, *Orthorhombic*, $a = 10.99153$ (12) \AA , $b = 13.26367$ (14) \AA , $c = 17.28232$ (16) \AA , $\alpha = \beta = \gamma = 90.00^\circ$, $V = 2519.56$ (4) \AA^3 , space group *P2(1)2(1)2(1)*, $Z = 4$, μ (Cu K α) = 0.912 mm^{-1} , 20419 reflections collected, 4036 independent reflections ($R_{\text{int}} = 0.0270$). The final R_1 value was 0.0297 [$I > 2\sigma(I)$]. The final $wR(F^2)$ value was 0.0769 [$I > 2\sigma(I)$]. The final R_1 value was 0.0310 (all data). The final $wR(F^2)$ value was 0.0781 (all data). The goodness of fit on F^2 was 1.069. Flack parameter = -0.09 (15). Crystallographic data of (*3S,7R*)-javaniside have been deposited at the Cambridge Crystallographic Data Centre (deposition number: CCDC 937396).

Acid hydrolysis: Indole alkaloids **1** and **2** (2 mg each) in 2 N HCl (5 mL) were heated at 80°C for 2 h, after which the residue was dissolved in pyridine (1 mL) and stirred with L-cysteine methyl ester hydrochloride (2 mg) at 60°C for 1 h. *O*-tolyl isothiocyanate (5 μL) was then added to the mixture and heated at 60°C for an additional 1 h. The reaction mixture was subsequently analyzed by HPLC and detected at 250 nm. Analytical HPLC was performed on a Cosmosil 5C₁₈-MS-II column (4.6 × 250 mm, 5 μm) at 20°C using CH₃CN-0.05% CH₃COOH in H₂O (25:75, 1.0 mL/min) as the mobile phase. Peaks were detected with a G1315D DAD. D-Glucose (t_R 16.4 min) was identified as the sugar moiety of indole alkaloids **1** and **2** by comparison with authentic samples of D-glucose (t_R 16.4 min) and L-glucose (t_R 14.9 min) [18].

Supplementary data: HRESIMS, UV, IR, 1D and 2D NMR spectra of indole alkaloids **1** and **2**, and quantum chemical CD calculations of **1** and **2**.

Acknowledgements – This work was supported financially by the Postdoctoral Science Foundation of China (No. 2015M572415).

- [5] Agomuoh AA, Ata A, Udenigwe CC, Aluko RE, Irenus I. (2013) Novel indole alkaloids from *Nauclea latifolia* and their renin-inhibitory activities. *Chemistry & Biodiversity*, **10**, 401-410.
- [6] Wu ZL, Zhao BX, Huang XJ, Tang GY, Shi L, Jiang RW, Liu X, Wang Y, Ye WC. (2014) Suffrutines A and B: a pair of Z/E isomeric indolizidine alkaloids from the roots of *Flueggea suffruticosa*. *Angewandte Chemie International Edition*, **53**, 5796-5799.
- [7] Liu ZW, Yang TT, Wang WJ, Li GQ, Tang BQ, Zhang QW, Fan CL, Zhang DM, Zhang XQ, Ye WC. (2013) Ervahainine A, a new cyano-substituted oxindole alkaloid from *Ervatamia hainanensis*. *Tetrahedron Letters*, **54**, 6498-6500.
- [8] Zhao BX, Wang Y, Li C, Wang GC, Huang XJ, Fan CL, Li QM, Zhu HJ, Chen WM, Ye WC. (2013) Flueggidine, a novel axisymmetric indolizidine alkaloid dimer from *Flueggea virosa*. *Tetrahedron Letters*, **54**, 4708-4711.
- [9] Zhao BX, Wang Y, Zhang DM, Huang XJ, Bai LL, Yan Y, Chen JM, Lu TB, Wang YT, Zhang QW, Ye WC. (2012) Virosaines A and B, two new birdcage-shaped Securinega alkaloids with an unprecedented skeleton from *Flueggea virosa*. *Organic Letters*, **14**, 3096-3099.
- [10] Zhao BX, Wang Y, Zhang DM, Jiang RW, Wang GC, Shi JM, Huang XJ, Chen WM, Che CT, Ye WC. (2011) Flueggines A and B, two new dimeric indolizidine alkaloids from *Flueggea virosa*. *Organic Letters*, **13**, 3888-3891.
- [11] Ouyang S, Wang L, Zhang QW, Wang GC, Wang Y, Huang XJ, Zhang XQ, Jiang RW, Yao XS, Che CT, Ye WC. (2011) Six new monoterpenoid indole alkaloids from the aerial part of *Gelsemium elegans*. *Tetrahedron*, **67**, 4807-4813.
- [12] Fan L, Fan CL, Wang Y, Zhang XQ, Zhang QW, Zhang JQ, Ye WC. (2010) Alkaloids from the leaves of *Nauclea officinalis*. *Acta Pharmaceutica Sinica*, **45**, 747-751.
- [13] Ma J, Hecht SM. (2004) Javaniside, a novel DNA cleavage agent from *Alangium javanicum* having an unusual oxindole skeleton. *Chemical Communications*, **40**, 1190-1191.
- [14] Pham VC, Ma J, Thomas SJ, Xu ZD, Hecht SM. (2005) Alkaloids from *Alangium javanicum* and *Alangium grisolleoides* that mediate Cu²⁺-dependent DNA strand scission. *Journal of Natural Products*, **68**, 1147-1152.
- [15] Wu M, Wu P, Xie HH, Wu GJ, Wei XY. (2011) Monoterpenoid indole alkaloids mediating DNA strand scission from *Turpinia arguta*. *Planta Medica*, **77**, 284-286.
- [16] Cong HJ, Zhao Q, Zhang SW, Wei JJ, Wang WQ, Xuan LJ. (2014) Terpenoid indole alkaloids from *Mappianthus iodoides* Hand.-Mazz.. *Phytochemistry*, **100**, 76-85.
- [17] Dolomanov OV, Bourhis LJ, Gildea RJ, Howard JAK, Puschmann H. (2009) OLEX2: a complete structure solution, refinement and analysis program. *Journal of Applied Crystallography*, **42**, 339-341.
- [18] Tanaka T, Nakashima T, Ueda T, Tomii K, Kouno I. (2007) Facile discrimination of aldose enantiomers by reversed-phase HPLC. *Chemical & Pharmaceutical Bulletin*, **55**, 899-901.

Lycopodium Alkaloids from Diphasiastrum complanatum

Yu Tang, Juan Xiong and Jin-Feng Hu*

Department of Natural Products Chemistry, School of Pharmacy, Fudan University, No. 826 Zhangheng Road, Shanghai 201203, PR China

jfhu@fudan.edu.cn

Received: August 20th, 2015; Accepted: October 2nd, 2015

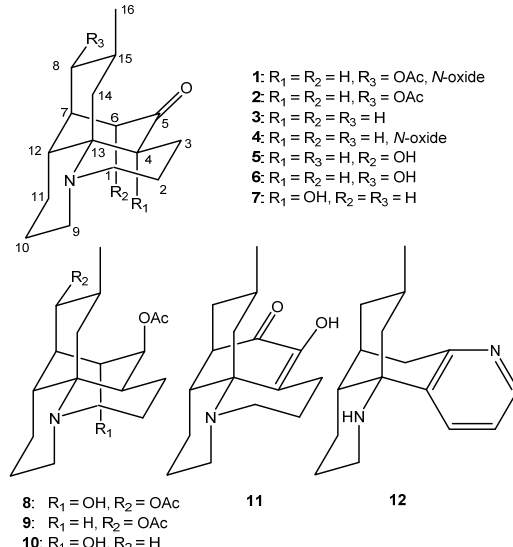
One new lycopodine-type *Lycopodium* alkaloid, dehydroisofawcettine N-oxide (**1**) and eleven known analogues (**2–12**) were isolated from the whole plant of *Diphasiastrum complanatum*. The new structure was established on the basis of spectroscopic methods, including 2D NMR techniques. The absolute configurations of **2** and its new N-oxide derivative (**1**) were deduced by chemical transformation combined with Cotton effects in their electronic circular dichroism (ECD) spectra.

Keywords: *Lycopodium* alkaloids, *Diphasiastrum complanatum*, Absolute configuration, Chemical transformation, ECD.

Diphasiastrum complanatum (L.) Holub (syn.: *Lycopodium complanatum* L.) belonging to the family Lycopodiaceae and commonly known as “Guo-Jiang-Long” in Chinese, is a club moss mainly distributed in temperate and subtropical areas. This plant has been used as a folk medicine for the treatment of arthritic pain, quadriplegia, contusion, and blood stasis [1]. Previous investigations of this plant led to the isolation of a number of *Lycopodium* alkaloids [2] with interesting bioactivities, such as enhancement of mRNA expression for nerve growth factor (NGF) [2d,2i], cytotoxicity against murine leukemia L1210 cells [2i], and antimicrobial activity [2i]. During the continuing program of discovery of novel bioactive alkaloids from club mosses [3], the chemical constituents of *D. complanatum* were reinvestigated. Herein described are the isolation and structural determination of one new (**1**) and eleven known (**2–12**) *Lycopodium* alkaloids (Figure 1) from the title plant.

The air-dried and pulverized whole plant of *D. complanatum* was extracted with 90% MeOH at room temperature and then worked up as usual [3,4] to give the crude alkaloid-containing extract. From this, 12 *Lycopodium* alkaloids were isolated and characterized (**1–12**, Figure 1). Comparing their spectroscopic data and physicochemical properties observed and reported, the known alkaloids were identified as dehydroisofawcettine (**2**) [5], lycopodine (**3**) [6], lycopodine N-oxide (**4**) [7], L.20 (= 6α-hydroxylycopodine, **5**) [8], clavolonine (**6**) [9,10], flabelliformine (**7**) [10], 6-*epi*-8β-acetoxylycoclavine (**8**) [11], acetylafawcettine (**9**) [6], lycoclavine (**10**) [12], 12-deoxyhuperzine O (**11**) [13], and lycodine (**12**) [14]. Among them, alkaloids **2**, **4**, **6**, **8** and **9** are reported here for the first time from the title plant.

Compound **1** showed an $[M+H]^+$ ion peak at m/z 322.2016 (calcd 322.2013) in its positive mode HRESIMS, corresponding to the molecular formula $C_{18}H_{27}NO_4$. The IR absorption bands at 1707 and 1733 cm^{-1} implied the presence of ester and ketone carbonyl groups. The ^1H and ^{13}C NMR data of **1** (Table 1), with the aid of an HSQC NMR experiment, showed the presence of one methyl doublet at δ_{H} 0.94 (3H, d, J = 6.2 Hz, Me-16; δ_{C} 19.0), eight sp^3 methylenes, five sp^3 methines (including one oxymethylene at δ_{H} 4.62 (1H, dd, J = 11.0, 4.1 Hz, H-8), δ_{C} 79.2), one sp^3 (δ 74.4) quaternary carbon, and one carbonyl group (δ_{C} 207.9) for the skeleton, along with signals assignable to an acetyl group [δ_{H} 2.06

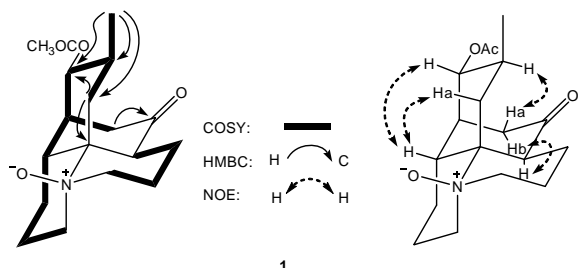
Figure 1: Chemical structures of compounds **1–12**.

(3H, s); δ_{C} 21.3 and 170.4]. The above spectroscopic data showed high similarity to those of a known lycopodine-type alkaloid, dehydroisofawcettine (**2**) [5]; however, the complete ^1H and ^{13}C NMR data of **2** have never been reported until the present study. Differing from **2**, the molecular formula of **1** contains one more oxygen atom. Meanwhile, the ^{13}C NMR shifts of C-1 (δ_{C} 64.4), C-9 (δ_{C} 59.8) and C-13 (δ_{C} 74.2) neighboring the N-atom in **1** were all shifted to lower field compared with the corresponding carbons [δ_{C} 47.0 (C-1), 46.9 (C-9) and 59.3 (C-13)] of compound **2** (see Experimental section). Thus, compound **1** was assumed to be the N-oxide derivative of **2**, which was confirmed by further detailed 2D NMR (COSY and HMBC) spectroscopic analyses of **1** (Figure 2). The relative configuration of **1** was then found to be the same as that of dehydroisofawcettine (**2**) from the magnitudes of $J_{\text{H}_8, \text{H}-15}$ (11.2 Hz) and $J_{\text{H}_{14a}, \text{H}-15}$ (13.0 Hz), and diagnostic NOE correlations of H-8/H-12 (δ 2.85, br d, J = 13.8 Hz), H-12/H_a-14 (δ 2.63, dd, J = 14.4, 14.4 Hz), H-15 (δ 1.56, m)/H_a-6 (δ 2.57, br d, J = 16.4 Hz), and H_b-6 (δ 2.35, dd, J = 16.4, 6.3 Hz)/H-4 (δ 3.01, dd, J = 12.2, 3.7 Hz) (Figure 2).

Table 1: ^1H (400 MHz) and ^{13}C (100 MHz) NMR data^{a,b} for alkaloid **1**.

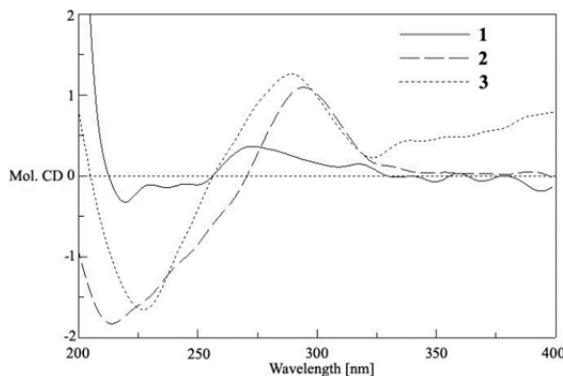
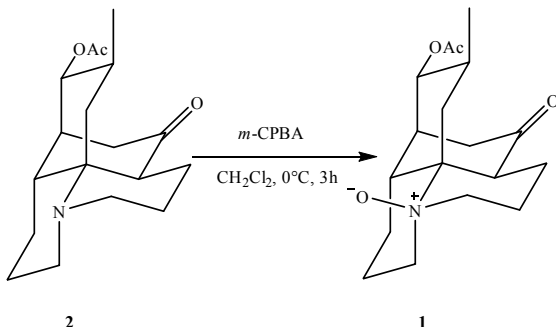
No.	δ_{H} , mult (J in Hz)	δ_{C}
1a	3.60, ddd (13.5, 13.5, 4.4)	64.4 CH ₂
1b	3.19, br d (13.5)	
2a	1.92, m	21.3 CH ₂
2b	1.85, m	
3a	2.22, br d (14.6)	17.5 CH ₂
3b	1.70, m, m	
4	3.01, dd (12.2, 3.7)	48.8 CH
5		207.9 C
6a	2.57, br d (16.4)	36.2 CH ₂
6b	2.35, dd (16.4, 6.3)	
7	2.44, m	39.1 CH
8	4.62, dd (11.0, 4.1)	79.1 CH
9a	3.96, ddd (12.6, 12.6, 3.0)	59.8 CH ₂
9b	3.08, br d (12.6)	
10a	2.78, m	20.1 CH ₂
10b	1.78, m	
11a	1.91, m	23.3 CH ₂
11b	1.68, m,	
12	2.85, br d (13.8)	36.4 CH
13		74.2 C
14a	2.63, dd (14.4, 14.4)	33.1 CH ₂
14b	2.10, dd (14.4, 5.0)	
15	1.56, m	30.4 CH
16	0.94, d (6.2)	19.0 CH ₃
8-OAc	2.06, s	21.3 CH ₃
		170.4 C

^aAssignments were made by a combination of 1D and 2D NMR experiments;
^bRecorded in CDCl₃.

**Figure 2:** COSY, key HMBC and NOE correlations of compound **1**.

As previously described by Ayer and Altenkirk [15], the lycopodine-like alkaloids with a carbonyl group at C-5 and in which the nitrogen lone pair is equatorial to ring A consistently display two Cotton effects above 200 nm, a positive around 288 nm due to $n \rightarrow \pi$ transition and a negative centered at 223 nm associated with σ -coupled p interaction. In good agreement with this assumption, the electronic circular dichroism (ECD) spectrum of dehydroisofawcettine (**2**) exhibited a positive Cotton effect at 295 nm ($\Delta\epsilon +1.09$) and a negative one at 214 nm ($\Delta\epsilon -1.85$), which matched well with that of lycopodine (**3**) [15], as depicted in Figure 3. Thus, the absolute configuration of **2** could be unequivocally determined as 4S,7S,8R,12R,13R,15S. In the case of alkaloid **1**, due to the disappearance of the nitrogen lone pair after oxidation, it is hard to judge the related Cotton effects since its ECD curve almost flattened (Figure 3). Nevertheless, the absolute configuration of **1** was established to be the same as that of **2** by chemical transformation. In a supplementary oxidation experiment, compound **2** was treated with one equivalent of *m*-CPBA to produce its *N*-oxide derivative (Scheme 1), which was identical to **1** by means of HPLC, optical rotation, and spectroscopic analyses. Accordingly, the structure of **1** was defined as (4S,7S,8R,12R,13R,15S)-dehydroisofawcettine *N*-oxide. Indeed, naturally occurring *N*-oxide derivatives of *Lycopodium* alkaloids have often been encountered [2h,7,16].

Similar to casuarinines A–J, lycodine-type alkaloids from *Lycopodiastrum casuarinoides* [3], all the isolates were evaluated for their neuroprotective and anti-acetylcholinesterase (AChE) effects, but none of them were active. They also did not show any significant cytotoxicity against human A-549 and NCI-H460 cancer cell lines.

**Figure 3:** ECD spectra of compounds **1**–**3**.**Scheme 1:** Chemical transformation from **2** to **1**.

Experimental

General experimental procedures: Optical rotations were measured on an Autopol IV automatic polarimeter, IR spectra on an Avatar 360 ESP FTIR spectrometer, ECD spectra on a JASCO-810 spectropolarimeter, and NMR spectra on a Bruker Avance III 400 MHz spectrometer. Chemical shifts are expressed in δ (ppm), and referenced to the residual solvent signals. ESIMS were measured on an Agilent 1100 series mass spectrometer, and HRESIMS on an AB SCIEX Triple TOF 5600+ spectrometer. Semi-preparative HPLC was performed on a Waters e2695 system coupled with a Waters 2998 Photodiode Array Detector and an ODS column (5 μm , 250 \times 10 mm, SunFire). Column chromatography (CC) was performed using silica gel (200–300 mesh, Kang-Bi-Nuo Silysia Chemical Ltd., Yantai, China), and Sephadex LH-20 (GE Healthcare Biosciences AB, Uppsala, Sweden). Silica gel-precoated plates (GF254, 0.25 mm, Kang-Bi-Nuo Silysia Chemical Ltd., Yantai, China) were used for TLC. Compounds were visualized using UV light (254 and/or 365 nm) and by spraying with Dragendorff's reagent.

Plant materials: The whole plant of *D. complanatum* was collected in October 2013 from Bijie in Guizhou Province of China. A voucher specimen (No. 20131007) was deposited at the Herbarium of the Department of Natural Products Chemistry, School of Pharmacy at Fudan University. The plant was identified by Prof. Qiang Luo (Guizhou University of Engineering Science, Bijie, Guizhou Province of China).

Extraction and isolation: The air-dried and pulverized whole plant of *D. complanatum* (1.6 kg) was extracted with 90% MeOH (5 \times 8 L) at room temperature, and the MeOH extract (170 g) was partitioned between EtOAc and 3% tartaric acid. The water-soluble portion, adjusted to pH 9 with sat. Na₂CO₃, was partitioned with CHCl₃. The CHCl₃-soluble portion (3.9 g) was loaded on a silica gel column, eluted with a gradient of CH₂Cl₂/MeOH (1:0–0:1) to

afford fractions 1–8. Fraction 2 (40 mg) was chromatographed on Sephadex LH-20 ($\text{CH}_2\text{Cl}_2/\text{MeOH}$, 2:1) to afford **2** (1.9 mg) and **11** (6.1 mg). Fraction 3 (90 mg) was subjected to silica gel CC ($\text{CH}_2\text{Cl}_2/\text{MeOH}$, 50:1) and then purified by semi-preparative HPLC [$\text{MeOH-H}_2\text{O}$ (containing 0.05% Et_2NH , v/v) 60:40, v/v; flow rate, 3.0 mL/min] to furnish **1** (1.7 mg, $t_{\text{R}} = 10.4$ min) and **4** (5.6 mg, $t_{\text{R}} = 12.0$ min). Compounds **3** (16.0 mg, $t_{\text{R}} = 13.1$ min) and **12** (2.7 mg, $t_{\text{R}} = 10.7$ min) were isolated from fraction 4 (80 mg) by semi-preparative HPLC [$\text{MeOH-H}_2\text{O}$ (containing 0.05% Et_2NH , v/v) 50:50, v/v; flow rate, 3.0 mL/min]. Fraction 5 (200 mg) was subjected to gel permeation chromatography (GPC) on Sephadex LH-20 ($\text{CH}_2\text{Cl}_2/\text{MeOH}$, 2:1) to afford **9** (29.5 mg). Compound **5** (7.2 mg, $t_{\text{R}} = 14.4$ min) was obtained from fraction 6 (210 mg) by semi-preparative HPLC [$\text{MeCN-H}_2\text{O}$ (containing 0.05% Et_2NH , v/v) 30:70, v/v; flow rate, 3.0 mL/min]. Fraction 7 (50 mg) was chromatographed on Sephadex LH-20 (MeOH) to furnish **6** (9.4 mg.). Fraction 8 (300 mg) was separated by Sephadex LH-20 (MeOH) and further purified by semi-preparative HPLC [$\text{MeCN-H}_2\text{O}$ (containing 0.05% Et_2NH , v/v) 45:55, v/v; flow rate, 3.0 mL/min] to afford **7** (6.1 mg, $t_{\text{R}} = 16.0$ min), **8** (2.1 mg, $t_{\text{R}} = 10.8$ min), and **10** (1.7 mg, $t_{\text{R}} = 20.4$ min).

Dehydroisofawcettine N-oxide (1)

$[\alpha]_D^{25} +30.0$ (c 0.1, MeOH).

IR (film): 3417, 2923, 1733, 1707, 1627, 1377, 1244, 1048 cm^{-1} .

^1H and ^{13}C NMR: Table 1.

HRESIMS: m/z [M+H]⁺ calcd for $\text{C}_{18}\text{H}_{27}\text{NO}_4$: 322.2013; found: 322.2016.

m-CPBA oxidation of dehydroisofawcettine (2): Similar to the reported literature [7], compound **2** (4.0 mg, 0.01312 mmol) was dissolved in CH_2Cl_2 (2 mL) to which *m*-CPBA (2.9 mg, 0.0142 mmol) was added. The reaction mixture was left at 0°C for 3 h and then evaporated to give a residue, which was applied to semi-preparative HPLC [$\text{MeOH-H}_2\text{O}$ (containing 0.05% diethylamine, v/v) 60:40, v/v; flow rate, 3.0 mL/min], giving 3.4 mg (yield 80%).

References

- [1] (a) Zhang X-C, Zhang L-B. (2004) *Flora of China*. Science Press. Beijing, Vol. 6, pp. 76-79; (b) Jiangsu New Medical College. (1986) *A Dictionary of the Traditional Chinese Medicine*. Science and Technology Press, Shanghai, pp. 872-873.
- [2] (a) Li H, Huang G, Zhan R, Jiang J, Liu Y, Chen Y. (2014) Studies on alkaloids of *Diphasiastrum complanatum* (L.) Holub. *Journal of Hainan Normal University* (Natural Science), **27**, 39-41; (b) Cheng J-T, Liu F, Li X-N, Wu X-D, Dong L-B, Peng L-Y, Huang S-X, He J, Zhao Q-S. (2013) Lycospidine A, a new type of *Lycopodium* alkaloid from *Lycopodium complanatum*. *Organic Letters*, **15**, 2438-2441; (c) Ishiuchi K, Kubota T, Ishiyama H, Hayashi S, Shibata T, Kobayashi J. (2011) Lyconadins C and F, new *Lycopodium* alkaloids from *Lycopodium complanatum*. *Tetrahedron Letters*, **52**, 289-292; (d) Ishiuchi K, Kubota T, Ishiyama H, Hayashi S, Shibata T, Mori K, Obara Y, Nakahata N, Kobayashi J. (2011) Lyconadins D and E, and complanadine E, new *Lycopodium* alkaloids from *Lycopodium complanatum*. *Bioorganic & Medicinal Chemistry*, **19**, 749-753; (e) Wu X-D, He J, Xu G, Peng L-Y, Song L-D, Zhao Q-S. (2009) Diphaladine A, a new *Lycopodium* alkaloid from *Diphasiastrum complanatum* (Lycopodiaceae). *Acta Botanica Yunnanica*, **31**, 93-96; (f) Ishiuchi K, Kubota T, Hayashi S, Shibata T, Kobayashi J. (2009) Lycopladine H, a novel alkaloid with fused-tetracyclic skeleton from *Lycopodium complanatum*. *Tetrahedron Letters*, **50**, 6534-6536; (g) Ishiuchi K, Kubota T, Hayashi S, Shibata T, Kobayashi J. (2009) Lycopladines F and G, new C_{16}N_2 -type alkaloids with an additional C_4N unit from *Lycopodium complanatum*. *Tetrahedron Letters*, **50**, 4221-4224; (h) Kubota T, Yahata H, Ishiuchi K, Obara Y, Nakahata N, Kobayashi J. (2007) Lycopladine E, a new C_{16}N_1 -type alkaloid from *Lycopodium complanatum*. *Heterocycles*, **74**, 843-848; (i) Ishiuchi K, Kubota T, Mikami Y, Obara Y, Nakahata N, Kobayashi J. (2007) Complanadines C and D, new dimeric alkaloids from *Lycopodium complanatum*. *Bioorganic & Medicinal Chemistry*, **15**, 413-417; (j) Ishiuchi K, Kubota T, Morita H, Kobayashi J. (2006) Lycopladine A, a new C_{16}N alkaloid from *Lycopodium complanatum*. *Tetrahedron Letters*, **47**, 3287-3289; (k) Ishiuchi K, Kubota T, Hoshino T, Obara Y, Nakahata N, Kobayashi J. (2006) Lycopladines B-D and lyconadin B, new alkaloids from *Lycopodium complanatum*. *Bioorganic & Medicinal Chemistry*, **14**, 5995-6000; (l) Morita H, Ishiuchi K, Haganuma A, Hoshino T, Obara Y, Nakahata N, Kobayashi J. (2005) Complanadine B, obscurumines A and B, new alkaloids from two species of *Lycopodium*. *Tetrahedron*, **61**, 1955-1960; (m) Ma X, Gang DR. (2004) The *Lycopodium* alkaloids. *Natural Product Reports*, **21**, 752-772; (n) Kobayashi J, Hirasawa Y, Yoshida N, Morita H. (2001) *Journal of Organic Chemistry*, **66**, 5901-5904; (o) Kobayashi J, Hirasawa Y, Yoshida N, Morita H. (2000) Complanadine A, a new dimeric alkaloid from *Lycopodium complanatum*. *Tetrahedron Letters*, **41**, 9069-9073.
- [3] Tang Y, Fu Y, Xiong J, Li M, Ma G-L, Yang G-X, Wei B-G, Zhao Y, Zhang H-Y, Hu J-F. (2013) Casuarinines A-J, lycodine-type alkaloids from *Lycopodiastrum casuarinoides*. *Journal of Natural Products*, **76**, 1475-1484.
- [4] Ma G-L, Yang G-X, Xiong J, Cheng W-L, Cheng K-J, Hu J-F. (2015) Salicifoxazines A and B, new cytotoxic tetrahydro-1,2-oxazine-containing tryptamine-derived alkaloids from the leaves of *Chimonanthus salicifolius*. *Tetrahedron Letters*, **56**, 4071-4075.
- [5] Burnell RH, Taylor DR. (1961) *Lycopodium* alkaloids-V, the structure and stereochemistry of fawcettine, clavoloneine and related alkaloids. *Tetrahedron*, **15**, 173-182.

of the *N*-oxide product of **2**. All the spectroscopic data (¹H NMR, ESIMS and $[\alpha]_D^{25}$) were identical with those of natural **1**.

Dehydroisofawcettine (2)

$[\alpha]_D^{25} +34.0$ (c 0.1, MeOH).

ECD ($c 5.65 \times 10^{-4}$ M, MeOH) λ_{max} ($\Delta\varepsilon$): 214 (-1.85), 295 (+1.09) nm.

¹H NMR (400 MHz, CDCl_3): δ 4.59 (1H, dd, $J = 11.0, 4.2$ Hz, H-8), 3.31 (1H, ddd, $J = 14.2, 14.2, 3.7$ Hz, H-1a), 3.14 (1H, ddd, $J = 12.4, 12.4, 2.7$ Hz, H-9a), 2.93 (1H, dd, $J = 11.8, 3.1$ Hz, H-4), 2.67 (1H, dd, $J = 13.9, 4.9$ Hz, H-14a), 2.63 (1H, br d, $J = 12.4$ Hz, H-9b), 2.55 (1H, dd, $J = 14.2, 4.9$ Hz, H-1b), 2.49 (1H, dd, $J = 17.9, 3.6$ Hz, H-6a), 2.33 (1H, d, $J = 17.9$ Hz, H-6b), 2.32 (1H, m, H-3a), 2.10 (1H, m, H-7), 2.07 (3H, s, CH_3CO), 1.88 (1H, m, H-2a), 1.84 (1H, m, H-10a), 1.77 (1H, m, H-12), 1.72 (1H, m, H-10b), 1.65 (1H, m, H-11a), 1.63 (1H, m, H-13b), 1.58 (1H, m, H-11b), 1.53 (1H, m, H-15), 1.39 (1H, br d, $J = 13.8$ Hz, H-2b), 1.09 (1H, dd, $J = 13.9, 13.9$ Hz, H-14b), 0.89 (3H, d, $J = 6.2$ Hz, Me-16);

¹³C NMR (100 MHz, CDCl_3): δ 212.6 (C-5, C), 170.8 (CH_3CO , C), 80.4 (C-8, CH), 59.3 (C-13, C), 47.0 (C-9, CH₂), 46.9 (C-1, CH₂), 43.3 (C-12, CH), 42.9 (C-4, CH), 41.6 (C-14, CH₂), 39.6 (C-7, CH), 37.0 (C-6, CH₂), 30.1 (C-15, CH), 25.9 (C-10, CH₂), 24.7 (C-11, CH₂), 21.1 (CH_3CO , CH₃), 19.2 (C-3, CH₂), 18.9 (C-16, CH₃), 18.5 (C-2, CH₂)

ESIMS: m/z 306 [M+H]⁺.

Supplementary data: NMR spectra of compounds **1** and **2** are available in electronic form on the publisher's website.

Acknowledgments - The authors gratefully acknowledge Prof. Qiang Luo (Guizhou University of Engineering Science, PR China) for the plant collection and identification. This work was supported by NSFC grants (Nos. 21472021, 81273401, 81202420), grants from the Ph.D. Programs Foundation of Ministry of Education (MOE) of China (Nos. 20120071110049, 20120071120049), and the National Basic Research Program of China (973 Program, Grant No. 2013CB530700).

- [6] Halldorsdottir ES, Palmadottir RH, Nyberg NT, Olafsdottir ES. (2013) Phytochemical analysis of alkaloids from the Icelandic club moss *Diphasiastrum alpinum*. *Phytochemistry Letters*, **6**, 355-359.
- [7] Pan K, Luo J-G, Kong L-Y. (2014) A new *Lycopodium* alkaloid from *Phlegmariurus fargesii*. *Chinese Journal of Natural Medicines*, **12**, 373-376.
- [8] Takayama H, Katakawa K, Kitajima M, Yamaguchi K, Aimi N. (2003) Ten new *Lycopodium* alkaloids having the lycopodane skeleton isolated from *Lycopodium serratum* Thunb. *Chemical and Pharmaceutical Bulletin*, **51**, 1163-1169.
- [9] Evans DA, Scheerer JR. (2005) Polycyclic molecules from linear precursors: stereoselective synthesis of clavolonine and related complex structures. *Angewandte Chemie International Edition*, **44**, 6038-6042.
- [10] Nakashima TT, Singer PP, Browne LM, Ayer WA. (1975) Carbon-13 nuclear magnetic resonance studies of some *Lycopodium* alkaloids. *Canadian Journal of Chemistry*, **53**, 1936-1942.
- [11] He J, Wu X-D, Liu F, Liu Y-C, Peng L-Y, Zhao Y, Cheng X, Luo H-R, Zhao Q-S. (2014) Lycopodine-type alkaloids from *Lycopodium japonicum*. *Natural Products and Bioprospecting*, **4**, 213-219.
- [12] Ayer WA, Law DA. (1962) *Lycopodium* alkaloids IV. The constitution and stereochemistry of lycoclavine, an alkaloid of *Lycopodium clavatum* var. *megastachyon*. *Canadian Journal of Chemistry*, **40**, 2088-2100.
- [13] Yang Y-F, Qu S-J, Xiao K, Jiang S-H, Tan J-J, Tan C-H, Zhu D-Y. (2010) *Lycopodium* alkaloids from *Huperzia serrata*. *Journal of Asian Natural Products Research*, **12**, 1005-1009.
- [14] (a) Tong X-T, Tan C-H, Ma X-Q, Jiang S-H, Zhu D-Y. (2003) *Lycopodium* alkaloids from *Huperzia miyoshiana*. *Natural Product Research and Development*, **15**, 383-386; (b) Anet FAL, Rao MV. (1960) The structure of lycodine. *Tetrahedron Letters*, **1**, 9-12.
- [15] Ayer WA, Altenkirk B, Burnell RH, Moinas M. (1969) Alkaloids of *Lycopodium lucidulum* Michx. structure and properties of alkaloid L.23. *Canadian Journal of Chemistry*, **47**, 449-455.
- [16] (a) Pan k, Luo J-G, Kong L-Y. (2013) Two new *Lycopodium* alkaloids from *Lycopodium obscurum*. *Helvetica Chimica Acta*, **96**, 1197-1201; (b) Katakawa K, Mito H, Kogure N, Kitajima M, Wongseripipatana S, Arisawa M, Takayama H. (2011) Ten new fawcettimine-related alkaloids from three species of *Lycopodium*. *Tetrahedron*, **67**, 6561-6567; (c) Wang H-B, Tan C-H, Tan J-J, Qu S-J, Chen Y-L, Li Y-M, Jiang S-H, Zhu D-Y. (2009) Two new *N*-oxide *Lycopodium* alkaloids from *Huperzia serrata*. *Natural Product Research*, **23**, 1363-1366; (d) Yin S, Fan C-Q, Wang X-N, Yue J-M. (2006) Lycodine-type alkaloids from *Lycopodium casuarinoides*. *Helvetica Chimica Acta*, **89**, 138-143.

Effects of Adding Vindoline and MeJA on Production of Vincristine and Vinblastine, and Transcription of their Biosynthetic Genes in the Cultured CMCs of *Catharanthus roseus*

Wenjin Zhang^{a,*}, Jiazeng Yang^{a,*}, Jiachen Zi^{a,#}, Jianhua Zhu^a, Liyan Song^b and Rongmin Yu^{a,b,#}

^aBiotechnological Institute of Chinese Materia Medica, Jinan University, Guangzhou 510632, China

^bCollege of Pharmacy, Jinan University, Guangzhou 510632, China

tyrm@jnu.edu.cn (RM Yu) and tzjc@jnu.edu.cn (JC Zi)

*These authors contributed equally to this work.

Received: August 15th, 2015; Accepted: October 31st, 2015

Vincristine and vinblastine were found by Liquid Chromatography-Mass Spectrometry (LC-MS) in *Catharanthus roseus*cambial meristem cells (CMCs) jointly treated with 0.25 mM vindolineand methyl jasmonate (MeJA), suggesting that *C. roseus* CMCs contain a complete set of the enzymes which are in response to convert vindoline into vincristine and vinblastine. Based on the facts that the transcript levels of vindoline-biosynthetic genes (*STR*, *SGD* and *D4H*) were up-regulated instead of being down-regulated by adding itself to the culture, and that the transcriptional factor *ORCA3* was up-regulated simultaneously, we further confirmed that the transcription of *STR*, *SGD*, *D4H* was manipulated by ORCA3.

Keywords: *Catharanthus roseus*, CMCs, TIAs, Quantitative RT-PCR, Precursor feeding, Gene expression profiling.

The terpene indole alkaloids (TIAs) from *Catharanthus roseus* are important secondary metabolites with diverse structures and biological activities [1,2]. In the complex biosynthetic process of TIAs, strictosidine aglycone is considered as a key intermediate from which at least two biosynthetic pathways are derived. From these two pathways, vindoline and cathenamine are synthesized, respectively. The coupling of vindoline and cathenamine finally leads to the production of bisindole alkaloids vincristine and vinblastine, and cathenamine is also hypothesized as the precursor of ajmalicine and serpentine. Previous results have proved that vindoline can be detected from CMCs of *C. roseus*,but not from either suspension cells or hairy roots due to deficiency of the corresponding enzymes in the latter two cells / tissues [3,4]. Unfortunately, vincristine and vinblastine are not found in the CMCs cultures which was possibly due to the low concentration of vindoline. Since the enzymes necessary for converting vindoline into vincristine and vinblastine have not been characterized yet, the levels of their transcription or expression could not be directly analyzed by biological methods, such as quantitative reverse transcription (RT)-PCR and Western blot. To clarify whether CMCs of *C. roseus* contain a complete set of response system of enzymes for converting vindoline into vincristine and vinblastine, vindoline was fed to the culture of CMCs of *C. roseus* in either the presence or absence of methyl jasmonate (MeJA). Also, the effects of excess vindoline on the transcription of the genes involved in its biosynthesis were investigated.

In the presence or absence of 250 mM MeJA, CMCs of *C. roseus* were treated with 0.5 mM vindoline for 12 h, 24 h and 36 h, respectively. Vinblastine and vincristine were observed by LC-MS. As time went on, the change in accumulation of both vindoline and catharanthine was not significantly observed, suggesting that the production and consumption of the two compounds were in a state of equilibrium (Figure 1). Interestingly, the treatment of vindoline enhanced the accumulation of catharanthine (Figure 1A). In general, additional feeding of one product can inhibit the transcription and translation of genes located at its up-stream steps due to a negative

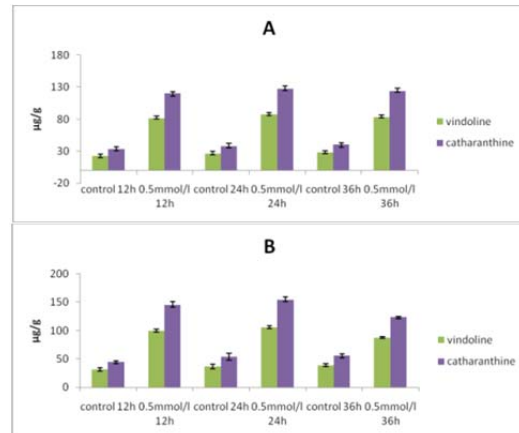


Figure 1: The accumulation of vindoline and catharanthine in *C. roseus* CMCs (A) treated with vindoline or (B) jointly treated with both vindoline and MeJA for 12, 24 and 36 h.

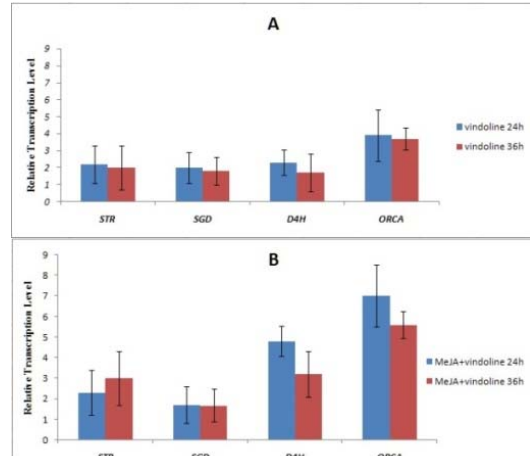


Figure 2: In comparison with untreated *C. roseus* CMCs, the relative transcription levels of *STR*, *SGD*, *D4H* and *ORCA3* in *C. roseus* CMCs (A) treated with either vindoline or (B) jointly treated with both vindoline and MeJA for 24 and 36 h, respectively.

feedback mechanism, which proposed that the transcription levels of the genes involved in the synthesis of vindoline were reduced due to the addition of vindoline. We monitored the transcription levels of *STR*, *SGD* and *D4H* in both vindoline-treated and vindoline-untreated CMCs by quantitative real time reverse transcription PCR (qRT-PCR) [5,6]. Unexpectedly, the transcription levels of *STR*, *SGD* and *D4H* were up-regulated by treated with vindoline. Eleven-day old CMCs were treated with either ethanol or 0.5 mM vindoline in ethanol, respectively. After 24 or 36 h, the CMCs were harvested and the transcript levels of *STR*, *SGD* and *D4H* were analyzed. For 24-h cells treated with vindoline enhanced the transcript levels of *STR*, *SGD* and *D4H* by 2.2, 2.0 and 2.3 folds of those of the ethanol-treated CMCs; for 36-h cells treated with vindoline led to 2.1-, 1.9- and 1.9-fold increases, respectively (Figure 2).

It has been reported that the transcriptional regulator ORCA3 is capable of manipulating the transcription of *STR*, *SGD* and *D4H* [7]. We monitored the change in *ORCA3* transcript level. The result indicated that in the CMCs with 24-h and 36-h treatment with vindoline, the transcription levels of *ORCA3* increased by 3.9 and 3.8 folds of those of the control cells, respectively (Figure 2A). Therefore, we supposed that vindoline may firstly enhance *ORCA3* transcription which not only overcomes the negative feedback effect caused by feeding vindoline, but also improves the transcription of *STR*, *SGD* and *D4H*. Transcription of genes responsible for biosynthesis of catharanthine might be up-regulated by *ORCA3* as well, which could be the reason that the treatment with vindoline enhanced the accumulation of catharanthine (Figure 1A). Regrettably, no enzyme involved in conversion of strictosidine aglycone to catharanthine has been characterized, so this assumption could not be verified.

MeJA can be used as an elicitor to enhance production of TIAs and transcription of their biosynthetic genes [3]. By jointly treating with 250 mM MeJA and 0.5 mM vindoline, enhancement of the accumulation of vindoline was not observed (Figure 1) and the transcript levels of *STR*, *SGD* and *D4H* increased by magnitudes comparable with those of treating solely with vindoline, while the transcript level of *ORCA3* was induced by 7 folds of that of the control cells (Figure 2). These results indicated that MeJA, in combination with vindoline, was not capable of enhancing the accumulation of vindoline and the transcript levels of its biosynthetic genes. However, in the presence of both vindoline and

MeJA, the further increase of the transcript level of *ORCA3*, together with the fact that vincristine and vinblastine were observed only in the CMCs treated with both MeJA and vindoline, indicated that *ORCA3* also improved the transcription of genes locating at downstream of vindoline, although these genes have not been characterized as yet. In conclusion, with treatment by both vindoline and MeJA, CMCs of *C. roseus* produced vinblastine and vincristine, suggesting that CMCs of *C. roseus* contain a complete set of the enzymes involved in conversion of vindoline to vinblastine and vincristine. However, CMCs cannot produce enough vindoline to yield vinblastine and vincristine in detectable amounts, and so feeding with vindoline is necessary. The transcriptions of the genes responsible for synthesizing vindoline, such as *STR*, *SGD* and *D4H*, are up-regulated by *ORCA3*, which may play a key role in manipulating the transcription of the genes involved in transforming vindoline into vinblastine and vincristine, as well.

Experimental

Plant material: CMCs of *C. roseus* were prepared in our research group [8]. Initially, these CMCs were cultured in solid MS medium with 1-naphthalene acetic acid (NAA, 2.0 mg/L), sucrose (10.0 g/L) and gelrite (4.0 g/L); the pH was regulated to 5.8. After that, cultures were sub-cultured every 12 days in 250 mL Erlenmeyer flasks in liquid MS medium. The cells were cultured at 25°C with a 12/12 h light / dark cycle, agitated at 100 rpm.

Extraction procedure: Alkaloids were extracted from medium and cells, respectively, following the reported method [9].

Analysis of TIAs: HPLC and LC-MS experiments were performed as previously report [3].

Monitor gene expression: The quantitative real time reverse transcription PCR (qRT-PCR) experiments were conducted as previously report [3].

Acknowledgments - This research work was financially supported by the National Natural Sciences Foundation of China (No. 81102771, 81274045 and 81573568) and Pearl River Scientific and Technological New Star Program of Guangzhou (No. 2014J2200004).

References

- [1] Dutta A, Sen J, Deswal R. (2013) New evidences about strictosidine synthase (*Str*) regulation by salinity, cold stress and nitric oxide in *Catharanthus roseus*. *Journal of Plant Biochemistry and Biotechnology*, **22**, 124-131.
- [2] Wang CT, Liu H, Gao XS, Zhang HX. (2009) Overexpression of G10H and ORCA3 in the hairy roots of *Catharanthus roseus* improves catharanthine production. *Plant Cell Reports*, **29**, 887-894.
- [3] Zhou P, Yang J, Zhu J, He S, Zhang W, Yu R, Zi J, Song L, Huang X. (2015) Effects of β-cyclodextrin and methyl jasmonate on the production of vindoline, catharanthine, and ajmalicine in *Catharanthus roseus* cambial meristematic cell cultures. *Applied Microbiology Biotechnology*, **99**:7035-7045.
- [4] Zhao J, Verpoorte R. (2007) Manipulating indole alkaloid production by *Catharanthus roseus* cell cultures in bioreactors: from biochemical processing to metabolic engineering. *Phytochemistry Review*, **6**, 435-457.
- [5] Peebles CA, Hughes EH, Shanks JV, San KY. (2009) Transcriptional response of the terpenoid indole alkaloid pathway to the overexpression of ORCA3 along with jasmonic acid elicitation of *Catharanthus roseus* hairy roots over time. *Metabolic Engineering*, **11**, 76-86.
- [6] Guo Z-G, Liu Y, Gong M-Z, Chen W, Li W-Y. (2012) Regulation of vinblastine biosynthesis in cell suspension cultures of *Catharanthus roseus*. *Plant Cell Tissue and Organ Culture*, **112**, 43-54.
- [7] Pan Q, Wang Q, Yuan F, Xing S. (2012) Overexpression of ORCA3 and G10H in *Catharanthus roseus* plants regulated alkaloid biosynthesis and metabolism revealed by NMR metabolomics. *Plos One*, **7**, 3038-3049.
- [8] Lee EK, Jin YW, Park JH, Yoo YM, Hong SM, Amir R. (2010) Cultured cambial meristematic cells as a source of plant natural products. *Nature Biotechnology*, **28**, 1213-1217.
- [9] Hisiger S, Jolicœur M. (2007) Analysis of *Catharanthus roseus* alkaloids by HPLC. *Phytochemistry Reviews*, **6**, 207-234.

Structures and Chemotaxonomic Significance of *Stemona* Alkaloids from *Stemona japonica*

Min Yi^a†, Xue Xia^a†, Hoi-Yan Wu^{b,c}, Hai-Yan Tian^a, Chao Huang^d, Paul Pui-Hay But^b, Pang-Chui Shaw^{b,c*} and Ren-Wang Jiang^a

^aCollege of Pharmacy, Jinan University, Guangzhou, 510632, P.R. China

^bSchool of Life Sciences, The Chinese University of Hong Kong, Shatin, Hong Kong SAR, P.R. China

^cInstitute of Chinese Medicine, The Chinese University of Hong Kong, Shatin, Hong Kong SAR, P.R. China

^dSinopharm Shenzhen Ltd., Shenzhen, P.R. China

† These authors contributed equally to this work.

trwjiang@jnu.edu.cn (R. W. J.); pcshaw@cuhk.edu.hk (P. C. S.)

Received: August 19th, 2015; Accepted: November 5th, 2015

A pair of new alkaloid stereo-isomers, stemocochinin (**1**) and isostemocochinin (**2**), was obtained from the roots of *Stemona japonica* Miq., along with seven known alkaloids, stemonamine (**3**), isostemonamine (**4**), maistemoneine (**5**), isomaistemoneine (**6**), croomine (**7**), stemonine (**8**), and protostemonine (**9**). The complete structure and stereochemistry of the pair of isomers were established by extensive analysis of the spectral data. Furthermore, our results indicated that *S. japonica* is chemically closer to *S. sessilifolia* than *S. tuberosa*, which are consistent with our previous DNA study on *Stemona* species.

Keywords: *Stemona japonica*, Stemona alkaloid, Chemotaxonomic significance, DNA phylogenetics.

Plants of the genus *Stemona*, belonging to the medicinally important family Stemonaceae, are a rich source of a class of structurally unique pyrrolo[1,2- α]azepine alkaloids known as Stemona alkaloids [1]. Three species in this genus, i.e. *S. tuberosa*, *S. japonica* and *S. sessilifolia*, are collectively recorded as Radix Stemona (‘Bai-Bu’ in Chinese) in the Chinese Pharmacopeia [2]. This herb is often used as an antitussive drug to treat respiratory disorders, such as cough and tuberculosis, and is also used as an anthelmintic agent for domestic animals [3]. The prominent clinical and pharmacological properties of these plants have prompted many phytochemical studies, and over one hundred Stemona alkaloids have been isolated from these herbs [4].

Our group has been engaged in this class of intriguing alkaloids for many years [5-8]. A series of alkaloids were identified from *S. tuberosa*, and some of them were found to show antitussive activities [9,10]. Interestingly, significant chemical diversity was observed for *S. tuberosa* collected from different places of production [5]. During our further systematic investigation of alkaloids from the genus *Stemona*, the chemical constituents of *S. japonica* were studied. A pair of stereoisomers, stemocochinin (**1**, Figure 1) and isostemocochinin (**2**), was isolated together with seven known alkaloids (**3-9**). Their chemical structures and stereochemistry were established by spectroscopic analysis. The chemotaxonomic significance of these alkaloids is discussed based on the distribution of these alkaloids in the genus and a DNA phylogenetic study.

A 95% ethanol extract of the herb was acidified with dilute hydrochloric acid. The acid soluble fraction was adjusted to pH 9 with ammonia solution, and then extracted with CH₂Cl₂. Compounds **1-9** were obtained from the CH₂Cl₂ fraction by silica gel column chromatography.

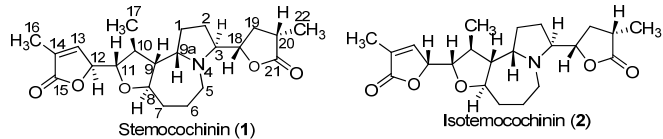


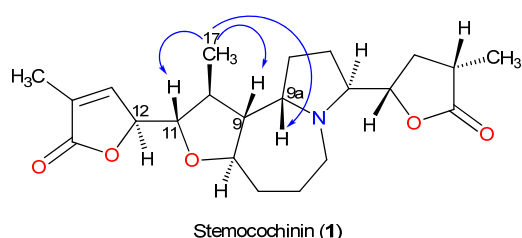
Figure 1: Chemical structures stemocochinin (**1**) and isostemocochinin (**2**).

Compound **1**, an amorphous powder, had the molecular formula C₂₂H₃₁NO₅, based on the quasimolecular ion [M+H]⁺ at m/z 389 in its EI-MS. The base peak at m/z 290 [M-C₅H₇O₂], a characteristic cleavage fragment of Stemona alkaloids, indicated the presence of an α -methyl- γ -lactone ring annexed to C-3. Another prominent peak at m/z 292 [M-C₅H₅O₂] can be attributed to the loss of the unsaturated α -methyl- γ -lactone ring from the molecular ion.

The ¹H NMR spectrum (Table 1) shows the presence of two primary methyl groups at δ_{H} 1.06, d, *J* = 6.6 Hz, H-17) and δ_{H} 1.25 (3H, d, *J* = 7.1 Hz, H-22), an olefinic methyl at δ_{H} 1.92 (3H, d, *J* = 2.4 Hz, H-16), four oxymethines at δ_{H} 3.89 (1H, m, H-8), 3.72 (1H, m, H-11), 4.83 (1H, dd, *J* = 6.4, 1.8 Hz, H-12) and 4.17 (1H, m, H-18), a *sp*² methine at δ_{H} 7.14 (1H, dq, *J* = 1.9, 1.5 Hz, H-13), a methine and two geminal protons attached to carbon atoms bearing a nitrogen function at δ_{H} 3.24 (1H, m, H-3), δ_{H} 3.45 (1H, dd, *J* = 15.6, 5.5 Hz, H-5 β) and δ_{H} 2.89 (1H, dd, *J* = 15.6, 11.7Hz, H-5 α). The ¹³C NMR and DEPT spectra of **1** show 22 carbon atoms: two lactonic carbonyl atoms (δ_{C} 179.5 and 174.1), two olefinic carbon atoms conjugated with carbonyl group (δ_{C} 146.9 and 130.7), four carbon atoms bearing oxygen (δ_{C} 80.1, 85.1, 83.2 and 83.1), six methylene groups (δ_{C} 26.8, 26.9, 47.3, 20.2, 35.2 and 34.3), three methyl groups (δ_{C} 10.7, 16.7 and 14.9) and four general methine carbons (δ_{C} 55.4, 58.9, 40.7 and 34.9). These spectroscopic data are reminiscent of the pentacyclic Stemoamide-type alkaloids bearing two lactone rings [11].

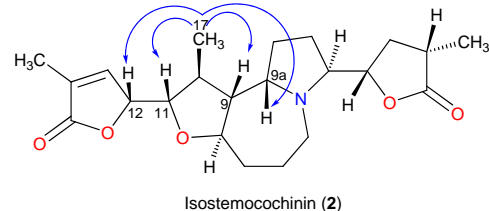
Table 1: The ^1H and ^{13}C NMR data of compounds **1** and **2** (J in Hz).

	Compound 1		Compound 2	
	^1H	^{13}C	^1H	^{13}C
1	1.75, m 1.58, m	26.8, t	1.81, m 1.56, m	26.8, t
2	1.89, m 1.41, m	26.9, t	1.90, m 1.37, m	26.9, t
3	3.24, m	64.5, d	3.21, m	64.4, d
5	3.45, dd (15.6,5.5) 2.89, dd (11.7,15.6)	47.3, t	3.44, dd, (15.6,5.2) 2.88, dd (11.4,15.6)	47.4, t
6	1.55, m 1.33, m	20.2, t	1.54, m 1.33, m	20.2, t
7	2.11, m 1.28, m	35.2, t	2.05, m 1.26, m	35.4, t
8	3.89, ddd (5.6,5.6,1)	80.1, d	3.79, m	80.5, d
9	1.99, ddd (4.7,10.2)	55.4, d	1.98, dd (5.2,10.6)	55.1, d
9a	3.65, m	58.9, d	3.64, dd (5.0,10.3)	59.1, d
10	1.82, m	40.7, d	2.19, m	39.6, d
11	3.52, m	85.1, d	3.77, m	83.4, d
12	4.83, m (6.4,1.8)	83.2, d	4.89, m (2.2, 1.8)	80.6, d
13	7.14,dq (1.9,1.5)	146.9, d	7.00, dq (1.8,1.5)	146.1, d
14		130.7, s		131.0, s
15		174.1, s		174.2, s
16	1.92,dd (1.5,1.8)	10.7, q	1.94, dd (1.8,1.8)	10.8, q
17	1.06,d, (6.6)	16.7, q	1.08, d (6.6)	15.9, q
18	4.17,m	83.1, d	4.15, m	83.5, d
19	2.37, m 1.53, m	34.3, t	2.36, m 1.52, m	34.4, t
20	2.62, m	34.9, d	2.69, m	35.0, d
21		179.5, s		179.4, s
22	1.25, d (6.9)	14.9, q	1.25,d (6.9)	14.9, q

**Figure 2:** Key ROESY correlations of **1**.

The full assignments and connectivities were determined by ^1H - ^1H COSY, HMQC and HMBC spectra. The ^1H - ^1H COSY spectrum established spin systems involving H-5, H-6, H-7, H-8, H-9, H-10, H-11, H-12, H-13 and H₃-16, and H-1, H-2, H-3, H-19, H-18, H-19, H-20 and H₃-22. The HMQC spectrum revealed a signal at δ_{H} 4.83 (H-12) attached to a carbon at δ_{C} 83.2 (C-12), and the HMBC spectrum showed H-12 correlated to C-11, C-13, C-14 and C-15, suggesting that the γ -lactone was formed by ring closure involving the oxygen atoms bridged to C-12 and C-15. Furthermore, the HMBC correlation H-12→C-11 suggested the location of this lactone at C-11. The HMBC correlation of the characteristic olefinic signal at δ_{H} 7.14 (H-13) to C-12, C-14, C-15 and C-16 suggested that the double bond is within the lactone ring and conjugated with the carbonyl group at C-15. Similarly, the HMQC spectrum revealed that the signal at δ_{H} 4.17 (H-18) was correlated with a carbon at δ_{C} 80.4 (C-18), and the HMBC spectrum showed that H-18 correlated with C-3, C-19, C-20 and C-21, suggesting that another γ -lactone attached to C-3 was formed by ring closure involving the oxygen atoms bridged to C-18 and C-21.

The stereochemistry of compound **1** was determined from the ROESY spectrum in which the protons of Me-17 had correlations with H-9a, H-11 and H-9, but not with H-12, indicating that Me-17, H-9a, H-11 and H-9 are on the same side and are β -orientated, whereas H-12 should be α -orientated (Figure 2). Accordingly, compound **1** was determined to be stemocochinin. This alkaloid has been reported before [11], but the full assignment of NMR data and detailed stereochemistry were not determined.

**Figure 3:** The key ROESY correlations of **2**.

Compound **2** had the same quasimolecular ion as that of **1** at m/z 389. It also showed the same prominent peaks at m/z 290 and 292 as alkaloid **1** in its ESI-MS. The ^1H -, ^{13}C - and DEPT-NMR spectra of **2** were similar to those of **1** except that the chemical shifts of H-10 and H-11 are slightly different (Table 1). Comparison of the ROESY spectra of alkaloids **1** and **2** revealed a significant difference. Clear correlation was observed between methyl-17 and H-12 in the ROESY spectrum (Figure 3) of alkaloid **2**, suggesting that H-12 should be β -orientated. Thus, the only difference between alkaloids **1** and **2** was the relative configuration of C-12, (*S* in **1** and *R* in **2**).

Accordingly, compound **2** was determined to be an isomer of stemocochinin (**1**) and was accorded the trivial name isostemocochinin (**2**).

The known alkaloids were identified as stemonamine (**3**) [13, 14], isostemonamine (**4**) [13], maistemone (**5**) [13-16], isomaistemone (**6**) [14, 17, 18], croomine (**7**) [12, 19, 20], stemonine (**8**) [21, 22] and protostemonine (**9**) [15, 21, 22] by comparing their MS and NMR spectral data with those reported in literature (Figure 1).

Six of the seven known alkaloids have been identified from *S. sessilifolia*, while only compound **7** has been isolated from *S. tuberosa* (Table 2), indicating that *S. japonica* is chemically closer to *S. sessilifolia* than to *S. tuberosa*. Current phytochemical results are consistent with our previous DNA study on *Stemona* species [23], which showed that the 5S rRNA sequence of *S. tuberosa* shares a similarity of 76% and 78.5% with those of *S. japonica* and *S. sessilifolia*, respectively. In contrast, the similarity between *S. japonica* and *S. sessilifolia* is 84.5%. Thus, both phytochemical and DNA phylogenetic data confirm a closer relationship between *S. japonica* and *S. sessilifolia* than *S. tuberosa*.

Table 2: Distribution of compounds **1-9** in the three *Stemona* species recorded in Chinese Pharmacopeia.

Compound	Name	Source	Reference
1	Stemocochinin	<i>S. japonica</i>	12
2	Isostemocochinin	<i>S. japonica</i>	Not found
3	Stemonamine	<i>S. japonica</i>	13
		<i>S. sessilifolia</i>	14
4	Isostemonamine	<i>S. japonica</i>	13
5	Maistemone	<i>S. japonica</i>	13,15
		<i>S. sessilifolia</i>	16,14
6	Isomaistemone	<i>S. sessilifolia</i>	14,17
		<i>S. japonica</i>	18
7	Croomine	<i>C. japonica</i>	19,12
		<i>S. tuberosa</i>	20
8	Stemonine	<i>S. japonica</i>	21,22
9	Protostemonine	<i>S. japonica</i>	15,21,22
		<i>S. sessilifolia</i>	14,17

Experimental

General procedure: TLC was performed on pre-coated silica gel GF254 plates (Qingdao Marine Chemical Factory, Qingdao, China). The NMR spectra were obtained on a Bruker 300 spectrometer with chemical shifts reported in ppm using TMS as an internal standard.

ESIMS were recorded on a Finnigan MAT TSQ 7000 instrument. Column chromatography (CC) was performed on silica gel (200–400 mesh, Qingdao Marine Chemical Plant, Qingdao, People's Republic of China). All solvents used in CC and high-performance liquid chromatography (HPLC) were of analytical grade (Shanghai Chemical Plant, Shanghai, People's Republic of China).

Plant material: The roots of *S. japonica* were collected in Guangxi Province, China in September 2004. The herbs (voucher specimen No. SJ-1) were identified at the Institute of Traditional Chinese Medicine and Natural Products, Jinan University.

Isolation of compounds 1-9: One kg of dried roots of *S. japonica* were ground and percolated with 95% EtOH at room temperature for 3 days, and then filtered and concentrated under reduced pressure. The residue was acidified with 500 mL of 4% HCl solution, and then extracted with Et₂O (400 mL x 3). The Et₂O was evaporated to give a crude non-alkaloid extract (6 g). The pH of the water layer was adjusted to 9–10 with 35% NH₄OH, and extracted with diethyl ether to give the total alkaloids (4.5 g). Part of these (4.0 g) was chromatographed on a silica gel column and eluted with CH₂Cl₂: MeOH: NH₄OH (94: 6: 0.04). The eluates were monitored by TLC and grouped into 6 fractions (Fr. 1 - Fr. 6). Fr. 1 was re-chromatographed on a silica gel column using *n*-hexane: EtOAc (6:4) as eluent to yield alkaloid **3** (10 mg). Fr. 2 was chromatographed on a silica gel column eluted with *n*-hexane:

EtOAc (5: 5) to give alkaloids **4** (12 mg), **5** (20 mg) and **6** (20 mg). Fr. 4 was chromatographed on a silica gel column eluted with *n*-hexane: EtOAc: acetone (2: 2: 0.5) to give alkaloids **7** (20 mg), **8** (26 mg) and **9** (93 mg). Fr. 6 was separated by silica gel CC eluting with *n*-hexane: EtOAc: acetone (2: 2: 1) to afford alkaloids **1** (20 mg) and **2** (40 mg).

Stemochocochinin (1)

Amorphous powder.

¹H and ¹³C NMR: Table 1.

FAB-MS: *m/z*: 390 [M+H]⁺.

EI-MS: *m/z*: 389 [M]⁺ (3), 292 [M-C₅H₅O₂]⁺ (100), 290 [M-C₅H₇O₂]⁺ (75), 278, 164, 134.

Isostemochocochinin (2)

Amorphous powder.

¹H and ¹³C NMR: Table 1.

FAB-MS: *m/z*: 390 [M+H]⁺.

EI-MS: *m/z*: 389 [M]⁺ (2), 292 [M-C₅H₅O₂]⁺ (75), 290 [M-C₅H₇O₂]⁺ (100), 278, 164, 136.

Acknowledgments - Thanks are due to Mr Po-Ming Hon at the Chinese University of Hong Kong for carrying out some of the work. This project was partially supported by the Guangdong Major Scientific and Technological Special Project for New Drug Development (2013A022100029).

References

- [1] (a) Pilli RA, Rossoa GB, de Oliveira Mda C. (2010) The chemistry of Stemona alkaloids: An update. *Natural Product Reports*, **27**, 1908-1937; (b) Wang FP, Chen QH. (2014) *Stemona* alkaloids: biosynthesis, classification, and biogenetic relationships. *Natural Product Communications*, **9**, 1809-1822.
- [2] Pharmacopoeia Commission of People's Republic of China. (2005) *The Pharmacopoeia of the People's Republic of China, Part 1*. Chemical Industry Publishing House, Beijing, P.R. China, 100.
- [3] Jiangsu New Medical College. (1977) *Dictionary of Chinese Traditional Medicine*. Shanghai People's Publishing House, P.R. China, 858-861.
- [4] Greger H. (2006) Structural relationships, distribution and biological activities of Stemona alkaloids. *Planta Medica*, **72**, 99-113.
- [5] Jiang RW, Hon PM, Xu YT, Chan YM, Xu HX, Shaw PC, But PPH. (2006) Isolation and chemotaxonomic significance of tuberostemospironine-type alkaloids from *Stemona tuberosa*. *Phytochemistry*, **67**, 52-57.
- [6] Jiang RW, Hon PM, Zhou Y, Chan YM, Xu YT, Xu HX, Greger H, Shaw PC, But PPH. (2006) Alkaloids and chemical diversity of *Stemona tuberosa*. *Journal of Natural Products*, **69**, 749-754.
- [7] Jiang RW, Hon PM, But PPH, Chung HS, Lin G, Ye WC, Mak TCW. (2002) Isolation and stereochemistry of two new alkaloids from *Stemona tuberosa* Lour. *Tetrahedron*, **58**, 6705-6712.
- [8] Jiang RW, Ye WC, Shaw PC, But PPH, Mak TCW. (2010) Absolute configuration of neostenine. *Journal of Molecular Structure*, **966**, 18-22.
- [9] Xu YT, Shaw PC, Jiang RW, Hon PM, Chan YM, But PPH. (2010) Antitussive and central respiratory depressant effects of *Stemona tuberosa*. *Journal of Ethnopharmacology*, **128**, 679-684.
- [10] Xu YT, Hon PM, Jiang RW, Cheng L, Li SH, Chan YP, Xu HX, Shaw PC, But PPH. (2006) Antitussive effects of *Stemona tuberosa* with different chemical profiles. *Journal of Ethnopharmacology*, **108**, 46-53.
- [11] Kaltenegger E, Brem B, Mereiter K, Kalchhauser H, Kählig H, Hofer O, Vajodaya S, Greger H. (2003) Insecticidal pyrido[1,2-a]azepine alkaloids and related derivatives from *Stemona* species. *Phytochemistry*, **63**, 803-816.
- [12] Tang CP, Chen T, Velten R, Jeschke P, Ebbinghaus-Kintzsch U, Geibel S, Ye Y. (2008) Alkaloids from stems and leaves of *Stemona japonica* and their insecticidal activities. *Journal of Natural Products*, **71**, 112-116.
- [13] Ye Y, Qin GW, Xu RS. (1994) Alkaloids of *Stemona japonica*. *Journal of Natural Products*, **57**, 665-669.
- [14] Yang XZ, Zhu JY, Tang CP, Ke CQ, Lin G, Cheng TY, Rudd JA, Ye Y. (2009) Alkaloids from roots of *Stemona sessilifolia* and their antitussive activities. *Planta Medica*, **75**, 174-177.
- [15] Ye Y, Xu RS. (1992) Studies on new alkaloids of *Stemona japonica*. *Chinese Chemical Letters*, **3**, 511-514.
- [16] Cong X, Zhao H, Guillaume D, Xu G, Lu Y, Zheng Q. (1995) Crystal structure and NMR analysis of the alkaloid protostemotinine. *Phytochemistry*, **40**, 615-617.
- [17] Guo A, Lin L, Deng Z, Cai S, Guo S, Lin W. (2008) New Stemona alkaloids from the roots of *Stemona sessilifolia*. *Chemistry & Biodiversity*, **5**, 598-605.
- [18] Zou CY, Fu HZ, Lei, HM, Li J, Lin W-H. (1999) New alkaloids from the roots of *Stemona japonica* Miq. *Journal of Chinese Pharmaceutical Sciences*, **8**, 185-190.
- [19] Lin WH, Cai MS, Ying BP, Feng R. (1993) Studies on the chemical constituents of *Croomia japonica* Miq. *Acta Pharmaceutica Sinica*, **28**, 202-206.
- [20] Lin LG, Leung HPH, Zhu JY, Tang CP, Ke CQ, Rudd JA, Lin G, Ye Y. (2008) Croomine- and tuberostemonine-type alkaloids from roots of *Stemona tuberosa* and their antitussive activity. *Tetrahedron*, **64**, 10155-10161.
- [21] Götz M, Strunz GM. (1975) Tuberostemonine and related compounds: The chemistry of Stemona alkaloids. In *Alkaloids MTP International Review of Sciences Organic Chemistry Series One Vol. 9* Giesner G. (Ed). Butterworths, London, UK, 143-160.
- [22] Ye Y, Qin GW, Xu RS. (1994) Alkaloids of *Stemona japonica*. *Phytochemistry*, **37**, 1205-1208.
- [23] Chan YM (2003) Molecular authentication and taxonomy of Radix Stemonae. MPhil thesis, the Chinese University of Hong Kong, Hong Kong SAR, China, 1-127.

Chemical Constituents of *Euonymus glabra*Jie Ren^a, Yang-Guo Xie^a, Xing Wang^a, Shi-Kai Yan^a, Hui-Zi Jin^{a,*} and Wei-Dong Zhang^{a,b,*}^aSchool of Pharmacy, Shanghai Jiao Tong University, Shanghai 200240, China^bDepartment of Phytochemistry, Second Military Medical University, Shanghai 200433, China

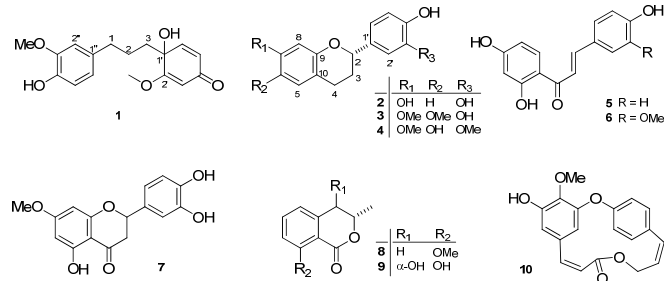
kimhz@sjtu.edu.cn (H.Z. Jin); wdzhangy@hotmail.com (W.D. Zhang)

Received: August 20th, 2015; Accepted: October 1st, 2015

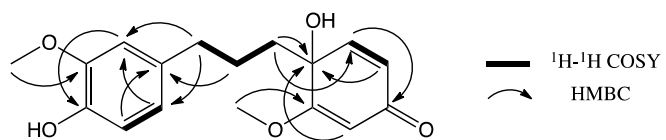
One new phenolic compound (**1**) and one new flavan (**2**), together with eight known compounds (**3–10**) were isolated from the stems and twigs of *Euonymus glabra* Roxb. Their structures were elucidated mainly on the basis of 1D and 2D spectroscopic methods and circular dichroism analysis. In addition, compounds **1–10** were tested for their inhibitory effects against LPS-induced NO production in RAW264.7 macrophages. Compounds **1–5** and **7** exhibited moderate inhibitory activities with IC₅₀ values ranged from 5.1 to 11.9 μM.

Keywords: *Euonymus glabra*, Euonyphenylpropane A, Flavan, NO production.

Euonymus glabra Roxb. (Celastraceae) is a deciduous shrub, which is mainly distributed in Xishuangbanna Dai Autonomous Prefecture in Yunnan province at an elevation of 900–1800 meters. It has been recorded that the twigs and leaves of this species are poisonous [1]. Previous investigations showed that *Euonymus* species exhibited a high diversity of both secondary metabolites (including sesquiterpenes, alkaloids, terpenoids, flavonoids) and biological activities (such as anti-tumor, anti-diabetes, and insecticidal effects [2]. In the continuing search for further bioactive natural products from this genus, phytochemical investigations of *E. glabra* were carried out and led to the isolation of one new phenolic compound euonyphenylpropane A (**1**), one new flavan (*2R*)-3',4',7-trihydroxyflavan (**2**), along with eight known compounds, griffinoid C (**3**) [5], griffinoid B (**4**) [5], isoliquiritigenin (**5**) [6], 2',4,4'-trihydroxy-3-methoxy-chalcone (**6**) [7], 7-O-methyl-eriodictyol (**7**) [8], (*R*)-(-)-mellein methyl ether (**8**) [9], *trans*-4-hydroxymellein (**9**) [10], and combretastatin D-3 (**10**) [11]. Here, we report the isolation and structural elucidation of these compounds, as well as their inhibitory activities against lipopolysaccharide (LPS)-induced nitric oxide (NO) production in RAW264.7 macrophages.

Figure 1: Structures of compounds **1–10**.

Compound **1** was obtained as a light yellow solid. Its molecular formula was determined to be C₁₇H₂₀O₅ by HRESIMS analysis (*m/z* 305.1392 [M+H]⁺), indicating eight degrees of unsaturation. The IR absorptions suggested the presence of hydroxyl groups (3448 cm⁻¹) and a conjugated carbonyl group (1445 cm⁻¹). The ¹H and ¹³C NMR spectral data showed great similarities to those of broussonone A [3], except for an additional methoxyl group in compound **1** (Table 1). HMBC correlation between δ_H 3.81 and C-3'' (δ_C 148.8)

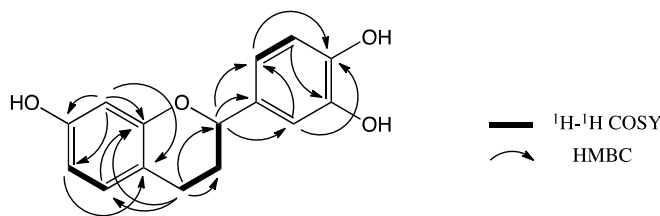
Figure 2: Key ¹H-¹H COSY and HMBC correlations of compound **1**.Table 1: ¹³C and ¹H NMR data [δ_H (*J* in Hz)] for compound **1**.

No.	δ _C	δ _H
1	36.1	2.5 m
2	26.7	1.26 m; 1.40 m
3	38.9	1.71 m; 1.95 m
1'	72.2	
2'	178.5	
3'	102.1	5.53 d (1.7)
4'	190.3	
5'	128.1	6.08 dd (10.0, 1.7)
6'	150.1	6.63 d (10.0)
1''	134.6	
2''	113.1	6.68 d (1.9)
3''	148.8	
4''	145.6	
5''	116.1	6.66 d (8.0)
6''	121.8	6.54 dd (8.0, 1.9)
2'-OMe	56.7	3.76 s
3'-OMe	56.4	3.81 s

¹³C and ¹H NMR data were measured in CD₃OD at 100 and 400 MHz, respectively.

was observed, which indicated that the additional methoxyl group was attached at C-3'' (Figure 2). Thus, the chemical structure of **1** was confirmed and this compound was named as euonyphenylpropane A.

Compound **2** was obtained as a light yellow solid. Its molecular formula C₁₅H₁₄O₄ was determined from the positive HR-ESIMS ion at *m/z* 259.0951 [M+H]⁺, indicating nine degrees of unsaturation. The IR spectrum exhibited absorption bands ascribed to hydroxy groups (3445 cm⁻¹) and benzene rings (1644 cm⁻¹). The ¹H NMR data of **2** exhibited two sets of ABX-substituted aromatic protons [ring A: δ_H 6.25 (1H, d, *J* = 2.4 Hz), 6.31 (1H, dd, *J* = 8.1, 2.4 Hz), 6.85 (1H, d, *J* = 8.1 Hz) and ring B: δ_H 6.72 (1H, dd, *J* = 8.0, 1.8 Hz), 6.75 (1H, d, *J* = 8.0 Hz), 6.85 (1H, d, *J* = 1.8 Hz)]. In addition, signals of an oxymethylene [δ_H 4.80 (1H, dd, *J* = 10.0, 2.5 Hz), δ_C 79.0] and two methylenes [δ_H 2.65, 2.80 (2H, m), δ_C 25.4; δ_H 1.90, 2.10 (2H, m), δ_C 31.3] were observed, which suggested compound **2** as a flavan.

Figure 3: Key ^1H - ^1H COSY and HMBC correlations of compound 2.Table 2: ^{13}C and ^1H NMR data [δ_{H} (J in Hz)] for compound 2.

No.	δ_{C}	δ_{H}
2	79.0	4.80 dd (10.0, 2.5)
3	31.3	1.90 m; 2.10 m
4	25.4	2.65 m; 2.80 m
5	130.9	6.85 d (8.1)
6	109.0	6.31 dd (8.1, 2.4)
7	157.5	
8	104.0	6.25 d (2.4)
9	157.1	
10	114.3	
1'	135.0	
2'	114.4	6.85 d (1.8)
3'	146.3	
4'	146.0	
5'	116.1	6.72 dd (8.0, 1.8)
6'	118.7	6.75 d (8.0)

^{13}C and ^1H NMR data were measured in CD_3OD at 100 and 400 MHz, respectively.

The corresponding carbon signals were assigned by HMQC experiment (Table 2). Analysis of the ^1H - ^1H COSY spectrum revealed the spin system of H-2/H₂-3/H₂-4 as shown in Figure 3. The chemical structure of compound 2 was further confirmed by the HMBC spectrum (Figure 3). In the CD spectrum, a positive Cotton effect observed at 280 nm indicated a 2*R* configuration, in comparison with published data [4] and 2 was defined as (2*R*)-3',4',7-trihydroxyflavan.

Compounds 1–10 were tested for their inhibitory effects against LPS-induced NO production in RAW264.7 macrophages with aminoguanidine as positive control. As shown in Table 2, compounds 1–5 and 7 exhibited moderate inhibitory activities with IC_{50} values ranged from 5.1 to 11.9 μM .

Table 3: Inhibitory effects of compounds 1–10 isolated from *E. glabra* against LPS-induced NO production in RAW264.7 macrophages.

Compounds	IC_{50} (μM)
1	10.3
2	8.1
3	11.9
4	5.1
5	11.9
6	20.1
7	5.4
8	21.8
9	19.3
10	19.1
aminoguanidine ^a	21.7

^aPositive control

Experimental

General procedures: TLC analysis utilized HSGF₂₅₄ silica gel plates (10–40 μm , Yantai, China). Column chromatography (CC) was performed using silica gel (100–200, 200–300 mesh, Yantai, China), silica gel H (10–40 μm , Qingdao, China) and Sephadex LH-20 (Pharmacia Co. Ltd.). Preparative HPLC (Shimadzu LC-6AD) was performed on a preparative column (Shimadzu PRC-ODS EV0233). 1D and 2D NMR spectra were recorded on Bruker Avance-400 spectrometers in either CD_3OD or $\text{DMSO}-d_6$ with TMS as internal standard. ESIMS were recorded on an Agilent LC/MSD Trap XCT spectrometer (Waters, USA), and HR-ESIMS on a Q-ToF micro YA019 mass spectrometer (Waters, USA). Optical rotations were recorded on a JASCO P-2000 polarimeter. IR spectra were

measured on a Bruker FTIR Vector 22 spectrometer with KBr pellets. CD spectra were determined on a JACSO J-815 spectrometer.

Plant material: The stems and twigs of *E. glabra* Roxb. were collected in Xishuangbanna Dai Autonomous Prefecture, Yunnan province, PR China, in August 2010, and were authenticated by Prof. Haiou Yang, Kunming Institute of Botany, Chinese Academy of Sciences. A voucher specimen (No. 201008SDWM) was deposited at the School of Pharmacy, Shanghai Jiao Tong University.

Extraction and isolation: Dried stems and twigs of *E. glabra* (4.5 kg) were powdered and extracted with 95% EtOH 3 times at room temperature and then evaporated under reduced pressure to give crude extract (350.0 g). This was further partitioned with light petroleum (PE), EtOAc and *n*-BuOH to obtain 3 fractions. The EtOAc fraction (90.7 g) was subjected to silica gel CC, and eluted with a step gradient of CH_2Cl_2 -MeOH (100:0–0:100) to yield 7 fractions (EA-A–EA-G). EA-A (3.9 g) was chromatographed on macroporous resin MCI (MeOH-H₂O, 4:1) and a silica gel column eluting with a step gradient of CH_2Cl_2 -MeOH (100:0–20:1), followed by a Sephadex LH-20 column (MeOH) to give 10 sub-fractions (EA-A1–EA-A10). EA-A5 was purified by preparative HPLC (MeOH-H₂O, 55:45) to yield compound 10 (5.0 mg). EA-A8 and EA-A9 were purified by preparative HPLC (MeOH-H₂O, 65:35) to obtain compounds 8 (5.0 mg) and 9 (3.5 mg), respectively. EA-B (7.0 g) was subjected to macroporous resin MCI (MeOH-H₂O, 4:1) and a silica gel column eluting with a step gradient of CH_2Cl_2 -MeOH (100:1–5:1) followed by Sephadex LH-20 column (MeOH) to give 9 sub-fractions (EA-B1–EA-B9). EA-B6 was further purified by silica gel CC eluting with CH_2Cl_2 -MeOH (100:1) to afford compounds 5 (5.3 mg) and 6 (3.2 mg). EA-B7 was purified by preparative HPLC (MeOH-H₂O, 60:40) to yield compound 3 (11.8 mg). EA-B8 was subjected to preparative HPLC (MeOH-H₂O, 60:40) to obtain compound 7 (1.6 mg). EA-C (7.1 g) was chromatographed on macroporous resin MCI (MeOH-H₂O, 4:1) and a silica gel column eluting with a step gradient of CH_2Cl_2 -MeOH (50:1–0:100) followed by a Sephadex LH-20 column (MeOH) to give 7 sub-fractions (EA-C1–EA-C7). EA-C7 was purified by preparative HPLC (MeOH-H₂O, 60:40) to yield compounds 1 (6.1 mg), 2 (5.2 mg) and 4 (7.8 mg).

Euonyphenylpropane A (1)

Light yellow solid.

$[\alpha]^{20}_{\text{D}}: -3.7$ (*c* 0.10, MeOH).

IR (KBr): 3448, 1620, 1505, 1645, 1455, 1383, 1189, 1121, 1075, 1032 cm^{-1} .

^1H and ^{13}C NMR: Table 1.

HR-ESIMS (positive) *m/z*: 305.1392 [M+H]⁺ (calcd for $\text{C}_{17}\text{H}_{21}\text{O}_5$, 305.1384).

(2*R*)-3',4',7-Trihydroxyflavan (2)

Light yellow solid.

$[\alpha]^{20}_{\text{D}}: +8.1$ (*c* 0.10, MeOH).

CD (1.0×10^{-4} M, MeOH): $\lambda (\Delta \epsilon) 280$ (2.1).

IR (KBr): 3445, 1644, 1383, 1189, 1153, 1119, 1077, 1022, 610 cm^{-1} .

^1H and ^{13}C NMR: Table 2.

HR-ESIMS (positive) *m/z*: 259.0951 [M+H]⁺ (calcd for $\text{C}_{15}\text{H}_{15}\text{O}_4$, 259.0965).

Determination of nitric oxide (NO) production: The assay was performed using the MTT method, as previously described [12–14].

Briefly, RAW264.7 cells grown on a 100 mm culture dish were harvested and seeded in 96-well plates (2×10^5 cells/well) for NO production. The plates were pretreated with various concentrations of samples for 30 min and incubated with LPS (1 μ g/mL) for 24 h. The amount of NO was determined by the nitrite concentration in the cultured RAW264.7 macrophage supernatants with the Griess reagent. The cell viability was evaluated by MTT [3-(4,5-dimethylthiazol-2-yl)-2,5-diphenyltetrazolium bromide, Sigma-Aldrich] reduction [15].

Acknowledgments - The work was supported by program NCET Foundation, NSFC (81230090 and 81102778), partially supported by Global Research Network for Medicinal Plants (GRNMP) and King Saud University, Shanghai Leading Academic Discipline Project (B906), FP7-PEOPLE-IRSES-2008 (TCMCANCER Project 230232), Key laboratory of drug research for special environments, PLA, and the Scientific Foundation of Shanghai China (12401900501), National Major Project of China (2011ZX09307-002-03), and National Key Technology R&D Program of China (2012BAI29B06).

References

- [1] Xishuangbanna Tropical Botanical Garden and Department of Ethnobotany, Kunming Institute of Botany, the Chinese Academy of Sciences. (1996) List of plants in Xishuangbanna. *The Nationalities Publishing House of Yunnan*, **6**, 299.
- [2] Ren J, Zhang YY, Jin HZ, Yu J, Zhou YY, Wu F, Zhang WD. (2014) Novel inhibitors of human DOPA decarboxylase extracted from *Euonymus glabra* Roxb. *ACS Chemical Biology*, **9**, 897-903.
- [3] Ahn JH, Liu Q, Lee C, Ahn MJ, Yoo HS, Hwang BY, Lee MY. (2012) A new pancreatic lipase inhibitor from *Broussonetia kazinoki*. *Bioorganic & Medicinal Chemistry Letters*, **22**, 2760-2763.
- [4] Yang Y, Zhang T, Xiao L, Chen RY. (2010) Two novel flavanoids from the leaves of *Morus alba* L. *Journal of Asian Natural Products Research*, **12**, 194-198.
- [5] Moosophon P, Kanokmedhakul S, Kanokmedhakul K, Buayairaksa M, Noichan J, Poopasit K. (2013) Antiplasmodial and cytotoxic flavans and diarylpropanes from the stems of *Combretum griffithii*. *Journal of Natural Products*, **76**, 1298-1302.
- [6] Yu HW, Hua J, Qin L, Xu Q. (2012) Study on chemical constituents of *Premna yunnanensis*. *Chinese Traditional Patent Medicine*, **34**, 300-303.
- [7] Bandeira PN, de Farias SS, Lemos TLG, Braz-Filho R, Santos HS, Albuquerque MRJR, Costa SMO. (2011) New isoflavone derivative and other flavonoids from the resin of *Amburana cearensis*. *Journal of the Brazilian Chemical Society*, **22**, 372-375.
- [8] Yang WX, Huang HY, Wang YJ, Jia ZY, Li LL. (2005) Study on chemical constituents in total saponin from *Trigonella foenum-graecum*. *China Journal of Chinese Materia Medica*, **30**, 1428-1430.
- [9] Klaiklay S, Rukachaisirikul V, Sukpondma Y, Phongpaichit S, Buatong J, Bussaban B. (2012) Metabolites from the mangrove-derived fungus *Xylaria cubensis* PSU-MA34. *Archives of Pharmacal Research*, **35**, 1127-1131.
- [10] Djoukeng JD, Polli S, Larignon P, Abou-Mansour E. (2009) Identification of phytotoxins from *Botryosphaeria obtusa*, a pathogen of black dead arm disease of grapevine. *European Journal of Plant Pathology*, **124**, 303-308.
- [11] Vongvanich N, Kittakoop P, Charoenchai P, Intamas S, Danwisetkanjana K, Thebtaranonth Y. (2005) Combretastatins D-3 and D-4, new macrocyclic lactones from *Getonia floribunda*. *Planta Medica*, **71**, 191-193.
- [12] Qin JJ, Jin HZ, Zhu JX, Fu JJ, Zeng Q, Cheng XR, Zhu Y, Shan L, Zhang SD, Pan YX, Zhang WD. (2010) New sesquiterpenes from *Inula japonica* Thunb. with their inhibitory activities against LPS-induced NO production in RAW264.7 macrophages. *Tetrahedron*, **66**, 9379-9388.
- [13] Nie LY, Qin JJ, Huang Y, Yan L, Liu YB, Pan YX, Jin HZ, Zhang WD. (2010) Sesquiterpenoids from *Inula linearifolia* inhibit nitric oxide production. *Journal of Natural Products*, **73**, 1117-1120.
- [14] Schmidt HHW, Kelm M. (1996) In *Methods in Nitric Oxide Research*. John Wiley & Sons, Ltd., London. Chapter 33, 491-497.
- [15] Denizot F, Lang R. (1986) Rapid colorimetric assay for cell growth and survival. Modifications to the tetrazolium dye procedure giving improved sensitivity and reliability. *Journal of Immunological Methods*, **89**, 271-277.

Isoprenylated Flavonoids with PTP1B Inhibition from *Ficus tikoua*Lu-Qin Wu^a, Chun Lei^a, Li-Xin Gao^b, Hai-Bing Liao^a, Jing-Ya Li^b, Jia Li^b and Ai-Jun Hou^{a,*}^aDepartment of Pharmacognosy, School of Pharmacy, Fudan University, 826 Zhang Heng Road, Shanghai 201203, PR China^bNational Center for Drug Screening, State Key Laboratory of Drug Research, Shanghai Institute of Materia Medica, Chinese Academy of Sciences, 189 Guo Shou Jing Road, Shanghai 201203, PR China

ajhou@shmu.edu.cn

Received: August 13th, 2015; Accepted: October 27th, 2015

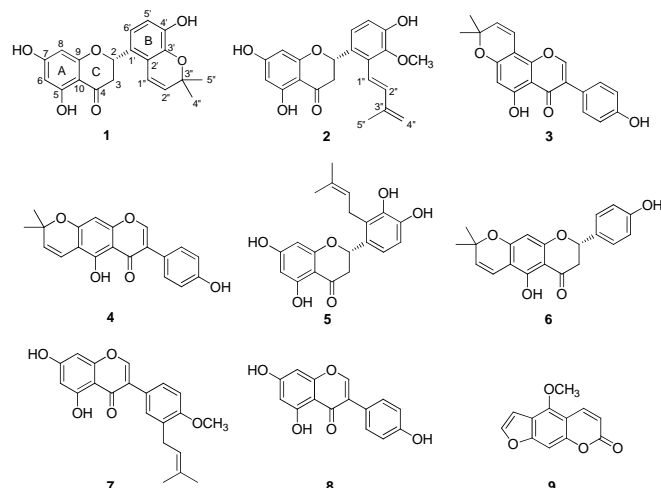
Two new isoprenylated flavanones, ficustikousins A and B (**1** and **2**), together with seven known compounds (**3–9**) were isolated from the whole plant of *Ficus tikoua* (Moraceae). The structures of the new compounds were elucidated on the basis of spectroscopic methods. Compounds **1–7** exhibited moderate inhibitory activities against PTP1B *in vitro*.

Keywords: *Ficus tikoua*, Moraceae, Isoprenylated flavonoids, Protein tyrosine phosphatase 1B.

Ficus tikoua Bur. belongs to the family Moraceae and is a creeping vine plant mainly distributed in south China, India, Vietnam and Laos [1]. This plant is used as traditional Chinese medicine and ethnomedicine in more than ten nationalities in China for the treatment of edema, jaundice, amenorrhea, and bruise [2,3]. Previous phytochemical studies on this plant resulted in the isolation of some flavonoids and phenolic glycosides, some of which showed antifungal and cytotoxic activities [4]. In the course of discovering structurally and biologically interesting compounds from the family Moraceae [5], we investigated the chemical constituents of *F. tikoua*.

Fractionation of an ethanol extract of this plant afforded eight flavonoids and one coumarin, including two new isoprenylated flavanones, ficustikousins A (**1**) and B (**2**), along with seven known compounds, derrone (**3**) [6a], alpinumisoflavone (**4**) [6b], (*S*)-5,7,3',4'-tetrahydroxy-2'-(3-methylbut-2-enyl)flavanone (**5**) [6c], (*S*)-paratocarpin K (**6**) [6d], 3'-(3-methylbut-2-enyl)biochanin A (**7**) [6e], genistein (**8**) [6f], and bergapten (**9**) [6g]. The known compounds **3–7** were isolated from this plant for the first time. Protein tyrosine phosphatase 1B (PTP1B) plays an important role in regulating the sensitivity of insulin signaling and fat metabolism and is considered to be a significant target in treating type 2 diabetes and obesity [7]. Recently, a series of isoprenylated flavonoids with PTP1B-inhibiting activities were isolated from the family Moraceae by our group [5a, d]. As a continuing research on the discovery of effective PTP1B inhibitors, compounds isolated from *F. tikoua* were evaluated *in vitro* for the inhibition on PTP1B enzyme activity. Compounds **1–7** showed moderate inhibitory effects. We herein report the structural elucidation and biological evaluation of these compounds.

Ficustikousin A (**1**), an optically active compound ($[\alpha]_D^{25} = -8.7$), was obtained as white amorphous powder. Its molecular formula was determined as $C_{20}H_{18}O_6$ by HRESIMS (m/z 353.1033 [$M - H^-$]; calcd. 353.1031). The IR spectrum of **1** indicated the presence of hydroxyl (3421 cm^{-1}), carbonyl (1653 cm^{-1}), and benzene ring (1539 and 1467 cm^{-1}) moieties. The UV spectrum showed absorption maxima at λ_{\max} 212 (sh), 231, 282 and 331 (sh) nm, which were similar to those of flavanones [8]. The 1H NMR

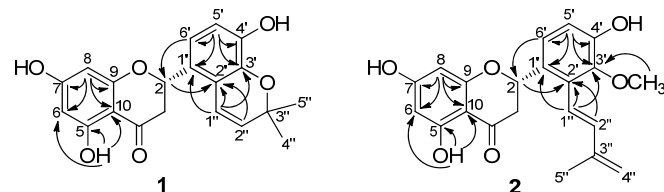
Figure 1: Structures of compounds **1–9**.

spectrum (Table 1) revealed signals of an ABX spin system at δ_H 5.73 (1H, dd, $J = 13.2, 2.8\text{ Hz}$, H-2), 3.21 (1H, dd, $J = 17.2, 13.2\text{ Hz}$, H-3), and 2.70 (1H, dd, $J = 17.2, 2.8\text{ Hz}$, H-3'), characteristic of ring C on a flavanone skeleton. It also showed resonances for a hydrogen-bonded hydroxyl group at δ_H 12.20 (1H, s), two *ortho*-coupled aromatic protons at δ_H 6.99 (1H, d, $J = 8.4\text{ Hz}$, H-6') and 6.79 (1H, d, $J = 8.4\text{ Hz}$, H-5'), two *meta*-coupled aromatic protons at δ_H 5.96 (2H, br s), and a 2,2-dimethylpyran ring at δ_H 6.81 (1H, d, $J = 10.0\text{ Hz}$, H-1"), 5.85 (1H, d, $J = 10.0\text{ Hz}$, H-2"), and 1.42, 1.43 (each 3H, s, H-3", 5"). The ^{13}C NMR spectrum (Table 1) exhibited 20 carbon signals attributable to one carbonyl group, eight quaternary sp^2 , one quaternary sp^3 , six methine sp^2 , one methine sp^3 , one methylene sp^3 , and two methyl carbon atoms. These spectroscopic data suggested that **1** is a monoprenylated flavanone. The two *ortho*-coupled protons at δ_H 6.99 and 6.79 were assigned to H-6' and H-5', respectively, as established by the HMBC correlations from H-6' (δ_H 6.99) to C-2 and from H-5' (δ_H 6.79) to C-1', C-3', C-4', and C-6' (Figure 2). The HMBC correlations from H-1" (δ_H 6.81) to C-1', C-2', and C-3' and from H-2" (δ_H 5.85) to C-2' indicated that the 2,2-dimethylpyran ring was fused at C-2' and

Table 1: ^1H and ^{13}C NMR Data (400 and 100 MHz, resp.) of compounds **1** and **2** in acetone-d₆ (δ in ppm, J in Hz).

Position	1		2	
	δ_{H}	δ_{C}	δ_{H}	δ_{C}
2	5.73, dd (13.2, 2.8)	77.3	5.65, dd (13.6, 2.8)	77.7
3	2.70, dd (17.2, 2.8) 3.21, dd (17.2, 13.2)	43.5	2.68, dd (17.2, 2.8) 3.31, dd (17.2, 13.6)	43.3
4		197.8		198.0
5		165.9		165.9
6	5.96, br s	97.4	5.96, d (2.0)	97.5
7		167.9		167.8
8	5.96, br s	96.4	5.99, d (2.0)	96.3
9		164.9		164.9
10		103.8		103.8
1'		126.3		129.3
2'		121.3		133.1
3'		141.5		146.9
4'		147.6		151.9
5'	6.79, d (8.4)	116.4	6.93, d (8.8)	123.2
6'	6.99, d (8.4)	120.0	7.32, d (8.8)	124.6
1''	6.81, d (10.0)	120.5	6.73, d (16.4)	116.5
2''	5.85, d (10.0)	133.3	6.81, d (16.4)	139.6
3''		77.0		143.7
4''	1.42, s ^a	28.0	5.06, br s	118.8
5''	1.43, s ^a	28.0	1.94, s	18.9
OH-5	12.20, s		12.17, s	
OMe-3'			3.71, s	60.9

^a Assignments are exchangeable.

**Figure 2:** Key HMBC (H→C) correlations of compounds **1** and **2**.

C-3'. The substitution of ring A was further supported by the HMBC correlations shown in Figure 2. The stereochemistry at C-2 was assigned as *S*-configuration by the ECD data with Cotton effects at 288 (−) and 330 (+) nm [8]. Thus, the structure of **1** was determined and named ficustikousin A.

Ficustikousin B (**2**), obtained as white amorphous powder, was assigned the molecular formula $\text{C}_{21}\text{H}_{20}\text{O}_6$ by HRESIMS (m/z 367.1202 [$\text{M} - \text{H}$]⁺; calcd. m/z 367.1187). The NMR spectroscopic data of **2** (Table 1) suggested a flavanone skeleton with the same rings A and C as those of **1**. It differed from **1** in the substituents on the ring B, as deduced from the NMR data of a 3-methylbutadienyl group [δ_{H} 6.73 (1H, d, $J = 16.4$ Hz, H-1'), 6.81 (1H, d, $J = 16.4$ Hz, H-2''), 5.06 (2H, br s, H₂-4''), and 1.94 (3H, s, H₃-5'); δ_{C} 116.5 (C-1''), 139.6 (C-2''), 143.7 (C-3''), 118.8 (C-4''), and 18.9 (C-5'')] and a methoxyl group [δ_{H} 3.71 (3H, s); δ_{C} 60.9 (OMe-3')]. In the HMBC spectrum (Figure 2), the correlations from H-1' to C-1', C-2' and C-3' and from H-2'' to C-2' indicated that the 3-methylbutadienyl group was attached to C-2'. The methoxyl group was located at C-3' according to the HMBC correlation from the methoxyl protons to C-3'. The (*E*)-configuration of the C(1'')=C(2'') bond was indicated by the coupling constant of H-1'' and H-2'' ($J = 16.4$ Hz). Compound **2** showed no Cotton effect in the ECD spectrum. The stereochemistry at C-2 was proposed to be *S*-configuration on the basis of the negative specific optical rotation ($[\alpha]_D^{25} = -5.0$) and the *trans* diaxial coupling constant of H-2 and H-3 ($J = 13.6$ Hz) [9]. Thus, the structure of **2** was assigned and named ficustikousin B.

The structures of compounds **3–9** were identified by comparison of their spectral data with those described in the literature.

Table 2: Inhibitory Effects of Compounds **1–7** against PTP1B.

Compound	$\text{IC}_{50} \pm \text{SD}$ (μM)
1	40.37 ± 4.66
2	16.33 ± 1.47
3	24.64 ± 0.57
4	11.16 ± 1.88
5	19.27 ± 3.26
6	25.12 ± 2.28
7	18.55 ± 0.74
Oleanolic acid	2.61 ± 0.59

The isolated compounds (**1–9**) were examined *in vitro* for the inhibition on PTP1B. Oleanolic acid is used as positive control in this test. The isoprenylated flavonoids (**1–7**) showed moderate PTP1B inhibitory activities (10 $\mu\text{M} < \text{IC}_{50} < 50 \mu\text{M}$) (Table 2).

In summary, two new isoprenylated flavanones and seven known compounds including five isoprenylated flavonoids were isolated from the whole plant of *F. tikoua*. Although isoprenylated flavonoids from *F. tikoua* had been reported previously [4a, b, c], the flavanones with 2,2-dimethylpyran moiety (**1** and **6**) and methylbutadienyl group (**2**) were found for the first time from this plant. Furthermore, isoprenylated flavonoids (**1–7**) were found to inhibit PTP1B, while flavonoid and coumarin without isoprenoid group (**8** and **9**) were inactive.

Experimental

General: Optical rotations were measured on Autopol IV. UV spectra were taken on a Hitachi U-2900 spectrophotometer. IR spectra were measured on a Nicolet Avatar 360 spectrometer with KBr pellets. ECD spectra were manipulated on a Jasco J-810 automatic digital polarimeter. NMR spectra were recorded on a Bruker DRX-400 and Varian Mercury Plus 400 instruments. ESIMS and HRESIMS were performed on an Agilent 1100 LC/MSD and on a Bruker Daltonics Apex 7.0 TESLA FTMS mass spectrometer, respectively. Column chromatography (CC) was performed on silica gel (200–300 mesh; Yantai Institute of Chemical Technology, Yantai, PR China), Sephadex LH-20 gel (GE Healthcare Bio-Science AB, Uppsala, Sweden), and Diaion HP-20 (Mitsubishi Chemical Co., Tokyo, Japan). TLC analysis was run on precoated silica gel GF254 plates (10–40 μm , Yantai Institute of Chemical Technology, Yantai, PR China), and spots were visualized by spraying with 10% H_2SO_4 in EtOH, followed by heating. Semi-preparative HPLC was run on an Agilent 1200 and a Promosil C₁₈ column (10 × 150 mm, 5 μm , Agela Technologies, China), using a UV detector set at 210 nm.

Plant material: The whole plant of *F. tikoua* was collected from Nanchong, Sichuan province, PR China, in August 2012. The plant material was identified by Dr. Yun Kang, Fudan University, and a voucher specimen (TCM 12-08-25 Hou) has been deposited in the Herbarium of the Department of Pharmacognosy, School of Pharmacy, Fudan University.

Extraction and isolation: The milled and air-dried plant material (4.7 kg) was percolated with 95% EtOH (20 L × 5 times) at room temperature. The filtrate was concentrated under reduced pressure to yield a residue (400 g), which was suspended in H_2O and extracted with EtOAc (2 L × 3 times). The EtOAc extract (96 g) was subjected to column chromatography (CC) on Diaion HP-20 eluted with 85% EtOH and then was applied to CC over silica gel eluted with a gradient system of $\text{CH}_2\text{Cl}_2/\text{MeOH}$ (100:1, 20:1, 9:1, 5:1, 2:1, v/v) to provide fractions 1–5. Fraction 1 (11 g) was purified by silica gel CC (petroleum ether (PE)/ Me_2CO 30:1, v/v) to give **9** (3.1 mg). Fraction 2 (8 g) was subjected successively to Sephadex LH-20 CC (MeOH), silica gel CC (PE/ Me_2CO 50:1, v/v),

and semi-preparative HPLC (MeOH/H₂O 7:3, v/v, flow rate 1 mL/min) to give **6** (7 mg, *t*_R 70 min) and **7** (6 mg, *t*_R 50 min). Purification of fraction 3 (3.3 g) by Sephadex LH-20 CC (MeOH) and semi-preparative HPLC (MeOH/H₂O 6:4, v/v, flow rate 1 mL/min) yielded **3** (20 mg, *t*_R 56 min) and **8** (4 mg, *t*_R 10 min). Fraction 4 (8.4 g) was subjected to Sephadex LH-20 CC (MeOH) to give fractions 4.1–4.5. Fraction 4.1 was isolated by semi-preparative HPLC (MeOH/H₂O 7:3, v/v, flow rate 1 mL/min) to provide **4** (3.9 mg, *t*_R 27 min) and **5** (8 mg, *t*_R 29 min). Fraction 4.3 was separated by semi-preparative HPLC (MeOH/H₂O 6:4, v/v, flow rate 1 mL/min) to give **2** (3.5 mg, *t*_R 67 min). Fraction 4.4 was purified by semi-preparative HPLC (MeOH/H₂O 5.5:4.5, v/v, flow rate 1 mL/min) to provide **1** (4 mg, *t*_R 46 min).

Ficustikousin A (**1**)

White amorphous powder.

[α]_D²⁵: -8.7 (c 0.2, MeOH).

IR (KBr) ν _{max}: 3421, 1653, 1539, 1467, 1327, 1287, 1157, 1087 cm⁻¹.

UV (MeOH) λ _{max} (log ε): 212 (sh 3.35), 231 (3.51), 282 (3.42), 331 (sh 2.95) nm.

ECD (MeOH) λ _{max} (Δε): 260 (+1.27), 288 (-1.39), 330 (+0.46) nm.

¹H and ¹³C NMR: Table 1.

HRESIMS: *m/z* 353.1033 [M – H]⁻; calcd for C₂₀H₁₇O₆: 353.1031.

References

- [1] Editorial Committee of Flora of China, Chinese Academy of Sciences. (1998) *Flora of China*. Science Press, Beijing, **23**, 156.
- [2] Wu JR, Qiu DW. (1993) *Colored illustration of commonly used Chinese traditional and herbal drugs*. Guizhou Science and Technology Publishing House, Guiyang, 170.
- [3] Guan YX, Yang XS, Tong LH, Yang B, Hao XJ. (2007) Chemical constituents in *Ficus tikoua* of Miao nationality. *Chinese Traditional and Herbal Drugs*, **38**, 342-344.
- [4] (a) Wei SP, Lu LN, Ji ZQ, Zhang JW, Wu WJ. (2012) Chemical constituents from *Ficus tikoua*. *Chemistry of Natural Compounds*, **48**, 484-485; (b) Wei SP, Wu WJ, Ji ZQ. (2012) New antifungal pyranosioflavone from *Ficus tikoua* Bur.. *International Journal of Molecular Sciences*, **13**, 7375-7382; (c) Jiang ZY, Li SY, Li WJ, Guo JM, Tian K, Hu QF, Huang XZ. (2013) Phenolic glycosides from *Ficus tikoua* and their cytotoxic activities. *Carbohydrate Research*, **382**, 19-24; (d) Wei SP, Luan JY, Lu LN, Wu WJ, Ji ZQ. (2011) A new benzofuran glucoside from *Ficus tikoua* Bur.. *International Journal of Molecular Sciences*, **12**, 4946-4952.
- [5] (a) Wang M, Gao XL, Wang J, Li JY, Yu MH, Li J, Hou AJ. (2015) Diels–Alder adducts with PTP1B inhibition from *Morus notabilis*. *Phytochemistry*, **109**, 140-146; (b) Hu X, Wu JW, Zhang XD, Zhao QS, Huang JM, Wang HY, Hou AJ. (2011) Isoprenylated flavonoids and adipogenesis-promoting constituents from *Morus nigra*. *Journal of Natural Products*, **74**, 816-824; (c) Hu X, Wu JW, Wang M, Yu MH, Zhao QS, Wang HY, Hou AJ. (2012) 2-Arylbenzofuran, flavonoid, and tyrosinase inhibitory constituents of *Morus yunnanensis*. *Journal of Natural Products*, **75**, 82-87; (d) Wang M, Yu BW, Yu MH, Gao LX, Li JY, Wang HY, Li J, Hou AJ. (2015) New isoprenylated phenolic compounds from *Morus laevigata*. *Chemistry & Biodiversity*, **12**, 937-945.
- [6] (a) Chibber SS, Sharma RP. (1980) Derrone, a new pyranosioflavone from *Derris robusta* seeds. *Phytochemistry*, **19**, 1857-1858; (b) Stewart M, Bartholomew B, Currie F, Abbiw DK, Latif Z, Sarker SD, Nash RJ. (2000) Pyranosioflavones from *Rinorea welwitschii*. *Fitoterapia*, **71**, 595-597; (c) Chauhan P, Saxena VK. (1987) A new prenylated flavanone from *Erythrina suberosa* roots. *Planta Medica*, **53**, 221-222; (d) Hano Y, Itoh N, Hanaoka A, Nomura T. (1995) Paratocarpins F-L, Seven new isoprenoid-substituted flavonoids from *Paratocarpus venenosus* Zoll. *Heterocycles*, **41**, 2313-2326; (e) Yenesew A, Midwo JO, Heydenreich M, Peter MG. (1998) Four isoflavones from the stem bark of *Erythrina saacleuxii*. *Phytochemistry*, **49**, 247-249; (f) Krishnamurti HG, Prasad JS. (1980) Isoflavones of *Moghania macrophylla*. *Phytochemistry*, **19**, 2797-2798; (g) El-Fishawy A, Zayed R, Afifi S. (2011) Phytochemical and pharmacological studies of *Ficus auriculata* Lour. *Journal of Natural Products*, **4**, 184-195.
- [7] (a) Zhang W, Li JY, Li J. (2006) Advance in the study about the inhibitors of PTP1B-a novel target for diabetes and obesity therapy. *Chinese Bulletin of Life Sciences*, **18**, 462-466; (b) Goldstein BJ, Bittner-Kowalczyk A, White MF, Harbeck M. (2000) Tyrosine dephosphorylation and deactivation of insulin receptor substrate-1 by protein tyrosine phosphatase 1B: Possible facilitation by the formation of a ternary complex with the Grb2 adaptor protein. *The Journal of Biological Chemistry*, **275**, 4283-4289.
- [8] Hano Y, Nomura T. (1983) Constituents of the Chinese crude drug “Sang-Bai-Pi” (Morus root barks) IV. Structures of four new flavonoids, Sanggenon H, I, J and K. *Heterocycles*, **20**, 1071-1076.
- [9] (a) Ma JP, Qiao X, Pan S, Shen H, Zhu GF, Hou AJ. (2010) New isoprenylated flavonoids and cytotoxic constituents from *Artocarpus tonkinensis*. *Journal of Asian Natural Products Research*, **12**, 586-592; (b) Kanokmedhakul S, Kanokmedhakul K, Nambuddee K, Kongsaeree P. (2004) New bioactive prenylflavonoids and dibenzocycloheptene derivative from roots of *Dendrolobium lanceolatum*. *Journal of Natural Products*, **67**, 968-972.
- [10] Shi L, Yu HP, Zhou YY, Du JQ, Shen Q, Li JY, Li J. (2008) Discovery of a novel competitive inhibitor of PTP1B by high-throughput screening. *Acta Pharmacologica Sinica*, **29**, 278-284.

Phenolic Derivatives from *Hypericum japonicum*Guoyong Luo^{a,b}, Min Zhou^a, Qi Ye^a, Jun Mi^c, Dongmei Fang^a, Guolin Zhang^{a,*} and Yinggang Luo^{a,*}^aChengdu Institute of Biology, Chinese Academy of Sciences, Chengdu 610041, PR China^bUniversity of the Chinese Academy of Sciences, Beijing 100049, PR China^cChengdu Nanshan Pharmaceutical Co., Ltd., Chengdu 610041, PR China

zhanggl@cib.ac.cn; yinggluo@cib.ac.cn

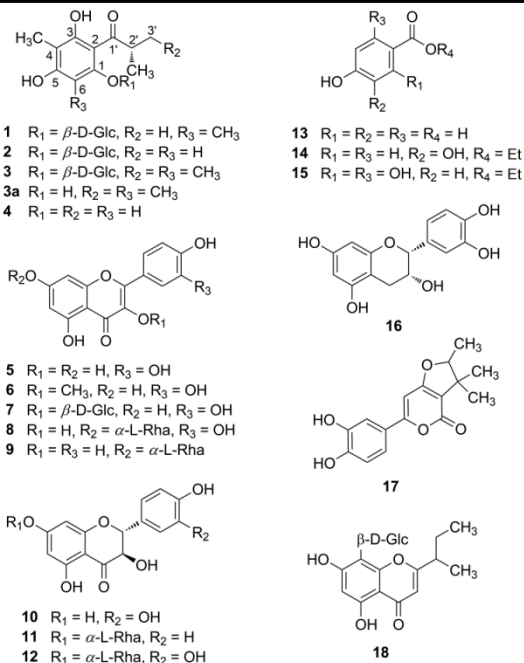
Received: May 17th, 2015; Accepted: June 17th, 2015

Three new acylphloroglucinol glycosides, hypericumols A - C, together with fifteen known phenolic derivatives, were isolated from the total phenolic extract of *Hypericum japonicum*. Hypericumols A, B, and C were characterized as 4,6-dimethyl-2-methylpropanoylphloroglucinol-1-O-β-D-glucopyranoside (**1**), 4-methyl-2-methylpropanoylphloroglucinol-1-O-β-D-glucopyranoside (**2**), and (2'S)-4,6-dimethyl-2-methylbutyrylphloroglucinol-1-O-β-D-glucopyranoside (**3**), respectively, on the basis of spectroscopic data interpretation and chemical degradation reaction.

Keywords: *Hypericum japonicum*, Hypericumol, Acylphloroglucinol, Flavonoid, Phenol.

Hypericum japonicum Thunb., di er cao or tian ji huang in Chinese, is an annual / perennial herbal plant [1]. It is widely distributed in Asia, Oceania, and North America [1]. The whole plant material has been used in traditional Chinese medicine for heat-relieving, detoxification, hemostasis, and detumescence [1]. Phytochemical and pharmacological investigations showed that the chemical components of *H. japonicum* have diverse biological activities such as antioxidant [2], antivirus [3], antitumor [4], antimicrobial [5], and hepatoprotection [2a, 6]. Flavonoids and chromones are the primary chemical components of *H. japonicum*, whereas phloroglucinols and xanthones are two characteristic metabolites present in *H. japonicum* [7]. Recent studies demonstrated that the total phenolic extract of *H. japonicum* showed potential application to cure chronic kidney disease (CKD), which may be attributed to its effects on interfering with renal fibrosis, and enhancing cellular and humoral immunity [8]. As part of our continuing interests in the chemistry of traditional Chinese medicines [9], here we report the isolation and structure characterization of three new acylphloroglucinol glycosides (**1** - **3**), together with fifteen known compounds, including an acylphloroglucinol (**4**), nine flavonoids (**5** - **12**, **16**), three benzoic acid derivatives (**13** - **15**), a pyrone (**17**), and a chromone glycoside (**18**), from the phenolic extract of *H. japonicum* (Figure 1).

Compound **1** was isolated as a yellowish gum. Its molecular formula $C_{18}H_{26}O_9$ was calculated from the $[M+Na]^+$ ion at *m/z* 409.1480 in its HRESIMS (positive ion mode). The hydroxyl and conjugated carbonyl groups were deduced from the IR bands at 3410 and 1615 cm^{-1} , respectively. Besides the ^1H NMR signals for a hexose moiety, two singlet methyls at $\delta_H = 2.03$ (3H, s) and 2.20 (3H, s), two doublet methyls at $\delta_H = 0.99$ (3H, d, $J = 6.9$ Hz) and 1.16 (3H, d, $J = 6.9$ Hz), and a heptet methine group at $\delta_H = 4.05$ (1H, h, $J = 6.9$ Hz) were recognized from the ^1H NMR spectrum (Table 1). In addition to the ^{13}C NMR signals for the groups mentioned above, seven downfield quaternary carbon signals ($\delta_C > 109$) were observed in the ^{13}C NMR spectrum (Table 1), which indicated the presence of a phenyl and a conjugated keto carbonyl group. Compound **1** might be an acylphloroglucinol derivative in view of its characteristic UV bands at 290 and 329 nm for acylphloroglucinol [10]. A 2-methyl propionyl group was established from the two doublet methyls, the

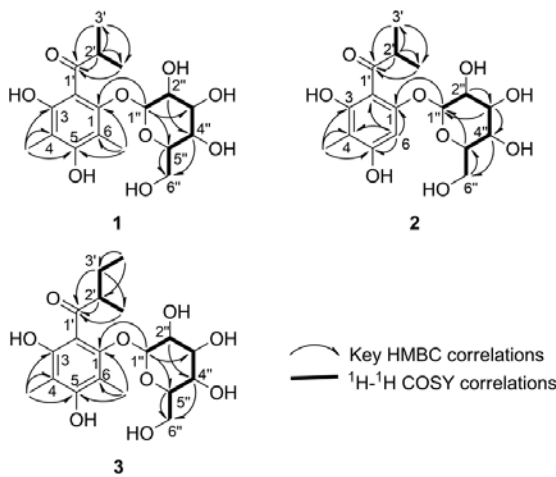
Figure 1. Chemical structures of phenolic derivatives from *Hypericum japonicum*.

heptet methine, and the keto carbonyl group on the basis of ^1H - ^1H COSY correlations of H-3' / H-2' / H-2'- CH_3 and the key HMBC correlations of H-2' / C-1', C-3', C-2'- CH_3 ; H-3' / C-1', C-2'- CH_3 ; and H-2'- CH_3 / C-1' shown in Figure 2. A 2,4-dimethyl-1,3,5-trihydroxyphenyl moiety was established from the key HMBC correlations of H-4- CH_3 / C-3, C-4, C-5 and H-6- CH_3 / C-1, C-5, C-6 (Figure 2). Acid hydrolysis of compound **1** afforded an acylphloroglucinol and D-glucose with β -orientation in view of the ^1H NMR signal of the anomeric proton at $\delta_H = 4.38$ (1H, d, $J = 7.7$ Hz). The 1-OH was glucosylated in view of the key HMBC correlation of H-1'' / C-1 (Figure 2). Thus compound **1**, named as hypericumol A, was characterized as 4,6-dimethyl-2-methylpropanoylphloroglucinol-1-O-β-D-glucopyranoside (Figure 1).

Table 1: NMR spectroscopic data of compounds **1** - **3** in CD₃OD.

	1	2	3	
	$\delta_{\text{H}}^{\text{a}}$	$\delta_{\text{C}}^{\text{b}}$	$\delta_{\text{H}}^{\text{a}}$	$\delta_{\text{C}}^{\text{b}}$
1		153.72, C		153.83, C
2		112.71, C		112.45, C
3		158.52, C		159.08, C
4		109.30, C		109.20, C
5		160.41, C		160.50, C
6		111.13, C	6.23, s	94.50, CH
4'-CH ₃	2.03, s	8.35, CH ₃	7.48, CH ₃	2.05, s
6'-CH ₃	2.20, s	9.43, CH ₃		2.21, s
1'		214.98, C		212.12, C
2'	4.05, h (6.9)	40.65, CH	4.05, h (6.7)	40.32, CH
3'	0.99 d (6.9) ^c	21.16, CH ₃	1.14, d (6.7) ^c	19.55, CH ₃
2'-CH ₃	1.16 d (6.9) ^c	17.87, CH ₃	1.15, d (6.7) ^c	20.42, CH ₃
3'-CH ₃				1.02, d (7.1)
1"	4.38 d (7.7)	105.64, CH	5.00, d (7.5)	101.60, CH
2"	3.48 dd (9.2, 7.7)	75.56, CH	3.51, dd (9.1, 7.5)	74.76, CH
3"	3.40 t (9.2)	77.67, CH	3.46, m	78.79, CH
4"	3.27 t (9.2)	72.04, CH	3.38,	71.23, CH
5"	3.10 ddd (9.2, 6.2, 2.7)	77.81, CH	3.44, m	78.37, CH
6"	3.73 dd (11.9, 2.7)	63.15, CH ₂	3.94, dd (12.0, 2.1)	62.56, CH ₂
	3.56 dd (11.9, 6.2)		3.71, dd (12.0, 5.7)	3.57, dd (11.9, 6.4)

^a Recorded at 400 MHz and reported in ppm. The coupling constants are reported in Hz; s, singlet; d, doublet; t, triplet; h, heptet; m, multiplet; ^b Recorded at 100 MHz; ^c Data in the same column are exchangeable.

**Figure 2.** ¹H-¹H COSY and HMBC correlations of compounds **1** - **3**.

Compound **2** showed similar IR and UV bands to that of compound **1**, which suggested that **2** might be an acylphloroglucinol derivative. The molecular formula of **2** was determined to be C₁₇H₂₄O₉ from the [M+Na]⁺ ion at *m/z* 395.1305 from the HRESIMS (positive ion mode). Comparison of the NMR data of compound **2** with that of compound **1** (Table 1) showed that a singlet methyl group of **1** was replaced by an aromatic proton at $\delta_{\text{H}} = 6.23$ (1H, s) to form **2**, which was consistent with the molecular formula of **2**. As shown in Figure 2, the spectroscopic data interpretation confirmed that the 6-methyl of **1** was replaced by the proton mentioned above to form **2**. Thus compound **2**, named as hypericumol B, was characterized as 4-methyl-2-methyl propanoylphloroglucinol-1-O-β-D-glucopyranoside (Figure 1).

Compound **3** had similar spectroscopic characteristics to that of compounds **1** and **2**. The molecular formula of **3**, C₁₉H₂₈O₉, was determined from the [M+Na]⁺ ion at *m/z* 423.1614 in its HRESIMS (positive ion mode). This indicated an additional CH₂ group present in the structure of **3**, relative to that of **1**. Comparison of the NMR signals of **3** with those of **1** showed that a doublet methyl of **1** was replaced by a triplet methyl at $\delta_{\text{H}} = 0.97$ (3H, t, *J* = 7.5 Hz) in **3**. A CH₂ group at $\delta_{\text{H}} = 1.90$ (1H, m) and 1.41 (1H, m) / $\delta_{\text{C}} = 25.94$ was deduced from the NMR spectroscopic data (Table 1) and it was confirmed to be adjacent to the triplet methyl group by the ¹H-¹H COSY and HMBC correlations (Figure 2). A 2-methylbutyryl group was established from a doublet methyl, a triplet methyl, a methine, a methylene, and a keto carbonyl group on the basis of detailed spectroscopic data interpretation (Figure 2). Acid hydrolysis of **3**

led to the identification of D-glucose and 4,6-dimethylmultifidol (**3a**) [11]. The absolute configuration of C-2' in **3a** was determined to be *S* by its optical rotation ([α]_D²⁰ +2.4), according to the empirical rule established by Pei *et al.* to determine the absolute configuration of 2-methylbutyrylphloroglucinols [12]. Thus, the structure of compound **3** was elucidated as (2'S)-4,6-dimethyl-2-methylbutyrylphloroglucinol-1-O-β-D-glucopyranoside. Compound **3** was a product of the acid hydrolysis of 4,6-dimethyl-1-O-[α-L-rhamnopyranosyl-(1→6)-β-D-glucopyranosyl]multifidol [13]. However, no spectroscopic data were reported and assigned to the product [13]. Here we report the compound as a naturally occurring product from the plant with detail spectroscopic data and named it as hypericumol C (**3**) (Figure 1).

The known compounds isolated from the phenolic extract were identified as 2-(2-methylpropionyl)-4-methylphloroglucinol (**4**) [14], quercetin (**5**) [15], 3-O-methylquercetin (**6**) [16], isoquercitrin (**7**) [17], quercetin-7-O-α-L-rhamnopyranoside (**8**) [18], kaempferol-7-O-α-L-rhamnopyranoside (**9**) [19], dihydroquercetin (**10**) [2c], dihydrokaempferol-7-O-α-L-rhamnopyranoside (**11**) [20], (2R,3R)-taxifolin-7-O-α-L-rhamnopyranoside (**12**) [21], *p*-hydroxybenzoic acid (**13**) [22], ethyl 3,4-dihydroxybenzoate (**14**) [23], ethyl 2,4,6-trihydroxybenzoate (**15**) [24], epicatechin (**16**) [25], saropyrone (**17**) [26], and 5,7-dihydroxy-2-(1-methylpropyl) chromone-8-β-D-glucopyranoside (**18**) [27] on the basis of spectroscopic analyses.

In summary, three new acylphloroglucinol glycosides and fifteen known phenolic natural products were isolated and identified from the phenolic extract of *H. japonicum*. Among them, quercetin (**5**), isoquercitrin (**7**), and dihydroquercetin (**10**) are the major chemical components of the extract. Quercetin (**5**) has been reported to recover renal amyloidosis and collagen deposition [28] and exhibit anti-fibrotic and kidney protection activities related to renal dysfunction [29], indicating its therapeutic potential in treating CKD. Meanwhile, oxidative stress induced by free radicals play a vital role in the progression of kidney diseases such as renal fibrosis and chronic renal failure [30], which suggested that antioxidant therapy using phenolic derivatives might be a practical strategy for CKD. The chemical investigations presented here support, in part, the potent application of the phenolic extract of *H. japonicum* in the treatment of CKD.

Experimental

General: Optical rotations were recorded on a Perkin-Elmer 341 automatic polarimeter. UV-Vis spectra were collected on a Perkin-Elmer Lambda 35 UV-Vis spectrometer with λ_{max} given in nanometers. IR spectra were recorded on a Perkin-Elmer Spectrum One spectrometer with ν_{max} given in cm⁻¹. NMR spectra were recorded on a Bruker Ascend 400 spectrometer with chemical shifts δ in ppm. HRESIMS were measured on a Bruker Bio TOF IIIQ (quadrupole time of flight) mass spectrometer and ESIMS on a Waters Xevo TQ (tandem quadrupole) mass spectrometer. Column chromatography (CC) was performed on silica gel (Qingdao Haiyang Chemical Co., Ltd., P. R. China (QHCC)), silica gel 60 (Merck, German), ODS gel (YMC Co., Ltd, Japan), or Sephadex LH-20 (GE Healthcare Bio-Sciences AB, Sweden). Thin layer chromatography (TLC) was conducted on plates precoated with 10 - 40 μm of silica gel GF254 from QHCC. Preparative HPLC separation was carried out on a LC3000 liquid chromatograph (Beijing Chuangxin Tongheng Science and Technology Co., Ltd) with a YMC C₁₈ column (20 × 250 mm; 10 μm), and semi-preparative HPLC on a Perkin-Elmer 200 liquid chromatograph with a Welch C₁₈ column (10 × 250 mm; 5 μm), and detected at 208 nm. All solvents were

commercially purchased and distilled under normal atmospheric pressure prior to use.

Extraction and isolation: The crude phenolic extract was provided by Chengdu Nanshan Pharmaceutical Co., Ltd. The crude extract was prepared, according to the following procedure. The whole plant material of *H. japonicum* was air-dried and extracted with 65% aqueous EtOH with refluxing. The filtrates were concentrated to remove EtOH under reduced pressure. The aqueous residue was subjected to CC on HPD100 macroporous resin eluted with H₂O, 30% and 80% EtOH, respectively. The eluents of 80% EtOH were collected and concentrated to afford the crude phenolic extract. This (350 g) was separated by CC over silica gel (160-200 mesh) eluted with light petroleum-acetone (2:1, 1:1, 0:1; v/v) to afford 15 sub-fractions S1 - S15. Fraction S3 (3.9 g) was subjected to preparative HPLC eluted with CH₃OH-H₂O (60:40, v/v; 15 mL/min) to give compound **14** (*t_R* = 7.6 min; 23 mg) and three sub-fractions S3B - S3D. Fraction S3B was purified with semi-preparative HPLC with CH₃CN-H₂O (31:69, v/v; 5 mL/min) as eluents to afford compound **15** (*t_R* = 30 min; 6 mg). Fraction S3D was separated by semi-preparative HPLC eluted with CH₃CN-H₂O (31:69, v/v; 5 mL/min) to afford compound **4** (*t_R* = 32 min; 70 mg). Fraction S4 was separated by preparative HPLC eluted with CH₃OH-H₂O (54:46, v/v; 20 mL/min) to give compounds **6** (*t_R* = 30 min; 60 mg) and **17** (*t_R* = 32 min; 6 mg), and four sub-fractions S4A - S4D. Fraction S4A was separated by semi-preparative HPLC eluted with CH₃OH-H₂O (38:62, v/v; 4 mL/min) to afford a sub-fraction S4A1 (*t_R* = 8 min) that was then subjected to CC on silica gel 60 (15 - 40 μm) eluted with CHCl₃-MeOH (10:1, v/v) to afford compound **13** (2 mg). Compound **5** (9.4 g) was precipitated from the light petroleum-acetone (2:1) solution of fraction S6. Compound **10** (3.8 g) was precipitated from the light petroleum-acetone (2:1) solution of fraction S7. The remaining sub-fraction of S7 was separated by CC over silica gel (160-200 mesh) with CHCl₃-MeOH (15:1, v/v) as solvent to give 4 sub-fractions S7A - S7D. Fraction S7B was subjected to preparative HPLC eluted with CH₃OH-H₂O (50:50, v/v; 15 mL/min) to afford compound **3** (*t_R* = 29 min; 63 mg) and 3 sub-fractions S7B1 - S7B3. Fraction S7B3 was separated by semi-preparative HPLC eluted with CH₃OH-H₂O (50:50, v/v; 3 mL/min) to afford subfraction S7B3C (*t_R* = 20 min) that was subjected to semi-preparative HPLC eluted with CH₃CN-H₂O (32:68, v/v; 3 mL/min) to give compounds **1** (*t_R* = 11 min; 463 mg) and **2** (*t_R* = 26 min; 6 mg). Compound **8** (88 mg) was crystallized from the methanol solution of fraction S9. Fraction S10 was separated over a self-packed ODS column using CH₃OH-H₂O (40:60, v/v) as solvent to give 4 sub-fractions S10A - S10D. Fraction S10C was subjected to semi-preparative HPLC with CH₃CN-H₂O (30:70, v/v; 4 mL/min) to afford compound **9** (*t_R* = 24 min; 26 mg) and a sub-fraction (*t_R* = 4 min) that was separated by semi-preparative HPLC with CH₃OH-H₂O (31:69, v/v; 3 mL/min) to afford compounds **11** (*t_R* = 40 min; 11 mg) and **18** (*t_R* = 44 min; 8 mg). Compound **7** (3.3

g) was precipitated from the methanol solution of fraction S15. The remaining sub-fraction of S15 was further subjected to CC over ODS eluted with CH₃OH-H₂O (28:72, v/v) to give a sub-fraction that was separated by semi-preparative HPLC with CH₃CN-H₂O (11:89, v/v; 5 mL/min) to afford compounds **16** (*t_R* = 16 min; 9 mg) and **12** (*t_R* = 24 min; 80 mg).

Hypericin A [4,6-dimethyl-2-methylpropanoylphloroglucinol-1-O-β-D-glucopyranoside] (1)

Yellowish gum.

[α]_D²⁰: +79 (*c* 0.23, MeOH).

UV (MeOH) λ_{max} (log ε): 290 (4.10), 329 (3.68) nm.

IR (KBr) ν_{max} : 3410, 2969, 2931, 2875, 1615, 1382, 1180, 1150, 1073, 1039 cm⁻¹.

¹H NMR and ¹³C NMR data: Table 1.

ESIMS (positive ion mode) *m/z*: 409.22 [M+Na]⁺, 425.12 [M+K]⁺.

ESIMS (negative ion mode) *m/z*: 385.31 [M-H]⁻, 223.19 [M-H-Glc]⁻.

HRESIMS (positive ion mode) *m/z*: 409.1480 (cacl for C₁₈H₂₆NaO₉, 409.1469, error -2.8 ppm).

Hypericin B [4-methyl-2-methyl propanoylphloroglucinol-1-O-β-D-glucopyranoside] (2)

Yellowish gum.

[α]_D²⁰: -93 (*c* 0.32, MeOH).

UV (MeOH) λ_{max} (log ε): 289 (4.00), 329 (3.49) nm.

IR (KBr) ν_{max} : 3430, 2974, 2933, 2880, 1622, 1384, 1242, 1100, 1080, 1042 cm⁻¹.

¹H NMR and ¹³C NMR data: Table 1.

ESIMS (positive ion mode) *m/z*: 395.19 [M+Na]⁺, 411.11 [M+K]⁺.

ESIMS (negative ion mode) *m/z*: 371.27 [M-H]⁻, 209.19 [M-H-Glc]⁻.

HRESIMS (positive ion mode) *m/z*: 395.1305 (cacl for C₁₇H₂₄NaO₉, 395.1313, error -1.9 ppm).

Hypericin C [(2'S)-4,6-dimethyl-2-methylbutyrylphloroglucinol-1-O-β-D-glucopyranoside] (3)

Yellowish gum.

[α]_D²⁰: +67 (*c* 0.22, MeOH).

UV (MeOH) λ_{max} (log ε): 290 (3.87), 329 (3.60) nm.

IR (KBr) ν_{max} : 3418, 2965, 2931, 2876, 1615, 1378, 1177, 1148, 1074, 1039 cm⁻¹.

¹H NMR and ¹³C NMR data: Table 1.

ESIMS (positive ion mode) *m/z*: 423.16 [M+Na]⁺, 439.09 [M+K]⁺.

ESIMS (negative ion mode) *m/z*: 399.25 [M-H]⁻, 237.18 [M-H-Glc]⁻.

HRESIMS (positive ion mode) *m/z*: 423.1614 (cacl for C₁₉H₂₈NaO₉, 423.1626, error -2.6 ppm).

Acknowledgments - We are grateful for financial support from the National New Drug Innovation Major Project of China (2011ZX09307-002-02) and the project KJF-EW-STS-026 from the Chinese Academy of Sciences.

References

- [1] Editorial committee of Flora of China, the Chinese Academy of Sciences. (1990) *Flora Reipublicae Popularis Sinicae*. Science Press, Beijing, 47.
- [2] (a) Zhang YQ, Huang MQ, Li H, Xu W, Chu KD, Zheng HY, Sha M, Chen LD. (2012) Hepatoprotective and antioxidant activity of the total flavonoids extraction from *Hypericum japonicum* by response surface methodology. *Latin American Journal of Pharmacy*, **31**, 1270-1278; (b) Samaga PV, Rai VR. (2013) Evaluation of pharmacological properties and phenolic profile of *Hypericum japonicum* Thunb. from Western Ghats of India. *Journal of Pharmacy Research*, **7**, 626-632; (c) Wang XW, Mao Y, Fan M, Ding AS, Wang NL, Yao XS. (2009) Isolation, identification and activity determination on the anti-hypoxic components of *Hypericum japonicum* Thunb. *Journal of Shenyang Pharmaceutical University*, **26**, 701-704.
- [3] (a) Zheng C, Liu M, Li J. (2014) Study on anti-HBV active ingredient of *Hypericum japonicum*. *Natural Product Research and Development*, **26**, 1350-1356; (b) Pan XJ, Yang K, Zeng JQ, Wei ZY, Chen C. (2009) Experimental study on anti-hepatitis B and anti-hepatoma effect of different extracts in serum of *Hypericum japonicum* Thunb. *in vitro*. *Lishizhen Medicine and Materia Medica Research*, **20**, 1076-1078; (c) Liu N, Hu XL, Meng YR, Zhu YT, Huang BS, Lin PZ. (2008) Effect of anti-influenza virus H3N2 of *Hypericum japonicum* *in vivo*. *Journal of Chinese Medicinal Materials*, **31**, 1022-1024.

- [4] (a) Zhang SD, Yin J, Li X, Zhang JG, Yue RC, Diao YY, Li HL, Wang H, Shan L, Zhang WD. (2014) Jacarehyperol A induced apoptosis in leukaemic cancer cell through inhibition the activity of Bcl-2 proteins. *BMC Cancer*, **14**, 689-699; (b) Liang S, Su WW, Wang YG, Peng W, Nie YC, Li PB. (2013) Effect of quercetin 7-rhamnoside on glycochenodeoxycholic acid-induced L-02 human normal liver cell apoptosis. *International Journal of Molecular Medicine*, **32**, 323-330.
- [5] (a) Li XF, Fu ZR, Wei Y, Yang T, Ouyang YZ. (2014) Research on antibacterial activity of total flavone in *Hypericum japonicum*. *Applied Chemical Industry*, **43**, 432-434; (b) Zuo GY, An J, Han J, Zhang YL, Wang GC, Hao XY, Bian ZQ. (2012) Isojacareubin from the Chinese herb *Hypericum japonicum*: potent antibacterial and synergistic effects on clinical methicillin-resistant *Staphylococcus aureus* (MRSA). *International Journal of Molecular Sciences*, **13**, 8210-8218; (c) An J, Zuo GY, Hao XY, Wang GC, Li ZS. (2011) Antibacterial and synergy of a flavanonol rhamnoside with antibiotics against clinical isolates of methicillin-resistant *Staphylococcus aureus* (MRSA). *Phytomedicine*, **18**, 990-993.
- [6] Wang N, Li PB, Wang YG, Peng W, Wu Z, Tian SY, Liang SL, Shen X, Su WW. (2008) Hepatoprotective effect of *Hypericum japonicum* extract and its fractions. *Journal of Ethnopharmacology*, **116**, 1-6.
- [7] Liu LS, Liu MH, He JY. (2014) *Hypericum japonicum* Thunb. ex Murray: phytochemistry, pharmacology, quality control and pharmacokinetics of an important herbal medicine. *Molecules*, **19**, 10733-10754.
- [8] (a) Wang Q, Mi J, Li XP, Liu JY, Bai XL. (2013) Effects of *Hypericum japonicum* total flavonoids on chronic renal failure rats induced by 5/6 nephrectomy. *Pharmacology and Clinics of Chinese Materia Medica*, **29**, 61-64; (b) Gao QL, Mei X, Yang DQ, Mi J, Liu WW, Zhao J, Zhang BC, Gao YX. (2014) The influence of herba *Hypericum japonicum* extract (MSN) on renal function and immune status of chronic renal failure model rats with five sixths kidney removal. *Asia-Pacific Traditional Medicine*, **10**, 7-9; (c) Liu WW, Gao YX, Zhao J, Tang SQ, Li XP. (2014) Research on influence of correlation genes on kidney fibrosis of 5/6 nephrectomized rats CRF model by MSN. *Pharmacy and Clinics of Chinese Materia Medica*, **5**, 28-30; (d) Zhao J, Liu WW, Yang DQ, Mei X, Li XP, Mi J, Gao YX. (2014) Study on interference of renal fibrosis by NSF in 5/6 nephrectomized rats. *Journal of Chengdu University of TCM*, **37**, 35-38.
- [9] (a) Luo YG, Zhou M, Ye Q, Pu Q, Zhang GL. (2012) Dihydroagarofuran derivatives from the dried roots of *Tripterygium wilfordii*. *Journal of Natural Products*, **75**, 98-102; (b) Luo YG, Pu X, Luo GY, Zhou M, Ye Q, Liu Y, Gu J, Qi HY, Li GY, Zhang GL. (2014) Nitrogen-containing dihydro- β -agarofuran derivatives from *Tripterygium wilfordii*. *Journal of Natural Products*, **77**, 1650-1657; (c) Luo GY, Yang Y, Zhou M, Ye Q, Liu Y, Gu J, Zhang GL, Luo YG. (2014) Novel 2-arylbenzofuran dimers and polyisoprenylated flavanones from *Sophora tonkinensis*. *Fitoterapia*, **99**, 21-27.
- [10] (a) Coskun M, Sakushima A, Nishibe S, Hisada S. (1982) Phloroglucinol derivatives of *Dryopteris abbreviata*. *Chemical and Pharmaceutical Bulletin*, **30**, 4102-4106; (b) Chang XL, Li W, Koike K, Wu LJ, Nikaido T. (2006) Phenolic constituents from the rhizomes of *Dryopteris crassirhizoma*. *Chemical and Pharmaceutical Bulletin*, **54**, 748-750.
- [11] Cheng Q, Snyder JK. (1991) Two new phloroglucinol derivatives with phosphodiesterase inhibitory activity from the leaves of *Eucalyptus robusta*. *Zeitschrift für Naturforschung B - A Journal of Chemical Sciences*, **46b**, 1275-1277.
- [12] Pei YH, Li X, Zhu TR. (1989) An empirical correlation between optical rotation and absolute configuration of optical active α -methylbutyrylphloroglucinols and its synthesis. *Acta Pharmaceutica Sinica*, **24**, 413-421.
- [13] Wang XW, Mao Y, Wang NL, Yao XS. (2008) A new phloroglucinol diglycoside derivative from *Hypericum japonicum* Thunb. *Molecules*, **13**, 2796-2803.
- [14] (a) Roelens F, Heldring N, Dhooge W, Bengtsson M, Comhaire F, Gustafsson JÅ, Treuter E, De Keukeleire D. (2006) Subtle side-chain modifications of the hop phytoestrogen 8-prenylnaringenin result in distinct agonist/antagonist activity profiles for estrogen receptors α and β . *Journal of Medicinal Chemistry*, **49**, 7357-7365; (b) Bohr G, Gerhäuser C, Knauf J, Zapp J, Becker H. (2005) Anti-inflammatory acylphloroglucinol derivatives from hops (*Humulus lupulus*). *Journal of Natural Products*, **68**, 1545-1548.
- [15] Mok SY, Lee S. (2013) Identification of flavonoids and flavonoid rhamnosides from *Rhododendron mucronulatum* for *albiflorum* and their inhibitory activities against aldose reductase. *Food Chemistry*, **136**, 969-974.
- [16] Fu P, Li TZ, Liu RH, Zhang W, Zhang C, Zhang WD, Chen HS. (2004) Studies on the flavonoids of *Hypericum japonicum* Thunb. ex Murray. *Chinese Journal of Natural Medicines*, **2**, 283-284.
- [17] Zhang J, Chu CJ, Li XJ, Yao S, Yan B, Ren HL, Xu NY, Liang ZT, Zhao ZZ. (2014) Isolation and identification of antioxidant compounds in *Vaccinium bracteatum* Thunb. by UHPLC-Q-TOF LC/MS and their kidney damage protection. *Journal of Functional Foods*, **11**, 62-70.
- [18] Wang PP, Luo J, Yang MH, Kong LY. (2013) Chemical constituents of *Lobelia chinensis*. *Chinese Traditional and Herbal Drugs*, **44**, 794-797.
- [19] Rho HS, Ahn SM, Lee BC, Kim MK, Ghimeray AK, Jin CW, Cho DH. (2010) Changes in flavonoid content and tyrosinase inhibitory activities in kenaf leaf extract after far-infrared treatment. *Bioorganic Medicinal Chemistry Letters*, **20**, 7534-7536.
- [20] (a) Cook RG, Haynes HF. (1960) Colouring matters of Australian plants VII. Flavonoid glycosides from *Exocarpus cupressiformis* Labill. *Australian Journal of Chemistry*, **13**, 150-155; (b) Wu W, Wang CZ, Li X, Li XR, Xu QM, Yang SL. (2011) Chemical constituents of antitumor active fraction of *Lysimachia clethroides*. *Chinese Traditional and Herbal Drugs*, **42**, 38-41.
- [21] Ishiguro K, Nagata S, Fukumoto H, Yamaki M, Takagi S, Isono K. (1991) A flavanonol rhamnoside from *Hypericum japonicum*. *Phytochemistry*, **30**, 3152-3153.
- [22] Zheng JX, Wang NL, Chen HF, Yao XS. (2007) Isolation and identification of phenolic constituents from *Selaginella uncinata* (Desv.) Spring. *Chinese Journal of Medicinal Chemistry*, **17**, 302-305.
- [23] Qiu YK, Dou DQ, Pei YP, Youshikawa M, Matsuda H, Chen YJ. (2005) Chemical constituents of *Opuntia dillenii*. *Journal of China Pharmaceutical University*, **36**, 213-215.
- [24] Sun ZH, Zhang CF, Zhang M. (2010) A new benzoic acid derivative from *Eclipta prostrata*. *Chinese Journal of Natural Medicines*, **8**, 244-246.
- [25] Shang XY, Li S, Wang YH, Wang SJ, Yang YC, Shi JG. (2007) Dihydroflavonol glycosides and flavan-3-ols from *Bauhinia aurea*. *China Journal of Chinese Materia Medica*, **32**, 815-818.
- [26] Ishiguro K, Nagata S, Fukumoto H, Yamaki M, Isono K, Yamagata Y. (1994) A 2-pyrone derivative from *Hypericum japonicum*. *Phytochemistry*, **37**, 283-284.
- [27] Wu QL, Wang SP, Du LJ, Zhang SM, Yang JS, Xiao PG. (1998) Chromone glycosides and flavonoids from *Hypericum japonicum*. *Phytochemistry*, **49**, 1417-1420.
- [28] Hsieh CL, Peng CC, Chen KC, Peng RY. (2013) Rutin (quercetin rutinoside) induced protein-energy malnutrition in chronic kidney disease, but quercetin acted beneficially. *Journal of Agriculture and Food Chemistry*, **61**, 7258-7267.
- [29] (a) Hu Q, Noor M, Wong YF, Hylands PJ, Simmonds MSJ, Xu Q, Jiang D, Hendry BM, Xu QH. (2009) In vitro anti-fibrotic activities of herbal compounds and herbs. *Nephrology Dialysis Transplantation*, **24**, 3033-3041; (b) Satyanarayana PSV, Singh D, Chopra S. (2001) Quercetin, a bioflavonoid, protects against oxidative stress-related renal dysfunction by cyclosporine in rats. *Methods and Findings in Experimental and Clinical Pharmacology*, **23**, 175-181.
- [30] (a) Rodrigo R, Rivera G. (2002) Renal damage mediated by oxidative stress: a hypothesis of protective effects of red wine. *Free Radical Biology and Medicine*, **33**, 409-422; (b) Qin J, Tao LJ. (2014) Progress in study on reactive oxygen species and renal fibrosis. *Journal of Clinical and Pathological Research*, **34**, 182-189.

Synthesis and Anti-Proliferative Effects of Quercetin Derivatives

Sami M.R. Al-Jabban^a, Xiaojie Zhang^a, Guanglin Chen^a, Ermias Addo Mekuria^b, Liva Harinandaina Rakotondraibe^b and Qiao-Hong Chen^{a,*}

^aDepartment of Chemistry, California State University, Fresno, 2555 E. San Ramon Ave., M/S SB70, Fresno, California 93740, USA

^bCollege of Pharmacy, Division of Medicinal Chemistry and Pharmacognosy, Ohio State University, 434 Parks Hall, 500 W 12th Ave., Columbus, OH 43210, USA

qchen@csufresno.edu

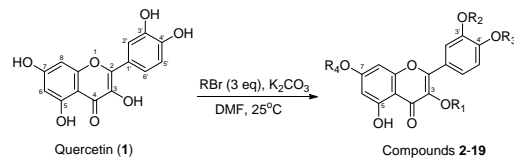
Received: June 29th, 2015; Accepted: August 12th, 2015

Prostate cancer is the most common diagnosed invasive cancer in American men and is the second leading cause of cancer-related deaths. Although there are several therapies successful in treating early, localized stage prostate cancer, current treatment of advanced metastatic castration-resistant prostate cancer remains ineffective due to inevitable progression of resistance to first-line treatment with docetaxel. The natural product quercetin (3,3',4',5,7-pentahydroxyflavone), a flavonoid compound ubiquitous in dietary plants, possesses evidenced potential in treating advanced metastatic castration-resistant prostate cancer. However, its poor bioavailability and moderate potency hinder its advancement into clinical therapy. In order to engineer quercetin derivatives with improved potency and pharmacokinetic profiles for the treatment of advanced metastatic prostate cancer, we started this study with creating a small library of alkylated derivatives of quercetin for *in vitro* evaluation. The biological data and chemical reactivity of quercetin and its derivatives reported in literature directed us to design 3,4',7-O-trialkylquercetins as our first batch of targets. Consequently, nine 3,4',7-O-trialkylquercetins, together with four 3,7-O-dialkylquercetins, four 3,3',4',7-tetraalkylquercetins, and one 3,3',4'-O-trialkylquercetin, were prepared by one step *O*-alkylation of commercially available quercetin mediated by potassium carbonate. Their structures were determined by 1D and 2D NMR data, and HRMS. Their anti-proliferative activities towards both androgen-refractory and androgen-sensitive prostate cancer cells were evaluated using WST-1 cell proliferation assay. The acquired structure-activity relationships indicate that 3,7-O-dialkylquercetins rather than 3,4',7-O-trialkylquercetins were much more potent than quercetin towards prostate cancer cells.

Keywords: Quercetin, Dietary natural product, Prostate cancer, Derivatives, Cell proliferation.

Prostate cancer, the most common diagnosed invasive cancer in American men, is the second leading cause of cancer-related deaths. Even though most patients can recover from localized androgen-sensitive prostate cancer after an appropriate therapy, the prostate cancer will unfortunately relapse in around 2-3 years after recovery from the early, androgen-sensitive stage [1]. At this point, prostate cancer is no longer responding to hormone therapy and/or has metastasized to different areas of the body. This was referred to as Hormone-Refractory Prostate Cancer or Androgen-Independent Prostate Cancer, and recently was designated as Castration-Resistant Prostate Cancer (CRPC). The US FDA did approve numerous drugs for the treatment of both androgen-dependent and castration-resistant prostate cancer. Sadly, there are no FDA-approved drugs that can actually cure advanced metastatic CRPC. The current first-line chemotherapy for CRPC, docetaxel, can barely increase survival by an average of 2.4 years [2]. The patients' inevitable progression of resistance to docetaxel makes it become an even less effective chemotherapeutic for advanced metastatic CRPC. Very recently, FDA approved cabazitaxel as a second-line treatment for the patients refractory to the first-line docetaxel chemotherapy due to the fact that cabazitaxel is the only available chemotherapeutic that can improve survival (even though by only 2.4 months) for docetaxel-resistant patients [3]. There is thus an urgent need to search for effective chemotherapeutics for clinical treatment of advanced metastatic castration-resistant prostate cancer.

Quercetin, 3,3',4',5,7-pentahydroxyflavone (**1** in Scheme 1), is a flavonoid compound ubiquitous in plant food sources [4]. Quercetin was capable of inhibiting cell growth in the mouse prostate cancer cell line TRAMP-C2 with an IC₅₀ of 20 μM [5-6]. Numerous studies demonstrated that quercetin was also capable of suppressing



Scheme 1: Synthesis of alkylated derivatives of quercetin.

Table 1: Alkyl groups for compounds 2-19.

Comps	R ₁	R ₂	R ₃	R ₄
2	Methyl	H	H	Methyl
3	Methyl	H	Methyl	Methyl
4	Methyl	Methyl	Methyl	Methyl
5	Ethyl	H	H	Ethyl
6	Ethyl	H	Ethyl	Ethyl
7	Ethyl	Ethyl	Ethyl	Ethyl
8	Ethyl	Ethyl	Ethyl	H
9	Propyl	H	H	Propyl
10	Propyl	H	Propyl	Propyl
11	Butyl	H	H	Butyl
12	Butyl	H	Butyl	Butyl
13	Butyl	Butyl	Butyl	Butyl
14	Pentyl	H	Pentyl	Pentyl
15	Hexyl	H	Hexyl	Hexyl
16	Isopropyl	H	Isopropyl	Isopropyl
17	Isopentyl	H	Isopentyl	Isopentyl
18	Benzyl	H	Benzyl	Benzyl
19	Benzyl	Benzyl	Benzyl	Benzyl

the growth of both androgen-sensitive (LNCaP) and androgen-refractory human prostate cancer cell lines (PC-3 and DU145) and that quercetin has no apparent toxicity against normal prostate epithelial cells [7-8]. Maggiolini and co-workers first demonstrated that quercetin functioned as agonists for the mutant androgen receptor (AR) T877A so that it could inhibit the proliferation of LNCaP cells at low concentration. However, high concentration of quercetin may independently cause significant cytotoxicity without involving hormone receptor expression [9].

Wang *et al.* reported that quercetin exhibited potential *in vivo* anti-prostate tumor efficacy in an androgen-sensitive LAPC-4 xenograft prostate tumor mouse model using severe combined immunodeficiency (SCID) mice. It inhibited tumor growth by 3% when 0.2% was administered as a supplement in diet and by 15% when 0.4% was taken [10]. Quercetin can also significantly reduce PC-3 tumor volume and weight in 6-week old BALB/cA nude mice. The average weight of prostate tumors decreased from 0.242 g for the control group to 0.099 g for the quercetin treated group, implying the *in vivo* anti-prostate tumor potential of quercetin [11]. The above-described cell-based and animal-based studies have evidenced that quercetin could be a good candidate for prostate cancer treatment. However, its poor bioavailability and moderate potency hinder its advancement into clinical therapy. In order to engineer quercetin derivatives with improved potency and a better pharmacokinetic profile for the treatment of advanced metastatic prostate cancer, we started this project by creating a small panel of alkylated derivatives of quercetin for *in vitro* evaluation. The structure-activity relationships will be used to direct our further structure modulation.

The structure-cytotoxicity relationships of methylquercetins summarized by Beutler *et al.* [12] showed that 3,4',7-trimethylquercetin possessed better cytotoxicity than quercetin and other methylquercetins. Intriguingly, Rao *et al.* [13] summarized that methylation of the five phenolic hydroxyl groups in quercetin occurred gradually with the following sequential positions order: 4'

$> 7 > 3 > 3' > 5$. The superposition of cytotoxic potency and chemical reactivity of quercetin derivatives directed us to synthesize a group of new 3,4',7-O-trialkylquercetins as our first batch of targets. Different alkyl groups were introduced to investigate the effect of their length and steric hindrance on the cell proliferation. The targets were proposed to be achieved by one-step alkylation of quercetin.

As shown in Scheme 1, we planned to synthesize our expected 3,4',7-O-trialkylquercetins by treating one equivalent of quercetin with three equivalents of alkyl halide using DMF as solvent and potassium carbonate as base. Reaction of quercetin with the appropriate alkyl halide did provide us with the expected 3,4',7-O-trialkylquercetins as the major products, but in moderate yields (less than 25%). Assignments of three alkyl groups were based on the key HMBC correlations between CH₂ protons of ethyl groups (δ 4.10, 4.10, and 4.22) and C-3, C-7, and C-4' in derivative **6** as summarized in Figure 1. Four 3,7-O-dialkylquercetins, four 3,3',4',7-O-tetraalkylquercetins, and one 3,3',4'-O-trialkylquercetin were also collected for structure-activity relationship studies. Similarly, the locations of the alkyl groups in 3,7-O-dibutylquercetin (**11**) and in 3,3',4'-O-triethylquercetin (**8**) were also confirmed by the existence of key correlations in their HMBC spectra (Figure 1). As shown in Table 2, all signals in the ¹H- and ¹³C-NMR spectra for compounds **6**, **8**, and **11** have been fully assigned based on the extensive interpretation of their COSY, HMQC, and HMBC data.

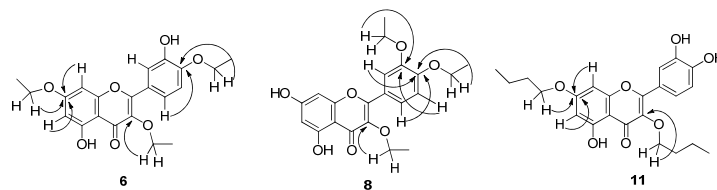


Figure 1: Key HMBC correlations in compounds **6**, **8**, and **11**.

Table 2: NMR data for derivatives **6**, **8**, and **11** (¹H NMR: 300 MHz; ¹³C NMR: 75 MHz).

Position	6 (CDCl ₃)		8 (acetone-d ₆)		11 (acetone-d ₆)	
	δ_c , type	δ_h , J in Hz	δ_c , type	δ_h , J in Hz	δ_c , type	δ_h , J in Hz
2	156.5, C		155.7, C		156.3, C	
3	138.7, C		137.5, C		137.7, C	
4	179.6, C		178.7, C		178.8, C	
4a	106.6, C		104.9, C		105.6 C	
5	162.6, C		162.3, C		162.0, C	
6	98.8, CH	6.33, d (1.8)	98.6, CH	6.26, s	97.9, CH	6.30, d (2.1)
7	165.4, C		164.3, C		165.1, C	
8	93.1, CH	6.42, d (1.8)	93.7, CH	6.51, s	92.2, CH	6.62, d (2.1)
8a	157.4, C		157.8, C		156.8, C	
1'	124.3, C		123.0, C		122.3, C	
2'	115.1, CH	7.72, br.s	113.8, CH	7.79, d (1.8)	115.7, CH	7.74, d (2.1)
3'	146.1, C		148.4, C		144.9, C	
4'	148.6, C		151.4, C		148.1, C	
5'	111.6, CH	6.94, d (9.3)	112.6, CH	7.12, d (8.4)	115.2 CH	7.00, d (8.4)
6'	122.2, CH	7.73, dd (9.3, 1.8)	122.2, CH	7.74, dd (8.4, 1.8)	121.4, CH	7.61, dd (8.4, 2.1)
3-O-CH ₂	64.8, CH ₂	4.10, q (6.9)	67.9, CH ₂	4.14, overlapped	-	-
CH ₃	15.2, CH ₃	1.45, t (6.9)	14.3, CH ₃	1.32, t (6.9)	-	-
7-O-CH ₂	65.3, CH ₂	4.10, q (6.9)	-	-	-	-
CH ₃	15.4, CH ₃	1.51, t (6.9)	-	-	-	-
7-O-CH ₂	-	-	-	-	68.3, CH ₂	4.14, t (6.6)
CH ₂	-	-	-	-	30.9, CH ₂	1.85-1.67, m
CH ₂	-	-	-	-	18.9, CH ₂	1.56-1.42, m
CH ₃	-	-	-	-	13.15 CH ₃	0.92, t (7.2)
3'-O-CH ₂	-	-	64.1, CH ₂	4.17, overlapped	-	-
CH ₃	-	-	14.2, CH ₃	1.43, t (6.9)	-	-
4'-O-CH ₂	69.2, CH ₂	4.22, q (6.9)	64.4, CH ₂	4.18, overlapped	-	-
CH ₃	16.2, CH ₃	1.36, t (6.9)	14.3, CH ₃	1.43, t (6.9)	-	-
3-O-CH ₂	-	-	-	-	71.9, CH ₂	4.05, t (6.6)
CH ₂	-	-	-	-	31.9, CH ₂	1.85-1.67, m
CH ₂	-	-	-	-	18.9, CH ₂	1.56-1.42, m
CH ₃	-	-	-	-	13.19 CH ₃	0.99, t (7.2)
3'-OH	-	5.81, s	-	-	-	-
5-OH	OH	12.68, s	-	12.81, s	8.50, brs	12.80, s
4'-OH	-	-	-	-	8.50, brs	8.50, brs

Among the eighteen quercetin derivatives that we prepared, five of them (**8, 14-17**) are new compounds. Derivatives **2-7, 9-13**, and **18-19** are known, but there are no reports available on their anti-proliferative activity against prostate cancer cell lines, even though their *in vitro* effects have been investigated on other cancer cell models [12, 14]. It should be pointed out that the 4',7-dialkylquercetins reported in Ref. [14] should be corrected as 3,7-dialkylquercetins based on our HMBC data of **11** (Figure 1).

The anti-proliferative effect of eighteen synthetic quercetin derivatives (at 50 μ M) was evaluated against both androgen-sensitive (LNCaP) and androgen-refractory (DU145 and PC-3) human prostate cancer cell lines. WST-1 cell proliferation assay was selected for this evaluation because of its easy operation in a microtiter plate without washing steps. The procedure is described in the Experimental Section and the absorbance was measured using a microplate reader (Synergy HT) at a wavelength of 430 nm. As shown in Table 3, alkylation of the hydroxyl groups at C-3, C-4', and C-7 in quercetin with short, linear alkyl groups (such as methyl groups in **3** and ethyl groups in **6**) slightly increases the anti-proliferative activity towards three human prostate cancer cell lines. However, potency was rapidly diminished when either branched alkyl groups (isopropyl in **16** and isopentyl in **17**) or linear lengthy groups (propyl in **10**, butyl in **12**, pentyl in **14**, and hexyl in **15**) were introduced into these three positions. Incorporation of ethyl groups to 3,3',4'-hydroxyl groups in quercetin (**8**) led to neither gain nor loss in its inhibitory rate. Surprisingly, all four 3,7-O-dialkylquercetins (**2, 5, 9**, and **11**) exhibited significantly higher inhibitory rate than quercetin against the three prostate cancer cell lines at both concentrations. They were over 2-11 times more potent than quercetin in the cell culture based on the comparison of their IC₅₀ values with that of quercetin (Table 3).

Table 3: Anti-proliferative activity of quercetin and its derivatives towards three cancer cell lines.

Compds	Inhibitory rate (%) @ 50 μ M			IC ₅₀ (μ M)		
	PC-3	DU145	LNCaP	PC-3	DU145	LNCaP
Quercetin	8	13	44	>100	>100	45.46 ± 1.31
2	64	40	80	22.27 ± 6.83	46.82 ± 3.69	13.23 ± 4.75
3	66	36	77	—	—	—
4	10	25	39	—	—	—
5	79	80	91	13.74 ± 1.62	12.59 ± 0.96	4.20 ± 0.96
6	25	32	50	—	—	—
7	0	16	9	—	—	—
8	6	8	48	—	—	—
9	95	91	96	17.68 ± 0.96	19.25 ± 2.21	6.42 ± 2.72
10	41	29	50	—	—	—
11	97	97	97	11.95 ± 1.12	18.63 ± 6.86	6.46 ± 1.10
12	0	0	0	—	—	—
13	0	0	0	—	—	—
14	0	19	7	—	—	—
15	0	5	0	—	—	—
16	25	30	40	—	—	—
17	3	13	0	—	—	—
18	0	19	11	—	—	—
19	0	3	16	—	—	—

Each experiment was performed at least thrice in duplicate.

In conclusion, eighteen alkylated derivatives of quercetin were prepared by a semi-synthesized approach. Their anti-proliferative activity was evaluated against three human prostate cancer cell lines using WST-1 cell proliferation assay. The structure-activity relationships acquired show i) that simultaneous introduction of three bulky or lengthy alkyl groups to C-3, C-4' and C-7 hydroxyl groups of quercetin led to a major loss of anti-proliferative activity in prostate cancer cells; and ii) that incorporation of two methyl groups in **2**, two ethyl groups in **5**, two propyl groups in **9**, and two butyl groups in **11** to C-3 and C-7 hydroxyl groups resulted in much more potent derivatives. Chemical manipulation of one phenolic hydroxyl group might be the best direction for the future.

Experimental

General: NMR spectra were obtained on a Bruker Fourier 300 spectrometer in CDCl₃ and CD₃COCD₃. The chemical shifts are given in δ (ppm) referenced to the respective solvent peak, and coupling constants are reported in Hz. All reagents and solvents were purchased from commercial sources and were used without further purification. Column chromatography was performed using silica gel (32-63 μ m). Preparative thin-layer chromatography (PTLC) separations were carried out on 1000 μ m AnalTech thin layer chromatography plates (Lot No.13401).

General procedure for the synthesis of alkylated quercetin derivatives: To a solution of quercetin hydrate (1.0 equiv.) in DMF was added anhydrous K₂CO₃ (3 equiv.), followed by the appropriate alkyl halide (3.0 equiv.). The reaction mixture was allowed to stir at room temperature for 12 to 48 h prior to being diluted with diethyl ether and ethyl acetate (300 mL in total, 1:1, v/v). The consequent mixture was rinsed with brine (30 mL × 5), and the organic layer was dried over anhydrous MgSO₄, filtered and concentrated *in vacuo* to give the corresponding crude product.

Preparation of methylated derivatives of quercetin (2, 3, and 4): These derivatives were prepared according to the general procedure from quercetin hydrate (320 mg, 1 mmol) in DMF (1 mL). PTLC purification of crude product, using 30% ethyl acetate in hexane as eluent, yielded compounds **2** (24 mg, 7% yield), **3** (83 mg, 24% yield), and **4** (21 mg, 6% yield).

3,7-O-Dimethylquercetin (2)

MP: 180-183°C.

IR (neat): 3244, 2923, 2852, 1653, 1605, 1559, 1506, 1456 cm⁻¹.

¹H NMR (300 MHz, CD₃COCD₃): 12.77 (s, 1H), 7.73 (d, J = 2.1 Hz, 1H), 7.61 (dd, J = 8.4, 2.1 Hz, 1H), 7.00 (d, J = 8.4 Hz, 1H), 6.64 (d, J = 2.4 Hz, 1H), 6.31 (d, J = 2.4 Hz, 1H), 3.93 (s, 3H), 3.88 (s, 3H).

¹³C NMR (75 MHz, CDCl₃): 178.7, 165.7, 161.9, 156.8, 156.1, 148.3, 145.0, 138.6, 122.1, 121.3, 115.5, 115.4, 105.7, 97.6, 91.9, 59.5, 55.5.

3,4',7-O-Trimethylquercetin (3)

MP: 151-153°C.

IR (neat): 3396, 2929, 1652, 1592, 1494 cm⁻¹.

¹H NMR (300 MHz, CDCl₃): 12.64 (s, 1H), 7.73 (dd, J = 8.7, 2.1 Hz, 1H), 7.70 (d, J = 2.1 Hz, 1H), 6.98 (d, J = 8.7 Hz, 1H), 6.46 (d, J = 2.1 Hz, 1H), 6.37 (d, J = 2.1 Hz, 1H), 5.73 (s, 1H), 4.00 (s, 3H), 3.89 (s, 6H).

¹³C NMR (75 MHz, CDCl₃): 179.5, 166.1, 162.6, 157.4, 156.2, 149.4, 146.2, 139.8, 124.3, 122.2, 115.0, 111.0, 106.7, 98.5, 92.8, 60.8, 56.7, 56.4.

3,3',4',7-O-Tetramethylquercetin (4)

MP: 136-137°C.

IR (KBr): 3580, 2933, 2839, 1652, 1589, 1496 cm⁻¹.

¹H NMR (300 MHz, CDCl₃): 12.64 (s, 1H), 7.73 (dd, J = 8.7, 1.8 Hz, 1H), 7.70 (s, 1H), 7.00 (d, J = 8.7 Hz, 1H), 6.45 (d, J = 1.8 Hz, 1H), 6.36 (d, J = 1.8 Hz, 1H), 3.98 (s, 6H), 3.88 (s, 3H), 3.87 (s, 3H).

¹³C NMR (75 MHz, CDCl₃): 179.4, 166.1, 162.7, 157.4, 156.5, 152.0, 149.4, 139.6, 123.6, 122.8, 111.9, 111.5, 106.7, 98.5, 92.9, 60.8, 56.7, 56.6, 56.5.

Preparation of ethylated quercetin derivatives (5, 6, 7, and 8): These derivatives were synthesized from quercetin hydrate (640 mg, 2 mmol) in DMF (2 mL). The crude product was purified through a

pad of silica gel, eluting with 33% ethyl acetate in hexanes, followed by repetitive PTLC, eluting with 33% ethyl acetate in hexanes and 5% methanol in DCM in hexane, to yield compounds **5** (56 mg, 8% yield), **6** (137 mg, 18% yield), **7** (57 mg, 7% yield), and **8** (15 mg, 2% yield).

3,7-O-Diethylquercetin (5)

MP: 155-156°C.

IR (KBr): 3210, 2980, 2929, 1654, 1590, 1496, 1339, 1206 cm⁻¹.

¹H NMR (300 MHz, CD₃COCD₃): 12.76 (s, 1H), 8.50 (br.s, 2H), 7.76 (d, *J* = 2.1 Hz, 1H), 7.68 (dd, *J* = 8.4, 2.1 Hz, 1H), 7.00 (d, *J* = 8.4 Hz, 1H), 6.55 (d, *J* = 2.1 Hz, 1H), 6.24 (d, *J* = 2.1 Hz, 1H), 4.15 (q, *J* = 6.9 Hz, 2H), 4.11 (q, *J* = 6.9 Hz, 2H), 1.40 (t, *J* = 6.9 Hz, 3H), 1.32 (t, *J* = 6.9 Hz, 3H).

¹³C NMR (75 MHz, CD₃COCD₃): 181.4, 167.5, 164.5, 159.4, 158.8, 150.7, 147.5, 140.1, 124.9, 124.0, 118.2, 117.9, 108.1, 100.5, 94.8, 70.4, 66.7, 17.5, 16.6.

3,4',7-O-Triethylquercetin (6)

MP: 123-124°C.

IR (neat): 3397, 2980, 2931, 2887, 1654, 1592, 1497 cm⁻¹.

¹H and ¹³C NMR: see Table 3.

HRMS-FAB: *m/z* [M + H]⁺ calcd for C₂₁H₂₃O₇: 387.1444; found: 387.1397; [M + Na]⁺ calcd for C₂₁H₂₂O₇Na: 409.1258; found: 409.1261.

3,3',4',7-O-Tetraethylquercetin (7)

MP: 121-122°C.

IR (neat): 2981, 2932, 1654, 1589, 1497 cm⁻¹.

¹H NMR (300 MHz, CDCl₃): 12.67 (s, 1H), 7.74 (d, *J* = 1.8 Hz, 1H), 7.71 (dd, *J* = 8.7, 1.8 Hz, 1H), 6.96 (d, *J* = 8.7 Hz, 1H), 6.40 (d, *J* = 2.1 Hz, 1H), 6.31 (d, *J* = 2.1 Hz, 1H), 4.18 (q, *J* = 6.9 Hz, 2H), 4.16 (q, *J* = 6.9 Hz, 2H), 4.08 (q, *J* = 6.9 Hz, 2H), 4.06 (q, *J* = 6.9 Hz, 2H), 1.500 (t, *J* = 6.9 Hz, 3H), 1.498 (t, *J* = 6.9 Hz, 3H), 1.44 (t, *J* = 6.9 Hz, 3H), 1.33 (t, *J* = 6.9 Hz, 3H).

¹³C NMR (75 MHz, CDCl₃): 180.8, 166.7, 163.9, 158.6, 158.1, 153.0, 150.0, 139.8, 124.9, 124.0, 115.5, 114.1, 107.8, 100.0, 94.4, 70.4, 66.7, 66.4, 66.1, 17.6, 16.7, 16.6, 16.5.

3,3',4'-O-Triethylquercetin (8)

MP: 170-172°C.

IR (neat): 3210, 3084, 2978, 2925, 1649, 1600, 1576, 1499, 1170 cm⁻¹.

¹H and ¹³C NMR: see Table 3.

Preparation of propylated derivatives of quercetin (9 and 10): These derivatives were synthesized from quercetin hydrate (200 mg, 0.59 mmol) in DMF (0.6 mL). The crude product was purified through a pad of silica gel, eluting with 33% ethyl acetate in hexanes, followed by repetitive PTLC, eluting with 33% ethyl acetate in hexanes, to yield compounds **9** (9 mg, 4% yield) and **10** (9 mg, 3.6 % yield).

3,7-O-Dipropylquercetin (9)

MP: 143-144°C.

IR (neat): 3352, 2965, 2878, 1654, 1590, 1496, 1205 cm⁻¹.

¹H NMR (300 MHz, CD₃COCD₃): 12.80 (s, 1H), 7.74 (d, *J* = 2.1 Hz, 1H), 7.61 (dd, *J* = 8.4, 2.1 Hz, 1H), 7.00 (d, *J* = 8.4 Hz, 1H), 6.62 (d, *J* = 2.1 Hz, 1H), 6.30 (d, *J* = 2.1 Hz, 1H), 4.09 (t, *J* = 6.6 Hz, 2H), 4.00 (t, *J* = 6.6 Hz, 2H), 1.84-1.71 (m, 4H), 1.05 (t, *J* = 7.2 Hz, 3H), 0.97 (t, *J* = 7.2 Hz, 3H).

¹³C NMR (75 MHz, CD₃COCD₃): 178.8, 165.1, 162.0, 156.8, 156.3, 148.2, 145.0, 137.7, 122.3, 121.4, 115.7, 115.2, 105.6, 97.9, 92.3, 73.8, 70.0, 23.1, 22.1, 9.9, 9.7.

3,4',7-O-Tripropylquercetin (10)

MP: 80-81°C.

IR (neat): 3320, 2965, 2877, 1654, 1597, 1497, 1207 cm⁻¹.

¹H NMR (300 MHz, CDCl₃): 12.69 (s, 1H), 7.73 (dd, *J* = 8.4, 2.1 Hz, 1H), 7.72 (s, 1H), 6.95 (d, *J* = 8.7 Hz, 1H), 6.45 (d, *J* = 2.1 Hz, 1H), 6.42 (d, *J* = 2.1 Hz, 1H), 5.73 (s, 1H), 4.12 (t, *J* = 6.6 Hz, 2H), 4.00 (t, *J* = 6.6 Hz, 2H), 3.98 (t, *J* = 6.6 Hz, 2H), 1.98-1.72 (m, 6H), 1.10 (t, *J* = 7.5 Hz, 3H), 1.07 (t, *J* = 7.5 Hz, 3H), 0.98 (t, *J* = 7.5 Hz, 3H).

¹³C NMR (75 MHz, CDCl₃): 179.0, 165.0, 161.9, 156.8, 155.7, 148.1, 145.5, 138.3, 123.7, 121.7, 114.5, 110.9, 106.0, 98.2, 92.5, 74.5, 70.5, 70.1, 23.4, 22.5, 22.3, 10.5, 10.43, 10.41.

Preparation of butylated derivatives of quercetin (11, 12, and 13):

These derivatives were synthesized from quercetin hydrate (426 mg, 1.26 mmol) in DMF (1.3 mL). The crude product was purified through a pad of silica gel, eluting with 33% ethyl acetate in hexanes, followed by repetitive PTLC, eluting with 33% ethyl acetate in hexanes, to yield compounds **11** (22 mg, 4% yield), **12** (42 mg, 7% yield), and **13** (16 mg, 2.4% yield).

3,7-O-Dibutylquercetin (11)

MP: 158-159°C.

IR (KBr): 3210, 2958, 2931, 2873, 1656, 1586, 1492, 1169 cm⁻¹.

¹H and ¹³C NMR: see Table 3.

3,4',7-O-Tributylquercetin (12)

MP: 66-68°C.

IR (neat): 3431, 2958, 2933, 2872, 1655, 1597, 1497, 1206 cm⁻¹.

¹H NMR (300 MHz, CDCl₃): 12.69 (s, 1H), 7.71 (d, *J* = 9.3 Hz, 1H), 7.69 (s, 1H), 6.93 (d, *J* = 9.3 Hz, 1H), 6.42 (d, *J* = 1.8 Hz, 1H), 6.32 (d, *J* = 2.1 Hz, 1H), 5.81 (br.s, 1H), 4.14 (t, *J* = 6.6 Hz, 2H), 4.02 (t, *J* = 6.6 Hz, 2H), 4.00 (t, *J* = 6.6 Hz, 2H), 1.91-1.69 (m, 6H), 1.60-1.38 (m, 6H), 1.02 (t, *J* = 7.2 Hz, 3H), 1.00 (t, *J* = 7.2 Hz, 3H), 0.93 (t, *J* = 7.2 Hz, 3H).

¹³C NMR (75 MHz, CDCl₃): 178.9, 165.0, 161.9, 156.8, 155.8, 148.1, 145.5, 138.3, 123.6, 121.6, 114.5, 110.9, 105.9, 98.2, 92.4, 72.6, 68.8, 68.4, 32.1, 31.1, 31.0, 19.21, 19.16, 19.12, 13.84, 13.83, 13.79.

3,3',4',7-O-Tetrabutylquercetin (13)

MP: 59-60°C.

IR (neat): 2957, 2933, 2873, 1661, 1589, 1500 cm⁻¹.

¹H NMR (300 MHz, CDCl₃): 12.71 (s, 1H), 7.73 (d, *J* = 2.1 Hz, 1H), 7.69 (dd, *J* = 8.4, 2.1 Hz, 1H), 6.98 (d, *J* = 8.4 Hz, 1H), 6.44 (d, *J* = 2.1 Hz, 1H), 6.35 (d, *J* = 2.1 Hz, 1H), 4.11 (t, *J* = 6.6 Hz, 2H), 4.09 (t, *J* = 6.6 Hz, 2H), 4.04 (t, *J* = 6.6 Hz, 2H), 4.00 (t, *J* = 6.6 Hz, 2H), 1.92-1.68 (m, 8H), 1.63-1.40 (m, 8H), 1.02 (t, *J* = 7.2 Hz, 6H), 1.00 (t, *J* = 7.2 Hz, 3H), 0.92 (t, *J* = 7.2 Hz, 3H).

¹³C NMR (75 MHz, CDCl₃): 178.9, 164.9, 162.0, 156.8, 156.2, 151.6, 148.5, 130.3, 123.0, 122.2, 114.1, 112.5, 105.9, 98.1, 92.6, 72.8, 69.2, 68.7, 68.4, 32.3, 31.3, 31.2, 31.0, 19.24, 19.17, 19.15, 13.89, 13.85, 13.79.

Preparation of 3,4',7-O-tripentylquercetin (14): This derivative was synthesized from quercetin hydrate (200 mg, 0.59 mmol) in DMF (10 mL). The crude product was subjected to PTLC purification eluting with 15% ethyl acetate in hexanes to yield compound **14** (19 mg, 7% yield).

3,4',7-O-Tripentylquercetin (14)

MP: 55-56°C.

IR (KBr): 3540, 2956, 2871, 1654, 1593, 1496 cm⁻¹.

¹H NMR (300 MHz, CDCl₃): 12.69 (s, 1H), 7.71 (dd, *J* = 9.3, 2.1 Hz, 1H), 7.70 (d, *J* = 2.1 Hz, 1H), 6.94 (d, *J* = 9.3 Hz, 1H), 6.43 (d, *J* = 2.1 Hz, 1H), 6.33 (d, *J* = 2.1 Hz, 1H), 5.77 (s, 1H), 4.14 (t, *J* = 6.6 Hz, 2H), 4.02 (t, *J* = 6.6 Hz, 2H), 4.00 (t, *J* = 6.6 Hz, 2H), 1.91–1.73 (m, 6H), 1.51 – 1.31 (m, 12H), 0.99–0.93 (overlapped, 6H), 0.90 (t, *J* = 6.6 Hz, 3H).

¹³C NMR (75 MHz, CDCl₃): 179.0, 165.0, 161.9, 156.8, 155.8, 148.1, 145.5, 138.3, 123.6, 121.6, 114.5, 110.9, 105.9, 98.2, 92.5, 73.0, 69.1, 68.7, 29.8, 28.8, 28.7, 28.12, 28.08, 28.06, 22.45, 22.43, 22.40, 13.4.

Preparation of 3,4',7-O-trihexylquercetin (15): This derivative was synthesized from quercetin hydrate (200 mg, 0.59 mmol) in DMF (10 mL). The crude product was subjected to PTLC purification eluting with 15% ethyl acetate in hexanes to yield compound **15** (20 mg, 6% yield).

3,4',7-O-Trihexylquercetin (15)

MP: 48–50°C.

IR (KBr): 3550, 2954, 2929, 2858, 1654, 1595, 1497 cm⁻¹.

¹H NMR (300 MHz, CDCl₃): 12.67 (s, 1H), 7.69 (d, *J* = 7.5 Hz, 1H), 7.68 (s, 1H), 6.93 (d, *J* = 7.5 Hz, 1H), 6.42 (d, *J* = 2.1 Hz, 1H), 6.32 (d, *J* = 2.1 Hz, 1H), 5.73 (s, 1H), 4.12 (t, *J* = 6.6 Hz, 2H), 4.01 (t, *J* = 6.6 Hz, 2H), 3.99 (t, *J* = 6.6 Hz, 2H), 1.89 – 1.70 (m, 6H), 1.42 – 1.20 (m, 18H), 0.81–0.98 (m, 9H).

¹³C NMR (75 MHz, CDCl₃): 179.1, 165.1, 162.1, 156.9, 156.0, 148.2, 145.6, 138.4, 123.8, 121.8, 114.6, 111.0, 106.1, 98.4, 92.6, 73.2, 69.2, 68.8, 31.74, 31.65, 30.2, 29.2, 29.1, 25.7, 22.7, 14.2.

HRMS-FAB: *m/z* [M + Na]⁺ calcd for C₃₃H₄₆O₇Na: 577.3136; found: 577.3127.

Preparation of 3,4',7-O-triisopropylquercetin (16): This derivative was synthesized from quercetin hydrate (200 mg, 0.59 mmol) in DMF (10 mL). PTLC purification of the crude product eluting with 15% ethyl acetate in hexanes generated compound **16** (18 mg, 7% yield).

3,4',7-O-Triisopropylquercetin (16)

MP: 62–64°C.

IR (KBr): 3428, 2976, 2932, 1652, 1589, 1492 cm⁻¹.

¹H NMR (300 MHz, CDCl₃): 12.73 (s, 1H), 6.76 (d, *J* = 8.6 Hz, 1H), 7.74 (s, 1H), 6.95 (d, *J* = 8.6 Hz, 1H), 6.42 (s, 1H), 6.33 (s, 1H), 5.78 (s, 1H), 4.79–4.69 (m, 1H), 4.69–4.54 (m, 2H), 1.45 (d, *J* = 7.0 Hz, 6H), 1.40 (d, *J* = 7.0 Hz, 6H), 1.23 (d, *J* = 7.0 Hz, 6H).

¹³C NMR (75 MHz, CDCl₃): 179.4, 164.0, 162.1, 157.0, 156.5, 146.8, 146.1, 136.9, 124.0, 122.1, 115.0, 112.1, 105.8, 99.0, 93.4, 75.3, 71.8, 70.8, 22.5, 22.2, 22.0.

HRMS-FAB: *m/z* [M + Na]⁺ calcd for C₂₄H₂₈O₇Na: 451.1733; found: 451.1727.

Preparation of 3,4',7-O-triisopentylquercetin (17): This derivative was synthesized from quercetin hydrate (200 mg, 0.59 mmol) in DMF (10 mL). The crude product was purified by repetitive PTLC eluting with 15% ethyl acetate in hexanes to yield compound **17** (24 mg, 8% yield).

3,4',7-O-Triisopentylquercetin (17)

MP: 75–76°C.

IR (KBr): 3540, 3054, 2957, 2871, 1653, 1594, 1464 cm⁻¹.

¹H NMR (300 MHz, CDCl₃): 12.67 (s, 1H), 7.69 (d, *J* = 8.6 Hz, 1H), 7.68 (s, 1H), 6.93 (d, *J* = 8.6 Hz, 1H), 6.42 (d, *J* = 2.4 Hz, 1H), 6.33 (d, *J* = 2.4 Hz, 1H), 5.72 (s, 1H), 4.15 (t, *J* = 6.4 Hz, 2H), 4.05 (t, *J* = 6.4 Hz, 2H), 4.02 (t, *J* = 6.4 Hz, 2H), 1.88 – 1.79 (m, 3H), 1.78 – 1.75 (m, 2H), 1.72 – 1.68 (m, 2H), 1.65 – 1.62 (m, 2H),

1.00 (d, *J* = 6.8 Hz, 6H), 0.97 (d, *J* = 6.8 Hz, 6H), 0.90 (d, *J* = 6.8 Hz, 6H).

¹³C NMR (75 MHz, CDCl₃): 179.1, 165.0, 162.0, 156.9, 155.9, 148.2, 145.6, 138.5, 123.7, 121.8, 114.6, 111.0, 106.1, 98.3, 92.6, 71.6, 67.6, 67.2, 39.0, 37.9, 37.7, 25.2, 25.1, 25.0, 22.7.

HRMS-FAB: *m/z* [M + Na]⁺ calcd for C₃₀H₄₀O₇Na: 535.2666; found: 535.2678.

Preparation of benzylated derivatives of quercetin (18 and 19): These two derivatives were synthesized from quercetin hydrate (200 mg, 0.59 mmol) in DMF (10 mL). PTLC purification of the crude product, using 15% ethyl acetate in hexanes as eluent, generated **18** (73 mg, 22% yield) and **19** (58 mg, 15% yield).

3,4',7-O-Tribenzylquercetin (18)

MP: 147–148°C.

IR (KBr): 3651, 3089, 3064, 3032, 2926, 2870, 1653, 1592, 1494 cm⁻¹.

¹H NMR (300 MHz, CDCl₃): 12.74 (s, 1H), 7.66 (s, 1H), 7.65 (d, *J* = 8.4 Hz, 1H), 7.45–7.28 (m, 15H), 6.96 (d, *J* = 8.4 Hz, 1H), 6.51 (s, 1H), 6.46 (s, 1H), 5.88 (s, 1H), 5.20 (s, 2H), 5.14 (s, 2H), 5.10 (s, 2H).

¹³C NMR (75 MHz, CDCl₃): 178.8, 164.5, 162.0, 156.7, 156.3, 148.0, 145.7, 137.7, 136.5, 135.9, 135.8, 128.94, 128.89, 128.75, 128.65, 128.4, 128.3, 128.2, 127.9, 127.5, 123.9, 121.9, 115.0, 111.6, 106.2, 98.7, 93.0, 74.3, 71.1, 70.5.

3,3',4',7-O-Tetrabenzylquercetin (19)

MP: 135–136°C.

IR (KBr): 3034, 2930, 1654, 1595, 1495 cm⁻¹.

¹H NMR (300 MHz, CDCl₃): 12.70 (s, 1H), 7.71 (d, *J* = 2.0 Hz, 1H), 7.55 (dd, *J* = 8.6, 2.0 Hz, 1H), 7.48–7.22 (m, 20H), 6.96 (d, *J* = 8.6 Hz, 1H), 6.46 (d, *J* = 2.0 Hz, 1H), 6.44 (d, *J* = 2.0 Hz, 1H), 5.25 (s, 2H), 5.13 (s, 2H), 5.04 (s, 2H), 4.99 (s, 2H).

¹³C NMR (75 MHz, CDCl₃): 178.9, 164.6, 162.2, 156.8, 151.2, 148.4, 137.0, 136.8, 136.5, 135.9, 128.94, 128.89, 128.75, 128.65, 128.5, 128.4, 128.2, 128.1, 127.6, 127.5, 127.3, 123.6, 122.8, 115.4, 113.8, 106.3, 98.7, 93.2, 74.5, 71.2, 71.0, 70.6.

Bioassay

Cell culture: All cell lines were initially purchased from American Type Culture Collection (ATCC™). The PC-3 prostate cancer cell line and the LNCaP prostate cancer cell line were routinely cultured in RPMI-1640 medium supplemented with 10% FBS and 1% penicillin/streptomycin. Cultures were maintained in 5% carbon dioxide at a temperature of 37°C. The DU-145 prostate cancer cells were routinely cultured in Eagle's Minimum Essential Medium (EMEM) supplemented with 10% FBS and 1% penicillin/streptomycin.

WST-1 cell proliferation assay: PC-3, DU-145, or LNCaP cells were plated in 96-well plates at a density of 3200 in each well in 200 μL of culture medium. The cells were then treated with either quercetin or synthesized quercetin derivatives separately at 2 different doses of 50 μM for 3 days, while equal treatment volumes of DMSO (0.25%) were used as vehicle control. The cells were cultured in a CO₂ incubator at 37°C for 3 days. Ten μL of the premixed WST-1 cell proliferation reagent (Clontech) was added to each well. After mixing gently for 1 min on an orbital shaker, the cells were incubated for an additional 3 h at 37°C. To ensure homogeneous distribution of color, it is important to mix gently on an orbital shaker for 1 min. The absorbance of each well was measured using a microplate reader (Synergy HT) at a wavelength of 430 nm. The IC₅₀ value is the concentration of each compound that inhibits cell proliferation by 50% under the experimental

conditions and is the average from at least triplicate determinations that are reproducible and statistically significant. For calculating the IC₅₀ values, a linear proliferative inhibition was made based on at least 5 dosages for each compound.

References

- [1] Richter E, Srivastava S, Dobi A. (2007) Androgen receptor and prostate cancer. *Prostate Cancer and Prostatic Diseases*, **10**, 114-118.
- [2] Roviello G, Petrioli R, Francini E. (2013) Time for a revision on the role of PSA response rate as a surrogate marker for median overall survival in docetaxel-based first-line treatment for patients with metastatic hormone-refractory prostate cancer. *International Journal of Biological Markers*, **28**, 326-328.
- [3] Paller CJ, Antonarakis ES. (2011) Cabazitaxel: a novel second-line treatment for metastatic castration-resistant prostate cancer. *Drug Design, Development and Therapy*, **5**, 117-124.
- [4] Sampson L, Rimm E, Hollman PC, de Vries JH, Katan MB. (2002) Flavonol and flavone intakes in US health professionals. *Journal of the American Dietetic Association*, **102**, 1414-1420.
- [5] Foster BA, Gingrich JR, Kwon ED, Madias C, Greenberg NM. (1997) Characterization of prostatic epithelial cell lines derived from transgenic adenocarcinoma of the mouse prostate (TRAMP) model. *Cancer Research*, **57**, 3325-3330.
- [6] Slusarz A, Shenouda NS, Sakla MS, Drenkhahn SK, Narula AS, MacDonald RS, Besch-Williford CL, Lubahn DB. (2010) Common botanical compounds inhibit the Hedgehog signaling pathway in prostate cancer. *Cancer Research*, **70**, 3382-3390.
- [7] Shenouda NS, Zhou C, Browning JD, Ansell PJ, Sakla MS, Lubahn DB, MacDonald RS. (2004) Phytoestrogens in common herbs regulate prostate cancer cell growth *in vitro*. *Nutrition and Cancer*, **49**, 200-208.
- [8] Alinkieel R, Bindukumar B, Reynolds JL, Sykes DE, Mahajan SD, Chadha KC, Schwartz SA. (2008) The dietary bioflavonoid, quercetin, selectively induces apoptosis of prostate cancer cells by down-regulating the expression of heat shock protein 90. *Prostate* (Hoboken, NJ, United States), **68**, 1773-1789.
- [9] Maggiolini M, Vivacqua A, Carpino A, Bonofiglio D, Fasanella G, Salerno M, Picard D, Ando S. (2002) The mutant androgen receptor T877A mediates the proliferative but not the cytotoxic dose-dependent effects of genistein and quercetin on human LNCaP prostate cancer cells. *Molecular Pharmacology*, **62**, 1027-1035.
- [10] Wang P, Vadgama JV, Said JW, Magyar CE, Doan N, Heber D, Henning SM. (2014) Enhanced inhibition of prostate cancer xenograft tumor growth by combining quercetin and green tea. *Journal of Nutritional Biochemistry*, **25**, 73-80.
- [11] Pratheeskumar P, Budhraja A, Son Y-O, Wang X, Zhang Z, Ding S, Wang L, Hitron A, Lee J-C, Xu M, Chen G, Luo J, Shi X. (2012) Quercetin inhibits angiogenesis mediated human prostate tumor growth by targeting VEGFR- 2 regulated AKT/mTOR/P70S6K signaling pathways. *PloS one*, **7**, e47516.
- [12] Beutler JA, Hamel E, Vlietinck AJ, Haemers A, Rajan P, Roitman JN, Cardellina JH, 2nd, Boyd MR. (1998) Structure-activity requirements for flavone cytotoxicity and binding to tubulin. *Journal of Medicinal Chemistry*, **41**, 2333-2338.
- [13] Rao KV, Owoyale JA. (1976) Partial methylation of quercetin: direct synthesis of tamarixetin, ombuin and ayanin. *Heterocyclic Chemistry*, **13**, 1293-1295.
- [14] Shi Z-H, Li N-G, Tang Y-P, Shi Q-P, Zhang W, Zhang P-X, Dong Z-X, Li W, Zhang X, Fu H-A, Duan J-A. (2014) Synthesis, biological evaluation and SAR analysis of O-alkylated analogs of quercetin for anticancer. *Bioorganic & Medicinal Chemistry Letters*, **24**, 4424-4427.

Acknowledgments - This work was financially supported by the California State University Fresno. Sami Jabban was supported in part by National Science Foundation (Award #: 1059994).

Compounds with Antifouling Activities from the Roots of *Notopterygium franchetii*

Chun Yu^{a,b}, Liqing Cheng^a, Zhongling Zhang^a, Yu Zhang^b, Chunmao Yuan^b, Weiwei Liu^b, Xiaojiang Hao^b, Weiguang Ma^{a,*} and Hongping He^{a,*}

(Chun Yu and Liqing Cheng contributed equally to this work)

^aSchool of Pharmacy, Yunnan University of TCM, Kunming 65050, China

^bState Key Laboratory of Phytochemistry and Plant Resources in West China, Kunming Institute of Botany, Chinese Academy of Sciences, Kunming 650201, China

hehongping@mail.kib.ac.cn, weiguangma@163.com

Received: September 24th, 2015; Accepted: November 2nd, 2015

In antifouling screening, the extract of *Notopterygium franchetii* de Boiss showed obvious activity. Two new phenylpropanoids (**1-2**) and five known coumarins (**3-7**) were isolated from the methanol extract of the roots of this species. The structures of the isolated compounds were determined on the basis of spectroscopic analysis. Compounds **1-2** showed definite antifouling activity against larval settlement of *Bugula neritina*.

Keywords: *Notopterygium franchetii*, Umbelliferae, Chemical constituent, Phenylpropanoids, Antifouling.

Notopterygium franchetii de Boiss, family Umbelliferae, is a traditional Chinese medicine. Its main constituents include essential oils, coumarins, amino acids, and organic acids [1]. Extracts of *N. franchetii* and some other species of *Notopterygium* have been reported to possess anti-inflammatory [2], antibacterial [3], antivirus [4], anti-thrombus [5], anti-arrhythmia [6] and anti-allergy [7] properties. We have carried out a study of the chemical constituents and their activities on marine fouling resistance, and now report the isolation and structure elucidation of two new phenylpropanoids (**1-2**), together with five known coumarins (**3-7**) from the dried roots of *N. franchetii*, and their antifouling activities against larval settlement of the barnacles *Balanus amphitrite* and *Bugula neritina*.

The methanol extract of the roots of the title plant was subjected to column chromatography to give two new phenylpropanoids (**1-2**), and five known coumarins, nodakenetin (**3**) [8], notopterol (**4**) [9], notoptol (**5**) [10], 5-[*E*,*S*]-7-hydroxy-3,7-dimethyl-2,5-octadienoxy]psoralen (**6**) [11] and 5-[*E*,*S*]-epoxy-3-hydroxy-3,7-dimethyl-6-octadienoxy]psoralen (**7**) [11]. The structures were elucidated by NMR, IR and UV spectroscopy and MS.

Compound **1** was isolated as a white amorphous powder with a molecular formula of C₂₀H₂₆O₅ (calcd. 346.1780) as determined by the [M]⁺ ion at *m/z* 346.1773 in the HR-EI-MS, together with eight degrees of unsaturation [12]. The IR spectrum showed hydroxyl at 3432 cm⁻¹ and a double bond at 1596 cm⁻¹, 1516 cm⁻¹, while the UV spectrum showed absorption maxima at λ_{max} 193, 217, 235 and 327 nm [13]. The ¹H NMR spectrum (Table 1) displayed three methyl singlet signals at δ_{H} 1.15 (3H, s), 0.91 (3H, s) and 0.89 (3H, s), a tri-substituted benzene ring signals at δ_{H} 7.35 (1H, d, *J* = 1.8), δ_{H} 7.15 (1H, dd, *J* = 8.1, 1.8) and δ_{H} 6.87 (1H, d, *J* = 8.1), a methoxyl group at δ_{H} 3.91 (3H, s), and a double bond at δ_{H} 7.59 (1H, d, *J* = 15.6), δ_{H} 6.42 (1H, d, *J* = 15.6); these last two protons had a *trans* form from the coupling constant (*J* = 15.6). The ¹³C NMR spectrum (Table 1) showed 20 carbon signals (four primary, two secondary, eight tertiary, and six quaternary), including one

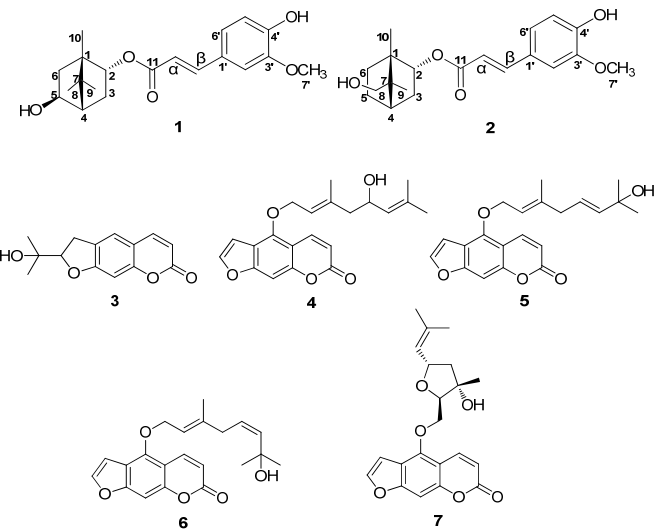


Figure 1: Isolated compounds from the roots of *Notopterygium franchetii*.

methoxyl carbon (δ_{C} 56.2), one carboxylic carbon (δ_{C} 167.6), eight aromatic carbons (δ_{C} 116.1, 145.4, 127.4, 111.1, 148.7, 150.0, 116.0, and 124.0). The HMBC correlation of H-7' (δ_{H} 3.91) with C-3' (δ_{C} 148.7) indicated that this methoxy group was at C-3' [14]. The correlations of H- β (δ_{H} 7.59) with C-2' (δ_{C} 111.1), C-6' (δ_{C} 124.0) and C-11 (δ_{C} 167.6) indicated that C- β (δ_{C} 145.4) was connected to C-1' (δ_{C} 127.4), and C- α (δ_{C} 116.1) with C-11 (δ_{C} 167.6). Analysis of the NMR data (Tables 1 and 2) of compound **1** revealed nearly identical structural features to those of (-)-bornyl ferulate [15], except that a methylene at C-5 was replaced by an oxygen-substituted methine, indicating that compound **1** is an analogue of (-)-bornyl ferulate. This was further confirmed by relevant ¹H-¹H COSY and HMBC data. The ¹H-¹H COSY correlations of a proton signal at δ_{H} 3.86 with H-4 (δ_{H} 1.74) and H-6a (δ_{H} 2.41) indicated this hydroxyl group at C-5 (δ_{C} 75.0). The planar structure of compound **1** was, therefore, determined as shown in Figure 1.

Table 1: NMR spectral data of compound **1** in CD₃COCD₃.

Position	δ_{H} (mult, J Hz) (600MHz)	δ_{C} (150 MHz)	HMBC
1		48.1 (s)	
2	4.88 (m)	78.6 (d)	C-6, C-10, C-11
3a	2.35 (m)	35.0 (t)	C-5, C-7
3b	0.85 (dd, 14.0, 3.3)		C-1, C-5
4	1.74 (d, 5.1)	53.4 (d)	
5	3.86 (m)	75.0 (d)	
6a	2.41 (m)	40.3 (t)	
6b	1.45 (dt, 13.4, 2.2)		
7		50.2 (s)	
8	1.15 (s)	21.1 (q)	C-1, C-4, C-9
9	0.91 (s)	20.2 (q)	C-1, C-4, C-8
10	0.89 (s)	13.4 (q)	C-2, C-6, C-9
11		167.6 (s)	
α	6.42 (d, 15.6)	116.1 (d)	
β	7.59 (d, 15.6)	145.4 (d)	C-2', C-6', C-11
1'		127.4 (s)	
2'	7.35 (d, 1.7)	111.1 (d)	
3'		148.7 (s)	
4'		150.0 (s)	
5'	6.87 (d, 8.1)	116.0 (d)	
6'	7.15 (dd, 1.8, 8.1)	124.0 (d)	C-2', C-4', C- β
7'	3.91 (s)	56.2 (q)	C-3'

Table 2: NMR spectral data of compound **2** and (-)-bornyl ferulate.

Position	(2) (CD ₃ COCD ₃)		(-)-bornyl ferulate (CDCl ₃)			
	δ_{H} (mult, J Hz) (600MHz)	δ_{C} (150 MHz)	Position	δ_{H} (mult, J Hz) (300 MHz)	δ_{C} (75 MHz)	
1		50.3 (s)	1		48.9 (s)	
2	4.00 (m)	76.3 (d)	2	5.02 (ddd, 10.0, 3.3, 1.8)	79.8 (d)	
3a	2.23 (m)	39.3 (t)	3a	2.41 (ddd, 13.8, 10.0, 4.0, 3.5)	36.8 (t)	
3b	0.97 (dd, 13.6, 3.6)		3b	1.05 (dd, 13.3, 3.3)		
4	1.89 (t, 4.5)	43.0 (d)	4	1.71 (m)	44.9 (d)	
5a	1.77 (m)	28.4 (t)	5a	1.78 (m)	28.0 (d)	
5b	1.30 (m)		5b	1.29 (m)		
6a	2.18 (dd, 9.1, 3.2)	26.6 (t)	6a	2.06 (m)	27.2 (t)	
6b	1.27 (m)		6b	1.31 (m)		
7		51.8 (s)	7		47.8 (s)	
8a	4.23 (d, 11.2)	68.0 (t)	8	0.90 (s)	19.7 (q)	
8b	4.03 (d, 11.2)					
9	1.01 (s)	14.2 (q)	9	0.94 (s)	18.8 (q)	
10	0.93 (s)	14.3 (q)	10	0.88 (s)	13.5 (q)	
11		167.7 (s)	11		167.0 (s)	
α	6.43 (d, 15.9)	115.9 (d)	α	6.31 (d, 15.9)	116.1 (d)	
β	7.61 (d, 15.9)	145.5 (d)	β	7.59 (d, 15.9)	144.3 (d)	
1'		127.4 (s)	1'		127.0 (s)	
2'	7.35 (d, 1.7)	111.1 (d)	2'	7.05 (d, 1.5)	109.3 (d)	
3'		148.7 (s)	3'		146.8 (s)	
4'		150.0 (s)	4'		147.8 (s)	
5'	6.86 (d, 8.2)	116.0 (d)	5'	6.91 (d, 8.2)	114.7 (d)	
6'	7.15 (dd, 1.8, 8.2)	123.9 (d)	6'	7.08 (dd, 2.2, 8.2)	123.0 (d)	
7'	3.91 (s)	56.2 (q)	7'	3.93 (s)	55.9 (q)	

The ROESY correlations of H-2 (δ_{H} 4.88) with H-3a (δ_{H} 2.35) and H-9 (δ_{H} 0.91) indicated that H-2, H-3a and H-9 were β -oriented. The correlation of H-5 (δ_{H} 3.86) with H-3b (δ_{H} 0.85) indicated that H-5 and H-3b were α -oriented. Herein, the OH at C-5 was β -oriented. Thus, the relative configuration of compound **1** was determined as shown in Figure 1.

Compound **2** was isolated as a white amorphous powder with a molecular formula of C₂₀H₂₆O₅ (calcd. 346.1780), as determined by the [M]⁺ peak at *m/z* 346.1779 in the HR-EI-MS, together with eight degrees of unsaturation. The IR spectrum showed hydroxyl at 3442 cm⁻¹ and double bond at 1631 cm⁻¹, 1516 cm⁻¹, while the UV spectrum showed absorption maxima at λ_{max} 202, 234 and 326 nm. Analysis of the NMR data (Table 2) of compound **2** revealed nearly identical structural features to those of (-)-bornyl ferulate [15], except that a methyl at C-8 was replaced by a hydroxymethyl,

indicating that compound **2** is an analogue of (-)-bornyl ferulate. This was further confirmed by relevant ¹H-¹H COSY and HMBC data. The HMBC correlations of H-8a (δ_{H} 4.23) and H-8b (δ_{H} 4.03) with C-9 (δ_{C} 14.2) indicated that the hydroxymethyl was at C-8 (δ_{C} 68.0). The planar structure of compound **2** was, therefore, determined as shown (Figure 1).

The ROESY correlation of H-2 (δ_{H} 4.00) with H-9 (δ_{H} 1.01) indicated H-2 and H-9 to be β -oriented, while H-8 should be α -oriented. Thus, the relative configuration of compound **2** was determined as shown in Figure 1.

Compounds **1**, **2** and **3-7** were evaluated for their antifouling activity against larval settlement of the barnacles *Balanus amphitrite* and *Bugula neritina*. Testing was performed in accordance with the method described by Kawahara [16]. Compounds **1** and **2** had activity against larval settlement of *Bugula neritina* with an EC₅₀ value of 25 $\mu\text{g}/\text{mL}$, which indicated that the -OH group of the bornyl moiety had no effect on the larval settlement. The attachment rate of the negative control group was 100%. The test results were read 12 hours after dosing. Specific results are shown in Table 3.

Experimental

General: The optical rotation data were measured on a JASCO P-1020 digital polarimeter (Jasco, Tokyo, Japan), UV-Vis spectra on a Shimadzu UV-2401 PC spectrophotometer, IR spectra on a Bruker Tensor-27 infrared spectrophotometer with a KBr disk, and ESI-MS and HR-EI-MS on Bruker HCT/E squire 3000 and Waters Autospec Premier P776 spectrometers, respectively. The NMR spectra were recorded on a Bruker Avance III-600 spectrometer with trimethylsilyl as internal standard. Column chromatography was performed on silica gel (200–300 and 300–400 mesh; Qingdao Marine Chemical Inc.), MCI gel CHP 20P (75–150 μm ; Mitsubishi Chemical Corporation), Sephadex LH-20 (40–70 μm ; Amersham Pharmacia Biotech AB), and Chromatorex Rp-C₁₈ gel (20–45 μm ; Merck). Compounds on thin layer chromatograms (TLC plates; Qingdao Marine Chemical Inc.) were visualized under UV light and by dipping into 5% H₂SO₄ in EtOH followed by heating.

Plant material: The dried roots of *Notopterygium franchetii* de Boiss were bought in Kunming Juhua market, Yunnan Province of China, in September 2012, and were identified by Mr Yu Chen (Kunming Institute of Botany, Chinese Academy of Sciences). A voucher specimen (H20120902) was deposited at the Key Laboratory of Phytochemistry and Plant Resources in West China, Kunming Institute of Botany, Chinese Academy of Sciences.

Extraction and isolation: The air-dried roots (15.0 kg) of *N. franchetii* were powdered and extracted 3 times with MeOH under reflux. The combined MeOH extracts were concentrated using a rotary evaporator to give the crude extract, which was suspended in water and then partitioned successively with light petroleum, ethyl acetate and *n*-butyl alcohol, sequentially.

The ethyl acetate portion (1.08 kg) was subjected to silica gel CC and eluted with light petroleum-acetone mixtures of increasing polarity (from 10:0 to 4:6) to yield 5 fractions (Fr.1-5) on the basis of TLC. Fr. 3 (22.5 g) was then separated on a silica gel column (light petroleum/ethyl acetate from 7.5:2.5 to 7:3) to obtain 13 fractions (Fr.3A–3M). Fr.3H (4.0 g) was separated over a MCI-gel column (MeOH/H₂O from 4:6 to 10:0) to obtain 11 fractions (Fr.3H1–3H11). Fr.3H4 (95.8 mg) was then separated on a silica gel column (light petroleum/ethyl acetate from 9.5:0.5) to obtain 7

(15.7 mg) [11]. Fr.3H6 (1.81 g) was then separated on a silica gel column (light petroleum/ethyl acetate, 9.5:0.5) to obtain 8 fractions (Fr.3H6A–3H6H). Fr.3H6B (200 mg) was purified by HPLC (MeOH/H₂O, 55:45) to obtain **1** (7.3 mg) and **2** (5.2 mg). Fr.3H7 (491.2 mg) was then separated on a silica gel column (light petroleum/ethyl acetate, 9.5:0.5) to obtain 9 fractions (Fr.3H7A–3H7I). Fr.3H7E (70 mg) was purified by HPLC to obtain **5** (15.7 mg) [10] and **6** (4.8 mg) [11]. Fr.3H7G (120 mg) was purified by HPLC to yield **3** (65.9 mg) [8] and **4** (14.0 mg) [9].

Compound (1)

White amorphous powder.

$[\alpha]_D^{16}$: -20.63 (*c* 0.34, MeOH).

UV (CH₃OH) λ_{max} (log ϵ): 327 (0.39).

¹H and ¹³C NMR: Table 1.

ESI-MS *m/z*: 369 [M+Na]⁺

HR-EI-MS *m/z*: 346.1773, C₂₀H₂₆O₅ (calcd. 346.1780).

Compound (2)

White amorphous powder.

$[\alpha]_D^{17}$: -19.05 (*c* 0.175, MeOH).

UV (CH₃OH) λ_{max} (log ϵ): 203 (0.43), 326 (0.40).

¹H and ¹³C NMR: Table 2.

References

- [1] Jin PP. (2011) Research progress of *Notopterygium incisum* Ting ex H. T. Chang. *Journal of Anhui Agricultural Sciences*, **39**, 815-816.
- [2] Li ZY, Zhang XS, Wang JL. (2003) Progress in researches on *Notopterygium* root. *Journal of Shaanxi College of Traditional Chinese Medicine*, **26**, 56-59.
- [3] Jin SF, Lin WM, Qiao J, Li WZ. (1981) Study on the pharmacological effects of *Notopterygium* injection. *Chinese Traditional Patent Medicine*, **4**, 41-41.
- [4] Guo YH, Sha M, Meng XS, Cao AM. (2005) The anti-viral studies of *Notopterygium incisum*. *Lishizhen Medicine and Materia Medica Research*, **16**, 198-199.
- [5] Lv EW, Ni ZM, He WJ, Ren ZH. (1981) Antithrombosis effect of nine kinds of traditional Chinese medicine. *Chinese Journal of Integrated Traditional and Western Medicine*, **1**, 101-103.
- [6] Cheng NZ, Shan ZY, Chen YP. (1998) Comparison antiarrhythmia effect of different water-soluble of *Notopterygium incisum*. *Chinese Journal of Basic Medicine in Traditional Chinese Medicine*, **4**, 43-43.
- [7] Sun YP, Xu Q. (2003) Effects of aqueous extract from rhizoma *Notopterygii* on the delayed-type hypersensitivity and inflammatory reactions and its mechanisms. *Journal of China Pharmaceutical University*, **34**, 51-54.
- [8] Zhao DF, Islam MN. (2012) *In vitro* antioxidant and anti-inflammatory activities of *Angelica decursiva*. *Archives of Pharmacal Research*, **35**, 179-192.
- [9] Kou GF, Zhang YB, Yang XW, Rong R. (2010) O-methylnotopterol, a new natural product from the roots and rhizomes of *Notopterygium incisum*. *China Journal of Chinese Materia Medica*, **35**, 1134-1136.
- [10] Kozawa M, Fukumoto M, Matsuyama Y. (1983) Chemical studies on the constituents of the Chinese crude drug “Qiang Huo”. *Chemical and Pharmaceutical Bulletin*, **31**, 2712-2717.
- [11] Wu SB, Zhao Y, Fan H, Hu YH, Hamann MT, Peng JN, Starks CM, O’Neil-Johnson M, Hu JF. (2008) New guaiane sesquiterpenes and furanocoumarins from *Notopterygium incisum*. *Planta Medica*, **74**, 1812-1817.
- [12] Su ZS, Wang P, Yuan W, Li SY. (2014) Chemical constituents from *Pterocarpus soyauxii*. *Natural Product Communications*, **9**, 1483-1486.
- [13] Rakata A, Laphookhieoa S, Cheenprachab S, Rithiwigrome T, Maneerata W. (2014) Antibacterial compounds from the roots of *Cratoxylum formosum* spp. *pruniflorum*. *Natural Product Communications*, **9**, 1487-1489.
- [14] Li RX, Niu SB, Guo LD, Zhang Y. (2014) Two new pyrone derivatives from the plant endophytic fungus *Exserohilum* sp. *Natural Product Communications*, **9**, 1497-1498.
- [15] Maldonado E, Apan MTR, Pérez-Castorena A L. (1998) Anti-inflammatory activity of phenyl propanoids from *Coreopsis mutica*. *Planta Medica*, **64**, 660-661.
- [16] Kawahara H, Tamura R, Ajioka S, Shizuri Y. (1999) Convenient assay for settlement-inducing substances of barnacle. *Marine Biotechnology*, **1**, 98-101.
- [17] Qi SH, Zhang S, Qian PY, Xiao ZH, Li MY. (2006) Ten new antifouling briarane diterpenoids from the South China Sea gorgonian *Junceella juncea*. *Tetrahedron*, **62**, 9123-9130.

ESI-MS *m/z*: 369 [M+Na]⁺

HR-EI-MS *m/z*: 346.1779, C₂₀H₂₆O₅ (calcd. 346.1780).

Marine fouling resistance assay: Activity testing was performed in accordance with the method described by Kawahara [16,17]. We used the larvae of the barnacles *Balanus amphitrite* and *Bugula neritina* as test larva. First, the larvae were cultured to the state of pre-attachment, and then the sample and a certain number of larvae were cultured together. Twelve h later, the number of non-attached and attached larvae was observed and counted under a microscope. Finally, the attachment rate of larvae was calculated. The experiment was conducted by Peiyuan Qian’s research group at Hong Kong University of Science and Technology.

Table 3: Activities of resistance to marine fouling of compounds **1** and **2**.

Compounds	Settlement bioassay of <i>Bugula neritina</i> larvae (EC ₅₀)	
	1	25
2		25

Acknowledgements - This work was supported financially by the National Natural Science Foundation of China (31170332). We thank Prof. Peiyuan Qian of Hong Kong University of Science and Technology for bioactivity testing.

New Isochromane Derivatives from the Mangrove Fungus *Aspergillus ustus* 094102

Peipei Liu^{a,1}, Cong Wang^{a,1}, Zhenyu Lu^{a,1}, Tonghan Zhu^a, Kui Hong^{b,*} and Weiming Zhu^{a,*}

^aKey Laboratory of Marine Drugs, Ministry of Education of China, School of Medicine and Pharmacy, Ocean University of China, Qingdao 266003, China

^bKey Laboratory of Combinatorial Biosynthesis and Drug Discovery, Ministry of Education of China, School of Pharmaceutical Sciences, Wuhan University, Wuhan 430071, China

¹The authors contributed equally to this paper

weimingzhu@ouc.edu.cn; kuihong31@gmail.com

Received: June 18th, 2015; Accepted: September 22nd, 2015

Four new isochromane derivatives (**1–4**) along with the known peniciphenol (**5**) and (*R*)-2-(hydroxymethyl)-3-(2-hydroxypropyl)phenol (**6**) were isolated from the EtOAc extract of the fermentation broth of the mangrove fungus, *Aspergillus ustus* 094102. The structures of the new compounds including the absolute configuration were elucidated on the basis of spectroscopic analysis, CD and ECD calculation. Compounds **1** and **2** exhibited α -glucosidase inhibition and anti-oxidation against DPPH radical with IC₅₀ values of 1.4 mM and 25.7 μ M, respectively.

Keywords: *Aspergillus ustus*, Isochromane derivatives, Anti-oxidation, α -Glucosidase inhibition.

Microorganisms in special niches have proved to be an important source of bioactive compounds. The mangrove is a typically special ecosystem at the junction of land and sea, in which there are abundant microorganisms that may produce structurally new and bioactive natural products [1–6]. Previously we identified cytotoxic drimane sesquiterpenes and isochromane derivatives from *Aspergillus ustus* 094102 isolated from the mud around the roots of the mangrove plant *Bruguiera gymnorhiza* [1]. Continuous study resulted in the isolation and identification of four new isocoumarin derivatives (**1–4**), as well as two known phenolic compounds, peniciphenol (**5**) [7] and (*R*)-2-(hydroxymethyl)-3-(2-hydroxypropyl)phenol (**6**) [8]. The new compound **1** exhibited α -glucosidase inhibition while new compound **2** showed anti-oxidative activity against 2,2-diphenyl-1-picrylhydrazyl (DPPH) radical with IC₅₀ values of 1.41 mM and 25.7 μ M, respectively.

Compound **1** was obtained as a colorless solid with a molecular formula of C₁₁H₁₂O₆ from the HRESIMS peak at *m/z* 239.0558 [M-H]⁻ (calcd 239.0556 for C₁₁H₁₁O₆). The IR spectrum indicated the presence of hydroxyl (3226 cm⁻¹), ester carbonyl groups (1751 cm⁻¹) and an aromatic ring (1595, 1482 cm⁻¹). The ¹H and ¹³C NMR along with DEPT spectra (Table 1, Figures S1–S3) exhibited signals for a methoxyl ($\delta_{\text{H/C}}$ 3.89/56.1), two oxygenated methylenes ($\delta_{\text{H/C}}$ 4.36 & 4.52/72.2, δ_{H} 4.46/50.9), one oxygenated methine ($\delta_{\text{H/C}}$ 4.75/62.6), one aromatic methine ($\delta_{\text{H/C}}$ 6.72/101.0), six sp³ quaternary carbons (δ_{C} 100.5, 144.0, 163.8, 115.7, 160.4, 169.0), and three exchangeable protons (δ_{H} 4.58, 5.95 & 11.36), indicating a penta-substituted benzopyrone skeleton in **1**. HMBC correlations (Figures 2 and S4) of H-3 (δ_{H} 4.36 & 4.52) to C-1 (δ_{C} 169.0), C-4 (δ_{C} 62.6) and C-4a (δ_{C} 144.0), along with HO-4 (δ_{H} 5.95) to C-3 (δ_{C} 72.2), C-4 and C-4a confirmed the skeleton as isochromane. In addition, the HMBC spectrum showed long distance ¹H-¹³C correlations from the methoxy proton (δ_{H} 3.89) to C-6 (δ_{C} 163.8), from H-5 (δ_{H} 6.72) to C-4, C-4a, C-1a (δ_{C} 100.5), C-6 (δ_{C} 163.8) and C-7 (δ_{C} 115.7), and from HO-9 (δ_{H} 4.58) to C-6, C-7 and C-8 (δ_{C} 160.4), locating the methoxy, hydroxymethyl and hydroxy groups at C-6,

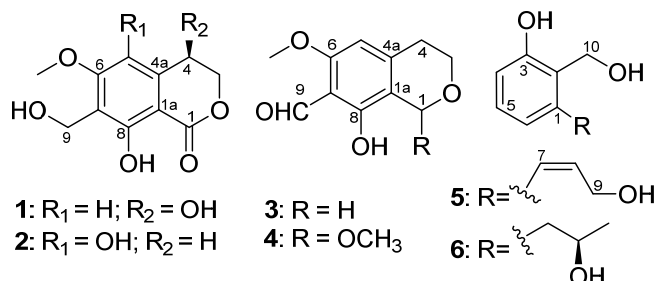


Figure 1: Chemical structures of compounds **1–6**.

C-7 and C-8, respectively. The absolute configuration was determined as *4R*- by ECD calculations using the time-dependent density functional theory (TD-DFT) method at the B3LYP/6-31G(d) level [9]. The results showed that the CD curve of **1** is matched well with the calculated ECD for *R*-**1** and opposite to that of *S*-**1** (Figure 3), indicating *R*-configuration. Thus, compound **1** was identified as (*R*)-4,8-dihydroxy-7-(hydroxymethyl)-6-methoxyisochroman-1-one.

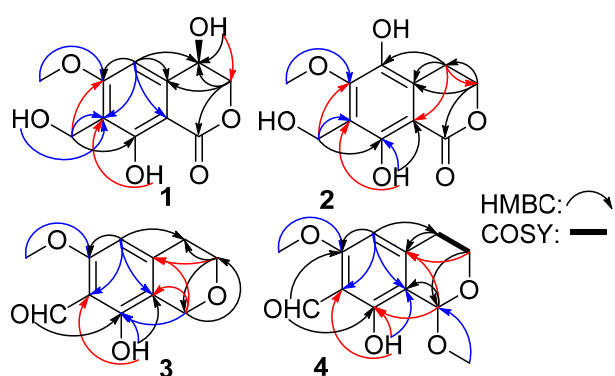
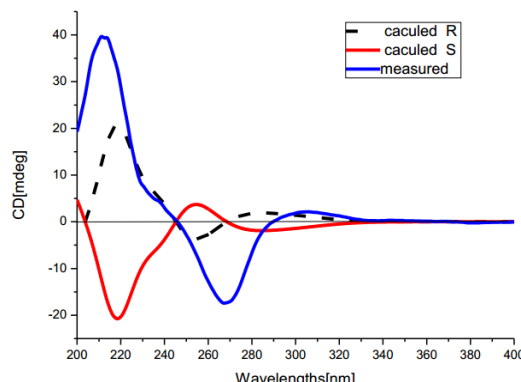


Figure 2: HMBC and ¹H-¹H COSY correlations of compounds **1–4**.

Table 1: ^1H (600 MHz) and ^{13}C (150 MHz) NMR data for compounds **1–3** in $\text{DMSO}-d_6$ and compound **4** in CDCl_3 (δ , ppm).

position	δ_{C}	1 δ_{H} (J in Hz)	2 δ_{H} (J in Hz)	3 δ_{H} (J in Hz)	4 δ_{H} (J in Hz)
1	169.0, qC		169.6, qC	62.4, CH ₂	93.8, CH
1a	100.5, qC		103.6, qC	114.8, qC	5.55, s
3	72.2, CH ₂	4.52, dd (11.5, 3.8) 4.36, dd (11.5, 5.5)	67.7, CH ₂	4.52, t (6.0)	115.6, qC
4	62.6, CH	4.75, m	21.5, CH ₂	2.95, t (6.0)	56.3, CH ₂
4a	144.0, qC		126.5, qC	146.0, qC	3.86, dd (15.4, 6.1)
5	101.0, CH	6.72, s	138.3, qC	102.2, CH	4.18, ddd (15.4, 12.1, 3.3)
6	163.8, qC		154.4, qC	160.0, qC	2.58, dd (17.6, 3.3 Hz); 3.00, ddd (17.6, 12.2, 6.1)
7	115.7, qC		120.8, qC	108.2, qC	
8	160.4, qC		154.4, qC	158.3, qC	
9	50.9, CH ₂	4.46, br d (3.5)	51.7, CH ₂	4.46, s	10.18, s
6-OMe	56.1, CH ₃	3.89, s	61.5, CH ₃	3.84, s	193.7, CH
1-Me				56.1, CH ₃	10.24, s
4-OH		5.95, d (5.3)			55.8, CH ₃
5-OH					3.86, s
8-OH		11.36, s			55.4, CH ₃
9-OH		4.58, t (3.5)			3.56, s

**Figure 3:** CD curve of **1** and the calculated ECD curves of *R*-**1** and *S*-**1**.

Compound **2** was obtained as a white solid with the same molecular formula as **1** from the HRESIMS peak at m/z 239.0549[M-H]⁻. The presence of hydroxyl, ester carbonyl groups and a benzene ring could be deduced from the IR absorptions at 3257, 1755, 1609, and 1465 cm^{-1} , respectively. The ^1H and ^{13}C NMR data classified by DEPT experiments (Table 1, Figures S5-S7) were closely related to compound **1**, except that the oxygenated sp^3 -methine and aromatic methine were replaced by a methylene ($\delta_{\text{H/C}}$ 2.95/21.5) and an aromatic quaternary carbon (δ_{C} 138.3), respectively. In addition, obvious up-field shifts for C-3, C-4a, C-6 and C-8 were observed while C-1a, C-7 and C-6-OMe shifted down-field. These data indicated that the HO- group at C-4 in **1** was moved to C-5 in compound **2**. This deduction was further supported by HMBC correlations of H-3 (δ_{H} 4.52) to C-1 (δ_{C} 169.6), C-4 (δ_{C} 21.5) and C-4a (δ_{C} 126.5), H-4 (δ_{H} 2.95) to C-1a (δ_{C} 103.6), C-3 (δ_{C} 67.7), C-4a and C-5 (δ_{C} 138.3), along with HO-9 (δ_{H} 4.75) to C-7 (δ_{C} 120.8), C-6 and C-8 (δ_{C} 154.4) (Figures 2 and S9). Thus, compound **2** was elucidated as 5,8-dihydroxy-7-(hydroxymethyl)-6-methoxyisochroman-1-one.

Compound **3** was obtained as a white solid with a molecular formula of $\text{C}_{11}\text{H}_{12}\text{O}_4$ from the HRESIMS peak at m/z 209.0839 [M+H]⁺ (calcd 209.0830 for $\text{C}_{11}\text{H}_{13}\text{O}_4$). The IR spectrum showed characteristic absorptions of -CHO at 2848, 2736 and 1695 cm^{-1} . The ^1H and ^{13}C NMR along with the DEPT spectra (Table 1, Figures S10-S12) exhibited signals for one methoxyl ($\delta_{\text{H/C}}$ 3.86/56.1), one aldehyde group ($\delta_{\text{H/C}}$ 10.18/193.9), one penta-substituted benzene nucleus ($\delta_{\text{H/C}}$ 6.45/102.2, 114.8, 146.0, 160.0, 108.2, and 158.3), two oxygenated methylenes ($\delta_{\text{H/C}}$ 4.54/62.4, 3.83/63.5), one methylene ($\delta_{\text{H/C}}$ 2.78/29.0), and a phenolic hydroxyl (δ_{H} 12.16), probably suggesting an isochroman skeleton. This deduction was confirmed by the HMBC correlations (Figures 2 and

S14) from H-1 (δ_{H} 4.54) to C-3 (δ_{C} 63.5), C-1a (δ_{C} 114.8) and C-4a (δ_{C} 146.0), from H-3 (δ_{H} 3.83) to C-1 (δ_{C} 62.4), C-4 (δ_{C} 29.0) and C-4a, and from H-4 (δ_{H} 2.78) to C-1a, C-4a, C-3 and C-5 (δ_{C} 102.2). In addition, the HMBC spectrum also showed long-distance ^1H - ^{13}C correlations from the aldehyde proton (δ_{H} 10.18) to C-7 (δ_{C} 108.2) and C-8 (δ_{C} 158.3), from the hydroxy proton (δ_{H} 12.16) to C-1a, C-7 and C-8, from the methoxy proton (δ_{H} 3.86) and C-6 (δ_{C} 160.0), and from H-5 (δ_{H} 6.45) to C-1a, C-4, C-6 and C-7, locating the methoxy, aldehyde and hydroxy protons at C-6, C-7 and C-8, respectively. Thus, compound **3** was determined as 8-hydroxy-6-methoxyisochromane-7-carbaldehyde.

Compound **4** was obtained as a white solid with a molecular formula of $\text{C}_{12}\text{H}_{14}\text{O}_5$ according to a HRESIMS peak at m/z 239.2445 [M+H]⁺ (calcd 239.2437 for $\text{C}_{12}\text{H}_{15}\text{O}_5$). The ^1H and ^{13}C NMR data (Table 1 and Figures S16-S18) were closely related to compound **3**, except for an additional methoxy ($\delta_{\text{H/C}}$ 3.56/55.4) and the replacement of the oxygenated methylene in **3** by a hemiacetal methine ($\delta_{\text{H/C}}$ 5.55/93.8). The key HMBC correlation of the methoxy proton to the hemiacetal methine carbon (C-1) located the methoxy group at C-1, indicating that compound **4** was a C-1 methoxylated derivative of **3** that was further confirmed by ^1H - ^1H COSY between H-3 and H-4 (Figures 2 and S20), along with almost the same HMBC pattern between **4** and **3** (Figures 2 and S21). The small $[\alpha]^{20}_D$ value -5.6 suggested that compound **4** might be a racemic mixture, which led us to carry out a chiral analysis. Unfortunately, compound **4** was not resolved by chiral HPLC analysis over chiralpak IA and chiralpak IC chiral columns (Figure S23). Thus, compound **4** was elucidated as (\pm) -8-hydroxy-1,6-dimethoxyisochromane-7-carbaldehyde.

Compounds **1–6** were assayed for their anti-oxidative activity against DPPH radical [10] and α -glucosidase inhibitory effects using *p*-nitrophenyl- α -glucopyranoside (pNPG) as substrate [11]. The results showed that compound **2** displayed anti-oxidation with an IC_{50} value of 25.7 μM , while compounds **1** and **3–6** were inactive ($\text{IC}_{50} > 400 \mu\text{M}$) compared with L-ascorbic acid (positive control, IC_{50} 16.5 μM) (Table 2, left). Compound **1** exhibited moderate α -glucosidase inhibition with an IC_{50} value of 1.41 mM compared with acarbose (positive control, IC_{50} 0.95 mM) (Table 2, right).

Experimental

General: Optical rotations were obtained on a JASCO P-1020 digital polarimeter. CD data were collected on a JASCO J-715 spectropolarimeter. UV spectra were recorded on a Beckman DU 640 spectrophotometer, and IR spectra on a Nicolet NEXUS 470 spectrophotometer as KBr discs. ^1H / ^{13}C NMR, DEPT, and

Table 2: DPPH radical scavenging activity (left) and α -glucosidase inhibition (right) of compounds **1–6**.

Compound	IC ₅₀ , μM	Compound	IC ₅₀ , mM ^a
1	>417	1	1.4
2	25.7	2	6.9
3	>481	3	-
4	>420	4	7.0
5	>556	5	-
6	>549	6	12.7
ascorbic acid	16.5	acarbose	0.9

^a - untested.

2D-NMR spectra were recorded on a JEOL JNM-ECP 600 spectrometer using TMS as internal standard; chemical shifts were recorded as δ values. ESI-MS were measured on a Q-TOF ULTIMA GLOBAL GAA076 LC mass spectrometer. HPLC was performed on an ODS RP-18 column [YMC-pack ODS-A, 10×250 mm, 5 μm , 4 mL/min].

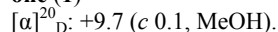
Fungal material: The fungus *Aspergillus ustus* 094102 was isolated and identified by Prof. Dr Kui Hong [1]. A reference culture of *A. ustus* 094102 is maintained at -80°C. Working stocks were prepared on Potato Dextrose agar slants and stored at 4°C.

Fermentation and extraction: *A. ustus* 094102 was incubated under static conditions at 30°C for 28 d in 100 × 1000 mL Erlenmeyer flasks containing liquid medium (300 mL/flask) composed of maltose (20 g/L), mannitol (20 g/L), glucose (10 g/L), monosodium glutamate (10 g/L), yeast extract (3 g/L), corn steep liquor (1 g/L), KH₂PO₄ (0.5 g/L), MgSO₄·7H₂O (0.3 g/L), and seawater, after adjusting its pH to 7.0. The fermentation broth (30 L) was filtered through cheesecloth to be separated into supernatant and mycelium. The supernatant was concentrated under reduced pressure to about 25% of the original volume and then extracted 3 times with EtOAc to give an EtOAc solution, while the mycelium was extracted 3 times with acetone. After removing the acetone by evaporation under vacuum, the obtained aqueous acetone solution was extracted 3 times with equal volumes of EtOAc. Both EtOAc solutions were combined and dried under vacuum to give 70.0 g of extract.

Purification: The EtOAc extract (70.0 g) was separated into 8 fractions on a silica gel column eluting with a stepwise gradient of light petroleum-CHCl₃-MeOH. Fraction 7 (2.2 g) was subjected to CC over an ODS column eluting with 30–80% MeOH/H₂O to provide 5 sub-fractions (Fr7.1-Fr7.5). Fr7.5 (0.2 g) was further purified on an ODS column with 60% MeOH/H₂O followed by semi-preparative HPLC to give compound **6** (7.7 mg, t_R 4.7 min, 55% MeOH/H₂O). Fraction 8 (5.3 g) was separated into 9 sub-fractions (Fr8.1-Fr8.9) on a silica gel column eluting with a stepwise gradient of CHCl₃-MeOH. Fr8.1 (0.1 g) was further purified by semipreparative HPLC with 55% MeOH/H₂O to give compound **5** (4.0 mg, t_R 7.5 min). Fr8.2 (1.1 g) was further separated on a Sephadex LH-20 column eluting with MeOH followed by semipreparative HPLC to give compound **2** (27.7 mg, t_R 4.4 min, 55% MeOH/H₂O). Fr8.3 (2.7 g) was further separated into 5 sub-fractions (Fr8.3.1-Fr8.3.5) on a RP-18 column eluting with 60% MeOH/H₂O. Fr8.3.4 (0.8 g) was then subjected to

chromatography over a Sephadex LH-20 column eluting with MeOH to afford 3 fractions (Fr8.3.4.1-Fr8.3.4.3). Fr8.3.4.1 (0.1 g) was further purified by semi-preparative HPLC with 55% MeOH/H₂O to give compound **3** (5.2 mg, t_R 14.6 min), while Fr8.3.4.2 (0.2 g) gave compounds **1** (12.6 mg, t_R 12.2 min) and **4** (9.3 mg, t_R 6.8 min) purified by semi-preparative HPLC with 55% MeOH/H₂O.

(R)-4,8-Dihydroxy-7-(hydroxymethyl)-6-methoxyisochroman-1-one (1)



IR (KBr): 3226, 2910, 1751, 1595, 1482, 1359, 1195, 1004 cm⁻¹.

UV/Vis $\lambda_{\text{max}}(\text{MeOH})$ nm (log ε): 305 (1.10), 270 (1.47), 219 (3.55).

CD λ_{max} (c 0.4, MeOH) ($\Delta\epsilon$) nm: 212 (+4.8), 268 (-2.1) and 306 (+0.26).

¹H and ¹³C NMR; Table 1.

HRESIMS: *m/z* [M - H]⁻ calcd for C₁₁H₁₁O₆: 239.0556; found: 239.0558.

5,8-Dihydroxy-7-(hydroxymethyl)-6-methoxyisochroman-1-one (2)

IR (KBr): 3257, 2926, 1755, 1609, 1465, 1361, 1206 cm⁻¹.

UV/Vis $\lambda_{\text{max}}(\text{MeOH})$ nm (log ε): 305 (1.21), 270 (1.47), 219 (3.65).

¹H and ¹³C NMR; Table 1.

HRESIMS: *m/z* [M - H]⁻ calcd for C₁₁H₁₁O₆: 239.0556; found: 239.0549.

8-Hydroxy-6-methoxyisochromane-7-carbaldehyde (3)

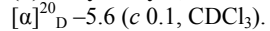
IR (KBr): 3254, 2925, 2848, 2736, 1695, 1602, 1458, 1323, 1193, 1085 cm⁻¹.

UV/Vis $\lambda_{\text{max}}(\text{MeOH})$ nm (log ε): 349 (1.10), 284 (2.89), 206 (3.38).

¹H and ¹³C NMR; Table 1.

HRESIMS: *m/z* [M + H]⁺ calcd for C₁₁H₁₃O₄: 209.0830; found: 209.0839.

(±)-8-Hydroxy-1,6-dimethoxy isochromane-7-carbaldehyde (4)



IR (KBr): 3228, 2947, 2851, 2746, 1705, 1599, 1448, 1356, 1202, 997 cm⁻¹.

UV/Vis $\lambda_{\text{max}}(\text{MeOH})$ nm (log ε): 349 (1.10), 284 (2.89), 206 (3.38).

¹H and ¹³C NMR; Table 1.

HRESIMS: *m/z* [M + H]⁺ calcd for C₁₂H₁₅O₅: 239.2447; found: 239.2445.

Supporting information: Bioassay protocols used, the NMR spectra of compounds **1–4**, the chiral separation picture of compound **4**. These materials are available free of charge via the Internet at <http://www.naturalproduct.us/>.

Acknowledgment - This work was supported by the National Natural Science Fund of China (Nos. 21172204, 41376148 & 81373298), the Natural Science Foundation of Shandong Province (No. 1405-910962180), the NSFC-Shandong Joint Fund for Marine Science Research Centers (No. U1406402), 863 programs of China (Nos. 2012AA092104 & 2013AA092901), and the Special Fund for Marine Scientific Research in the Public Interest of China (No. 201405038).

References

- [1] Lu Z, Wang Y, Miao C, Liu P, Hong K, Zhu W. (2009) Sesquiterpenoids and benzofuranoids from the marine-derived fungus *Aspergillus ustus* 094102. *Journal of Natural Products*, **72**, 1761-1767.
- [2] Lu Z, Zhu H, Fu P, Wang Y, Zhang Z, Lin H, Liu P, Zhuang Y, Hong K, Zhu W. (2010) Cytotoxic polyphenols from the marine-derived fungus *Penicillium expansum*. *Journal of Natural Products*, **73**, 911-914.
- [3] Peng X, Wang Y, Sun K, Liu P, Yin X, Zhu W. (2011) Cerebrosides and 2-pyridone alkaloids from the halotolerant fungus *Penicillium chrysogenum* grown in a hypersaline medium, *Journal of Natural Products*, **74**, 1298-1302.

- [4] Wang J, Lu Z, Liu P, Wang Y, Li J, Hong K, Zhu W. (2012) Cytotoxic polyphenols from the fungus *Penicillium expansum* 091006 endogenous with mangrove plant *Excoecaria agallocha*. *Planta Medica*, **78**, 1861-1866.
- [5] Fan Y, Wang Y, Liu P, Fu P, Zhu T, Wang W, Zhu W. (2013) Indole-diterpenoids with anti-H1N1 activity from the aciduric fungus *Penicillium camemberti* OUCMDZ-1492. *Journal of Natural Products*, **76**, 1328-1336.
- [6] Kong F, Wang Y, Liu P, Dong T, Zhu W. (2014) Thiodiketopiperazines from the marine-derived fungus *Phoma* sp. OUCMDZ-1847. *Journal of Natural Products*, **77**, 132-137.
- [7] Kuramochi K, Tsubaki K, Kuriyama I, Mizushina Y, Yoshida H, Takeuchi T, Kamisuki S, Sugawara F, Kobayashi S. (2013) Synthesis, structure, and cytotoxicity studies of some fungal isochromananes. *Journal of Natural Products*, **76**, 1737-1745.
- [8] Trisuwan K, Rukachaisirikul V, Sukpondma Y, Phongpaichit S, Preedanon S, Sakayaroj J. (2010) Furo [3, 2-h] isochroman, furo [3, 2-h] isoquinoline, isochroman, phenol, pyranone, and pyrone derivatives from the sea fan-derived fungus *Penicillium* sp. PSU-F40. *Tetrahedron*, **66**, 4484-4489.
- [9] Stephens PJ, Pan JJ, Krohn KJ (2007) Determination of the absolute configurations of pharmacological natural products via density functional theory calculations of vibrational circular dichroism: the new cytotoxic iridoid prismatomerin. *Journal of Organic Chemistry*, **72**, 7641-7649.
- [10] Wang WL, Lu ZY, Tao HW, Zhu TJ, Fang YC, Gu QQ, Zhu WM. (2007) Isoechinulin-type alkaloids, variecolorins A-L, from halotolerant *Aspergillus variecolor*. *Journal of Natural Products*, **70**, 1558-1564.
- [11] Nampoothiri SV, Prathapan A, Cherian OL, Raghu KG, Venugopalan VV, Sundaresan A. (2011) *In vitro* antioxidant and inhibitory potential of *Terminalia bellerica* and *Emblica officinalis* fruits against LDL oxidation and key enzymes linked to type 2 diabetes. *Food and Chemical Toxicology*, **49**, 125-131.

Pericocins A–D, New Bioactive Compounds from *Periconia* sp.

Yue-Hua Wu^{a,1}, Gao-Keng Xiao^{a,1}, Guo-Dong Chen^a, Chuan-Xi Wang^a, Dan Hu^a, Yun-Yang Lian^b, Feng Lin^b, Liang-Dong Guo^c, Xin-Sheng Yao^{a,*} and Hao Gao^{a,*}

^aInstitute of Traditional Chinese Medicine and Natural Products, College of Pharmacy, Jinan University, Guangzhou 510632, China

^bFujian Key Laboratory of Screening for Novel Microbial Products, Fujian Institute of Microbiology, Fuzhou 350007, China

^cState Key Laboratory of Mycology, Institute of Microbiology, Chinese Academy of Sciences, Beijing 100190, China

tghao@jnu.edu.cn (H. Gao); tyaoxs@jnu.edu.cn (X.-S. Yao)

Received: September 29th, 2015; Accepted: November 2nd, 2015

One new dihydroisocoumarin, pericocin A (**1**), one new chromone, pericocin B (**2**), and two new α -pyrone derivatives, pericocins C–D (**3–4**), together with two known compounds, 3-(2-oxo-2*H*-pyran-6-yl)propanoic acid (**5**) and (*E*)-3-(2-oxo-2*H*-pyran-6-yl)acrylic acid (**6**), were isolated from the culture of the endolichenic fungus *Periconia* sp.. Their structures were elucidated by spectroscopic methods. All these compounds are derived from the polyketone biosynthetic pathway. Compound **1** was obtained as a mixture of enantiomers. The antimicrobial activity of compounds **1–5** was tested against *Escherichia coli*, *Staphylococcus aureus*, *Aspergillus niger*, and *Candida albicans*. Compounds **1–5** showed moderate antimicrobial activity against *A. niger* and weak activity against *C. albicans*.

Keywords: *Periconia* sp., Endolichenic fungus, Pericocin, Antimicrobial activity.

The *Periconia* genus is a rich source of bioactive compounds, such as cell-adhesion inhibitors (macrosphelides and peribysins) [1a–1d], antimicrobial agents (periconicins) [2a,2b], cytotoxic cytochalasans (periconiasins) [3a], and anti-inflammatory agents (periconianones) [3b]. In our early chemical investigation of a strain of this genus (19-4-2-1), some sesquiterpenes were isolated [3c,3d]. To search for more new bioactive secondary metabolites, a continuing chemical investigation of the strain (19-4-2-1) was carried out, which led to the isolation of four new compounds, pericocins A–D (**1–4**), along with two known compounds, 3-(2-oxo-2*H*-pyran-6-yl)propanoic acid (**5**) and (*E*)-3-(2-oxo-2*H*-pyran-6-yl)acrylic acid (**6**) (Figure 1). Herein, we report the isolation and structure elucidation, together with the antimicrobial activity of **1–5**.

Compound **1** was obtained as a white powder. The HR-ESI-MS showed a quasi-molecular ion peak at *m/z* 271.0587 [$M + Na$]⁺, which indicated that the molecular formula should be $C_{13}H_{12}O_5$ (eight degrees of unsaturation). The ¹³C NMR spectrum showed 13 carbons signals, which was consistent with the deduction of the HRESIMS. Combined with the DEPT-135 experiment, the carbons can be classified into six sp^2 quaternary carbons [including two ester carbonyl/carboxyl carbons (δ_C 171.0, 169.6)], four sp^2 methine carbons, one oxygenated sp^3 methine carbon (δ_C 79.0), one sp^3 methylene carbon (δ_C 33.1), and one methyl carbon (δ_C 15.4). The ¹H NMR spectrum displayed four olefinic/aromatic proton signals [δ_H 7.35 (1H, d, *J* = 7.5 Hz), 6.95 (1H, dd, *J* = 15.7, 4.7 Hz), 6.72 (1H, d, *J* = 7.5 Hz), and 6.16 (1H, d, *J* = 15.6 Hz)], one oxymethine signal [δ_H 5.32 (1H, m)], one methylene signal [δ_H 3.17 (1H, dd, *J* = 16.3, 3.8 Hz), 3.02 (1H, dd, *J* = 16.3, 10.6 Hz)], and one methyl signal [δ_H 2.21 (3H, s)]. All the proton resonances were assigned to relevant carbon atoms through the HSQC experiment. An analysis of the ¹H–¹H COSY spectrum revealed the presence of two isolated spin-systems corresponding to the C-4–C-3–C-9–C-10 and C-5–C-6 subunits. Combined with the ¹H–¹H COSY analysis and

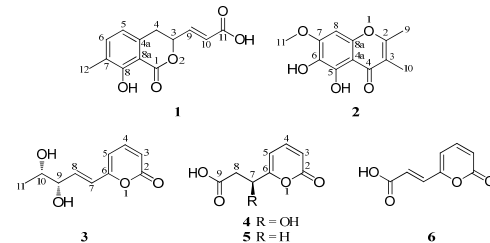


Figure 1: Chemical structures of **1–6**.

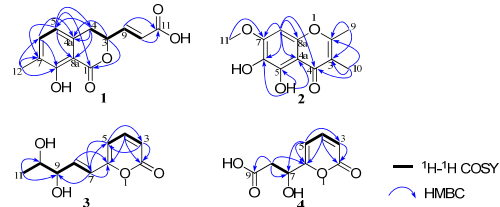


Figure 2: ¹H–¹H COSY and key HMBC correlations of **1–4**.

the molecular formula, the HMBC correlations from H-3 to C-1/C-4a, from Ha-4/Hb-4 to C-4a/C-5/C-8a, from H-5 to C-1/C-4/C-7/C-8a, from H-6 to C-8/C-4a, from H-9/H-10 to C-11, and from H₃-12 to C-6/C-7/C-8 deduced the planar structure of **1**, as shown in Figure 2, and the assignments of all proton and carbon resonances are shown in Table 1. In an optical rotation experiment, compound **1** showed almost no optical activity. Compound **1** displayed a single peak in achiral analytical HPLC, but two peaks (20.8 min with relative peak area of 22.3% and 24.0 min with relative peak area of 77.7%) in chiral HPLC analysis, which indicated that **1** is a mixture of enantiomers. The geometry of the Δ^9 double bond was determined as 9*E* by the value of $^3J_{H-9/H-10}$ (15.7 Hz) observed in the ¹H NMR spectrum. Based on the above analysis, the structure of **1** was established as (*E*)-3-(8-hydroxy-7-methyl-1-oxoisochroman-3-yl)acrylic acid, and named pericocin A.

Compound **2** was obtained as a white powder. The HR-ESI-MS showed a quasi-molecular ion peak at m/z 237.0769 [$M + H$]⁺, which indicated that the molecular formula should be $C_{12}H_{12}O_5$ (seven degrees of unsaturation). The ¹³C NMR spectrum showed 12 carbons signals, which was consistent with the deduction of the HRESIMS. Combined with the DEPT-135 experiment, the carbons can be classified into eight sp^2 quaternary carbons [including one α,β -conjugated keto carbonyl carbon (δ_C 181.4)], one sp^2 methine carbon (δ_C 90.3), one methoxyl carbon (δ_C 56.2), and two methyl carbons (δ_C 18.3, 8.8). The ¹H NMR spectrum displayed one olefinic/aromatic proton signal [δ_H 6.68 (1H, s)], one methoxyl signal [δ_H 3.87 (3H, s)], two methyl signals [δ_H 2.39 (3H, br s), 1.92 (3H, br s)], and two exchangeable hydrogen proton signals [δ_H 12.71 (1H, s), 8.61 (1H, s)]. All the non-exchangeable proton resonances were assigned to relevant carbon atoms through the HSQC experiment. Combined with the molecular formula, the HMBC correlations from H-8 to C-4/C-6/C-7/C-4a/C-8a, from H₃-9 to C-2/C-3, from H₃-10 to C-2/C-3/C-4, from H₃-11 to C-7, and from 5-OH to C-5/C-6/C-4a deduced the structure of **2** as shown in Figure 2; the assignments of all proton and carbon resonances are shown in Table 1. Based on the above analyses, the structure of **2** was established as 5,6-dihydroxy-7-methoxy-2,3-dimethyl-4*H*-chromen-4-one, and named pericocin B.

Compound **3** was obtained as a brown oil. The HR-ESI-MS showed a quasi-molecular ion peak at m/z 197.0809 [$M + H$]⁺, which indicated that the molecular formula should be $C_{10}H_{12}O_4$ (five degrees of unsaturation). The ¹³C NMR spectrum showed 10 carbons signals, which was consistent with the deduction of the HRESIMS. Combined with the DEPT-135 experiment, the carbons can be classified into two sp^2 quaternary carbons, five sp^2 methine carbons, two sp^3 oxygenated methine carbons (δ_C 76.6, 71.5), and one methyl carbon (δ_C 18.9). The ¹H NMR spectrum displayed five olefinic/aromatic proton signals [δ_H 7.50 (1H, dd, J = 9.2, 6.7 Hz), 6.74 (1H, dd, J = 15.7, 5.4 Hz), 6.38 (1H, d, J = 15.7 Hz), 6.30 (1H, d, J = 6.7 Hz), and 6.22 (1H, d, J = 9.3 Hz)], two oxymethine signals [δ_H 4.09 (1H, br t, J = 5.0 Hz), 3.72 (1H, quint, J = 6.3 Hz)], and one methyl signal [δ_H 1.18 (3H, d, J = 6.4 Hz)]. All the proton resonances were assigned to relevant carbon atoms through the HSQC experiment. An analysis of the ¹H-¹H COSY spectrum revealed the presence of two isolated spin-systems corresponding to the C-3-C-4-C-5 and C-7-C-8-C-9-C-10-C-11 subunits. When **3** was tested in DMSO-*d*₆ (Table S4, Supporting Information), exchangeable protons were observed and two additional spin-systems (H-9 and 9-OH, H-10 and 10-OH) were revealed. Combined with the ¹H-¹H COSY analysis, the molecular formula, and the HMBC correlations from H-3 to C-2/C-5, from H-4 to C-2/C-6, from H-5 to C-3/C-7, from H-7 to C-5/C-6/C-9, from H-8 to C-6, and from H₃-11 to C-9/C-10 deduced the planar structure of **3** as shown in Figure 2; the assignments of all proton and carbon resonances are shown in Table 1.

The geometry of the Δ^7 double bond was determined as 7*E* by the value of $^3J_{H_7/H_8}$ (15.7 Hz) observed in the ¹H NMR spectrum. In the ROESY experiment in DMSO-*d*₆ (Table S4, Supporting Information), the observed correlations between H-9 and 10-OH/H₃-11, between H₃-11 and H-8, and between H-10 and 9-OH/H-8 signified that the relative configuration of **3** was *threo* (Figure 3), combined with the value of $^3J_{H_9/H_{10}}$ (6.1 Hz). The absolute configuration of the 9,10-diol moiety in **3** was determined by the *in situ* dimolybdenum CD method. On addition of Mo₂(OAc)₄ to a solution of **3** in DMSO, a metal complex as an auxiliary chromophore was produced. The induced CD of the complex was obtained by subtracting the inherent CD. The observed sign of the

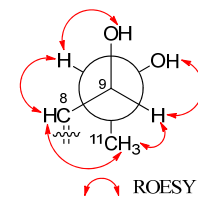


Figure 3: key ROESY correlations in DMSO-*d*₆ of **3**.

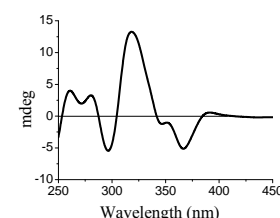


Figure 4: CD spectrum of **3** in DMSO containing Mo₂(OAc)₄ with the inherent CD spectrum subtracted.

Cotton effect in the induced spectrum comes from the chirality of the vic-diol moiety expressed by the sign of the O-C-C-O torsion angle. In this study, positive Cotton effects were observed at 310 and 400 nm, respectively. The induced CD spectrum (Figure 4) permitted the assignment of 9*S* and 10*S* on the basis of the empirical rule proposed by Snatzke [4a,b]. Thus, the structure of **3** was established as 6-((3*S*,4*S*,*E*)-3,4-dihydroxypent-1-en-1-yl)-2*H*-pyran-2-one, and named pericocin C.

Compound **4** was obtained as a brown oil. The HR-ESI-MS showed a quasi-molecular ion peak at m/z 185.0447 [$M + H$]⁺, which indicated that the molecular formula should be $C_8H_9O_5$ (five degrees of unsaturation). The ¹³C NMR spectrum showed 8 carbon signals, which was consistent with the deduction of the HRESIMS. Combined with the DEPT-135 experiment, the carbons can be classified into three sp^2 quaternary carbons, three sp^2 methine carbons, one oxygenated sp^3 methine carbon (δ_C 68.3), and one sp^3 methylene carbon (δ_C 40.9). The ¹H NMR spectrum displayed three olefinic/aromatic proton signals [δ_H 7.52 (1H, dd, J = 9.3, 6.6 Hz), 6.45 (1H, d, J = 6.6 Hz), and 6.22 (1H, d, J = 9.3 Hz)], one oxymethine signal [δ_H 4.80 (1H, dd, J = 8.6, 4.4 Hz)], and one methylene signal [δ_H 2.82 (1H, dd, J = 15.7, 4.4 Hz), 2.63 (1H, dd, J = 15.7, 8.6 Hz)]. All the proton resonances were assigned to relevant carbon atoms through the HSQC experiment. An analysis of the ¹H-¹H COSY spectrum revealed the presence of two isolated spin-systems corresponding to the C-3-C-4-C-5 and C-7-C-8 subunits. Combined with the ¹H-¹H COSY analysis and the molecular formula, the HMBC correlations from H-3 to C-2, from H-4 to C-2/C-6, from H-5 to C-3/C-6/C-7, and from H₂-8 to C-6/C-7/C-9 deduced the planar structure of **4** as shown in Figure 2; the assignments of all proton and carbon resonances are shown in Table 1.

The absolute configuration at C-7 of compound **4** was assigned by comparison of the Cotton effect and specific rotation with those of nodulisporipyrone A [5a], whose absolute configuration at C-7 was *R*. The CD spectrum of nodulisporipyrone A showed a positive Cotton effect at 280 nm, whereas a negative Cotton effect was seen in the CD spectrum of **4**. Likewise, nodulisporipyrone A showed a positive specific rotation ($[\alpha]_D^{23} +67.6$), whereas **4** gave a negative value ($[\alpha]_D^{27} -49.7$). Therefore, the absolute configuration of **4** was assigned as 7*S*. Based on the above analyses, the structure of **4** was established as (S)-3-hydroxy-3-(2-oxo-2*H*-pyran-6-yl)propanoic acid, and named pericocin D.

Table 1: ^1H NMR and ^{13}C NMR data of **1–4** (δ in ppm, J in Hz).

No.	1 (CD ₃ OD)		2 (DMSO- <i>d</i> ₆)		3 (CD ₃ OD)		4 (CD ₃ OD)	
	δ_{C} (150 MHz)	δ_{H} (600 MHz)	δ_{C} (100 MHz)	δ_{H} (400 MHz)	δ_{C} (100 MHz)	δ_{H} (400 MHz)	δ_{C} (100 MHz)	δ_{H} (400 MHz)
1	171.0							
2			163.3		164.1		164.1	
3	79.0	5.32, m		113.6	114.9	6.22, d (9.3)	114.9	6.22, d (9.3)
4	33.1	3.17, dd (16.3, 3.8), Ha 3.02, dd (16.3, 10.6), Hb		181.4	146.4	7.50, dd (9.2, 6.7)	146.1	7.52, dd (9.3, 6.6)
4a	137.7			104.0				
5	118.8	6.72, d (7.5)		146.0	106.1	6.30, d (6.7)	103.2	6.45, d (6.6)
6	138.4	7.35, d (7.5)		129.5	160.6		167.5	
7	126.3			154.2	123.1	6.38, d (15.7)	68.3	4.80, dd (8.6, 4.4)
8	161.5			90.3	6.68, s	138.7	6.74, dd (15.7, 5.4)	40.9
8a	108.6			149.6				
9	144.1	6.95, dd (15.7, 4.7)		18.3	2.39, br s	76.6	4.09, br t (5.0)	173.9
10	124.9	6.16, d (15.6)		8.8	1.92, br s	71.5	3.72, quint (6.3)	
11	169.6			56.2	3.87, s	18.9	1.18, d (6.4)	
12	15.4	2.21, s						
5-OH					12.71, s			
6-OH					8.61, s			

The structures of 3-(2-oxo-2*H*-pyran-6-yl)propanoic acid (**5**), and (*E*)-3-(2-oxo-2*H*-pyran-6-yl)acrylic acid (**6**) were confirmed by comparison of their NMR data with literature values [5b,6a]. Compounds **1–5** were tested for antimicrobial activity against *Escherichia coli*, *Staphylococcus aureus*, *Aspergillus niger*, and *Candida albicans*, using tobramycin (bacteria) and cycloheximide (fungi) as the positive controls. Compounds **1–5** displayed moderate activities against *A. niger* and weak activities against *C. albicans* (Table 2).

Table 2: Antimicrobial activity of **1–5** (MIC, $\mu\text{g/mL}$).

compounds	Bacteria		Fungi	
	<i>S. aureus</i>	<i>E. coli</i>	<i>A. niger</i>	<i>C. albicans</i>
1	>1000	>1000	31	500
2	>1000	>1000	31	500
3	>1000	>1000	31	500
4	>1000	>1000	31	500
5	>1000	>1000	31	500
Tobramycin ^a	<16	<16	nt	nt
Cycloheximide ^b	nt	nt	<16	<16

^aPositive control (bacteria). ^bPositive control (fungi). nt: not tested

This work reports the isolation of six metabolites, including four new compounds {one dihydroisocoumarin (**1**), one chromone (**2**), and two α -pyrone derivatives (**3–4**)}, and two known compounds (α -pyrone derivatives (**5–6**)). To our best knowledge, compounds **3–6** are the first α -pyrone derivatives from *Periconia* fungi.

Experimental

General: UV, JASCO V-550 UV/Vis spectrophotometer; IR, JASCO FT/IR-480 plus Fourier transform infrared spectrometer; HR-ESI-MS, Waters Synapt G2 TOF mass spectrometer; NMR, Bruker AV-400 and Bruker AV-600 spectrometers; CC, Sephadex LH-20 (Pharmacia) and ODS (60–80 mm, YMC); TLC, precoated silica gel plates (SGF₂₅₄, 0.2 mm, Yantai Chemical Industry Research Institute). The analytical HPLC was performed on a Shimadzu HPLC system equipped with a LC-20AB pump, and a SPD-20A diode array detector (Shimadzu) using a Phenomenex Gemini C18 column (5 μm , 4.6 mm \times 250 mm, Phenomenex Inc.). The chiral analytical HPLC was performed on a Shimadzu HPLC system equipped with a LC-20AB pump, and a SPD-20A diode array detector (Shimadzu) using a Phenomenex Lux Amylose-2 column (5 μm , 4.6 mm \times 250 mm, Phenomenex Inc.) at 1.0 ml/min under 60%MeOH-H₂O (0.1%HCOOH). The semi-preparative HPLC was performed on a Shimadzu LC-6AD system equipped with an LC-6AD pump and a SPD-M20A detector (Shimadzu), using a YMC Park ODS-A column (5 μm , 10 mm \times 250 mm, YMC).

Fungal material: The strain of *Periconia* sp. (No.19-4-2-1) was isolated by one of the authors (L.D. Guo) from the lichen *Parmelia* sp. collected from Changbai Mountain, Jilin Province, China, in August 2006. The fungus strain was identified as *Periconia* sp. based on the morphological characteristics and sequence analysis of the internal transcribed spacer (ITS) regions ITS1-5.8S-ITS2 (GenBank accession No. KP873157). The strain was assigned the accession number 19-4-2-1 in the culture collection at the Institute of Traditional Chinese Medicine and Natural Products, College of Pharmacy, Jinan University, Guangzhou. The fungus was cultured on slants of potato dextrose agar at 25°C for 5 days. Agar plugs were used to inoculate 4 Erlenmeyer flasks (250 mL), each containing 100 mL of potato dextrose broth. Four flasks of the inoculated media were incubated at 25°C on a rotary shaker at 200 rpm for 5 days to prepare the seed culture. Fermentation was carried out in 20 Erlenmeyer flasks (500 mL), each containing 70 g of rice. Distilled H₂O (105 mL) was added to each flask, and the rice was soaked overnight before autoclaving at 120°C for 30 min. After cooling to room temperature, each flask was inoculated with 5.0 mL of the spore inoculum and incubated at room temperature for 45 days.

Extraction and isolation: The culture was extracted thrice with EtOAc, and the organic solvent was evaporated to dryness under vacuum to afford a crude extract (33.4 g). This was dissolved in 90%, v/v, aqueous MeOH (500 mL) and partitioned against the same volume of cyclohexane to afford a cyclohexane fraction (C, 24.5 g) and an aqueous MeOH fraction (W, 8.7 g). The aqueous MeOH fraction (W, 8.7 g) was separated by ODS CC eluting with MeOH-H₂O (30:70, 50:50, 70:30, and 100:0, v/v) to afford 4 fractions (W1 to W4). Fraction W2 (2.3 g) was subjected to ODS CC with a gradient of MeOH-H₂O (35:65, 40:60, 45:55, 50:50, 55:45, and 100:0 v/v) to give 8 sub-fractions (W2a–W2h). Sub-fraction W2e (533.6 mg) was separated by Sephadex LH-20 (MeOH) and semi-preparative HPLC (55% MeOH-H₂O) to yield **1** (5.3 mg). Purification of sub-fraction W2d (199.9 mg) was carried out by Sephadex LH-20 (MeOH) and semi-preparative HPLC (45% MeOH-H₂O) to yield **2** (6.9 mg). Fraction W1 (1.96 g) was subjected to ODS CC with a gradient of MeOH-H₂O (10:90, 15:85, 20:80, 25:75, 30:70, 35:65, 40:60, 45:55, and 100:0 v/v) to give 6 sub-fractions (W1a–W1f). Sub-fraction W1a (392.2 mg) was purified by semi-preparative HPLC (15% MeOH-H₂O) to yield **3** (29.9 mg), **4** (13.1 mg), **5** (35.5 mg), and **6** (3.5 mg).

Pericocin A (**1**)

White powder.

IR (KBr): 1698, 1676, 1427, 1287, 1138, 974 cm⁻¹.

UV (MeOH) λ_{max} (log ϵ): 210 (4.20), 252 (3.58), 320 (3.36) nm.

¹H and ¹³C NMR: Table 1.

HR-ESI-MS: *m/z* 271.0587 [M + Na]⁺ (calcd for C₁₃H₁₂O₅Na, 271.0582).

Pericocin B (2)

White powder.

IR (KBr): 3566, 3472, 1671, 1484, 1250, 1094, 803 cm⁻¹.

UV (MeOH) λ_{max} (log ε): 211 (4.27), 240 (4.05), 295 (3.75) nm.

¹H and ¹³C NMR: Table 1.

HR-ESI-MS: *m/z* 237.0769 [M + H]⁺ (calcd for C₁₂H₁₃O₅, 237.0763).

Pericocin C (3)

Brown oil.

[α]_D²⁷: +9.9 (c 1.0, MeOH).

IR (KBr): 3429, 2979, 1712, 1650, 1538, 1378, 1110, 804 cm⁻¹.

UV (MeOH) λ_{max} (log ε): 205 (3.98), 229 (3.96), 327 (3.90) nm.

¹H and ¹³C NMR: Table 1.

HR-ESI-MS: *m/z* 197.0809 [M + H]⁺ (calcd for C₁₀H₁₃O₄, 197.0814).

Pericocin D (4)

Brown oil.

[α]_D²⁷: -49.7 (c 1.0, MeOH).

IR (KBr): 3401, 1716, 1634, 1558, 1402, 813 cm⁻¹.

UV (MeOH) λ_{max} (log ε): 204 (3.22), 297 (3.41) nm.

CD (*c* 2.0 × 10⁻⁴ M, MeOH) λ_{max} (Δε): 231 (-0.85), 286 (-3.39).

¹H and ¹³C NMR: Table 1.

HR-ESI-MS: *m/z* 185.0447 [M + H]⁺ (calcd for C₈H₉O₅, 185.0450).

References

- [1] (a) Yamada T, Iritani M, Doi M, Minoura K, Ito T, Numata A. (2001) Absolute stereostructures of cell-adhesion inhibitors, macrosphelides C, E-G and I, produced by a *Periconia* species separated from an *Aplysia* sea hare. *Journal of the Chemical Society, Perkin Transactions 1*, 3046-3053; (b) Yamada T, Iritani M, Minoura K, Numata A. (2002) Absolute stereostructures of cell adhesion inhibitors, macrosphelides H and L, from *Periconia byssoides* OUPS-N133. *The Journal of Antibiotics*, **55**, 147-154; (c) Yamada T, Iritani M, Minoura K, Kawai K, Numata A. (2004) Peribysins A-D, potent cell-adhesion inhibitors from a sea hare-derived culture of *Periconia* species. *Organic and Biomolecular Chemistry*, **2**, 2131-2135; (d) Yamada T, Doi M, Miura A, Harada W, Hiramura M, Minoura K, Tanaka R, Numata A. (2005) Absolute stereostructures of cell-adhesion inhibitors, peribysins A, E, F and G, produced by a sea hare-derived *Periconia* sp. *The Journal of Antibiotics*, **58**, 185-191.
- [2] (a) Kim S, Shin DS, Lee T, Oh KB. (2004) Periconicins, two new fusicoccane diterpenes produced by an endophytic fungus *Periconia* sp. with antibacterial activity. *Journal of Natural Products*, **67**, 448-450; (b) Shin DS, Oh MN, Yang HC, Oh KB. (2005) Biological characterization of periconicins, bioactive secondary metabolites, produced by *Periconia* sp. OBW-15. *Journal of Microbiology and Biotechnology*, **15**, 216-220.
- [3] (a) Zhang D, Ge H, Xie D, Chen R, Zou JH, Tao X, Dai J. (2013) Periconiasins A-C, new cytotoxic cytochalasans with an unprecedented 9/6/5 tricyclic ring system from endophytic fungus *Periconia* sp. *Organic Letters*, **15**, 1674-1677; (b) Zhang D, Ge H, Zou JH, Tao X, Chen R, Dai J. (2014) Periconianone A, a new 6/6/6 carbocyclic sesquiterpenoid from endophytic fungus *Periconia* sp. with neural anti-inflammatory activity. *Organic Letters*, **16**, 1410-1413; (c) Wu YH, Chen GD, Wang CX, Hu D, Li XX, Lian YY, Lin F, Guo LD, Gao H. (2015) Pericoterpenoid A, a new bioactive cadinane-type sesquiterpene from *Periconia* sp. *Journal of Asian Natural Products Research*, **17**, 671-675; (d) Wu YH, Chen GD, He RR, Wang CX, Hu D, Wang GQ, Guo LD, Yao XS, Gao H. (2015) Pericolactines A-C, a new class of diterpenoid alkaloids with unusual tetracyclic skeleton. *Scientific Reports*, **5**, 17082.
- [4] (a) Bari LD, Pescitelli G, Pratelli, C, Pini D, Salvadori P. (2001) Determination of absolute configuration of acyclic 1,2-diols with Mo₂(OAc)₄. 1. Snatzke's method revisited. *Journal of Organic Chemistry*, **66**, 4819-4825; (b) Gorecki M, Jablonska E, Kruszewska A, Suszczynska A, Urbanczyk-Lipkowska Z, Gerards M, Morzycki JW, Szczepak WJ, Frelek J. (2007) Practical method of the absolute configuration assignment of tert/tert 1,2-diols using their complexes with Mo₂(OAc)₄. *Journal of Organic Chemistry*, **72**, 2906-2916.
- [5] (a) Zhao Q, Wang CX, Yu Y, Wang GQ, Zheng QC, Chen GD, Lian YY, Lin F, Guo LD, Gao H. (2015) Nodulisporipyrones A-D, new bioactive α-pyrone derivatives from *Nodulisporium* sp. *Journal of Asian Natural Products Research*, **17**, 567-575; (b) Poole PR, Whitaker G. (1997) Biotransformation of 6-pentyl-2-pyrone by *Botrytis cinerea* in liquid cultures. *Journal of Agricultural and Food Chemistry*, **45**, 249-252.
- [6] (a) Cooney JM, Lauren DR. (1999) Biotransformation of the *Trichoderma* metabolite 6-*n*-pentyl-2H-pyran-2-one (6PAP) by selected fungal isolates. *Journal of Natural Products*, **62**, 681-683; (b) Groblacher B, Maier V, Kunert O, Bucar F. (2012) Putative mycobacterial efflux inhibitors from the seeds of *Aframomum melegueta*. *Journal of Natural Products*, **75**, 1393-1399; (c) Shen CC, Syu WJ, Li SY, Lin CH, Lee GH, Sun CM. (2002) Antimicrobial activities of naphthazarins from *Arnebia euchroma*. *Journal of Natural Products*, **65**, 1857-1862.

New Benzenoids from the Roots of *Lindera aggregata*Guo-Hao Ma^{a,#}, Che-Wei Lin^{a,#}, Hsin-Yi Hung^b, Sheng-Yang Wang^c, Po-Chuen Shieh^d and Tian-Shung Wu^{b,d*}^aDepartment of Chemistry, National Cheng Kung University, Tainan, 701, Taiwan^bSchool of Pharmacy, National Cheng Kung University Hospital, College of Medicine, National Cheng Kung University, Tainan, 701, Taiwan^cCore Laboratory of Plant Metabolomics, Biotechnology Center and Department of Forestry, National Chung Hsing University, Kou Kung Road, Taichung 402, Taiwan^dDepartment of Pharmacy, Tajen University, Pintung 907, Taiwan

#The authors contributed equally to this work.

tswu@mail.ncku.edu.tw

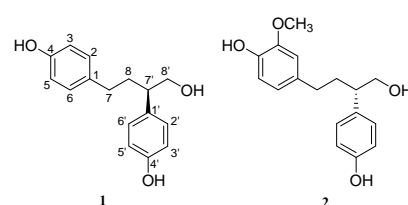
Received: October 8th, 2015; Accepted: October 22nd, 2015

Two new benzenoids, linderagatin A and B (**1-2**), were isolated from the roots of *Lindera aggregata*. Their structures were elucidated on the basis of 1D (¹H, ¹³C) and 2D NMR (COSY, NOESY, HSQC and HMBC) spectra. Moreover, their absolute configurations were established from ECD spectra compared with previous reports.

Keywords: *Lindera aggregata*, Lauraceae, Benzenoids, NMR spectroscopy, ECD.

Lindera aggregata (Sims) Kosterm (Lauraceae), also known as Wu Yao, a famous traditional Chinese medicine, has been used to treat abdominal distension and pain, acute asthma, and rheumatic diseases [1, 2]. In addition, recent studies showed the plant has other pharmacological effects, such as antioxidant [3], increased insulin sensitivity [3], anti-tumor [4] and anti-inflammatory [5]. Previous phytochemical studies on Wu Yao have led to the isolation of sesquiterpenes [6], alkaloids [7, 8], flavonoids [9] and lignans [10]. In this study, two new benzenoids, linderagatin-A (**1**) and linderagatin-B (**2**), were isolated from *L. aggregata*, as well as 27 known compounds, *N-trans*-feruloyltyramine (**3**) [11], *N-cis*-feruloyltyramine (**4**) [11], *N-trans*-feruloylmethoxytyramine (**5**) [12], thalifoline (**6**) [13], yuzirine (**7**) [14], linderagrigrine-A (**8**) [8], northalifoline (**9**) [15], (+)-boldine (**10**) [16], (+)-*N*-methyllaurotetanine (**11**) [17], (+)-isoboldine (**12**) [11], 3-hydroxy-1-(4-hydroxyphenyl)propan-1-one (**13**) [18], *p*-hydroxybenzoic acid (**14**) [12], 4-hydroxy-3-methoxy acetophenone (**15**) [19], methyl 3,5-dimethoxy-4-hydroxy-benzoate (**16**) [20], vanillic acid (**17**) [12], tyrosol (**18**) [21], 2-(4-hydroxy-3-methoxyphenyl)ethanol (**19**) [22], 2-(4-hydroxy-3,5-dimethoxyphenyl)ethanol (**20**) [23], 3-hydroxy-1-(4-hydroxyphenyl)propan-1-one (**21**) [18], rel-(2 α , 3 β)-7-*O*-methylcedrusin (**22**) [24], (-)-lyoniresinol (**23**) [25], hydroxylindestrenolide (**24**) [6], 2,6-dimethoxy-*p*-quinone (**25**) [26], evofolin-B(**26**) [27], (-)-boscialin (**27**) [28], methyl dihydrophaseate (**28**) [29], and 6'-*O*-vanilloyltachioside (**29**) [30]. Here, we report the structure elucidation of the two new benzenoids.

Linderagatin-A (**1**) was obtained as a colorless powder. Its molecular formula was determined as C₁₆H₁₈O₃ on the basis of its positive HRESIMS (*m/z* 281.1153 [M + Na]⁺; calc. 281.1154). The complete ¹H and ¹³C NMR data are shown in Table 1. The ¹H NMR spectrum showed two sets of AA'XX' systems at δ_H 7.07 (2H, d, *J* = 8.4 Hz, H-2', 6'), 6.79 (2H, d, *J* = 8.4 Hz, H-3', 5'), as well as signals at 6.94 (2H, d, *J* = 8.4 Hz, H-2, 6) and 6.72 (2H, d, *J* = 8.4 Hz, H-3, 5). Furthermore, two methylene groups at δ_H 3.60 (2H, m, H-8') and 2.37 (2H, m, H-7), and a methine group at δ_H 2.64 (1H, m,

Figure 1: Structure of compounds **1-2**.Table 1: ¹H and ¹³C NMR spectroscopic data of compounds **1** (acetone-*d*₆) and **2** (CDCl₃).

position	1^a	2^b
	δ _C	δ _H (<i>J</i> in Hz)
1	134.1	133.9
2	130.0	6.94 d (8.4)
3	115.8	6.72 d (8.4)
3-OCH ₃		55.9
4	156.2	143.6
5	115.8	6.72 d (8.4)
6	130.0	6.94 d (8.4)
7	33.3	2.37 m
8a	35.2	2.11 m
8b		1.76 m
1'	134.7	134.0
2'	129.8	7.07 d (8.4)
3'	115.9	6.79 d (8.4)
4'	156.6	154.4
5'	115.9	6.79 d (8.4)
6'	129.8	7.07 d (8.4)
7'	48.3	2.64 m
8'	67.9	3.60 m
		47.1
		67.7
		3.69 m

H-7') were found, while methylenes at δ_H 2.11 (1H, m, H-8a) and 1.76 (2H, m, H-8b) were observed in the ¹H NMR and HSQC spectra. Moreover, the COSY spectrum showed correlations that indicated the presence of the spin systems H-7, H-8, H-7' and H-8' with a partial -CH₂CH₂(CH)CH₂OH structure. In the HMBC experiment, the signal at δ_H 6.94 (H-2, 6) correlated with the carbons at δ_C 33.3 (C-7), and the signal at δ_H 7.07 (H-2', 6') correlated with δ_C 48.3 (C-7'). The above results showed that C-7

and C-7' are substituted with a *p*-hydroxybenzyl group. Furthermore, the absolute configuration of **1** was determined from the ECD spectrum, in which positive Cotton effects at 206, 212 and 217 nm suggested that the absolute configuration at C-7' of **1** is opposite to that of *S*(+)-2-phenyl-1-butanol. Therefore, the absolute configuration at C-7' were determined as 7'R. [31].

Linderagatin-B (**2**) was isolated as colorless syrup and its molecular formula was determined to be C₁₇H₂₀O₄ on the basis of its positive HRESIMS (*m/z* 311.1261 [M + Na]⁺; calc. 311.1259). The ¹H and ¹³C NMR spectra of **2** (Table 1) were similar to those of **1**, except for the H-3 proton being replaced by a methoxyl group, the signal for which was observed at δ_H 3.85 (s, 3-OCH₃) in the ¹H NMR spectrum and at δ_C 55.9 (3-OCH₃) in the ¹³C NMR spectrum. In the HMBC spectrum, the proton signal at δ_H 6.59 (H-2) correlated with carbons at δ_C 33.1 (C-7), and HMBC correlations of peaks at δ_H 7.10 (H-2') with δ_C 47.1 (C-7') were also found. The above results showed that C-7 and C-7' are substituted with a benzyl group. In addition, the proton signals at δ_H 6.59 (H-2) and 6.60 (H-6) were correlated with carbon at δ_C 143.6 (C-4) in the HMBC spectrum. And the proton signals at δ_H 3.85 (3-OCH₃) and 6.80 (H-5) were correlated with carbon at δ_C 146.3 (C-3). The methoxy group was thus assigned at C-3 by the NOESY correlation between δ_H 6.59 (H-2) and the methyl signal at δ_H 3.85 (3H, s, 3-OCH₃). The absolute configuration of **2** at C-7' was assigned from the ECD spectrum, which showed negative Cotton effects at 207, 212, and 219 nm similar to those of *S*(+)-2-phenyl-1-butanol in ethanol, indicating a 7'S configuration. [31]

Experimental

General: Optical rotations were measured with a JASCO P-2000 digital polarimeter in a 0.5 dm cell. UV spectra were obtained with a Hitachi UV-3210 spectrophotometer, and IR spectra with a Shimadzu FTIR Prestige-21 spectrometer. The ECD spectra were recorded on a JASCO J-720 spectrometer, and the ¹H and ¹³C NMR spectra on a Bruker AVIII-400 with TMS as the internal reference, and chemical shifts expressed in δ (ppm). The ESIMS and HRESIMS were taken on a Bruker Daltonics APEX II 30e spectrometer. Silica gel (70–230 and 230–400 mesh; Merck) and Diaion HP-20 resin (Mitsubishi, Chemical, Tokyo, Japan) were used for column chromatography (CC), and silica gel 60 F₂₅₄ (Merck) for TLC.

Plant material: The roots of *Lindera aggregata* were collected from Huisun Forest Area, Ren Ai Township, Nantou County, Taiwan. The plant material was identified and authenticated by Assoc. Prof. Dr Chang-Sheng Kuoh, Department of Life Sciences, National Cheng Kung University. A voucher specimen (TSWu-20100601) was deposited in the Department of Chemistry, Natural Cheng Kung University, Tainan, Taiwan.

Extraction and isolation: The ground air-dried whole plants of *L. aggregata* (12.5 kg) were extracted with MeOH at 60°C by refluxing for 8 h. The MeOH extracts were combined and evaporated under reduced pressure to give ca. 1160 g residue.

References

- [1] Gan LS, Zheng YL, Mo JX, Liu X, Li XH, Zhou CX. (2009) Sesquiterpene lactones from the root tubers of *Lindera aggregata*. *Journal of Natural Product*, **72**, 1497–1501.
- [2] Cheng XL, Ma SC, Wei F, Wang GL, Xiao XY, Lin RC. (2007) A new sesquiterpene isolated from *Lindera aggregata* (Sims) Kosterm. *Chemical and Pharmaceutical Bulletin*, **55**, 1390–1392.
- [3] Wang F, Gao Y, Zhang L, Bai B, Hu YN, Dong ZJ, Zhai QW, Zhu HJ, Liu JK. (2010) A pair of windmill-shaped enantiomers from *Lindera aggregata* with activity toward improvement of insulin sensitivity. *Organic Letters*, **12**, 3196–3199.

The residue was suspended in water and then partitioned with EtOAc. After removing the solvent, the EtOAc-soluble portion (340 g) underwent partition extraction with 5% aqueous HCl solution. The HCl-aqueous solution was treated with 5% NH₄OH_(aq) to obtain a phase with pH 9 and then extracted with EtOAc. The organic layer was evaporated under reduced pressure to yield an alkaloid fraction residue (40 g). This was subjected to CC over silica gel and eluted with *n*-hexane and acetone by step gradients to afford 16 fractions on the basis of TLC analysis. Fraction 11 was separated by CC with benzene–ethyl acetate (19:1) to afford **15** (1.4 mg), **16** (7.7 mg), **24** (4.9 mg), and **25** (4.9 mg). Separation of fraction 13 was performed by silica gel chromatography with CHCl₃–MeOH (20:1) to give **1** (4.0 mg), **2** (2.3 mg), **3** (6.5 mg), **4** (2.2 mg), **5** (13.1 mg), **6** (1.4 mg), **7** (3.2 mg), **14** (0.8 mg), **17** (3.5 mg), **18** (5.3 mg), **19** (2.6 mg), **20** (2.7 mg), **21** (1.6 mg), **22** (8.6 mg), **26** (2.1 mg), **27** (14.9 mg), and **28** (3.0 mg). Fraction 14 was purified by CC with CHCl₃–MeOH (15:1) to afford **9** (4.7 mg) and **23** (3.4 mg). Fraction 15 was purified by CC with CHCl₃–MeOH (9:1) to give **10** (93.2 mg), **11** (5.4 mg), **12** (6.0 mg) and **29** (2.1 mg).

Linderagatin-A (**1**)

Colorless powder;

[α]_D: +99.0 (c 0.20, MeOH)

CD[θ]: [θ]₁₉₆+405, [θ]₁₉₉−61, [θ]₂₀₃−91, [θ]₂₀₆ +71, [θ]₂₁₀−413, [θ]₂₁₂ +329, [θ]₂₁₅ +423, [θ]₂₁₇+337, [θ]₂₂₄−133, [θ]₂₃₁ +175, [θ]₂₃₆+163, [θ]₂₄₀−113, [θ]₂₅₁+123, [θ]₂₆₇+153, [θ]₂₈₀+1380, [θ]₂₈₇+1602 (c 7.4 × 10^{−4}, EtOH)

IR ν_{max} (KBr) cm^{−1}: 3356, 2924, 2854, 1652, 1458 cm^{−1}.

UV (MeOH): λ_{max} (log ε): 218 (3.6), 229 (3.5, sh), 273 (3.5), 282 (3.4, sh) nm.

¹H and ¹³C NMR: Table 1.

ESI-MS *m/z* (rel. int. %): 281([M+Na]⁺)

HR ESI-MS *m/z* (rel. int. %): 281.1153 ([M+Na]⁺) (calcd for C₁₆H₁₈O₃Na, 281.1154).

Linderagatin-B (**2**)

Colorless powder.

[α]_D: −58.3 (c 0.11, MeOH).

CD[θ]: [θ]₁₉₆+300, [θ]₁₉₉−191, [θ]₂₀₂+167, [θ]₂₀₇−148, [θ]₂₁₀−413, [θ]₂₁₂−295, [θ]₂₁₉−64, [θ]₂₂₄+532, [θ]₂₂₉+671, [θ]₂₄₁−369, [θ]₂₅₂+161, [θ]₂₅₆+159, [θ]₂₆₉+300, [θ]₂₈₄+300, [θ]₂₉₃+300 (c 4.9 × 10^{−4}, EtOH)

IR ν_{max} (KBr) cm^{−1}: 3333, 2928, 2855, 1608, 1454 cm^{−1}

UV (MeOH): λ_{max} (log ε): 217 (3.8), 232 (3.7, sh), 277 (3.6) nm.

¹H and ¹³C NMR: Table 1.

ESI-MS *m/z* (rel. int. %): 331([M+Na]⁺)

HR ESI-MS *m/z* (rel. int. %): 311.1261 ([M+Na]⁺) (calcd for C₁₇H₂₀O₄Na, 311.1259).

Supplementary data: NMR spectra (¹H and ¹³C NMR, COSY, NOESY, HSQC, and HMBC) for compounds **1** and **2**.

Acknowledgments – Financial support for this work was provided by the Ministry of Science and Technology of R.O.C. Special thanks Dr Wu, Yi-Hung, Experimental Forest, National Chung Hsing University, for collecting the plant material.

- [4] Lin CT, Chu FH, Chang ST, Chueh PJ, Su YC, Wu KT, Wang SY. (2007) Secoaggregatalactone-A from *Lindera aggregata* induces apoptosis in human hepatoma hep G2 cells. *Planta Medica*, **73**, 1548-1553.
- [5] Zhang CF, Sun QS, Wang ZT, Chou GX. (2001) Studies on constituents of the leaves of *Lindera aggregata* (Sims) Kosterm. *Zhongguo Zhong Yao Za Zhi*, **26**, 765-767.
- [6] Kouno I, Hirai A, Jiang ZH, Tanaka T. (1997) Bisequiterpenoid from the root of *Lindera strychnifolia*. *Phytochemistry*, **46**, 1283-1284.
- [7] Kazuka M, Yoshikawa M, Sawada T. (1984) Alkaloids From *Lindera strychnifolia*. *Journal of Natural Products*, **47**, 1063-1063.
- [8] Kuo PC, Li YC, Hwang TL, Ma GH, Yang ML, Lee EJ, Wu TS. (2014) Synthesis and structural characterization of an anti-inflammatory principle purified from *Lindera aggregata*. *Tetrahedron Letters*, **55**, 108-110.
- [9] Zhang CF, Sun QS, Zhao YY, Zheng W. (2001) Studies on flavonoids from leaves of *Lindera aggregata* (Sims) Kosterm. *Chinese Journal of Medicinal Chemistry*, 274-276.
- [10] Ichino K, Tanaka H, Ito K. (1988) A lignan from *Lindera praecox*. *Phytochemistry*, **27**, 1906-1907.
- [11] Chang YC, Chen CY, Chang FR, Wu YC. (2001) Alkaloids from *Lindera glauca*. *Journal of the Chinese Chemical Society*, **48**, 811-815.
- [12] Chen CY, Wang YD, Wang HM. (2010) Chemical constituents from the roots of *Synsepalum dulcificum*. *Chemistry of Natural Compounds*, **46**, 448-449.
- [13] Lia Q, Zhang SQ, Wang SC, Zhoua MZ. (2009) Efficient synthesis of thalifoline and its analogs. *Synthetic Communications*, **39**, 1752-1758.
- [14] Ziyaev R, Irgashev T, Israilov IA, Abdullaev ND, Yunusov MS, Yunusov SY. (1977) Alkaloids of *Ziziphus jujuba* the structure of juziphine and juzirine. *Chemistry of Natural Compounds*, **13**, 204-207.
- [15] Chou CJ, Lin LC, Chen KT, Chen CF. (1994) Norththalifoline, a new isoquinolone alkaloid from the pedicels of *Lindera megaphylla*. *Journal of Natural Products*, **57**, 689-694.
- [16] Jackman LM, Trewella JC, Moniot JL, Shamma M, Stephens RL, Wenkert E, Leboeuf M, Cavé A. (1979) The carbon-13 NMR spectra of aporphine alkaloids. *Journal of Natural Products*, **42**, 437-449.
- [17] Chen CY, Chang FR, Wu YC. (1997) The constituents from the stems of *Annona cherimola*. *Journal of the Chinese Chemical Society*, **44**, 313-319.
- [18] Achenbach H, Waibel R, Addae-mensah I.. (1983) Lignans and other constituents from *Carissa edulis*. *Phytochemistry*, **22**, 749-753.
- [19] Asghar SF, Rehman HU, Rahman AU. (2010) Phytochemical investigations on *Iris germanica*. *Natural Product Research*, **24**, 131-139.
- [20] Hristea EN, Covaci-Cîmpeanu IC, Ionita G, Ionita P, Draghici C, Caaproiu MT, Hillebrand M, Constantinescu T, Balaban AT. (2009) Reactions of 2,2-diphenyl-1-picrylhydrazyl (DPPH) with two syringyllic phenols or one aroxide derivative. *European Journal of Organic Chemistry*, **2009**, 626-634.
- [21] Takaya Y, Furukawa T, Miura S, Akutagawa T, Hotta Y, Ishikawa N, Niwa M. (2007) Antioxidant constituents in distillation residue of Awamori spirits. *Journal of Agricultural and Food Chemistry*, **55**, 75-79.
- [22] Kodaira H, Ishikawa M , Komoda Y, Nakajima T. (1983) Isolation and identification of anti-platelet aggregation principles from the bark of *Fraxinus japonica* BLUME. *Chemical and Pharmaceutical Bulletin*, **31**, 2262-2268.
- [23] Yang F, Lian G, Yu B. (2010) Synthesis of raphanuside, an unusual oxathiane-fused thioglucoside isolated from the seeds of *Raphanus sativus* L. *Carbohydrate Research*, **345**, 309-314.
- [24] Seidel V, Bailleul F, Waterman PG. (2000) Novel oligorhamnosides from the stem bark of *Cleistopholis glauca*. *Journal of Natural Products*, **63**, 6-11.
- [25] Hanawa F, Shiro M, Hayash Y. (1997) Heartwood constituents of *Betula maximowicziana*. *Phytochemistry*, **45**, 589-595.
- [26] Chang YC, Chang FR, Wu YC. (2000) The Constituents of *Lindera Glauca*. *Journal of the Chinese Chemical Society*, **47**, 373-380.
- [27] Wu TS, Yeh JH, Wu PL. (1995) The heartwood constituents of *Tetradium glabrifolium*. *Phytochemistry*, **40**, 121-124.
- [28] Wattanapiromsakul C, Forster PI, Waterman PG. (2003) Alkaloids and limonoids from *Bouchardatia neurococca*: systematic significance. *Phytochemistry*, **64**, 609-615.
- [29] Cui B, Nakamura M, Kinjo J, Nohara T. (1993) Chemical constituents of *Astragalus semen*. *Chemical and Pharmaceutical Bulletin*, **64**, 178-182.
- [30] Yang XW, Wang JS, Ma YL, Xiao HT, Zuo YQ, Lin H, He HP, Li L, Hao XJ. (2007) Bioactive phenols from the leaves of *Baccaurea ramiflora*. *Planta Medica*, **73**, 1415-1417.
- [31] Cymerman CJ, Pereira Jr. WE, Halpern B, Westley JW. (1971) Optical rotatory dispersion and absolute configuration—XVII α -Alkylphenylacetic acids. *Tetrahedron*, **27**, 1173-1184.

12-Membered Resorcylic Acid Lactones Isolated from *Saccharicola bicolor*, an Endophytic Fungi from *Bergenia purpurascens*

Da-Le Guo^{a,c}, Min Zhao^{a,c}, Shi-Ji Xiao^b, Bing Xia^a, Bo Wan^a, Yu-Cheng Gu^d, Li-Sheng Ding^a and Yan Zhou^{a*}

^aKey Laboratory of Mountain Ecological Restoration and Bioresource Utilization, Chengdu Institute of Biology, Chinese Academy of Sciences, Chengdu 610041, P. R. China

^bPharmacy School, Zunyi Medical College, Zunyi 563000, P. R. China

^cUniversity of Chinese Academy of Sciences, Beijing 100049, P. R. China

^dSyngenta Jealott's Hill International Research Centre, Berkshire RG42 6EY, UK

zhouyan@cib.ac.cn

Received: August 21st, 2015; Accepted: November 2nd, 2015

Two new resorcylic acid lactones, 13-hydroxyhidroresorcylide (**1**) and 12-hydroxyhidroresorcylide (**2**), along with four known congeners (**3-6**) were isolated from *Saccharicola bicolor*, an endophytic fungus from *Bergenia purpurascens*. Their structures were elucidated by interpretation of the spectroscopic evidence.

Keywords: *Saccharicola bicolor*, *Bergenia purpurascens*, Resorcylic acid lactone.

Resorcylic acid lactones (RALs) are a class of fungal polyketides that have a core structure of a β -resorcylic acid chromophore bearing a side-chain in the form of a lactone ring. The first isolated RAL is radicicol in 1953 [1]. Since then, more than 40 naturally occurring RALs have been reported. These have showed antifungal [2], antimarial [3] and cytotoxic [4] activities. Due to their attractive biological activities, RALs had provoked interest in drug development. In the course of our ongoing research on the discovery of unique compounds from Tibetan plant endophytes, *Saccharicola bicolor*, an endophytic fungus, has been isolated from *Bergenia purpurascens*. The chemical investigation of its fermentation broth led to the isolation of two new resorcylic acid lactones namely 13-hydroxyhidroresorcylide (**1**) and 12-hydroxyhidroresorcylide (**2**), and four known congeners (**3-6**). Details of the isolation and structure elucidation of these compounds are discussed below.

Compound **1** was isolated as a yellow gum. Its molecular formula was assigned as C₁₆H₂₀O₆ on the basis of HRESIMS by the pseudo-molecular ion peak at *m/z* 309.1331 [M+H]⁺ (calcd. 309.1333). The IR spectrum showed the presence of phenolic hydroxyl (3502 cm⁻¹), methylene (2925.6, 2854.6 cm⁻¹), and lactone (1640.6 cm⁻¹) groups. ¹H, ¹³C, H-H COSY and HSQC NMR spectral data indicated the presence of a *m*-dihydroxybenzene unit [δ _H 6.25 (d, *J* = 2.5 Hz), 6.11 (d, *J* = 2.5 Hz); δ _C 166.6, 163.9, 140.5, 114.0, 106.3, 102.9], a CH₃CHCH₂CH(CH₂)₃ system [δ _H 5.08 (1H, m), 3.65 (1H, m), 2.85 (1H, m), 2.33 (1H, m), 2.08 (2H, m), 1.88 (1H, m), 1.62 (2H, m), 1.58 (1H, m), 1.34 (3H, d, *J* = 6.1 Hz); δ _C 73.3, 68.6, 44.1, 43.7, 38.2, 21.3, 20.7], a lactone carbonyl (δ _C 172.4), a methylene [δ _H 4.79 (1H, d, *J* = 18.6Hz), 3.60 (1H, d, *J* = 18.6Hz); δ _C 50.7] and a ketone group (δ _C 211.6). HMBC correlations between H-10 and C-9 were observed and the aliphatic system was linked to the ketone. Both HMBC cross peaks between H-8 (δ 4.79, 3.60) and C-9 (δ 211.6), C-7(δ 140.5), and between H-6 (δ 6.11) and C-8 (δ 50.7) placed the insular methylene between the aromatic ring and the ketone. HMBC correlations from H-6 (δ 6.11), H-4 (δ 6.25) and H-15 (δ 5.08) to the lactone carbonyl (δ _C 172.4) were observed and located the lactone between C-2 and C-15.

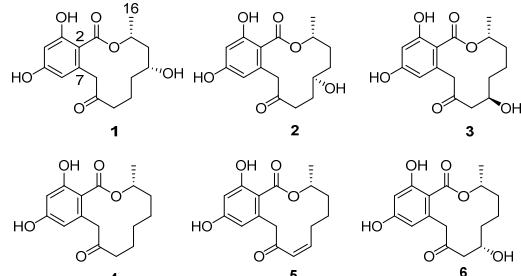
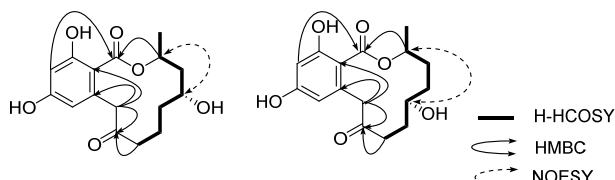


Figure 1: Compounds **1-6** isolated from *Saccharicola bicolor*.

The relative stereochemistry of **1** was established by NOESY correlations of relevant protons as in Figure 2. Both presence of the NOE interaction between H-15 (δ 5.08) and H-13 (δ 3.65) and the absence of the NOE correlation between 15-methyl (δ 1.34) and H-13 indicated that H-15 and H-13 were in the same orientation. Therefore, the structure of **1** (13-hydroxyhidroresorcylide) was determined as shown in Figure 1.

Compound **2** was obtained as a yellow gum, and its molecular formula was determined as C₁₆H₂₀O₆ from the [M+H]⁺ ion peak at *m/z* 309.1333 (calcd. 309.1333) in the HRESIMS with seven degrees of unsaturation. The NMR data of **2** were similar to those of **1** with the difference of a hydroxyl located on the saturated chain system CH₃CH(CH₂)₂CH(CH₂)₂ [δ _H 5.22 (1H, m), 3.73 (1H, m), 2.94 (1H, m), 2.20 (1H, m), 2.18 (1H, m), 1.94 (1H, ddd, *J*=13.8, 9.0, 4.5 Hz), 1.67 (2H, m), 1.49 (1H, m), 1.30 (3H, d, *J* = 6.3 Hz); δ _C 73.7, 70.5, 36.9, 30.3, 30.0, 29.9, 19.0]. The final structure was established by the 2D NMR experiments including HMQC and HMBC spectra. The relative stereochemistry of **2** was established by NOESY correlations of relevant protons as in Figure 2. Both the presence of a NOE interaction between H-15 and H-12 and the absence of the NOE correlation between 15-methyl and H-12 indicated that H-15 and H-12 were on the same side of the twelve-membered ring. The structure of **2** (12-hydroxyhidroresorcylide) was thus elucidated as shown in Figure 1.

**Figure 2:** The H-H COSY, key HMBC, and NOESY correlations of **1** and **2**.**Table 1:** ^1H (400 MHz) and ^{13}C (100 MHz) NMR data in CD_3OD of **1** and **2**.

Position	1	2	δ_{H} (J in Hz)	δ_{C}
1	-	172.4	-	172.3
2	-	106.3	-	106.6
3	-	166.6	-	166.6
4	6.25, d (2.5)	102.9	6.25, d (2.5)	103.0
5	-	163.9	-	163.9
6	6.11, d (2.5)	114.0	6.12, d (2.5)	113.7
7	-	140.5	-	140.0
8	4.79, d (18.6), 3.60, d (18.6)	50.7	4.73, d (18.8), 3.78, d (18.8)	52.3
9	-	211.6	-	211.0
10	2.08, 1.58 m	44.1	2.94, 2.20, m	36.9
11	1.62 (2H), m	38.2	2.18, m, 1.94, ddd (13.8, 9.0, 4.5)	29.9
12	2.08, 1.88, m	20.7	3.73, m	70.5
13	3.65, m	68.6	1.67 (2H), m	30.0
14	2.33, 2.85, m	43.7	1.49, 1.67, m	30.3
15	5.08, m	73.3	5.22, m	73.7
16	1.34, d (6.1)	21.3	1.30, d (6.3)	19.0

Experimental

General: Optical rotations were determined on a JASCO P-1020 polarimeter at room temperature. UV spectra were recorded on a Perkin-Elmer Lambda 35 UV-VIS spectrophotometer, and IR spectra on a Perkin-Elmer FT-IR spectrometer (KBr). 1D and 2D NMR were carried out on a Bruker-Ascend-400 MHz instrument at 300 K, with TMS as internal standard. HRESIMS were recorded on a Bruker MicrO TOF-Q II mass spectrometer. Preparative HPLC was performed on a Waters 2545 equipped with a Waters 2489 detector on Kromasil RP-C18 column (10 × 250 mm). Column chromatography (CC) was performed with silica gel and Sephadex LH-20. All the solvents used were of analytical grade.

Fungal material: The title strain was isolated from the root of *Bergenia purpurascens*, collected from a suburb of Lhasa, Tibet Autonomous Region, People's Republic of China. The culture was grown on potato dextrose agar (PDA) and distinguished morphologically as *Saccharicola* sp., which was further reinforced by 18S rDNA sequence with a 99% identity to *Saccharicola bicolor*. The strain (GenBank accession no. KT367526) has been preserved at Chengdu Institute of Biology, Chinese Academy of Sciences, China.

References

- [1] Delmotte P, Delmotte-Plaque J. (1953) A new antifungal substance of fungal origin. *Nature*, **171**, 344.
- [2] Nair MSR, Carey ST. (1980) Metabolites of pyrenomycetes XIII: Structure of (+) hypothemycin, an antibiotic macrolide from *Hypomyces trichothecoides*. *Tetrahedron Letters*, **21**, 2011-2012.
- [3] Isaka M, Suyarnsestakorn C, Tanticharoen M, Kongsaeree P, Thebtaranonth Y. (2002) Aigialomycins A-E, new resorcylic macrolides from the marine mangrove fungus *Aigialus parvus*. *The Journal of Organic Chemistry*, **67**, 1561-1566.
- [4] Isaka M, Yangchum A, Intamas S, Kocharin K, Jones EBG, Kongsaeree P, Prabpai S. (2009) Aigialomycins and related polyketide metabolites from the mangrove fungus *Aigialus parvus* BCC 5311. *Tetrahedron*, **65**, 4396-4403.

Fungal culture and extraction: This fungus was cultivated on a 4.8 L scale using 500 mL Erlenmeyer flasks containing 200 mL of the seed PDA medium for 3 days. The fermentations were carried out in 60 Fernbach flasks each containing 200 g rice. Distilled water (200 mL) was added to each flask, and the contents were soaked overnight before autoclaving at 121°C for 30 min. The flasks were cooled to room temperature, inoculated with 3.0 mL of spore inoculum, and incubated for 21 days at 25°C. The fermented substrate in each flask was first fragmented with a spatula and then extracted 3 times with light petroleum, followed by EtOAc. The EtOAc solution was dried under vacuum and yielded 14 g extract.

Fractionation and isolation: The EtOAc residue (14 g) was separated into 4 fractions by CC on silica gel (300-400 mesh), eluting stepwise with a $\text{CHCl}_3/\text{MeOH}$ gradient (CHCl_3 , $\text{CHCl}_3/\text{MeOH}$: 10:1 (v/v), $\text{CHCl}_3/\text{MeOH}$: 3:1 (v/v), MeOH). LC-MS analysis was performed on these fractions. The third fraction (eluted with MeOH) was selected. Sephadex LH-20 separation of this fraction ($\text{CHCl}_3/\text{MeOH}$: 1:1, v/v) afforded 3 sub-fractions (Fr.1-Fr.3). Fr.2 was further purified on a Waters preparative HPLC equipped with a Kromasil RP-C18 column (10 × 250 mm, ID × L; MeOH/H₂O: 55:45, v/v), which led to the separation of **1** (10.3 mg), **2** (4.5 mg), **3** (4.6 mg), **4** (11.3 mg), **5** (7.3 mg) and **6** (4.7 mg).

13-Hydroxyhidroresorcylide (1)

$[\alpha]_D^{20} -19.4$ (*c* 0.1, MeOH).

IR (KBr): 3502.2, 2925.6, 1640.6, 1260.8 cm^{-1} .

UV/Vis λ_{max} (MeOH) nm ($\log \epsilon$): 302.6 (3.48), 263.8 (3.74), 221.1(4.08).

^1H and ^{13}C NMR (CD_3OD): Table 1.

HRESIMS: m/z [M + H⁺] calcd. for $\text{C}_{16}\text{H}_{20}\text{O}_6$: 309.1333; found: 309.1331.

12-Hydroxyhidroresorcylide (2)

$[\alpha]_D^{20} +25.1$ (*c* 0.1, MeOH).

IR (KBr): 3383.9, 2936.3, 1645.9, 1622.1, 1261.8 cm^{-1} .

UV/Vis λ_{max} (MeOH) nm ($\log \epsilon$): 302.6 (3.52), 263.8 (3.76), 221.1 (4.10).

^1H and ^{13}C NMR (CD_3OD): Table 1.

HRESIMS: m/z [M + H⁺] calcd. for $\text{C}_{16}\text{H}_{20}\text{O}_6$: 309.1333; found: 309.1331.

Acknowledgments - This work was financially supported by grants from the National Natural Sciences Foundation of China (21302180, 21572219) and a Syngenta Postgraduate Fellowship awarded to Da-Le Guo.

Phenylpropanoid Glycosides from the Leaves of *Ananas comosus*

Wen-Hao Chen, Xiao-Juan Huang, Huo-Ming Shu, Yang Hui, Fei-Yan Guo, Xiao-Ping Song, Ming-Hui Ji^{*}
and Guang-Ying Chen^{*}

Key Laboratory of Tropical Medicinal Plant Chemistry of the Ministry of Education, Chemistry and Chemical Engineering, Hainan Normal University, Haikou 571158, P.R. China

Wen-Hao Chen and Xiao-Juan Huang contributed equally to this work.

jimh66@163.com; chgying123@163.com

Received: October 1st, 2015; Accepted: November 18th, 2015

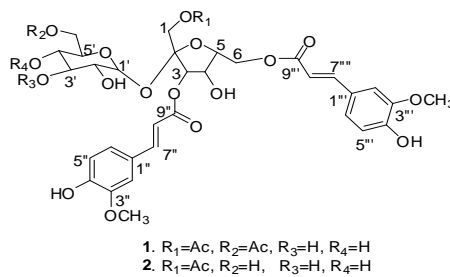
Two new phenylpropanoid glycosides, named β -D-(1-O-acetyl-3,6-O-diferuloyl) fructofuranosyl α -D-6'-O-acetylglucopyranoside (**1**) and β -D-(1-O-acetyl-3,6-O-diferuloyl) fructofuranosyl α -D-glucopyranoside (**2**), along with two known analogues (**3-4**) and four glycerides (**5-8**), were isolated from the EtOAc extract of the leaves of *Ananas comosus*. Their structures were elucidated on the basis of 1D- and 2D-NMR analyses, as well as HR-ESI-MS experiments. Compounds **1-4** showed significant antibacterial activities against *Staphylococcus aureus* and *Escherichia coli*.

Keywords: *Ananas comosus*, Bromeliaceae, Phenylpropanoid glycosides, Antibacterial activities.

Ananas comosus L. (family Bromeliaceae) is a perennial herbaceous plant that is employed in a traditional Chinese medicinal preparation to treat stomach upsets and as an anti-diarrheal [1]. Modern pharmacological studies on *A. comosus* leaves indicated that they could have anti-oxidant, blood sugar lowering, blood lipid reducing and antibiotic activities [2]. Previous chemical studies on the leaves of *A. comosus* have led to the isolation of an array of structurally interesting compounds, including phenylpropanoids, glycerides, amides and triterpenes [3].

The ongoing investigation, seeking stronger antibacterial compounds from *A. comosus*, led to the isolation, from the EtOAc extract of the leaves, of two new phenylpropanoid glycosides, named β -D-(1-O-acetyl-3,6-O-diferuloyl) fructofuranosyl α -D-6'-O-acetylglucopyranoside (**1**) and β -D-(1-O-acetyl-3,6-O-diferuloyl) fructofuranosyl α -D-glucopyranoside (**2**), together with two known analogues and four glycerides. The known compounds were identified as 2-feruloyl- α -D-glucopyranosyl-(1'→2)-3,6-O-feruloyl- β -D-fructofuranoside (**3**) [4], β -D-(1-O-acetyl-3,6-O-diferuloyl)fructofuranosyl α -D-2',4',6'-triacyetylglucopyranoside (**4**) [5], 1-O-p-coumaroyl-3-O-caffeoyleglycerol (**5**) [6], 1-O-feruloyl-3-O-p-coumaroylglycerol (**6**) [7], 1-O-feruloyl-3-O-caffeoyleglycerol (**7**) [6], and 1,3-O-diferuloylglycerol (**8**) [7] (Figure 1). We present herein the isolation, structural elucidation, and antibacterial activity of these compounds.

Compound **1** was obtained as a colorless amorphous solid with the elemental composition C₃₆H₄₂O₁₉, established by high-resolution MS. The ¹H NMR spectrum (Table 1) suggested that **1** contained two feruloyl moieties, represented by signals of two sets of *trans* olefinic protons [δ _H 6.40 (1H, d, *J* = 16.0 Hz), 7.66 (1H, d, *J* = 16.0 Hz); 6.46 (1H, d, *J* = 16.0 Hz), 7.72 (1H, d, *J* = 16.0 Hz)], two sets of 1,3,4-trisubstituted aromatic ring protons [δ _H 7.20 (1H, d, *J* = 1.8 Hz), 6.80 (1H, d, *J* = 8.0 Hz), 7.10 (1H, dd, *J* = 1.8, 8.0 Hz); 7.25 (1H, d, *J* = 1.8 Hz), 6.83 (1H, d, *J* = 8.0 Hz), 7.12 (1H, dd, *J* = 1.8, 8.0 Hz)], and two methoxy groups [δ _H 3.89 (3H, s), 3.90 (3H, s)]. Signals in the ¹³C NMR spectrum (Table 1) at δ _C 90.2, 74.34, 72.03, 71.8, 71.9, 65.0; 65.2, 105.3, 81.1, 73.8, 78.3, and 64.8 suggested the presence of a disaccharide moiety [5]. Alkaline and



1. R₁=Ac, R₂=Ac, R₃=H, R₄=H
2. R₁=Ac, R₂=H, R₃=H, R₄=H
3. R₁=H, R₂=H, R₃=H, R₄=H
4. R₁=Ac, R₂=Ac, R₃=Ac, R₄=Ac

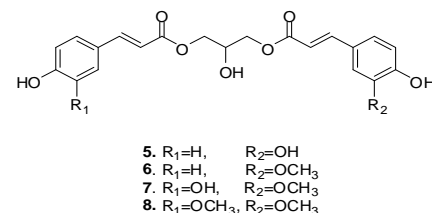


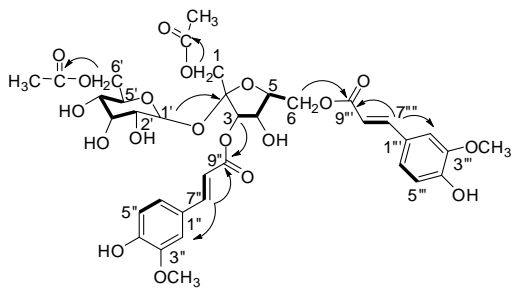
Figure 1: Structures of compounds **1-8**.

acid hydrolysis of **1** gave sucrose and a mixture of glucose and fructose, which were identified by direct comparison with authentic samples on TLC. A characteristic doublet signal with a small coupling constant at δ _H 5.66 (1H, d, *J* = 3.7 Hz) in the ¹H NMR spectrum that was ascribed to the anomeric proton in the α -glucopyranose unit [8, 9] also supported the presence of a sucrose moiety in **1**. Furthermore, ¹H- and ¹³C-NMR spectra (Table 1) revealed the presence of two acetyl groups [δ _H 2.07 (3H, s), 2.05 (3H, s); δ _C 20.9, 20.8] located in the sucrose moiety. The position of bond conjugation of the feruloyls and the acetyl groups on the sucrose was assigned by HMBC experiment. This HMBC spectrum (Figure 2) enabled the assignments of two feruloyl moieties located at positions 3 and 6 on the fructose unit of sucrose, since the methine proton (δ _H 5.56) of position 3 and one *trans* olefinic proton (δ _H 7.72) of position 7" on a feruloyl moiety gave cross-peaks with the same carbonyl carbon (δ _C 168.3), and one set of the methylene protons (δ _H 4.50, 2H) of position 6 and another *trans* olefinic proton

Table 1: ^1H - and ^{13}C NMR data for compounds **1** and **2** in CD_3OD (δ in ppm, J in Hz)^{a,b)}

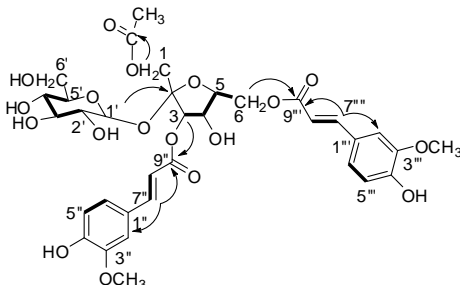
NO.	1		2	
	δ_{H}	δ_{C}	δ_{H}	δ_{C}
1	4.54, 4.60 (m)	65.2, CH_2	4.19, 4.45 (m)	65.6, CH_2
2		105.2, C		104.9, C
3	5.56 (m)	78.3, CH	5.50 (d, 8.0)	78.9, CH
4	4.50 (m)	81.1, CH	4.50 (m)	81.2, CH
5	3.45 (m)	73.8, CH	3.45 (m)	74.3, CH
6	4.10, 4.50 (m)	64.8, CH_2	4.10, 4.50 (m)	65.7, CH_2
1'	5.66 (d, 3.6)	90.2, CH	5.49 (d, 3.6)	92.9, CH
2'	3.65 (m)	71.8, CH	3.65 (m)	71.9, CH
3'	4.16 (m)	74.3, CH	4.16 (m)	74.8, CH
4'	3.82 (dd, 9.0, 9.0)	72.0, CH	3.82 (dd, 9.0, 9.0)	73.0, CH
5'	3.34 (m)	71.9, CH	3.34 (m)	72.1, CH
6'	4.14, 4.20 (m)	65.0, CH_2	4.10, 4.19 (m)	65.5, CH_2
1''		127.5, C		127.5, C
2''	7.25 (d, 1.8)	111.8, CH	7.25 (d, 1.8)	111.9, CH
3''		149.3, C		149.4, C
4''		150.8, C		150.8, C
5''	6.82 (d, 8.2)	115.2, CH	6.82 (d, 8.2)	115.1, CH
6''	7.12 (dd, 1.6, 7.6)	124.4, CH	7.12 (dd, 1.6, 7.6)	124.3, CH
7''	7.72 (d, 16.0)	147.9, CH	7.72 (d, 16.0)	147.9, CH
8''	6.48 (d, 16.0)	116.4, CH	6.39 (d, 16.0)	116.5, CH
9''		168.3, C		168.3, C
1'''		127.7, C		127.6, C
2'''	7.19 (d, 1.8)	111.7, CH	7.19 (d, 1.8)	111.6, CH
3'''		149.3, C		149.3, C
4'''		150.6, C		150.7, C
5'''	6.80 (d, 8.2)	114.6, CH	6.80 (d, 8.2)	114.4, CH
6'''	7.08 (dd, 1.6, 7.6)	124.1, CH	7.08 (dd, 1.6, 7.6)	124.1, CH
7'''	7.67 (d, 16.0)	147.0, CH	7.67 (d, 16.0)	147.1, CH
8'''	6.41 (d, 16.0)	116.4, CH	6.41 (d, 16.0)	116.4, CH
9'''		168.8, C		168.8, C
3''-OCH ₃	3.90 (s)	56.5, CH_3	3.90 (s)	56.4, CH_3
3'''-OCH ₃	3.89 (s)	56.5, CH_3	3.89 (s)	56.4, CH_3
1-CO		172.4, C		173.0, C
6'-CO		172.8, C		
1-OAc	2.07 (s)	20.8, CH_3	2.08 (s)	20.9, CH_3
6'-OAc	2.05 (s)	20.9, CH_3		

^{a)} The ^1H NMR were measured at 400 MHz and ^{13}C NMR at 100 MHz; ^{b)} The assignments were based upon DEPT135, ^1H - ^1H COSY, HSQC and HMBC spectra.

**Figure 2:** Selected ^1H - ^1H COSY (—) and HMBC (→) correlations of compound **1**.

(δ_{H} 7.67) of position 7'' with the same carbonyl carbon (δ_{C} 168.8). Also, the methylene protons of position 6' (δ_{H} 4.14 and 4.20) on the glucose and methylene protons of position 1 (δ_{H} 4.54 and 4.60) on the fructose showed cross-peaks with respective acetyl carbonyl carbons (δ_{C} 172.8, 172.4). On the basis of these spectroscopic data and chemical evidence, the structure of compound **1** was determined to be β -D-(1-*O*-acetyl-3,6-*O*-diferuloyl) fructofuranosyl α -D-6'-*O*-acetylglucopyranoside.

Compound **2**, obtained as a colorless amorphous solid with elemental composition $\text{C}_{34}\text{H}_{40}\text{O}_{18}$, was also a phenylpropanoid glycoside. The ^1H and ^{13}C NMR spectra (Table 1) suggested that **2** possesses a structure similar to **1**, containing glucose (Glc) and fructose (Fru) units, and two feruloyl moieties [*trans* olefinic protons: δ_{H} 6.39 (1H, d, J = 15.6 Hz), 7.65 (1H, d, J = 15.6 Hz); 6.44 (1H, d, J = 16.0 Hz), 7.72 (1H, d, J = 16.0 Hz); 1,3,4-trisubstituted aromatic ring protons: δ_{H} 7.19 (1H, d, J = 1.6 Hz), 6.80 (1H, d, J = 8.0 Hz), 7.08 (1H, dd, J = 1.6, 8.0 Hz; 7.25 (1H, d, J = 1.6 Hz), 6.82 (1H, d, J = 8.0 Hz), 7.12 (1H, dd, J = 1.6, 8.0 Hz);

**Figure 3:** Selected ^1H - ^1H COSY (—) and HMBC (→) correlations of compound **2**.

two methoxy groups: δ_{H} 3.89 (3H, s) and 3.90 (3H, s), but only one acetate group (δ_{H} 2.07, 3H, s) was present in **2**. Acid and alkaline hydrolysis, followed by TLC, indicated that **2** contained a sucrose moiety. The HMBC spectrum (Figure 3) of **2** revealed long range couplings between the oxygenated methine and methylene protons at positions 3 and 6 of the fructose, as well as the *trans* olefinic protons at positions 8'' and 8''' of two feruloyl groups, and their respective carbonyl carbons (^1H / ^{13}C /H: δ 5.50/168.3/6.39 for the C-3 group), so these two feruloyl groups were located at C-3 and C-6, the same as **1** [10]. Analogously, couplings between the methyl protons of one acetyl groups, as well as methylene protons at 1 of the sucrose core and its carbonyl carbon (^1H / ^{13}C /H: 2.08/173.0/4.19) indicated that the acetyl group was at C-1 [11]. These data confirmed that the substantial differences between **2** and **1** were in the interchange of the C-6' acetyl group and hydroxy group, so the structure of **2** was β -D-(1-*O*-acetyl-3,6-*O*-diferuloyl) fructofuranosyl α -D-glucopyranoside.

The structures of compounds **3-8** were identified by comparison of their spectral data with those described in the literature. As stated before, the occurrence of natural phenolic diglycerides is restricted to species of Gramineae, Liliaceae, Sparganiaceae and Bromeliaceae [6]. The presence of the phenylpropanoid glycosides (**1-4**) and glycerides (**5-8**) could contribute to chemotaxonomic studies of the *Ananas* genus.

The antibacterial activities of all the isolates (**1-8**) from the leaves of *A. comosus* were evaluated using the 96-well plate method [13] and the results are given in terms of the concentration of the sample decreasing minimal inhibitory concentration (MIC). All the tested samples had different activity against different bacteria. Preliminary antibacterial activity screening revealed that four of the isolated phenylpropanoid glycosides (**1-4**) exhibited significant activity against *S. aureus* and *E. coli*, with MIC values ranging from 0.16 to 0.62 $\mu\text{g}/\text{mL}$; while **6** and **7** showed good inhibition of *S. aureus* and *M. luteus*, as shown in Table 2.

Table 2: Minimal inhibitory concentration (MIC) of compounds **1-8**.

Comps	MIC ($\mu\text{g}/\text{mL}$)				
	<i>S. aureus</i>	<i>S. albus</i>	<i>E. coli</i>	<i>B. subtilis</i>	<i>M. luteus</i>
1	0.16	5.00	0.31	0.62	2.50
2	0.16	10.00	0.16	0.31	1.25
3	0.16	2.50	0.62	10.00	1.25
4	0.16	1.25	0.16	10.00	5.00
5	0.62	0.62	10.0	10.00	N
6	0.31	1.25	5.00	2.50	0.62
7	0.62	2.50	5.00	1.25	0.62
8	0.62	0.62	1.25	10.00	N
CPFX ^a	0.16	0.31	0.16	0.16	0.31

^a CPFX (ciprofloxacin) was used as positive control.

Experimental

General experimental procedure: NMR spectra: Bruker AV 400 spectrometer {400 (^1H) and 100 MHz (^{13}C)}; δ in ppm rel. to TMS

as internal standard, *J* in Hz. ESI-MS: Bruker Esquire 6000 Ion Trap mass spectrometer and HR-ESI-MS: Bruker Daltonics Apex-Ultra 7.0 T mass spectrometer; in m/z. Column chromatography (CC): silica gel (SiO_2 , 200–300 mesh; Qingdao Haiyang Chemical Group Co.), and sephadex LH-20 (Pharmacia). TLC: Precoated SiO_2 GF-254 (10–40 μm) plates (Qingdao Haiyang Chemical Group Co.).

Plant material: *A. comosus* leaves were collected in Wanning, Hainan Province of China, and identified by Professor Qiong-xin Zhong of Hainan Normal University. A voucher specimen has been deposited at the Key Laboratory of Tropical Medicinal Plant Chemistry of the Ministry of Education, Hainan Normal University.

Extraction and isolation: Air-dried leaves (20.0 kg) of *A. comosus* were finely cut and extracted 3 times (each for 7 days) with 95% EtOH at room temperature. Evaporation of the solvent under reduced pressure produced the EtOH extract. This was dissolved in H_2O and partitioned with light petroleum and EtOAc. The EtOAc soluble fraction (300 g) was initially subjected to column chromatography (CC) on silica gel, and then eluted with a step gradient of light petroleum/EtOAc (10/0-0/10, v/v) to give 10 fractions. Fraction 7 (15.6 g) was decolorized on a Sephadex LH-20 (CHCl_3 -MeOH, 2:3, v/v) column and then chromatographed on a silica gel column (CHCl_3 -MeOH, 6:1-1:1) to afford 6 fractions (fractions 7.1-7.6). Compounds **1** (7.0 mg) and **3** (7.4 mg) were obtained from fraction 7.2 by reversed-phase silica gel CC, and compounds **2** (7.2 mg) and **4** (6.8mg) from fraction 7.4 by reversed-phase silica gel CC. Fraction 4 (14.6g) was decolorized on Sephadex LH-20 (CHCl_3 -MeOH, 1:1, v/v) to obtain a sub-fraction, which was further isolated and purified by silica gel CC (CHCl_3 - Me_2CO , 4:1-1:1, v/v), and Sephadex LH-20 (CHCl_3 -MeOH, 2:3, v/v) to afford compounds **5** (10.5 mg), **6** (12.1 mg), **7** (9.0 mg) and **8** (7.5 mg).

References

- [1] Song LL. (1999) *Chinese Herbs*. SST Press, 2000 Shanghai, PRC, Chapter 8, p. 7357 (in Chinese).
- [2] (a) Xie WD, Xing DM, Sun H, Wang W, Ding Y, Du LJ. (2005) The effects of *Ananas comosus* L. leaves on diabetic-dyslipidemic rats induced by alloxan and a high fat/high-cholesterol diet. *The American Journal of Chinese Medicine*, **33**, 95-105; (b) Xie WD, Wang W, Sun H, Xing DM, Cai GP, Du LJ. (2007) Hypolipidemic mechanisms of *Ananas comosus* L. leaves in mice: different from fibrates but similar to statins. *Journal of Pharmacological Sciences*, **103**, 267-274.
- [3] (a) Wang W, Ding Y, Xing DM, Wang JP, Du LJ. (2006) Studies on phenolic constituents from leaves of pineapple (*A. comosus*). *China Journal of Chinese Materia Medica*, **31**, 1242-1244; (b) Wang JP, Wang HY, Du LJ, Ding Y, Xing DM, Wang W. (2007) New cerebroside from leaves of pineapple. *China Journal of Chinese Materia Medica*, **32**, 401-403; (c) Ma C, Xiao SY, Li ZG, Wang W, Du LJ. (2007) Characterization of active phenolic components in the ethanolic extract of *Ananas comosus* L. leaves using high-performance liquid chromatography with diode array detection and tandem mass spectrometry. *Journal of Chromatography A*, **1165**, 39-44.
- [4] Yan LL, Gao WY, Zhang YJ, WangY. (2008) A new phenylpropanoid glycosides from *Paris polyphylla* var. *yunnanensis*. *Fitoterapia*, **79**, 306-307.
- [5] Osamu S., Setsuko S., Motoyoshi S, Yan N, Hua WY. (1996) Chemical constituents of Chinese folk medicine “San Leng”, *Sparganium stoloniferum*. *Journal of Natural Products*, **59**, 242-245.
- [6] Delaporte RH, Guzen KP, Laverde Jr A, dos Santos AR, Sarragiotto MH. (2006) Phenylpropanoid glycerols from *Tillandsia streptocarpa* Baker (Bromeliaceae). *Biochemical Systematics and Ecology*, **34**, 599-602.
- [7] Shimomura HK, Sashida YK, Mimaki YR. (1987) Phenolic glycerides from *Lilium auratum*. *Phytochemistry*, **26**, 844-875.
- [8] Binkley WW, Horton D, Bhacca NS. (1969) Physical studies on oligosaccharides related to sucrose. I. N.M.R. studies on the peracetates of sucrose, 1-ketose and nystose. *Carbohydrate Research*, **10**, 245-248.
- [9] Linscheid M, Wendisch D, Strack D. (1980) The structures of sinapic acid esters and their metabolism in cotyledons of *Raphanus sativus*. *Zeitschrift fuer Naturforschung*, **35c**, 907-914.
- [10] Yao HK, Ya WH, Chia CL. (2005) Cytotoxic phenylpropanoid glycosides from the stems of *Smilax china*. *Journal of Natural Products*, **68**, 1475-1478.
- [11] Sun XZ, Zimmermann ML, Campagne JM, Sneden AT. (2000) New sucrose phenylpropanoid esters from *Polygonum perfoliatum*. *Journal of Natural Products*, **63**, 1094-1097.
- [12] Solis PN, Wright CW, Anderson MM, Gupta MP, Phillipson JD. (1993) Antimicrobial activity and brine shrimp lethality bioassay of the leaves extract of *Dillenia indica* Linn. *Planta Medica*, **59**, 250-252.

β -D-(1-O-Acetyl-3,6-O-diferuloyl) fructofuranosyl α -D-6'-O-acetylglucopyranoside (1)

$[\alpha]_D$: + 16.9 (c 0.1, DMSO)

^1H and ^{13}C NMR: Table 1.

HRESI-MS: m/z 777.2241 [M-H]⁻, calcd. for $\text{C}_{36}\text{H}_{41}\text{O}_{19}$: 777.2248

β -D-(1-O-Acetyl-3,6-O-diferuloyl)fructofuranosyl- α -D-glucopyranoside (2)

$[\alpha]_D$: + 19.5 (c 0.1, DMSO)

^1H and ^{13}C NMR: Table 1.

HRESI-MS: m/z 735.2149 [M-H]⁻, calcd. for $\text{C}_{34}\text{H}_{39}\text{O}_{18}$: 735.2152

Antibacterial activity assay: Five bacterial strains, *Staphylococcus aureus*, *Bacillus subtilis*, *Escherichia coli*, *Micrococcus luteus*, and *Staphylococcus albus*, were used for the assay using standard agar diffusion tests [13]. Ciprofloxacin (CPFX) was the positive control. The results are presented as minimum inhibitory concentrations (MIC) in Table 2.

Supplementary data: NMR (^1H and ^{13}C NMR, DEPT135, HSQC, HMBC, ^1H - ^1H COSY and NOESY) and IR spectroscopic, and HR-ESI-MS data for the new compounds (**1-2**).

Acknowledgments - This work was financially supported by the 973 Program, Ministry of Science and Technology of China (Grant No. 2014CB560714), the National Natural Science Foundation of China (21202030), the Application technology research and development and demonstration of Hainan Province (ZDXM20130020), the National Natural Science Foundation of Hainan Province (214028, 20152036) and in part by the Science and Technology Project of Social Development of Hainan Province (2015SF36) and the University Scientific Research project of Hainan Province (HNKY2014-40).

Tannins and Antioxidant Activities of the Walnut (*Juglans regia*) Pellicle

Tian-Peng Yin^{a,1}, Le Cai^{a,1}, Yang Chen^b, Ying Li^a, Ya-Rong Wang^b, Chuan-Shui Liu^a and Zhong-Tao Ding^{a,*}

^aKey Laboratory of Medicinal Chemistry for Natural Resource, Ministry of Education, School of Chemical Science and Technology, Yunnan University, Kunming, Yunnan 650091, PR China

^bDepartment of Pharmaceutical Sciences, Zunyi Medical University Zhuhai Campus, Zhuhai 519041, PR China

¹The authors contributed equally to this paper

ztding@ynu.edu.cn

Received: August 13th, 2015; Accepted: October 6th, 2015

The total phenolic content and antioxidant activities of the acetone extract and derived fractions from the walnut (*Juglans regia*) pellicle were estimated. The BuOH fraction exhibited the strongest antioxidant activity with the highest phenolic content. A phytochemical investigation of this fraction led to the isolation of three tannins, 2,3-hexahydroxydiphenoylgucose (1), pedunculagin (2) and 2,3,4,6-tetragalloylgucose (3). Pedunculagin showed high content and powerful activity, which implied that this compound plays an important role in the antioxidant activity of the walnut pellicle.

Keywords: *Juglans regia*, Pellicle, Antioxidant, Phenolic, Tannin, Pedunculagin.

Walnut, the fruits of *Juglans regia* L. (Juglandaceae), is a highly nutritious food, which has been found to be an excellent source of multiple health-beneficial components, such as polyunsaturated fatty acids, tocopherols, phenolics, hormone and melatonin [1-3]. The increased consumption of walnuts has been correlated with reduced risk of cardiovascular disease, cancer and diabetes [4, 5]. The walnut kernel, which is officially listed in the Chinese Pharmacopoeia, has long been utilized to treat cough, stomachache and cancer in traditional Chinese medicine. Though rich in unsaturated fatty acids, walnuts are readily preserved from oxidation, which may be attributed to the protective property of the pellicle. Previous studies revealed that a large amount of phenolics possessing significant antioxidant activities exist in the walnut pellicle [6, 7]. In addition, the total phenolic content and antioxidant activity of the walnut pellicle were much higher than the kernel [8]. The antioxidant ingredients in the pellicle probably aid in stabilizing the walnut kernel against decomposition. Therefore, this investigation was conducted to elucidate the protective mechanism of the pellicle and to supply more scientific evidence of antioxidant activity for the further research and development of walnut.

Several studies concluded that walnuts possess higher antioxidant capacity than any other nuts [9], and this antioxidant capacity is presumably a product of phenolics, especially hydrolysable tannins located mainly in the pellicle [10]. The total phenolic content (TPC) of the fractions from the walnut pellicle followed the order BuOH fraction > EtOAc fraction > crude extract > light petroleum (PE) fraction > water fraction (Table 1). It revealed that phenolics in the walnut pellicle were more extractable with highly polar solvents [11, 12]. Combined with the previous studies, the major phenolics in the walnut pellicle were assigned to be tannins.

Plant phenolics, particularly phenolic acids, tannins and flavonoids, are known to be potent antioxidants, which could effectively scavenge free radicals, break radical chain reactions and chelate metal ions [13]. Three methods were utilized to evaluate the antioxidant activities of the fractions from the walnut pellicle.

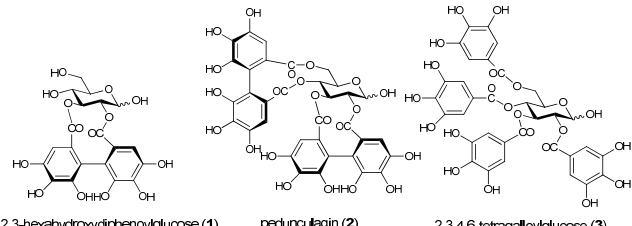


Figure 1: Structures of tannins from the walnut pellicle.

2,2'-Diphenyl-1-picrylhydrazyl (DPPH) has been widely used to estimate the radical scavenging activity of natural antioxidants since it can accommodate a large number of samples in a short period and is sensitive enough to detect active principles at low concentrations. As observed in Table 1, the BuOH fraction of the walnut pellicle showed the highest radical scavenging activity, followed by the EtOAc fraction, crude extract, PE fraction and water fraction. The IC₅₀ value of the BuOH fraction (2.09 ± 0.05 µg/mL) was very close to that of the positive control, gallic acid (1.42 ± 0.02 µg/mL).

Tannins function as primary antioxidants and secondary antioxidants, which could chelate metal ions and interfere with one of the reaction steps in the Fenton reaction and thereby retard oxidation [14]. The Fe²⁺ chelating activities decreased in the order BuOH fraction > EtOAc fraction > crude extract > water fraction > PE fraction, which were similar to those of the DPPH assay (Table 1). The result revealed that the BuOH fraction from the walnut pellicle could chelate Fe²⁺ effectively, which was probably due to the presence of tannins.

The hydroxyl radical has been reported to be the most harmful reactive oxygen species that is responsible for the oxidative injury of biomolecules. It is generated from the Fenton reaction in the presence of transition metals such as Fe²⁺ and Cu²⁺ [15]. Similarly, the BuOH fraction showed the highest hydroxyl radical scavenging (HRS) activity, followed by the EtOAc fraction, crude extract, PE fraction and water fraction (Table 1). It can be concluded that the

extracts showed strong hydroxyl radical scavenging activity probably due to their Fe^{2+} chelating capability [16].

To demonstrate that the extracts' strong antioxidant activity was attributed to the large amount of phenolics, the correlation analysis between total phenolic content and antioxidant activity was carried out. The correlation between IC_{50} of DPPH and TPC was very strong ($y = 63.8698 - 0.2029x$, $R^2 = 0.8282$), and so was that between the IC_{50} of HRS and TPC ($y = 418.7180 - 1.2384x$, $R^2 = 0.7578$). The correlation between the IC_{50} of Fe^{2+} chelating activity and TPC was also remarkable ($y = 77.6002 - 0.2538x$, $R^2 = 0.6945$). The results suggested the strong antioxidant activity of walnut pellicle could be attributed to its high phenolic content.

Table 1: Total phenolic content and antioxidant activity of acetone extract and its derived soluble fractions from the walnut pellicle.

Sample	IC ₅₀ (μg/mL)			
	TPC	DPPH	HRS	Fe ²⁺
Crude extract	122.5 ± 5.7	32.1 ± 1.7	146.7 ± 5.5	21.9 ± 0.8
PE fraction	19.7 ± 2.1	87.8 ± 2.9	453.1 ± 15.4	81.9 ± 1.3
EtOAc fraction	188.9 ± 8.7	14.9 ± 1.0	123.6 ± 3.5	15.5 ± 0.5
BuOH fraction	344.1 ± 13.5	2.09 ± 0.05	74.6 ± 2.6	6.42 ± 0.27
Water fraction	95.4 ± 7.9	55.6 ± 2.0	369.3 ± 9.8	37.3 ± 1.1
Gallic acid	—	1.42 ± 0.02	15.9 ± 2.3	—
EDTA	—	—	—	5.32 ± 0.19

To obtain the tannin compounds, which might be the main contributors to the high antioxidant activity of the walnut pellicle, a phytochemical investigation of the BuOH fraction was performed. Three hydrolyzable tannins were isolated and identified as 2,3-hexahydroxydiphenylglucose (**1**) [17], pedunculagin (**2**) [18], and 2,3,4,6-tetragalloylglucose (**3**) [19], by comparison of the MS, ¹H and ¹³C NMR spectral data with those reported in the literature (Figure 1). Compound **3** was isolated from this species for the first time. The isolated tannins exhibited significant high radical scavenging activity and had a decreasing order **1** (5.10 ± 0.09 μM) > **2** (5.69 ± 0.10 μM) > gallic acid (7.51 ± 0.06 μM) > **3** (11.35 ± 0.14 μM). Compounds **1** and **2** were more effective than gallic acid in terms of DPPH radical-scavenging activity, which was attributed to the galloyl groups present in the structure [20].

According to the UPLC chromatogram, pedunculagin (**2**) (6.97 ± 0.09 mg/g sample) is the major compound in walnut pellicle. The quantities of compounds **1** (0.57 ± 0.03 mg/g sample), **3** (0.96 ± 0.03 mg/g sample), and gallic acid (1.05 ± 0.05 mg/g sample) in walnut pellicle were also quantified. The result revealed that pedunculagin (**2**) may play a vital role in the antioxidant activity of the walnut pellicle, while the other tannins and gallic acid may also contribute to the enhanced activity. Additionally, the stabilizing or protective effect of the pellicle to the walnut kernel may mainly be attributed to the preferential oxidation of these easily oxidizable tannins [6].

Experimental

General experimental procedures: A Shimadzu UV–Vis 2550 spectrometer (Shimadzu, Kyoto, Japan) was used for colorimetric measurements and collection of UV spectra. ESI-MS analyses were recorded with an Agilent G3250AA (Agilent, Santa Clara, USA) and Auto Spec Premier P776 spectrometer (Waters, Milford, USA). NMR spectra were acquired with a Bruker AM-500 spectrometer (Bruker, Karlsruhe, Germany) using TMS as the internal reference. A Waters semipreparative HPLC system equipped with a Waters 2487 dual λ absorbance detector, a Waters delta 600 quaternary pump, a Waters Spherisorb ODS2 (C₁₈) Semi-Prep column (S10, 20 mm × 250 mm, 5 μm, Waters, Milford, USA), and an Empower 3

HPLC workstation (Waters) was used for semipreparative HPLC. Silica gel (200–300 mesh and 300–400 mesh; Qingdao Marine, Qingdao, China), middle chromatogram isolated gel (MCI, Greenherbs, Beijing, China), and Sephadex LH-20 (GE Healthcare, Fairfield, USA) were used for column chromatography (CC). GF254 plates (Qingdao Marine, Qingdao, China) were used for thin layer chromatography, and compounds were visualized either under UV light or by spraying with 10% H₂SO₄ in ethanol followed by heating. DPPH and ferrozine were obtained from J&K Scientific Ltd (Beijing, China), gallic acid from Aladdin-Reagent (Shanghai, China), CD₃OH from Sigma-Aldrich (Shanghai, China), and CH₃CN and CH₃OH (HPLC grade) from Fisher Chemicals (New Jersey, USA). Deionized water (resistivity ≥ 18.25 MΩ·cm) was purified with a You Pu purity water system (You Pu, Chengdu, China).

Plant materials: The pellicle of *J. regia* was collected from Kunming City in Yunnan Province, China, in August 2011. The samples were identified by Professor Shu-gang Lu at the School of Life Sciences at Yunnan University in Kunming City, China. A voucher specimen (No. LCS-02) is deposited at the Key Laboratory of Medicinal Chemistry for Natural Resources, Ministry of Education in Kunming City of China.

Extraction and isolation: Air-dried and powdered pellicle of *J. regia* (1.8 kg) was extracted with 80% aqueous acetone at room temperature (3 × 5 L, each extraction 24 h). Removal of the solvent under reduced pressure afforded the crude extract (450 g), which was partitioned successively with PE, EtOAc, and BuOH to yield soluble fractions in PE (210 g), EtOAc (44 g), BuOH (144 g), and water (52 g), respectively. Five g samples were collected from each fraction for the antioxidant experiments. The remainders were used to study the fractions' chemical components.

The BuOH fraction was subjected to silica gel CC, elution with a CHCl₃–CH₃OH gradient system (200:1 to 1:1, v/v) to give 8 fractions (FrC1–FrC8). FrC5 (1.2 g) was subjected to MCI gel CC (CH₃OH–H₂O, 1:1, v/v), Sephadex LH-20 CC (CH₃OH) and semipreparative HPLC (CH₃OH–H₂O, 3:2, v/v) to provide **1** (40 mg). FrC6 (1.5 g) was subjected to silica gel CC (EtOAc–CH₃OH, 10:1, v/v) and then purified by MCI CC (CH₃OH–H₂O, 1:1, v/v) to provide **2** (252 mg) and **3** (28 mg).

Total phenolic content: The TPC was determined according to the Folin-Ciocalteau method [21]. Folin-Ciocalteau reagent was prepared according to a previously described method [22]. A total of 15 μL of extract solution was added to 2.25 mL Folin-Ciocalteau reagent, which had been prediluted by a factor of 10 with deionized water. Five min later, 3.0 mL of Na₂CO₃ (7.5%, w/v) solution was added and the mixture was allowed to stand for 30 min at room temperature. The absorbance was measured at 765 nm. TPC was expressed as mg gallic acid equivalents/g dry extract (mg GAE/g Ex) and calculated according to the calibration curve obtained from a standard solution of gallic acid at various concentrations.

DPPH assay: The DPPH assay was assessed by using a previously published method [23]. A total of 3.9 mL DPPH (0.075 mM) was mixed with 0.1 mL sample at various concentrations. The mixture was shaken and incubated at 25°C in the dark, and the absorbance of the reaction mixture was measured at 515 nm after 30 min. The DPPH radical scavenging activity was calculated by the following equation: inhibition = $(1 - A_s/A_0) \times 100\%$; where A₀ is the absorbance of DPPH without any sample, and A_s is the absorbance of a sample with DPPH in it. Inhibition was the scavenging effect, and the 50% absorbance reduction (IC₅₀) was measured from a

curve relating concentration to the absorbance of a sample. Gallic acid was used as a reference standard.

Fe²⁺ chelating activity: The Fe²⁺ chelating assay was assessed by using a previously published method [24, 25]. Briefly, samples at various concentrations in CH₃OH (0.4 mL) were added to a solution of 2 mM FeCl₂ (0.05 mL). The reaction was initiated by the addition of 5 mM ferrozine (0.2 mL), and the total volume was adjusted to 4 mL with CH₃OH. The mixture was shaken vigorously and left standing at room temperature for 10 min; absorbance of the solution was then measured at 562 nm. The Fe²⁺ chelating activity was calculated by the following equation: inhibition = $(1 - A_s/A_o) \times 100\%$; where A_o is the absorbance of the control which contains FeCl₂ and ferrozine, and A_s is the absorbance in the presence of the sample or standard. EDTA was used as a reference standard.

HRS assay: The HRS assay was conducted by a Fenton reaction method [26]. Briefly, the reaction mixture containing 0.2 mL of acidic chrome blue K (0.2 mM), 1.2 mL of FeSO₄ (0.4 mM), 1.0 mL of H₂O₂ (0.03%, v/v), 1.2 mL of phosphate buffer (0.1 mM, pH = 5.5) and 1.0 mL of samples at various concentrations was incubated at room temperature for 15 min, and the absorbance was measured at 520 nm. Hydroxyl radical scavenging activity was calculated by the following equation: inhibition = $[(A_s - A_o) / (A - A_o)] \times 100\%$; where A_s is the absorbance in the presence of the sample, A_o is the absorbance of the control in the absence of the sample, and A is the absorbance without the sample and Fenton reaction system. Gallic acid was used as a reference standard.

Tannins determined by UPLC: Air-dried and powdered pellicle of *J. regia* (1.0000 g) was extracted 3 times with 80% aqueous acetone at room temperature, for 24 h each time. The resulting crude extract

and the authentic samples were prepared as solutions (10.00 mg/mL and 1.00 mg/mL, respectively). All sample solutions were filtered through a 0.45 μm filter before injection into the ACQUITY UPLC system equipped with a QSM (quaternary solvent manager), a UPL PDA (photodiode array) detector, a CHA column thermostat, a SDI sample manager, a reversed phase Symmetry1 C₁₈ column (T3, 2.1 mm × 100 mm, 1.8 μm; Waters, Milford, USA), and an Empower 3 UPLC workstation (Waters). The optimal mobile phase for the analysis was a gradient elution system consisting of solvent A (H₂O, 1.0% acetic acid) and solvent B (CH₃CN). The gradient program was as follows: 0-3 min, 0-5% solvent B; 3-6 min, 5-10% solvent B; 6-10 min, 10%-15% solvent B; 10-20 min, 15%-100% solvent B; 20-21 min, 100%-0 solvent B. The flow rate was 0.5 mL/min, the column temperature was set at 30 °C, and the injection volume was 5 μL. The UV detection wavelength was monitored at 280 nm. The identification of peaks was confirmed by the UV absorptions and retention times of authentic samples. The sample analyte content (C_s, mg/g dry sample) was calculated according to the equation C_s = (C_a × V) / M, where C_a is the analyte content (mg/mL) based on the calibration curve, V (mL) is the final volume of sample, and M is the sample weight (g).

Statistical analysis: The results were determined as the mean ± SD for at least 3 replicates for each sample. Statistical analysis was performed using SPSS. A significant difference was evaluated at a level of p < 0.05.

Acknowledgments - This work was financially supported by a grant from the Program for Changjiang Scholars and Innovative Research Team in University (No. IRT13095) and a grant from the National Natural Science Foundation of China (No. 21162046).

References

- [1] Grace MH, Warlick CW, Neff SA, Lila MA. (2014) Efficient preparative isolation and identification of walnut bioactive components using high-speed counter-current chromatography and LC-ESI-IT-TOF-MS. *Food Chemistry*, **158**, 229-238.
- [2] Matlawska I, Bylka W, Widz-Tyszkiewicz E, Stanisz B. (2015) Determination of the juglone content of *Juglans regia* leaves by GC/MS. *Natural Product Communications*, **10**, 1239-1242.
- [3] Paudel P, Prabodh Satyal P, Dosoky NS, Maharjan S, Setzer NW. (2013) *Juglans regia* and *J. nigra*, two trees important in traditional medicine: a comparison of leaf essential oil compositions and biological activities. *Natural Product Communications*, **8**, 1481-1486.
- [4] Pan A, Sun Q, Manson JE, Willett WC, Hu FB. (2013) Walnut consumption is associated with lower risk of type 2 diabetes in women. *The Journal of Nutrition*, **143**, 512-518.
- [5] Feldman EB. (2002) The scientific evidence for a beneficial health relationship between walnuts and coronary heart disease. *The Journal of Nutrition*, **132**, 1062-1101.
- [6] Jurd L. (1956) Plant polyphenols. I. The polyphenolic constituents of the pellicle of the walnut (*Juglans regia*). *Journal of the American Chemical Society*, **78**, 3445-3448.
- [7] Jurd L. (1958) Plant polyphenols. III. The isolation of a new ellagitannin from the pellicle of the walnut. *Journal of the American Chemical Society*, **80**, 2249-2252.
- [8] Arranz S, Pérez-Jiménez J, Saura-Calixto F. (2007) Antioxidant capacity of walnut (*Juglans regia* L.): contribution of oil and defatted matter. *European Food Research and Technology*, **227**, 425-431.
- [9] Li L, Tsao R, Yang R, Liu C, Zhu H, Young JC. (2006) Polyphenolic profiles and antioxidant activities of heartnut (*Juglans ailanthifolia* var. *cordiformis*) and Persian walnut (*Juglans regia* L.). *Journal of Agricultural and Food Chemistry*, **54**, 8033-8040.
- [10] Pellegrini N, Serafini M, Salvatore S, Del Rio D, Bianchi M, Brighenti F. (2006) Total antioxidant capacity of spices, dried fruits, nuts, pulses, cereals and sweets consumed in Italy assessed by three different *in vitro* assays. *Molecular Nutrition and Food Research*, **50**, 1030-1038.
- [11] Liu J, Wang CN, Wang ZZ, Zhang C, Lu S, Liu JB. (2011) The antioxidant and free-radical scavenging activities of extract and fractions from corn silk (*Zea mays* L.) and related flavone glycosides. *Food Chemistry*, **126**, 261-269.
- [12] You Q, Chen F, Wang X, Sharp JL, You YR. (2012) Analysis of phenolic composition of Noble muscadine (*Vitis rotundifolia*) by HPLC-MS and the relationship to its antioxidant capacity. *Journal of Food Science*, **77**, 1115-1123.
- [13] Kaisoon O, Siriamornpun S, Weerapreeyakul N, Meeso N. (2011) Phenolic compounds and antioxidant activities of edible flowers from Thailand. *Journal of Functional Foods*, **3**, 88-99.
- [14] Amarowicz R. (2007) Tannins: the new natural antioxidants. *European Journal of Lipid Science and Technology*, **109**, 549-551.
- [15] Kao TH, Chen BH. (2006) Functional components in soybean cake and their effects on antioxidant activity. *Journal of Agriculture and Food Chemistry*, **54**, 7544-7555.
- [16] Li S, Zhao Y, Zhang L, Zhang X, Huang L, Li D, Niu C, Yang Z, Wang Q. (2012) Antioxidant activity of *Lactobacillus plantarum* strains isolated from traditional Chinese fermented foods. *Food Chemistry*, **135**, 1914-1919.
- [17] Okuda T, Yoshida T, Hatano T, Yazaki K, Ashida M. (1980) Ellagittannins of the Casuarinaceae, Stachyuraceae and Myrtaceae. *Phytochemistry*, **21**, 2871-2874.

- [18] Okuda T, Yoshida T, Ashida M, Yazaki K. (1983) Tannins of *Casuarina* and *Stachyurus* species. Part 1. Structures of pendunculagin, casuarictin, strictinin, casuarinin, casuariin, and stachyurin. *Journal of the Chemical Society, Perkin Transactions 1*, 1765-1772.
- [19] Khanbabaei K, Lötzerich K. (1997) Efficient total synthesis of the natural products 2,3,4,6-tetra-O-galloyl-D-glucopyranose, 1,2,3,4,6-penta-O-galloyl- β -D-glucopyranose and the unnatural 1,2,3,4,6-penta-O-galloyl- α -D-glucopyranose. *Tetrahedron*, **53**, 10725-10732.
- [20] Cai YZ, Mei S, Jie X, Luo Q, Corke H. (2006) Structure-radical scavenging activity relationships of phenolic compounds from traditional Chinese medicinal plants. *Life Science*, **78**, 2872-2888.
- [21] Singleton VL, Rossi JA. (1965) Colorimetry of total phenolics with phosphomolybdic-phosphotungstic acid reagents. *American Journal of Enology and Viticulture*, **16**, 144-158.
- [22] Huang D, Ou B, Prior RL. (2005) The chemistry behind antioxidant capacity assays. *Journal of Agricultural and Food Chemistry*, **53**, 1841-1856.
- [23] He JM, Yin TP, Chen Y, Cai L, Tai ZG, Li ZJ, Liu CS, Wang YR, Ding ZT. (2015) Phenolic compounds and antioxidant activities of edible flowers of *Pyrus pashia*. *Journal of Functional Foods*, **17**, 371-379.
- [24] Miceli N, Trovato A, Dugo P, Cacciola F, Donato P, Marino A, Bellinghieri V, La Barbera TM, Guvenc A, Taviano MF. (2009) Comparative analysis of flavonoid profile, antioxidant and antimicrobial activity of the berries of *Juniperus communis* L. var. *communis* and *Juniperus communis* L. var. *saxatilis* Pall. from Turkey. *Journal of Agricultural and Food Chemistry*, **57**, 6570-6577.
- [25] Yin TP, Cai L, Fang HX, Fang YS, Li ZJ, Ding ZT. (2015) Diterpenoid alkaloids from *Aconitum vilmorinianum*. *Phytochemistry*, **116**, 314-319.
- [26] Fu FE, Wang XH, Li F, Cao QE. (2008) A method for screening of antioxidant activities of resina draconis *in vitro* and its applications. *Chinese Journal of Analysis Laboratory*, **28**, 2009-2011.

Chemical Constituents of *Cordyceps cicadae*Zhi-Bo Chu^a, Jun Chang^b, Ying Zhu^{a,*} and Xun Sun^{b,*}^aSchool of Pharmacy, Zhejiang Chinese Medical University, 548 Binwen Road, Hangzhou 310053, China^bSchool of Pharmacy, Fudan University, 826 Zhangheng Road, Shanghai 201203, China

zhuyinggw@163.com, sunxunf@shmu.edu.cn

Received: September 30th, 2015; Accepted: November 5th, 2015

One new bifuran derivative (**1**), together with fourteen known compounds, were isolated from *Cordyceps cicadae* X. Q. Shing. The known compounds included nine nucleosides, uracil (**2**), uridine (**3**), 2'-deoxyuridine (**4**), 2'-deoxyinosine (**5**), guanosine (**6**), 2'-deoxyguanosine (**7**), thymidine (**8**), adenosine (**9**), and 2'-deoxyadenosine (**10**); three amino acids tryptophan (**11**), phenylalanine (**12**), and tyrosine (**13**); and two dopamine analogues *N*-acetylnoradrenaline (**14**) and its dimer, *trans*-2-(3',4'-dihydroxyphenyl)-3-acetylamo-7-(*N*-acetyl-2"-amino-ethylene)-1,4-benzodioxane (**15**). Their structures were decisively elucidated by spectroscopic analysis, including 1D and 2D NMR techniques.

Keywords: *Cordyceps cicadae*, Bifuran derivative, Nucleoside, Amino acid, Dopamine analogue.

Cordyceps cicadae X. Q. Shing (Clavicipitaceae, Ascomycotina), named 'Chan Hua', an anamorph of *Isaria cicadae* Miq, is a major parasitic fungus growing on the nymphs of *Cicada flammata* Distant, *Platyleura kaempferi* Fabricius, *Crytotympana pustulata* Fabricious, *Platylomia pieli* Kato and *Oncotympana maculatellollis* Motsch [1]. As a traditional Chinese medicine used for thousands of years, 'Chan Hua' is reported to possess antitumor, antibacterial, immunoregulatory and sedative effects, and is widely used in the treatment of fever, infantile convulsion, palpitation and dizziness [2]. Some bioactive constituents, for example, polysaccharides, galactomannan, ISP-1 (myriocin) and cyclodepsipeptides have been isolated from *C. cicadae* [3]. Cordycepin, adenosine derivatives, aromatic 4-*O*-methylglucosides, cyclopentenone and furan derivative were reported from the cultivated mycelia of *C. cicadae* [4]. As part of our investigation on biologically active constituents from Chinese traditional medicines [5], *C. cicadae* was exhaustively studied. A crude extract of the drug was chromatographed repeatedly on the MCI gel CHP 20P, HW-40F, normal phase silica gel, Sephadex LH-20, and reversed phase silica gel. As a result, one new heterocyclic compound, 5,5'-di (2-ethyl-hexyloxy)-5,5'-bifuran (**1**) (Figure 1), was obtained, together with fourteen known compounds. Herein, we report the isolation and structural elucidation of compound **1**.

Compound **1** was obtained as colorless oil. The positive ESI-MS showed quasimolecular ion peaks at *m/z* 391 [$M + H$]⁺ and 803 [2*M* + Na]⁺, indicating a molecular weight of 390. The molecular formula of **1** was determined to be $C_{24}H_{38}O_4$ from the HR-ESI-MS ion peak at *m/z* 413.2659 [$M + Na$]⁺ (calcd 413.2662), and ¹H and ¹³C NMR spectroscopic data. The low-field part of the ¹H NMR spectrum (Table 1) indicated the presence of four olefinic protons at δ 7.734, 7.726, 7.628, and 7.620 (d, *J* = 5.6 Hz). The high-field region of the spectrum showed two oxygenated methylenes at δ 4.229 (4H, m), two methines at δ 1.681 (2H, m), eight methylenes at δ 1.392-1.423 (8H, m), and four methyl groups at δ 0.961 (6H, t, *J* = 7.5 Hz) and 0.932 (6H, t, *J* = 7.5 Hz). The ¹³C NMR spectrum showed two quaternary carbons at δ 169.23 and 133.59, and two methine carbons at δ 132.37 and 129.86, which suggested an oxygenated furan ring. There was evidence of an oxygenated methylene carbon at δ 69.02, one methine carbon at δ 40.13, four methylene carbons at δ 31.60, 30.12, 24.04, and 24.92, and two

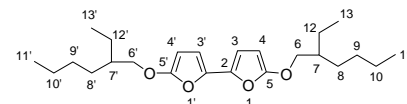


Figure 1: The structure of compound **1**.

Table 1: NMR data of compound **1**.

position	¹ H ^a	¹³ C ^b	¹ H- ¹ H COSY	HMBC (H→C)
2, 2'		133.59 s		
3, 3'	7.734, 7.726 d (5.6)	129.86 d	H-4	C-2, 4, 5
4, 4'	7.628, 7.620 d (5.6)	132.37 d	H-3	C-2, 3
5, 5'		169.23 s		
6, 6'	4.229 m	69.02 t	H-7	C-5, 7, 8, 12
7, 7'	1.681 m	40.13 d	H-6, 8, 12	C-6, 8, 9, 12, 13
8, 8'	1.421 m	31.60 t	H-7, 9	C-6, 7
9, 9'	1.392 m	30.12 t	H-8, 10	C-10
10, 10'	1.395 m	24.04 t	H-9, 11	C-9, 11
11, 11'	0.932 t (7.5)	14.45 q	H-10	C-9, 10
12, 12'	1.423 m	24.92 t	H-7, 13	C-6, 7, 8, 13
13, 13'	0.961 t (7.5)	11.44 q	H-12	C-7, 12

^a 400 MHz, CD₃OD; chemical shifts in ppm relative to TMS; coupling constant (*J*) in Hz.
^b 100 MHz, CD₃OD; multiplicity was established from DEPT data.

terminal methyl carbons at δ 14.45 and 11.44, which were derived from the alkoxy moiety. Based on the ESI-MS, compound **1** was proved as a dimer of a furan derivative. The 2-ethyl-hexyloxy moiety was established unambiguously by ¹H-¹H COSY, HMQC and HMBC experiments, in which long-range correlations were observed not only between H-7 (δ 1.681) and five carbons (C-6, C-8, C-9, C-12 and C-13), but also between H-11 (δ 0.932) and two carbons (C-9 and C-10). Moreover, the long-range correlations between the oxygenated methylene H-6, 6' (δ 4.229) and oxygenated quaternary olefin carbons C-5, 5' (δ 169.23) indicated that 2-ethyl-hexyloxy was substituted at C-5 and C-5' of each furan ring. The two furan rings were linked at C-2 and C-2' by a C-C bond, because the olefin methine signals at δ 7.734 and 7.726 (H-3, 3') showed cross peaks with a quaternary olefin carbon at δ 133.59 (C-2, 2') by *J*₂ and *J*₃ correlation. Consequently, compound **1** was identified as 5,5'-di (2-ethyl-hexyloxy)-5,5'-bifuran.

It is worth mentioned that Baek *et al.* reported a bifuran derivative from *Chrysanthemum coronarium* L. [6] and Guo *et al.* reported bifuran derivatives from *Cyathula officinalis* Kuan [7]. However, the peak of H-4 and H-4' of the furan was assigned as dd peaks with

coupling constants of either 5.6 Hz or 5.6 and 3.3 Hz. In fact, the peak of H-4 (H-3) was not completely overlapped by H-4' (H-3') of the furan because of a steric effect. Therefore, the aromatic protons of the furan should be assigned as four doublet peaks with a coupling constant of 5.6 Hz, respectively.

Fourteen known compounds were also isolated, including nine nucleosides, uracil (**2**), uridine (**3**), 2'-deoxyuridine (**4**), 2'-deoxyinosine (**5**), guanosine (**6**), 2'-deoxyguanosine (**7**), thymidine (**8**), adenosine (**9**), 2'-deoxyadenosine (**10**); three amino acid tryptophan (**11**), phenylalanine (**12**), and tyrosine (**13**); and two dopamine analogues, *N*-acetylnoradrenaline (**14**), and its dimer, *trans*-2-(3',4'-dihydroxyphenyl)-3-acetylamino-7-(*N*-acetyl-2"-amino-ethylene)-1,4-benzodioxane (**15**) were isolated from *C. cicadae*.

Experimental

General: Optical rotation, Perkin-Elmer 241 automatic digital polarimeter; UV, Shimadzu UV-260 instrument; IR, Perkin-Elmer 599B instrument; NMR, Bruker DRX-400 spectrometer; (¹H 400 MHz and ¹³C 100 MHz). ESI-MS, Quattro instrument. Reverse-phase chromatography utilized TSK gel Toyopearl HW-40F (30-60 µm, Toso Co., Ltd.), MCI gel CHP 20P (75-150 µm, Mitsubishi Chemical Industries Co., Ltd.) and Cosmosil 75 C18-OPN (42-105 µm, Nacalai Tesque Inc.) columns. TLC was performed using precoated silica gel 60 F254 plates (0.2 mm, Merck).

Plant material: *Cordyceps cicadae* X. Q. Shing was collected in Zhejiang Province, People's Republic of China in 2014, and authenticated by Dr Xie H. A voucher specimen has been deposited in the Herbarium of our lab (DNPC 2014006).

Extraction and isolation: *C. cicadae* (2 kg) was extracted 3 times with 70% aqueous acetone at room temperature (3 × 10 L). The solvent was evaporated under reduced pressure to 1 L and filtered through celite. The filtrate was concentrated *in vacuo* to yield 65 g of a gummy residue. This was dissolved in 400 mL water, and subjected to MCI gel CHP 20P (8 × 60 cm) eluting with a MeOH/H₂O gradient with a flow rate of 15 mL/min to obtain fractions 1 [1.0 L, H₂O], 2 [0.6 L, MeOH/H₂O (10:90)], 3 [0.6 L, MeOH/H₂O (30:70)], 4 [0.6 L, MeOH/H₂O (50:50)], 5 [0.7 L,

MeOH/H₂O (70:30)], 6 [1.0 L, MeOH], 7 [1.0 L, MeCOMe/H₂O (60:40)], and 8 [1.0 L, MeCOMe]. Fraction 2 (6.4 g) was chromatographed on Toyopearl HW-40F (6 × 60 cm) using water as eluent to obtained 6 fractions 2A-2F (eluent volume: 200 mL/fraction). Fraction 2C (0.3 g) was further purified by MCI gel CHP 20P (5 × 40 cm, eluted with H₂O→30% MeOH) and Cosmosil 75 C₁₈-OPN (4 × 30 cm, eluted with H₂O→30% MeOH) to give **13** (26 mg). Fraction 3 (5.8 g) was chromatographed on Toyopearl HW-40F (6 × 60 cm) using water as eluent to obtained 5 fractions 3A-3E (eluent volume: 200 mL/fraction). Fraction 3C (0.8 g) was purified by MCI gel CHP 20P (5 × 40 cm, eluted with 10-50% MeOH) and Cosmosil 75 C₁₈-OPN (4 × 30 cm, eluted with H₂O→50% MeOH) to give **3** (10 mg), **4** (15 mg), **5** (6 mg), **6** (11 mg), **7** (8 mg), and **9** (25 mg). Fraction 4 (6.2 g) was chromatographed on Toyopearl HW-40F (6 × 60 cm) using water as eluent to obtained 6 fractions 4A-4F (eluent volume: 200 mL/fraction). Fraction 4C (0.8 g) was further purified by MCI gel CHP 20P (5 × 40 cm, eluted with 20-60% MeOH) and Cosmosil 75 C₁₈-OPN (4 × 30 cm, eluted with H₂O→60% MeOH) to give **2** (6 mg), **8** (9 mg), **10** (18 mg), **11** (45 mg), **12** (30 mg) and **14** (6 mg). Fraction 8 (6.8 g) was chromatographed on LH-20 (4 × 200 cm) using methanol as eluent to obtained 6 fractions 8A-8F (eluent volume: 200 mL/fraction). Fraction 8C (0.4 g) was subjected to CC on silica gel to give **1** (15 mg) and **15** (11 mg).

5, 5'-Di (2-ethyl-hexyloxy)-5, 5'-bifuran (1)

Colorless oil.

[α]_D²⁰: 0 (c 0.10, MeOH).

IR (KBr) ν_{max} : 3100, 1660, 1245, 1230 cm⁻¹.

UV (MeOH) λ_{max} (log ε): 241 (3.89), 274 (3.14) nm;

¹H and ¹³C NMR: Table 1.

ESI-MS: *m/z* 391 [M + H]⁺, 803 [2M + Na]⁺.

HR-ESI-MS: *m/z* 413.2659 [M + Na]⁺ (calcd. for C₂₄H₃₈O₄Na, 413.2662).

Acknowledgments - This project was supported financially by the National Natural Science Foundation of China (No. 21242003), Specialized Research Fund for the Doctoral Program of Higher Education (No. 20120071120047).

References

- [1] Zeng WB, Yu H, Ge F, Yang JY, Chen ZH, Wang YB, Dai YD, Adams A. (2014) Distribution of nucleosides in populations of *Cordyceps cicadae*. *Molecules*, **19**, 6123-6141.
- [2] Nanjing University of Chinese Medicine. (2006) *The Dictionary of Chinese Traditional Medicine*. Shanghai Press of Science and Technology, Shanghai, 3597-3598.
- [3] (a) Kiho T, Ito M, Nagai K, Hara C, Ukai S. (1988) Polysaccharides in fungi. XXII. a water soluble polysaccharide from the alkaline extract of the insect-body portion of Chan hua (fungus: *Cordyceps cicadae*). *Chemical & Pharmaceutical Bulletin*, **36**, 3032-3037; (b) Ukai S, Matsuura S, Hara C, Kiho T, Hirose K. (1982) Structure of a new galactomannan from the ascocarps of *Cordyceps cicadae* Shing. *Carbohydrate Research*, **101**, 109-116; (c) Fujita T, Inoue K, Yamamoto S, Ikumoto T, Sasaki S, Toyama R, Chiba K, Hoshino Y, Okumoto T. (1994) Fungal metabolites. Part II. A potent immunosuppressive activity found in *Isaria sinclairii* metabolite. *Journal of Antibiotics*, **47**, 208-215; (d) Kuo YC, Lin LC, Don MJ, Liao HF, Tsai YP, Lee GH, Chou CJ. (2002) Cyclodepsipeptide and dioxomorpholine derivatives isolated from the insect-body portion of the fungus *Cordyceps cicadae*. *Journal of Chinese Medicine*, **13**, 209-219; (e) Wang J, Zhang DM, Jia JF, Peng QL, Tian HY, Wang L, Ye WC. (2014) Cyclodepsipeptides from the ascocarps and insect-body portions of fungus *Cordyceps cicadae*. *Fitoterapia*, **97**, 23-27.
- [4] (a) Furuya T, Hirotani M, Matsuzawa M. (1983) N6-(2-hydroxyethyl) adenosine, a biologically active compound from cultured mycelia of *Cordyceps* and *Isaria* species. *Phytochemistry*, **22**, 2509-2512; (b) Zhang SW, Xuan LJ. (2007) Five aromatics bearing a 4-O-methylglucose unit from *Cordyceps cicadae*. *Helvetica Chimica Acta*, **90**, 404-410; (c) Zhang SW, Xuan LJ. (2008) Cyclopentenone and furan derivative from the mycelia of *Cordyceps cicadae*. *Journal of Antibiotics*, **61**, 43-45.
- [5] (a) Jiang K, Bai JQ, Chang J, Tan JJ, Qu SJ, Luo HF, Tan CH, Zhu DY. (2014) Three new 24-nortriterpenoids from the roots of *Ilex asprella*. *Helvetica Chimica Acta*, **97**, 64-69; (b) Chang J, Chu ZB, Song J, Jin L, Sun X. (2015) Two novel isoquinoline alkaloids from the seedling of *Corydalis decumbens*. *Tetrahedron Letters*, **56**, 225-228.
- [6] Song MC, Yang HJ, Jeong TS, Kim KT, Baek NI. (2008) Heterocyclic compounds from *Chrysanthemum coronarium* L. and their inhibitory activity on hACAT-1, hACAT-2, and LDL-oxidation. *Archives of Pharmacal Research*, **31**, 573-578.
- [7] Liu J, Xu J, Zhao XJ, Gao WY, Zhang SZ, Guo YQ. (2010) A new heterocyclic compound from *Cyathula officinalis* Kuan. *Chinese Chemical Letters*, **21**, 70-72.

A New Bithiophene from the Root of *Echinops grijsii*

Fang-Pin Chang^{a,f}, Chien-Chih Chen^b, Hui-Chi Huang^c, Sheng-Yang Wang^d, Jih-Jung Chen^e, Chang-Syun Yang^c, Chung-Yi Ou^f, Jin-Bin Wu^{f,**}, Guan-Jhong Huang^{c,**} and Yueh-Hsiung Kuo^{c,g,*}

^aThe Ph.D. Program for Cancer Biology and Drug Discovery, China Medical University and Academia Sinica, Taichung 404, Taiwan

^bDepartment of Nursing and Department of Biotechnology, Hungkuang University, Taichung 443, Taiwan

^cDepartment of Chinese Pharmaceutical Sciences and Chinese Medicine Resources, China Medical University, Taichung 404, Taiwan

^dDepartment of Forestry, National Chung Hsing University, Taichung 402, Taiwan

^eDepartment of Pharmacy, Tajen University, Pingtung, Taiwan 907

^fSchool of Pharmacy, China Medical University, Taichung 404, Taiwan

^gDepartment of Biotechnology, Asia University, Taichung 404, Taiwan

** Authors made equal contribution to this article.

kuoyh@mail.cmu.edu.tw

Received: August 19th, 2015; Accepted: November 5th, 2015

A new bithiophene, 5-(4-hydroxy-3-methoxy-1-butynyl)-2,2'-bithiophene (**1**), and sixteen known thiophenes: 2-(3,4-dihydroxybut-1-ynyl)-5-(penta-1,3-diynyl)thiophene (**2**), α-terthienyl (**3**), 5-(3,4-dihydroxybut-1-ynyl)-2,2'-bithiophene (**4**), 5-acetyl-2,2'-bithiophene (**5**), 5-formyl-2,2'-bithiophene (**6**), methyl 2,2'-bithiophene-5-carboxylate (**7**), 5-(but-3-en-1-ynyl)-2,2'-bithiophene (**8**), 5-(4-isovaleroxybut-1-ynyl)-2,2'-bithiophene (**9**), cardopatine (**10**), isocardopatine (**11**), 5-(3-hydroxy-4-isovaleroxybut-1-ynyl)-2,2'-bithiophene (**12**), 5-(3-hydroxymethyl-3-isovaleroxyprop-1-ynyl)-2,2'-bithiophene (**13**), 5-(4-hydroxy-1-butynyl)-2,2'-bithiophene (**14**), 5-(4-acetoxy-1-butynyl)-2,2'-bithiophene (**15**), 2,2'-bithiophene-5-carboxylic acid (**16**) and 2-(4-hydroxybut-1-ynyl)-5-(penta-1,3-diynyl)thiophene (**17**) were isolated from the roots of *Echinops grijsii* Hance. Among them, compounds **6**, **7** and **16** were isolated from a natural source for the first time. Compounds **2**, **4** and **14** exhibited significant anti-inflammatory activity against nitrite of LPS-stimulated production in the RAW 264.7 cell line.

Keywords: *Echinops grijsii*, Bithiophene, 5-(4-Hydroxy-3-methoxy-1-butynyl)-bithiophene, Anti-inflammatory.

Echinops grijsii Hance (Compositae) is a perennial medicinal herb and the only native species of *Echinops* from Taiwan [1]. The roots of this plant have been used to clear heat, expel miasma and stimulate milk secretion. It was recorded in the Chinese Pharmacopoeia (2005 edition) as Yuzhou Loulu [2]. Previous chemical investigation of the roots of *E. grijsii* demonstrated the presence of thiophenes, steroids, triterpenes and essential oils [3]. Thiophenes have been proven to possess anti-inflammatory [2], anti-tumor [4] and anti-viral [5] activities. The MeOH extract of the roots showed a significant anti-inflammatory activity. Thus, the constituents of *E. grijsii* were investigated. This paper deals with the structure elucidation of a new compound and the anti-inflammatory activity of the isolates.

Silica gel column chromatography of the MeOH extract of dried roots of *E. grijsii* led to the isolation of a new compound: 5-(4-hydroxy-3-methoxy-1-butynyl)-2,2'-bithiophene (**1**), as well as sixteen known compounds: 2-(3,4-dihydroxybut-1-ynyl)-5-(penta-1,3-diynyl)thiophene (**2**) [6], α-terthienyl (**3**), 5-(3,4-dihydroxybut-1-ynyl)-2,2'-bithiophene (**4**), 5-acetyl-2,2'-bithiophene (**5**) [1], 5-formyl-2,2'-bithiophene (**6**) [7], methyl 2,2'-bithiophene-5-carboxylate (**7**) [8], 5-(but-3-en-1-ynyl)-2,2'-bithiophene (**8**), 5-(4-isovaleroxybut-1-ynyl)-2,2'-bithiophene (**9**), cardopatine (**10**), isocardopatine (**11**), 5-(3-hydroxy-4-isovaleroxybut-1-ynyl)-2,2'-bithiophene (**12**) [1], 5-(3-hydroxymethyl-3-isovaleroxyprop-1-ynyl)-2,2'-bithiophene (**13**) [9], 5-(4-hydroxy-1-butynyl)-2,2'-bithiophene(**14**) [1], 5-(4-acetoxy-1-butynyl)-2,2'-bithiophene (**15**)

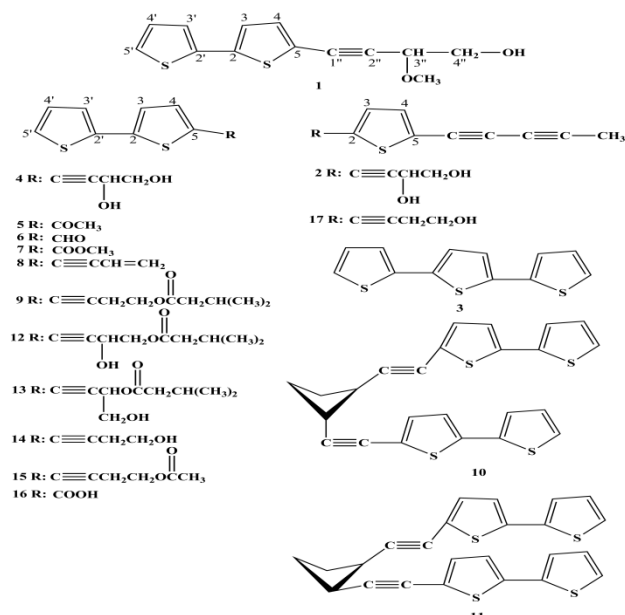


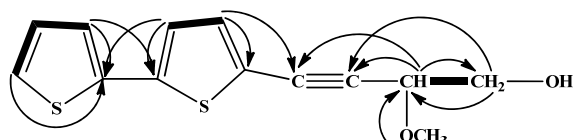
Figure 1: The chemical structures of compounds 1-17.

[10], 2,2'-bithiophene-5-carboxylic acid (**16**) [11] and 2-(4-hydroxybut-1-ynyl)-5-(penta-1,3-diynyl)thiophene (**17**) [12] (Figure 1).

Table 1: ^1H - and ^{13}C -NMR data (CDCl_3) of **1**. δ in ppm, J in Hz.

Position	^1H NMR (400 MHz, δ , CDCl_3)	^{13}C NMR (50 MHz, δ , CDCl_3)
1		
2		139.5
3	7.13 (1H, d, $J=3.8$ Hz)	133.8
4	7.00 (1H, d, $J=3.8$ Hz)	128.2
5		122.3
1'		
2'		136.5
3'	7.17 (1H, d, $J=3.6$ Hz)	124.6
4'	7.02 (1H, dd, $J=5.1, 3.6$ Hz)	123.6
5'	7.24 (1H, d, $J=5.1$ Hz)	125.4
1"		90.0
2"		80.7
3"	4.31 (1H, t, $J=5.7$ Hz)	73.0
4"	3.82 (1H, d, $J=5.7$ Hz)	65.3
OCH ₃	3.52 (3H, s)	57.3

The numbers in parentheses are J values in Hz

**Figure 2:** ^1H - ^1H COSY (—) and key HMBC ($^1\text{H} \rightarrow ^{13}\text{C}$) correlation of **1**.

Compound **1** was obtained as a yellow oil. Its molecular formula $\text{C}_{13}\text{H}_{12}\text{O}_2\text{S}_2$ was determined by the pseudomolecular ion peak at m/z 262.9758 [$\text{M}-2\text{H}$]⁺ in the HR-ESIMS. The structure of **1** was established by analysis of ^1H and ^{13}C NMR, HMQC, COSY and HMBC spectral data. The UV absorption maximum at λ_{max} 333 nm showed the presence of a bithiophene group conjugated with an acetylene functionality [13]. The IR spectrum showed the presence of hydroxy (3431 cm^{-1}), alkyne (2214 cm^{-1}), and bithiophene (802, 696 cm^{-1}).

The ^1H NMR spectrum showed characteristic signals of 5-substituted 2,2'-bithiophene protons at δ 7.24 (1H, d, $J=5.1$ Hz, H-5'), 7.17 (1H, d, $J=3.6$ Hz, H-3'), 7.13 (1H, d, $J=3.8$ Hz, H-3), 7.02 (1H, dd, $J=5.1, 3.6$ Hz, H-4') and 7.00 (1H, d, $J=3.8$ Hz, H-4) [13]. Additionally, signals of CH₂CH protons appeared at δ 4.31 (1H, t, $J=5.7$ Hz, H-3'') and 3.82 (2H, d, $J=5.7$ Hz, H-4''); proton signals that appeared at δ 3.52 (3H, s) indicated the presence of a methoxy group. The ^{13}C NMR spectrum of **1** exhibited 13 carbon signals including eight bithiophene carbons appearing at δ 139.5, 136.5, 133.8, 128.2, 125.4, 124.6, 123.6 and 122.3, along with the vinyl carbons at δ 90.0 and 80.7. Two oxygenated carbons appeared at δ 73.0 and 65.3, and one methoxy carbon at δ 57.3 (Table 1).

The COSY and HMBC experiments gave ^1H - ^1H and ^1H - ^{13}C direct correlations of **1** (Figure 2). The correlation between H-4 (δ 7.00) / C-5 (δ 122.3) and C-1" (δ 90.0), H-3" (δ 4.31) / C-1" (δ 90.0), C-2" (δ 80.7) and C-4" (δ 65.3) indicated that the CHCH₂OH group was connected with the vinyl group, which was connected with the bithiophene at C-5. The ^1H NMR and ^{13}C NMR spectral data of compound **1** were very similar to those of **4**. The only difference was that the correlation between the methoxy group (δ 3.52) with C-3" (δ 73.0) indicated that the methoxy group was connected at C-3". From the above evidence, the structure of **1** was established as 5-(4-hydroxy-3-methoxy-1-butynyl)-2,2'-bithiophene.

Compounds **1-17** were tested for anti-inflammatory activity against the RAW 264.7 cell line. Compounds **2**, **4** and **14** exhibited significant activity, with IC₅₀ values of 2.5, 20.0 and 6.7 $\mu\text{g}/\text{mL}$ (Table 2).

Table 2: Cell viability and *in vitro* anti-inflammatory activities of compounds from *E. grijsii* against nitrite of LPS-stimulated production in RAW 264.7 cell.

Compds	IC ₅₀ ($\mu\text{g}/\text{mL}$)	Cell viability (% of control)
2	2.5	98.5 \pm 3.4
4	20.0	82.7 \pm 4.0
14	6.7	93.1 \pm 2.7
indomethacin	65.4	

Experimental

Plant material: The roots of *E. grijsii* were bought from the Shan You herb store in Nantou country in September 2010. The plant material was identified by assistant professor Shyh-Shyun Huang from the school of Pharmacy, China Medical University.

Extraction and isolation: The roots of *E. grijsii* (10 kg) were crushed into pieces and extracted with methanol (50 L \times 3) at ambient temperature and concentrated under vacuum to yield the MeOH extract (2.5 kg). Part of this (1 kg) was partitioned between EtOAc-H₂O to give EtOAc-soluble (100 g) and H₂O-soluble fractions. The EtOAc-soluble fraction was chromatographed over silica gel eluted with *n*-hexane and a gradient of *n*-hexane-EtOAc. The eluent was collected in constant volumes, and combined into 32 fractions based on TLC results. Fraction 10 (obtained with *n*-hexane: EtOAc = 90:10, amount 2 g) was re-separated by HPLC to yield **1** (1.46 mg), **5** (2.15 mg), **6** (13.75 mg), **7** (2.42 mg), **8** (24.74 mg), **9** (2.89 mg), **10** (4.53 mg), **11** (17.54 mg), **12** (3.82 mg), **13** (5.67 mg), 5-(4-hydroxy-1-butynyl)-2,2'-bithiophene (**14**) (3.1 mg), **15** (2.6 mg) and **17** (1.99 mg). Fraction 16 (obtained with *n*-hexane: EtOAc = 70:30, amount 1.2 g) was re-separated by Sephadex LH-20 and HPLC to yield **2** (63.6 mg), **3** (43.49 mg), **4** (77.64 mg) and **16** (112.07 mg).

General: UV spectra were obtained with a Shimadzu Pharmaspec-1700 UV-Visible spectrophotometer, optical rotations with a Jasco P-1020 polarimeter, and infrared spectra with a Shimadzu IR prestige-21 Fourier transform infrared spectrophotometer. ^1H - and ^{13}C -NMR spectra were recorded with Bruker DRX-400 and DRX-200 FT-NMR spectrometers. HRESIMS data were generated at the Mass Spectrometry Laboratory of the Chung Hsing University. Column chromatography was performed using LiChroCART Si gel (5 μM) and SephadexTMLH-20. HPLC details: detector: IOTA 2, pump: P230 HPLC PUMP, column: Phenomenex 250 \times 10.00 mm 5 micron. TLC analysis was carried out using aluminum pre-coated Si plates and the compounds were visualized using a UV lamp at $\lambda = 254$ nm and $\lambda = 365$ nm.

Cell viability: Cells (2×10^5) were cultured in a 96-well plate containing DMEM supplemented with 10% FBS for 1 day to become nearly confluent. Then cells were cultured with compounds **1-17** in the presence of 100 ng/mL LPS (lipopolysaccharide) for 24 h. After that, the cells were washed twice with DPBS and incubated with 100 μL of 0.5 mg/mL MTT for 2 h at 37°C. The medium was then discarded and 100 μL dimethyl sulfoxide (DMSO) was added. After 30-min incubation, absorbance at 570 nm was read using a microplate reader (Molecular Devices, Sunnyvale, CA, USA).

Measurement of nitric oxide/nitrite: NO production was indirectly assessed by measuring the nitrite levels in the cultured media and serum determined by a colorimetric method based on the Griess reaction. The cells were incubated with compounds **1-17** (2.5, 5.0, 10.0 and 20 $\mu\text{g}/\text{mL}$) in the presence of LPS (100 ng/mL) at 37°C for 24 h. Then, cells were dispensed into 96-well plates, and 100 μL of each supernatant was mixed with the same volume of Griess reagent (1% sulfanilamide, 0.1% naphthylethylenediamine dihydrochloride and 5% phosphoric acid) and incubated at room temperature for 10

min; the absorbance was measured at 540 nm with a Micro-Reader (Molecular Devices). Serum samples were diluted 4 times with distilled water and deproteinized by adding 1/20 volume of zinc sulfate (300 g/L) to a final concentration of 15 g/L. After centrifugation at 10,000 × g for 5 min at room temperature, 100 µL supernatant was applied to a microtiter plate well, followed by 100 µL of Griess reagent. After 10 min of color development at room temperature, the absorbance was measured at 540 nm with a Micro-Reader. By using sodium nitrite to generate a standard curve, the concentration of nitrite was measured from the absorbance at 540 nm.

5-(4-Hydroxy-3-methoxy-1-butynyl)-2,2'-bithiophene (1)

Yellow oil

References

- [1] Lin YL, Huang RL, Kuo YH, Chen CF. (1999) Thiophenes from *Echinops grijsii* Hance. *The Chinese Pharmaceutical Journal*, **51**, 201-211.
- [2] Jin W, Shi Q, Hong C, Cheng Y, Ma Z, Qu H. (2008) Cytotoxic properties of thiophenes from *Echinops grijsii* Hance. *Phytomedicine: International Journal of Phytotherapy and Phytopharmacology*, **15**, 768-774.
- [3] Lin CC, Lin CH. (1993) Pharmacological and pathological studies on Taiwan folk medicine (IX): The hepatoprotective effect of the methanolic extract from *Echinops grijsii*. *The American Journal of Chinese Medicine*, **21**, 33-44.
- [4] Lambert JDH, Campbell G, Arnason JT, Majak W. (1991) Herbicidal properties of alpha-terthienyl, a naturally occurring phototoxin. *Canadian Journal of Plant Science*, **71**, 215-218.
- [5] Menelaou MA, Fronczeck FR, Hjortso MA, Morrison AF, Foroozesh M, Thibodeaux TM, Flores HE, Fisher NH. (1991) NMR spectral data of benzofurans and bithiophenes from hairy root cultures of *Tagetes patula* and the molecular structure of isoeparin. *Spectroscopy Letters*, **24**, 1405-1413.
- [6] Shi J, Zhang X, Jiang H. (2010) 2-(Penta-1,3-diynyl)-5-(3,4-dihydroxybut-1-ynyl)thiophene, a novel NQO1 inducing agent from *Echinops grijsii* Hance. *Molecules*, **15**, 5273-5281.
- [7] Lu Z, Li C, Fang T, Lia G, Bo Z. (2013) Triindole-cored star-shaped molecules for organic solar cells. *Journal of Materials Chemistry A*, **1**, 7657-7665.
- [8] Klingstedt T, Shirani H, Mahler J, Wegenast-Braun BM, Nyström S, Goedert M, Jucker M, Nilsson KPR. (2015) Distinct spacing between anionic groups: An essential chemical determinant for achieving thiophene-based ligands to distinguish β-amyloid or tau polymorphic aggregates. *Chemistry (Weinheim an Der Bergstrasse, Germany)*, **21**, supporting Information, 7-8.
- [9] Wang Y, Li X, Meng DL, Li ZL, Zhang P, Xu J. (2006) Thiophenes from *Echinops latifolius*. *Journal of Asian Natural Products Research*, **8**, 585-588.
- [10] Norton RA, Finlayson AJ, Towers GHN. (1985) Thiophene production by crown gall and callus tissues of *Tagetes patula*. *Phytochemistry*, **24**, 719-722.
- [11] Kilbinger AFM, Schenning APHJ, Goldoni F, Feast WJ, Meijer EW. (2000) Chiral aggregates of α,ω-disubstituted sexithiophenes in protic and aqueous media. *Journal of the American Chemical Society*, **122**, 1820-1821.
- [12] Abegaz BM. (1991) Polyacetylenic thiophenes and terpenoids from the roots of *Echinops pappii*. *Phytochemistry*, **30**, 879-881.
- [13] Zhang P, Jin WR, Shi Q, He H, Ma ZJ, Qu HB. (2008) Two novel thiophenes from *Echinops grijsii* Hance. *Journal of Asian Natural Products Research*, **10**, 977-981.

MP: 101-103°C.

$[\alpha]_D$: +0.78 (*c* 0.23, CHCl_3).

IR (KBr): 3431, 2214, 802, 696 cm^{-1} .

UV λ_{max} (MeOH) nm (log ε): 234 (3.80), 280 (4.52), 324 (3.45).

^1H and ^{13}C NMR: Table 1.

HR-ESI-MS: *m/z* 262.9758 [M-2H]⁺, calcd for $\text{C}_{13}\text{H}_{12}\text{O}_2\text{S}_2$.

Acknowledgments - This study was kindly supported by Grants to the NSC99-2320-B-039-022-MY2 from National Science Council of the Republic of China, and CMU under the Aim for Top University Plan of the Ministry of Education, Taiwan, and Taiwan Ministry of Health and Welfare Clinical Trial and Research Center of Excellence (MOHW104-TDU-B-212-113002).

Cyclic Lipopeptides with Herbicidal and Insecticidal Activities Produced by *Bacillus clausii* DTM1

Da-Le Guo^a, Bo Wan^a, Shi-Ji Xiao^b, Sarah Allen^c, Yu-Cheng Gu^c, Li-Sheng Ding^a and Yan Zhou^{a,*}

^aKey Laboratory of Mountain Ecological Restoration and Bioresource Utilization, Chengdu Institute of Biology, Chinese Academy of Sciences, Chengdu 610041, P. R. China

^bSchool of Pharmacy, Zunyi Medical College, Zunyi 563000, P. R. China

^cSyngenta, Jealott's Hill International Research Centre, Berkshire RG42 6EY, UK

zhouyan@cib.ac.cn

Received: April 29th, 2015; Accepted: October 23rd, 2015

Seven cyclic lipopeptide biosurfactants (**1-7**) were isolated for the first time from the fermentation broth of endophytic *Bacillus clausii* DTM1 and were identified as anteisoC₁₃[Val7] surfactin-(L-Glu)-O-methyl-ester (**1**), anteisoC₁₂[Val7] surfactin (**2**), anteisoC₁₅[Val7] surfactin (**3**), isoC₁₄[Leu7] surfactin (**4**), anteisoC₁₂[Leu7] surfactin (**5**), nC₁₃[Leu7] surfactin (**6**), and anteisoC₁₄[Leu7] surfactin-(L-Glu)-O-methyl-ester (**7**). **1** has not been isolated before as a natural product from any source. Plate-based herbicide and insecticide bioassays showed that all compounds exhibited interesting insecticidal and herbicidal activities.

Keywords: *Bacillus clausii*, Surfactin, Insecticidal, Herbicidal.

The secondary metabolites of *Bacillus* species are known for their ability to control plant diseases through various mechanisms [1]. It is also documented that *Bacillus* species have the potential to synthesize a wide variety of metabolites with antibacterial and/or antifungal activity, which is one determinant of their ability to control plant diseases when applied as a biological control agent [1-4]. For instance, *B. subtilis*, the most studied species, is known to have strong antifungal activity by producing fungicidal and fungistatic peptides [3]. However, to the best of our knowledge, there have been limited studies on the activity of these peptides for controlling insects and weeds [5-7]. *B. clausii*, as one of the *Bacillus* species, has rarely been studied.

In this study, seven cyclic lipopeptides were isolated from the fermentation broth of *B. clausii* DTM1, and were identified as surfactin isomers. Of these seven, compound **1** was isolated as a natural product for the first time (although it had been prepared before by esterification of valine-7 surfactin isomer with a chain length of 13 carbons, but its spectral data have not been previously reported [8]). The complete assignments of ¹H and ¹³C NMR spectral data have been achieved by various 2D NMR experiments including ¹H-¹H COSY, HSQC, HMBC and ROESY.

Compound **1** was obtained as a white gum. Its molecular formula was assigned as C₅₁H₈₉N₇NaO₁₃ on the basis of the HRESIMS. In the ¹H NMR spectrum, seven NH and seven α -H signals showed the presence of seven amino acid units. A strong signal at 81.21 indicated the presence of a fatty acid chain. The ¹³C NMR spectrum showed 10 ester/amide carbonyl signals and 7 α -C signals. Amino acid units were identified as glutamic acid (Glu \times 1), aspartic acid (Asp \times 1), valine (Val \times 2) and leucine (Leu \times 3) on the basis of ¹H-¹H COSY analysis. The HMBC correlation between the signals at 83.57 (the ¹H signal of OCH₃) and 173.8 (the residual CO of Glu1) established that the carboxyl group of Glu 1 was esterified. The substitution type of the branching methyl in the hydroxyl fatty acid chain was identified as anteiso by a ¹³C NMR experiment using the method described by Lin *et al.* [9]. The sequence of the amino acid units and the fatty acid unit were assigned by a ROSEY experiment.

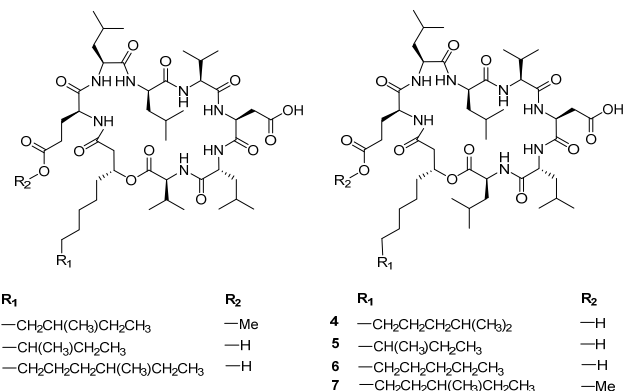


Figure 1: Structures of compounds **1-7**.

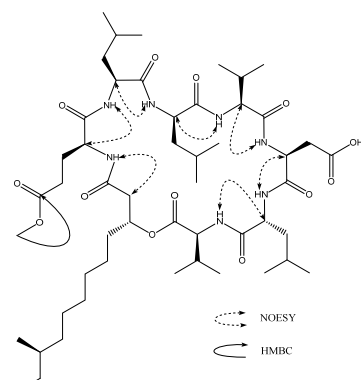


Figure 2: Key HMBC and NOESY of compound 1.

Thus, the primary structure was established. The configurations of the amino acid units were confirmed as L-Glu (\times 1), L-Val (\times 2), L-Leu (\times 1), L-Asp (\times 1), and D-Leu (\times 2) by Marfey's reaction [10], and assigned as L-, L-, D-, L-, L-, D-, and L-, from N- to C-terminal according to previous biogenesis research. The absolute stereochemistry of the β -hydroxyl function of the fatty acid chain

Table 1: ^1H and ^{13}C -NMR spectral data of compound **1^a**.

Name	Position	δH	δC	Name	Position	δH	δC
Glu1	NH	7.82 (d, 6.6)		Leu6	$\alpha\text{-C}$	4.55(m)	49.6
	C=O		170.71		$\beta\text{-C}$	2.73(dd,5.10,16.6)/2.58(dd,8.8,16.6)	35.7
	$\alpha\text{-C}$	4.17(m)	52.39		$\delta\text{-C=O}$		171.6
	$\beta\text{-C}$	1.79(m)/1.93(m)	27.1				
	$\gamma\text{-C}$	2.24(m)	29.7				
	$\delta\text{-C=O}$		173.8		$\alpha\text{-C}$	4.51(m)	50.7
	$\delta\text{-OCH}_3$	3.57	51.3		$\beta\text{-C}$	1.52(m)	41.1
	NH	7.99(d, 5.7)			$\gamma\text{-C}$	1.52(m)	24.2
	C=O		172.8		$\delta\text{-C}$	0.84(m)	21.6/22.0
	$\alpha\text{-C}$	4.17(m)	51.9				
Leu2	$\beta\text{-C}$	1.52(m)	39.4	Val7	NH	8.23 (d, 8.2)	
	$\gamma\text{-C}$	1.52(m)	24.2		C=O		171.7
	$\delta\text{-C}$	0.84(m)	22.9/22.8		$\alpha\text{-C}$	4.09 (m)	50.7
	NH	8.29(d,7.1)			$\beta\text{-C}$	2.07(m)	29.4
	C=O		172.60		$\gamma\text{-C}$	0.84(m)	17.8/19.0
Leu3	$\alpha\text{-C}$	4.17(m)	51.8	Fatty acid 1			169.9
	$\beta\text{-C}$	1.52(m)	39.4		2	2.48(m)/2.33(m)	41.6
	$\gamma\text{-C}$	1.52(m)	24.2		3	5.06(m)	71.4
	$\delta\text{-C}$	0.84(m)	22.8/22.6		4	1.60(m)	33.5
	NH	7.74(d, 8.3)			5	1.22(m)	24.3
Val4	C=O		171.0		6-8	1.21(m)	28.6-29.0
	$\alpha\text{-C}$	4.02(m)	58.6		9	1.05(m)/1.25(m)	35.9
	$\beta\text{-C}$	1.99(m)	30.1		10	1.28(m)	33.6
	$\gamma\text{-C}$	0.84(m)	17.8/19.0		11	1.21(m)	26.3
	NH	8.15(d,7.4)			12	0.82(m)	11.1
Asp5	C=O		169.9		13	0.83(m)	19.0

^aMeasured in DMSO-*d*₆ at 400MHz for ^1H NMR and at 100 MHz for ^{13}C NMR.

was (R) according to previous biogenesis research [11] and confirmed by comparing the specific rotation with known compounds [12]. The structure of **1** was determined to be a methylated product of [Val7] surfactin isomer with a chain length of 13 carbons.

The structures of compounds **2-7** were identified by comparison of their spectral data with those described in the literature [12, 13].

The bioassay, arranged by Syngenta, has been described in earlier work [14, 15] and the results are given in Table 2. All the compounds showed activity against aphid species. It has been speculated that surfactin isomers interact with cuticle lipid molecules of aphids and induce cuticle membrane perturbation [5]. Compound **6** was also active against *Plutella xylostella*. Compounds **2-6** were active on *Poa annua*, and this is the first report of surfactin's activity against this plant species. Compounds **1** and **7** showed weaker activity against *P. annua*, which may be due to the methyl esterification of [Glu-1].

Due to the development of resistant mutants and new physiological races of pests and pathogens, many synthetic pesticides are gradually becoming ineffective. This creates a need to find alternative ways to control farm pests and pathogens. Natural products such as surfactins, which have activity against not only plant pathogens but also pests and weeds, make them an ideal biocontrol agent. *B. clausii* might be a valuable source which could be commercialized as mentioned above.

Table 2: Herbicidal and insecticidal activities of compounds **1-7**.

Compd.	Herbicidal activity		Insecticidal activity		
	<i>Poa annua</i>	<i>Arabidopsis thaliana</i>	<i>Aphid</i> species	<i>Plutella xylostella</i>	<i>Diabrotica balteata</i>
1	49 ^a	0	99	0	0
2	99	0	99	0	0
3	99	0	99	0	0
4	99	0	99	0	0
5	99	0	99	0	0
6	99	0	99	99	0
7	49	0	99	0	0

a. Data are presented as the means of the assessment scores across two replicates for the herbicide assays and three replicates for the insecticide assays.

Experimental

General: Perkin-Elmer-241 polarimeter; Perkin-Elmer Lambda 35 UV-VIS spectrophotometer; Perkin-Elmer one FT-IR spectrometer (KBr); Bruker-Ascend-400 MHz instrument at 300 K, with TMS as

internal standard; preparative HPLC utilized a Waters equipped with a Kromasil RP-C18 column(10 × 250 mm, ID×L) and a UV detector; columns were of either silica gel (300-400 mesh) or Sephadex LH-20; all the solvents used were of analytical grade.

Material and cultivation of Bacillus strain: The bacterial strain was isolated using PDA from the plant *Dracocephalum tanguticum* Maxim., and was identified as *Bacillus clausii* by characterization and complete 16S rRNA gene sequence. The strain (Genbank accession number was KR632489) has been preserved at Chengdu Institute of Biology, Chinese Academy of Sciences, China. This bacterium was cultivated on a 30 L scale using 1L Erlenmeyer flasks containing 400 mL of the seed PDA medium for 3 days and fermentation medium (soluble starch 0.8%, peptone 0.5%, NaCl 0.2%, CaCO₃ 0.2%, MgSO₄·7 H₂O 0.05%, K₂HPO₄ 0.05%) for 14 days at 28°C on a rotary shaker (250rpm).

Extraction and isolation of compounds: The fermentation broth (30 L) of *B. clausii* was filtered. The filtrate was extracted with EtOAc and the solvent was removed under vacuum. The EtOAc residue (18 g) was separated into 4 fractions by CC on silica gel (300-400 mesh), eluting stepwise with a CHCl₃/MeOH gradient (CHCl₃, CHCl₃/MeOH: 10:1, v/v, CHCl₃/MeOH: 3:1, v/v, MeOH). The fourth fraction (eluted with MeOH) was separated by Sephadex LH-20 (CHCl₃/MeOH: 1:1, v/v) to afford 3 fractions (Fr.1-Fr.3). Fr.1 was further purified on a Waters preparative HPLC equipped with a Kromasil RP-C18 column (10 × 250 mm, ID × L; MeOH/H₂O: 90:10, v/v) to afford **1** (8.3 mg), **2** (12.5 mg), **3** (82.6 mg), **4** (53.3 mg), **5** (34.7 mg), **6** (28.4 mg) and **7** (18.5 mg).

Herbicide assays: The compounds were tested for herbicidal activity against *Arabidopsis thaliana* at 10 ppm and *Poa annua* at 32 ppm. Test plates were stored for 7 days in a controlled environment cabinet. They were scored as 0 or 99, where 99 = herbicidal effect, and 0 = no effect.

Insecticide assays: The compounds were tested for activity against an aphid species at 1000 ppm on a leaf-piece based assay, and against *Plutella xylostella* and *Diabrotica balteata* at 500 ppm in artificial diet assays. Compounds were applied to feeding aphids, or prior to infestation with *P. xylostella* and *D. balteata* larvae.

Positive control compounds were included in each test: thiamethoxam and indoxacarb for insecticide assays and norflurazon for herbicide assays (S21 and S22 in supplementary information). Test plates were stored in a controlled environment cabinet for 6 days for the aphid species, 5 days for *D. balteata* and 9 days for *P. xylostella*. Mortality was assessed relative to control wells using a 2 band system (0 or 99 where 99 = significant mortality ($\geq 70\%$), 0 = mortality not significant/no effect($\leq 70\%$)).

Compound **1**

MP: 137-139°C.

[α]_D²⁰: -14 (c 1.00, MeOH).

IR (KBr): 3421, 2957, 2927, 1657, 1534, 1205, 1018, 592 cm⁻¹.

UV/Vis λ_{max} (MeOH) nm (log ε): 206 (1.38).

^1H NMR and ^{13}C NMR: Table 1.

HR-ESI-MS *m/z*: 1030.6359 (calcd. 1030.6411 for [C₅₁H₈₉N₇NaO₁₃]⁺)

Appendix - Supplementary data associated with this article including UV, IR, HR-ESIMS, ^1H , ^{13}C NMR spectra and Positive control data can be found on line.

Acknowledgments - This work was financially supported by grants from the National Natural Sciences Foundation of China (21302180, 21402187, 21572219 and 21572221) and a Syngenta Postgraduate Fellowship awarded to Da-Le Guo.

References

- [1] Ramarathnam R, Bo S, Chen Y, Fernando WGD, Gao XW, de Kievit T. (2007) Molecular and biochemical detection of fengycin- and bacillomycin D-producing *Bacillus* spp., antagonistic to fungal pathogens of canola and wheat. *Canadian Journal of Microbiology*, **53**, 901-911.
- [2] Moyne AL, Shelby R, Cleveland TE, Tuzun S. (2001) Bacillomycin D: an iturin with antifungal activity against *Aspergillus flavus*. *Journal of Applied Microbiology*, **90**, 622-629.
- [3] Liu C, Sheng JP, Chen L, Zheng YY, Lee DYW, Yang Y, Xu MS, Shen L. (2015) Biocontrol activity of *Bacillus subtilis* isolated from *Agaricus bisporus* mushroom compost against pathogenic fungi. *Journal of Agricultural and Food Chemistry*, **63**, 6009-6018.
- [4] Zhao ZZ, Wang QS, Wang KM, Brian K, Liu CH, Gu YC. (2010) Study of the antifungal activity of *Bacillus vallismortis* ZZ185 *in vitro* and identification of its antifungal components. *Bioresource Technology*, **101**, 292-297.
- [5] Yun DC, Yang SY, Kim YC, Kim IS, Kim YH. (2013) Identification of surfactin as an aphicidal metabolite produced by *Bacillus amyloliquefaciens* G1. *Journal of the Korean Society for Applied Biological Chemistry*, **56**, 751-753.
- [6] Ghribi D, Elleuch M, Abdelkefi L, Ellouze-Chaabouni S. (2012) Evaluation of larvicidal potency of *Bacillus subtilis* SPB1 biosurfactant against *Ephestia kuhniella* (Lepidoptera: Pyralidae) larvae and influence of abiotic factors on its insecticidal activity. *Journal of Stored Products Research*, **48**, 68-72.
- [7] Geetha I, Paily KP, Manonmani AM. (2012) Mosquito adulticidal activity of a biosurfactant produced by *Bacillus subtilis* subsp. *subtilis*. *Pest Management Science*, **68**, 1447-1450.
- [8] Kowall M, Vater J, Kluge B, Stein T, Franke P, Ziessow D. (1998) Separation and characterization of surfactin isoforms produced by *Bacillus subtilis* OKB 105. *Journal of Colloid and Interface Science*, **204**, 1-8.
- [9] Lin SC, Minton MA, Sharma MM, Georgiou G. (1994) Structural and immunological characterization of a biosurfactant produced by *Bacillus licheniformis* JF-2. *Applied and Environment Microbiology*, **60**, 31-38.
- [10] Marfey P. (1984) Determination of D-amino acids. II. Use of a bifunctional reagent, 1,5-difluoro-2,4-dinitrobenzene. *Carlsberg Research Communications*, **49**, 591-596.
- [11] Nagai S, Okimura K, Kaizawa N, Ohki K, Kanatomo S. (1996) Study on surfactin, a cyclic depsipeptide. II. synthesis of surfactin B2 produced by *Bacillus natto* KMD 2311. *Chemical & Pharmaceutical Bulletin*, **44**, 5-10.
- [12] Tang JS, Gao H, Hong K, Yu Y, Jiang MM, Lin HP, Ye WC, Yao XS. (2007) Complete assignments of ¹H and ¹³C NMR spectral data of nine surfactin isomers. *Magnetic Resonance in Chemistry*, **45**, 792-796.
- [13] Liu XY, Yang SZ, Mu BZ. (2009) Production and characterization of a C15-surfactin-O-methyl ester by alipopeptide producing strain *Bacillus subtilis* HSO121. *Process Biochemistry*, **44**, 1144-1151.
- [14] Zhang MZ, Chen Q, Mulholland N, Beattie D, Irwin D, Gu YC, Yang GF, Clough J. (2012) Synthesis and fungicidal activity of novel pimprinine analogues. *European Journal of Medicinal Chemistry*, **53**, 283-291.
- [15] Chen JL, Tang W, Che JY, Chen K, Yan G, Gu YC, Shi DQ. (2015) Synthesis and biological activity evaluation of novel α-amino phosphonate derivatives containing a pyrimidinyl moiety as potential herbicidal agents. *Journal of Agricultural and Food Chemistry*, **63**, 7219-7229.

Synthesis of (*6R,12R*)-6,12-Dimethylpentadecan-2-one, the Female-Produced Sex Pheromone from Banded Cucumber Beetle *Diabrotica balteata*, Based on a Chiron Approach

Wei Shen, Xiang Hao, Yong Shi* and Wei-Sheng Tian*

CAS Key Laboratory of Synthetic Chemistry of Natural Substances, Shanghai Institute of Organic Chemistry, Chinese Academy of Sciences, 345 Lingling Road, Shanghai 200032, China

shiong81@sioc.ac.cn; wstian@sioc.ac.cn

Received: August 14th, 2015; Accepted: August 18th, 2015

Herein we describe a synthesis of (*6R,12R*)-6,12-dimethylpentadecan-2-one (**5**), the female produced sex pheromone of banded cucumber beetle *Diabrotica balteata* Le Conte, from (*R*)-4-methyl- δ -valerolactone, a methyl-branched chiron.

Keywords: Sex pheromone, (*6R,12R*)-6,12-dimethylpentadecan-2-one, Methyl-branched chiron, (*R*)-4-Methyl- δ -valerolactone, Synthesis.

Pheromones are species-specific biofunctional molecules that are used for communication between individuals within the same species, and thus are useful tools for pest control. Among various pheromones, those with one or more chiral methyl-branched units [1]—such as compounds **1–5**, Figure 1—attract us most, for we have developed several methyl chirons from industrial waste and been interested in applying them to the syntheses of natural products [2]. Herein we report a synthesis of (*6R,12R*)-6,12-dimethylpentadecan-2-one (**5**) from (*R*)-4-methyl- δ -valerolactone (**6**).

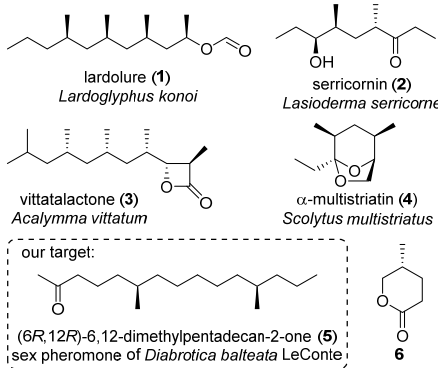
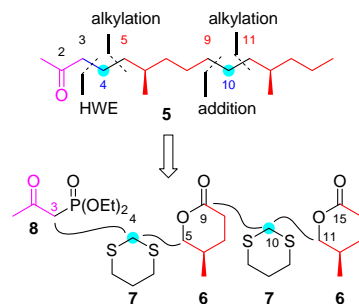


Figure 1: Chemical structures of chiral methyl-branched pheromones **1–5**.

Ketone **5** is the female produced sex pheromone of banded cucumber beetle (BCB) *Diabrotica balteata* Le Conte, the larvae of which are serious pests of a variety of agricultural crops such as curbits and sweet potatoes. The structure of **5** was elucidated by spectroscopic analyses and confirmed by synthesis [3]. The stereochemistry was provided by Mori's synthesis of all the four possible isomers and further affirmed by two other stereoselective syntheses [4].

Our synthetic plan is depicted in Scheme 1. Both lactone **6** and 1,3-dithiane **7** were to be used twice. The former was to form the C5–C9 and C11–C15 units in **5**, and the latter to act as linking point for fragments **6** and diethyl (2-oxopropyl)phosphonate (**8**).

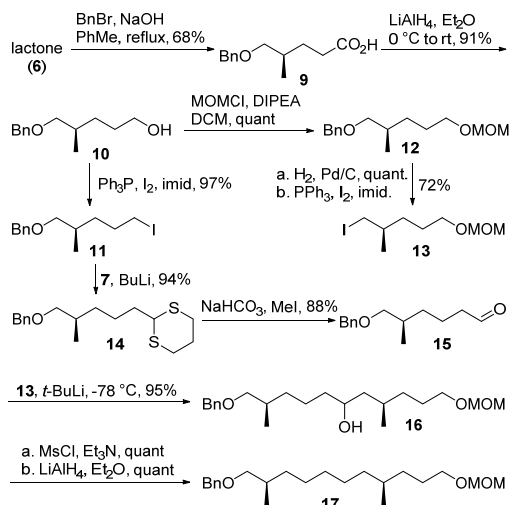


Scheme 1: Synthetic plan for (*6R,12R*)-6,12-dimethylpentadecan-2-one (**5**).

As shown in Scheme 2, our synthesis commenced with opening the lactone ring of **6**. Treatment of **6** with NaOH and BnBr in refluxing toluene successfully delivered acid **9** in 68% yield on a 0.2 mol scale. After reducing the acid with LiAlH₄, removal of the exposed hydroxyl group in resultant **10** was investigated and found to be low-yielding due to the low boiling point of the product (*ca* 142°C). Therefore we decided to postpone this step to a later stage of the synthesis. Compound **10** was first protected as the MOM ether, then the benzyl group was removed by catalytic hydrogenation and the newly exposed OH was converted to iodide, giving **13** in 72% overall yield. In another direction, **10** was directly converted to iodide **11**, which was then treated with lithio dithiane to afford **14** in high yield.

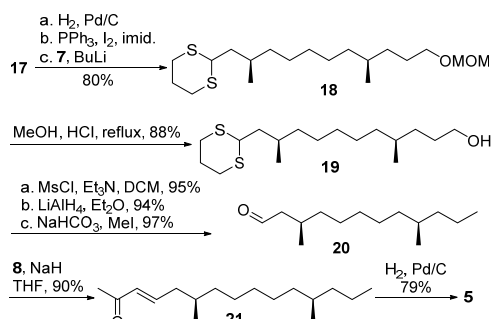
With **13** and **14** in hand, we first tried to couple them directly by preparing the anion of **14** and then reacting with **13**, but found this reaction to be low-yielding and irreproducible. Therefore, dithiane **14** was unmasked (NaHCO₃, MeI, MeCN, water) [5] and the resultant aldehyde **15** was coupled with the lithio derivative of **13** [6] to give **16** in high yield as a mixture of epimers. The unneeded hydroxyl group on **16** was removed by transforming to mesylate and reducing it with LiAlH₄ [7], affording **17** in nearly quantitative yield.

Then the benzyl ether of **17** was cleaved and the exposed hydroxyl group was transformed to iodide and coupled with 1,3-dithiane anion again to deliver **18** in 80% overall yield. The unneeded hydroxyl group at the right side was again removed in good yield.



Scheme 2: Synthesis of 17.

via cleaving the MOM ether with HCl, preparing the corresponding mesylate of **19**, and reducing it with LiAlH₄. The dithiane moiety was unmasked to give aldehyde **20** in high yield and then underwent Horner–Wadsworth–Emmons olefination with **8** to give enone **21**, which was subjected to catalytic hydrogenation to deliver **5** in 79% yield. The spectroscopic properties of the synthetic **5** are consistent with those reported ($[\alpha]_D^{24}$: -0.395 (*c* 0.41, CHCl₃); reported in reference 4d: $[\alpha]_D^{23}$: -0.40 (*c* 0.40, CHCl₃)).

Scheme 3: Completion of the synthesis of (6*R*,12*R*)-6,12-dimethylpentadecan-2-one (5).

In conclusion, we have achieved a synthesis of (6*R*,12*R*)-6,12-dimethylpentadecan-2-one (**5**), the female produced sex pheromone of BCB *Diabrotica balteata* Le Conte, in 17 steps with an overall yield of 20% from (*R*)-4-methyl- δ -valerolactone (**6**). Although the synthesis is relatively longer than previous ones, the reactions used herein are simpler and easier to handle.

Experimental

General: All reactions sensitive to air or moisture were performed in flame-dried round bottom flasks with rubber septum under a positive pressure of either argon or nitrogen atmosphere, unless otherwise noted. Air and moisture-sensitive liquids and solutions were transferred via syringe and stainless steel cannula. Reactions were monitored by thin-layer chromatography (TLC) carried out on silica gel plates using UV light as visualizing agent and an ethanolic solution of phosphomolybdic acid, and heat as developing agents. NMR spectra were recorded on a Bruker AMX-300 instrument and calibrated using TMS or residual undeuterated solvent as an internal reference [¹H NMR: TMS (0.00); ¹³C NMR: CDCl₃ (77.16)]. The following abbreviations were used to explain the multiplicities: s = singlet, d = doublet, t = triplet, q = quartet, br = broad.

(*R*)-5-(Benzoyloxy)-4-methylpentanoic acid (9): To a solution of lactone **6** (23.0 g, 0.20 mol) in toluene (400 mL) were added NaOH (24 g, 0.60 mol) and BnBr (37.6 g, 0.22 mol). The flask was equipped with a Dean–Stark trap, heated to reflux for 20 h, cooled, added water (200 mL), and acidified with HCl aqueous solution. The mixture was separated and the aqueous layer was extracted with diethylether (150 mL×2). The combined organic layers were washed with brine, dried over Na₂SO₄, filtered, and concentrated under reduced pressure. Purification via flash column chromatography on silica gel (PE/EA: 3/1) afforded acid **10** (30.4 g, 68%) as a colorless liquid.

$[\alpha]_D^{27}$: +1.68 (*c* 1.26, CHCl₃).

IR (KBr): 3033, 2962, 1708, 1496, 1454, 1276, 1100, 938, 738, 714 cm⁻¹.

¹H NMR (300 MHz, CDCl₃): 7.26–7.35 (m, 5H), 4.50 (s, 2H), 3.31 (d, 2H, *J* = 5.7 Hz), 2.36–2.43 (m, 2H), 1.78–1.88 (m, 2H), 1.47–1.55 (m, 1H), 0.95 (d, 3H, *J* = 5.7 Hz)

MS (EI, 70 eV): *m/z* (%) = 222 [M⁺] (100)

Anal. Calcd for C₁₃H₁₈O₃: C, 70.24; H, 8.16. Found C, 70.28; H, 8.27.

(*R*)-5-(Benzoyloxy)-4-methylpentan-1-ol (10): To a suspension of LiAlH₄ (1.23 g, 32 mmol) in dry diethylether (50 mL) was added dropwise a solution of acid **9** (6.0 g, 27 mmol) in diethylether (20 mL) at 0°C. The mixture was then stirred at room temperature and quenched with Na₂SO₄•10H₂O after which—TLC showed complete consumption of **9**. The mixture was filtered and washed with diethylether. The filtrate was concentrated and purified via flash column chromatography on silica gel (PE/EA: 5/1) to give **10** (5.09 g, 91%) as a colorless liquid.

$[\alpha]_D^{28}$: +2.03 (*c* 1.26, CHCl₃).

IR (KBr): 2934, 2864, 1497, 1454, 1364, 1099, 1073, 1029, 736, 698 cm⁻¹.

¹H NMR (300 MHz, CDCl₃): 7.26–7.35 (m, 5H), 4.50 (s, 2H), 3.60–3.64 (m, 2H), 3.25–3.35 (m, 2H), 2.27 (bs, 1H), 1.47–1.81 (m, 4H), 1.16–1.21 (m, 1H), 0.93 (d, 3H, *J* = 6.6 Hz).

MS (EI, 70 eV): *m/z* (%) = 208 [M⁺] (100).

Anal. Calcd for C₁₃H₂₀O₂: C, 74.96; H, 9.68. Found C, 74.92; H, 9.73.

(*R*)-1-Benzoyloxy-5-iodo-2-methylpentane (11): To a solution of PPh₃ (393 mg, 1.5 mmol) and imidazole (204 mg, 3.0 mmol) in dry CH₂Cl₂ (15 mL) was added I₂ (381 mg, 1.5 mmol) at 0°C. The mixture was stirred for 30 min before a solution of **10** (104 mg, 0.50 mmol) in CH₂Cl₂ (2 mL) was added. The mixture was stirred at ambient temperature and quenched with water after TLC showed complete consumption of **10**. The mixture was diluted with CH₂Cl₂ (50 mL), washed with a saturated solution of Na₂S₂O₃ (20 mL) and brine (20 mL) sequentially, dried over Na₂SO₄, filtered, and concentrated under reduced pressure. Flash column chromatography on silica gel (PE/EA: 80/1) afforded **11** (154 mg, 97%) as a colorless liquid.

$[\alpha]_D^{28}$: +4.55 (*c* 1.03, CHCl₃).

IR (KBr): 3064, 3030, 2957, 2854, 1496, 1454, 1363, 1222, 1179, 1099, 1029, 843, 736, 697, 611, 415 cm⁻¹.

¹H NMR (300 MHz, CDCl₃): 7.25–7.38 (m, 5H), 4.49 (s, 2H), 3.23–3.32 (m, 2H), 3.12–3.18 (m, 2H), 1.75–1.88 (m, 3H), 1.49–1.57 (m, 1H), 1.21–1.29 (m, 1H), 0.92 (d, 3H, *J* = 6.9 Hz).

¹³C NMR (75 MHz, CDCl₃): 138.52, 128.24, 127.43, 127.39, 75.44, 72.90, 34.57, 32.69, 31.09, 17.05, 7.21

HRMS-EI: *m/z* [M⁺] calcd for C₁₃H₁₉OI: 318.0481; found: 318.0480.

(*R*)-1-Benzoyloxy-5-methoxymethoxy-2-methylpentane (12): To a solution of **10** (15.0 g, 72 mmol) in dry CH₂Cl₂ (150 mL) were added iPr₂NEt (23.9 mL, 144 mmol) and MOMCl (11.3 mL, 144

mmol) at 0°C. The mixture was stirred at ambient temperature and quenched with water after TLC showed that **10** was completely consumed. The mixture was diluted with CH₂Cl₂, separated, washed with brine, dried over Na₂SO₄, filtered, and concentrated under reduced pressure. Flash column chromatography on silica gel (PE/EA: 30/1) afforded **12** (18.8 g, quantitative) as a colorless liquid.

[α]_D²⁴: +0.24 (*c* 0.80, CHCl₃).

IR (KBr): 2932, 2876, 1497, 1454, 1207, 1152, 1110, 1048, 919, 737, 698, 415, 410, 402 cm⁻¹.

¹H NMR (300 MHz, CDCl₃): 7.26-7.39 (m, 5H), 4.62 (s, 2H), 4.51 (s, 2H), 3.24-3.61 (m, 7H), 1.48-1.83 (m, 4H), 1.19-1.27 (m, 1H), 0.97 (d, 3H, *J* = 6.9 Hz)

¹³C NMR (75 MHz, CDCl₃): 138.71, 128.24, 127.35, 96.33, 75.63, 72.91, 68.01, 65.80, 55.01, 33.30, 30.10, 27.15, 17.03.

MS (EI, 70 eV): *m/z* (%) = 252 [M⁺] (100).

HRMS-EI: *m/z* [M+Na⁺] calcd for C₁₅H₂₄O₃: 275.1623; found: 275.1625.

(R)-5-(Methoxymethoxy)-2-methylpentan-1-ol: A reaction flask containing **12** (18.6 g, 74 mmol), Pd/C (5%, 3.0 g), and MeOH (150 mL) was evacuated and back-filled with hydrogen (1 atm). The reaction mixture was stirred at ambient temperature under hydrogen for 3 days and then filtered over a plug of silica gel topped with Celite (MeOH eluent). The filtrate was concentrated and purified by flash column chromatography on silica gel (PE/EA: 10/1) to give the title compound (11.3 g, quantitative) as a colorless liquid.

[α]_D²⁴: +10.5 (*c* 1.04, CHCl₃).

IR (KBr): 2935, 2878, 1466, 1386, 1216, 1153, 1111, 1046, 920, 414, 402 cm⁻¹.

¹H NMR (300 MHz, CDCl₃): 4.62 (s, 2H), 3.38-3.55 (m, 4H), 3.36 (s, 3H), 2.71 (t, 1H, *J* = 5.4 Hz), 1.43-1.72 (m, 4H), 1.11-1.23 (m, 1H), 0.92 (d, 3H, *J* = 6.6 Hz).

¹³C NMR (75 MHz, CDCl₃): 96.15, 67.92, 67.61, 54.90, 35.37, 29.43, 26.92, 16.40.

MS (ESI): *m/z* = 185 [M+Na⁺].

(R)-1-Iodo-5-(methoxymethoxy)-2-methylpentane (13): To a solution of PPh₃ (19.65 g, 75 mmol) and imidazole (10.2 g, 75 mmol) in dry CH₂Cl₂ (100 mL) was added I₂ (19.1 g, 75 mmol) at 0°C. The mixture was stirred for 20 min before a solution of (*R*)-5-(methoxymethoxy)-2-methylpentan-1-ol (4.0 g, 24 mmol) in CH₂Cl₂ (15 mL) was added. The mixture was stirred at ambient temperature and quenched with water after TLC showed complete consumption of the starting material. The mixture was diluted with CH₂Cl₂ (150 mL), washed with a saturated solution of Na₂S₂O₃ (100 mL) and brine sequentially, dried over Na₂SO₄, filtered, and concentrated under reduced pressure. Flash column chromatography on silica gel (PE/EA: 20/1) afforded **13** (4.9 g, 72%) as a colorless liquid.

[α]_D²⁴: +0.18 (*c* 1.82, CHCl₃).

IR (KBr): 2931, 2882, 1458, 1379, 1196, 1145, 1111, 1044, 919, 415, 409, 402 cm⁻¹.

¹H NMR (300 MHz, CDCl₃): 4.56 (s, 2H), 3.45-3.50 (m, 2H), 3.31 (s, 3H), 3.08-3.20 (m, 2H), 1.36-1.58 (m, 4H), 1.18-1.130 (m, 1H), 0.94 (d, 3H, *J* = 6.6 Hz).

¹³C NMR (75 MHz, CDCl₃): 96.39, 67.64, 55.14, 36.18, 34.55, 27.13, 20.49, 17.40.

MS (EI, 70 eV): *m/z* (%) = 211 [M-C₂H₅O₂]⁺ (100).

(R)-2-(5-(Benzyl)-4-methylpentyl)-1,3-dithiane (14): To a solution of 1,3-dithiane (**7**) (151 mg, 1.26 mmol) in anhydrous THF (8 mL) at 0°C under argon was added a solution of *n*-BuLi (1.5 M in pentane, 0.86 mL, 1.38 mmol). The mixture was stirred for 30 min and added to a solution of **11** (200 mg, 0.63 mmol) in THF (3.0 mL)

and warmed to room temperature. After **11** was fully consumed, the reaction was quenched with water, extracted with EtOAc (30 mL × 3), the extracts combined, washed with brine, dried over Na₂SO₄, filtered, and concentrated under reduced pressure. Flash column chromatography on silica gel (PE/EA: 50/1) afforded **14** (184 mg, 94%) as a colorless liquid.

[α]_D²⁴: +0.89 (*c* 0.92, CHCl₃).

IR (KBr): 3030, 2934, 2901, 2856, 1496, 1454, 1423, 1363, 1276, 1180, 1100, 1028, 909, 845, 737, 698, 414 cm⁻¹.

¹H NMR (300 MHz, CDCl₃): 7.22-7.34 (m, 5H), 4.48 (s, 2H), 4.03 (t, 1H, *J* = 6.9 Hz), 3.19-3.31 (m, 2H), 2.72-2.89 (m, 4H), 2.05-2.17 (m, 1H), 1.68-1.92 (m, 4H), 1.40-1.61 (m, 3H), 1.04-1.19 (m, 1H), 0.92 (d, 3H, *J* = 6.3 Hz).

¹³C NMR (75 MHz, CDCl₃): 138.60, 128.17, 127.37, 127.27, 75.60, 72.80, 47.44, 35.54, 33.15, 32.99, 30.33, 25.89, 23.87, 16.90.

MS (ESI): *m/z* = 349 [M+K⁺].

HRMS-MALDI: *m/z* [M+Na⁺] calcd for C₁₇H₂₆OS₂: 333.1323; found: 333.1316.

(R)-6-(Benzyl)-5-methylhexanal (15): To a solution of **14** (8.01 g, 25.8 mmol) in MeCN/water (80 mL/24 mL) were added MeI (16 mL, 258 mmol) and NaHCO₃ (21.7 g, 258 mmol) at room temperature. The mixture was stirred for 12 h, concentrated under reduced pressure, dissolved in water, extracted with EtOAc (100 mL × 3), the extracts combined, washed with brine, dried over Na₂SO₄, filtered, and concentrated under reduced pressure. Flash column chromatography on silica gel (PE/EA: 20/1) afforded **15** (4.98 g, 88%) as a colorless liquid.

[α]_D²⁴: +3.54 (*c* 1.08, CHCl₃).

IR (KBr): 3035, 2856, 2721, 1725, 1496, 1455, 1363, 1100, 1029, 738, 698, 463, 451, 415 cm⁻¹.

¹H NMR (300 MHz, CDCl₃): 9.74 (t, 1H, *J* = 1.5 Hz), 7.25-7.35 (m, 5H), 4.49 (s, 2H), 3.23-3.33 (m, 2H), 2.39-2.44 (m, 2H), 1.44-1.81 (m, 4H), 1.14-1.18 (m, 1H), 0.93 (d, 3H, *J* = 6.6 Hz).

¹³C NMR (75 MHz, CDCl₃): 202.60, 138.61, 128.26, 127.46, 127.40, 75.52, 72.96, 44.06, 33.31, 33.10, 19.47, 16.88.

MS (EI, 70 eV): *m/z* (%) = 221 [M+H⁺] (100).

HRMS-MALDI: *m/z* [M+Na⁺] calcd for C₁₄H₂₀O₂: 243.1361; found: 243.1360.

(2R,8R)-1-(Benzyl)-11-(methoxymethoxy)-2,8-dimethylundecan-6-ol (16): Under argon, to a solution of **13** (2.48 g, 9.10 mmol) in dry diethylether/pentane (20 mL/30 mL) was added a solution of *t*-BuLi (1.5 M in pentane, 12.7 mL, 19.1 mmol) at -78°C. The mixture was stirred at -78°C for 5 min and then at room temperature for 1 h. At -78°C, to the resultant solution was added a solution of **15** (800 mg, 3.64 mmol) in diethylether/pentane (8 mL/12 mL). The mixture was stirred at room temperature and quenched with water after **15** was consumed completely. The mixture was separated and the aqueous layer was extracted with diethylether (60 mL × 3). The combined organic layers were washed with brine, dried over Na₂SO₄, filtered, and concentrated under reduced pressure. Flash column chromatography on silica gel (PE/EA: 5/1) gave **16** (1.27 g, 95%) as an inseparable mixture of epimers.

IR (KBr): 3031, 2930, 2873, 1497, 1455, 1213, 1153, 1111, 1045, 919, 736, 698, 434, 416, 403 cm⁻¹.

¹H NMR (300 MHz, CDCl₃): 7.12-7.20 (m, 5H), 4.48 (s, 2H), 4.36 (s, 2H), 3.46-3.51 (m, 1H), 3.35-3.40 (m, 1H), 3.22 (s, 3H), 3.08-3.19 (m, 2H), 0.98-1.64 (m, 15H), 0.76-0.80 (m, 6H).

¹³C NMR (75 MHz, CDCl₃): 138.74, 128.26, 127.49, 127.38, 96.37, 75.84, 72.92, 69.43, 55.12, 45.14, 38.61, 35.55, 35.41, 29.59, 28.42, 27.02, 22.91, 19.20, 17.05, 16.53.

HRMS-MALDI: *m/z* [M+Na⁺] calcd for C₂₂H₃₈O₄: 389.2668; found: 389.2670.

(2*R*,8*R*)-1-(Benzylxyloxy)-11-(methoxymethoxy)-2,8-dimethylundecan-6-yl methanesulfonate: To a solution of **16** (290 mg, 0.79 mmol) in dry CH_2Cl_2 (5 mL) were added MsCl (0.10 mL, 1.2 mmol) and Et_3N (0.17 mL, 1.2 mmol) at 0°C. Then the mixture was stirred at room temperature for 3 h and diluted with CH_2Cl_2 (50 mL). The solution was washed with water and brine sequentially, dried over Na_2SO_4 , filtered, and concentrated under reduced pressure. Flash column chromatography on silica gel (PE/EA: 20/1) afforded the title compound (355 mg, inseparable mixture of epimers, 100%) as a colorless liquid.

$[\alpha]_D^{24}:+1.68$ (*c* 1.26, CHCl_3).

IR (KBr): 3031, 2935, 2872, 1497, 1455, 1356, 1336, 1175, 1110, 1030, 971, 906, 792, 739, 699, 610, 528, 415, 409 cm^{-1} .

^1H NMR (300 MHz, CDCl_3): 7.26-7.39 (m, 5H), 4.79-4.82 (m, 1H), 4.61 (s, 2H), 4.49 (s, 2H), 3.49-3.56 (m, 2H), 3.35 (s, 3H), 3.24-3.30 (m, 2H), 2.98 (t, 3H, *J* = 2.1 Hz), 1.14-1.80 (m, 14H), 0.92-0.98 (m, 6H).

^{13}C NMR (75 MHz, CDCl_3): 138.67, 128.27, 127.48, 127.41, 96.36, 82.42, 82.35, 75.41, 72.96, 67.89, 67.86, 65.48, 65.28, 55.14, 55.08, 41.82, 41.72, 38.72, 35.55, 34.90, 33.69, 33.39, 33.31, 33.05, 29.28, 28.92, 27.00, 26.95, 22.22, 19.69, 19.24, 17.00.

MS (EI, 70 eV): m/z (%) = 467 [$\text{M}+\text{Na}^+$] (100).

(2*R*,8*S*)-1-Benzylxyloxy-11-methoxymethoxy-2,8-dimethylundecane (17): To a suspension of LiAlH_4 (600 mg, 1.58 mmol) in dry diethylether (10 mL) was added dropwise a solution of the above prepared mesylate (350 mg, 0.79 mmol) in diethylether (5 mL) at 0°C. The mixture was then stirred at room temperature for 12 h and quenched with $\text{Na}_2\text{SO}_4 \cdot 10\text{H}_2\text{O}$ after TLC showed complete consumption of **9**. The mixture was filtered and washed with diethylether. The filtrate was concentrated and purified via flash column chromatography on silica gel (with hexane) to give **17** (285 mg, 100%) as a colorless oil.

$[\alpha]_D^{24}:-1.20$ (*c* 0.82, CHCl_3).

IR (KBr): 3032, 2957, 2928, 2856, 1497, 1455, 1378, 1261, 1208, 1111, 1047, 920, 801, 736, 697, 417, 404 cm^{-1} .

^1H NMR (300 MHz, CDCl_3): 7.25-7.38 (m, 5H), 4.62 (t, 2H, *J* = 1.5 Hz), 4.50 (s, 2H), 3.48-3.55 (m, 2H), 3.37 (s, 3H), 3.20-3.35 (m, 2H), 1.72-1.76 (m, 1H), 1.54-1.64 (m, 2H), 1.08-1.19 (m, 13H), 0.85-0.91 (m, 6H)

^{13}C NMR (75 MHz, CDCl_3): 138.84, 128.27, 127.48, 127.36, 96.38, 76.02, 72.93, 68.25, 55.07, 36.96, 33.66, 33.45, 33.39, 32.62, 30.25, 27.29, 27.01, 26.96, 19.59, 17.15

MS (EI, 70 eV): m/z (%) = 305 [$\text{M}-\text{C}_2\text{H}_5\text{O}^+$] (100)

HRMS-MALDI: m/z [$\text{M}-\text{C}_2\text{H}_5\text{O}^+$] calcd for $\text{C}_{22}\text{H}_{38}\text{O}_3$: 305.2481; found: 305.2487.

(2*R*,8*S*)-11-(Methoxymethoxy)-2,8-dimethylundecan-1-ol: A reaction flask containing **17** (2.30 g, 6.57 mmol), Pd/C (10%, 300 mg), and MeOH (30 mL) was evacuated and back-filled with hydrogen (1 atm). The reaction mixture was stirred at ambient temperature under hydrogen for 24 h and then filtered over a plug of silica gel topped with Celite (MeOH eluent). The filtrate was concentrated and purified by flash column chromatography on silica gel (PE/EA: 5/1) to give the title compound (1.67 g, 98%) as a colorless liquid.

$[\alpha]_D^{28}:+6.54$ (*c* 0.99, CHCl_3).

IR (KBr): 2928, 2857, 1465, 1379, 1214, 1153, 1112, 1046, 921, 418, 410 cm^{-1} .

^1H NMR (300 MHz, CDCl_3): 4.62 (d, 2H, *J* = 0.9 Hz), 3.38-3.56 (m, 4H), 3.36 (s, 3H), 1.73-1.78 (m, 1H), 1.52-1.66 (m, 3H), 1.07-1.19 (m, 12H), 0.86-0.92 (m, 6H).

^{13}C NMR (75 MHz, CDCl_3): 96.33, 68.30, 68.23, 66.07, 55.04, 36.90, 35.72, 33.33, 33.11, 32.56, 30.19, 27.25, 26.94, 19.56, 16.56.

MS (EI, 70 eV): m/z (%) = 215 [$\text{M}-\text{C}_2\text{H}_5\text{O}^+$] (100).

HRMS-MALDI: m/z [$\text{M}-\text{MeO}^+$] calcd for $\text{C}_{15}\text{H}_{32}\text{O}_3$: 229.2168; found: 229.2164.

(2*R*,8*S*)-1-Iodo-11-(methoxymethoxy)-2,8-dimethylundecane: To a solution of PPh_3 (487 mg, 1.86 mmol) and imidazole (253 mg, 3.72 mmol) in dry CH_2Cl_2 (10 mL) was added I_2 (473 mg, 1.86 mmol) at 0°C. The mixture was stirred for 20 min before a solution of alcohol (160 mg, 0.62 mmol) in CH_2Cl_2 (2 mL) was added. The mixture was stirred at ambient temperature and quenched with water after TLC showed complete consumption of the starting material. The mixture was diluted with CH_2Cl_2 (40 mL), washed with a saturated solution of $\text{Na}_2\text{S}_2\text{O}_3$ (20 mL) and brine sequentially, dried over Na_2SO_4 , filtered, and concentrated under reduced pressure. Flash column chromatography on silica gel (PE/EA: 20/1) afforded the title compound (210 mg, 92%) as a colorless liquid.

$[\alpha]_D^{24}:-2.76$ (*c* 0.77, CHCl_3).

IR (KBr): 2928, 2855, 1460, 1378, 1195, 1153, 1112, 1046, 920, 417, 404 cm^{-1} .

^1H NMR (300 MHz, CDCl_3): 4.63 (s, 2H), 3.51 (d, 2H, *J* = 7.2 Hz), 3.36 (s, 3H), 3.13-3.26 (m, 2H), 1.49-1.61 (m, 2H), 1.12-1.43 (m, 14H), 0.97 (d, 3H, *J* = 6.3 Hz), 0.86 (d, 3H, *J* = 6.6 Hz).

^{13}C NMR (75 MHz, CDCl_3): 96.37, 68.22, 66.04, 55.06, 36.88, 36.42, 34.71, 33.37, 32.58, 29.94, 27.28, 26.82, 20.59, 19.58, 17.95.

MS (EI, 70 eV): m/z (%) = 325 [$\text{M}-\text{MOM}^+$] (100).

2-(*(2R,8S)-11-(Methoxymethoxy)-2,8-dimethylundecyl*)-1,3-dithiane (18): To a solution of 1,3-dithiane **7** (2.27 g, 18.9 mmol) in anhydrous THF (40 mL) at 0°C under argon was added a solution of *n*-BuLi (2.5 M in hexane, 7.56 mL, 18.9 mmol). The mixture was stirred for 30 min and added to a solution of previously prepared iodide (1.40 g, 3.78 mmol) in THF (10 mL) and warmed to room temperature. After the starting material was fully consumed, the reaction was quenched with water, extracted with EtOAc (30 mL × 3), combined, washed with brine, dried over Na_2SO_4 , filtered, and concentrated under reduced pressure. Flash column chromatography on silica gel (PE/EA: 50/1) afforded **18** (1.22 g, 89%) as a pale yellow liquid.

$[\alpha]_D^{24}:-6.49$ (*c* 0.55, CHCl_3).

IR (KBr): 2928, 2856, 1465, 1423, 1378, 1276, 1243, 1153, 1111, 1046, 919, 417, 404 cm^{-1} .

^1H NMR (300 MHz, CDCl_3): 4.63 (s, 2H), 4.08-4.13 (m, 1H), 3.51 (t, 2H, *J* = 6.9 Hz), 3.37 (s, 3H), 2.78-2.92 (m, 4H), 2.08-2.17 (m, 1H), 1.43-1.92 (m, 6H), 1.11-1.39 (m, 13H), 0.85-0.92 (m, 6H).

^{13}C NMR (75 MHz, CDCl_3): 96.36, 68.24, 55.06, 45.57, 42.55, 36.93, 36.75, 33.37, 32.60, 30.57, 30.36, 30.13, 29.57, 27.28, 26.99, 26.75, 26.12, 19.58, 19.39.

MS (EI, 70 eV): m/z (%) = 362 [M^+] (100)

HRMS-EI: m/z [M^+] calcd for $\text{C}_{19}\text{H}_{38}\text{O}_2\text{S}_2$: 362.2313; found: 362.2322.

(4*S,10R*)-11-(1,3-Dithian-2-yl)-4,10-dimethylundecan-1-ol (19): A solution of **18** (90 mg, 0.25 mmol) in acidified MeOH (5 mL, two drops of HCl) was heated at reflux for 5 h and concentrated under reduced pressure. The residue was purified by flash column chromatography on silica gel (PE/EA: 10/1) to give **19** (70 mg, 88%) as a colorless liquid.

$[\alpha]_D^{24}:-9.59$ (*c* 0.45, CHCl_3).

IR (KBr): 2927, 2855, 1461, 1423, 1378, 1276, 1057, 908, 411 cm^{-1} .

^1H NMR (300 MHz, CDCl_3): 4.05-4.10 (m, 1H), 3.60 (t, 2H, *J* = 6.6 Hz), 2.74-2.88 (m, 4H), 2.07-2.13 (m, 1H), 1.07-1.83 (m, 20H), 0.80-0.92 (m, 6H).

^{13}C NMR (75 MHz, CDCl_3): 63.37, 45.55, 42.51, 36.88, 36.72, 32.87, 32.55, 30.56, 30.34, 30.30, 30.07, 29.52, 26.93, 26.85, 26.71, 26.10, 19.60, 19.38.

MS (EI, 70 eV): m/z (%) = 318 [M^+] (100).

HRMS-EI: m/z [M^+] calcd for $C_{17}H_{34}OS_2$: 318.2051; found: 318.2053.

(4*S*,10*R*)-11-(1,3-Dithian-2-yl)-4,10-dimethylundecyl methanesulfonate: To a solution of **19** (770 mg, 2.42 mmol) in dry CH_2Cl_2 (30 mL) were added $MsCl$ (0.28 mL, 3.63 mmol) and Et_3N (0.50 mL, 3.63 mmol) at 0°C. Then the mixture was stirred at room temperature for 5 h and diluted with CH_2Cl_2 (40 mL). The solution was washed with water and brine sequentially, dried over Na_2SO_4 , filtered, and concentrated under reduced pressure. Flash column chromatography on silica gel (PE/EA: 10/1) afforded the title compound (910 mg, 95%) as a colorless liquid.

$[\alpha]_D^{24}$: -5.81 (*c* 0.43, $CHCl_3$).

IR (KBr): 2928, 2854, 1465, 1423, 1356, 1276, 1176, 919, 823, 528, 410 cm^{-1} .

1H NMR (300 MHz, $CDCl_3$): 4.22 (t, 2H, J = 6.6 Hz), 4.08-4.13 (m, 1H), 3.02 (s, 3H), 2.79-2.92 (m, 4H), 2.09-2.18 (m, 1H), 1.63-1.88 (m, 5H), 1.12-52 (m, 14H), 0.83-0.92 (m, 6H).

^{13}C NMR (75 MHz, $CDCl_3$): 70.50, 45.54, 42.52, 37.34, 36.72, 35.93, 32.50, 32.32, 30.57, 30.35, 30.03, 29.93, 29.53, 29.31, 26.90, 26.72, 26.11, 19.43, 19.38, 19.24.

MS (EI, 70 eV): m/z (%) = 396 [M^+] (100).

HRMS-EI: m/z [M^+] calcd for $C_{18}H_{36}O_3S_3$: 396.1827; found: 396.1821.

2-((2*R*,8*R*)-2,8-Dimethylundecyl)-1,3-dithiane: To a suspension of $LiAlH_4$ (239 mg, 6.3 mmol) in dry diethylether (30 mL) was added, dropwise, a solution of mesylate (830 mg, 2.1 mmol) in diethylether (10 mL) at 0°C. The mixture was then stirred at room temperature and quenched with $Na_2SO_4 \cdot 10H_2O$ after TLC showed complete consumption of **9**. The mixture was filtered and washed with diethylether. The filtrate was concentrated and purified via flash column chromatography on silica gel (with hexane) to give the title compound (592 mg, 94%) as a colorless oil.

$[\alpha]_D^{24}$: -9.10 (*c* 0.63, $CHCl_3$).

IR (KBr): 2956, 2927, 2855, 1465, 1423, 1378, 1275, 1243, 1185, 909, 418 cm^{-1} .

1H NMR (300 MHz, $CDCl_3$): 4.08-4.13 (m, 1H), 2.79-2.92 (m, 4H), 2.10-2.16 (m, 1H), 1.67-1.89 (m, 3H), 1.47-1.52 (m, 1H), 1.05-1.36 (m, 15H), 0.82-0.93 (m, 9H).

^{13}C NMR (75 MHz, $CDCl_3$): 45.59, 42.58, 39.39, 37.04, 36.78, 32.46, 30.59, 30.39, 30.18, 29.60, 27.03, 26.78, 26.15, 20.12, 19.66, 19.41, 14.40.

MS (EI, 70 eV): m/z (%) = 302 [M^+] (100).

HRMS-EI: m/z [M^+] calcd for $C_{17}H_{34}S_2$: 302.2102; found: 302.2099.

(3*R*,9*R*)-3,9-Dimethylundecanal (20): To a solution of dithiane (44 mg, 0.15 mmol) in MeCN/water (3 mL/1 mL) were added MeI (0.19 mL, 3 mmol) and $NaHCO_3$ (252 mg, 3 mmol) at room temperature. The mixture was stirred for 10 h, concentrated under

reduced pressure, dissolved in water, extracted with diethylether (20 mL × 3), the extracts combined, washed with brine, dried over Na_2SO_4 , filtered, and concentrated under reduced pressure. Flash column chromatography on silica gel (PE/EA: 10/1) afforded **20** (30 mg, 97%) as a colorless liquid.

$[\alpha]_D^{24}$: +5.54 (*c* 0.81, $CHCl_3$).

IR (KBr): 2985, 2928, 2857, 2711, 1729, 1464, 1379, 1261, 1018, 804, 471, 430, 413 cm^{-1} .

1H NMR (300 MHz, $CDCl_3$): 9.75 (t, 1H, J = 2.1 Hz), 2.17-2.44 (m, 2H), 2.03-2.07 (m, 1H), 1.02-1.38 (m, 15H), 0.95 (d, 3H, J = 6.6 Hz), 0.82-0.89 (m, 6H).

^{13}C NMR (75 MHz, $CDCl_3$): 203.14, 51.09, 39.40, 37.03, 36.94, 32.46, 30.07, 28.20, 27.00, 20.13, 19.99, 19.65, 14.40.

MS (EI, 70 eV): m/z (%) = 212 [M^+] (100).

HRMS-EI: m/z [M^+] calcd for $C_{14}H_{28}O$: 212.2140; found: 212.2143.

(6*R*,12*R,E*)-6,12-Dimethylpentadec-3-en-2-one (21): To a suspension of NaH (60%, 9.0 mg, 0.22 mmol) in anhydrous THF (2 mL) was added a solution of phosphonate **8** (42 mg, 0.22 mmol) in THF (1 mL) at 0°C. The mixture was stirred for 10 min and added to a solution of aldehyde **20** (30 mg, 0.14 mmol) in THF (1 mL). The solution was stirred at room temperature for 6 h, quenched with water, extracted with $EtOAc$ (20 mL × 3), combined, washed with brine, dried over Na_2SO_4 , filtered, and concentrated under reduced pressure. Flash column chromatography on silica gel (PE/EA: 30/1) afforded enone **21** (32 mg, 90%) as a colorless oil.

$[\alpha]_D^{24}$: -3.41 (*c* 0.42, $CHCl_3$).

IR (KBr): 2958, 2928, 2872, 2856, 1701, 1678, 1629, 1465, 1379, 1361, 1252, 1180, 980, 616, 543 cm^{-1} .

1H NMR (300 MHz, $CDCl_3$): 6.74-6.82 (m, 1H), 6.05 (d, 1H, J = 15.9 Hz), 1.98-2.23 (m, 5H), 1.03-1.35 (m, 16H), 0.80-0.89 (m, 9H).

^{13}C NMR (75 MHz, $CDCl_3$): 198.61, 147.52, 132.39, 39.98, 39.41, 37.05, 36.73, 32.64, 32.48, 30.17, 27.06, 26.89, 20.14, 19.66, 14.41.

MS (EI, 70 eV): m/z (%) = 253 [$M+H^+$] (100).

(6*R*,12*R*)-6,12-Dimethylpentadecan-2-one (5): A reaction flask containing **21** (30 mg, 0.13 mmol), Pd/C (10%, 30 mg), and $MeOH$ (5 mL) was evacuated and back-filled with H_2 (1 atm). The reaction mixture was stirred at ambient temperature under hydrogen for 2 days and then filtered over a plug of silica gel topped with Celite ($MeOH$ eluent). The filtrate was concentrated and purified by flash column chromatography on silica gel (PE/EA: 100/1) to give **5** (24 mg, 79%) as a colorless liquid.

$[\alpha]_D^{24}$: -0.395 (*c* 0.41, $CHCl_3$).

IR (KBr): 2957, 2928, 2856, 1720, 1464, 1409, 1378, 1362, 1164, 726, 435, 419 cm^{-1} .

1H NMR (300 MHz, $CDCl_3$): 2.38 (t, 2H, J = 7.8 Hz), 2.12 (s, 3H), 1.43-1.62 (m, 2H), 1.01-1.40 (m, 18H), 0.80-0.89 (m, 9H).

^{13}C NMR (75 MHz, $CDCl_3$): 209.36, 44.14, 39.41, 37.08, 36.90, 36.64, 36.51, 32.65, 32.47, 30.33, 29.84, 29.48, 27.09, 27.06, 21.43, 20.13, 19.67, 19.54, 19.22, 14.40.

MS (EI, 70 eV): m/z (%) = 254 [M^+] (100).

References

- [1] Ando T, Yamakawa, R. (2015) Chiral methyl-branched pheromones. *Natural Product Reports*, **32**, 1007-1041.
- [2] (a) Tian WS, Shi Y. (2010) The study of resource chemistry. *Progress in Chemistry*, **22**, 538-556; (b) Huang XG, Li T, Lin JR, Jin RH, Tian WS. (2007) Synthesis of the C(7)-C(13) fragment of matsuone, a sex pheromone of the matsuococcus pine bast scales. *Chinese Journal of Organic Chemistry*, **27**, 428-430; (c) Li T, Huang XG, Lin JR, Jin RH, Tian WS. (2007) Total synthesis of (2*R*,6*R*)-2,6,10-trimethylundecan-1-ol with (*R*)-5-methyl-delta-valerolactone from the industrial waste. *Acta Chimica Sinica*, **65**, 1165-1171; (d) Zhang SJ, Dong HD, Gui JH, Tian WS. (2012) Stereoselective synthesis of the insect growth regulator (*S*)-(+) hydrodroprene through Suzuki-Miyaura cross-coupling. *Tetrahedron Letters*, **53**, 1882-1884; (e) Wang C, He CY, Shi Y, Xiang H, Tian WS. (2015) Synthesis of tribolure, the common aggregation pheromone of four *Tribolium* flour beetles. *Chinese Journal of Chemistry*, **33**, 627-631; (f) Zhang SJ, Shi Y, Tian WS. (2015) Synthesis of C1-C9 domain of the nominal didemnaketal A. *Chinese Journal of Chemistry*, **33**, 663-668.
- [3] (a) Guss PL, Tumlinson JH, Sonnet PE, McLaughlin JR. (1983) Identification of a female-produced sex pheromone from the southern corn rootworm, *Diabrotica undecimpunctata howardi* Barber. *Journal of Chemical Ecology*, **9**, 1363-1375; (b) Chuman T, Guss PL, Doolittle RE,

- [4] McLaughlin JR, Krysan JL, Schalk JM, Tumlinson JH. (1987) Identification of female-produced sex pheromone from banded cucumber beetle, *Diabrotica balteata* LeConte (Coleoptera: Chrysomelidae). *Journal of Chemical Ecology*, **13**, 1601-1616.
- [5] Mori K, Igarashi Y. (1988) Pheromone synthesis. CIX. Synthesis of the four stereoisomers of 6,12-dimethyl-2-pentadecanone, the sex pheromone of *Diabrotica balteata* Le Conte. *Liebigs Annalen der Chemie*, 717-720; (b) Enders D, Jandeleit B, Prokopenko OF. (1995) Convergent synthesis of (*R,R*)-6,12-dimethylpentadecan-2-one, the female sex pheromone of the banded cucumber beetle by iron mediated chirality transfer. *Tetrahedron*, **51**, 6273-6284; (c) Chow S, Kitching W. (2001) Hydrolytic kinetic resolution of mono- and bisepoxides as a key step in the synthesis of insect pheromones. *Chemical Communications*, 1040-1041; (d) Chow S, Kitching W. (2002) Hydrolytic kinetic resolution of terminal mono- and bis-epoxides in the synthesis of insect pheromones: routes to (−)-(R)- and (+)-(S)-10-methyldodecyl acetate, (−)-(R)-10-methyl-2-tridecanone, (−)-(R)-(Z)-undec-6-en-2-ol (Nostrenol), (−)-(1*R*,7*R*)-1,7-dimethylnonyl propanoate, (−)-(6*R*,12*R*)-6,12-dimethylpentadecan-2-one, (−)-(2*S*,11*S*)-2,11-diacetoxytridecane and (+)-(2*S*,12*S*)-2,12-diacetoxytridecane. *Tetrahedron: Asymmetry*, **13**, 779-793.
- [6] Takahashi S, Ogawa N, Koshino H, Nakata T. (2005) Total synthesis of the proposed structure for pyragonicin. *Organic Letters*, **7**, 2783-2786.
- [7] Krebs O, Taylor RJK. (2005) Synthesis of the eastern portion of ajudazol a based on Stille coupling and double acetylene carbocupration. *Organic Letters*, **7**, 1063-1066.
- [7] Semmelhack MF, Jiang Y, Ho D. (2001) Synthesis of the amino sugar from C-1027. *Organic Letters*, **3**, 2403-2406.

A Rapid Study of Botanical Drug–Drug Interaction with Protein by Re-ligand Fishing using Human Serum Albumin–Functionalized Magnetic Nanoparticles

Lin-Sen Qing^a, Ying Xue^a, Li-Sheng Ding^a, Yi-Ming Liu^b, Jian Liang^a and Xun Liao^{a,*}

^aChengdu Institute of Biology, Chinese Academy of Sciences, Chengdu, Sichuan, China, 610041

^bJackson State University, Mississippi, USA, 39217

liaoxun@cib.ac.cn

Received: July 9th, 2015; Accepted: November 16th, 2015

A great many active constituents of botanical drugs bind to human serum albumin (HSA) reversibly with a dynamic balance between the free- and bound-forms in blood. The curative or side effect of a drug depends on its free-form level, which is always influenced by other drugs, combined dosed or multi-constituents of botanical drugs. This paper presented a rapid and convenient methodology to investigate the drug-drug interactions with HSA. The interaction of two steroid saponins, dioscin and *pseudo*-protodioscin, from a botanical drug was studied for their equilibrium time and equilibrium amount by re-ligand fishing using HSA functionalized magnetic nanoparticles. A clear competitive situation was obtained by this method. The equilibrium was reached soon about 15 s at a ratio of 0.44: 1. Furthermore, the interaction of *pseudo*-protodioscin to total steroid saponins from DAXXK was also studied. The operation procedures of this method were faster and more convenient compared with other methods reported.

Keywords: Drug–drug interaction, Re-ligand fishing, Dioscin, *Pseudo*-protodioscin, Human serum albumin–functionalized magnetic nanoparticles.

Botanical drugs are often mixtures of many active ingredients that could bind to human serum albumin (HSA) reversibly with a dynamic balance of the free- and bound-form in blood. The drug distribution of the free- or bound-form will probably be affected by the competitive binding with HSA, which is directly related to the curative or side effect. Therefore, it is of great importance to study botanical drug–drug interactions.

There has been much research on interactions between drugs and HSA using classical methods such as equilibrium dialysis [1], ultrafiltration [2], X-ray crystallography [3], and mass spectrometry [4], as well as some spectroscopic methods [5]. However, these methods are only suitable for pure compound study, not being able to detect multiple ingredients in a complex matrix. As for herb-drug interaction, the present studies concentrate mainly on the change in the curative effect of the drug, as well as the activity of CPY450 [6–8], while very few studies are involved in the interaction between each single component. Herein we demonstrate that re-ligand fishing could be applied to study the drug-drug interactions, which is based on ligand fishing experiments with HSA functionalized magnetic nanoparticles (HSA–MNPs) used in our previous research [9–12]. Ligand fishing based on receptor theory had been proposed as a new method for drug–protein interaction using a protein immobilized on the surface of MNPs for the isolation of ligands from a mixture of compound extracts [13]. Correspondingly, re-ligand fishing was defined as HSA–MNPs saturated binding with one drug in advance and then ligand fish other drugs in the second ligand fishing experiment.

“Di Ao Xin Xue Kang” capsule (DAXXK), manufactured from the total steroid saponins extract of *Dioscorea nipponica* and *D. panthaica*, is a popular botanical medicine in China for prevention and treatment of coronary heart disease by inhibiting platelet aggregation [14]. It is an interesting phenomenon that a single saponin either inhibits or induces platelet aggregation [15, 16], while the total steroid saponins has an obvious platelet aggregation

inhibition activity due to multicomponent effective ingredients synergy and/or antagonistic action [17, 18]. There has been some research on the interaction between certain proteins with saponins from *D. nipponica* [19–21]. However, the interactions with HSA by individual steroid saponins have never been reported. Thus, in the present work, the drug–drug interaction with HSA between the two main constituents of DAXXK, dioscin and *pseudo*-protodioscin (ppd), were studied by re-ligand fishing using *pseudo*-protodioscin pre-saturated HSA–MNPs (ppd-HSA–MNPs). Mass spectrometry (MS) using an electrospray ionization source (ESI) was chosen for detection.

Different drugs, even with few structural differences, have different binding capacity to HSA. As shown in Fig 1, dioscin is an isospirostanol type steroid saponin with F ring closed, and *pseudo*-protodioscin (ppd) is a furostanol type steroid saponin with F ring opened. It was reported that dioscin is the inhibitor of platelet aggregation while *pseudo*-protodioscin is not. Dioscin and *pseudo*-protodioscin are two main ingredients of DAXXK. Thus, it is of great interest to investigate the dioscin–*pseudo*-protodioscin interaction with HSA by re-ligand fishing experiment.

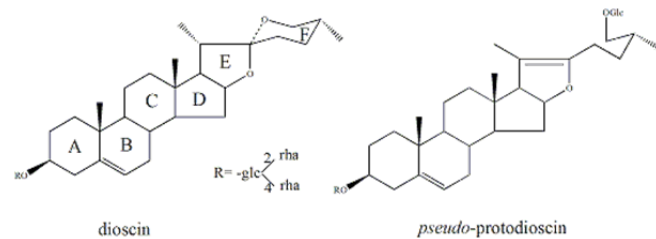


Figure 1: Chemical structures of dioscin and *pseudo*-protodioscin.

Our previous study revealed that dioscin had a greater affinity to HSA than *pseudo*-protodioscin [12]. Thus, HSA–MNPs pre-saturated with *pseudo*-protodioscin (ppd-HSA–MNPs) was used to ligand fish dioscin in this study. An excessive amount of *pseudo*-

protodioscin was used to ensure that all the HSA binding sites were saturated with *pseudo*-protodioscin. The de-binding wash of the ppd-HSA-MNPs was performed in 1 mL buffer containing 50% acetonitrile by vigorous shaking. The supernatant was carefully removed and saved for MS analysis. The existence of *pseudo*-protodioscin de-bound from ppd-HSA-MNPs was revealed by the peak at m/z 1029 [M-H]⁻, which could easily be assigned as *pseudo*-protodioscin; this was confirmed by MS².

Dioscin and *pseudo*-protodioscin were competitively bound with HSA at the same site. The dynamic interaction process and equilibrium amount of these two constituents could be rapidly reached using the ppd-HSA-MNPs re-ligand fish dioscin. It was anticipated that the ratio of dioscin/*pseudo*-protodioscin would be increased as the re-ligand fishing time increased, until the equilibrium point arrived. The re-ligand fishing time in five experiments, 3 s, 5 s, 10 s, 15 s and 25 s, was set as the different interaction time points for these two drug constituents. Their de-binding wash solutions were named as A2-1, A2-2, A2-3, A2-4 and A2-5, respectively. The peak at m/z 867 [M-H]⁻ in the mass spectrum could be easily assigned to dioscin, which was confirmed by MS². The mass spectra of A2-1, A2-2, A2-3, A2-4 and A2-5 showed the peaks of dioscin and *pseudo*-protodioscin, the height ratios of which correspond to their competitive binding; the results are summarized in Table 1. It was obvious that the height ratio of dioscin/*pseudo*-protodioscin was gradually increased with the re-ligand fishing time.

To calculate the amount of dioscin and *pseudo*-protodioscin, an eleven-point calibration curve was obtained with standard solutions at concentration ratios ranging from 8 : 1 to 1 : 128. Peak heights were used for the calculation. Linear regression analysis of the results yielded the following equations for the ratio of dioscin/*pseudo*-protodioscin: $Y = 8.4247 X + 0.0157$, $r^2 = 0.998$, where Y was the peak height ratio of dioscin/*pseudo*-protodioscin, X was the concentration ratio of dioscin/*pseudo*-protodioscin, and r^2 was the correlation coefficient. The concentration ratio of dioscin/*pseudo*-protodioscin calculated by peak heights was determined in solutions A2-1, A2-2, A2-3, A2-4 and A2-5, as shown in Table 1, which reflected the dynamic interaction process intuitively. The equilibrium was reached after about 15 s at a ratio of 0.44 : 1.

Among the steroidal saponins exhibiting activity for the prevention and treatment of coronary heart disease in DAXXK, there are two categories, the furostanol type and the isospirostanol type. Dioscin is the most important isospirostanol type and *pseudo*-protodioscin the most important furostanol type; both are determined in the Chinese Pharmacopoeia assay [14]. In this current study, further studies of the total steroidal saponins from DAXXK were conducted by comparison of ligand fishing results (de-binding wash solution B1) using HSA-MNPs and re-ligand fishing using ppd-HSA-MNPs (de-binding wash solution B2).

Table 1: Height ratios and concentration ratios of dioscin/*pseudo*-protodioscin at the different interaction times.

Solution	Re-ligand fishing time(s)	Height Ratio (dioscin/ <i>pseudo</i> -protodioscin)	Con. Ratio (dioscin/ <i>pseudo</i> -protodioscin)
A 1	0	0	0
A 2-1	3	1.03	0.12
A 2-2	5	1.72	0.20
A 2-3	10	3.57	0.42
A 2-4	15	3.70	0.44
A 2-5	25	3.70	0.44

Although dozens of steroidal saponins are present in DAXXK, only three, i.e. dioscin (m/z 687 [M-H]⁻), *pseudo*-protodioscin (m/z 1029 [M-H]⁻) and gracillin (m/z 883 [M-H]⁻) were bound to HSA significantly in the ligand fishing experiment. The ratio of dioscin/*pseudo*-protodioscin in the B1 solution was 0.54: 1, calculated by peak heights. By contrast, the ratio changed to 0.07: 1 in the re-ligand fishing experiment (B2 solution). This result indicated that the equilibrium was changed significantly in the presence of some outside source of *pseudo*-protodioscin and the drug-drug interaction of each constituent in DAXXK was serious. Further, it was reported that both dioscin and *pseudo*-protodioscin were degradation products of 26-O- β -D-glucopyranosyl-(25R)-furost-5-en-3 β ,22 ξ ,26-triol-3-O- β -D-glucopyranosyl-(1 \rightarrow 3)- β -D-glucopyranosyl-(1 \rightarrow 4)-[α -L-rhamnopyranosyl-(1 \rightarrow 2)]- β -D-glucopyranoside in *D. panthaica* [22]. The assay standard for DAXXK in the Chinese Pharmacopoeia is the content of *pseudo*-protodioscin and total saponins [14]. However, unlike modern therapeutic drugs that are single active pure compounds, DAXXK is an herbal medicine that contains many active ingredients, and the chemical compositions always vary depending on the variety, origin, harvesting time and processing technique. Hence, the strong binding ingredients such as dioscin should be integrated into the quality control standard. It is necessary to monitor the drug blood concentration in clinical use, especially with combined use with narrow therapeutic index drugs (for example warfarin, digoxin). Furthermore, this work can be important for the evaluation of the pharmaceutical effect of a herb medicine containing multi-components.

In summary, a rapid and convenient methodology was presented to determine the balance ratio and balance time of dioscin/*pseudo*-protodioscin interaction with HSA by re-ligand fishing using human serum albumin-functionalized magnetic nanoparticles. The equilibrium was reached soon after 15 s at the amount ratio of 0.44: 1. Furthermore, the interaction of *pseudo*-protodioscin to total steroidal saponins from DAXXK was also studied. The procedures with the aid of mass spectrometry detection were very sensitive, quick and convenient. These results revealed that re-ligand fishing coupled with MS detection could be applied to investigate the botanical drug-drug interactions.

Experimental

Preparation of HSA-MNPs: HSA functionalized MNPs (HSA-MNPs) were prepared following the procedures reported previously [9-12]. Briefly, magnetic nanoparticles were prepared by co-precipitation with a molar ratio of Fe^{2+} : Fe^{3+} = 1: 2 at pH 10. MNPs were first coated with SiO_2 using TEOS. Secondly, the particles were dispersed in APTMS solution to add -NH₂ to the SiO_2 ; the resultant particles were then dispensed in the GD solution to provide -CHO to the surface. Finally, the -CHO coated MNPs were incubated with HSA to obtain HSA functionalized MNPs. HSA-MNPs were suspended in NH₄Ac solution and kept at 4°C before use.

Re-ligand fishing experiments

Saturated binding *pseudo*-protodioscin to HSA-MNPs (ppd-HSA-MNPs): A 225 $\mu\text{g}/\text{mL}$ solution of *pseudo*-protodioscin was prepared using ammonium acetate buffer solution (10 mM/L, pH 7.4). One mL *pseudo*-protodioscin solution and 100 μL HSA-MNPs were added to a 4 mL Eppendorf tube. The tube was vigorously shaken for 2 min using a vortex oscillator, and then put aside for magnetic separation for 1 min. The supernatant was removed. The HSA-MNPs were washed 3 times with 1 mL of buffer solution, each by vigorously shaking for 1 min, and then the supernatants

were removed after magnetic separation. Hence, the pseudo-protodioscin saturated binding HSA-MNPs (ppd-HSA-MNPs) were obtained.

Detection binding amount of pseudo-protodioscin in ppd-HSA-MNPs: The de-binding wash of the ppd-HSA-MNPs was performed in 1 mL buffer containing 50% acetonitrile by vigorous shaking for 2 min. The supernatant was carefully removed and saved (A1) for mass spectrometric analysis.

Re-ligand fish dioscin using ppd-HSA-MNPs for different times: A 0.55 µg/mL solution of dioscin was prepared using ammonium acetate buffer solution (10 mM/L, pH 7.4). One mL dioscin solution was added to a 4 mL Eppendorf tube containing 100 µL ppd-HSA-MNPs. The tube was vigorously shaken for 3 s (re-ligand fish time investigated) using a vortex oscillator, and then put aside for magnetic separation for 1 min. The supernatant was removed. The ppd-HSA-MNPs were washed 3 times with 1 mL of buffer solution each by vigorous shaking for 1 min, and then the supernatants were removed, after magnetic separation. Finally, the de-binding wash was performed in 1 mL buffer containing 50% acetonitrile by vigorous shaking for 2 min. The supernatant was carefully removed and saved (A2-1).

Another 4 experiments were undertaken using the parallel procedures above as well. Four de-binding solutions A2-2, A2-3,

A2-4 and A2-5 were obtained for mass spectrometric analysis by prolonging the re-ligand fishing time from 3 s (A2-1) to 5 s (A2-2), 10 s (A2-3), 15 s (A2-4) and 25 s (A2-5), respectively.

Re-ligand fish total steroid saponins using ppd-HSA-MNPs: First, a comparative ligand fishing experiment was made using HSA-MNPs. One mL DAXXK solution and 100 µL HSA-MNPs were added to a 4 mL Eppendorf tube. After vigorous shaken, magnetic separation, and buffer wash, the 50% acetonitrile de-binding wash solution (B1, ligand fishing) was obtained for comparison with B2 below.

Then, a 52 µg/mL solution of the DAXXK solution was prepared using ammonium acetate buffer solution (10 mM/L, pH 7.4). One mL dioscin solution was added to a 4 mL Eppendorf tube containing 100 µL ppd-HSA-MNPs. The 50% acetonitrile de-binding wash solution (B2, re-ligand fishing) was obtained following the same procedure. All the experiments above were repeated 3 times.

Acknowledgments - Financial support from the National Natural Science Foundation of China (21072184 and 21202161), and China Postdoctoral Science Foundation (2013T60863) are gratefully acknowledged.

References

- [1] Taboada P, Mosquera V, Russo JM, Sarmiento F, Jones MN. (1999) Interaction between penicillins and human serum albumin: A thermodynamic study of micellar-like clusters on a protein. *Langmuir*, **16**, 934-938.
- [2] Zlotos G, Oehlmann M, Nickel P, Holzgrabe U. (1998) Determination of protein binding of gyrase inhibitors by means of continuous ultrafiltration. *Journal of Pharmaceutical and Biomedical Analysis*, **18**, 847-858.
- [3] Zhu L, Yang F, Chen L, Meehan EJ, Huang M. (2008) A new drug binding subsite on human serum albumin and drug-drug interaction studied by X-ray crystallography. *Journal of Structural Biology*, **162**, 40-49.
- [4] Schmidt AC, Steier S. (2010) Some critical aspects in the determination of binding constants by electrospray ionisation mass spectrometry as the example of arsenic bindings to sulphur-containing biomolecules. *Journal of Mass Spectrometry*, **45**, 870-879.
- [5] Mandeville JS, Froehlich E, Tajmir-Riahi HA. (2009) Study of curcumin and genistein interactions with human serum albumin. *Journal of Pharmaceutical and Biomedical Analysis*, **49**, 468-474.
- [6] Qiu Z, Wang L, Dai Y, Ren W, Jiang W, Chen X, Li N. (2015) The potential drug-drug interactions of ginkgolide B mediated by renal transporters. *Phytotherapy Research*, **29**, 662-667.
- [7] Milić N, Milosević N, Golocorbin Kon S, Božić T, Abenavoli L, Borrelli F. (2014) Warfarin interactions with medicinal herbs. *Natural Product Communications*, **9**, 1211-1216.
- [8] Miladinović DL, Ilić BS, Mihajilov-Krstev TM, Jović JL, Marković MS. (2014) *In vitro* antibacterial activity of *Libanotis montana* essential oil in combination with conventional antibiotics. *Natural Product Communications*, **9**, 281-286.
- [9] Qing LS, Shan XQ, Xu XM, Xue Y, Deng WL, Li BG, Wang XL, Liao X. (2010) Rapid probe and isolation of bioactive compounds from *Dioscorea panaica* using human serum albumin functionalized magnetic nano-particles (HSA-MNPs)-based ligand fishing coupled with electrospray ionization mass spectrometry. *Rapid Communications in Mass Spectrometry*, **24**, 3335-3339.
- [10] Qing LS, Tang N, Xue Y, Liang J, Liu YM, Liao X. (2012) Identification of enzyme inhibitors using therapeutic target protein-magnetic nanoparticle conjugates. *Analytical Methods*, **4**, 1612-1615.
- [11] Qing LS, Xue Y, Deng WL, Liao X, Xu XM, Li BG, Liu YM. (2011) Ligand fishing with functionalized magnetic nanoparticles coupled with mass spectrometry for herbal medicine analysis. *Analytical and Bioanalytical Chemistry*, **399**, 1223-1231.
- [12] Qing LS, Xue Y, Zheng Y, Xiong J, Liao X, Ding LS, Li BG, Liu YM. (2011) Ligand fishing from *Dioscorea nipponica* extract using human serum albumin functionalized magnetic nanoparticles. *Journal of Chromatography A*, **1217**, 4663-4668.
- [13] Moaddel R, Marszał MP, Bighi F, Yang Q, Duan X, Wainer IW. (2007) Automated ligand fishing using human serum albumin-coated magnetic beads. *Analytical Chemistry*, **79**, 5414-5417.
- [14] Chinese Pharmacopoeia Commission. (2010) Pharmacopoeia of the People's Republic of China. China Medical Science Press, Beijing, China, 671.
- [15] Fu YL. Master's thesis. (2007) The characteristic of steroid saponins on platelet aggregation through structure-activity assay and mechanism study. Military Medical Science Academy of the Chinese People's Liberation Army.
- [16] Zhao NX, Han YM, Zhang SJ. (2011) Antithrombotic components in *Dioscorea nipponica*. *Chinese Traditional and Herbal Drugs*, **42**, 652-655.
- [17] Su W. (2012) DAXXK intervention clinical trials of aspirin resistance and its mechanism. *China Pharmaceuticals*, **21**, 26-28.
- [18] Li ZM., Xu XJ, Yin CH. (2002) Experimental research of DAXXK on thromboi. *Lishizhen Medicine and Materia Medica Research*, **13**, 390-391.
- [19] Ali Z, Smillie TJ, Khana IA. (2013) 7-Oxodioscin, a new spirostane steroid glycoside from the rhizomes of *Dioscorea nipponica*. *Natural Product Communications*, **8**, 319-321.
- [20] Yu H, Zheng L, Xu L, Yin L, Lin Y, Li H, Liu K, Peng J. (2015) Potent effects of the total saponins from *Dioscorea nipponica* Makino against streptozotocin-induced type 2 diabetes mellitus in rats. *Phytotherapy Research*, **29**, 228-240.
- [21] Lu F, Liu L, Yu DH, Li XZ, Zhou Q, Liu SM. (2014) Therapeutic effect of Rhizoma *Dioscoreae Nipponicae* on gouty arthritis based on the SDF-1/CXCR 4 and p38 MAPK pathway: an *in vivo* and *in vitro* study. *Phytotherapy Research*, **28**, 280-288.
- [22] Geng, Y, Tan NH, Zhou J, Kong LY. (2004) Isolation and identification of steroid saponins from the fresh rhizomes of *Dioscorea panaica*. *Chinese Journal of Natural Medicines*, **2**, 25-27.

Serum Metabolomic Profiling of Rats by Intervention of *Aconitum soongaricum*

Fan Zhang^{a*}, Jiao Liu^a, Jun Lei^a, Wenjing He^b and Yun Sun^b

^aSchool of Pharmacy, North Sichuan Medical University, Nanchong 637000, Sichuan, P. R. China

^bDepartment of Traditional Chinese Medicine, Xinjiang Medical University, Urumqi 830011, Xinjiang, P. R. China

zhangfan596@163.com

Received: August 1st, 2015; Accepted: September 29th, 2015

To understand the toxic mechanism and to find the changes in the endogenous metabolites of *Aconitum soongaricum* Staf for clinical detection, a combination of ¹H NMR spectroscopy and multivariate statistical analysis was applied to examine the metabolic profiles of the blood serum samples collected from the rat model. In total, thirteen biomarkers of *A. soongaricum* were found and identified. It turned out that *A. soongaricum* treatment may partially disorder the metabolism. The study has shown the potential application of NMR-based metabolomic analysis in providing further insights into the toxicity caused by *A. soongaricum*.

Keywords: Ranunculaceae, *Aconitum soongaricum*, Metabolomic Profiling, Biomarkers, Nuclear Magnetic Resonance.

Aconitum soongaricum Staf, family Ranunculaceae, is well known for its anti-inflammatory and analgesic effect, and is widely used in the north of China as an analgesic for neuralgia, toothache, arthritis and other pains [1a-d]. However, as this plant contains *Aconitum* alkaloids, it has been reported that it has resulted in several poisoning accidents [2a,b]. To understand the toxic mechanism and to find the changes in endogenous metabolites for clinical detection, NMR based metabolomics was conducted to investigate the intervention effects of *A. soongaricum* on mice. Metabolomics analysis was carried out on serum samples, while orthogonal partial least squares-discriminant analysis (OPLS-DA) was employed to investigate the toxic effects of *A. soongaricum* and to detect related potential biomarkers [3a-c].

In this study, rats were fed with *A. soongaricum* and the biochemical variations in the serum from these rats were investigated by high resolution ¹H NMR spectroscopy. This procedure has provided an insight into the systematic metabolism after use of *A. soongaricum*. Results of this study have validated the applicability of NMR based metabolomics in the study of toxicity and biomarkers detection. In total, thirteen biomarkers were found and identified (Table 1). It turned out that *A. soongaricum* treatment may partially disorder the metabolism. Besides, NMR based metabolomics proved to be a powerful tool for investigating the pharmacodynamic effects of natural products and underlying mechanisms.

OPLS-DA analysis of endogenous metabolites in rat serum at different times after administration showed that there were significant differences in serum metabolites in each time group. It can be seen from the OPLS-DA analysis of different time groups that the 2d group is far away from the others in the space, but the 2d and 5d groupswere closer in the plane and space, while the 2d group can be separated completely from the 9d and 13d groups in the score plot. The 9 d and 13 d groups are gradually approaching the blank group, the results showing that the effects of *A. soongaricum* on rats occurred within two days after the administration, but then they gradually recovered.

Table 1: Potential biomarkers of *A. soongaricum* detected by NMR.

No.	Metabolites	Reference value, ¹ H NMR, δ	Measured value, ¹ H NMR, δ
1	β -Glucose	3.24(dd)	3.24(dd)
		3.40(t)	3.40(t)
		4.64(d)	4.64(d)
2	α -Glucose	3.53(dd)	3.53(dd)
		3.72(dd)	3.72(dd)
		3.83(dd)	3.83(dd)
3	VLDL	5.23(d)	5.23(d)
		0.85(m)	0.85(m)
		0.88(m)	0.88(m)
4	LDL	1.27(m)	1.27(m)
		1.26(m)	1.26(m)
		4.25(m)	4.25(m)
5	Lactic acid	1.33(d)	1.32(d)
		4.11(q)	4.11(q)
6	Creatine	3.03(s)	3.03(s)
		3.93(s)	3.92(s)
7	Trimethylamine oxide	3.27(s)	3.26(s)
8	β -Hydroxybutyric acid	1.19(d)	1.19(d)
9	Glycine	3.57(s)	3.55(s)
10	Alanine	1.47(d)	1.47(d)
11	Glutamic acid	3.76(q)	3.76(q)
12	Pyruvic acid	2.13(m)	2.13(m)
13	Acetoacetic acid	2.38(s)	2.36(s)
		2.27(s)	2.27(s)

The variable metabolites in the serum of different time groups were VLDL, LDL, glucose, lactic acid, creatine, trimethylamine oxide, glycine, glutamic acid, alanine, β -hydroxybutyric acid, pyruvic acid and acetoacetic acid. The levels of glucose, glycine, and glutamic acid were decreased in the 2 d, 5 d and 9 d groups comparing with the blank group; these metabolites were obviously decreased in the day after administration, but were restored to normal levels in 13 d. The levels of VLDL, LDL and lactic acid were decreased 2 d after administration, but increased significantly in 9 d. The levels of creatine and trimethylamine oxide were increased compared with the blank group and trimethylamine oxide was obviously increased in 9 d. The levels of β -hydroxybutyric acid and acetoacetic acid

Table 2: The change of metabolites at different times.

No.	Metabolites	2d	5d	9d	13d
1	β -Glucose	↓↓	↓	↓	—
2	α -Glucose	↓↓	↓	↓	—
3	VLDL	↓	↓	↑↑	↑
4	LDL	↓	↓	↑↑	↑
5	Lactic acid	↓	↓	↑↑	↑
6	Creatine	↑	↑	↑	↑
7	Trimethylamine oxide	↑	↑	↑↑	↑
8	β -Hydroxybutyric acid	↑↑	↑	↑	—
9	Glycine	↓↓	↓	↓	—
10	Alanine	↓↓	↓	↓	↓
11	Glutamic acid	↓↓	↓	↓	—
12	Pyruvic acid	—	—	↓	—
13	Acetoacetic acid	↑↑	↑	↑	—

Concentration compared with the blank group was not obvious; ↑ and ↓ concentration increase or decrease compared with the blank group; ↑↑ and ↓↓ concentration increase or decrease compared with the blank group was significant.

were increased obviously in 2d and higher than the blank group, while levels of pyruvic acid were decreased in 9d compared with the blank group (Table 2).

In this study, metabolomics have been used to highlight the metabolic effect of *A. soongaricum* treatment in the rat model. NMR based metabolomics has been shown to be an efficient technique to investigate the metabolic perturbation due to *A. soongaricum* poisoning. The changes in endogenous metabolites in serum samples from models of different groups of rats were identified by OPLS-DA. The toxicity of *A. soongaricum* was proven to be selective and affected a number of metabolic pathways. To complement the current study, future proteomic and immunohistochemistry studies may provide further insights into the metabolic mechanism and discover more effective treatments for toxicity detection. In summary, the current results indicate that ^1H NMR based metabolomics have the potential to uncover the metabolic response of *A. soongaricum* toxicity that could provide better understanding of the metabolic biomarkers.

Experimental

Plant material: The fresh roots of *A. soongaricum* were collected in Narat Grassland, Xinjiang Province of China in July 2012 and were identified by Prof. Fan Zhang (North Sichuan Medical University, Sichuan, P. R. China) [4a]. A voucher specimen (ZGEWT20120801) was deposited at the Xinjiang Museum of Traditional Chinese Medicine and Ethnomedicine.

Animal handling and sample collection: Sixty-six healthy SPF Sprague-Dawley rats (200 ± 20 g weight) were provided by North Sichuan Medical University. All rats were housed individually in metabolic cages. The animal room was maintained under controlled condition (a 12 h light-dark cycle with constant temperature and humidity). All efforts were made to minimize animal suffering. After acclimatization for one week, the rats were randomly separated into 11 groups, i.e. 2 h group, 6 h group, 2 d group, 3 d group, 5 d group, 7 d group, 9 d group, 11 d group, 13 d group, 14 d group and blank group ($n=6$). The blank group was given normal diet and clean water throughout the experiment, while the model groups were fed with the dose of 170 mg/kg, which was confirmed by acute toxicity test [4b]. After 2 h, 6 h, 2 d, 3 d, 5 d, 7 d, 9 d, 11 d, 13 d and 14 d, respectively, the blood was drawn from orbit using a syringe and the blood was left to clot at room temperature for 30 min. Serum samples were centrifuged (12,000 rpm) for 15 min at 4°C to remove particulate contaminants and then stored at -80°C until further analysis.

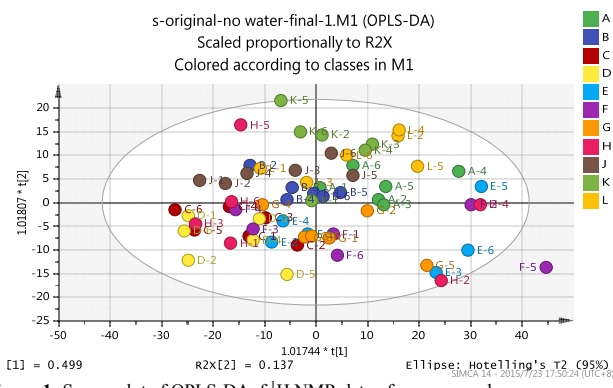


Figure 1: Scores plot of OPLS-DA of ^1H NMR data of serum samples.

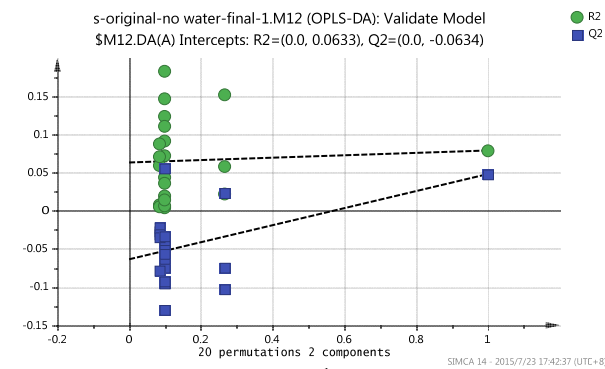


Figure 2: Permutations plot of OPLS-DA of ^1H -NMR data of serum samples.

Sample preparation and ^1H NMR spectroscopy: For ^1H NMR analysis, 500 μL of serum samples was mixed with 200 μL phosphate buffer solution (0.2M $\text{Na}_2\text{HPO}_4/\text{NaH}_2\text{PO}_4$, pH 7.4, 20% D_2O) to reduce pH variation across samples. In addition, 1×10^{-3} mol/L TSP (3-(trimethylsilyl)propionic-2,2,3,3-d4 acid sodium salt) was used as an internal reference standard at δ 0.0. The mixture was then transferred into a 5 mm NMR tube. The ^1H NMR measurements of the serum samples were performed using a Varian NMR system 600 MHz spectrometer equipped with a triple resonance probe. The experimental temperature was set to 298 K and the 90° pulse length was calibrated individually for each sample. For the serum samples, an additional Carr-Purcell-Meiboom-Gill (CPMG) spin-echo pulse train was incorporated into the NOESYPR sequence with a relaxation delay-90°-(τ -180°- τ) n-acquire. A total of 128 scans with a spectral width of 10 kHz were collected for all NMR experiments. The acquired signals were zero filled to 32k before Fourier transformation. For data analysis, metabolites in the Metabolomic Responses to *A. soongaricum* rat serum ^1H NMR spectra were assigned with reference to published data and HMDB database (<http://www.hmdb.ca/>).

Data preprocessing of NMR spectra and pattern recognition: The collected NMR spectra were phased and baseline corrected using the software Topspin 2.0 (Bruker, Germany)(Figure 1). All NMR spectra were also peak-aligned manually using in-house software to minimize variation due to peak shift. The chemical shift regions of δ 4.6-6.0 (water resonances), δ 0.0-0.2 (TSP resonance) and the regions which are peak-free for all spectra were excluded from further analysis. Table S1 shows the raw spectral data of serum samples. Then each spectrum was binned into segments by adaptive binning method. To account for variations in sample concentration, the spectra were normalized using group aggregating normalization technique. The NMR spectral data were converted to Microsoft Excelformat and imported into SIMCA software (version 14.0, Umetrics, Sweden) for multivariate analysis.

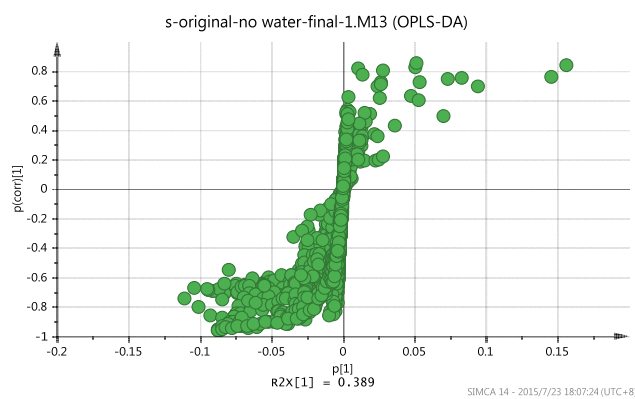


Figure 3: S-plots of OPLS-DA of ^1H -NMR data of serum samples.

Orthogonal partial least squares discriminant analysis (OPLS-DA) is a regression method that uses binary variables Y to indicate class membership. The OPLS-DA projects the original variables X (metabolic concentrations) to latent variables that focus on class separation, thus obtaining a better classification. The quality of the

models is described by R^2X and Q^2 values. R^2X is defined as the proportion of variance in the data explained by the models and indicates goodness of fit, and Q^2 is defined as the proportion of variance in the data predictable by the model and indicates predictability. The metabolites with high variable importance in the projection values in each OPLS-DA models are selected to investigate further their quantitative changes in all groups.

OPLS-DA of blood serum samples: OPLS-DA analysis of blood serum samples showed that the samples clustered based on studied groups (Figure 1). To investigate further the metabolic patterns and identify potential characteristic metabolites, group comparisons were carried out using OPLS-DA (Figures 2 and 3).

Supplementary data: S1 Table. Raw spectral data of serum samples.

Acknowledgments - The work was financially supported by the Chinese National Natural Science Foundation (81160547, 81460637), and the Doctoral Foundation of North Sichuan Medical University (201402).

References

- [1] (a) Chinese Academy of Sciences of Editorial Committee of flora of China. (1979) In *The flora of China (ZhongguoZhiwuzhi)*. Sciences Publishing House, Beijing, **27**, 308; (b) Xu X, Huangerhan B. (2009) In *Plant records of Kazakh medicine (HasakeYaozhi)*. Ethnic Publishing House, Beijing, **1**, 45; (c) Cai DM, Liu Y, Zhang F. (2011) Research survey of *Aconitum* grown in Xinjiang. *Xinjiang Journal of Traditional Chinese Medicine*, **29**, 74-75; (d) Zhang F, Yang LJ, Cai DM, Liu Y. (2012) Analysis of the diterpenoid alkaloids in *Aconitum soongaricum* Staph by HPLC and TLC. *Natural Product Research & Development*, **24**, 924-927.
- [2] (a) Jia XG, Zhou Q, Wang GP, Li XJ, He J. (2012) Toxic symptom and clinical rescue of *Aconitum*. *Xinjiang Journal of Traditional Chinese Medicine*, **30**, 67-70; (b) Li H, Chen WM, Chen X, Wang H, Li XQ. (2010) Poisonous weed species and their harmfulness in the grassland of Yili regions, Xinjiang Uygur Autonomous region of China. *Pratacultural Science*, **27**, 171-173.
- [3] (a) Nicholson JK, Connelly J, Lindon JC, Holmes E. (2002) Metabonomics: a platform for studying drug toxicity and gene function. *Nature Reviews*, **1**, 153-161; (b) Zhao LC, Zhang XD, Wang HY, Lin DH. (2011) ^1H NMR-based metabonomic analysis of metabolic changes of serum and liver in zucker obese rats. *Analytical Letters*, **44**, 1579-1590; (c) Fages A, Pontoizeau C, Jobard E, Lévy P, Bartosch B, Elena-Herrmann B. (2013) Batch profiling calibration for robust NMR metabonomic data analysis. *Analytical & Bioanalytical Chemistry*, **405**, 8819-8827.
- [4] (a) Cai DM, Liu Y, WUFUER H, Zhang F. (2011) Morphological and histological identification of Kazak medicinal herb *Aconitum soongaricum* Staph. *Journal of Chinese Medicinal Materials*, **34**, 876-878; (b) Yang LJ, Zhang F, Cai DM, Liu Y. (2012) Analysis on the acute toxicity of *Aconitum soongaricum* Staph in mice. *Lishizhen Medicine & Materia Medica Research*, **23**, 2542-2543.

Re-evaluation of ABTS^{•+} Assay for Total Antioxidant Capacity of Natural Products

Jian-Wei Dong, Le Cai*, Yun Xing, Jing Yu and Zhong-Tao Ding

Key Laboratory of Medicinal Chemistry for Natural Resource, Ministry of Education, School of Chemical Science and Technology, Yunnan University, Kunming 650091, P.R. China

caile@ynu.edu.cn

Received: June 23rd, 2015; Accepted: November 4th, 2015

2,2'-Azino-bis(3-ethylbenzothiazoline-6-sulfonic acid) diammonium salt radical cation (ABTS^{•+}) is a stable free radical frequently used for estimating the total antioxidant capacity (TAC) of natural products. The existing methods for ABTS^{•+} radical-scavenging activity assays are diverse in pre-diluting solvents and reaction time, which lead to errors in the TAC estimations. To develop an effective and universal method for estimating the ABTS^{•+} capacity accurately and reasonably, five pre-dilution solvents [methanol, ethanol, phosphate buffer ($\text{Na}_2\text{HPO}_4\text{-NaH}_2\text{PO}_4$, 200 mM, pH = 7.4), PBS buffer ($\text{Na}_2\text{HPO}_4\text{-NaH}_2\text{PO}_4\text{-NaCl}$, 200 mM, pH = 7.4), and distilled water] and different reaction times were investigated in ABTS^{•+} assays of five typical antioxidants. The results showed that the solvent effects were very significant. When using different pre-diluting solvents, different detection wavelengths should be selected. ABTS^{•+} assay could be measured within 2-10 min to obtain a rough result, which was mostly 6 min in the literature. However, full and accurate evaluation of antioxidant reactivity rather than capacity requires recording ABTS^{•+} loss continuously during the whole reaction period. The present study makes a recommendation for estimating the ABTS^{•+} capacity accurately and reasonably.

Keywords: ABTS, Solvent, Reaction time, Phenolic compound, Recommendation.

Reactive oxygen species (ROS), a collective term often used to include oxygen radicals [superoxide ($\text{O}_2^{\cdot-}$), hydroxyl (OH^{\cdot}), peroxy (RO_2^{\cdot}) , and alkoxyl (RO^{\cdot})] and certain nonradicals that either are oxidizing agents and/or are easily converted into radicals, such as HOCl, ozone (O_3), peroxy nitrite (ONOO^-), singlet oxygen (${}^1\text{O}_2$), and H_2O_2 [1], may cause cell aging, cardiovascular diseases, mutagenic changes, and cancerous tumor growth [2]. Antioxidants are compounds that can delay the oxidation of other molecules by inhibiting either the initiation or propagation of oxidizing chain reactions caused by free radicals and thereby may reduce oxidative damage to the human body [3]. Phenolic substances, which exist in plant tissues as secondary metabolites, can be categorized into simple phenols, phenolic acids (both hydroxybenzoic acids and hydroxycinnamic acids), flavonoids, lignins and tannins. These substances are responsible for color, bitterness, acerbic taste, flavour, odor and antioxidant properties [4].

2,2'-Azino-bis(3-ethylbenzothiazoline-6-sulfonic acid) diammonium salt radical cation (ABTS^{•+}), a stable free radical, is frequently used for estimating the total antioxidant capacity (TAC) of natural products, including crude extracts [5-9], polyphenols [10], phenolic acids [11], flavonoids [12], and others [13]. The original ABTS^{•+} radical-scavenging assay was measured according to the activation of metmyoglobin with hydrogen peroxide in the presence of ABTS to produce the radical cation, in the presence or absence of antioxidants [14]. With the improving technology for determination of the blue ABTS^{•+} chromophore produced through the reaction between ABTS and potassium persulfate (Figure 1), a feasible method was established according to a maximal absorption of ABTS^{•+} at wavelengths of 645 nm, 734 nm, and 815 nm [15, 16]; the original method measured at 415 nm [17, 18].

Until 1999, the applicable and universal ABTS^{•+} method for the study of both water-soluble and lipid-soluble antioxidants, pure compounds, and food extracts, including flavonoids, hydroxycinnamates, carotenoids, and plasma antioxidants, was

proposed by Re *et al.* [14]. This ABTS^{•+} assay was measured by a colorimetric method at 734 nm, and the extent of decolorization as a percentage inhibition of the ABTS^{•+} radical cation was determined as a function of concentration and time and calculated relative to the reactivity of Trolox, as a standard, under the same conditions. Recently, the LC-ABTS^{•+} assay is frequently used for ABTS^{•+} radical-scavenging activity. He *et al.* [19, 20] identified the phenolic compounds from pomegranate (*Punica granatum* L.) seed residues and investigated their antioxidant capacities by HPLC-ABTS^{•+} assay; Kalili *et al.* [21] reported that the combination of LC × LC separation with an on-line radical scavenging assay increased the likelihood of identifying individual radical scavenging species in comparison with the conventional LC-ABTS^{•+} assay.

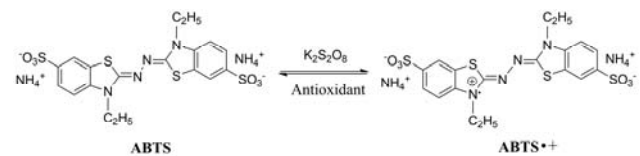


Figure 1: Reaction mechanism of ABTS and the oxygen radical (ABTS^{•+}).

However, in the course of the application of the ABTS^{•+} method, some problems appeared. First, the pre-diluting solvents in ABTS^{•+} assay are various in the existing literature. For example, Bangoura *et al.* [22] and Shao *et al.* [23] selected PBS buffer solution ($\text{Na}_2\text{HPO}_4\text{-NaH}_2\text{PO}_4\text{-NaCl}$, 200 mM, pH = 7.4) as the solvent and the absorbance of ABTS^{•+} assay measured at 734 nm. Gursoy *et al.* [24] reported that ABTS^{•+} free radical-scavenging assay was measured after ABTS^{•+} dilution with phosphate buffer (0.1M, pH 7.4). Luo *et al.* [10] diluted the ABTS^{•+} with 95% ethanol, and determined the absorbance at 734 nm. Siddhuraju [25] reported the ABTS^{•+} solution diluted in ethanol (1:89, v/v) and used an absorbance at 734 nm. However, our previous research revealed that the ABTS^{•+} solution diluted with ethanol had maximal absorption at 753 nm [26]. It is inaccurate to measure the absorbance at 734 nm in either ethanol or the other solvents.

Although Dawidowicz and Olszowy discussed the importance of solvent type in estimating antioxidant properties of phenolic compounds by ABTS⁺ assay [27], only three solvents (methanol, ethanol and propanol) were discussed in detail. The solvents frequently-used in ABTS⁺ assay, including PBS and phosphate buffer, were not reported and discussed to our knowledge. Secondly, the reaction time is an important factor causing errors in estimating the ABTS⁺ free radical-scavenging activity. ABTS⁺ can be quenched by both electron (fast) and hydrogen atom transfer (slow) like DPPH [28]. That is to say, the reaction time of different antioxidants with ABTS⁺ is not same. In the literature, 6 min of reaction time were employed universally, which could cause error in the ABTS⁺ radical-scavenging, especially for complex samples (e.g. crude extracts). Therefore, it is necessary to investigate the proper reaction time for the ABTS⁺ capacity determination of different antioxidants.

This paper deals with the effects of different solvents and different reaction times on ABTS⁺ assay. In this study, five pre-diluting solvents [methanol, ethanol, phosphate buffer (PB, Na₂HPO₄-NaH₂PO₄, 200 mM, pH = 7.4), PBS buffer, and distilled water] and different reaction times (0-30 min) were investigated in ABTS⁺ assays for five antioxidants.

Effects of the solvents: ABTS⁺ has a maximal absorption at 734 nm according to the literature [14, 22]. However, the maximal absorption wavelengths of ABTS⁺ in different solvents are not the same, which might be ascribed to a red or blue shift caused by solvent effects. Although Dawidowicz and Olszowy [27] have reported the methanol, ethanol, and propanol effects, other solvents are frequently used to pre-dilute ABTS⁺. In the present study, ABTS⁺ solution was diluted with PBS buffer, PB, H₂O, MeOH, and EtOH, respectively. The UV-Vis spectra of pre-diluting ABTS⁺ solutions were scanned in the range of 500-1000 nm. Figure 2 shows that the ABTS⁺ solutions diluted with PBS buffer, PB, and H₂O have the same maximal absorption at 734 nm, but MeOH pre-dilution of ABTS⁺ has a maximal absorption at 745 nm, and the EtOH pre-dilution, a maximal absorption at 753 nm. Therefore, it is unsuitable for the literature methods [10, 24] to measure ABTS⁺ capacity at the same wavelength (734 nm) without regard to the solvent effects. Additionally, the linearity coefficients between absorptions and concentrations were analyzed and are shown in Table 1. The results reveal that all the above pre-diluting ABTS⁺ have good linearity coefficients ($r^2 \geq 0.998$), indicating that all of the above solvents could be used for pre-diluting ABTS⁺. However, when using different pre-diluting solvents, the corresponding maximal absorption wavelengths for detection were varied.

Effects of reaction time: The same as with the DPPH free radical, ABTS⁺ could be quenched by both electron (fast) and hydrogen atom transfer (slow) [28, 29]. That is to say, the time of various antioxidants quenching ABTS⁺ is different. However, most existing methods used for ABTS⁺ assay are measured after 6 min

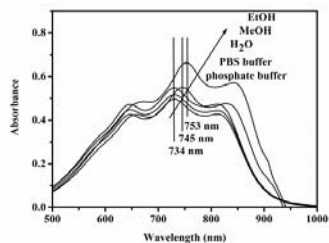


Figure 2: UV-Vis spectra (500-1000 nm) of ABTS⁺ solution diluted with different solvents.

Table 1: Linearity analysis of ABTS⁺ solutions at different concentrations (2.2-140 μ M).^a

Pre-diluting solvents	Linear equation (correlation coefficient)
PBS	$A = -0.00717 + 0.00748 C$ ($r^2 = 0.99999$)
PB	$A = -0.01641 + 0.00769 C$ ($r^2 = 0.99848$)
H ₂ O	$A = -0.00477 + 0.00781 C$ ($r^2 = 0.99987$)
MeOH	$A = -0.01316 + 0.00806 C$ ($r^2 = 0.99985$)
EtOH	$A = 0.00261 + 0.00936 C$ ($r^2 = 0.99962$)

^a Abbreviation: A , the absorbance of ABTS⁺ solution at different concentrations; C , the concentration of ABTS⁺ solution.

of reaction time, which provide little chemical information about the antioxidants. In the present study, the ABTS⁺ scavenging activity of five familiar antioxidants, gallic acid, ferulic acid, caffeic acid, phenol, and glutathione were determined under different reaction times, as shown in Figure 3A. The reaction rate (k_1) at different times is shown in Figure 3B. The results reveal that ABTS⁺ could be quenched very rapidly by phenol, but very slowly by glutathione. Gallic acid, ferulic acid, and caffeic acid also quench ABTS⁺ very rapidly, but it takes them a longer time to reach a steady state. The ABTS⁺ scavenging activity of glutathione is very weak, especially within a short reaction time, indicating that glutathione quenches ABTS⁺ according to hydrogen atom transfer. That is to say, the antioxidants like glutathione need longer time to accomplish the reaction. According to our experiments, the six minutes of reaction time used in the literature is too long for reaching a slow reaction state, and it is difficult for the majority of compounds to obtain a steady state within a limited time. It can be concluded from Figure 3 that ABTS assay could be measured within 2-10 min to obtain a rough result. To get more accurate and reliable results, a time-varying measurement is recommended.

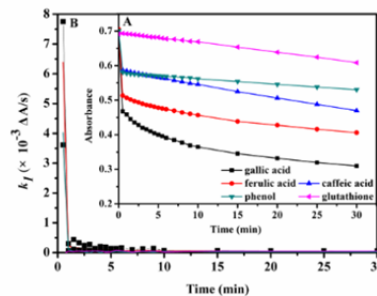


Figure 3: Absorbance (A) and reaction rate (k_1) (B) of ABTS⁺ solution mixed with antioxidants (5 μ M) at different time.

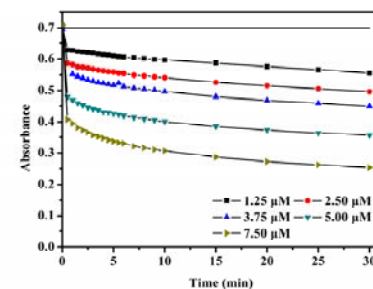


Figure 4: Absorbance of ABTS⁺⁺ solution mixed with gallic acid at different concentrations.

Effects of concentration of antioxidants: The reaction needs more time when the antioxidants have a high concentration, according to a previous report by Xie and Schaich [28]. In the present study, gallic acid was selected to determine the effects of the concentration of the antioxidant on the reaction time. The concentrations of gallic acid ranged from 1.25 μ M to 7.50 μ M. The results in Figure 4 show that the time of reaching a stationary state becomes longer with higher concentrations. The stationary state could not be reached within a stationary time for different concentrations of antioxidants.

Therefore, the absorbance of the ABTS^{•+} assay could not be measured at a stationary reaction time, and a time-varying measurement is encouraged to obtain accurate results.

Antioxidant assay: The ABTS^{•+} scavenging activity of five antioxidants, gallic acid, ferulic acid, caffeic acid, phenol, and glutathione were measured using five different solvents (PBS buffer solution, PB, H₂O, MeOH, and EtOH) to pre-dilute ABTS^{•+} radical solution, respectively. The absorbance was recorded at the corresponding maximum absorption wavelength. The results in Table 2 (IC₅₀ [APR] and I_{7.5}) reveal that phenolic acids and phenol exhibit similar ABTS^{•+} radical-scavenging capacity in the five solvents. Additionally, good linear relationships between inhibition and antioxidant concentrations of three phenolic acids and phenol could be obtained at an inhibition of about 50%. For a limited range of concentrations, a reliable linear relationship does exist between antioxidant concentration and percentage inhibition according to the literature [30, 31]. Carmona-Jiménez *et al.* [32] reported that the IC₅₀ can be obtained accurately when a reliable linear relationship exists. Therefore, the five different solvents might be alternative solvents for pre-diluting ABTS^{•+} radical solution in the ABTS^{•+} radical-scavenging assay.

Table 2: The compounds' properties and their ABTS^{•+} radical-scavenging capacity.

Compound	gallic acid	ferulic acid	caffeic acid	phenol	glutathione
#-OH ^a	3	1	2	1	0
E ₇ (V) ^b	0.55	0.60	0.54	0.90	0.24
IC ₅₀ (APR) of ABTS ^{•+} ^c	PBS 4.5 (0.22)	5.7 (0.18)	7.9 (0.13)	8.9 (0.11)	nd ^d
	PB 3.9 (0.26)	5.3 (0.19)	7.7 (0.13)	8.7 (0.12)	nd ^d
	H ₂ O 4.5 (0.22)	4.2 (0.24)	9.7 (0.10)	11.6 (0.09)	nd ^d
	MeOH 4.9 (0.20)	5.7 (0.17)	8.1 (0.12)	nd ^e	nd ^d
	EtOH 5.6 (0.18)	5.5 (0.39)	8.4 (0.12)	10.0 (0.10)	nd ^d
IC ₅₀ (APR) of DPPH ^d	- 9.5 (0.10)	84 (0.012)	21 (0.05)	nr ^f	nd ^d
I _{7.5} (%) ^e	PBS 78.5	64.1	49.6	42.3	14.6
	PB 86.3	67.1	49.3	42.9	11.6
	H ₂ O 76.5	73.6	40.6	32.0	2.4
	MeOH 75.6	60.1	47.4	36.5	1.9
	EtOH 69.4	65.3	44.9	38.0	1.1

^a Number of reactive -OH groups; ^b Redox potential at pH 7; ^c IC₅₀ of ABTS^{•+} is expressed as μM , APR=1/IC₅₀; ^d IC₅₀ of DPPH is obtained from the literature [28] and expressed as μM , APR=1/IC₅₀; ^e Inhibition of ABTS^{•+} at the concentration of 7.5 μM . ^f no reaction; ^g response too low to determine stoichiometry accurately.

It is interesting that phenol (monohydric phenol) exhibited moderate ABTS^{•+} radical-scavenging activity, but exhibited no DPPH radical-scavenging activity (Table 2). Ferulic acid has stronger APR than caffeic acid in the ABTS^{•+} assay, which might be caused by the higher redox potential of ferulic acid (E₇: ferulic acid > caffeic acid); this further supported the view that ABTS^{•+} can be quenched by both electron and hydrogen atom transfer. The above results imply that accurate ABTS^{•+} antioxidant capacity could not be obtained from a stationary time measurement because of the existence of diverse samples, especially for mixture samples and crude extracts of plants.

Recommendations for the use of ABTS^{•+} assay in the evaluation of total antioxidant activity: The ABTS^{•+} assay has been used extensively to compare and rank the antioxidant effectiveness of a wide range of natural extracts in thousands of studies. Nonetheless, results reported here raise serious questions about its validity for quantitating and comparing the activity of antioxidants with different sizes and structures, and especially for ranking their relative reactivity. Hence, some recommendations for the use of the ABTS^{•+} assay according to the results of the present study are listed as follow: (1) When using different pre-diluting solvents, the corresponding maximal absorption wavelengths for detection should be selected; (2) Although ABTS^{•+} antioxidant capacity could be measured within 2-10 min to obtain a rough result, to obtain more accurate and reliable results, a time-varying measurement is recommended, with calculation of reaction kinetics from early response.

Experimental

Reagents and instruments: 2,2'-Azino-bis(3-ethylbenzothiazoline-6-sulfonic acid) diammonium salt (ABTS) was obtained from J&K Scientific Ltd. (Beijing, China), gallic acid and ferulic acid from Sigma-Aldrich Co. LLC (Shanghai, China), and caffeic acid, phenol, and glutathione from Aladdin Chemistry Co. Ltd (Shanghai, China). The water (resistivity $\geq 18.25 \text{ M}\Omega\text{/cm}$) used was purified with a purity water system (Chengdu, China). A Shimadzu UV-Vis 2401 PC spectrophotometer was used for recording the UV-Vis spectra and absorbance in colorimetric methods.

Reagent preparation: ABTS (38.4 mg) was dissolved in 10 mL 2.5 mM potassium persulfate and the mixture was reacted in the dark at room temperature for 12-16 h to prepare ABTS^{•+} solution. This was diluted with methanol, ethanol, PB (Na₂HPO₄-NaH₂PO₄, 200 mM, pH = 7.4), PBS buffer (Na₂HPO₄-NaH₂PO₄-NaCl, 200 mM, pH = 7.4), and distilled water, respectively, to obtain an absorbance of 0.70 ± 0.02 for ABTS^{•+} colorimetric method.

Sample preparation: Stock solutions (2 mM) were prepared in methanol, and then diluted with methanol to obtain serial concentration solutions. In the present study, all antioxidant sample concentrations noted are final reaction concentrations.

Effects of the solvents: The ABTS^{•+} was diluted 50 times with methanol, ethanol, PB (Na₂HPO₄-NaH₂PO₄, 200 mM, pH = 7.4), PBS buffer (Na₂HPO₄-NaH₂PO₄-NaCl, 200 mM, pH = 7.4), and distilled water, respectively. The absorbance of the ABTS^{•+} solutions pre-diluted to different concentrations with the above solvents was measured in the wavelength range from 500 nm to 1000 nm.

Effects of reaction time: ABTS^{•+} was diluted with PBS buffer solution to obtain an absorbance in the range of 0.70 ± 0.02 . Ten μL of 2 mM antioxidant samples (5 μM , final concentration) and 90 μL distilled water were added to the tube, then 3.9 mL of diluting ABTS^{•+} solution was added and vibrated vigorously. The mixture was transferred to the cuvette, and the absorbance at 734 nm was measured rapidly. The absorbance was recorded successively every 30 s (0-6 min), 1 min (6-10 min), and 5 min (10-30 min), respectively. The initial absorbance was recorded by replacing the sample with methanol. The reaction rate (k_1) was obtained from the absorbance drop (ΔA_i) for every time unit (Δt) and calculated as follows: $k_1 = \Delta A_i / \Delta t (\Delta A/\text{s})$.

Effects of concentration of the antioxidants: Gallic acid solutions at different concentrations were selected to determine the effects of the concentration of the antioxidants on ABTS^{•+} assay. The absorbance was measured as above.

ABTS free radical-scavenging activity assays: One hundred μL of each sample in methanol at various concentrations (2.5, 5.0, 7.5, 10.0, and 15.0 μM , final concentration) was added to 3.9 mL of pre-diluting ABTS^{•+} (absorbance at 0.70 ± 0.02) and vibrated vigorously. Then the reaction mixture was incubated at room temperature for 2-10 min, and the absorbance was recorded at the corresponding maximum absorption wavelength (734 nm for PBS, PB solution, and H₂O, 745 nm for MeOH, and 753 nm for EtOH). The ABTS free radical-scavenging activity was expressed by inhibition (%), calculated as follows: $I\% = (A_{\text{blank}} - A_{\text{sample}})/A_{\text{blank}} \times 100$; where A_{sample} was the absorbance of ABTS solution mixed with sample and A_{blank} was the absorbance of ABTS solution mixed with solvent. The IC₅₀ value was defined as the effective concentration at which the DPPH radical was scavenged by 50% and the antiradical power (ARP) was calculated as follow: ARP = 1/IC₅₀.

Acknowledgments - This work was financially supported with a grant from the Natural Science Foundation of China (No.

81460648) and a grant from the Program for Changjiang Scholars and Innovative Research Team in University (IRT13095).

References

- [1] Cekic SD, Cetinkaya A, Avan AN, Apak R. (2013) Correlation of total antioxidant capacity with reactive oxygen species (ROS) consumption measured by oxidative conversion. *Journal of Agricultural and Food Chemistry*, **61**, 5260-5270.
- [2] Ozyurek M, Guclu K, Apak R. (2011) The main and modified CUPRAC methods of antioxidant measurement. *Trends in Analytical Chemistry*, **30**, 652-664.
- [3] Namiki M. (1990) Antioxidants/anti-mutagens in food. *Critical Reviews in Food Science and Nutrition*, **29**, 273-300.
- [4] Kartika H, Li QX, Wall MM, Nakamoto ST, Iwaoka WT. (2007) Major phenolic acids and total antioxidant activity in Mamaki leaves, *Pipturus albidus*. *Journal of Food Science*, **72**, 696-701.
- [5] Dong JW, Cai L, Xiong J, Chen XH, Wang WY, Shen N, Liu BL and Ding ZT. (2015) Improving the antioxidant and antibacterial activities of fermented *Bletilla striata* with *Fusarium avenaceum* and *Fusarium oxysporum*. *Process Biochemistry*, **50**, 8-13.
- [6] Dong JW, Cai L, Zhu XF, Huang X, Yin TP, Fang HX, Ding ZT. (2014) Antioxidant activities and phenolic compounds of cornhusk, corncob and stigma maydis. *Journal of the Brazilian Chemical Society*, **25**, 1956-1964.
- [7] Cretu E, Salminen J-P, Karonen M, Miron A, Charalambous C, Constantinou AI, Aprotosoaie AC. (2014) *In vitro* antioxidant activity and phenolic content of *Cedrus brevifolia* bark. *Natural Product Communications*, **9**, 481-482.
- [8] Hung PV, Maeda T, Miyatake K, Morita N. (2009) Total phenolic compounds and antioxidant capacity of wheat graded flours by polishing method. *Food Research International*, **42**, 185-190.
- [9] Sacchetti G, Di Mattia C, Pittia P, Martino G. (2008) Application of a radical scavenging activity test to measure the total antioxidant activity of poultry meat. *Meat Science*, **80**, 1081-1085.
- [10] Luo W, Zhao M, Yang B, Shen G, Rao G. (2009) Identification of bioactive compounds in *Phyllanthus emblica* L. fruit and their free radical scavenging activities. *Food Chemistry*, **114**, 499-504.
- [11] Wang X, Li X, Chen D. (2011) Evaluation of antioxidant activity of isoferulic acid *in vitro*. *Natural Product Communications*, **6**, 1285-1288.
- [12] Khanama UKS, Obab S, Yanaseh E, Murakamic Y. (2012) Phenolic acids, flavonoids and total antioxidant capacity of selected leafy vegetables. *Journal of Functional Foods*, **4**, 979-987.
- [13] Zan LF, Bao HY, Bau T, Li Y. (2015) A new antioxidant pyrano[4,3-c][2]benzopyran-1,6-dione derivative from the medicinal mushroom *Fomitiporia ellipsoidea*. *Natural Product Communications*, **10**, 315-316.
- [14] Re R, Pellegrini N, Proteggente A, Pannala A, Yang M, Rice-Evans C. (1999) Antioxidant activity applying an improved ABTS radical cation decolorization assay. *Free Radical Biology & Medicine*, **26**, 1231-1237.
- [15] Miller NJ, Rice-Evans CA, Davies MJ, Gopinathan V, Milner A. (1993) A novel method for measuring antioxidant capacity and its application to monitoring the antioxidant status in premature neonates. *Clinical Science*, **84**, 407-412.
- [16] Miller NJ, Rice-Evans CA. (1994) Total antioxidant status in plasma and body fluids. *Methods in Enzymology*, **234**, 279-293.
- [17] Liu YR, Li WG, Chen LF, Xiao BK, Yang JY, Yang L, Zhang CG, Rong-Qing Huang RQ, Dong JX. (2014) ABTS⁺ scavenging potency of selected flavonols from *Hypericum perforatum* L. by HPLC-ESI/MS QQQ: Reaction observation, adduct characterization and scavenging activity determination. *Food Research International*, **58**, 47-58.
- [18] Nakano S, Tanaka K, Oki R, Kawashima T. (1999) Flow-injection spectrophotometry of manganese by catalysis of the periodate oxidation of 2,2'-azinobis(3-ethylbenzothiazoline-6-sulfonic acid). *Talanta*, **49**, 1077-1082.
- [19] He L, Xu HG, Liu X, He WH, Yuan F, Hou ZQ, Gao YX. (2011) Identification of phenolic compounds from pomegranate (*Punica granatum* L.) seed residues and investigation into their antioxidant capacities by HPLC-ABTS⁺ assay. *Food Research International*, **44**, 1161-1167.
- [20] He L, Zhang XF, Xu HG, Xu C, Yuan F, Knez Z, Novakb Z, Gao YX. (2012) Subcritical water extraction of phenolic compounds from pomegranate (*Punica granatum* L.) seed residues and investigation into their antioxidant activities with HPLC-ABTS⁺ assay. *Food and Bioproducts Processing*, **90**, 215-223.
- [21] Kalili KM, De Smet S, van Hoeylandt T, Lynen F, de Villiers A. (2014) Comprehensive two-dimensional liquid chromatography coupled to the ABTS radical scavenging assay: a powerful method for the analysis of phenolic antioxidants. *Analytical and Bioanalytical Chemistry*, **406**, 4233-4242.
- [22] Bangoura ML, Nsor-Atindana J, Ming ZH. (2013) Solvent optimization extraction of antioxidants from foxtail millet species' insoluble fibers and their free radical scavenging properties. *Food Chemistry*, **141**, 736-744.
- [23] Shao Y, Wu Q-n, Duan J-a, Yue W, Gu W, Wang X. (2014) Optimisation of the solvent extraction of bioactive compounds from *Lophatherum gracile* Brongn. using response surface methodology and HPLC-PAD coupled with pre-column antioxidant assay. *Analytical Methods*, **6**, 170-177.
- [24] Gursoy N, Sarikurkcu C, Cengiz M, Solak MH. (2009) Antioxidant activities, metal contents, total phenolics and flavonoids of seven *Morchella* species. *Food and Chemical Toxicology*, **47**, 2381-2388.
- [25] Siddhuraju P. (2006) The antioxidant activity and free radical-scavenging capacity of phenolics of raw and dry heated moth bean (*Vigna aconitifolia*) (Jacq.) Marechal seed extracts. *Food Chemistry*, **99**, 149-157.
- [26] Dong JW, Zhao LX, Cai L, Fang HX, Chen XH, Ding ZT. (2014) Antioxidant activities and phenolics of fermented *Bletilla formosana* with eight plant pathogen fungi. *Journal of Bioscience and Bioengineering*, **118**, 396-399.
- [27] Dawidowicz AL, Olszowy M. (2013) The importance of solvent type in estimating antioxidant properties of phenolic compounds by ABTS assay. *European Food Research and Technology*, **236**, 1099-1105.
- [28] Xie J, Schaich KM. (2014) Re-evaluation of the 2,2-diphenyl-1-picrylhydrazyl free radical (DPPH) assay for antioxidant activity. *Journal of Agricultural and Food Chemistry*, **62**, 4251-4260.
- [29] Dawidowicz AL, Olszowy M. (2012) Mechanism change in estimating of antioxidant activity of phenolic compounds. *Talanta*, **97**, 312-317.
- [30] Buenger J, Ackermann H, Jentzsch A, Mehling A, Pfitzner I, Reiffen KA, Schroeder KR, Wollenweber U. (2006) An interlaboratory comparison of methods used to assess antioxidant potentials. *International Journal of Cosmetic Science*, **28**, 135-146.
- [31] Locatelli M, Gindro R, Travaglia F, Coisson JD, Rinaldi M, Arlorio M. (2009) Study of the DPPH[·]-scavenging activity: Development of a free software for the correct interpretation of data. *Food Chemistry*, **114**, 889-897.
- [32] Carmona-Jimenez Y, Garcia-Moreno MV, Igartuburu JM, Garcia Barroso C. (2014) Simplification of the DPPH assay for estimating the antioxidant activity of wine and wine by-products. *Food Chemistry*, **165**, 198-204.

Chemical Synthesis of the Echinopine Sesquiterpenoids

Xiao-Yu Liu and Yong Qin*

Key Laboratory of Drug Targeting and Drug Delivery Systems of the Ministry of Education, Department of Chemistry of Medicinal Natural Products, West China College of Pharmacy, Sichuan University
No. 17, Duan 3, Remin Nan Road, Chengdu 610041, P.R. China

yongqin@scu.edu.cn

Received: October 6th, 2015; Accepted: October 30th, 2015

As new members of the sesquiterpenoid family, echinopines A and B were found to possess an unprecedented [3/5/5/7] carbon framework, which has stimulated considerable interest among the chemistry community since their isolation. This review article documents chronologically the steps towards chemical synthesis of the echinopine sesquiterpenoids, showcasing different strategies by resorting to the toolkit of organic chemistry.

Keywords: Echinopine, Natural product, Sesquiterpenoid, Total synthesis.

1. Introduction

Throughout the long research history of natural products, the terpenoids constitute the largest family, with the most diversified structures created by Mother Nature. Notable features associated with their chemical structures and therapeutic applications have made them a permanently pursued theme among the synthetic chemists worldwide [1,2].

Echinopines A (**1**) and B (**2**) (Figure 1), two closely related sesquiterpenoids with remarkable architectural novelties, were isolated from the roots of *Echinops spinosus* by Shi, Kiyota, and co-workers in 2008 [3]. Based upon spectroscopic analyses, the structures of echinopines A (**1**) and B (**2**) were established as shown in Figure 1, which represents the first example of a unique [3/5/5/7] carbon framework. Biogenetically, the unprecedented skeleton of echinopine sesquiterpenoids was proposed to originate from a guaiane-type precursor **3** (Scheme 1) [3]. Key steps concerning their biosynthetic pathways involved a C11→C13 rearrangement followed by successive C15–C13 and C13–C4 bond formations.

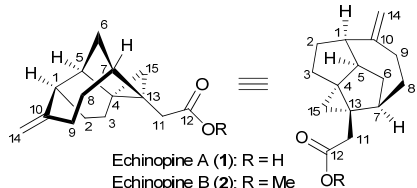
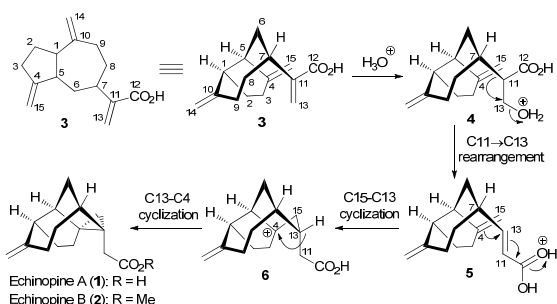


Figure 1: Structures of echinopines A (1) and B (2).



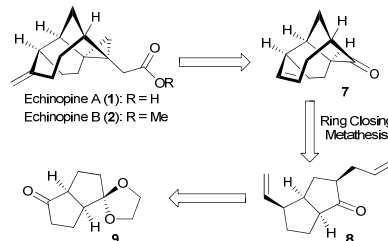
Scheme 1: Proposed biosynthesis of the echinopine sesquiterpenoids.

In spite of the lack of reported biological activities, echinopines attracted many synthetic interests immediately by their novel structures. Thus far, five successful total syntheses [4–8], together with two interesting formal syntheses [9,10], have been achieved. To the best of our knowledge, a logical summary concerning this topic is missing in the literature. This review aims to highlight these accomplishments described to date towards the fascinating echinopine sesquiterpenoids.

2. Chemical synthesis of echinopines

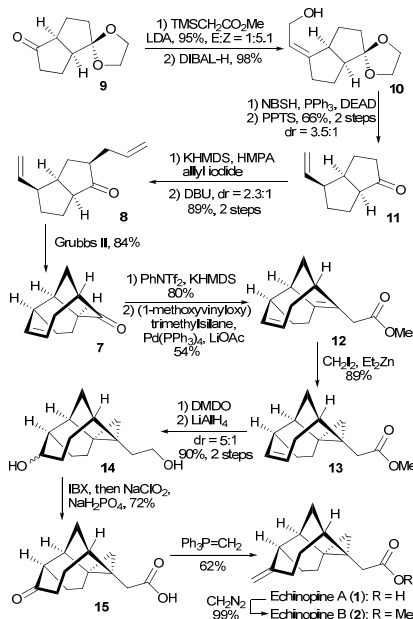
2.1 Magauer-Tiefenbacher's total synthesis of (+)-echinopines A and B

The first total synthesis of (+)-echinopines A and B was reported by Magauer, Mulzer, and Tiefenbacher in 2009 [4]. Their approach features an intermolecular cyclopropanation to form the cyclopropane, as well as a ring closing metathesis (RCM) to construct the seven-membered ring. As illustrated in Scheme 2, the precursor **8** could be synthesized from the known optically pure bicyclic intermediate **9**.



Scheme 2: Retrosynthetic analysis by Magauer *et al.*

The synthesis commenced with the preparation of bicycle **9** from 1,5-cyclooctadiene based on the literature method [11]. Subsequent Peterson olefination [12] and reduction of the ester afforded allylic alcohol **10** (Scheme 3). Transformation of **10** to the requisite terminal alkene was secured by a Myers' [3,3]-rearrangement protocol [13], which was followed by removal of acetal protection, resulting in the unmasked ketone as a separable diastereomeric mixture (3.5:1). The major and desired isomer **11** was subjected to allylation and epimerization to furnish the key intermediate **8**. Ring closing metathesis of the latter under the conditions of Grubbs II catalyst generated the [5/5/7]-tricyclic framework **7** (84%).

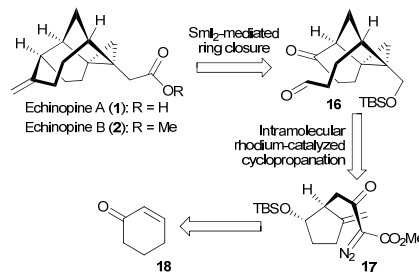


Scheme 3: The first total synthesis of (+)-echinopines A and B.

The remaining task was to introduce the side chain and cyclopropane unit. To this end, the authors developed two routes to the advanced intermediate **14**; the shorter one is shown in Scheme 3. Specifically, palladium-catalyzed coupling reaction of the corresponding vinyl triflate derived from **7** with (1-methoxyvinyloxy)trimethylsilane [14] provided ester **12**. Regioselective cyclopropanation [15,16], followed by epoxidation and LiAlH₄ reduction, delivered the tetracyclic diol **14**. After global oxidation, Wittig methylation of the resulting ketone ultimately led to the production of (+)-echinopine A (**1**), which could be converted to (+)-echinopine B (**2**) on exposure to diazomethane. The absolute configuration of echinopines was determined through the synthesis, together with a single crystal X-ray diffraction analysis of **1**. Thus, the first synthesis of enantiomerically pure echinopine sesquiterpenoids was achieved starting from the known bicyclic compound **9**. The highlight of this pioneering approach was embodied in forging of the seven-membered ring by RCM to access the bridged core structure.

2.2 Nicolaou-Chen's total synthesis of echinopines A and B

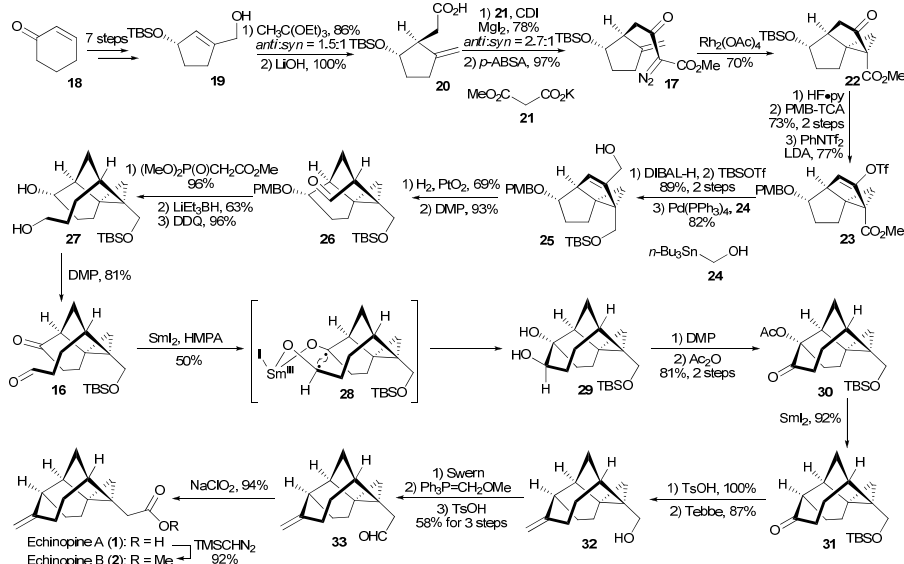
Shortly after the first total synthesis, Nicolaou, Chen and co-workers reported their endeavors on echinopine synthesis [5]. The retrosynthetic analysis is outlined in Scheme 4, which relied on an intramolecular cyclopropanation and a SmI₂-mediated [17] ring closure to establish the crucial cyclopropane and cycloheptane, respectively.



Scheme 4: Nicolaou-Chen's bond disconnection towards echinopines.

The functionalized cyclopentyl allylic alcohol **19** was prepared by a ring contraction process from the commercial cyclohexenone (**18**) at the beginning stage of the synthesis (Scheme 5). Compound **19** could be further transformed into the unsaturated carboxylic acid **20** through Jonson-Claisen rearrangement [18], followed by saponification. The latter was then subjected to homologation and subsequently reacted with *p*-ABSA to give the key intermediate **17**. As anticipated, the intramolecular cyclopropanation of diazo **17** took place smoothly with catalytic Rh₂(OAc)₄, affording the [3/5/5] tricyclic system (**22**) as a single isomer in 70% yield.

Further functional group manipulations of **22**, including Stille coupling of enol triflate with hydroxymethylstannane **24** and a stereocontrolled hydrogenation, furnished aldehyde **26**. Next, Horner-Wadsworth-Emmons reaction of the aldehyde followed by reduction of the resultant α,β -unsaturated ester and deprotection of PMB afforded diol **27**. After oxidation of diol to keto aldehyde **16**, the stage was set for the intramolecular pinacol coupling. Consequently, the core structure **29** was successfully established (as a single diastereoisomer) under the conditions of SmI₂-HMPA, through the proposed transition state **28**.

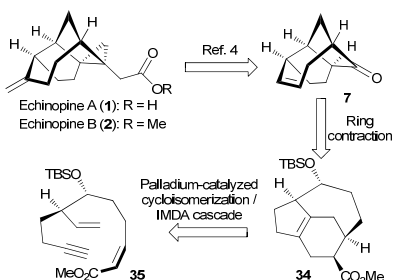


Scheme 5: Total synthesis of echinopines by Nicolaou, Chen and co-workers.

Having the tetracyclic framework **29** secured, the final stage of the synthesis was relatively easy. Oxidation of the secondary alcohol followed by removal of the tertiary acetate mediated by SmI_2 gave rise to ketone **31**. Prior to homologation of the side chain, an exocyclic olefin was installed through Tebbe olefination. A routine procedure was then applied to convert alcohol **32** to aldehyde **33** with homologation of one more carbon. Finally, echinopine A (**1**) was obtained after oxidation of the aldehyde to acid by using NaClO_2 , while echinopine B (**2**) was realized by further esterification. The synthesis was achieved in both forms employing enantiomeric or racemic intermediate **19** [5].

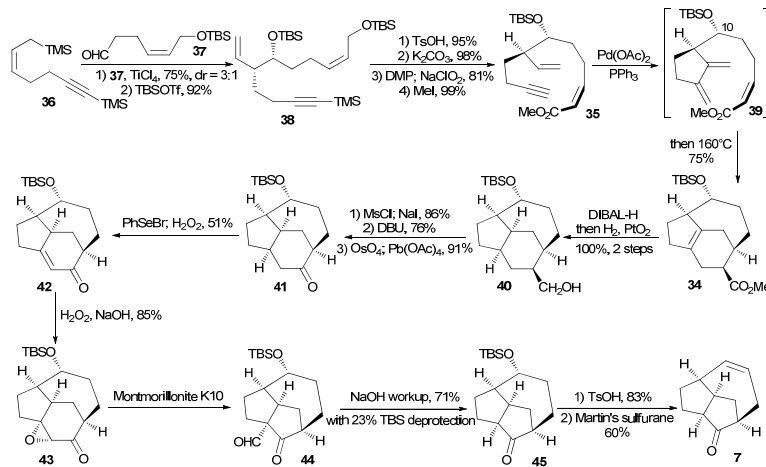
2.3 Chen's synthesis of echinopines A and B

Continuous studies by Chen and co-workers led to a conceptually different approach [9] to the intriguing sesquiterpenoids compared with the aforementioned synthesis. Inspired by the biosynthetic proposal [3], a [5/6/7] carbocyclic framework (i.e., the hypothetical intermediate **6**, Scheme 1) was associated with the planned chemical synthesis of echinopines A (**1**) and B (**2**). In this context, a ring contraction event could enable the central [5/6/7] core of the natural products. As shown in Scheme 6, the desired [5/6/7] tricyclic system **34** was envisioned to be constructed from the linear substrate **35** by a palladium-mediated cycloisomerization/intramolecular Diels-Alder cycloaddition sequence.



Scheme 6: Palladium-catalyzed cascade strategy from Chen group.

To access the acyclic precursor **35**, a crucial Hosomi-Sakurai reaction [19] was realized between allylsilane **36** and aldehyde **37** in the presence of TiCl_4 ; and the resulting alcohol ($\text{dr} = 3:1$) was silylated to afford **38** (Scheme 7). Subsequent functional group manipulations could smoothly give rise to the enyne **35**. Upon treatment of **35** with $\text{Pd}(\text{OAc})_2/\text{PPh}_3$ at 80°C , the diene enoate **39** was detected, which could be further converted into the tricycle **34**



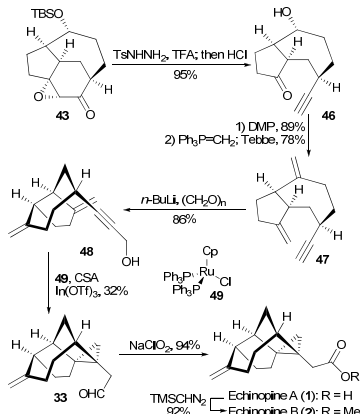
Scheme 7: Chen's formal synthesis of echinopines.

(75%) in one-pot with prolonged heating at 160°C by intramolecular Diels-Alder cycloaddition. A selective *endo*-cycloaddition was observed, while the configuration at C10 proved to be insignificant for the stereochemical outcome of the sequence.

Further elaboration commenced with a two-step reduction (DIBAL-H; H_2/PtO_2) of **34** with high efficiency. The hydroxymethyl group in compound **40** was converted to ketone **41** through the sequence of iodination, elimination, and oxidative cleavage. Preparation of an epoxy ketone would be the next task, which was envisaged to serve as the appropriate substrate for the corresponding ring contraction process. After introduction of enone *via* the well-established α -selenation/oxidative elimination sequence, **42** underwent epoxidation by treatment with $\text{H}_2\text{O}_2/\text{NaOH}$, furnishing epoxy ketone **43**. Based on the method of Sheldon [20], keto aldehyde **44** was obtained from **43** in the presence of montmorillonite K10, which after basic aqueous workup, resulted in deformylation to provide tricyclic ketone **45** (71%) together with the TBS deprotection product (23%). Finally, global desilylation (TsOH , 83%) followed by dehydration using Martin's sulfurane delivered the known intermediate **7** [4], constituting a formal synthesis of echinopines A (**1**) and B (**2**). In addition, an auxiliary-based aldol reaction strategy provided the same intermediate **38** in its optically active form, thus enabling an asymmetric version of this synthetic approach [9].

Alternatively, Chen's group developed a novel endgame towards echinopines starting from intermediate **43** [6], which for the first time showcased the $[5/7] \rightarrow [3/5/5/7]$ ring-forming sequence by a bio-inspired late-stage intramolecular cyclopropanation strategy (Scheme 8). With an improved synthesis of epoxy ketone **43**, an Eschenmoser fragmentation [21] was envisioned to realize the bond cleavage. As such, alkynyl ketone **46** was obtained *via* treatment with TsNNH_2 followed by acidic workup, setting the stage for $[5/7] \rightarrow [3/5/5/7]$ skeletal conversion. Prior to that, oxidation of the hydroxyl group followed by subsequent double methylation of the diketone afforded diene-yne **47**. The cycloisomerization precursor **48** was produced by a lithium chemistry to introduce the terminal hydroxymethyl group. After extensive investigations, the conditions reported by the group of Trost [$\text{CpRu}(\text{PPh}_3)_2\text{Cl}$, CSA, $\text{In}(\text{OTf})_3$] [22] was revealed to be successful to furnish the tetracycle **33** with a modest yield. Lastly, echinopines A (**1**) and B (**2**) could be formed through the same procedures as described before.

Central to Chen's novel approach towards echinopines was the use of two transition-metal-catalyzed enyne cycloisomerizations. Especially the ruthenium-mediated intramolecular cyclopropanation was successfully demonstrated in a complex molecular system, which resembled the late-stage bond formations in the proposed biosynthetic pathway for the echinopine framework.



Scheme 8: Synthesis of echinopines by a bio-inspired strategy.

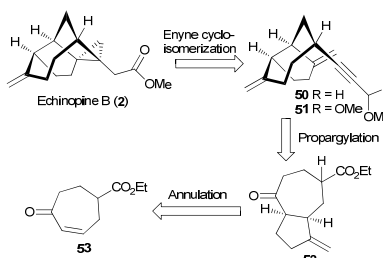
2.4 Vanderwal's synthesis of echinopine B

Another synthesis of echinopine B (**2**), employing a bio-inspired conversion of a *cis*-guaiane precursor bearing a [3/5]-bicycle into the [3/5/5/7] skeleton, was achieved by the team of Vanderwal in 2012 [7]. While the core of echinopines was established through an enyne cycloisomerization [23] from **50/51**, the bicyclic **52** was accessible by an annulation of cycloheptenone **53** (Scheme 9).

Starting from ketone **54**, a standard ring expansion process was carried out to generate the δ -substituted cycloheptenone **53** with a 46% overall yield (Scheme 10). Since the one-step annulation by Piers protocol [24] was unsuccessful, the group adopted a stepwise procedure, beginning with installation of a vinyl chain through conjugate addition of cuprate **55** ($\text{dr} = 6.5:1$). The relative stereochemical outcome between the two centers could not be fully determined by NMR spectroscopy at this stage. The synthesis was continued by transforming the silyl ether into tosylate ester **56** before the annulation took place. Under the condition of LDA, the *cis*-fused bicyclo[5.3.0]decane **52** was prepared in 25–40% yield, along with a near 30% recovery of the starting material. After Wittig olefination of compound **52**, the resultant ester was subjected to DIBAL-H reduction, followed by treatment with Ohira-Bestmann reagent [25], leading to the diene-ynе **58** as a mixture of diastereomers (4.5:1). A control experiment indicated epimerization occurred under the Ohira-Bestmann conditions.

With bicyclic **58** in hand, the terminal alkyne was then functionalized to propargylic ether **50** upon exposure to *n*-BuLi/MOMCl. The key cycloisomerization was realized in the

presence of PtCl_2 [26], delivering the tetracyclic core of echinopine in 56% yield. On the basis of the successful cyclopropanation, it could be concluded that the conjugate addition (**53**→**56**) might give the undesired stereoisomer predominantly, which was corrected during the alkynylation to enable the desired cycloisomerization. Since the two-carbon chain was attached to the core as an enol ether, a direct oxidation using PCC formed the methyl carboxylate [27],



Scheme 9: Retrosynthetic analysis of echinopine B by Vanderwal *et al.*

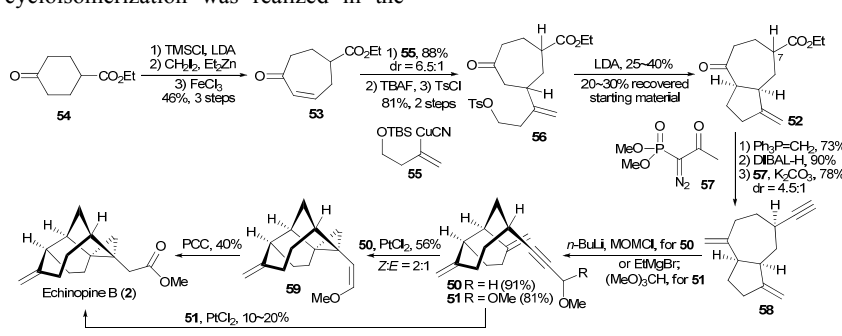
providing racemic echinopine B. Alternatively, a propargylacetal **51** was introduced from **58**, and its cycloisomerization could straightforwardly afford echinopine B, although with less efficiency (10~20% yield).

By use of the enyne cycloisomerization, together with a facile synthesis of [5/7]-bicyclic system **52**, Vanderwal's accomplishments provided a very concise solution to the synthetic issue of echinopines.

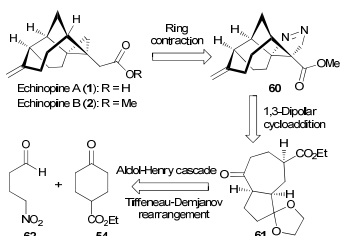
2.5 Liang's synthesis of echinopines

Liang and co-workers described a new synthesis of echinopines in 2013 [8], taking advantage of an intramolecular 1,3-dipolar cycloaddition and ring contraction sequence for the core construction. From a retrosynthetic viewpoint, the *cis*-fused bicyclo[5.3.0]decane system (**61**) could be formed through a tandem aldol-Henry reaction, followed by a Tiffeneau-Demjanov rearrangement (Scheme 11) [28].

In the forward synthesis, an aldol-Henry cascade between 4-nitrobutanal **62** and ketone **54** was employed as the launch point, with subsequent oxidation of the resulting secondary alcohol, giving access to *trans*-decaline **63a** and **63b** as a pair of isomers (Scheme 12). The undesired **63a** could be epimerized to **63b** upon treatment with Et_3N , which offered a scalable and efficient preparation of **63b** from the commercially available **54**. After ketone protection and nitro reduction, subjecting amine **64** to the Tiffeneau-Demjanov rearrangement conditions [29] delivered *cis*-fused [5/7]-bicycle **61** (77%) through the diazo intermediate **65**. The short sequence for supplying the bicyclo[5.3.0]decane system set the stage for the following chemistry.

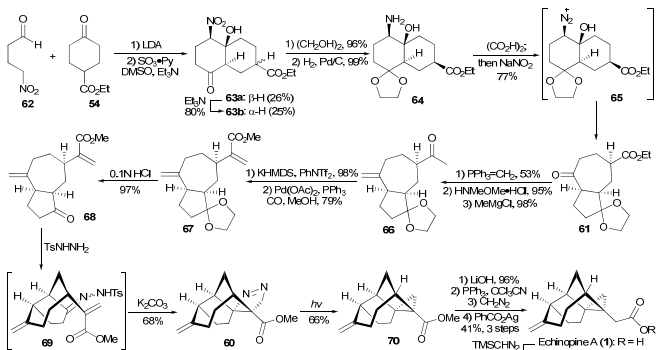


Scheme 10: A concise synthesis of echinopine B *via* a cycloisomerization strategy.



Scheme 11: Liang's bond disconnection towards echinopines.

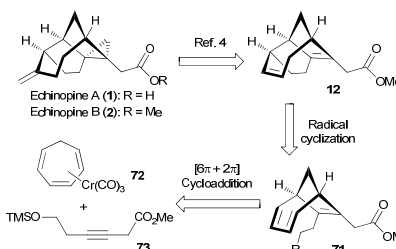
Several conventional transformations were involved before the designed 1,3-dipolar cycloaddition took place. Specifically, Wittig methylation of **61** followed by a Weinreb ketone synthesis [30] furnished the olefinic ketone **66**. The latter was converted into unsaturated ester **67** efficiently *via* a palladium-catalyzed carbonylation of the vinyl triflate. After cleavage of the dioxolane, tosylhydrazone **69** was formed and ready for the 1,3-dipolar cycloaddition. Gratifyingly, upon exposure to K_2CO_3 , **69** underwent the cycloaddition smoothly to give the advanced intermediate **60** [31]. The anticipated ring contraction was realized by a light-induced decomposition of pyrazoline to cyclopropane [32], leading to the echinopine framework **70** in 66% yield. After hydrolysis of the ester to carboxylic acid in **70**, the synthesis of echinopine A (**1**) was completed through an Arndt-Eistert homologation process [33], while echinopine B (**2**) was obtained by further methylation.

Scheme 12: Total synthesis of echinopines by Liang *et al.*

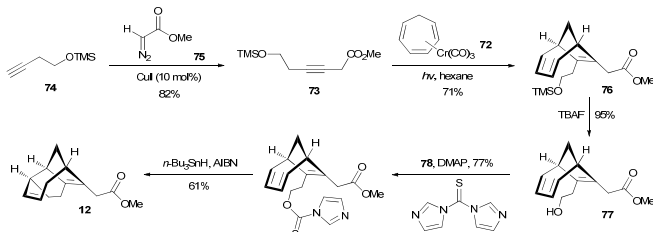
The Liang group demonstrated a new entry to the *cis*-fused bicyclo[5.3.0]decane system from an aldol-Henry cascade reaction followed by a Tiffeneau-Demjanov rearrangement. This critical building block was ultimately elaborated to echinopines by a 1,3-dipolar cycloaddition with subsequent light-induced ring contraction. The crucial 1,3-dipolar cycloaddition between diazo alkane and alkene functionalities established the structural complexity rapidly, representing its second application in natural product synthesis [34].

2.6 Misra's formal synthesis of echinopines

For a given molecule, there can be various ways for bond disconnection. In the case of echinopines, aside from the aforementioned synthesis, Misra *et al* disclosed a distinct strategy very recently [10]. The target sesquiterpenoids could be accessed from intermediate **12** according to Magauer *et al* [4], in which the five-membered ring could be forged by a radical cyclization of compound **71** (Scheme 13). The crucial bicyclo[4.2.1]nonane core could in turn be assembled via a $[6\pi + 2\pi]$ cycloaddition of cycloheptatriene tricarbonyl chromium complex **72** and alkyne **73** [35].



Scheme 13: Retrosynthetic analysis of echinopines by Misra and co-workers.



Scheme 14: Formal synthesis of echinopines by Misra and co-workers.

After a successful model study showing the feasibility of the $[6\pi + 2\pi]$ cycloaddition/radical cyclization sequence, the authors initiated their efforts towards echinopines A and B. As depicted in Scheme 14, the substituted alkynoate **73** was easily prepared on a multigram scale from alkyne **74** and diazoester **75**, by harnessing Fu's C–H insertion method in the presence of catalytic CuI [36]. Under photolytic conditions, the key $[6\pi + 2\pi]$ cycloaddition between **72** and **73** proceeded with excellent stereo- and regioselectivity, leading to the bicyclic intermediate **76** in 71% yield. Next, desilylation followed by treatment with 1,1'-(thiocarbonyl)diimidazole (**78**) afforded thioxoester **79** smoothly. Thus, the stage was set for the radical cyclization. After screening of the conditions, it was found that slow addition of the *n*-Bu₃SnH/AIBN mixture to the refluxing solution of **79** ultimately gave the desired product **12** in 61% yield. Synthesis of the known tricyclic intermediate **12**, which was previously prepared by Magauer and co-workers, represents a new formal synthesis of the echinopine sesquiterpenoids.

As mentioned above, Misra *et al.* have accomplished the formal synthesis of echinopines A and B in an extremely concise manner, by reaching the known intermediate **12** in only five steps. Remarkably, the utility of a photo-induced $[6\pi + 2\pi]$ cycloaddition to construct the bicyclo[4.2.1]nonane system was of great significance to this synthesis.

3 Conclusions

The echinopine sesquiterpenoids have attracted the attention of synthetic laboratories worldwide, being reflected in the chemical synthesis published almost each year since the report of their isolation. The major achievements have been highlighted in this review, which illustrate the evolution of creative strategies and applications of modern chemical methodologies. We hope the endeavors in this field will not only serve to enrich our education in synthesis design and execution, but also as the launching point for a better understanding of the biological activities and medicinal profiles of these intriguing compounds.

Acknowledgments - We gratefully acknowledge financial support from the National Natural Science Foundation of China (21321061, 21132006, 21572139, and 21502126).

References

- [1] Maimone TJ, Baran PS. (2007) Modern synthetic efforts toward biologically active terpenes. *Nature Chemical Biology*, **3**, 396–407.
- [2] Jansen DJ, Shenvi RA. (2014) Synthesis of medicinally relevant terpenes: reducing the cost and time of drug discovery. *Future Medicinal Chemistry*, **6**, 1127–1148.
- [3] Dong M, Cong B, Yu SH, Sauriol F, Huo CH, Shi QW, Gu YC, Zamir LO, Kiyota H. (2008) Echinopines A and B: sesquiterpenoids possessing an unprecedented skeleton from *Echinops spinosus*. *Organic Letters*, **10**, 701–704.
- [4] Magauer T, Mulzer J, Tiefenbacher K. (2009) Total syntheses of (+)-echinopine A and B: determination of absolute stereochemistry. *Organic Letters*, **11**, 5306–5309.
- [5] Nicolaou KC, Ding H, Richard JA, Chen DYK. (2010) Total synthesis of echinopines A and B. *Journal of the American Chemical Society*, **132**, 3815–3818.
- [6] Peixoto PA, Richard JA, Severin R, Chen DYK. (2011) Total synthesis of echinopines A and B: exploiting a bioinspired late-stage intramolecular cyclopropanation. *Organic Letters*, **13**, 5724–5727.
- [7] Michels TD, Dowling MS, Vanderwal CD. (2012) A synthesis of echinopine B. *Angewandte Chemie International Edition*, **51**, 7572–7576.
- [8] Xu W, Wu S, Zhou L, Liang G. (2013) Total syntheses of echinopines. *Organic Letters*, **15**, 1978–1981.
- [9] Peixoto PA, Richard JA, Severin R, Tseng CC, Chen DYK. (2011) Formal asymmetric synthesis of echinopine A and B. *Angewandte Chemie International Edition*, **50**, 3013–3016.
- [10] De S, Misra S, Rigby JH. (2015) Formal total synthesis of echinopines A and B via Cr(0)-promoted [6π + 2π] cycloaddition. *Organic Letters*, **17**, 3230–3232.
- [11] Zhong YW, Lei XS, Lin GQ. (2002) Amino alcohols with the bicyclo[3.3.0]octane scaffold as ligands for the catalytic enantioselective addition of diethylzinc to aldehydes. *Tetrahedron: Asymmetry*, **13**, 2251–2255.
- [12] Peterson DJ. (1968) Carbonyl olefination reaction using silyl-substituted organometallic compounds. *The Journal of Organic Chemistry*, **33**, 780–784.
- [13] Myers AG, Zheng B. (1996) An efficient method for the reductive transposition of allylic alcohols. *Tetrahedron Letters*, **37**, 4841–4844.
- [14] Carfagna C, Musco A, Sallesse G, Santi R, Fiorani T. (1991) Palladium-catalyzed coupling reactions of aryl triflates or halides with ketene trimethylsilyl acetals. A new route to alkyl 2-arylalkanoates. *The Journal of Organic Chemistry*, **56**, 261–263.
- [15] Tang P, Qin Y. (2012) Recent applications of cyclopropane-based strategies to natural product. *Synthesis*, **44**, 2969–2984.
- [16] Chen DYK, Pouwer RH, Richard JA. (2012) Recent advances in the total synthesis of cyclopropane-containing natural products. *Chemical Society Reviews*, **41**, 4631–4642.
- [17] Nicolaou KC, Ellery SP, Chen JS. (2009) Samarium diiodide mediated reactions in total synthesis. *Angewandte Chemie International Edition*, **48**, 7140–7165.
- [18] Johnson WS, Werthemann L, Bartlett WR, Brocksom TJ, Li TT, Faulkner DJ, Petersen MR. (1970) Simple stereoselective version of the Claisen rearrangement leading to trans-trisubstituted olefinic bonds. Synthesis of squalene. *Journal of the American Chemical Society*, **92**, 741–743.
- [19] Hosomi A, Endo M, Sakurai H. (1976) Allylsilanes as synthetic intermediates. II. Syntheses of homoallyl ethers from allylsilanes and acetals promoted by titanium tetrachloride. *Chemistry Letters*, **5**, 941–942.
- [20] Elings J, Lempers H, Sheldon R. (2000) Solid-acid catalyzed rearrangement of cyclic α,β-epoxy ketones. *European Journal of Organic Chemistry*, 1905–1911.
- [21] Eschenmoser A, Felix D, Ohloff G. (1967) Eine neuartige fragmentierung cyclischer α,β-ungesättigter carbonyl-systeme; synthese von exalton und rac-Muscon aus cyclododecanon vorläufige mitteilung. *Helvetica Chimica Acta*, **50**, 708–713.
- [22] Trost BM, Breder A, O'Keefe BM, Rao M, Franz AW. (2011) Propargyl alcohols as β-oxocarbonoid precursors for the ruthenium-catalyzed cyclopropanation of unactivated olefins by Redox isomerization. *Journal of the American Chemical Society*, **133**, 4766–4769.
- [23] Watsonand IDG, Toste FD. (2012) Catalytic enantioselective carbon-carbon bond formation using cycloisomerization reactions. *Chemical Science*, **3**, 2899–2919.
- [24] Piers E, Karunaratna V. (1989) Organotin-based bifunctional reagents: 4-chloro-2-lithio-1-botene and related substances: Methylenecyclopentane annotations. Total synthesis of (±)- $\delta^{9(12)}$ -capnellene. *Tetrahedron*, **45**, 1089–1104.
- [25] Müller S, Liepold B, Roth GJ, Bestmann HJ. (1996) An improved one-pot procedure for the synthesis of alkynes from aldehydes. *Synlett*, 521–522.
- [26] Ye L, Chen Q, Zhang J, Michelet V. (2009) PtCl₂-catalyzed cycloisomerization of 1,6-enynes for the synthesis of substituted bicyclo[3.1.0]hexanes. *The Journal of Organic Chemistry*, **74**, 9550–9553.
- [27] Piancatelli G, Scettriand A, D'Auria M. (1977) Pyridinium chlorochromate in the organic synthesis: a convenient oxidation of enol-ethers to esters and lactones. *Tetrahedron Letters*, **18**, 3483–3484.
- [28] Weller T, Seebach D, Davis RE, Laird BB. (1981) 3-Hydroxy-4-nitro-cyclohexanone aus ketonen und 4-nitrobuttersäurechlorid. eine ringerweiternde fünfringanelierung. *Helvetica Chimica Acta*, **64**, 736–760.
- [29] Fattori D, Henry S, Vogel P. (1993) The Demjanov and Tiffeneau-Demjanov one-carbon ring enlargements of 2-aminomethyl-7-oxabicyclo[2.2.1]heptane derivatives. The stereo- and regioselective additions of 8-oxabicyclo[3.2.1]oct-6-en-2-one to soft electrophiles. *Tetrahedron*, **49**, 1649–1664.
- [30] Nahmand S, Weinreb SM. (1981) N-methoxy-n-methylamides as effective acylating agents. *Tetrahedron Letters*, **22**, 3815–3818.
- [31] Taber DF, Guo P. (2008) Convenient access to bicyclic and tricyclic diazenes. *The Journal of Organic Chemistry*, **73**, 9479–9481.
- [32] Van Aukenand TL, Rinehart Jr. KL. (1962) Stereochemistry of the formation and decomposition of 1-pyrazolines. *Journal of the American Chemical Society*, **84**, 3736–3743.
- [33] Kirmse W. (2002) 100 Years of the Wolff rearrangement. *European Journal of Organic Chemistry*, 2193–2256.
- [34] Schultz AG, Puig S. (1985) The intramolecular diene-carbene cycloaddition equivalence and an enantioselective Birch reduction-alkylation by the chiral auxiliary approach. Total synthesis of (±)- and (−)-longifolene. *The Journal of Organic Chemistry*, **50**, 915–916.
- [35] Rigby JH, Henshilwood JA. (1991) Transition metal template controlled cycloaddition reactions. An efficient chromium(0)-mediated [6π + 2π] cycloaddition. *Journal of the American Chemical Society*, **113**, 5122–5123.
- [36] Suarez A, Fu GC. (2004) A straightforward and mild synthesis of functionalized 3-alkenoates. *Angewandte Chemie International Edition*, **43**, 3580–3582.

Synergistic Effects of Dietary Natural Products as Anti-Prostate Cancer Agents

Bao Vue, Sheng Zhang and Qiao-Hong Chen*

Department of Chemistry, California State University, Fresno, 2555 E. San Ramon Ave., M/S SB70, Fresno, California 93740, USA

qchen@csufresno.edu

Received: August 14th, 2015; Accepted: October 15th, 2015

This review is to describe synergistic effects of various combinations of dietary natural products including curcumin, quercetin, soybean isoflavones, silibinin, and EGCG that have potential for the treatment of prostate cancer. These data can provide valuable insights into the future rational design and development of synergistic and/or hybrid agents for potential treatment of prostate cancer.

Keywords: Dietary natural product, Synergy, Combination therapy, Prostate cancer.

1. Introduction

Dietary habit has been identified as one of the risk factors for prostate cancer as evidenced by several epidemiological studies. For example, Asian traditional food has been demonstrated to be correlated with the low incidence of prostate cancer in Asian men in contrast to soaring risk of prostate cancer in the Asian immigrants who live in the United States [1]. A variety of dietary agents (e.g. curcumin, quercetin, and silibinin) with diverse chemical structures (Figure 1) have been verified by *in vitro* cell-based and *in vivo* animal studies to possess the potential for preventing and treating prostate cancer [2-3]. The safety profiles enable these dietary natural products to be qualified as drug candidates. However, their moderate potency and poor bioavailability impede them in becoming effective chemotherapeutics when taken alone [4-5]. Combination therapy might be an important strategy to overcome this problem in order to achieve enhanced overall clinical efficacy with acceptable clinical toxicity. Indeed, synergistic inhibition of growth, proliferation, and apoptosis of prostate cancer cells has been evident when using combinations of one dietary natural product with another natural product or with well-established chemotherapeutics. This review summarizes the synergistic effects of dietary anti-prostate cancer agents including curcumin, quercetin, soybean isoflavones, silibinin, and (-)-epigallocatechin-3-gallate (EGCG, Figure 1). These data can provide valuable insights into future rational design and development of synergistic and/or hybrid agents for potential treatment of prostate cancer.

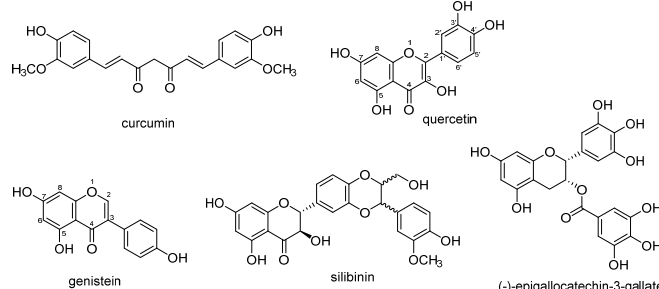


Figure 1: Structures of curcumin, quercetin, genistein, silibinin, and EGCG.

2. Synergistic effects of curcumin as anti-prostate cancer agents

Curcumin (Figure 1), derived from *Curcuma longa* (turmeric) that has long been used for food flavoring and Ayurvedic medicine, represents a dietary natural product possessing potential in preventing and treating prostate cancer [2]. As summarized below, several studies have established the synergistic effects of curcumin in combination with either other natural products or clinical used chemotherapeutics as anti-prostate cancer agents.

2.1 Synergistic effects of curcumin with isoflavones: Genistein (4',5,7-trihydroxyisoflavone, Figure 1) and daidzein (4',7-dihydroxyisoflavone, Figure 2) are two chief isoflavones that were exclusively obtained from soybeans. When they were used for the respective single agent treatment, soybean milk, genistein, and daidzein were capable of inhibiting prostate cancer cell growth *in vitro* and tumor xenograft growth *in vivo* [6].

Combined ingestion of soy isoflavones and curcumin has been unveiled by Ide and co-workers to substantially downregulate serum prostate-specific antigen levels for men who received biopsies in one clinical study [7]. Further investigation by the same research group indicated that the combination treatment of isoflavones and curcumin led to additive suppression of cell proliferation through activation of DNA damage response in LNCaP prostate cancer cells [8]. The synergism was also observed recently between curcumin and genistein in growth suppression of androgen-insensitive human prostate cancer cells [9]. Additionally, combined administration of curcumin and genistein exhibited more noticeable of the capability to inhibit cell proliferation and to induce apoptosis in androgen-insensitive PC-3 human prostate cancer cells than the respective single-agent treatment [10].

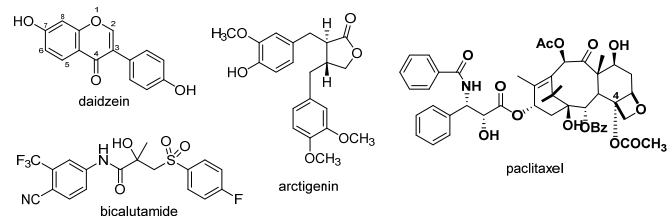


Figure 2: Structures of daidzein, bicalutamide, arctigenin, and paclitaxel.

2.2 Synergistic effects of curcumin with EGCG: EGCG stands for (-)-epigallocatechin-3-gallate (Figure 1) and is the most abundant flavan-3-ol in green tea. EGCG has been shown by various *in vitro* and animal studies to possess potential for preventing and treating prostate cancer [11]. The combination of 5-10 μ M curcumin and 40 μ M EGCG has been revealed by one study to improve synergistically the *in vitro* antiproliferative effects by 40% in androgen-sensitive LNCaP prostate cancer cells as compared with their individual treatments [12]. The synergism between curcumin and EGCG was linked to enhanced cell apoptosis induction and cell cycle perturbation through upregulation of multiple critical carcinogenesis-involved signaling pathways (e.g. PI3k/Akt and nuclear factor kappa B).

2.3 Synergistic effects of curcumin with arctigenin: Arctigenin (Figure 2) is a plant lignan derived mainly from *Arctium lappa* of the Asteraceae family that is commonly used in traditional Chinese medicine for the treatment of inflammation-associated diseases. The *in vitro* antiproliferative property of arctigenin has been evidenced in several cancer cell lines [12]. The cell proliferation inhibition and cell apoptosis induction of the combination treatment of curcumin and arctigenin towards androgen-sensitive LNCaP human prostate cancer cells was appreciably enhanced as compared with their individual treatment [12]. Additionally, the effect of curcumin and arctigenin in combination and alone on several vital signaling pathways relevant to cell proliferation and apoptosis has been examined. The data showed that combination treatment was capable of enhancing the ratio of Bax (pro-apoptotic protein) to Bcl-2 (anti-apoptotic protein), increasing the phosphorylation suppression of nuclear factor kappa B, and reducing the level of p-I κ B.

2.4 Synergistic effects of curcumin with TRAIL: TRAIL, also designated as Apo2L, is a cytokine member of the tumor necrosis factor family and plays as an extracellular signal that activates apoptosis in a variety of cancer cell lines, but exhibits little toxicity to normal cells [13]. In combination with its *in vivo* antitumor efficacy towards human tumor xenografts in nude mice, TRAIL is regarded as an appealing cytokine for the treatment of advanced cancers, such as advanced, metastatic prostate cancer [14]. However, TRAIL alone is not efficient enough for the treatment due to its drug resistance and moderate potency. The combination of TRAIL and dietary natural products with safety profiles might provide an alternative to chemotoxic agents to treat prostate cancer.

Curcumin has been shown in both *in vitro* and *in vivo* studies to sensitize both androgen-sensitive (LNCaP) and androgen-insensitive (PC-3) human prostate cancer cells to TRAIL-induced apoptosis [15-16]. This sensitization was demonstrated by a follow-up study to be associated with downregulation of Akt-regulated nuclear factor- κ B (NF- κ B) and NF- κ B dependent anti-apoptotic proteins, including Bcl-2, Bcl-xL, and XIAP [17]. The in-depth *in vivo* animal experiment verified that curcumin and TRAIL combination appreciably reduced the growth of PC-3 prostate tumor xenografts in Balb/c nude mice by reducing the tumor growth rate to 139% and 147% for TRAIL-treated and curcumin-treated group, respectively, to 59% for the combined treatment group [16].

2.5 Synergistic effects of curcumin with adenoviral mutants: Adenoviruses have been identified as oncolytic virotherapeutic agents that can selectively replicate in and destroy cancer cells, but causing no harm to normal cells. Numerous viral mutants have been established as potential anti-prostate cancer agents, featuring clinical safety profiles. However, the clinical efficacy when administered alone needs to be improved due to its moderate potency. Combination administration of curcumin and tumor

selective adenoviral mutant (Ad5) can amplify the cytotoxicity three to eight times towards both virus-sensitive 22Rv1 and virus-insensitive PC-3 human prostate cancer lines. This suggests that curcumin and Ad5 served as a potential combination of chemotherapy and oncolytic virotherapy [18].

2.6 Synergistic effects of curcumin with bicalutamide: Treatment of androgen-sensitive LNCaP prostate cancer cells with bicalutamide (Figure 2), a nonsteroidal androgen receptor antagonist, at 10 μ M for 24 hours resulted in notable suppression of cell proliferation. Significant antiproliferative effects of bicalutamide towards androgen-insensitive human prostate cancer cell lines (PC-3 and DU145) can only be observed at higher concentration and prolonged exposure time (30 μ M, 72 hours). Intriguingly, a profound synergy has been observed between curcumin at low doses (10-20 μ M) and bicalutamide in both androgen-sensitive and androgen-insensitive prostate cancer cell lines [19]. The potential underlying mechanism was correlated with phosphorylation escalation of extracellular signal-regulated kinase 1/2 (ERK1/2) and stress-activated protein kinase (SAPK)/Jun amino-terminal kinase (JNK).

2.7 Synergistic effects of curcumin with paclitaxel: Curcumin has been demonstrated *in vitro* to considerably potentiate the cytotoxicity of paclitaxel (Figure 2), a naturally occurring microtubule stabilizer and well-known clinically used anticancer drug, towards two androgen-insensitive DU145 and PC-3 human prostate cancer cell lines [20]. Intriguingly, this synergy can be affected by the treatment schedule. Sequential treatment with curcumin followed by paclitaxel yielded more significant synergism than concurrent treatment with curcumin/paclitaxel and sequential treatment with paclitaxel followed by curcumin [21]. The synergism between curcumin and paclitaxel in PC-3 prostate cancer cells was evidenced to be correlated with upregulation of p21WAF1/CIP1 expression and downregulation of paclitaxel-induced nuclear factor kappa B.

2.8 Synergistic effects of curcumin with radiotherapy: The limitation of radiotherapy, a frequent therapy for prostate cancer, is radio resistance. Radiotherapy failure has been more often observed in the prostate cancer patients with abnormal p53. Sensitization of curcumin on radiotherapy has been examined in one study [22]. It was concluded that the combination of curcumin and radiation can synergistically reduce cell viability and proliferation relative to either curcumin or radiation alone in both wild type p53-containing LNCaP and mutant p53-containing PC-3 human prostate cancer cell lines. Additionally, a synergistic effect independent of p53 status was also observed between curcumin and radiation towards clonogenic cell death in both LNCaP and PC-3 human prostate cancer cell lines.

3. Synergistic effects of quercetin as anti-prostate cancer agents

Quercetin, 3,3',4',5,7-pentahydroxyflavone (Figure 1), is an ubiquitous flavonol widely occurring in a variety of edible vegetables and fruits. Several *in vitro* cell based evaluations indicate that quercetin processes cytotoxic and antiproliferative effects against a panel of prostate cancer cell lines, but not obvious toxicity towards normal prostate epithelial cells [3a]. The *in vivo* anti-prostate tumor efficacy of quercetin has also been attested to by several animal experiments [23]. Combination treatment of quercetin with either other natural products or well-known chemotherapeutics was believed to be one good strategy to overcome its moderate potency and poor bioavailability.

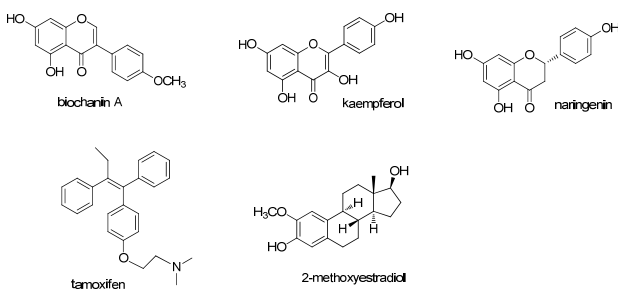


Figure 3: Structures of biochanin A, kaempferol, naringenin, tamoxifen, and 2-methoxyestradiol.

3.1 Synergistic effects of quercetin with genistein: One clinical trial (ClinicalTrials.gov Identifier: NCT01538316) is investigating the effectiveness of the combination of genistein and quercetin in reducing the level of prostate-specific antigen (PSA) in patients with rising PSA.

3.2 Synergistic effects of quercetin with genistein and biochanin A: It is believed that combinations of different subclasses of flavonoids might provide either additive or synergistic activity *in vitro* and *in vivo* when compared with single-flavonoid treatment. Kumar *et al.* systematically investigated the synergistic effects of two-flavonoid and three-flavonoid combinations among quercetin, genistein, and biochanin A (Figure 3) on suppressing cell proliferation of three prostate cancer cell lines (PC-3, DU145, and LNCaP). The findings of this study showed (i) the two-flavonoid combinations at 25 μ M (12.5 μ M of each flavonoid) only exhibited additive effects in inhibiting prostate cancer cell proliferation; and (ii) the three-flavonoid combination (8.33 μ M of quercetin, genistein, and biochanin A, respectively) can synergistically repress cell proliferation in three prostate cancer cell lines [24]. The androgen-insensitive PC-3 and DU145 human prostate cancer cell lines are more responsive to the combination treatments than the androgen-sensitive LNCaP cell line. Both two-flavonoid and three-flavonoid combinations can cause synergistic apoptosis and cell cycle arrest at the G₁ phase of PC-3 prostate cancer cells as evidenced by flow cytometric analysis [24]. Further investigation of the molecular mechanism revealed that the synergistic effects in PC-3 cells are associated with (i) the downregulation of c-myc, PCNA, mitogen activated protein kinase (MAPK)/ERK-1/2 signaling, and PI3K/AKT signaling pathway, and (ii) upregulation of ER- β gene and MAPK/c-Jun N-terminal kinase signaling. The synergistic inhibition of cell-cycle in PC-3 cells is correlated with gene expression downregulation of cyclins D1 and E. The synergistic apoptosis contributed by the flavonoid combinations is related to the cooperative upregulation of caspase-3 and pro-apoptotic protein Bax, and to the collaborative downregulation of anti-apoptotic protein Bcl-2 in PC-3 cells [24].

3.3 Synergistic effects of quercetin with green tea catechins: The combination of quercetin with epigallocatechin gallate (EGCG, Figure 1) only exerts additive instead of synergistic effects in controlling proliferation of CWR22Rv1 and PC-3 prostate cancer cells [25-26]. Intriguingly, a three-flavonoid combination consisting of quercetin, EGCG, and genistein can synergistically inhibit the CWR22Rv1 prostate cancer cell proliferation [25]. In contrast, androgen-sensitive LNCaP prostate cancer cells are more responsive to the treatment of quercetin combined with EGCG. The combination treatment acts synergistically in inhibiting proliferation, apoptosis, and cell cycle regulation of LNCaP cells [26]. Combination treatment of PC-3 and LNCaP prostate cancer cells with quercetin plus EGCG led to synergistically increased cellular absorption and decreased methylation of both EGCG and

quercetin [26]. Additionally, the combination of quercetin and EGCG synergistically suppresses the self-renewal activities of prostate cancer stem cells, activates apoptosis, and prevents cancer stem cells' migration and invasion [27].

The *in vivo* antitumor efficacy of green tea catechins has been shown to be improved by quercetin. A Phase I clinical study (ClinicalTrials.gov Identifier: NCT01912820) is designated to translate these preclinical results into a clinical setting by assessing the possible bioavailability improvement of quercetin and green tea catechins in combination.

3.4 Synergistic effects of quercetin with kaempferol: The only structural difference between kaempferol (3,4',5,7-tetrahydroxyflavone, Figure 3) and quercetin is that kaempferol lacks the 3'-OH group in quercetin. Kaempferol has been revealed to have antiproliferative effects towards prostate cancer cells with IC₅₀ values ranging from 10 to 55 μ M [28]. Quercetin and kaempferol have been demonstrated to inhibit synergistically proliferation of androgen-sensitive LNCaP and androgen-insensitive PC-3 human prostate cancer cells [29].

3.5 Synergistic effects of quercetin with naringenin: Naringenin (Figure 3) is a naturally occurring flavonoid belonging to the flavanone subclass, which only exhibits weak antiproliferative effects towards prostate cancer cells [29b]. Its synergistic effect on cell proliferation suppression towards the androgen-sensitive LNCaP prostate cancer cell line has been identified [29a].

3.6 Synergistic effects of quercetin with arctigenin: As mentioned in section 2.3, arctigenin is a naturally occurring lignan with promising antiproliferative activity towards prostate cancer cells. Arctigenin has been demonstrated to exhibit 10- to 20-fold stronger antiproliferative potency than quercetin in both LAPC-4 and LNCaP prostate cancer cell lines. LNCaP cells were more refractory to arctigenin than LAPC-4 cells. The treatment with arctigenin in combination with quercetin synergistically inhibits the cell proliferation in both prostate cancer cell lines. Cell proliferation suppression was enhanced by 30% in both cell lines by a combination treatment with arctigenin (1 μ M) and quercetin (20 μ M) as compared with the treatments with the individual compounds. The combination index values were in a range of 0.5-0.7 for LAPC-4 cells, and 0.2-0.8 for LNCaP cells [30]. The combination of quercetin plus arctigenin also led to the synergistic phosphorylation inhibition of multiple signaling molecules in LAPC-4 prostate cancer cells as determined by the intracellular signaling array analysis, as well as by Western blot analysis [30]. The synergistic downregulation of androgen receptor and prostate specific antigen in LAPC-4 cells was generated by the combination treatment as examined by qRT-PCR analysis and Western blot analysis. Additionally, the synergistic migration suppression of LAPC-4 and LNCaP prostate cancer cells was noticeably enhanced by the combination treatment [30].

3.7 Synergistic effects of quercetin with tamoxifen: Tamoxifen (Figure 3), a specific antagonist of the estrogen receptor, has been demonstrated to be capable of potentiating the cytotoxic effect of chemotherapeutic agents in prostate cancer cell lines [31]. The *in vivo* synergistic efficacy of combined tamoxifen (10 mg/kg/week) plus quercetin (200 mg/kg/day) has been examined in CWR22 prostate tumor xenografts in severe combined immune deficient (SCID) mice. The results showed that combined tamoxifen with quercetin appreciably prolonged the appearance time of tumors by four days, reduced the final tumor volume by 73%, and lowered the tumor weight at the endpoint by 67%. As compared with the

individual agent treatment, a statistically significant synergism between quercetin and tamoxifen was established. The synergistic antitumor efficacy is linked with the modulation of angiogenesis [32].

3.8 Synergistic effects of quercetin with 2-methoxyestradiol: 2-Methoxyestradiol (Figure 3), an endogenous metabolite of 17 β -estradiol, has been revealed to inhibit growth and activate apoptosis of both androgen-sensitive and androgen-insensitive human prostate cancer cells by arresting cell cycle regulation in the G2/M phase [33]. One clinical study identified that 2-methoxyestradiol has a good safety profile for humans, but poor bioavailability as a drug candidate [34]. Wang *et al.* examined the growth inhibitory effects of sixteen combinations of quercetin (5, 10, 20, 40 μ M) and 2-methoxyestradiol (0.5, 1, 3, 5 μ M) towards androgen-sensitive LNCaP and androgen-insensitive PC-3 human prostate cancer cell lines. Combination index values were in a range of 0.36-2.18 for LNCaP cells, and 0.32-1.77 for PC-3 cells. The combination index values indicated that synergistic effects can only be achieved when combining lower doses of quercetin (5 and 10 μ M) with higher doses of 2-methoxyestradiol (3 and 5 μ M) for LNCaP cells, and mixing higher doses of quercetin (20 and 40 μ M) with higher doses of 2-methoxyestradiol (3 and 5 μ M) for PC-3 cells [35]. The combination treatment for 48 hours significantly enhanced the apoptosis induction through regulation of anti-apoptotic Bcl-2 and proapoptotic Bax as compared with two individual treatments [35]. Additionally, the synergistic cell cycle regulation in the G2/M phase was also observed by treating LNCaP and PC-3 cells with quercetin plus 2-methoxyestradiol.

3.9 Synergistic effects of quercetin with TRAIL: Combination treatment of quercetin (100 μ M) and the death ligand TRAIL (10-100 ng/mL) for 24 hours generated strong synergistic cytotoxicity and apoptosis induction in androgen-insensitive DU-145 and PC-3 human prostate cancer cell lines, as determined by Annexin V and PI staining assays. The PC-3 cell line was illustrated to be more sensitive to the synergy of quercetin with TRAIL than the DU145 cell line even though these two cell lines are both tumorigenic and independent of wild-type p53. This disparity was assumed to be caused by an inherent dissimilarity in TRAIL sensitivity [36]. Further Western blot analysis displayed that the quercetin-induced sensitization to TRAIL-mediated DU145 cell apoptosis is linked to the upregulation of caspases -3, -8, and -9 [36-38]. Downregulation of survivin (anti-apoptotic protein) gene expression in both DU145 and PC-3 cell lines in an ERK-MSK1 dependent pathway was suggested to be a vital molecular mechanism associated with the apoptosis synergism between quercetin and TRAIL. Upregulation of DR5 (decoy receptor 5) protein expression by quercetin through enhancing transcription and protein stability has also been demonstrated by Jung *et al.* to be associated with its potentiating effect on the apoptosis of prostate cancer cells induced by TRAIL [37]. However, Kim and Lee did not observe any alteration of DR5 in their study when treating prostate cancer cells with quercetin in combination with TRAIL [38]. The combination of quercetin plus TRAIL has been revealed to exhibit a stronger synergistic cytostatic effect than synergistic cytotoxicity. The overriding feature of the combination is that the synergistic apoptosis is triggered by a mixture of an apoptotic "sensitizer" (quercetin) and an apoptotic "inducer" (TRAIL) [36].

2. Synergistic effects of soybean isoflavones as anti-prostate cancer agents

4.1 Synergistic effects of genistein with daidzein: As indicated previously, genistein and daidzein are two isoflavones exclusively isolated from soybeans [6]. The only structural difference between

genistein (Figure 1) and daidzein (Figure 2) is that daidzein lacks the hydroxyl group at C-5 of genistein. Genistein has been elicited to be more potent than daidzein in suppressing cell growth and proliferation of various prostate cancer cells [39]. Interestingly, the combination of daidzein and genistein exhibited greater anti-proliferative and apoptotic effects than the respective single agent treatment towards androgen-sensitive LNCaP and its derived C4-2B human prostate cancer cell lines [40]. It is especially worth noting that an apparent apoptosis induction in C4-2B prostate cancer cells can be caused by the combination of genistein (50 μ M) and daidzein (25-50 μ M), but not individual genistein or daidzein. The synergism between genistein and daidzein might be contributed by their shared molecular mechanism of actions through modulating cell cycle and angiogenesis related genes and by the multi-target mechanism underlying the anti-proliferative effect of genistein.

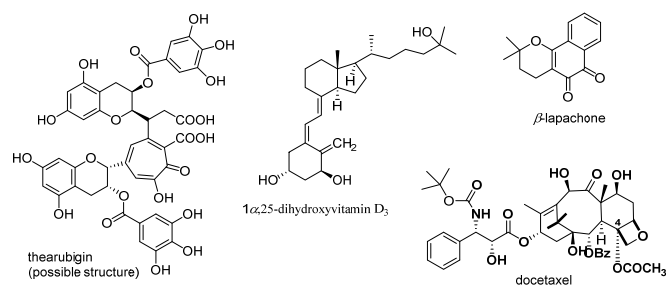


Figure 4: Structures of thearubigin, 1 α ,25-dihydroxyvitamin D₃, β -lapachone, and docetaxel.

4.2 Synergistic effects of soybean isoflavones with tea: In one *in vivo* animal study carried out by Zhou and co-workers in 2003, it was concluded that prostate tumor progression and metastasis can be synergistically suppressed by soy isoflavones (with genistein as its major chemical component) and tea (both green and black tea) in androgen-sensitive LNCaP human prostate tumor xenografts in severe combined immune deficient (SCID) mice [41]. They observed that (i) treatment of mice with soy phytochemicals and black tea in combination led to a 1.46-times greater effect on tumorigenicity rate than their additive effect; and (ii) combination treatment of soy phytochemicals and tea (both black and green tea) synergistically suppressed tumor metastasis to lymph nodes with ratios of 2.13 and 1.87. The synergistic effects might be linked to effective reduction of both testosterone and DHT in serum.

4.3 Synergistic effects of genistein with thearubigin: Thearubigin (Figure 4) is synonymous with black tea polyphenols, which are transformed from green tea catechins (flavan-3-ols) catalyzed by polyphenol oxidase during tea leaf fermentation [42]. Thearubigin alone (up to 25 μ g) neither showed any apparent cell growth inhibition nor DNA distribution change of cell cycle modulation in an androgen-insensitive prostate cancer cell line. However, a combination of thearubigin and genistein (1:40) appreciably enhanced cell growth suppression and cell cycle arrest at the G2/M phase as compared with the genistein-treated group [43]. Additionally, exposure of PC-3 prostate cancer cells to a combination of 2.5 μ g/mL of genistein and 0.0625 μ g/mL of thearubigin resulted in cell growth suppression by 33%. No cell growth inhibition was observed from either thearubigin-treated (0.0625 μ g/mL) or genistein-treated (2.5 μ g/mL) groups. This result thus confirmed the synergism between thearubigin and genistein. The molecular mechanism underlying the synergism is still elusive. Sakamoto *et al.* pointed out that genistein, but not thearubigin, can directly regulate the cell cycle. However, thearubigin in conjugation with genistein can synergistically cause cell cycle arrest at the G2/M phase and therefore repress cell growth.

4.4 Synergistic effects of genistein with 1 α ,25-dihydroxyvitamin D₃: Vitamin D deficiency has been hypothesized to be one of the primary risks for prostate cancer [44]. This hypothesis was not only corroborated by the correlation between the low incidence of prostate cancer and the vitamin D-rich Asian diet, but also confirmed by the antiproliferative effect of 1 α ,25-dihydroxyvitamin D₃ (the most bioactive metabolite of vitamin D, Figure 4) against androgen-sensitive LNCaP human prostate cancer cells [45]. The inhibition of 1 α ,25-dihydroxyvitamin D₃ on prostate cancer cell proliferation is linked to the nuclear vitamin D receptor. The soy isoflavone genistein (0.1 to 1 μ M) and 1 α ,25-dihydroxyvitamin D₃ (0.1 to 0.5 nM) have been demonstrated by Cramer and co-workers to possess synergistic effects on suppressing the growth of primary human prostatic epithelial cells and androgen-sensitive LNCaP human prostate cancer cells through cell cycle arrest [46]. The further mechanism exploration from the same research group demonstrated that 1 α ,25-dihydroxyvitamin D₃ and genistein can act jointly to enhance the stability and subsequently the protein level of vitamin D receptor; and to escalate the levels of cell cycle inhibitor p21 that is essential to the anti-proliferative effects of both genistein and 1 α ,25-dihydroxyvitamin D₃. Accordingly, modulation of nuclear vitamin D signaling was concluded as one mechanism for the synergism between genistein and 1 α ,25-dihydroxyvitamin D₃ [47].

4.5 Synergistic effects of genistein with β -lapachone: β -Lapachone (Figure 4) is an abundant naturally occurring quinone and can be readily obtained from *Tabebuia avellaneda*, the lapacho tree native to South America. β -Lapachone has been shown to be a distinct Topo I inhibitor that suppresses the relevant enzymatic activity through directly binding to Topo I. Additionally, β -lapachone has been revealed to be capable of suppressing cell growth and promoting cell apoptosis in both androgen-sensitive and insensitive human prostate cancer cells [48]. The androgen-insensitive PC-3 human prostate cancer cells have been shown to be significantly more responsive to the combined administration of genistein and β -lapachone when compared with the respective single-agent treatment [49]. Additionally, genistein and β -lapachone have been demonstrated to act synergistically to induce apoptosis in the PC-3 cell line.

4.6 Synergistic effects of genistein with sodium selenite: The anti-prostate cancer potential of selenite has been established based on various *in vitro* cell-based assays, *in vivo* animal experiments, and human clinical studies [50]. In search of a combination of anti-prostate cancer agents with different underlying mechanisms, Zhao *et al.* evaluated the synergistic effects of genistein and selenite. The data revealed that the combination of genistein and selenite can synergistically induce cell apoptosis, cause cell cycle arrest at the G₂/M phase, and modulate relevant signaling pathways in both androgen-sensitive LNCaP (p53-positive) and insensitive PC-3 (p53-negative) human prostate cancer cells [50]. The synergism was assumed to be partly due to their distinct molecular mechanisms. For example, selenite was shown to activate cell apoptosis but was not involved in cell cycle modulation. In contrast, genistein can cause both apoptosis activation and cell cycle modulation at the G₂/M phase, which was contributed in part by downregulation of AKT [50].

4.7 Synergistic effects of GCP with docetaxel: GCP, with the isoflavones genistein and daidzein as the main chemical components, stands for a genistein combined polysaccharide that is marketed as a nutritional supplement. GCP with an enhanced absorption rate of genistein in the small intestine is generated from soybean extract catalyzed by mycelia. Docetaxel (Figure 4),

working by mainly promoting the polymerization of tubulin to microtubules and microtubule stabilization, is the current FDA-approved gold standard, first-line treatment for castration-resistant prostate cancer. The limitation of docetaxel's clinical efficacy is that it can barely prolong a maximum 2-3 years of survival for a prostate cancer patient [51]. Even worse, approximately 30,000 US men die each year of castration-resistant prostate cancer due to the inevitable progression of resistance to first-line treatment with docetaxel [52]. To explore the possible advantage of GCP in combination with docetaxel for the treatment of castration-resistant prostate cancer, the *in vitro* antiproliferative and apoptotic effects of the combination of GCP and docetaxel were examined by Burich *et al.* in one androgen-sensitive LNCaP prostate cancer cell line and three androgen-insensitive CWR22Rv1, PC-3, and LNCaP-R273H prostate cancer cell lines. The results showed that GCP can potentiate docetaxel in inhibiting cell proliferation and promoting cell apoptosis in the four prostate cancer cell lines [53]. However, the degree of synergism between GCP and docetaxel is dependent on the administration schedule. Much greater synergism was observed in the LNCaP cell model when docetaxel rather than GCP was administered first in the sequential treatment.

4.8 Synergistic effects of GCP with bicalutamide: GCP could also synergistically enhance the *in vitro* antiproliferative effects of androgen receptor antagonist bicalutamide (Figure 2) in androgen-dependent LNCaP and androgen-independent LNCaP-R273H prostate cancer cell lines [53]. The LNCaP-R273H model, established from its parental LNCaP cell line by constitutive expression of the p53 gain-of-function mutation R273H, may better represent patient prostate tumor cells after progression to androgen insensitive. Parental LNCaP prostate cancer cells have been demonstrated to be far more responsive than the variant LNCaP-R273H subline to individual treatment with either GCP or bicalutamide. Intriguingly, both prostate cancer cell lines were well-sensitized to the combination of GCP and bicalutamide.

3. Synergistic effects of silibinin as anti-prostate cancer agents

Silymarin is a commercially available herb preparation that is extracted from the seeds of *Silybum marianum* (L.) Gaertn. Seven flavonolignans compose the critical chemical components of silymarin, with silibinin (a 1:1 mixture of diastereomers silybin A and silybin B, Figure 1) as the most abundant one [54]. The medicinal values of silymarin and silibinin as chemotherapeutics to treat hepatotoxicity have been extensively explored, especially in Europe and Asia [55]. Since 1998, the anti-prostate cancer potential of silymarin and silibinin has been evidenced by several *in vitro* cell-based evaluations and *in vivo* animal studies [56]. Their liver protective function, antiproliferative effects, and antitumor efficacy suggest the potential of silymarin and silibinin for clinical use, along with currently established cancer therapies, to improve synergistically the efficacy while alleviating toxicity for prostate cancer patient treatment [57]. Silymarin has already been used by cancer patients to eliminate the hepatotoxicity caused by several chemotherapies [58]. The synergistic effects of silibinin and chemotherapeutic drugs on cell proliferation, cell cycle modulation, and apoptosis activation in various cancer cell lines have been reviewed by Raina and Agarwal [59]. As described in the following subsections, silymarin and silibinin have been reported to be synergized with well-established chemotherapeutic agents including cisplatin, carboplatin, doxorubicin, docetaxel, and mitoxantrone as anti-prostate cancer agents.

5.1 Synergistic effects of silibinin with cisplatin/carboplatin: Cisplatin and carboplatin belong to two platinum complexes that act as cytotoxic chemotherapeutics with molecular mechanism

underlying cytotoxicity similar to that of alkylating agents. Cisplatin [*cis*-diamminedichloroplatinum(II)] is a well-known and commonly used cytotoxic chemotherapy drug that was introduced into clinical trials in 1972. Its capability to form DNA adducts mainly contributes to the cytotoxicity of cisplatin [60]. However, its clinical efficacy is largely compromised by its high toxicity [61]. Carboplatin is another cytotoxic platinum complex with its full name as *cis*-diammine[1,1-cyclobutane-dicarboxylato]platinum. Compared with cisplatin, carboplatin has a better safety profile but no considerable effect towards castration-resistant prostate cancer [62]. Silibinin has been reported to potentiate cisplatin and carboplatin in inhibiting cell proliferation and activating cell apoptosis in the androgen-insensitive DU145 human prostate cancer cells. The synergistic effects on apoptosis were further confirmed by the results that the cleaved levels of PARP and Caspases 3, 7, and 9 were also synergistically upregulated by the combination regimen. The combination of silibinin (50-100 μ M) with either cisplatin (2 μ g/mL) or carboplatin (20 μ g/L) has also been reported to cause synergistic cell cycle arrest at the G₂-M phase and downregulate the relevant proteins of Cdc2, cyclin B1, and Cdc25C. It is worth noting that exposure of DU145 cells to cisplatin, carboplatin, and silibinin alone resulted in cell cycle arrest at G₂-M, S, and G₁ phases, respectively. Both immunocytochemical and Western immunoblotting analyses indicated that combination treatment with silibinin and platinum complex led to a noticeable increase in the levels of cytosolic cytochrome *c* [63].

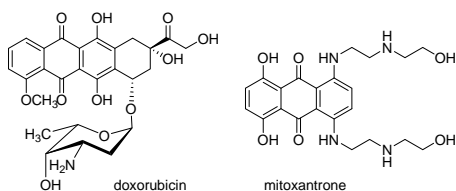


Figure 5: Structures of doxorubicin and mitoxantrone.

5.2 Synergistic effects of silibinin with doxorubicin: Doxorubicin (Figure 5) is a well-known chemotherapeutic for a variety of cancers targeting topoisomerase II; its clinical efficacy, however, is limited by its high systemic toxicity. The synergism between silibinin and doxorubicin has been examined against both androgen-insensitive DU145 and androgen-sensitive LNCaP human prostate cancer cell lines [64]. The results showed that treatment with silibinin (25-100 μ M) and doxorubicin (15-25 nM) alone or in combination led to considerable cell growth suppression in a dose-dependent manner in both prostate cancer cell lines. However, DU145 cells are much more sensitive to the synergistic effects of silibinin and doxorubicin than LNCaP cells. It was established that the combination treatment of silibinin (100 μ M) and doxorubicin (25 nM) generated a profound synergistic effect on inhibition of DU145 cell growth with combination index values in a range of 0.23-0.59. In contrast, almost no synergistic effect of silibinin (25 μ M) and doxorubicin (15 nM) was observed on suppression of LNCaP cell growth with a combination index of 0.929. The perceived synergistic effects on growth suppression of DU145 cells were linked to intense cell cycle perturbation at the G₂-M phase. The combination treatment caused up to 88% cell arrest in the G₂-M phase while silibinin treatment alone caused G₁ arrest, and doxorubicin alone only caused moderate G₂-M arrest (41%). Mechanistically, the combination of silibinin and doxorubicin can synergistically downregulate the G₂-M cell cycle related protein expression, including cdc25C, cdc2/p34 and cyclin B1, and cdc2/p34 kinase activity affiliated with histone H1. Additionally, the combination treatment can also act synergistically in promoting DU145 cell apoptosis [65].

5.3 Synergistic effects of silibinin with docetaxel/mitoxantrone: Docetaxel (Figure 4) is a well-established anticancer drug and inhibits cell division mainly through binding to and stabilizing microtubules. Docetaxel represents the first cytotoxic chemotherapeutic that offers survival benefit for patients with castration-resistant prostate cancer. For this reason, the US Food and Drug Administration (FDA) approved docetaxel in combination with prednisone in 2004 for the first-line treatment in patients with castration-resistant prostate cancer [66]. However, an average 2.4 years of survival improvement and drug resistance make docetaxel less effective in the clinical use [67]. Chemotherapy with mitoxantrone (Figure 5), an inhibitor of topoisomerase II, has been shown to alleviate symptoms, but not prolong survival rate of patients with advanced castration-resistant prostate cancer [68]. In one study, only additive or even antagonistic effects on cell proliferation inhibition were observed when treating three human prostate cancer cell lines with silibinin in combination with docetaxel, with combination index values of 0.898-2.54 for DU145 cells, 0.921-2.32 for LNCaP cells, and 0.895-4.47 for PC-3 cells [69]. In contrast, the combination treatment of silibinin and mitoxantrone has been demonstrated to have noticeable synergy with combination index values in a range of 0.515-0.929 for DU145 cells, 0.521-0.967 for LNCaP cells, and 0.413-2.65 for PC-3 cells. The only exception is that antagonism was observed in the treatment of PC-3 cells with a low dose of mitoxantrone (e.g. 25 nM) in combined with silibinin [69]. To explore the molecular mechanism underlying the synergy between silibinin and mitoxantrone, the levels of caspase-3 and caspase-7 were evaluated. The results revealed that the combination treatment synergistically and significantly induced the apoptosis of three prostate cancer cell lines.

4. Synergistic effects of green tea catechins as anti-prostate cancer agents

Green tea crude extracts have been designated as green tea catechins that consist of a group of naturally occurring flavan-3-ols, with (-)-epigallocatechin-3-gallate (EGCG) as the most abundant one. Green tea catechins and EGCG have been demonstrated by several *in vitro* cell-based assays and *in vivo* animal studies to have potential in preventing and treating prostate cancer [11]. Several studies as shown in the following subsections have suggested that either green tea catechins or EGCG might be even more effective as anti-prostate agents when they synergistically act with other natural or non-natural compounds. The synergistic apoptosis induced by combinations of EGCG with anti-cancer drugs in various cancer cells (including prostate cancer cells) has been systematically reviewed [70].

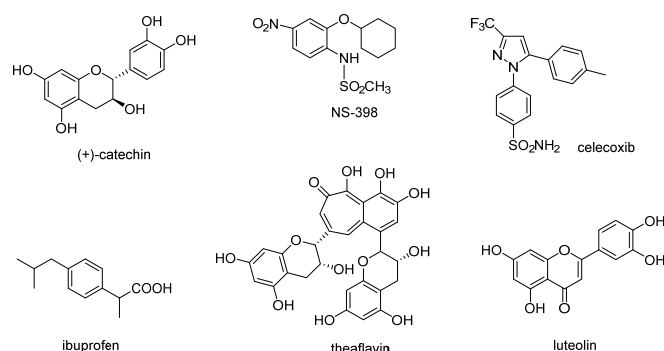


Figure 6: Structures of catechin, NS-398, celecoxib, ibuprofen, theaflavin, and luteolin.

6.1 Synergistic effects of EGCG with selective COX-2 inhibitors [71]: Cyclooxygenase (COX) is a critical enzyme that catalyzes the

transformation of arachidonic acid to prostaglandins. Highly expressed in prostate cancer tissue, prostaglandins are believed to serve as an essential role in the cell proliferation of prostate cancer. COX-2 is an inductive isoform and has been revealed to affect the proliferation and apoptosis of prostate cancer cells [72]. Consequently, COX-2 inhibitors have been proposed to be useful for potential chemotherapy for prostate cancer. (+)-Catechin (Figure 6) is the simplest flava-3-ol derived from green tea, which showed certain cell proliferation suppression at a high concentration (100 μ M) toward LNCaP and DU145 (but not PC-3) prostate cancer cell lines. Zaslau and co-workers reported that catechin and NS398 (a selective COX-2 inhibitor, Figure 6) would act synergistically to inhibit prostate cancer cell proliferation [72a]. Adhami and co-workers also explored the combinatorial effect of (-)-epigallocatecatechin-3-gallate (EGCG) and selective COX-2 inhibitors (NS-398 and celecoxib, Figure 6) in both *in vitro* human prostate cancer cell models and *in vivo* prostate cancer CWR22Rv1 xenografts in athymic nude mice [71]. The *in vitro* synergism between EGCG and NS-398 was established because the combination treatment enhanced cell growth suppression and apoptosis activation, which was also supported by increased expression of Bax, pro-caspase-6, and pro-caspase-9, and poly(ADP-ribose) polymerase cleavage. Additionally, the suppression of proliferator activated receptor γ and nuclear factor- κ B were also enhanced as compared with their additive effects. Combination administration of EGCG and celecoxib in *in vivo* tumor xenografts led to improved anti-tumor efficacy, and decreased PSA levels and insulin-like growth factor-1 levels.

6.2 Synergistic effects of EGCG with ibuprofen: Ibuprofen (Figure 6) is a well-established non-steroidal anti-inflammatory drug (NASID) that functions *via* inhibiting cyclooxygenase (COX) enzymes. Administration of ibuprofen was associated with low incidence of prostate cancer probably due to its ability to suppress COX enzymes [73]. The *in vitro* study has revealed that ibuprofen can inhibit cell proliferation and activate cell apoptosis in LNCaP prostate cancer cells [74]. The synergism between EGCG and ibuprofen has been established by *in vitro* cell-based assays, in which they can act synergistically in inhibiting cell proliferation and inducing cell apoptosis in both androgen-insensitive and sensitive (PC-3, DU145, and LNCaP) prostate cancer cell lines [75]. The further underlying mechanism investigation indicated that combined treatment of PC-3 cells can synergistically upregulate protein phosphatase 1 activity and subsequently activate alternative splicing of anti-apoptotic proteins Bcl-X and Mcl-1 [75b].

6.3 Synergistic effects of green tea catechins with black tea theaflavin: As mentioned previously, EGCG represents the most copious flava-3-ol in green tea while theaflavin (Figure 6) is the major flavonoid polymer in black tea. Interestingly, EGCG and theaflavin can function synergistically to decrease the growth rate of prostate cancer as compared with either EGCG or theaflavin alone. This synergism may be caused by functionally supplemented mechanisms of EGCG and theaflavin [76].

6.4 Synergistic effects of green tea catechins with luteolin: It has been demonstrated that prostate cancer progression can be driven by the existence of myofibroblasts and that EGCG may suppress the myofibroblast differentiation relevant to prostate cancer [77]. Luteolin, 3',4',5,7-tetrahydroxyflavone (Figure 6), is another ordinary flavone and can be readily obtained from a variety of vegetables and fruits, as well as traditional Chinese medicines [78]. Several *in vitro* and *in vivo* studies have shown its potential in preventing and treating prostate cancer [79]. Luteolin can potentiate EGCG to upregulate fibronectin expression in prostate fibroblast

cell lines [77]. Consequently, myofibroblast phenotypes and extracellular matrix contraction (a promoter of cancer cell invasion) mediated by TGF- β can be synergistically suppressed by combinations of EGCG and luteolin at micromolar concentrations. Mechanistically, EGCG and luteolin can individually downregulate ERK and Rho that are downstream signalings induced by TGF- β and are essential for fibronectin expression [77]. Additionally, EGCG and luteolin have been shown to reverse synergistically fibronectin expression induced by TGF- β . These findings suggested that the combination of EGCG and luteolin might be clinically useful in preventing and reversing prostate cancer progression *via* targeting the tumor microenvironment rather than the tumor itself.

6.5 Synergistic effects of EGCG with TRAIL: TRAIL is known to inhibit cell proliferation in PC-3 instead of LNCaP prostate cancer cells. The synergism between EGCG and TRAIL has been identified according to the following experimental findings: (i) combination treatment of EGCG and TRAIL enhanced antiproliferative effects towards TRAIL refractory LNCaP cells as compared with the single-agent treatments; (ii) the combination treatment led to escalated apoptosis of LNCaP cells relative to effects caused by the single treatments; and (iii) the combination treatment resulted in a synergistic suppression of the invasion and migration of LNCaP cells [80]. The improved apoptosis contributed by the combined treatment is linked to both intrinsic and extrinsic pathways through several molecular mechanisms. For example, the apoptosis was found to be accompanied by the increased poly(ADP-ribose)polymerase cleavage and pro-apoptotic proteins, together with reduced anti-apoptotic proteins.

6.6 Synergistic effects of EGCG with taxanes: The combination of EGCG and either paclitaxel (Figure 2) or docetaxel (Figure 4) generated synergistic efficacy *in vitro* and *in vivo* [81]. The *in vitro* cell-based studies have unveiled that EGCG (30 μ M) in combination with either paclitaxel (6.25 nM) or docetaxel (3.12 nM) exhibited synergistic effects in inhibiting proliferation and activating apoptosis of PC-3ML human prostate cancer cells. The *in vivo* animal studies indicated that the synergistic effects in suppressing PC-3ML tumor xenograft growth were generated for the combined treatment with EGCG and docetaxel in severe combined immunodeficient mice. In addition to attenuating the preexisting PC-3ML tumor xenografts, the combined treatment increased disease-free survival rates to greater than 90%. EGCG combined with either paclitaxel or docetaxel through intraperitoneal injection (i.p.) promoted a considerable enhancement in apoptosis rates, as determined by TUNEL assays. The *in vitro* cell-based assays and *in vivo* mechanism studies in mice have also revealed that EGCG and either paclitaxel or docetaxel can act synergistically to upregulate certain apoptotic genes [81].

6.7 Synergistic effects of EGCG with doxorubicin: Doxorubicin is a well-known chemotherapeutic for a variety of cancers. Low doses of doxorubicin have been demonstrated by *in vitro* studies to act synergistically with EGCG in inhibiting cell proliferation and colony forming of PC-3ML human prostate cancer cells. The synergism between EGCG and doxorubicin was also verified by *in vivo* animal studies in mice implanted with advanced, metastatic PC-3ML human prostate cancer cells. The data showed that the combined treatment led to synergistic suppression of tumor xenograft growth, elimination of tumors, and enhancement of mouse survival rates [82]. Additionally, EGCG was also demonstrated to escalate doxorubicin retention by the prostate cancer cells *in vitro* and by the metastatic tumor xenografts *in vivo*.

6.8 Synergistic effects of EGCG with cisplatin: As described in section 5.1, cisplatin is a well-known and commonly used cytotoxic chemotherapy drug that processes promising efficacy but high toxicity. EGCG (25 μ M) has been evidenced to induce synergistically apoptosis of PC-3 prostate cancer cells in combination with cisplatin (2.5 μ M) as compared with the effects caused by treating the individual agent alone [83].

6.9 Synergistic effects of EGCG with free Zn²⁺: Zinc is an essential trace element. The elevated level of intracellular zinc has been demonstrated to be linked with decreased proliferation and increased apoptosis of prostate cancer cells [84]. The antiproliferative activities of Zn²⁺/EGCG mixture and zinc-EGCG complex were examined on an androgen-insensitive PC-3 human prostate cancer cell line. It was revealed that free Zn²⁺ can potentiate the antiproliferative effect of EGCG on PC-3 cells [85].

References

- [1] (a) Shimizu H, Ross RK, Bernstein L, Yatani R, Henderson BE, Mack TM. (1991) Cancers of the prostate and breast among Japanese and white immigrants in Los Angeles County. *British Journal of Cancer*, **63**, 963-966; (b) Mills PK, Beeson WL, Phillips RL, Fraser GE. (1989) Cohort study of diet, lifestyle, and prostate cancer in Adventist men. *Cancer*, **64**, 598-604.
- [2] Chen Q-H. (2015) Curcumin-based anti-prostate cancer agents. *Anti-Cancer Agents in Medicinal Chemistry*, **15**, 138-156.
- [3] (a) Aalinkeel R, Bindukumar B, Reynolds JL, Sykes DE, Mahajan SD, Chadha KC, Schwartz SA. (2008) The dietary bioflavonoid, quercetin, selectively induces apoptosis of prostate cancer cells by down-regulating the expression of heat shock protein 90. *Prostate (Hoboken, NJ, United States)*, **68**, 1773-1789; (b) Singh RP, Raina K, Sharma G, Agarwal R. (2008) Silybinin inhibits established prostate tumor growth, progression, invasion, and metastasis and suppresses tumor angiogenesis and epithelial-mesenchymal transition in transgenic adenocarcinoma of the mouse prostate model mice. *Clinical Cancer Research*, **14**, 7773-7780.
- [4] Prasad S, Tyagi AK, Aggarwal BB. (2014) Recent developments in delivery, bioavailability, absorption and metabolism of curcumin: the golden pigment golden spice. *Cancer Research and Treatment*, **46**, 2-18.
- [5] Ali BH, Marrif H, Noureldayem SA, Bakheit AO, Blunden G. (2006) Some biological properties of curcumin: a review. *Natural Product Communications*, **1**, 509-521.
- [6] van Die MD, Bone KM, Williams SG, Pirotta MV. (2014) Soy and soy isoflavones in prostate cancer: a systematic review and meta-analysis of randomized controlled trials. *BJU International*, **113**, E119-E130.
- [7] Ide H, Tokiwa S, Sakamaki K, Nishio K, Isotani S, Muto S, Hama T, Masuda H, Horie S. (2010) Combined inhibitory effects of soy isoflavones and curcumin on the production of prostate-specific antigen. *Prostate (Hoboken, NJ, United States)*, **70**, 1127-1133.
- [8] Ide H, Yu J, Lu Y, China T, Kumamoto T, Koseki T, Muto S, Horie S. (2011) Testosterone augments polyphenol-induced DNA damage response in prostate cancer cell line, LNCaP. *Cancer Science*, **102**, 468-471.
- [9] Aditya NP, Shim M, Lee I, Lee Y, Im M-H, Ko S. (2013) Curcumin and genistein coloaded nanostructured lipid carriers: *in vitro* digestion and antiprostate cancer activity. *Journal of Agricultural and Food Chemistry*, **61**, 1878-1883.
- [10] Aditya NP, Shim M, Yang H, Lee Y, Ko S. (2014) Antiangiogenic effect of combined treatment with curcumin and genistein on human prostate cancer cell line. *Journal of Functional Foods*, **8**, 204-213.
- [11] Henning SM, Wang P, Heber D. (2011) Chemopreventive effects of tea in prostate cancer: Green tea versus black tea. *Molecular Nutrition & Food Research*, **55**, 905-920.
- [12] Wang P, Wang B, Chung S, Wu Y, Henning SM, Vadgama JV. (2014) Increased chemopreventive effect by combining arctigenin, green tea polyphenol and curcumin in prostate and breast cancer cells. *RSC Advances*, **4**, 35242-35250.
- [13] Pitti RM, Marsters SA, Ruppert S, Donahue CJ, Moore A, Ashkenazi A. (1996) Induction of apoptosis by Apo-2 ligand, a new member of the tumor necrosis factor cytokine family. *Journal of Biological Chemistry*, **271**, 12687-12690.
- [14] Ashkenazi A, Dixit VM. (1999) Apoptosis control by death and decoy receptors. *Current Opinion in Cell Biology*, **11**, 255-260.
- [15] (a) Deeb D, Xu YX, Jiang H, Gao X, Janakiraman N, Chapman RA, Gautam SC. (2003) Curcumin (diferuloyl-methane) enhances tumor necrosis factor-related apoptosis-inducing ligand-induced apoptosis in LNCaP prostate cancer cells. *Molecular Cancer Therapeutics*, **2**, 95-103; (b) Deeb DD, Jiang H, Gao X, Divine G, Dulchavsky SA, Gautam SC. (2005) Chemosensitization of hormone-refractory prostate cancer cells by curcumin to TRAIL-induced apoptosis. *Journal of Experimental Therapeutics and Oncology*, **5**, 81-91.
- [16] Andrzejewski T, Deeb D, Gao X, Danyluk A, Arbab Ali S, Dulchavsky Scott A, Gautam Subhash C. (2008) Therapeutic efficacy of curcumin/TRAIL combination regimen for hormone-refractory prostate cancer. *Oncology Research*, **17**, 257-267.
- [17] Deeb D, Jiang H, Gao X, Al-Holou S, Danyluk AL, Dulchavsky SA, Gautam SC. (2007) Curcumin [1,7-bis(4-hydroxy-3-methoxyphenyl)-1-6-heptadine-3,5-dione; C21H20O6] sensitizes human prostate cancer cells to tumor necrosis factor-related apoptosis-inducing ligand/Apo2L-induced apoptosis by suppressing nuclear factor- κ B via inhibition of the prosurvival Akt signaling pathway. *Journal of Pharmacology and Experimental Therapeutics*, **321**, 616-625.
- [18] Adam V, Ekblad M, Sweeney K, Mueller H, Busch KH, Johnsen CT, Kang NR, Lemoine NR, Hallden G. (2012) Synergistic and selective cancer cell killing mediated by the oncolytic adenoviral mutant Ad $\Delta\Delta$ and dietary phytochemicals in prostate cancer models. *Human Gene Therapy*, **23**, 1003-1015.
- [19] Li J, Xiang ST, Zhang QH, Wu JJ, Tang Q, Zhou JF, Yang LJ, Chen ZQ, Hann SS. (2015) Combination of curcumin and bicalutamide enhanced the growth inhibition of androgen-independent prostate cancer cells through SAPK/JNK and MEK/ERK1/2-mediated targeting NF- κ B/p65 and MUC1-C. *Journal of Experimental & Clinical Cancer Research*, **34**, 1-21.
- [20] Hour T-C, Chen J, Huang C-Y, Guan J-Y, Lu S-H, Pu Y-S. (2002) Curcumin enhances cytotoxicity of chemotherapeutic agents in prostate cancer cells by inducing p21WAF1/CIP1 and C/EBP β expressions and suppressing NF- κ B activation. *Prostate (New York, NY, United States)*, **51**, 211-218.
- [21] Cabrespina-Faugeras A, Bayet-Robert M, Bay J-O, Chollet P, Barthomeuf C. (2010) Possible benefits of curcumin regimen in combination with taxane chemotherapy for hormone-refractory prostate cancer treatment. *Nutrition and Cancer*, **62**, 148-153.
- [22] Nayak BK, Krishnegowda NK, Galindo CA, Meltz ML, Swanson GP. (2010) Synergistic effect between curcumin (diferuloylmethane) and radiation on clonogenic cell death independent of p53 in prostate cancer cells. *Journal of Cancer Science & Therapy*, **2**, 171-181.

5. Conclusion

These data can provide valuable insights into future design and development of multi-targeting and synergistic agents for potential treatment of prostate cancer. However, most currently available data are only derived from *in vitro* evaluations. The molecular mechanism of the underlying synergism is still elusive. The in-depth mechanism investigation of the synergism of dietary natural products and the rational application of the synergism to the design of hybrid molecules would thus be a good future direction for the development of potential anti-prostate cancer agents.

Acknowledgments – The authors are grateful to the financial support from the California State University (CSU)-Fresno, and to the ASI at CSU-Fresno for a Graduate Research Grant Award (to S. Zhang).

- [23] (a) Firdous A, Sharmila G, Balakrishnan S, Raja Singh P, Suganya S, Srinivasan N, Arunakaran J. (2014) Quercetin, a natural dietary flavonoid, acts as a chemopreventive agent against prostate cancer in an *in vivo* model by inhibiting the EGFR signaling pathway. *Food & Function*, **5**, 2632-2645; (b) Poyil P, Budhraja A, Son Y-O, Wang X, Zhang Z, Ding S, Wang L, Hitron A, Lee J-C, Xu M, Chen G, Luo J, Shi X. (2012) Quercetin inhibits angiogenesis mediated human prostate tumor growth by targeting VEGFR-2 regulated AKT/mTOR/P70S6K signaling pathways. *PLoS One*, **7**, e47516; (c) Wu K, Ning Z, Zhou J, Wang B, Fan J, Zhu J, Gao Y, Wang X, Hsieh J-T, He D. (2014) 2'-Hydroxyflavanone inhibits prostate tumor growth through inactivation of AKT/STAT3 signaling and induction of cell apoptosis. *Oncology reports*, **32**, 131-138.
- [24] Kumar R, Verma V, Jain A, Jain RK, Maikhuri JP, Gupta G. (2011) Synergistic chemoprotective mechanisms of dietary phytoestrogens in a select combination against prostate cancer. *Journal of Nutritional Biochemistry*, **22**, 723-731.
- [25] Hsieh T-C, Wu JM. (2009) Targeting CWR22Rv1 prostate cancer cell proliferation and gene expression by combinations of the phytochemicals EGCG, genistein and quercetin. *Anticancer Research*, **29**, 4025-4032.
- [26] Wang P, Heber D, Henning SM. (2012) Quercetin increased the antiproliferative activity of green tea polyphenol (-)-epigallocatechin gallate in prostate cancer cells. *Nutrition and Cancer*, **64**, 580-587.
- [27] Tang S-N, Singh C, Nall D, Meagher D, Shankar S, Srivastava RK. (2010) The dietary bioflavonoid quercetin synergizes with epigallocatechin gallate (EGCG) to inhibit prostate cancer stem cell characteristics, invasion, migration and epithelial-mesenchymal transition. *Journal of Molecular Signaling*, **5**, 14.
- [28] (a) Haddad AQ, Venkateswaran V, Viswanathan L, Teahan SJ, Fleshner NE, Klotz LH. (2006) Novel antiproliferative flavonoids induce cell cycle arrest in human prostate cancer cell lines. *Prostate cancer and prostatic diseases*, **9**, 68-76; (b) Tsimploulou C, Demetzos C, Hadzopoulou-Cladaras M, Pantazis P, Dimas K. (2012) *In vitro* activity of dietary flavonol congeners against human cancer cell lines. *European Journal of Nutrition*, **51**, 181-190.
- [29] (a) Campbell JK, King JL, Harmston M, Lila MA, Erdman JW. (2006) Synergistic effects of flavonoids on cell proliferation in Hepa-1c1c7 and LNCaP cancer cell lines. *Journal of Food Science*, **71**, S358-S363; (b) Knowles LM, Zigrossi DA, Tauber RA, Hightower C, Milner JA. (2000) Flavonoids suppress androgen-independent human prostate tumor proliferation. *Nutrition and Cancer*, **38**, 116-122.
- [30] Wang P, Phan T, Gordon D, Chung S, Henning SM, Vadgama JV. (2015) Arctigenin in combination with quercetin synergistically enhances the antiproliferative effect in prostate cancer cells. *Molecular Nutrition & Food Research*, **59**, 250-261.
- [31] Lin C-C, Hsu C-H, Chen J, Tsai T-C, Cheng A-L, Pu Y-S. (2001) A pilot study of AFL-T (doxorubicin, 5-fluorouracil, leucovorin, and tamoxifen) combination chemotherapy for hormone-refractory prostate cancer. *Anticancer Research*, **21**, 1385-1390.
- [32] Ma Z, Nguyen TH, Huynh TH, Do PT, Huynh H. (2004) Reduction of CWR22 prostate tumor xenograft growth by combined tamoxifen-quercetin treatment is associated with inhibition of angiogenesis and cellular proliferation. *International Journal of Oncology*, **24**, 1297-1304.
- [33] Kumar AP, Garcia GE, Slaga TJ. (2001) 2-Methoxyestradiol blocks cell-cycle progression at G2/M phase and inhibits growth of human prostate cancer cells. *Molecular Carcinogenesis*, **31**, 111-124.
- [34] Sweeney C, Liu G, Yiannoutsos C, Kolesar J, Horvath D, Staab MJ, Fife K, Armstrong V, Treston A, Sidor C, Wilding G. (2005) A phase II multicenter, randomized, double-blind, safety trial assessing the pharmacokinetics, pharmacodynamics, and efficacy of oral 2-methoxyestradiol capsules in hormone-refractory prostate cancer. *Clinical Cancer Research*, **11**, 6625-6633.
- [35] Wang G, Song L, Wang H, Xing N. (2013) Quercetin synergizes with 2-methoxyestradiol inhibiting cell growth and inducing apoptosis in human prostate cancer cells. *Oncology Reports*, **30**, 357-63.
- [36] Kim YH, Lee DH, Jeong JH, Guo ZS, Lee YJ. (2008) Quercetin augments TRAIL-induced apoptotic death: involvement of the ERK signal transduction pathway. *Biochemical Pharmacology*, **75**, 1946-1958.
- [37] Jung YH, Heo J, Lee YJ, Kwon TK, Kim YH. (2010) Quercetin enhances TRAIL-induced apoptosis in prostate cancer cells via increased protein stability of death receptor 5. *Life Sciences*, **86**, 351-357.
- [38] Kim YH, Lee YJ. (2007) TRAIL apoptosis is enhanced by quercetin through Akt dephosphorylation. *Journal of Cellular Biochemistry*, **100**, 998-1009.
- [39] Xiong P, Wang R, Zhang X, DeLa Torre E, Leon F, Zhang Q, Zheng S, Wang G, Chen Q-H. (2015) Design, synthesis, and evaluation of genistein analogues as anti-cancer agents. *Anti-Cancer Agents in Medicinal Chemistry*, **15**, 1197-1203.
- [40] Dong X, Xu W, Sikes RA, Wu C. (2013) Combination of low dose of genistein and daidzein has synergistic preventive effects on isogenic human prostate cancer cells when compared with individual soy isoflavone. *Food Chemistry*, **141**, 1923-1933.
- [41] Zhou J-R, Yu L, Zhong Y, Blackburn GL. (2003) Soy phytochemicals and tea bioactive components synergistically inhibit androgen-sensitive human prostate tumors in mice. *Journal of Nutrition*, **133**, 516-521.
- [42] Haslam E. (2003) Thoughts on thearubigins. *Phytochemistry*, **64**, 61-73.
- [43] Sakamoto K. (2000) Synergistic effects of thearubigin and genistein on human prostate tumor cell (PC-3) growth via cell cycle arrest. *Cancer Letters (Shannon, Ireland)*, **151**, 103-109.
- [44] Schwartz GG, Hulka BS. (1990) Is vitamin D deficiency a risk factor for prostate cancer? (Hypothesis). *Anticancer Research*, **10**, 1307-1311.
- [45] Zhuang S-H, Burnstein KL. (1998) Antiproliferative effect of 1 α ,25-dihydroxyvitamin D₃ in human prostate cancer cell line LNCaP involves reduction of cyclin-dependent kinase 2 activity and persistent G1 accumulation. *Endocrinology*, **139**, 1197-1207.
- [46] Rao A, Woodruff RD, Wade WN, Kute TE, Cramer SD. (2002) Genistein and vitamin D synergistically inhibit human prostatic epithelial cell growth. *Journal of Nutrition*, **132**, 3191-3194.
- [47] Rao A, Coan A, Welsh J-E, Barclay WW, Koumenis C, Cramer SD. (2004) Vitamin D receptor and p21/WAF1 are targets of genistein and 1,25-dihydroxyvitamin D₃ in human prostate cancer cells. *Cancer Research*, **64**, 2143-2147.
- [48] Planchon SM, Wuerzberger S, Frydman B, Witiak DT, Hutson P, Church DR, Wilding G, Boothman DA. (1995) β -Lapachone-mediated apoptosis in human promyelocytic leukemia (HL-60) and human prostate cancer cells: a p53-independent response. *Cancer Research*, **55**, 3706-3711.
- [49] Kumi-Diaka J, Saddler-Shawnette S, Aller A, Brown J. (2004) Potential mechanism of phytochemical-induced apoptosis in human prostate adenocarcinoma cells: Therapeutic synergy in genistein and β -lapachone combination treatment. *Cancer Cell International*, **4**, 5.
- [50] Zhao R, Xiang N, Domann FE, Zhong W. (2009) Effects of selenite and genistein on G2/M cell cycle arrest and apoptosis in human prostate cancer cells. *Nutrition and Cancer*, **61**, 397-407.
- [51] (a) Corcoran C, Rani S, O'Brien K, O'Neill A, Prencipe M, Sheikh R, Webb G, McDermott R, Watson W, Crown J, O'Driscoll L. (2012) Docetaxel-resistance in prostate cancer: evaluating associated phenotypic changes and potential for resistance transfer via exosomes. *PLoS One*, **7**, e50999; (b) Yap TA, Zivi A, Omlin A, de Bono JS. (2011) The changing therapeutic landscape of castration-resistant prostate cancer. *Nature Reviews Clinical Oncology*, **8**, 597-610.
- [52] Torre Lindsey A, Bray F, Siegel Rebecca L, Ferlay J, Lortet-Tieulent J, Jemal A. (2015) Global cancer statistics, 2012. *CA: A Cancer Journal for Clinicians*, **65**, 87-108.
- [53] Burich RA, Holland WS, Vinall RL, Tepper C, de Vere White RW, Mack PC. (2008) Genistein combined polysaccharide enhances activity of docetaxel, bicalutamide and Src kinase inhibition in androgen-dependent and independent prostate cancer cell lines. *BJU International*, **102**, 1458-1466.

- [54] Kim N-C, Graf TN, Sparacino CM, Wani MC, Wall ME. (2003) Complete isolation and characterization of silybins and isosilybins from milk thistle (*Silybum marianum*). *Organic & Biomolecular Chemistry*, **1**, 1684-1689.
- [55] Flora K, Hahn M, Rosen H, Benner K. (1998) Milk thistle (*Silybum marianum*) for the therapy of liver disease. *American Journal of Gastroenterology*, **93**, 139-143.
- [56] Zi X, Agarwal R. (1999) Silibinin decreases prostate-specific antigen with cell growth inhibition via G1 arrest, leading to differentiation of prostate carcinoma cells: implications for prostate cancer intervention. *Proceedings of the National Academy of Sciences of the United States of America*, **96**, 7490-7495.
- [57] Comelli MC, Mengs U, Schneider C, Prosdocimi M. (2007) Toward the definition of the mechanism of action of silymarin: activities related to cellular protection from toxic damage induced by chemotherapy. *Integrative Cancer Therapies*, **6**, 120-129.
- [58] Werneke U, Earl J, Seydel C, Horn O, Crichton P, Fannon D. (2004) Potential health risks of complementary alternative medicines in cancer patients. *British Journal of Cancer*, **90**, 408-413.
- [59] Raina K, Agarwal R. (2007) Combinatorial strategies for cancer eradication by silibinin and cytotoxic agents: efficacy and mechanisms. *Acta pharmacologica Sinica*, **28**, 1466-1475.
- [60] Bellon SF, Coleman JH, Lippard SJ. (1991) DNA unwinding produced by site-specific intrastrand crosslinks of the antitumor drug cis-diamminedichloroplatinum(II). *Biochemistry*, **30**, 8026-8035.
- [61] Drelichman A, Oldford J, Al-Sarrat M. (1985) Evaluation of cyclophosphamide, adriamycin, and cis-platinum (CAP) in patients with disseminated prostatic carcinoma. A phase II study. *American Journal of Clinical Oncology*, **8**, 255-259.
- [62] Trump DL, Marsh JC, Kvols LK, Citrin D, Davis TE, Hahn RG, Vogl SE. (1990) A phase II trial of carboplatin (NSC 241240) in advanced prostate cancer, refractory to hormonal therapy. An Eastern Cooperative Oncology Group pilot study. *Investigational New Drugs*, **8 Suppl 1**, S91-S94.
- [63] Dhanalakshmi S, Agarwal P, Glode LM, Agarwal R. (2003) Silibinin sensitizes human prostate carcinoma DU145 cells to cisplatin- and carboplatin-induced growth inhibition and apoptotic death. *International Journal of Cancer*, **106**, 699-705.
- [64] Tyagi AK, Singh RP, Agarwal C, Chan DCF, Agarwal R. (2002) Silibinin strongly synergizes human prostate carcinoma DU145 cells to doxorubicin-induced growth inhibition, G2-M arrest, and apoptosis. *Clinical Cancer Research*, **8**, 3512-3519.
- [65] Singh RP, Agarwal R. (2004) Prostate cancer prevention by silibinin. *Current Cancer Drug Targets*, **4**, 1-11.
- [66] McKeage K. (2012) Docetaxel: a review of its use for the first-line treatment of advanced castration-resistant prostate cancer. *Drugs*, **72**, 1559-1577.
- [67] Bahl A, Masson S, Birtle A, Chowdhury S, de Bono J. (2014) Second-line treatment options in metastatic castration-resistant prostate cancer: A comparison of key trials with recently approved agents. *Cancer Treatment Reviews*, **40**, 170-177.
- [68] Gravis G, Salem N, Bladou F, Viens P. (2007) Prostate cancer and chemotherapy. *Bulletin du Cancer*, **94** (Suppl. FMC, 6), F21-F28.
- [69] Flraig TW, Su LJ, Harrison G, Agarwal R, Glode LM. (2007) Silibinin synergizes with mitoxantrone to inhibit cell growth and induce apoptosis in human prostate cancer cells. *International Journal of Cancer*, **120**, 2028-2033.
- [70] Fujiki H, Suganuma M. (2012) Green tea: An effective synergist with anticancer drugs for tertiary cancer prevention. *Cancer Letters (New York, NY, United States)*, **324**, 119-125.
- [71] Adhami VM, Malik A, Zaman N, Sarfaraz S, Siddiqui IA, Syed DN, Afaq F, Pasha FS, Saleem M, Mukhtar H. (2007) Combined inhibitory effects of green tea polyphenols and selective cyclooxygenase-2 inhibitors on the growth of human prostate cancer cells both *in vitro* and *in vivo*. *Clinical Cancer Research*, **13**, 1611-1619.
- [72] (a) Farivar-Mohseni H, Kandzari SJ, Zaslau S, Riggs DR, Jackson BJ, McFadden DW. (2004) Synergistic effects of Cox-1 and -2 inhibition on bladder and prostate cancer *in vitro*. *American Journal of Surgery*, **188**, 505-510; (b) Kamijo T, Sato T, Nagatomi Y, Kitamura T. (2001) Induction of apoptosis by cyclooxygenase-2 inhibitors in prostate cancer cell lines. *International Journal of Urology*, **8**, S35-S39.
- [73] Platz EA, Rohrmann S, Pearson JD, Corrada MM, Watson DJ, De Marzo AM, Landis PK, Metter EJ, Carter HB. (2005) Nonsteroidal anti-inflammatory drugs and risk of prostate cancer in the Baltimore longitudinal study of aging. *Cancer Epidemiology, Biomarkers & Prevention*, **14**, 390-396.
- [74] Andrews J, Djakiew D, Krygier S, Andrews P. (2002) Superior effectiveness of ibuprofen compared with other NSAIDs for reducing the survival of human prostate cancer cells. *Cancer Chemotherapy and Pharmacology*, **50**, 277-284.
- [75] (a) Kim MH, Chung J. (2007) Synergistic cell death by EGCG and ibuprofen in DU-145 prostate cancer cell line. *Anticancer Research*, **27**, 3947-3956; (b) Kim MH. (2008) Protein phosphatase 1 activation and alternative splicing of Bcl-X and Mcl-1 by EGCG + ibuprofen. *Journal of Cellular Biochemistry*, **104**, 1491-1499.
- [76] Kobalka Andrew J, Keck Rick W, Jankun J. (2015) Synergistic anticancer activity of biologicals from green and black tea on DU 145 human prostate cancer cells. *Central-European Journal of Immunology*, **40**, 1-4.
- [77] Gray AL, Stephens CA, Bigelow RL, Coleman DT, Cardelli JA. (2014) The polyphenols (-)-epigallocatechin-3-gallate and luteolin synergistically inhibit TGF-beta-induced myofibroblast phenotypes through RhoA and ERK inhibition. *PLoS One*, **9**, e109208.
- [78] Lin Y, Shi R, Wang X, Shen H-M. (2008) Luteolin, a flavonoid with potential for cancer prevention and therapy. *Current Cancer Drug Targets*, **8**, 634-646.
- [79] Zhou Q, Yan B, Hu X, Li X-B, Zhang J, Fang J. (2009) Luteolin inhibits invasion of prostate cancer PC3 cells through E-cadherin. *Molecular Cancer Therapeutics*, **8**, 1684-1691.
- [80] Siddiqui IA, Malik A, Adhami VM, Asim M, Hafeez BB, Sarfaraz S, Mukhtar H. (2008) Green tea polyphenol EGCG sensitizes human prostate carcinoma LNCaP cells to TRAIL-mediated apoptosis and synergistically inhibits biomarkers associated with angiogenesis and metastasis. *Oncogene*, **27**, 2055-2063.
- [81] Stearns Mark E, Wang M. (2011) Synergistic effects of the green tea extract epigallocatechin-3-gallate and taxane in eradication of malignant human prostate tumors. *Translational Oncology*, **4**, 147-156.
- [82] Stearns ME, Amatangelo MD, Varma D, Sell C, Goodyear SM. (2010) Combination therapy with epigallocatechin-3-gallate and doxorubicin in human prostate tumor modeling studies inhibition of metastatic tumor growth in severe combined immunodeficiency mice. *American Journal of Pathology*, **177**, 3169-3179.
- [83] Hagen RM, Chedea VS, Mintoff CP, Bowler E, Morse HR, Ladomery MR. (2013) Epigallocatechin-3-gallate promotes apoptosis and expression of the caspase 9a splice variant in PC3 prostate cancer cells. *International Journal of Oncology*, **43**, 194-200.
- [84] Huang L, Kirschke Catherine P, Zhang Y. (2006) Decreased intracellular zinc in human tumorigenic prostate epithelial cells: a possible role in prostate cancer progression. *Cancer Cell International*, **6**, 10.
- [85] Sun S-I, He G-Q, Yu H-N, Yang J-G, Borthakur D, Zhang L-C, Shen S-R, Das UN. (2008) Free Zn²⁺ enhances inhibitory effects of EGCG on the growth of PC-3 cells. *Molecular Nutrition & Food Research*, **52**, 465-471.

***Ligustrum lucidum* and its Constituents : A Mini-Review on the Anti-Osteoporosis Potential**

Chun-Tao Che^{a,*} and Man-Sau Wong^b

^aDepartment of Medicinal Chemistry and Pharmacognosy, College of Pharmacy, University of Illinois at Chicago, Chicago, Illinois 60612, USA

^bDepartment of Applied Biology and Chemical Technology, The Hong Kong Polytechnic University, Hong Kong

chect@uic.edu

Received: September 17th, 2015; Accepted: September 26th, 2015

Osteoporosis is a metabolic bone disorder commonly occurred in aging populations, particularly postmenopausal women and patients who undergo long-term steroid or anti-estrogen therapies. Given the rapid growth of the aging population, the prevalence of bone loss, and the huge medical and healthcare cost involved, demand for alternative approaches for the promotion of bone health is pressing. With the advent of global interest in complementary and alternative medicine and natural products, Chinese medicine serves as a viable source that offers benefits to improve and maintain bone health. This review summarizes the scientific information on the Chinese medicinal herb *Ligustrum lucidum* and its chemical components as potential therapy for osteoporosis.

Keywords: *Ligustrum lucidum*, Ligustri Lucidi Fructus, Nu-Zhen-Zi, Osteoporosis, Anti-osteoporotic activity, Bone health.

Osteopenia (low bone density) and osteoporosis ("porous bone") are metabolic bone disorders commonly occurred in aging populations, particularly postmenopausal women and patients who undergo long-term steroid or anti-estrogen therapies. Although postmenopausal women are at greater risk, osteopenia/osteoporosis can strike at any age of both genders. The disease is characterized by thinning of bones, with reduction in bone mass and bone mineral density, as well as microarchitectural deterioration of the bone tissue due to depletion of calcium and bone protein. The clinical result is loss of bone strength, thus making bone more fragile and vulnerable to fracture, which often happens in the hip, spine, and wrist. Worldwide, osteoporosis is estimated to affect 200 million women, approximately one-tenth of women aged 60 and one-fifth of women aged 70 [1]. Although the overall prevalence of fragility fractures is higher in women, men generally have higher rates of fracture related mortality. The National Osteoporosis Foundation projected that by 2020, 14 million Americans over the age of 50 are expected to have osteoporosis and another 47 million to have low bone mass, accounting for 55% of the population 50 years of age and older [2].

A comprehensive bone health management plan usually includes non-pharmacologic measures such as balanced diet, adequate calcium and vitamin D intake, exercise and fall prevention, together with pharmacologic therapy [3]. For osteoporosis prevention and treatment, less than ten FDA-approved drugs are currently available. They fall into two major classes, the anti-resorptive and the anabolic drugs. Anti-resorptive medications such as the bisphosphonates (alendronate, ibandronate, risedronate, and zoledronic acid), calcitonin, denosumab (a receptor activator of nuclear factor- κ B ligand [RANKL] inhibitor), selective estrogen receptor modulator (raloxifene), and estrogen (with or without progesterone) slow down the process of bone loss; and the anabolic drug such as the recombinant form of parathyroid hormone (teriparatide) enhances bone formation [4-6]. However, the long-term safety of many of these anti-osteoporosis drugs has posted some concerns; for example, potentially serious adverse effects of bisphosphonate therapy have been reported [7-12]. Only a small number of investigational drugs are currently in the pipeline of development [13, 14].

Apart from drug therapy, hormone replacement therapy is effective in increasing bone density and reducing the risk of fracture, and it is an effective regimen for the prevention and treatment of postmenopausal osteoporosis. Nevertheless, the use of estrogenic hormones has been severely limited by concerns for the increased risk of breast, endometrial and ovarian cancers, heart attack, and stroke [15]. Dietary supplementation of calcium and vitamin D is often included as part of the treatment plan, yet calcium and vitamin D alone or in combination are ineffective in reducing fractures in the absence of pharmacologic agents [16, 17].

Studies in Canada [18] and Australia [19] indicated that over 50% of osteoporosis patients go for complementary and alternative medicines, with up to 10% seeking treatment from herbal therapy or Chinese medicine. Soy isoflavone [20-23], red clover [24] and black cohosh [25] are commonly used by postmenopausal women with or without osteoporosis. Indeed, botanicals prepared as dietary supplements hold promise for use and there is considerable interest because the general population is receptive to the use of natural products for long-term treatment, and the cost for dietary supplements is more affordable to the elderly population.

The dried fruit of *Ligustrum lucidum* Ait. (Oleaceae), known in herbal medicine as "Ligustri Lucidi Fructus" and in Chinese medicine as "Lu-Zhen-Zi", is a tonic drug ("good-for-health") often included in herbal prescriptions for vitalizing the "liver and kidney" functions as well as nourishing the "Yin component" in these organs. It is indicated for "weakness of the loin and knees" [26], which may represent a symptom of bone deterioration. Indeed, the Chinese medical theory states that "the kidney serves to strengthen the bone" [27] and, therefore, the use of *Lucidum* fruits as a kidney-tonifying agent among the elderly to improve skeletal strength is supported by substantial ethnomedical evidence.

To the best of our knowledge, the first reports on the osteoprotective activity of *L. lucidum* were published by Zhang *et al.* [28, 29]. In the studies, an extract of *L. lucidum* fruits was given to three-month-old ovariectomized rats four weeks after surgical operation and continued for fourteen weeks. Results showed that

both bone turnover and calcium balance were improved. Thus, treatment with the plant extract suppressed bone turnover markers such as serum osteocalcin and urinary deoxypyridinoline. It also decreased urinary and fecal calcium excretion as well as increased the bone calcium content. In addition, the mRNA expressions of renal calbindin-D9K and calbindin-D28K were up-regulated. These findings suggested the involvement of both vitamin D metabolism and calcium reabsorption. Indeed, in aged (eleven-month old) female rats treated with the ethanol extract of *L. lucidum* fruits, serum levels of 1,25-dihydroxyvitamin D₃ and the mRNA expression of duodenal calcium binding protein CaBP-9k were increased; renal CaBP-28K mRNA expression was also up-regulated [30]. In a study to investigate whether the plant extract could improve bone properties in aged animals, both sham- and ovariectomized ten-month-old female rats were treated with the extract for 12 weeks, at three levels of dietary calcium contents. The *L. lucidum* extract significantly improved bone mineral density and content at tibial and femoral diaphysis as well as the lumbar vertebrae (LV-2) in rats fed with diets containing either low calcium (0.1%) or medium calcium (0.6%) level; the biomechanical strength of the tibial diaphysis was also improved [31]. In a similar experiment, eight-week treatment in ovariectomized aged rats also prevented the loss of bone mineral density [32].

In a retinoic acid-induced osteoporosis rat model, treatment with *L. lucidum* led to an increase of serum calcium and phosphorus contents, together with lowered alkaline phosphatase and tartrate-resistant acid phosphatase levels, as well as improved bone microarchitecture [33].

When the osteoblast-like UMR-106 cells were treated with the plant extract, increased formation of calcified matrix and increased extracellular calcium and phosphorus deposition were observed. These results suggested that *L. lucidum* extract could improve bone properties possibly via the enhancement of differentiation and mineralization of osteoblasts [31]. Indeed, *in vitro* study using human bone marrow mesenchymal stem cells treated with an ethanol extract of *L. lucidum* displayed stimulatory activity on osteogenic differentiation, evidenced by an increase in alkaline phosphatase activity and shortening of time needed for mineralization. The mRNA expressions of osteoblast differentiation regulatory genes involved in the Wnt signaling, such as β -catenin, bone morphogenetic protein (BMP)-2, cyclin D1, MT1-MMP, osteoprotegerin (OPG) and TBX3, were up-regulated, thus enhancing osteogenesis [34]. The aqueous extract of the same plant materials also demonstrated promoting effects on both human and rat mesenchymal stem cells as shown by enhanced alkaline phosphatase activity, mineralization level, and the expression of osteopontin [35]. In osteoblast-like MC3T3-E1 cells, an extract of *L. lucidum* increased cell viability and promoted cell differentiation by up-regulating the OPG and RANKL mRNA and protein expressions [36].

The improved calcium balance after treatment was found to associate, at least in part, with an increase of circulating levels of 1,25-dihydroxyvitamin D₃ via up-regulating the 25-hydroxyvitamin D 1 α -hydroxylase activity [37]. At the same time, the renal mRNA expression of 25-hydroxyvitamin D 24-hydroxylase was suppressed [38]. These findings suggested that the protective effects of the ethanol extract on bone could be accounted for by its direct actions on the vitamin D system, including the biosynthesis of 1,25-dihydroxyvitamin D₃ and the expression of vitamin D-dependent calcium transport protein expression. In a subsequent study, the plant extract was separated into ethyl acetate-soluble and water-soluble fractions by solvent extraction. The results indicated that the

Table 1: Secondary metabolites in the fruit of *Ligustrum lucidum* known prior to 2011 (Adopted and translated based on the information available in [44])

Compound
PHENYLETHANOIDS
Salidroside
TRITERPENOIDS
α -Amyrin
β -Amyrin
Betulin
3-O-Acetyl-12-hydroxydammar-24-ene
(20S)-3-O-Acetyl-dammar-24-en-3 β ,20-diol
3-O-Acetyl- 20,25-epoxydammaren-3 β ,24 α -diol
(20S,24R)-3-O-Acetyl-24-hydroperoxydammar-25-en-3 β ,20-diol
3 β ,12-Dihydroxydammar-24-ene
20,25-Epoxydammaren-3 β ,24 α -diol
(20S)-25-Hydroperoxydammar-23(E)-en-3 β ,20-diol
3 β -O-Palmitoyl-dammar-24-en-12-ol
Fouquierol
Ligustrin
Lupeol
Ocotillo II 3-O-palmitate
Oleanolic acid
Oleanolic acid 3-acetate
Oleanolic acid ethyl acetate
2 α -Hydroxyoleanolic acid
2 α -Hydroxy-3 β -O-(trans-p-coumaroyl)-oleanolic acid
Oliganthas A
Tomentic acid
Ursolic acid
Ursolic acid 3-acetate
3-O-Acetyl-19-hydroxyursolic acid
2 α -Hydroxyursolic acid
3 β -Hydroxyursolic acid ethyl ester
α -Ursonic acid methyl ester
SECOIRIDOIDS
Ligustroside
10-Hydroxyligustroside
Ligustrosidic acid
Ligustuloside A
Ligustuloside B
Lucidumoside A
Lucidumoside B
Nu(e)zhenide
10-Hydroxynuzhenide
Nuezhenide acid
Nuezhenegalaside
Isonuezhenide
Neonuezhenide
Oleoside dimethyl ester
Oleoside 7- β -D-glucosyl-11-methyl diester
10-Hydroxyoleoside 7,11-dimethyl ester
Oleuropein
10-Hydroxyoleuropein
Oleuropeinic acid
Specnuezhenide
FLAVONOIDS
Apigenin
Apigenin 7-O- β -D-glucopyranoside
Apigenin 7-O-(6 \prime -acetyl)- β -D-glucopyranoside
Apigenin-7-O- β -D-rutinoside
Cosmosin
Eriodictyol
Kaemotrol
Luteolin
Luteolin 7-O- β -D-glucopyranoside
Quercetin
Taxifolin

water fraction inhibited urinary and fecal calcium excretion in mature female rats. However, it is noteworthy that the enhancement of calcium absorption by the water fraction was not associated with an increase in serum 1,25-dihydroxyvitamin D₃ levels, but serum parathyroid hormone levels [39].

Apart from the aged and/or ovariectomized animals, the extract of *L. lucidum* was found to benefit bone mass acquisition during early life of the animals. Thus, when an ethanol extract of *L. lucidum* was given to one-month old male and female rats for 4 months, improvements in bone mineral density, bone microarchitecture and bone mechanical properties were observed (compared with control).

Table 2: Additional secondary metabolites found in the fruit of *Ligustrum lucidum*

Compound	Reference
PHENYLETHANOIDS	
Acteoside (verbacoside)	[59]
Cimiduhurinine	[60]
2-(3,4-Dihydroxyphenyl)-ethanol	[60]
2-(3,4-Dihydroxyphenyl)-ethyl-O- β -D-glucopyranoside	[60]
Osmanthuside H	[60]
Tyrosol	[59, 61]
Tyrosol acetate	[61]
Hydroxytyrosol	[59, 61]
TRITERPENOIDS	
Crataegolic acid	[60]
Dammarenediol-II	[60]
Dammarenediol-II 3-O-palmitate	[60]
(20S)-Dammar-23-en-3 β ,20,25-triol	[62]
(20S,24R) 24-Hydroperoxydammar-25-en-3 β ,20-diol	[62]
(20S,24R) 3-O-Acetyl-24-hydroperoxydammar-25-en-3 β ,20-diol	[62]
(20S,24R)-24-Hydroperoxydammar-25-en-3 β ,20-diol	[60]
3-O-cis-p-Coumaroylmaslinic acid	[63]
3-O-trans-p-Coumaroylmaslinic acid	[63]
Oleanolic acid methyl ester	[63]
3-Keto-oleanolic acid	[63]
Oliganthas A	[60]
19 α -Hydroxyursolic acid	[63]
19 α -Hydroxyursolic acid 3-acetate	[63]
SECOIRIDOIDS	
p-Hydroxyphenethyl 7- β -D-glycosylelenolic acid ester	[64]
1'''-O- β -D-glucosylformoside	[65]
Gl 3	[59, 61, 65, 66]
Jaspolyside methyl ester	[66]
6'-O-trans-Cinnamoyl-8-epikingisidic acid	[67]
6'-O-cis-Cinnamoyl-8-epikingisidic acid	[67]
Liguside A	[65]
Liguside B	[65]
Isoligustrosidic acid	[67]
8(Z)-Nuezhenide A	[65]
Nuzhenal A	[67]
Nuzhenal B	[67]
Oleouezhenide	[65, 66]
Oleopolynezhenide	[67]
Iso-oleouezhenide	[66]
Nicotiflorine	[64]
6'''-Acetylnicotiflorine	[64]
6'-Elenolylnicotiflorine	[64]
Oleonin	[68]
Methyloleoside 7-ethyl ester	[66]
Oleoside 11-methyl ester	[64]
Oleoside7-ethyl-11-methyl diester	[64]

In addition, *L. lucidum* treatment increased bone formation marker osteocalcin (OCN), decreased the bone-resorbing marker CTX-1, while increasing serum 25-hydroxyvitamin D₃. The vitamin D metabolism- and calcium absorption-related gene expressions (1 α -vitamin D hydroxylase, vitamin D receptor, calcium transporter calbindin-D9K, and transient receptor potential vanilloid 6) were up-regulated. These results suggested that the extract had beneficial effects on peak bone mass acquisition during early life of the animals and the improvement of bone mechanical properties by favoring calcium metabolism [40, 41].

In diabetic mice, feeding with an aqueous extract of *L. lucidum* was found to protect against excessive urinary calcium excretion and trabecular bone deterioration. The underlying mechanism might be attributed to the regulation of duodenal calcium transporting proteins and renal calcium-sensing receptor [42].

The volatile oil obtained from *L. lucidum* fruits exhibited *in vitro* osteoblastic activity by stimulating the proliferation and alkaline phosphatase activity of rat calvarial osteoblasts [43]. The main components in the volatile oil included (Z,Z)-9,12-octadecadienoic acid, *n*-hexadecanoic acid, (E)-9-octadecenoic acid, α -cadinol, 4-hexyl-2,5-dihydro-2,5-dioxo-3-furanacetic acid, and (E)-8-octadecenoic acid methyl ester [43]. A number of phenylethanoids, secoiridoids, flavonoids and triterpenoids have been identified from

Table 3: Osteo-active secondary metabolites in the fruit of *Ligustrum lucidum*.

Compound	Biological activity	Reference
PHENYLETHANOIDS		
Tyrosol (3)	Protect UMR-106 cells against H ₂ O ₂ -induced injury	[59]
Hydroxytyrosol (4)	Increase alkaline phosphatase activity in UMR-106 cells; Protect UMR-106 cells against H ₂ O ₂ -induced injury	[59, 61]
Salidroside (5)	Promote UMR-106 cell proliferation; Increase alkaline phosphatase activity in UMR-106 cells	[59, 61]
Acteoside (6)	Promote UMR-106 cell proliferation; Increase alkaline phosphatase activity in UMR-106 cells	[59]
SECOIRIDOIDS		
Oleoside dimethyl ester (7)	Promote UMR-106 cell proliferation	[61]
Oleoside7-ethyl-11-methyl diester (8)	Promote UMR-106 cell proliferation	[61]
Oleuropein (9)	Promote UMR-106 cell proliferation; Increase alkaline phosphatase activity in UMR-106 cells	[59]
Nu(e)zhenide (10)	Promote UMR-106 cell proliferation; Increase alkaline phosphatase activity in UMR-106 cells	[61]
Specneuzhenide (11)	Promote UMR-106 cell proliferation; Increase alkaline phosphatase activity in UMR-106 cells	[59]
G13 (12)	Promote UMR-106 cell proliferation; Increase alkaline phosphatase activity in UMR-106 cells	[59, 61]
FLAVONOIDS		
Luteolin 7-O- β -D-glucopyranoside (13)	Promote UMR-106 cell proliferation; Increase alkaline phosphatase activity in UMR-106 cells	[59]
Apigenin (14)	Promote UMR-106 cell proliferation; Increase alkaline phosphatase activity in UMR-106 cells; Protect UMR-106 cells against H ₂ O ₂ -induced injury	[59]
Apigenin 7-O- β -D-glucopyranoside (15)	Promote UMR-106 cell proliferation; Increase alkaline phosphatase activity in UMR-106 cells; Protect UMR-106 cells against H ₂ O ₂ -induced injury	[59]
Apigenin 7-O-acetyl- β -D-glucopyranoside (16)	Promote UMR-106 cell proliferation; Increase alkaline phosphatase activity in UMR-106 cells	[59]

the fruit of *L. lucidum* and they were summarized in several review articles [44-47]. Since most of these review articles were published in the Chinese language, the chemical ingredients as highlighted by Huang and Wang [44] are listed in Table 1.

In recent years, further phenylethanoids, triterpenoids and secoiridoids have been reported and they are included in Table 2. Several ingredients of *L. lucidum* fruits have been demonstrated to display potential anti-osteoporosis activities in cell-based and/or animal models. Thus, oleanolic acid (1) and its glycosidic and synthetic derivatives have been known to be inhibitors of osteoclast formation [48-51]. They inhibited the formation of osteoclast-like multinucleated cells induced by 1 α , 25-dihydroxyvitamin D₃. Oleanolic acid acetate was demonstrated to inhibit receptor activator of nuclear factor- κ B (RANKL)-induced osteoclast differentiation; and it attenuated lipopolysaccharide-induced bone erosion in mice [52]. Apart from the anti-osteoclastogenic activity, oleanolic acid was found to be able to promote osteoblastic differentiation and change the gene expression profile of bone marrow stromal cells obtained from rats with corticosterone-induced osteoporosis [53]. In ovariectomized rats, oleanolic acid exerted osteoprotective effect by increasing the population of osteoblasts as well as the levels of osteocalcin and the Runt-related protein-2. It also stimulated the osteoblastic differentiation of bone mesenchymal stem cells *in vitro*. Gene expression profile analysis suggested that the effect might be related to the Notch signaling pathway [54].

Another triterpene ingredient of *L. lucidum*, ursolic acid (**2**), has been found to stimulate osteoblast differentiation and mineralization by activating osteoblast-specific genes such as mitogen-activated protein kinases, nuclear factor- κ B, and activator protein-1 [55]. It also promoted bone formation in a mouse calvarial bone formation model [55]. In addition, recent studies showed that ursolic acid was able to inhibit RANKL-induced osteoclast differentiation [56-58] and down-regulate the NFATc1-regulated osteoclast marker genes [58]. Using a mouse model of titanium particle-induced osteolysis, ursolic acid protected calvarial bone loss and decreased the population of tartrate-resistant acid phosphatase (TRAP)-positive osteoclasts [58].

Two screening and bioactivity-guided isolation reports on the osteoprotective activity of *L. lucidum* have identified fourteen active compounds [59, 61]. While the screening results are considered to be preliminary at this time, the active compounds were found to promote the proliferation of osteoblast-like UMR-106 cells, increase the alkaline phosphatase activity, and/or protect the cells from hydrogen peroxide-induced damage (Table 3). The chemical structures of these osteo-active compounds are shown in Figure 1.

Among the four active phenylethanoids, tyrosol (**3**) and hydroxytyrosol (**4**) are also present in olive oil [69-71], which has been reported to possess anti-osteoporosis property when tested in ovariectomized rats [72]. Salidroside (**5**) is a major bioactive ingredient of *Rhodiola* plants and is well known for its adaptogenic potential for use in high-altitude environment [73, 74]. The inhibitory effect of this compound on diabetes-related osteoporosis has been described [75]. Acteoside (**6**), also known as verbascoside, is a phenylethanoid glycoside possessing pharmacologically beneficial properties such as antioxidant, anti-inflammatory, antitumor, and neuroprotective activities [76, 77].

For the secoiridoids, oleuropein (**9**) is also present in olive oil [69-71]. Together with the phenylethanoids, it is considered to be the active principle. The structure of specnuezhenide (**11**) differs from nu(e)zhenide (**10**) by replacing the glucose with galactose. Both compounds were demonstrated to possess proliferative activity in the osteoblast-like UMR-106 cells and they enhanced the alkaline phosphatase activity [59, 61]. Compound GI 3 (**12**) can be considered as a dimeric derivative of nu(e)zhenide; it displayed similar *in vitro* activities. It is noteworthy that nu(e)zhenide (**10**), specnuezhenide (**11**) and GI 3 (**12**) contain the salidroside moiety in their structures. It will, therefore, be of interest to determine whether the salidroside portion of the molecule acts as a pharmacophore for the osteoprotective activity.

The flavonoids apigenin (**14**) and two glucoside derivatives (**15** and **16**), as well as luteolin 7- O - β -D-glucopyranoside (**13**), were found to be active in UMR-106 cells [59, 61].

All in all, available information strongly suggests that the fruit of *Ligustrum lucidum* possesses osteoprotective property and it may be useful in promoting bone health. The beneficial effects seem to be associated with improved calcium balance, modulation of vitamin D metabolism, as well as osteoblastogenic and anti-osteoclastogenic activities. Yet the exact mechanisms remain to be elucidated. Further studies on the potentials of this plant drug and its chemical ingredients for use in the improvement of age-related changes in calcium homeostasis and development of anti-osteoporosis remedies are warranted.

Acknowledgments – The authors thank Professor Xin-Sheng Yao (Jinan University, Guangzhou, China) and Professor Ping Chung Leung (the Chinese University of Hong Kong) for collaboration on the studies of bone health. The skillful assistance of Dr Xiaoli Dong (Hong Kong Polytechnic University) and Dr Ming Zhao (the Chinese University of Hong Kong) in carrying out the experimental studies of *Ligustrum lucidum* is acknowledged.

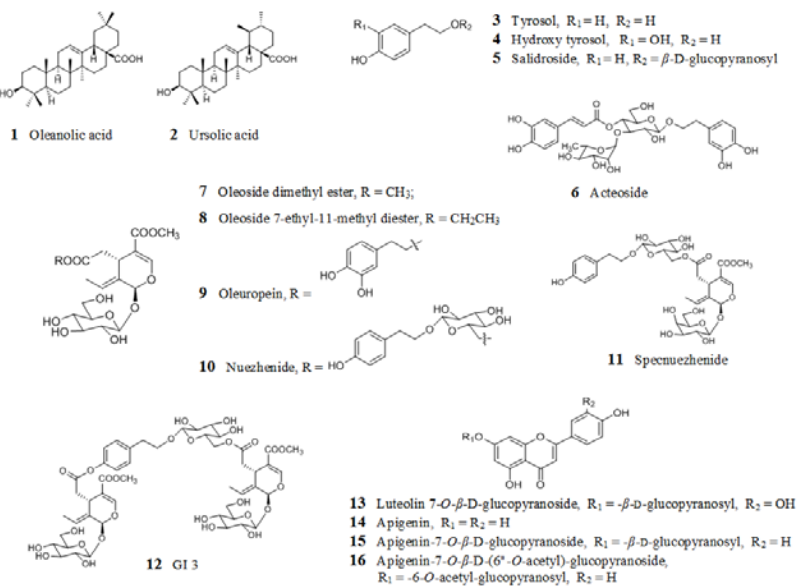


Figure 1: Chemical structures of osteo-active compounds from *Ligustrum lucidum* fruits.

References

- [1] Anon. (2015) International Osteoporosis Foundation: Facts and statistics about osteoporosis and its impact. International Osteoporosis Foundation.
- [2] Anon. (2015) National Osteoporosis Foundation Prevalence Report. National Osteoporosis Foundation.
- [3] Tella SH, Gallagher JC. (2014) Prevention and treatment of postmenopausal osteoporosis. *Journal of Steroid Biochemistry and Molecular Biology*, **142**, 155-170.

- [4] Sandhu SK, Hampson G. (2011) The pathogenesis, diagnosis, investigation and management of osteoporosis. *Journal of Clinical Pathology*, **64**, 1042-1050.
- [5] Sweet MG, Sweet JM, Jeremiah MP, Salazka SS. (2009) Diagnosis and treatment of osteoporosis. *American Family Physician*, **79**, 193-200.
- [6] Rachner TD, Kholas S, Hofbauer LC. (2011) Osteoporosis: now and the future. *Lancet*, **377**, 1276-1287.
- [7] Hollick RJ, Reid DM. (2011) Role of bisphosphonates in the management of postmenopausal osteoporosis: an update on recent safety anxieties. *Menopause International*, **17**, 66-72.
- [8] Park-Wyllie LY, Mamdani MM, Juurlink DN, Hawker GA, Gunraj N, Austin PC, Whelan DB, Weiler PJ, Laupacis A. (2011) Bisphosphonate use and the risk of subtrochanteric or femoral shaft fracture in older women. *The Journal of the American Medical Association*, **305**, 783-789.
- [9] Lewiecki EM. (2011) Safety of long-term bisphosphonate therapy of the management of osteoporosis. *Drugs*, **71**, 791-814.
- [10] Watts NB, Diab DL. (2010) Long-term use of bisphosphonates in osteoporosis. *Journal of Clinical Endocrinology and Metabolism*, **95**, 1555-1565.
- [11] Kos M. (2011) Bisphosphonates promote jaw osteonecrosis through facilitating bacterial colonization. *Medical Hypotheses*, **77**, 214-215.
- [12] Knopp-Sihota JA, Cummings GG, Homik J, Voaklander D. (2013) The association between serious upper gastrointestinal bleeding and incident bisphosphonate use: a population-based nested cohort study. *BMC Geriatrics*, **13**, 36.
- [13] Honig S. (2010) Osteoporosis, new treatment and updates. *Bulletin of the New York University Hospital for Joint Diseases*, **68**, 166-170.
- [14] Silva BC, Bilezikian JP. (2011) New approaches to the treatment of osteoporosis. *Annual Review of Medicine*, **62**, 307-322.
- [15] Bowring CE, Francis RM. (2011) National Osteoporosis Society's position statement on hormone replacement therapy in the prevention and treatment of osteoporosis. *Menopause International*, **17**, 63-65.
- [16] Spangler M, Phillips BB, Ross MB, Moores KG. (2011) Calcium supplementation in postmenopausal women to reduce the risk of osteoporotic fractures. *American Journal of Health-System Pharmacy*, **68**, 309-318.
- [17] Quesada-Gomez JM, Blanch-Rubio J, Diaz-Curiel M, Diez-Perez A. (2011) Calcium citrate and vitamin D in the treatment of osteoporosis. *Clinical Drug Investigation*, **31**, 285-298.
- [18] Chong CA, Diaz-Granados N, Hawker GA, Jamal S, Josse RG, Cheung AM. (2007) Complementary and alternative medicine use by osteoporosis clinic patients. *Osteoporosis International*, **18**, 1547-1556.
- [19] Mak JCS, Faux S. (2010) Complementary and alternative medicine use by osteoporotic patients in Australia (CAMEO-A): a prospective study. *Journal of Alternative and Complementary Medicine*, **16**, 579-584.
- [20] Newton KM, Grady D. (2011) Soy isoflavones for prevention of menopausal bone loss and vasomotor symptoms. *Archives in Internal Medicine*, **171**, 1369-1370.
- [21] Levis S, Strickman-Stein N, Ganjei-Azar P, Xu P, Doerge DR, Krischer J. (2011) Soy isoflavones in the prevention of menopausal bone loss and menopausal symptoms. A randomized, double-blind trial. *Archives in Internal Medicine*, **171**, 1363-1369.
- [22] Taku K, Melby MK, Nishi N, Omori T, Kurzer MS. (2011) Soy isoflavones for osteoporosis: An evidence-based approach. *Maturitas*, **70**, 333-338.
- [23] Castelo-Branco C, Cancelo-Hidalgo MJ. (2011) Isoflavones: effects on bone health. *Climacteric*, **14**, 204-211.
- [24] Lethaby LE, Marjoribanks J, Kronenberg F, Roberts H, Eden J. (2013) Phytoestrogens for menopausal vasomotor symptoms. *Cochrane Database of Systematic Reviews*, (12):CD001395.
- [25] Depypere HT, Comhaire FH. (2014) Herbal preparation for the menopause: Beyond isoflavones and black cohosh. *Maturitas*, **77**, 191-194.
- [26] Anon. (2010) Ligustri Lucidi Fructus. In *Chinese-Pharmacopoeia, 2010 Chinese Edition, Part 1*, Chinese Medical and Pharmaceutical Press, Beijing (China), p. 43.
- [27] Kong YC. (2010) *Huangdi Neijing: a synopsis with commentaries*, The Chinese University Press, Hong Kong, p.131.
- [28] Zhang Y, Lai WP, Leung PC, Wu CF, Yao XS, Wong MS. (2006) Effects of Fructus Ligustri Lucidi extract on bone turnover and calcium balance in ovariectomized rats. *Biological Pharmaceutical Bulletin*, **29**, 291-296.
- [29] Zhang Y, Huang W, Chen B, Leung PC, Wu CF, Yao XS. (2006) Effect of Fructus Ligustri Lucidi on calcium metabolism and vitamin D-dependent gene expressions in ovariectomized rats. *Zhongcaoyao*, **37**, 558-561.
- [30] Zhang Y, Lai WP, Leung PC, Che CT, Wong MS. (2008) Improvement of Ca balance by Fructus Ligustri Lucidi extract in aged female rats. *Osteoporosis International*, **19**, 235-242.
- [31] Zhang Y, Leung PC, Che CT, Chow HK, Wu CF, Wong MS. (2008) Improvement of bone properties and enhancement of mineralization by ethanol extract of Fructus Ligustri Lucidi. *British Journal of Nutrition*, **99**, 494-502.
- [32] Ko CH, Siu WS, Lau CP, Lau CBS, Fung KP, Leung PC. (2010) Osteoprotective effects of Fructus Ligustri Lucidi aqueous extract in aged ovariectomized rats. *Chinese Medicine*, **5**, 39.
- [33] Kang X, Li Z, Zhang WH, Zhou Q, Liu RH, Wang XJ. (2013) Study on the effect of combination of Epimedii Folium and Ligustri Lucidi Fructus on osteoporosis rats induced by retinoic acid. *Zhongguo Zhongyao Zazhi*, **38**, 4124-4128.
- [34] Li G, Zhang XA, Zhang JF, Chan CY, Yew DTW, He ML, Lin MCM, Leung PC, Kung HF. (2010) Ethanol extract of Fructus Ligustri Lucidi promotes osteogenesis of mesenchymal stem cells. *Phytotherapy Research*, **24**, 571-576.
- [35] Li G, Chan CY, Zhang JF, Zhang XA, Yew DTW, He ML, Lin MCM, Leung PC, Kung HF. (2008) The aqueous extract of Fructus Ligustri Lucidi regulates the differentiation of mesenchymal stem cells. *International Journal of Integrative Biology*, **3**, 182-190.
- [36] Li Q, Fan YS, Gao ZQ, Fan K, Liu ZJ. (2015) Effect of Fructus Ligustri Lucidi on osteoblastic like cell-line MC3T3-E1. *Journal of Ethnopharmacology*, **170**, 88-95.
- [37] Dong XL, Zhang Y, Favus MJ, Che CT, Wong MS. (2010) Ethanol extract of Fructus Ligustri Lucidi increases circulating 1,25-dihydroxyvitamin D3 by inducing renal 25-hydroxyvitamin D-1alpha hydroxylase activity. *Menopause*, **17**, 1174-1181.
- [38] Zhang Y, Dong XL, Leung PC, Che CT, Wong MS. (2008) Fructus Ligustri Lucidi extract improves calcium balance and modulates the calcitropic hormone level and vitamin D-dependent gene expression in aged ovariectomized rats. *Menopause*, **15**, 558-565.
- [39] Dong XL, Zhao M, Wong KK, Che CT, Wong MS. (2012) Improvement of calcium balance by Fructus Ligustri Lucidi extract in mature female rats was associated with the induction of serum parathyroid hormone levels. *British Journal of Nutrition*, **108**, 92-101.
- [40] Lyu Y, Feng X, Zhao P, Wu Z, Xu H, Fang Y, Hou Y, Denney L, Xu Y, Feng H. (2014) Fructus Ligustri Lucidi ethanol extract increases bone mineral density and improves bone properties in growing female rats. *Journal of Bone Mineral Metabolism*, **32**, 616-626.
- [41] Feng X, Ying L, Wu Z, Fang Y, Xu H, Zhao P, Xu Y, Feng H. (2014) Fructus ligustri lucidi ethanol extract improves bone mineral density and properties through modulating calcium absorption-related gene expression in kidney and duodenum of growing rats. *Calcified Tissue International*, **94**, 433-441.
- [42] Zhang Y, Diao TY, Wang L, Che CT, Wong MS. (2014) Protective effects of water fraction of Fructus Ligustri Lucidi extract against hypercalcemia and trabecular bone deterioration in experimentally type 1 diabetic mice. *Journal of Ethnopharmacology*, **158 (Pt A)**, 239-245.
- [43] Wu YB, Lin XH, Wu JG, Yi J, Zheng YZ, Wu JZ. (2011) Volatile components of fruits of *Ligustrum lucidum* Ait. stimulate proliferation and differentiation of rat calvarial osteoblasts. *African Journal of Biotechnology*, **10**, 8662-8668.
- [44] Huang XP, Wang WC. (2011) Chemical constituents of *Ligustrum lucidum* fruits: research advances. *Guoji Yaoxue Yanjiu Zazhi*, **38**, 47-51.
- [45] Zhao L, Feng Y. (2012) Advances in research on triterpenoids and iridoids of Ligustri Lucidi Fructus. *Guangdong Yaoxueyuan Xuebao*, **28**, 107-110.

- [46] Zhang J, Wang X, Deng Z, Li X. (2013) Advances in research on chemical components and pharmacological effects of Chinese medicine *Ligustrum lucidum* fruit. *Xiandai Zhongxiyi Jiehe Zazhi*, **22**, 4100-4101.
- [47] Gao L, Li CY, Wang Z, Liu X, You Y, Wei H, Guo T. (2015) Ligustrum Lucidi Fructus as a traditional Chinese medicine: a review of its phytochemistry and pharmacology. *Natural Products Research*, **29**, 493-510.
- [48] Li JX, Hareyama T, Tezuka Y, Zhang Y, Miyahara T, Kadota S. (2005) Five new oleanolic acid glycosides from *Achyranthes bidentata* with inhibitory activity on osteoclast formation. *Planta Medica*, **71**, 673-679.
- [49] Zhang Y, Li JX, Zhao J, Wang SZ, Pan Y, Tanaka K, Kadota S. (2005) Synthesis and activity of oleanolic acid derivatives, a novel class of inhibitors of osteoclast formation. *Bioorganic and Medicinal Chemistry Letters*, **15**, 1629-1632.
- [50] Li JF, Zhao YJ, Cai MM, Li XF, Li JX. (2009) Synthesis and evaluation of a novel series of heterocyclic oleanolic acid derivatives with anti-osteoclast formation activity. *European Journal of Medicinal Chemistry*, **44**, 2796-2806.
- [51] Li JF, Chen SJ, Zhao Y, Li JX. (2009) Glycoside modification of oleanolic acid derivatives as a novel class of anti-osteoclast formation agents. *Carbohydrate Research*, **344**, 599-605.
- [52] Kim JY, Cheon YH, Oh HM, Rho MC, Erkhembaatar M, Kim MS, Lee CH, Kim JJ, Choi MK, Yoon KH, Lee MS, Oh J. (2014) Oleanolic acid acetate inhibits osteoclast differentiation by downregulating PLCgamma2-Ca(2+)-NFATc1 signaling and suppresses bone loss in mice. *Bone*, **60**, 104-111.
- [53] Bian Q, Huang JH, Yang Z, Ning Y, Zhao YJ, Wang YJ, Shen ZY. (2011) Effects of active ingredients in three kidney-tonifying Chinese herbal drugs on gene expression profile of bone marrow stromal cells from a rat model of corticosterone-induced osteoporosis. *Zhongxiyi Jiehe Xuebao*, **9**, 179-185.
- [54] Bian Q, Liu SF, Huang JH, Yang Z, Tang DZ, Zhou Q, Ning Y, Zhao YJ, Lu S, Shen ZY. (2012) Oleanolic acid exerts an osteoprotective effect in ovariectomy-induced osteoporotic rats and stimulates the osteoblastic differentiation of bone mesenchymal stem cells *in vitro*. *Menopause*, **19**, 225-233.
- [55] Lee SU, Park SJ, Kwak HB, Oh J, Min YK, Kim SH. (2008) Anabolic activity of ursolic acid in bone: stimulating osteoblast differentiation *in vitro* and inducing new bone formation *in vivo*. *Pharmacological Research*, **58**, 290-296.
- [56] Tan H, Furuta S, Nagata T, Ohnuki K, Akasaka T, Shirouchi B, Sato M, Kondo R, Shimizu K. (2014) Inhibitory effects of the leaves of loquat (*Eriobotrya japonica*) on bone mineral density loss in ovariectomized mice and osteoclast differentiation. *Journal of Agricultural and Food Chemistry*, **62**, 836-841.
- [57] Tan H, Ashour A, Katakura Y and Shimizu K. (2015) A structure-activity relationship study on antiosteoclastogenesis effect of triterpenoids from the leaves of loquat (*Eriobotrya japonica*). *Phytomedicine*, **22**, 498-503.
- [58] Jiang C, Xiao F, Gu X, Zhai Z, Liu X, Wang W, Tang T, Wang Y, Zhu Z, Dai K, Qin A, Wang J. (2015) Inhibitory effects of ursolic acid on osteoclastogenesis and titanium particle-induced osteolysis are mediated primarily via suppression of NF-kappaB signaling. *Biochimie*, **111**, 107-118.
- [59] Huang Y, Wu Y, Wu J, Yi J, Zhang Q, Chen T, Wu J. (2014) Chemical constituents from *Ligustrum lucidum* differentially promote bone formation and prevent oxidative damage in osteoblastic UMR-106 cells. *Latin American Journal of Pharmacy*, **33**, 258-265.
- [60] Huang XJ, Yin ZQ, Ye WC, Shen WB. (2010) Chemical constituents from fruits of *Ligustrum lucidum*. *Zhongguo Zhongyao Zazhi*, **35**, 861-864.
- [61] Chen Q, Yang L, Zhang G, Wang F. (2013) Bioactivity-guided isolation of antiosteoporotic compounds from *Ligustrum lucidum*. *Phytotherapy Research*, **27**, 973-979.
- [62] Xu XH, Yang NY, Qian SH, Xie N, Duan JA. (2008) Dammarane triterpenes from *Ligustrum lucidum*. *Journal of Asian Natural Product Research*, **10**, 33-37.
- [63] Feng J, Feng Z, Wang J, Cui Y. (2011) Triterpenoids from the fruits of *Ligustrum lucidum*. *Zhongyaocai*, **34**, 1540-1544.
- [64] Yang NY, Xu XH, Ren DC, Duan JA, Xie N, Tian LJ, Qian SH. (2010) Secoiridoid constituents from the fruits of *Ligustrum lucidum*. *Helvetica Chimica Acta*, **93**, 65-71.
- [65] Huang XJ, Wang Y, Yin ZQ, Ye WC. (2010) Two new dimeric secoiridoid glycosides from the fruits of *Ligustrum lucidum*. *Journal of Asian Natural Product Research*, **12**, 685-690.
- [66] Fu G, Ip FCF, Pang H, Ip NY. (2010) New secoiridoids from *Ligustrum lucidum* induce ERK and CREB phosphorylation in cultured cortical neurons. *Planta Medica*, **76**, 998-1003.
- [67] Aoki S, Honda Y, Kikuchi T, Miura T, Sugawara R, Yaoita Y, Kikuchi M, Machida K. (2012) Six new secoiridoids from the dried fruits of *Ligustrum lucidum*. *Chemical and Pharmaceutical Bulletin*, **60**, 251-256.
- [68] Huang XJ, Wang L, Shao M, Hu SZ, Jiang RW, Yao XS, Li YL, Yin ZQ, Wang Y, Ye WC. (2013) Oleonin, the first secoiridoid with alpha-configuration from *Ligustrum lucidum*. *RSC Advances*, **3**, 16300-16303.
- [69] Barbaro B, Toietta G, Maggio R, Arciello M, Tarocchi M, Galli A, Balsano C. (2014) Effects of the olive-derived polyphenol oleuropein on human health. *International Journal of Molecular Sciences*, **15**, 18508-18524.
- [70] Sacchi RP, A., Savarese M, Vitaglione P, Fogliano V. (2014) Extra virgin olive oil: from composition to "molecular gastronomy". *Cancer Treatment and Research*, **159**, 325-338.
- [71] Mellou E, Zweigenbaum JA, Mitchell AE. (2015) Ultrahigh-pressure liquid chromatography triple-quadrupole tandem mass spectrometry quantitation of polyphenols and secoiridoids in California-style black ripe olives and dry salt-cured olives. *Journal of Agricultural and Food Chemistry*, **63**, 2400-2405.
- [72] Saleh NK, Saleh HA. (2011) Olive oil effectively mitigates ovariectomy-induced osteoporosis in rats. *BMC Complementary and Alternative Medicine*, **11**, 10.
- [73] Panossian A, Wikman G, Sarris J. (2010) Roseroot (*Rhodiola rosea*): traditional use, chemical composition, pharmacology and clinical efficacy. *Phytomedicine*, **17**, 481-493.
- [74] Choe KI, Kwon JH, Park KH, Oh MH, Kim MH, Kim HH, Cho SH, Chung EK, Ha SY, Lee MW. (2012) The antioxidant and antiinflammatory effects of phenolic compounds isolated from the root of *Rhodiola sachalinensis* A. Bor. *Molecules*, **17**, 11484-11494.
- [75] Zhang SC, Wang SQ, Zhao S. (2009) The effect of salidroside on leptin expression of diabetic rats with osteoporosis. *Chinese Journal of Pathophysiology*, **25**, 787-788.
- [76] He J, Hu XP, Zeng Y, Li Y, Wu HQ, Qiu RZ, Ma WJ, Li T, Li CY, He ZD. (2011) Advanced research on acteoside for chemistry and bioactivities. *Journal of Asian Natural Product Research*, **13**, 449-464.
- [77] Alipieva K, Korkina L, Orthan IE, Georgiev MI. (2014) Verbascoside: a review of its occurrence, (bio)synthesis and pharmacological significance. *Biotechnology Advances*, **32**, 1065-1076.

Alice, Benzene, and Coffee: The ABCs of Ecopharmacognosy

Geoffrey A. Cordell

Natural Products Inc., Evanston, IL, 60203, USA and Department of Pharmaceutics, College of Pharmacy, University of Florida, Gainesville, FL, 32610, USA

pharmacog@gmail.com

Received: July 31st, 2015; Accepted: August 12th, 2015

The sesquicentennial celebrations of the publication of “Alice’s Adventures in Wonderland” and the structure of benzene offer a unique opportunity to develop a contemporary interpretation of aspects of Alice’s adventures, illuminate the symbolism of benzene, and contextualize both with the globalization of coffee, transitioning to how the philosophy and sustainable practices of ecopharmacognosy may be applied to modulating approaches to the quality, safety, efficacy, and consistency (QSEC) of traditional medicines and dietary supplements through technology integration, thereby improving patient-centered health care.

Keywords: Alice in Wonderland, Benzene, Coffee, Ecopharmacognosy, Traditional medicines, Quality control, Technology integration, Global health care.

“Everything’s got a moral, if only you can find it.” said the Duchess to Alice.

We begin our allegoric thoughts with Alice and Benzene. The year 2015 marks the sesquicentennial of two, apparently disparate, events. In 1865, August Kekulé published an iconic paper in French (for he was then a Professor in Ghent, Belgium) suggesting that the structure of benzene contained a six-membered ring of carbon atoms with alternating single and double bonds, each with an attached hydrogen [1, 2]. Describing the origin of his idea twenty-five years later, Kekulé indicated that the benzene ring shape had come to him from a dream of a snake seizing its own tail, mimicking the ancient Egyptian symbol, the ouroboros.

Coincidentally, at about the same time, across the North Sea in England, the Oxford University mathematician Charles Lutwidge Dodgson, writing under the pseudonym Lewis Carroll, was publishing the most famous and widely-translated “children’s” books, “Alice’s Adventures in Wonderland” and “Through the Looking Glass” [3]. The audacities of Kekulé’s and Carroll’s vivid imaginations have survived and thrived, and in 2015 are being celebrated following 150 years of global impact. Molecular architecture, rabbit holes, and dreams..... What can their connections be with our contemporary challenges in traditional medicine on this disappearing Earth? This brief contribution attempts to tie these two “events” together in an allegoric manner, offering a contemporary interpretation of aspects of Alice’s adventures, and illuminating the symbolism of benzene, with a relationship to the globalization of coffee, and transitioning to the global need for the philosophy and practices of ecopharmacognosy as integral to a patient-centered approach for advancing the status of traditional medicines (TMs) in integrated health care systems.

Alice’s story begins with curiosity after she meets the White Rabbit wearing a waistcoat and looking at a pocket watch (“..this watch is exactly two days slow.”). As if on a shamanistic journey, she shrinks in size and follows him deep down a hidden hole into a world where her orderly, mundane, upper-class existence becomes completely discombobulated. Since the beginning of the industrial revolution about 260 years ago in England, we have inexorably descended our own “rabbit-hole”, accelerating in the past 150 years, to our contemporary life on Earth. Aspects of that incredible

progress make abundant sense, and the continuously evolving scientific realities have dramatically and spectacularly extended our human and technological capacities throughout all aspects of society, including the extension of life expectancy which has risen from 47 years in 1950-1955 to 69 years in 2005-2010 [4].

Alice in her “Wonderland” of endless surprises and quirks represents us in ours; the wholeness of the single human race in a continuously changing, almost unpredictable world. In that wondrous and alien world, she almost completely loses both her orientation and her power of independent decision-making. Her leader in the unexpected and bizarre environment of Wonderland is the White Rabbit; for us it is burgeoning technology. We are challenged to ask whether we have now lost control of the applicability of our technology over the past 150 years [5], and the recent movie “Ex Machina”, directed by Garland, provides a fascinatingly evocative and dramatic cautionary tale of creating truly humanistic, artificial intelligence systems as our pathway progresses. How did Alice get out of the deep rabbit hole and of Wonderland and return to her mundane and structured upper-class English life? She was woken up by a whirling pack of cards....it was all a dream. Can we be awakened from our dream-like stupor and take charge of global health care for the majority? Or are we already too deeply somnolent and transfixed by our technological prowess to consider serving the minority? One situational difference is that the rabbit-hole into which Alice fell was animal-created, “zoogenic”, whereas *our* “hole” is anthropogenic, a human-created, altered environment. Alice didn’t have to change her habits to restore balance to her environment; we must.

Benzene, a distillate of coal tar [6], results from the decay, over hundreds of millions of years, of Earth’s primordial forests. The availability and continued use of benzene as a synthetic precursor, and in gasoline fuels (at the 0.62% level in the US), epitomizes human civilization taking from the Earth, and not returning to the Earth. It recognizes our deep societal dependence on depleting Earth’s finite gifts, such as coal and oil. Benzene is the synthetic base for styrene, phenol, nylon fibers, lubricants, dyes, detergents, drugs, and pesticides, etc. It is an integral (now essential) aspect of an evolving global lifestyle; one which has turned into a continuing destructive saga of the very source of everything that supports us. Ironically, like the ouroboros, we are continuously “eating” our own

tails! As such, benzene represents the antithesis of sustainability; for its primary source, bituminous coal, may only last another 100 years [7]. Ironically though, in the obverse context, we could equally now deploy the ouroboros symbol, as it was originally used in Egypt, to represent the reincarnation (recycling) of the human state. We can extend that concept to the recycling of waste to reduce the rate of depletion of our planetary resources for future generations.

A similar dichotomy of philosophy and practice exists with coffee. The coffee bean (berry) is derived from either *Coffea arabica* L. or *C. canephora* Pierre ex A. Froehner (Rubiaceae). Beginning in Ethiopia in the 15th century, and moving into Yemen [8], and then to Arabia and Persia, coffee as a consumed beverage spread to Venice, where it was deemed a Christian drink by Pope Clement VIII in 1600. The first coffee house in England appeared in 1650, and within 25 years, 3,000 existed [9]. Brazil, where cultivation began in 1822, is by far the world's largest producer (33.1%). Coffee is now grown in more than 70 countries, and engages over 100 million people [8]. It is the second-most valuable commodity exported by developing countries [10].

Coffee serves as a representative example of the philosophical culmination of the concept of transitioning a plant from the forest into a global commodity (globalization). The continued, expanding daily consumption of coffee by billions of people illuminates the underlying assumptions of the global evolution of coffee as *the* marketed beverage in four ways: i) that the coffee contents are of good quality and not contaminated; ii) that they are safe when taken on a chronic basis, iii) that they are effective on continued use, and iv) that they are consistent on a day-to-day basis. These are the fundamental principles of quality, safety, efficacy, and consistency (QSEC) which should, at the global level, underpin the sciences of patient-centered traditional medicines. In addition, because it has been globalized as a stimulant beverage over hundreds of years [9], coffee is produced in a sustainable, and in many places organic, manner, through widespread cultivation, at a level of approximately 12 billion pounds per year.

Coffee also serves as a classic example of a non-sustainable and controversial commodity. Because of issues related to the susceptibility of *C. arabica* to infestation, particularly by coffee leaf rust *Hemileia vastatrix* and the coffee berry borer beetle (*Hypothenemus hampei*), a variety of pesticides is required for cultivation. Growing in open-fields compared with shaded, under canopy, cultivation [11], the need for extensive deforestation, as well as the extreme water requirements (est. 140 L) to produce the beans for one cup of coffee [12], provide important lessons through which to lessen the environmental impact as traditional medicines are transitioned into cultivated global commodities.

Alice, Benzene, and Coffee, each provide important background concepts as we look at the future development of traditional medicines. The last aspect to be introduced is the term "ecopharmacognosy", a word 25 years in development [13] over the course of numerous articles [13-34], including some on that precise topic [30, 32, 34]. "Pharmacognosy" is defined as "the study of biologically active natural products" [17]. Therein, the constituent sciences of pharmacognosy are unlimited by the source material (plant, marine, microbial, insect, mammalian, etc.), or the research area (information systems, botanical, analytical, chemical, biosynthetic, biological, pharmacological, clinical, economic, legal, regulatory, etc.). This inherently suggests that to be successful in bringing focus to the implications for, and outcomes of, pharmacognosy research, a highly integrated and collaborative approach is needed.

In London, in March 2012, the "State of the Planet Declaration" was promulgated by the "Planet under Pressure" Conference [35]. It sought support for a societal contract to encompass: i) global sustainability analyses based in science, ii) integrated, international, and solutions-oriented research, implemented and involving government, society, scientists, and the private sector, and iii) enhanced dialog on issues of global sustainability. More recently, in July 2015, the Rockefeller Foundation–*Lancet* Commission on planetary health released a report on Planetary Health [4], calling for societies to "address the drivers of environmental change by promoting sustainable and equitable patterns of consumption, reducing population growth, and harnessing the power of technology for change."

As a series of global sciences requiring, as a fundamental aspect of success, the continuing availability and judicious use of natural resources, it was astounding and distressing to acknowledge that pharmacognosy and its practices had barely considered "sustainability" as a conscious and evident component in our daily scientific research ideas and practices. There was a discussion sponsored by the World Health Organization on the conservation of medicinal plants in 1988 [36] and more recently aspects of "sustainable medicines" were discussed [25-28]; the need for awareness is much greater. Based on this situation, it was deduced that the profile and consciousness of the environmental and sustainability issues surrounding TMs needed to be raised, and hence a new term to integrate philosophy and practice was developed.

Thus "ecopharmacognosy" was born and introduced at a scientific meeting in Lublin, Poland in May, 2012. It is defined as "the study of sustainable, biologically active natural products" [30,32,34]. It offers a philosophical approach and a system of practices which stresses environmental concerns in natural product research from the perspective of the types of materials which should be studied, to opportunities for changing the practices used for their botanical, chemical, biological, and clinical assessment, to assuring a high QSEC product for the patient and the practitioner. It also embraces aspects of naturally-resourced agricultural practices, and the development of marine, bacterial, and fungal systems for scientific and economic development.

This brief and somewhat droll essay will attempt to coalesce some of the most well-known quotes and concepts from *Alice's Adventures in Wonderland* (AAIW) as a personal allegory for the considered use of our natural resources, with a more eco-centric view of developing Earth's natural medicinal resources, considering the patient-centered view of coffee as a pathway to develop a broad vision for traditional medicine enhancement within more integrated health care systems. Perhaps for some readers who are not familiar with "Alice's Adventures in Wonderland" this may be initially confusing. "Then you should say what you mean," the March Hare went on." I will.

We all are aware of the Doomsday clock.....since 1947 a philosophical construct which "indicates" how close Earth is to nuclear disaster, based on the levels of war and conflict in its various forms around the world, and since 2007 to the impending disaster from climate change. It is presently set at 11.57 pm [37]. When Alice first meets the White Rabbit in her real world, he is concerned about how late it is as he scurries off down the hole. The White Rabbit is OUR timepiece for getting things done in time (his watch is two days slow remember!), suggesting that we look now at how late it is becoming to restore our world towards a semblance of sanity. For the truth is, as the grinning Cheshire cat states, "We are all mad here", in the way we use Earth's resources.

Since 2000, the World Health Organization has been promoting the evidence-based assessment of traditional medicine practices [38], and the Beijing Declaration of 2008 encouraged countries to: i) respect, preserve, and promote knowledge and practices of TM; ii) formulate national policies, regulations and standards, as part of integrated health systems to ensure the appropriate, safe and effective use of TMs, and iii) promote TM research and innovation [39]. Further support has come from “The Regional Strategy for Traditional Medicine in the Western Pacific (2011-2020)” [40] and the “WHO traditional medicine strategy: 2014-2023” [41], which have also placed significant emphasis on the sustainability aspects of developing traditional medicines. These strategy documents challenge countries to introduce policies and practices which will ensure the availability and improve the status of TM in their respective health-care systems, based on a continuum of evidence-based approaches, in order to narrow the overt gaps in health care practices.

The economic and health care outcome gaps between traditional medicine and allopathic medicine globally are vast [30, 42-47]. The additional challenges for enhancing TM based on an evidence-based, patient-centered approach entail an exploration from a scientific perspective of the many myths which are associated with, and in some respects inhibit, unbiased TM research and development [32-34], to address the desperate need for quality control systems for TMs [13, 29, 31, 33], and to examine the profound necessity to assure the supply of critically-needed traditional medicines through sustainable sourcing [25, 26, 29, 32, 33] for the majority of patients in the world. That those situations even exist in the 21st century reflect another deep-seated “madness”, a failure to bring even a semblance of equality to our health-care priorities globally, and an irrational view of natural resource sustainability, namely, the enduring “myth” that the plants will always be there.

When we speak of “sustainable medicines”, the reference is to both natural and synthetic medicinal agents [25-28]. For the patient, accessibility to treatment is critical for healing, and must embrace both affordability and sustainability. In addition, the patient requirement is for a safe and effective regimen for healing; the source of the medicine is irrelevant. The costs of allopathic medicines have risen well beyond the index of inflation [48]. Stunningly, there are a number of medical treatment protocols which have been approved by the USFDA in recent years where the annual patient/insurance company cost is in excess of \$200,000 [49]. Meanwhile, at the global level, we are unable to deliver the simple drug aspirin (at less than 5 cents per dose) to those in pain. Drug resistance against cancer chemotherapeutics, antibiotics, antimalarials, anti-AIDS, and other infectious diseases is increasing steadily, but is not being addressed as a priority by the global pharmaceutical drug companies for economic reasons. Similarly, systematic drug discovery for the global major killer diseases and for tropical (orphan) diseases is not on the radar of Big Pharma, or even WHO; although the Gates Foundation and a recent Drugs for Neglected Diseases Initiative (www.dndi.org) will hopefully be impactful over time. Typically, and quite absurdly, these health care issues have been deemed to be addressed by the countries where the disease is prevalent; a truly inhumane and unethical decision with unrealistic expectations when only a handful of countries has the capacity to “discover” new medicinal agents for therapeutic use. Their typical resource is their plants and the medicinal knowledge associated with them, accumulated over time.

Let us return to our allegoric tale and to the sustainability of plant-based traditional medicine systems. It is fascinating that the dodo is one of the animals mentioned and depicted in *AAIW*; speculated to

be because of Do-do-Dodgson’s stammer [3]. The dodo, endemic to Mauritius, in 1662 became the first recorded extinction of a species caused by the actions of humans. It serves here as a profound reminder of the fragility of nature, and of the facile detrimental outcomes of the irrational urge for human dominance over nature. Today, there is a global system in place actively reviewing and recording the status of disappearing animals, plants, and other species, under the auspices of the International Union for Conservation of Nature. On these Red Lists of threatened and endangered species are (as of 2011) an estimated 9,568 plants of 61,900 recognized medicinal plant species. One of the priority activities recommended by WHO [40, 41, 50] is for countries to invest in assessing the availability and projected future access and supply chain for the needed TMs for their respective systems; some have done so [51, 52]. In the former instance, 39 of the most widely-used medicinal plant species were classified as threatened. The European Union has also recently issued a Red List of medicinal plants [53]. It was estimated that 31% of the medicinal plant species were in decline, principally due to wild-crafting.

The most powerful biological effects in *AAIW* are those produced by the mushroom, which is introduced to Alice by the caterpillar, who sits atop it, smoking a hookah. For us, Caterpillar is the local medicine practitioner, curandero, hakim, shaman, etc. The left part of the mushroom causes Alice to grow larger, while the right part causes her to diminish in size. She eats these parts in turn to “control” her height. The mushroom represents what in pharmacognosy are known to be the very powerful attributes of biologically active natural products; on one hand to promote disease, to cause profound toxicity, even death, and on the other to overcome toxicity, treat disease, and restore homeostasis.

The mushroom is also an allegory for the impact of what we ingest (physically and metaphorically) on global population dynamics. Over the past two centuries, humanity has been taking the left part of the mushroom, which has allowed the global population to grow larger (to 7.4 billion in 2015), stay healthier, have more mothers and children surviving, and to live longer. Disease, famine, war, natural events, and some naturally-derived products for male and female fertility regulation, and social and personal reassessments of family size have caused a modulated population growth, or even a diminishing population, as seen in countries like Russia, Japan, Germany, and Bulgaria [54].

Those are effects derived from the right part of the mushroom. The mushroom also suggests that, through nature, an acceptable balance for Earth’s population can be found. It is distressingly clear that such a balanced view of humanity is not on the agenda of any of the major international agencies or religions at this time. Maybe their leaders have not yet met any White Rabbits with watches indicating how behind the current time they are! For the dream seems to be of an Earth filled beyond sustainable capacity with healthy people. In this regard, Caterpillar asks Alice, “*What size do you want to be?*” As a human species, what is our answer for Earth’s population? We have already passed, or are close to passing, several tipping points for a sustainable population of Earth [55-57], such is the measure of our “overshoot”. This occurs when the population exceeds the carrying capacity that an environment can maintain indefinitely. Even optimistic estimates for what population Earth could support for extended periods are low (ca. 4 billion; passed in July, 1974) based on an ecological footprint, and much lower (ca. 1 billion; passed in August, 1804) based on a thermodynamic footprint [58].

Alice takes the left part of the mushroom that makes her grow taller to a point where she completely fills the little room she is in and then can’t move. “*There’s no room to grow up any more here*” she

cries out. Some of the major cities in the world (Beijing, Manila, Delhi, Sao Paolo, Dhaka) are like that now, houses are cramped, streets are thronged with people, cars cause endless traffic jams, and combined with industrialization, produce stunning levels of pollution, and in war zones, refugees live with many families to a single tent. Like Alice, we too are losing our freedom of movement. Earth's population is projected to rise to 10 billion by 2045. The oceans are rising, and are becoming distinctly more acidic, as a result of climate modulation (global warming) [59-61]. Major cities, such as Bangkok [62] and Venice [63], are sinking at alarming rates, and the future fate of needed medicinal plants in low-lying regions of the world is poorly studied [64, 65]. We can all shed tears, buckets of them, as we travel and observe what has happened to the state of our planet in our lifetimes. So when Alice swims in the pool of her tears with the dormouse (now an endangered species in England, by the way) she does so reflecting our tears for our environmental and biodiversity losses, now, and for the future generations. In terms of health care and medicinal agents, there are no solutions at present for delivering traditional and synthetic medicines in a sustainable manner to this exploding patient base.

Interestingly, and as a slight diversion from the main discussion, there are a number of direct associations with pharmacognosy present in the original drawings for *AAIW* by John Tenniel. There is for example a foxglove depicted in the meeting with the Cheshire Cat, and also when Alice is carrying the piglet. Then there is the powerful mushroom upon which the caterpillar sits, and chamomile is also cited. There is also the reference to the children down a well living on treacle, which was originally an extract of medicinal plants. And there is the warning on the first bottle that Alice encounters which is labeled "Drink me". "*Better read it first, for if one drinks too much from a bottle marked "Poison", it's almost certain to disagree with one sooner or later*", says Alice. This is an admirable admonition (read the label!) to the patient taking any medicine, particularly one where the plant material is known to have toxic effects at higher doses. It is a reminder too that the notion of "more is better", does not apply to the dosing of traditional medicines, a topic in itself of great controversy. With the differential effects of the mushroom evident, the important relationship between stereochemistry (handedness) and biological activity is also raised, where one enantiomer may have a completely different, even opposite biological effect, than the other enantiomer [66-68].

At one point in the narrative, Alice ponders the question, "*What is a mustard?*" Is it a mineral, an animal, or a vegetable? A reasonable question for a young, sheltered girl from an "upstairs" environment, for which the answer is actually not trivial, beyond being "vegetable" [69]. Her question though is a reminder to consider, and be grateful for, the items in our daily lives which we take for granted, and which are derived from nature without us thinking about them. In a contemporary context, consider, for example, how many readers of this article are aware of the origins and processing of cochineal and its uses or its' potential for sustainable development to provide the natural rouges and lipsticks for the faces of an expanding world? [70, 71].

Speaking of red, Alice witnesses the presaging of GMOs, for there in the garden are three playing cards (spades, of course) painting the white roses red at the behest of the Queen. Biotechnology has revealed approaches to a new scenario, where colors and biologically useful metabolites can be modulated and potentiated in biosynthetic terms, and deleterious compounds minimized or eliminated in content; a highly effective demonstration of the

principles of ecopharmacognosy, since expensive methods of separation and purification can be reduced.

Gryphons (griffins) are, according to legend, half eagle, and half lion. They are characterized by their power, extreme alertness and being stirred into rapid and fatally aggressive action at the slightest sound or movement, so as to alert the community. In *AAIW*, Carroll's gryphon is dozing, in spite of everything going on around. In our allegory, this is a clear reference to our lack of awareness and active concern, of not seeing and hearing the long standing, and increasingly loud indications from Nature itself, and those humanistic scientists concerned about nature, that aggressive corrective action in our behavior is needed.

Perhaps the most relevant scene to Earth's contemporary situation in *AAIW* is the Mad Hatters' Tea Party, where the time never changes (it is always six o'clock, and thus the time for tea). At the tea party, the participants (the Mad Hatter, the March Hare, and Dormouse) move around the table at each tea time, and always a new tea service is used. It is a classic example of our profligate consumption, as we move around our substantially disposable, non-reusable world, and of how, only very slowly, is global thinking at the political level concerning the sustainability and re-using of our resources (washing the dishes in *AAIW*) evolving. This scene can also be viewed as illustrating that changing time, actually moving through time as the world turns, requires the continuous reassessment of the *status quo*, whereas if time stands still, so does the *status quo*. For traditional medicines, it is this very *status quo* situation, which must shift to a patient-centered perspective for the benefit of humanity; we are already two days too slow (!), and need to move to a different time where the product and science and technology coalesce for the benefit of the patient. We, in consideration of future generations, have to wake up, "smell the coffee", and change our habits and practices to improve the role of traditional medicine in global health care.

The Preamble to the Constitution of the World Health Organization [72] states that "the highest attainable standard of health is one of the fundamental rights of every human being without distinction of race, religion, political belief, economic or social condition". Only when a population is healthy and not ravaged by disease, whether acute (Ebola) or chronic (malaria), can social and economic development be linked to effective and appropriate resource use [73]. About 80% of the plant resources used for traditional medicines in commerce are wild-crafted, and many are typically offered in an open manner in a local market, with little or no quality control, marginal concerns for safety, and almost no consideration afforded as to the age of the plant, and its changing efficacy and consistency. For most of the population of the world, this scene is their primary health care *status quo*, and has been for at least 4,000 years since the times of the early Chinese and Persian physicians until the present day [28]. As a global natural product health care community, we should be deeply embarrassed and ashamed by this appalling patient care situation.

In developed countries, the status of a patient-centric system for dietary supplements and traditional medicines is no better (and in some respects is even worse). A recent action by the Attorney General for New York State offers a glimmer of hope that even in the United States, where dietary supplement quality control is notoriously poor, and that of traditional medicines even worse, positive movement is possible [74]. In this instance, four large companies, GNC, Walgreen's, Walmart, and Target, were determined (through some not particularly well-conducted science) to have sold fraudulent dietary supplements; indeed 80% of the

package contents were not as labeled. Stunningly, several industry-related groups [75], not the retailers, went on the defensive, rather than acknowledging that, irrespective of the quality of the science, this is a huge, long-standing, industry-wide issue. Numerous instances of fraud in dietary supplements have been identified recently [76-83]. When products are recalled by the FDA, they may remain on the market for over four years and still contain synthetic adulterants, including those products from US manufacturers [84]. However, it seems unlikely that, absent US Congressional action, concerted industry reform in terms of research investment and an enhanced commitment to real quality control (QSEC) will follow voluntarily. The present system is based entirely on the trust between the manufacturer and the patient; a trust which is now essentially dissipated. From the patient perspective, the opportunity for the dietary supplement manufacturing industry to change effectively the *status quo* as an evidence-based commitment to US patient health care has been lost. Similarly to when Alice is "lost" in Wonderland, the situation begs the very core question for the global traditional medicine and the dietary supplement industry:

"Would you tell me, please, which way I ought to go from here?" asked Alice. "That depends a good deal on where you want to get to," said the Cat.

Louis Sullivan, perhaps the most famous early American architect, who was based in Chicago, wrote, in an essay in 1896 concerning the design of tall buildings, that "...form ever follows function. That is the law." [85]. In practical terms, therefore, know what the building is for, and then design its form to meet the functional requirements. So what then is to be the perceived function of (eco)pharmacognosy? For what, as a conglomeration of diverse and integrated scientific applications, will it accept responsibility in terms of meeting the needs of those patients who choose to take natural products for their health care? Will it redefine itself, as this author has urged for more than 25 years, or will it forever be engulfed at the junction of *status quo* and societal health care responsibility; frozen at, indeed by, the abyss of change?

Traditional medicines, TM practitioners, and their patients around the world are in a state of deep flux, moving down the long pathway of information and experimentation from an inherently knowledge-based system, to an experience-based system, and eventually to an evidence-based system. It is well-known that the existing frameworks for the development, regulation, quality control, and sale of traditional medicines, dietary supplements and phytotherapeutics, in spite of burgeoning sales, are not scientifically or societally acceptable because they are not patient-centered. The patient, who we as individuals all are, should be assured of the continued availability of quality, safe, effective, consistent (QSEC), and affordable traditional medicine products based on the results of evidence-based research and sustainability.

In the mid-1950s, before the global Japanese brands were renowned for their product quality, W. Edwards Deming, an American management expert, introduced a focus on continuous quality improvement to enhance the performance and product quality of Japanese industry [86]. One of his aphorisms from that time is "Quality begins with intent". Another dictum is that "We have lived in a world..... of defective products. It is time to adopt a new philosophy." [86]. In terms of the global quality control of traditional medicines and dietary supplements, we are still stuck living in a time of defective products. Moreover, the manufacturing industry, as the New York case showed, cannot grasp that it is their responsibility to change voluntarily their practices and their products to lead the improvements that are anticipated by the

patient. The *status quo* places the patient in the unacceptable position of "buyer beware", with no reliable resources to consult. Now is indeed the time for a new philosophy, a new intent for the quality of traditional medicines and dietary supplements; the existing paradigm must change [13, 28, 29, 31, 32, 33]. The patient must be assured of QSEC in a trustworthy product as an essential moral and ethical responsibility. Less than that is an ethical misstep by the manufacturer, the provider, and a moral dilemma for the practitioner. Therefore, evidence-based research, focused on the development of sustainably-resourced, standardized traditional medicines and dietary supplements, as well as those essential oils used in aromatherapy and cosmeceutical products, is fundamental. In this way, appropriate biological and clinical studies can be conducted for the health benefit of the patient, and the assurances of the practitioner. There is a need also to label products, in an appropriate manner, to reflect the standards being applied to placing the product in the market place, and how sustainable is its sourcing.

There are numerous practical examples of ecopharmacognosy. Long-term resourcing of traditional medicines (and those for drug discovery) is an early stage development question. Consideration of a bark or a root material offers very different long-term challenges for sustainability than the corresponding development of a leaf or fruit. Following the principles of "green chemistry", ecopharmacognosy could embrace six applicable and practical principles [26, 87], so that the global use of plants in traditional medicine can transition a "forest economy" to a "field economy", just as coffee has done [88-95]. Some other examples of the practical application of ecopharmacognosy include: i) the improved use of information systems to delineate what has been done and what needs to be done (not wasting resources by reinventing the wheel!); ii) reducing the energy requirements for plant material extraction; iii) reducing the reliance on non-recyclable chromatographic supports and solvents; iv) determining the significance of individual plants in complex plant matrices to conserve species use; v) using network pharmacology [96, 97] to develop new uses for established and sustainable plants, vi) studying the waste products of the industrial processing of plants for new applications; vii) developing natural pesticides and insecticides from renewable resources, viii) assessing whole organisms, plants, and microbial systems as renewable catalytic reagents showing high yield and high enantioselectivity for organic chemical processes [98-101]; ix) re-energizing the development of natural dyestuffs from sustainable resources; and x) investigating well-established commercial crops, such as turmeric, ginger, oregano, garlic, cinnamon, caraway, etc. for new biological responses. One recent study found that an aqueous extract of caraway seed could have an obesity-reducing effect [102, 103]. Finally, microfluidic, lab-on-a-chip approaches to the chemical and biological assessment of plant samples in the field (previously referred to as "pharmacognosy in a suitcase") [25-27, 29, 30, 34] would save significantly on the drying, transportation, and macro-analytic processes required to evaluate the optimal time for accessing plant materials for therapeutic purposes based on the levels of their bioactive agents. Similarly, hyperspectral imaging using drone technology and/or remote sensing devices based on Raman technology could play a significant role in the field determination of important biological molecules, as has already been achieved with collagen [104, 105].

Conclusions

Using the allegories based on *Alice's Adventures in Wonderland*, the dreamt discovery of the structure of benzene, and the globalization of coffee, new insights regarding the future, evidence-based directions of traditional medicine, are presented from the perspective of patient needs and expectations.

Acknowledgments – Comments on this concept for discussing ecopharmacognosy were received over several years from colleagues in several countries, including the UK, Poland, Sri

Lanka, India, Brazil, Peru, Japan, Thailand, Malaysia, and Jamaica. Their input is recognized and greatly appreciated.

References

- [1] Kekulé FA. (1865) Sur la constitution des substances aromatiques. *Bulletin de la Société Chimique de Paris*, **3**, 98-110.
- [2] Kekulé FA. (1866) Untersuchungen über aromatische Verbindungen. *Liebigs Annalen der Chemie und Pharmacie*, **137**, 129-136.
- [3] Carroll, L. (1999) *The Annotated Alice. The Definitive Edition*. Gardner M. (Ed). W.W. Norton Company, Inc. New York, NY, USA, pp. 352.
- [4] The Rockefeller Foundation-Lancet Commission on Planetary Health. *Safeguarding human health in the Anthropocene epoch: report of The Rockefeller Foundation-Lancet Commission on planetary health*. July 16, 2015, pp. 56. Available at <http://www.thelancet.com/commissions/planetary-health>. Accessed on July 17, 2015.
- [5] Cordell GA, Colvard MD. (2012) Natural products and traditional medicine - turning on a paradigm. *Journal of Natural Products*, **75**, 514-525.
- [6] Hofmann AW. (1845) Über eine sichere Reaction auf Benzol. *Annalen der Chemie und Pharmacie*, **55**, 200-205.
- [7] <http://riverbasinenergy.com/pages/the-future-of-coal/how-long-will-coal-last.php>. Accessed on July 9, 2015.
- [8] Vega FE. (2008) The rise of coffee. *American Scientist*, **96**, 138-145.
- [9] <http://www.history.co.uk/study-topics/history-of-london/londons-coffee-houses>. Accessed July 9, 2015.
- [10] Talbot JM. (2004) *Grounds for Agreement: The Political Economy of the Coffee Commodity Chain*. Rowman & Littlefield, Lanham, MD, USA, pp. 50.
- [11] Janzen DH. (Ed) (1983) *Costa Rican Natural History*. University of Chicago Press, Chicago, IL, USA, pp. 823.
- [12] <http://environment.nationalgeographic.com/environment/freshwater/change-the-course/water-footprint-calculator/>. Accessed July 9, 2015.
- [13] Cordell GA. (2015) Ecopharmacognosy and the globalization of traditional medicines. *International Journal of Traditional Knowledge*, in press.
- [14] Cordell GA. (1987) Pharmacognosy: far from dead. *American Druggist*, March, 96-98.
- [15] Cordell GA. (1987) Pharmacognosy: far from dead. *Thai Journal of Pharmaceutical Sciences*, **12**, 221-224.
- [16] Cordell GA. (1990) Pharmacognosy - a high tech pharmaceutical science. *Pharmacia*, **30**, 169-181.
- [17] Cordell GA. (1993) Pharmacognosy - new roots for an old science. In *Studies in Natural Products Chemistry, Volume 13. Bioactive Natural Products (Part A)*, Atta-ur-Rahman, Basha FZ, (Eds), Elsevier, Amsterdam, The Netherlands, 629-675.
- [18] Cordell GA. (1995) Changing strategies in natural products chemistry. *Phytochemistry*, **40**, 1585-1612.
- [19] Cordell GA. (2000) Biodiversity and drug discovery - a symbiotic relationship. *Phytochemistry*, **55**, 463-480.
- [20] Cordell GA. (2001) The yin and yang of natural products in the new millennium. *Acta Manilana*, **49**, 1-4.
- [21] Cordell GA. (2004) Accessing our gifts from nature, now and in the future. Part III. *Revista Química*, **19**, 33-41.
- [22] Cordell GA, Colvard MD. (2005) Some thoughts on the future of ethnopharmacology. *Journal of Ethnopharmacology*, **100**, 5-14.
- [23] Cordell GA, Colvard MD. (2007) Natural products in a world out-of-balance., *Arkivoc vii*, 97-115.
- [24] Cordell GA. (2008) Natural products research - a view through the looking glass. *Science and Culture*, **74**, 11-16.
- [25] Cordell GA. (2009) Sustainable drugs and global health care. *Química Nova*, **32**, 1356-1364.
- [26] Cordell GA. (2011) Sustainable medicines and global health care. *Planta Medica*, **77**, 1129-1138.
- [27] Cordell GA. (2011) Phytochemistry and traditional medicine - a revolution in process. *Phytochemistry Letters*, **4**, 391-398.
- [28] Cordell GA. (2011) Plant medicines key to global health. *Chemical & Engineering News*, June 27, 52-56.
- [29] Cordell GA. (2012) New strategies in traditional medicine. In *Medicinal Plants: Diversity and Drugs*. Rai M, Cordell GA, Martinez JL, Marinoff M, Rastrelli L, (Eds). CRC Press, Boca Raton, FL, USA, 1-45.
- [30] Cordell GA. (2014) Ecopharmacognosy: exploring the chemical and biological potential of nature for human health. *Journal of Biology and Medicinal Natural Product Chemistry*, **4**, 1-21.
- [31] Cordell GA. (2014) Phytochemistry and traditional medicine - the revolution continues. *Phytochemistry Letters*, **10**, 28-40.
- [32] Cordell GA. (2015) Ecopharmacognosy - the responsibilities of natural product research to sustainability. *Phytochemistry Letters*, **11**, 332-346.
- [33] Guo DA, Wu W-Y, Ye M, Liu X, Cordell GA. (2015) A holistic approach to the quality control of traditional Chinese medicines. *Science*, **347**, S29-S31.
- [34] Cordell GA. (2015) Ecopharmacognosy. In *Ethnopharmacology – A Reader*. Heinrich M, Jäger A. (Eds). Wiley Science Publishers, Chichester, UK, in production.
- [35] Brito L, MS Smith MS. (2012) State of the planet declaration. In *Proceedings of the 'Planet under Pressure' Conference, London*. 26-29.
- [36] Akerele O, Heywood, VH. (1991) *The Conservation of Medicinal Plants: Proceedings of an International Consultation, 21-27 March 1988 held at Chiang Mai, Thailand*. Cambridge University Press, Cambridge, UK, pp. 384.
- [37] Doomsday Clock. (2015) https://en.wikipedia.org/wiki/Doomsday_Clock. Accessed July 9, 2015.
- [38] WHO. (2002) http://whqlibdoc.who.int/hq/2002/WHO_EDM_TRM_2002.1.pdf. Accessed on July 9, 2015.
- [39] WHO. (2008) http://www.who.int/medicines/areas/traditional/congress/beijing_declaration/en/. Accessed on July 9, 2015.
- [40] WPRO. (2011) http://www.wpro.who.int/traditional_medicine/about/en/. Accessed on July 9, 2015.
- [41] WHO. (2014) http://www.who.int/medicines/publications/traditional/trm_strategy14_23/en/. Accessed on July 9, 2015.
- [42] World Health Organization. (1998) *The World Health Report 1998: Life in the 21st Century A Vision for All*. World Health Organization, Geneva, Switzerland, pp. 241.
- [43] Evans T, Whitehead M, Diderichsen F, Bhuiya A, Wirth M, Whitehead M. (2001) *Challenging inequities in health: from ethics to action*. Oxford University Press, Oxford, UK, pp. 368.
- [44] Lee J.-W. (2003) Global health improvement and WHO: shaping the future. *The Lancet*, **362**, 2083-2088.
- [45] Frenk J, Chen L. (2011) Overcoming gaps to advance global health equity: a symposium on new directions for research. *Health Research Policy and Systems*, **9**, 11.
- [46] Balarajan Y, Selvaraj S, Subramanian SV. (2011) Health care and equity in India. *The Lancet*, **377**, 505-515.
- [47] Holtz C. (Ed). (2013) *Global Health Care: Issues and Policies*. Jones & Bartlett Learning Publishers, Burlington, MA, USA, pp. 614.
- [48] Thomas K. (2012) Brand name drug prices rise sharply, report says. <http://www.nytimes.com/2012/11/29/business/cost-of-brand-name-prescription-medicines-soaring.html>. Accessed on July 9, 2015.
- [49] Williams S. (2014) The 5 most expensive drugs in the world. <http://www.fool.com/investing/general/2014/10/26/the-5-most-expensive-drugs-in-the-world.aspx>. Accessed on July 9, 2015.
- [50] IUCN/WHO/WWF. (1993) Guidelines for the Conservation of Medicinal Plants. IUCN, Gland, Switzerland, pp. 38.
- [51] Reddy KN, Reddy CS. (2008) First red list of medicinal plants of Andhra Pradesh, India - conservation assessment and management planning. *Ethnobotanical Leaflets*, **12**, 103-107.

- [52] Williams VL, Victor JE, Crouch NR. (2013) Red listed medicinal plants of South Africa: status, trends, and assessment challenges. *South African Journal of Botany*, **86**, 23-35.
- [53] Allen D, Bilz M, Leaman DJ, Miller RM, Timoshyna A, Window J. (2014) European Red List of Medicinal Plants. European Union, Luxembourg, pp. 75.
- [54] https://en.wikipedia.org/wiki/List_of_countries_by_population_growth_rate. Accessed on July 11, 2012.
- [55] Murray J, King D. (2012) Climate policy: oil's tipping point has passed. *Nature*, **481**, 433-435.
- [56] Kiron D, Kruschwitz N, Haanaes K, von Streng Velken I. (2012) Sustainability nears a tipping point. *MIT Sloan Management Review*, **53**, 69-74.
- [57] Boettiger C, Hastings A. (2013) Tipping points: from patterns to predictions. *Nature*, **493**, 157-158.
- [58] Chefurka PS. (2013) Sustainability. <http://www.paulchefurka.ca/Sustainability.html>. Accessed on July 10, 2015.
- [59] Orr JC, Fabry VJ, Aumont O, Bopp L, Doney SC, Feely RA, Gnanadesikan A, Gruber N, Ishida A, Joos F, Key RM, Lindsay K, Maier-Reimer E, Matear R, Monfray P, Mouchet A, Najjar RG, Plattner G-K, Rodgers KB, Sabine CL, Sarmiento JL, Schlitzer R, Slater RD, Totterdell IJ, Weirig M-F, Yamanaka Y, Yool A. (2005) Anthropogenic ocean acidification over the twenty-first century and its impact on calcifying organisms. *Nature*, **437**, 681-686.
- [60] Doney SC, Fabry VJ, Feely RA, Kleypas JA. (2009) Ocean acidification: the other CO₂ problem. *Annual Review of Marine Science*, **1**, 169-192.
- [61] McCulloch M, Falter J, Trotter J, Montagna P. (2012) Coral resilience to ocean acidification and global warming through pH up-regulation. *Nature Climate Change*, **2**, 623-627.
- [62] Phien-Wej N, Giao PH, Nutalaya P. (2006) Land subsidence in Bangkok, Thailand. *Engineering Geology*, **82**, 187-201.
- [63] Lewis T. (2013) Venice's gradual sinking charted by satellites. <http://www.livescience.com/39979-venice-gradual-sinkingcharted-by-satellites.html>. Accessed on July 11, 2015.
- [64] Kirilenko AP, Sedjo RA. (2007) Climate change impacts on forestry. *Proceedings of the National Academy of Sciences*, **104**, 19697-19702.
- [65] Cavalieri C. (2009) The effects of climate change on medicinal and aromatic plants. *Herbal Gram*, **81**, 44-57.
- [66] Waldeck B. (1993) Biological significance of the enantiomeric purity of drugs. *Chirality*, **5**, 350-355.
- [67] Biellmann JF. (2003) Enantiomeric steroids: synthesis, physical, and biological properties. *Chemical Reviews*, **103**, 2019-2034.
- [68] Garrison AW. (2006) Probing the enantioselectivity of chiral pesticides. *Environmental Science & Technology*, **40**, 16-23.
- [69] Antol MN. (1999) *The Incredible Secrets of Mustard: The Quintessential Guide to the History, Lore, Varieties, and Healthful Benefits of Mustard*. Avery Publishing Group, Knoxville, TN, USA, pp. 228.
- [70] Eisner T, Nowicki S, Goetz M, Meinwald J. (1980) Red cochineal dye (carminic acid): its role in nature. *Science*, **208**, 1039-1042.
- [71] Campana MG, Robles García NM, Tuross N. (2015) America's red gold: multiple lineages of cultivated cochineal in Mexico. *Ecology and Evolution*, **5**, 607-617.
- [72] WHO (1946) The Constitution of the World Health Organization. http://www.who.int/governance/eb/WHO_Constitution_en.pdf. Accessed on July 11, 2015.
- [73] Mitchell RJ, Bates P. (2011) Measuring health-related productivity loss. *Population Health Management*, **14**, 93-98.
- [74] O'Connor A. (2015) New York Attorney General Targets Supplements at Major Retailers. New York Times, February 3. http://well.blogs.nytimes.com/2015/02/03/new-york-attorney-general-targets-supplements-at-major-retailers/?_r=0. Accessed on July 12, 2015.
- [75] http://www.nutraceuticalsworld.com/contents/view_breaking-news/2015-02-03/new-york-ag-targets-herbal-supplements-at-major-retailers/. Accessed on July 12, 2015.
- [76] Cohen PA, Benner C, McCormick D. (2012) Use of a pharmaceutically adulterated dietary supplement, Pai You Guo, among Brazilian-born women in the United States. *Journal of General Internal Medicine*, **27**, 51-56.
- [77] Harel Z, Harel S, Wald R, Mamdani M, Bell CM. (2013) The frequency and characteristics of dietary supplement recalls in the United States. *JAMA Internal Medicine*, **173**, 929-930.
- [78] Posadzki P, Watson L, Ernst E. (2013) Contamination and adulteration of herbal medicinal products (HMPs): an overview of systematic reviews. *European Journal of Clinical Pharmacology*, **69**, 295-307.
- [79] Wheatley VM, Spink J. (2013) Defining the public health threat of dietary supplement fraud. *Comprehensive Reviews in Food Science and Food Safety*, **12**, 599-613.
- [80] Campbell N, Clark JP, Stecher VJ, Thomas JW, Callanan AC, Donnelly BF, Goldstein I, Kaminetsky JC. (2013) Adulteration of purported herbal and natural sexual performance enhancement dietary supplements with synthetic phosphodiesterase type 5 inhibitors. *The Journal of Sexual Medicine*, **10**, 1842-1849.
- [81] Song F, Monroe D, El-Demerdash A, Palmer C. (2014) Screening for multiple weight loss and related drugs in dietary supplement materials by flow injection tandem mass spectrometry and their confirmation by liquid chromatography tandem mass spectrometry. *Journal of Pharmaceutical and Biomedical Analysis*, **88**, 136-143.
- [82] Zhu Q, Cao Y, Cao Y, Chai Y, Lu F. (2014) Rapid on-site TLC-SERS detection of four antidiabetes drugs used as adulterants in botanical dietary supplements. *Analytical and Bioanalytical Chemistry*, **406**, 1877-1884.
- [83] Gilard V, Balyssac S, Tinaugus A, Martins N, Martino R, Malet-Martino M. (2015) Detection, identification and quantification by ¹H NMR of adulterants in 150 herbal dietary supplements marketed for improving sexual performance. *Journal of Pharmaceutical and Biomedical Analysis*, **102**, 476-493.
- [84] Cohen PA, Maller G, DeSouza R, Neal-Kababick J. (2014) Presence of banned drugs in dietary supplements following FDA recalls. *Journal of the American Medical Association*, **312**, 1691-1693.
- [85] Sullivan LH. (1896) The tall office building artistically considered, *Lippincott's Magazine*, March.
- [86] Deming WE. (2000) *Out of the Crisis*. MIT Press, Cambridge, MA, USA, pp. 507.
- [87] Cordell GA, Michel J. (2007) Sustainable drugs and women's health. In *Proceedings of the Third Women's Health and Asian Traditional Medicine Conference and Exhibition*. Rao AN. (Ed), Kuala Lumpur, Malaysia, 15-27.
- [88] Schippmann UWE, Leaman D, Cunningham AB. (2006) A comparison of cultivation and wild collection of medicinal and aromatic plants under sustainability aspects. *Frontis*, **17**, 75-95.
- [89] Lange D. (2004) Medicinal and aromatic plants: trade, production and management of botanical resources. *Acta Horticulturae*, **629**, 177-197.
- [90] Anastas PT, Warner JC. (1998) *Green Chemistry: Theory and Practice*. Oxford University Press, New York, NY, USA, pp. 152.
- [91] De Silva T. (1997) Industrial utilization of medicinal plants in developing countries. In *Medicinal Plants for Forest Conservation and Health Care*. FAO, Rome, Italy, 34-44.
- [92] Dubey NK, Kumar R, Tripathi P. (2004) Global promotion of herbal medicine: India's opportunity. *Current Science*, **86**, 37-41.
- [93] Hamilton AC. (2004) Medicinal plants, conservation and livelihoods. *Biodiversity and Conservation*, **13**, 1477-1517.
- [94] Canter PH, Thomas H, Ernst E. (2005) Bringing medicinal plants into cultivation: opportunities and challenges for biotechnology. *Trends in Biotechnology*, **23**, 180-185.
- [95] Lubbe A, Verpoorte R. (2011) Cultivation of medicinal and aromatic plants for specialty industrial materials. *Industrial Crops and Products*, **34**, 785-801.

- [96] Li S, Zhang B. (2013) Traditional Chinese medicine network pharmacology: theory, methodology and application. *Chinese Journal of Natural Medicines*, **11**, 110-120.
- [97] Zheng CS, Xu XJ, Ye HZ, Wu GW, Li XH, Xu HF, Liu XX. (2013) Network pharmacology-based prediction of the multi-target capabilities of the compounds in Taohong Siwu decoction, and their application in osteoarthritis. *Experimental and Therapeutic Medicine*, **6**, 125-132.
- [98] Sousa JSN, Machado LL, de Mattos MC, Solange S, Lemos TLG, Cordell, GA. (2006) Bioreduction of aromatic aldehydes and ketones using *Manihot* species, *Phytochemistry*, **67**, 1637-1643.
- [99] Cordell GA, Lemos TLG, Monte FJQ, de Mattos MC. (2007) Vegetables as chemical reagents. *Journal of Natural Products*, **70**, 478-492.
- [100] Assunção JCC, Machado LL, Lemos TLG, Cordell GA, Monte FJQ. (2008) Sugar cane juice for the reduction of carbonyl compounds, *Journal of Molecular Catalysis B – Enzymatic*, **52-53**, 194-198.
- [101] Fonseca AM, Monte FJQ, Braz-Filho R, de Mattos MC, Oliveira MCF, Cordell GA, Lemos TLG. (2009) Coconut juice (*Cocos nucifera*) - a new biocatalyst system for organic synthesis. *Journal of Molecular Catalysis B – Enzymatic*, **57**, 78-82.
- [102] Kazemipoor M, Radzi CJM, Hajifarji M, Hearian B, Mosadegh M, Cordell, GA. (2013) Anti-obesity effect of caraway extract on overweight and obese women: a randomized triple-blind, placebo-controlled clinical trial. *Evidence-based Complementary and Alternative Medicine*, id 928582, 8 pp.
- [103] Kazemipoor M, Radzi CJM, Hajifarji M, Cordell GA. (2014) Preliminary safety evaluation and biochemical efficacy of *Carum carvi*: a triple-blind, placebo-controlled clinical trial. *Phytotherapy Research*, **28**, 1456-1460.
- [104] Pestle WJ, Ahmad F, Vesper B, Cordell GA, Colvard MD. (2014) Ancient bone collagen assessment by hand-held vibrational spectroscopy. *Journal of Archaeological Science*, **42**, 381-389.
- [105] Pestle WJ, Brennan V, Sierra R, Smith EK, Vesper BJ, Cordell GA, Colvard MD. (2015) Hand-held Raman spectroscopy as a prescreening tool for archaeological bone. *Journal of Archaeological Science*, **58**, 113-120.

Additions and Corrections

Natural Product Communications 10 (7), 1175-1177 (2015)

Title: Cytotoxic and Antimalarial Alkaloids from the Twigs of *Dasymaschalon obtusipetalum*

Authors: Atchara Jaidee, Thanika Promchai, Kongkiat Trisuwan, Surat Laphookhieo, Roonglawan Rattanajak, Sumalee Kamchonwongpaisan, Stephen G. Pyne and Thunwadee Ritthiwigrom*

Received: February 1st, 2015; **Accepted:** April 6th, 2015

- After publishing the above paper we became aware of the following reference indicating that the correct name for the plant species that we studied is *Dasymaschalon yunnanense* and the name *D. obtusipetalum* is now regarded as a heterotypic synonym.

Guo, X., Wang, J., Xue, B., Thomas, D.C., Su, Y. C. F., Tan, Y. H., Saunders, R. M. K., "Reassessing the taxonomic status of two enigmatic *Desmos* species (Annonaceae): Morphological and molecular phylogenetic support for a new genus, *Wangia*," *Journal of Systematics and Evolution*, **52**, 1-15 (2014).

Stephen Pyne
Senior Professor of Chemistry
School of Chemistry
Faculty of Science, Medicine and Health
Building 18/Room 121
University of Wollongong NSW 2522 Australia
T +61 2 4221 3511 | **F** +61 2 4221 4287

Natural Product Communications

Manuscripts in Press Volume 10, Number 12 (2015)

Influence of Tanshinone IIA on the Apoptosis of Human Esophageal EC-109 Cells

Yan-qin Zhu, Bai-Yan Wang, Fang Wu, Yong-kang An and Xin-qiang Zhou
Cordycepin, a Natural Antineoplastic Agent, Induces Apoptosis of Breast Cancer Cells via Caspase-dependent Pathways
Di Wang, Yongfeng Zhang, Jiahui Lu, Yang Wang, Junyue Wang, Qingfan Meng, Robert J. Lee, Di Wang and Lesheng Teng

Polyphenols and Volatile Compounds in Commercial Chokeberry (*Aronia melanocarpa*) Products

Annalisa Romani, Pamela Vignolini, Francesca Ieri and Daniela Heimler

Cytotoxic and Pro-apoptotic Activities of Sesquiterpene Lactones from *Inula britannica*

Ping Xiang, Xin Guo, Yang-Yang Han, Jin-Ming Gao and Jiang-Jiang Tang

Antifungal and Cytotoxic Assessment of Lapachol Derivatives Produced by Fungal Biotransformation

Eliane O. Silva, Antonio Ruano-González, Raquel A. dos Santos, Rosario Sánchez-Maestre, Niegé A. J. C. Furtado, Isidro G. Collado and Josefina Aleu

A New Taraxastane-type Triterpenoid from *Cleistocalyx operculatus*

Phan Minh Giang, Vu Thi Thu Phuong and Truong Thi To Chinh

Antimicrobial Metabolites from a Marine-Derived Actinomycete in Vietnam's East Sea

Quyen Vu Thi, Van Hieu Tran, Huong Doan Thi Mai, Cong Vinh Le, Hong Minh Le, Brian T. Murphy, Van Minh Chau and Van Cuong Pham

Cycloartane-Type Saponins from *Astragalus tmeoleus* var. *tmeoleus*

Sibel Avunduk, Anne-Claire Mitaïne-Offer, Tomofumi Miyamoto, Chiaki Tanaka, and Marie-Aleth Lacaille-Dubois

A New Antibacterial Tetrahydronaphthalene Lignanamide, Foveolatamide, from the Stems of *Ficus foveolata*

Wirot Meerungrueang and Parkphoom Panichayupakaranant

Anti-allergic Inflammatory Triterpenoids Isolated from the Spikes of *Prunella vulgaris*

Hyun Gyu Choi, Tae Hoon Kim, Sang-Hyun Kim and Jeong Ah Kim

Trocheliolide B, a New Cembranoidal Diterpene from the Octocoral *Sarcophyton trocheliophorum*

Kuan-Ming Liu, Yu-Hsuan Lan, Ching-Chyuan Su and Ping-Jyun Sung

Chemical Composition and Antimicrobial Activity of the Essential Oil from Aerial Parts of Algerian *Pulicaria mauritanica*

Mohammed Gherib, Chahrased Bekhechi, Fewzia Atik Bekkara, Ange Bighelli, Joseph Casanova and Félix Tomi

Volatile Components of the Stressed Liverwort *Conocephalum conicum*

Nurunajah Ab Ghani, Agnieszka Ludwiczuk, Nor HadianiSmail and Yoshinori Asakawa

Phytochemical and Biological Investigations of *Conradina canescens*

Noura S. Dosoky, Debra M. Moriarity and William N. Setzer

Steroidal Glucosides from the Rhizomes of *Tacca chantrieri* and Their Inhibitory Activities of NO Production in BV2 Cells

Pham Hai Yen, Vu Thi Quynh Chi, Dong-Cheol Kim, Wonmin Ko, Hyunchol Oh, Youn-Chul Kim, Duong Thi Dung, Nguyen Thi Viet Thanh, Tran Hong Quang, Nguyen Thi Thanh Ngan, Nguyen Xuan Nhem^a, Hoang Le Tuan Anh, Chau Van Minh and Phan Van Kiem

Molecular Docking and Binding Mode Analysis of Plant Alkaloids as *in vitro* and *in silico* Inhibitors of Trypanothione Reductase from *Trypanosoma cruzi*

Alonso J. Argüelles, Geoffrey A. Cordell and Helena Maruenda

Synthesis of a Novel 1,2,4-Oxadiazole Diterpene from the Oxime of the Methyl Ester of 1 β ,13-Epoxydihydroquinopimaric Acid

Elena V. Tretyakova, Elena V. Salimova, Victor N. Odinokov and Usein M. Dzhemilev

Influence of Merosesquiterpenoids from Marine Sponges on Seedling Root Growth of Agricultural Plants

Elena L. Chaikina, Natalia K. Utkina and Mikhail M. Anisimov

A New Geranylated Chalcone from *Andrographis lobelioides*

Manne Sumalatha, Aluru Rammohan, Duvvuru Gunasekar, Alexandre Deville and Bernard Bodo

Isolation and Characterization of Sclerienone C from *Scleria striatinus*

Kennedy D. Nyongbela, Felix L. Makolo, Thomas R. Hoye and Simon MN Efange

Inhibition of Alpha-Glucosidase by Synthetic Derivatives of Lupane, Oleanane, Ursane and Dammarane Triterpenoids

El'mira F. Khusnutdinova, Irina E. Smirnova, Gul'nara V. Giniyatullina, Natal'ya I. Medvedeva, Emil Yu. Yamansarov, Dmitri V. Kazakov, Oxana B. Kazakova, Pham T. Linh, Do Quoc Viet and Do Thi Thu Huong

Profiling and Metabolism of Sterols in the Weaver Ant Genus *Oecophylla*

Nanna H. Vidkjær, Karl-Martin V. Jensen, René Gislum and Inge S. Fomsgaard

Origanum vulgare and *Thymbra capitata* Essential Oils from Spain: Determination of Aromatic Profile and Bioactivities

Alejandro Carrasco, Enrique Perez, Ana-Belen Cutillas, Ramiro Martinez-Gutierrez, Virginia Tomas and Jose Tudela

Xanthones from *Garcinia propinqua* Roots

Pornphimol Meesakul, Acharavadee Pansanit, Wisanu Maneerat, Tawanun Sripisut, Thunwadee Ritthiwigrom, Theeraphan Machan, Sarot Cheenpracha and Surat Laphookhieo

A New Cytotoxic Clerodane Diterpene from *Casearia graveolens* Twigs

Pornphimol Meesakul, Thunwadee Ritthiwigrom, Sarot Cheenpracha, Tawanun Sripisut, Wisanu Maneerat, Theeraphan Machan and Surat Laphookhieo

In vivo Cytotoxicity Studies of Amaryllidaceae Alkaloids

Jerald J. Nair, Jaume Bastida and Johannes van Staden

Acetophenones Isolated from *Acronychia pedunculata* and their Anti-proliferative Activities

Chihiro Ito, Takuya Matsui, Yoshiaki Ban, Tian-Shung Wu, and Masataka Itoigawa

Electron Ionization Mass Spectrometry-based Metabolomics Studies of *Sophora flavescens* can Identify the Geographical Origin of Root Samples

Ryuichiro Suzuki, Hisahiro Kai, Yoshihiro Uesawa, Koji Matsuno, Yoshihito Okada and Yoshiaki Shirataki

New Bioactive Semisynthetic Derivatives of 31-Norlanostenol and Obtusifoliol from *Euphorbia officinarum*

Maria Bailen, Mourad Daoubi Khamlichi, Ahmed Benharref, Rafael A. Martinez-Diaz and Azucena Gonzalez-Coloma

Absolute Stereochemistry of the β -Hydroxy Acid Unit in Hantapeptins and Trungapeptins

Deepak Kumar Gupta, Gary Chi Ying Ding, Yong Chua Teo and Lik Tong Tan

Qualitative and Quantitative Analysis of Flower Pigments in Chocolate Cosmos, *Cosmos atrosanguineus*, and its Hybrids

Kotarou Amamiya and Tsukasa Iwashina

Chemical Composition of the Essential Oil of *Bupleurum fontanesii* (Apiaceae) Growing Wild in Sicily and its Activity on Microorganisms Affecting Historical Art Crafts

Simona Casiglia, Maurizio Bruno, Federica Senatore and Felice Senatore

Pterocarpans from *Derris laxiflora*

Shih-Chang Chien, Hsi-Lin Chiu, Wei-Yi Cheng, Yong-Han Hong, Sheng-Yang Wang, Jyh-Horng Wu, Chun-Ching Shih, Jung-Chun Liao and Yueh-Hsiung Kuo

Natural Product Communications

2015

Volume 10

Natural Product Communications 10 (1-12) 1-2204 (2015)

**ISSN 1934-578X (print)
ISSN 1555-9475 (online)**

Natural Product Communications

Contents of Volume 10 2015

Number 1

10th Anniversary issue

<u>Anniversary Message</u>	i-ii
<u>Editorial Board Members</u>	iii-vi
Expedient Access to Enantiopure Cyclopentanoid Natural Products: Total Synthesis of (-)-Cyclonerodiol Carmen Pérez Morales, M. Mar Herrador, José F. Quílez del Moral and Alejandro F. Barrero	1
Identification of Sesquiterpene Lactones in the Bryophyta (Mosses) <i>Takakia</i>: <i>Takakia</i> Species are Closely Related Chemically to the Marchantiophyta (Liverworts) Yoshinori Asakawa, Kaeko Nii and Masanobu Higuchi	5
Chemotypes of <i>Ligularia vellerea</i>, its Hybrids, and <i>L. melanothyrs</i> Anna Shimizu, Kyosuke Inoue, Mayu Ichihara, Ryo Hanai, Yoshinori Saito, Yasuko Okamoto, Motoo Tori, Xun Gong and Chiaki Kuroda	9
neo-Clerodane Diterpenoids from <i>Scutellaria altissima</i> Petko I. Bozov and Josep Coll	13
Phytotoxicity of Triterpenes and Limonoids from the Rutaceae and Meliaceae. 5α,6β,8α,12α-Tetrahydro-28-norisotoonafolin – a Potent Phytotoxin from <i>Toona ciliata</i> Liliane Nebo, Rosa M. Varela, José M. G. Molinillo, Vanessa G. P. Severino, André L. F. Sarria, Cristiane M. Cazal, Maria Fátima das Graças Fernandes, João B. Fernandes and Francisco A. Macías	17
Triterpene Glycosides of Sea Cucumbers (Holothuroidea, Echinodermata) as Taxonomic Markers Vladimir I. Kalinin, Sergey A. Avilov, Alexandra S. Silchenko and Valentin A. Stonik	21
Amurensiosides L-P, Five New Cardenolide Glycosides from the Roots of <i>Adonis amurensis</i> Satoshi Kubo, Minpei Kuroda, Akihito Yokosuka, Hiroshi Sakagami and Yoshihiro Mimaki	27
UV-protective Effects of Phytoecdysteroids from <i>Microsorum grossum</i> Extracts on Human Dermal Fibroblasts Raimana Ho, Taivini Teai, Alain Meybeck and Phila Raharivelomanana	33
Spirostane-type Saponins from <i>Dracaena fragrans</i> « Yellow Coast » Abdelmalek Rezgui, Anne-Claire Mitaine-Offer, Tomofumi Miyamoto, Chiaki Tanaka and Marie-Aleth Lacaille-Dubois	37
Secondary Metabolites from a Strain of <i>Alternaria tenuissima</i> Isolated from Northern Manitoba Soil Chukwudi S. Anyanwu and John L. Sorensen	39
Chemical Prospection of Important Ayurvedic Plant <i>Tinospora cordifolia</i> by UPLC-DAD-ESI-QTOF-MS/MS and NMR Manju Bala, Praveen Kumar Verma, Shiv Awasthi, Neeraj Kumar, Brij Lal and Bikram Singh	43
Kopsiyunnanines J1 and J2, New Strychnos-type Homo-Monoterpenoid Indole Alkaloids from <i>Kopsia arborea</i> Mariko Kitajima, Tetsuya Koyama, Yuqiu Wu, Noriyuki Kogure, Rongping Zhang and Hiromitsu Takayama	49
Diversity in the Flavonoid Composition of <i>Stellera chamaejasme</i> in the Hengduan Mountains Kei Shirai, Yasuko Okamoto, Motoo Tori, Takayuki Kawahara, Xun Gong, Teruaki Noyama, Eiji Watanabe and Chiaki Kuroda	53
Constituents of Indonesian Medicinal Plant <i>Averrhoa bilimbi</i> and Their Cytochrome P450 3A4 and 2D6 Inhibitory Activities Lidyawati Auw, Subehan, Sukrasno, Shigetoshi Kadota and Yasuhiro Tezuka	57
Flavonoids from <i>Curcuma longa</i> Leaves and their NMR Assignments Chia-Ling Jiang, Sheng-Fa Tsai and Shoei-Sheng Lee	63
Phytochemical Analysis and Biological Evaluation of Selected African Propolis Samples from Cameroon and Congo Danai Papachroni, Konstantia Graikou, Ivan Kosalec, Harilaos Damianakos, Verina Ingram and Ioanna Chinou	67
Improved Chromatographic Fingerprinting Combined with Multi-components Quantitative Analysis for Quality Evaluation of <i>Penthorum chinense</i> by UHPLC-DAD Wangping Deng, Tongtong Xu, Min Yang, Yajun Cui and De-an Guo	71
Anthocyanins of <i>Hibiscus sabdariffa</i> Calyces from Sudan Lucie Cahliková, Badreldin H. Ali, Lucie Havliková, Mirek Ločárek, Tomáš Siatka, Lubomír Opletal and Gerald Blunden	77
Maqui berry vs Sloe berry – Liquor-based Beverage for New Development Amadeo Gironés-Vilaplana, Diego A. Moreno and Cristina García-Viguera	81
Phytochemical Profile of the Aerial Parts of <i>Sedum sediforme</i> and Anti-inflammatory Activity of Myricitrin Daniel Winekenstädde, Apostolis Angelis, Birgit Waltenberger, Stefan Schwaiger, Job Tchoumtchoua, Stefanie König, Oliver Werz, Nektarios Aligiannis, Alexios-Leandros Skaltsounis and Hermann Stuppner	83

Diarylheptanoids of <i>Curcuma comosa</i> with Inhibitory Effects on Nitric Oxide Production in Macrophage RAW 264.7 Cells	
Nilubon Sornkaew, Yuan Lin, Fei Wang, Guolin Zhang, Ratchanaporn Chokchaisiri, Ailian Zhang, Kanjana Wongkrajang, Parichat Suebsakwong, Pawinee Piyachaturawat and Apichart Suksamarn	89
Rapid Dereplication and Identification of the Bioactive Constituents from the Fungus, <i>Leucocoprinus birnbaumii</i>	
Robert Brkljača and Sylvia Urban	95
Pterandric Acid – its Isolation, Synthesis and Stereochemistry	
Muhammad A. Haleem, Simone C. Capellari, Beryl B. Sympson and Anita J. Marsaioli	99
Cardanol, Long Chain Cyclohexenones and Cyclohexenols from <i>Lannea schimperi</i> (Anacardiaceae)	
Dorothy A. Okoth and Neil A. Koobanally	103
Pulvinulin A, Graminin C, and <i>cis</i>-Gregatin B – New Natural Furanones from <i>Pulvinula</i> sp. 11120, a Fungal Endophyte of <i>Cupressus arizonica</i>	
E. M. Kithsiri Wijeratne, Yaming Xu, A. Elizabeth Arnold and A. A. Leslie Gunatilaka	107
Potent Anti-Calmodulin Activity of Cyclotetradepsipeptides Isolated from <i>Isaria fumosorosea</i> Using a Newly Designed Biosensor	
Abraham Madariaga-Mazón, Martín González-Andrade, Conchita Toriello, Hortensia Navarro-Barranco and Rachel Mata	113
Mutagenesis of Lysines 156 and 159 in Human Immunodeficiency Virus Type 1 Integrase (IN) Reveals Differential Interactions between these Residues and Different IN Inhibitors	
David C. Crosby, Xiangyang Lei, Charles G. Gibbs, Manfred G. Reinecke, and W. Edward Robinson, Jr.	117
Herbal Medicinal Products versus Botanical-Food Supplements in the European market: State of Art and Perspectives	
Anna Rita Bilia	125
Chemical Composition and Biological Activity of Essential Oils of <i>Dracocephalum heterophyllum</i> and <i>Hyssopus officinalis</i> from Western Himalaya	
Iris Stappen, Jürgen Wanner, Nurhayat Tabanca, David E. Wedge, Abbas Ali, Vijay K. Kaul, Brij Lal, Vikas Jaitak, Velizar K. Gochev, Erich Schmidt and Leopold Jirovetz	133
Cytotoxic Active Constituents of Essential Oils of <i>Curcuma longa</i> and <i>Curcuma zanthorrhiza</i>	
Erich Schmidt, Boris Ryabchenko, Juergen Wanner, Walter Jäger and Leopold Jirovetz	139
Antimicrobial Activity of Nerolidol and its Derivatives against Airborne Microbes and Further Biological Activities	
Sabine Krist, Daniel Banovac, Nurhayat Tabanca, David E. Wedge, Velizar K. Gochev, Jürgen Wanner, Erich Schmidt and Leopold Jirovetz	143
Chemical Composition and Antifungal Activity of <i>Aaronsohnia pubescens</i> Essential Oil from Algeria	
Ahmed Makhloufi, L. Ben Larbi, Abdallah Moussaoui, Hamadi A. Lazouni, Abderrahmane Romane, Jürgen Wanner, Erich Schmidt, Leopold Jirovetz and Martina Höferl	149
Radical Scavenging and Antioxidant Activities of Essential Oil Components – An Experimental and Computational Investigation	
Farukh S. Sharopov, Michael Wink and William N. Setzer	153

Accounts/Reviews

Enzyme-Mediated Synthesis of Sesquiterpenes	
Stefano Serra	157
Triterpenoids as Neutrophil Elastase Inhibitors	
Dom Guillaume, Thi Ngoc Tram Huynh, Clément Denhez, Kim Phi Phung Nguyen and Azzaq Belaaouaj	167
Mechanistic Insights to the Cytotoxicity of Amaryllidaceae Alkaloids	
Jerald J. Nair, Lucie Rárová, Miroslav Strnad, Jaume Bastida and Johannes van Staden	171
Review of β-carboline Alkaloids from the Genus <i>Aspidosperma</i>	
Tanya H. Layne, Joy S. Roach and Winston F. Tinto	183
Natural Flavonoids as Potential Herbal Medication for the Treatment of Diabetes Mellitus and its Complications	
Jian Chen, Sven Mangelinckx, An Adams, Zheng-tao Wang, Wei-lin Li and Norbert De Kimpe	187
Lignins of Bioenergy Crops: a Review	
Yadhu N. Guragain, Alvaro I. Herrera, Praveen V. Vadlani and Om Prakash	201
Plant Chemical Defenses: Are all Constitutive Antimicrobial Metabolites Phytoanticipins?	
M. Soledade C. Pedras and Estifanos E. Yaya	209
Sponge Derived Bromotyrosines: Structural Diversity through Natural Combinatorial Chemistry	
Hendrik Niemann, Andreas Marmann, Wenhan Lin and Peter Proksch	219

Number 2

NPC-CSPR issue

Antitumor Constituents of the Wetland Plant <i>Nymphoides peltata</i>: A Case Study for the Potential Utilization of Constructed Wetland Plant Resources	
Yuanda Du, Renqing Wang, Haijie Zhang and Jian Liu	233
Preparation and Characterization of Colon-Targeted Particles of <i>Pulsatilla chinensis</i> Saponins	
Zhenhua Chen, Yongmei Guan, Leilei Zhou, Ying Xu, Ming Yang and Hongning Liu	237
Ursolic Acid and Oleanolic Acid from <i>Eriobotrya fragrans</i> Inhibited the Viability of A549 Cells	
Yuan Yuan, Yongshun Gao, Gang Song and Shunquan Lin	239

Protective Effect of Compound K on Diabetic Rats	243
Xiaotong Shao, Na Li, Jinzhuo Zhan, Hui Sun, Liping An and Peige Du	
New Cytotoxic Triterpene Glycoside from the East China Sea Cucumber <i>Holothuria nobilis</i>	247
Jia-Jia Zhang, Qi-Ke Zhu, Jun Wu and Hui-Wen Zhang	
Ovarian Cancer HO-8910 Cell Apoptosis Induced by Crocin <i>in vitro</i>	249
Dan Xia	
Effect of Puerarin on Expression of Fas/FasL mRNA in Pulmonary Injury induced by Ischemia-Reperfusion in Rabbits	253
Mengxiao Zheng, Dong Song, Ziyin Luo, Zhongqiu Lu, Yiming Wu and Wantie Wang	
Proanthocyanidin from Grape Seed Extract Inhibits Airway Inflammation and Remodeling in a Murine Model of Chronic Asthma	257
Dan-Yang Zhou, Su-Rong Fang, Chun-Fang Zou, Qian Zhang and Wei Gu	
Protective Effect of Silymarin against Rapamycin-induced Apoptosis and Proliferation Inhibition in Endothelial Progenitor Cells	263
Peng Zhang, Guohua Han, Pei Gao, Kun Qiao, Yusheng Ren, Chun Liang, Bing Leng and Zonggui Wu	
Cs₂CO₃-Catalyzed Synthesis of N-Sulfonyl-Substituted Allenamides	267
Li Zheqi	
Theoretical Studies on the Mechanism of the Azido-Tetrazole of Azido-s-triazine	269
Xiao-Qin Liang, Jin-Jun Zhou, Yan Zheng and Feng Ma	
Isolation and Identification of a Polygalacturonase Inhibiting Protein from <i>Isatidis</i> root	273
Guanzhen Gao, Qian Wang, Jianwu Zhou, Huiqin Wang, Lijing Ke and Pingfan Rao	

Original Paper

Antibacterial Triterpenoids from the Bark of <i>Sonneratia alba</i> (Lythraceae)	277
Harizon, Betry Pujiastuti, Dikdik Kurnia, Dadan Sumiarsa, Yoshihito Shiono, and Unang Supratman	
Hypotensive and Bradycardic Effects of Quinovic Acid Glycosides from <i>Aspidosperma fendleri</i> in Spontaneously Hypertensive Rats	281
Omar Estrada, Juan M. González-Guzmán, María M. Salazar-Bookman, Alfonso Cardozo, Eva Lucena, and Claudia P. Alvarado-Castillo	
Chemical Composition and <i>in vitro</i> Cytotoxic and Antileishmanial Activities of Extract and Essential Oil from Leaves of <i>Piper cernuum</i>	285
Tabata M. Capello, Euder G. A. Martins, Camyla F. de Farias, Carlos R. Figueiredo, Alisson L. Matsuo, Luiz Felipe D. Passero, Diogo Oliveira-Silva, Patricia Sartorelli and João Henrique G. Lago	
Synthesis and Antihyperlipidemic Activity of Piperic Acid Derivatives	289
Rong A, Narisu Bao, Zhaorigetu Sun, Gereltu Borjijahan, Yanjiang Qiao and Zhuang Jin	
A New Benzylisoquinoline Alkaloid from <i>Leontice altaica</i>	291
Janar Jenis, Alfarius Eko Nugroho, Akiyo Hashimoto, Jun Deguchi, Yusuke Hirasawa, Chin Piow Wong, Toshio Kaneda, Osamu Shiota and Hiroshi Morita	
Quantitative Analysis of Bioactive Carbazole Alkaloids in <i>Murraya koenigii</i>	293
Trapti Joshi, Rohit Mahar, Sumit K. Singh, Piush Srivastava, Sanjeev K. Shukla, Dipak K. Mishra, R.S. Bhatta and Sanjeev Kanojiya	
Anthocephaline, a New Indole Alkaloid and Cadambine, a Potent Inhibitor of DNA Topoisomerase IB of <i>Leishmania donovani</i> (LdTOP1LS), Isolated from <i>Anthocephalus cadamba</i>	297
Ashish Kumar, Somenath Roy Chowdhury, Kumar Kalyan Jatte, Tulika Chakrabarti, Hemanta K Majumder, Tarun Jha and Sibabrata Mukhopadhyay	
Phosphodiesterase Inhibitory Activity of the Flavonoids and Xanthones from <i>Anaxagorea luzonensis</i>	301
Chalisa Sabphon, Prapapan Temkithawon, Kornkanok Ingkaninan and Pattara Sawasdee	
Xanthone Derivatives from the Fermentation Products of an Endophytic Fungus <i>Phomopsis</i> sp.	305
Yanlin Meng, Yuchun Yang, Ying Qin, Congfang Xia, Min Zhou, Xuemei Gao, Gang Du ^{and} Qiufen Hu	
Coumarins from <i>Murraya paniculata</i> var. <i>zollingeri</i> Endemic to the Timor Islands	309
Naoko Teshima, Hiromi Yamada, Motoharu Ju-ichi, Tahan Uji, Takeshi Kinoshita and Chihiro Ito	
A New Geranylbenzofuranone from <i>Zanthoxylum armatum</i>	313
Vinod Bhatt, Vishal Kumar, Bikram Singh and Neeraj Kumar	
A New Antioxidant Pyrano[4,3-c] [2]benzopyran-1,6-dione Derivative from the Medicinal Mushroom <i>Fomitiporia ellipsoidea</i>	315
Li Feng Zan, Hai Ying Bao, Tolgor Bau and Yu Li	
Anti-inflammatory Anthraquinones from the Crinoid <i>Himerometra magnipinna</i>	317
Yen-You Lin, Su-June Tsai, Michael Y. Chiang, Zhi-Hong Wen and Jui-Hsin Su	
Phenolic Compounds from <i>Limonium pruinosum</i>	319
Sihem Boudermine, Nicola Malafronte, Teresa Mencherini, Tiziana Esposito, Rita Patrizia Aquino, Noureddine Beghidja, Samir Benayache, Massimiliano D'Ambola and Antonio Vassallo	
Two New Compounds from <i>Paeonia lactiflora</i>	323
QingHu Wang, Nayintai Dai, Narenchaoketu Han and Wuliji Ao	
Arylalkanones from <i>Horsfieldia macrobotrys</i> are Effective Antidiabetic Agents Achieved by α-Glucosidase Inhibition and Radical Scavenging	325
Rico Ramadhan and Preecha Phuwapraisiran	
Metabolomic Characterization of a Low Phytic Acid and High Anti-oxidative Cultivar of Turmeric	329
Ken Tanaka, Masanori Arita, Donghan Li, Naoaki Ono, Yasuhiro Tezuka and Shigehiko Kanaya	
The Cardioprotective Effects of Resveratrol in Rats with Simultaneous Type 2 Diabetes and Renal Hypertension	335
Masoud Mozafari, Ali Akbar Nekooeian, Elaheh Mashghoolzeh and Mohammad Reza Panjeshahin	

A Specific Process to Purify 2-Methyl-D-Erythritol-4-Phosphate Enzymatically Converted from D-Glyceraldehyde-3-Phosphate and Pyruvate	339
Shao-Qing Yang, Jian Deng, Qian-Qian Wu, Heng Li and Wen-Yun Gao	
Two New Ramulosin Derivatives from the Entomogenous Fungus <i>Truncatella angustata</i>	341
Shenxi Chen, Zhuowei Zhang, Li Li, Xingzhong Liu and Fengxia Ren	
Anti-inflammatory and Cytotoxic Compounds from <i>Solanum macaonense</i>	345
Chia-Lin Lee, Tsong-Long Hwang, Chieh-Yu Peng, Chao-Jung Chen, Chao-Lin Kuo, Wen-Yi Chang and Yang-Chang Wu	
<i>Crassostrea gigas</i> Oyster Shell Extract Inhibits Lipogenesis via Suppression of Serine Palmitoyltransferase	349
Nguyen Khoi Song Tran, Jeong Eun Kwon, Se Chan Kang, Soon-Mi Shim and Tae-Sik Park	
Using the Gene Expression Signature of Scutellarin VN Isolated from <i>Scutellaria barbata</i> to Elucidate its Anticancer Activities	353
Do Thi Thao, Chi-Ying Huang, Kuan-Ting Lin, Do Thi Phuong, Nguyen Thi Nga, Nguyen Thi Trang, Nguyen Thi Cuc, Nguyen Xuan Cuong, Nguyen Hoai Nam and Chau Van Minh	
Comparison of Different Methodologies for Detailed Screening of <i>Taraxacum officinale</i> Honey Volatiles	357
Igor Jerković, Zvonimir Marijanović, Marina Kranjac and Ani Radonić	
Volatile Constituents from the Leaves, Fruits (Berries), Stems and Roots of <i>Solanum xanthocarpum</i> from Nepal	361
Prabodh Satyal, Samjhana Maharjan and William N. Setzer	
Essential Oil Constituents of <i>Etlingera yunnanensis</i> and <i>Hornstedtia sanhan</i> grown in Vietnam	365
Dao T. M. Chau, Do N. Dai, Tran M. Hoi, Tran H. Thai, Tran D. Thang and Isiaka A. Ogunwande	
Chemical Constituents of Essential Oils from the Leaves, Stems, Roots and Fruits of <i>Alpinia polyantha</i>	367
Le T. Huong, Tran D. Thang and Isiaka A. Ogunwande	
Volatile Constituents of the Fruit and Roots of <i>Cymbopogon olivieri</i>	369
Jinous Asgarpanah, Setareh Bahrani and Elham Bina	
Composition of Essential Oils Isolated from the Needles of <i>Pinus uncinata</i> and <i>P. uliginosa</i> Grown in Poland	371
Radosław Bonikowski, Konrad Celiński, Aleksandra Wojnicka-Półtorak and Tomasz Małysiński	
Essential Oil Composition and Antimicrobial Activity of <i>Vismia macrophylla</i> Leaves and Fruits Collected in Táchira-Venezuela	375
Alexis Buitrago, Janne Rojas, Luis Rojas, Judith Velasco, Antonio Morales, Yonel Peñaloza and Clara Díaz	

Number 3

Flavonoids: Colors, Functions and Activities (Guest Editor: Tsukasa Iwashina)

Extraction of Pinocembrin from Leaves of Different Species of <i>Eucalyptus</i> and its Quantitative Analysis by qNMR and HPTLC	379
Isha Saraf, Alka Choudhary, Ram Jee Sharma, Karthik Dandi, Karen J. Marsh, William J. Foley and Inder Pal Singh	
Anti-inflammatory Compounds from <i>Ampelopsis cantoniensis</i>	383
Nguyen Van Thu, To Dao Cuong, Tran Manh Hung, Hoang Van Luong, Mi Hee Woo, Jae Su Choi, Jeong-Hyung Lee, Jeong Ah Kim and Byung Sun Min	
Convergent Synthesis of Moslosooflavone, Isowogonin and Norwogonin from Chrysins	387
Lin-Lin Jing, Xiao-Fei Fan, Zheng-Ping Jia, Peng-Cheng Fan and Hui-Ping Ma	
Tangeretin Triggers Melanogenesis through the Activation of Melanogenic Signaling Proteins and Sustained Extracellular Signal-Regulated Kinase in B16/F10 Murine Melanoma Cells	389
Hoon Seok Yoon, Hee-Chul Ko, Sang Suk Kim, Kyung Jin Park, Hyun Joo An, Young Hun Choi, Se-Jae Kim, Nam-Ho Lee and Chang-Gu Hyun	
Flavonoids from <i>Artocarpus anisophyllus</i> and their Bioactivities	393
Siti Mariam Abdul Lathiff, Noraini Jemaon, Siti Awanis Abdullah and Shajarahtunnur Jamil	
<i>Chrysanthemum indicum</i> Attenuates Cisplatin-induced Nephrotoxicity both <i>in vivo</i> and <i>in vitro</i>	397
Tae-Won Kim, Young-Jung Kim, So-Ra Park, Chang-Seob Seo, Hyekyung Ha, Hyeun-Kyoo Shin and Ju-Young Jung	
Foliar Flavonoids from <i>Tanacetum vulgare</i> var. <i>boreale</i> and their Geographical Variation	403
Ayumi Uehara, Shinobu Akiyama and Tsukasa Iwashina	
Altitudinal Variation of Flavonoid Content in the Leaves of <i>Fallopia japonica</i> and the Needles of <i>Larix kaempferi</i> on Mt. Fuji	407
Yoshinori Murai, Hiroaki Setoguchi, Junichi Kitajima and Tsukasa Iwashina	
Quantitative Flavonoid Variation Accompanied by Change of Flower Colors in <i>Edgeworthia chrysanthia</i>, <i>Pittosporum tobira</i> and <i>Wisteria floribunda</i>	413
Megumi Ono and Tsukasa Iwashina	
New Kaempferol 3,7-Diglycosides from <i>Asplenium ruta-muraria</i> and <i>Asplenium altajense</i>	417
Tsukasa Iwashina, Junichi Kitajima, Takayuki Mizuno, Sergey V. Smirnov, Oyunchimeg Damdinsuren and Katsuhiko Kondo	
New Flavonol Glycosides from the Leaves and Flowers of <i>Primula sieboldii</i>	421
Nana Hashimoto, Ryo Ohsawa, Junichi Kitajima and Tsukasa Iwashina	
Flavone C-Glucosides Responsible for Yellow Pigmentation Induced by Low Temperature in Bracts of <i>Zantedeschia aethiopica</i>	425
Masayoshi Nakayama, Masaji Koshioka, Tadao Kondo and Kiyotoshi Imizu	
Flavonoids and their Qualitative Variation in <i>Calystegia soldanella</i> and Related Species (Convolvulaceae)	429
Yoshinori Murai, Hiroaki Setoguchi, Eiichiro Ono and Tsukasa Iwashina	

A New Triglycosyl Flavonoid Isolated from Leaf Juice of <i>Kalanchoe gastonis-bonnieri</i> (Crassulaceae)	433
Sônia Soares Costa, Maria Fernanda Paresqui Corrêa and Livia Marques Casanova	
Flavonoids from <i>Stellaria nemorum</i> and <i>Stellaria holostea</i>	437
Elena Ancheeva, Georgios Daletos, Rini Muharini, Wen Han Lin, Leonid Teslov and Peter Proksch	
Novel C-Xylosylflavones from the Leaves and Flowers of <i>Iris gracilipes</i>	441
Takayuki Mizuno, Tsunashi Kamo, Nobuhiro Sasaki, Hiroshi Yada, Yoshinori Murai and Tsukasa Iwashina	
Constituents of the Leaves of <i>Verbascum blattaria</i>	445
I-Soo Youn, Ah-Reum Han, Mark S. Roh and Eun-Kyoung Seo	
Anthocyanins and Other Flavonoids as Flower Pigments from Eleven <i>Centaurea</i> Species	447
Tamaki Mishio, Kosaku Takeda and Tsukasa Iwashina	
Flower Color Changes in three Japanese <i>Hibiscus</i> Species: Further Quantitative Variation of Anthocyanin and Flavonols	451
Satoshi Shimokawa, Tsukasa Iwashina and Noriaki Murakami	
Anthocyanins in the Bracts of <i>Curcuma</i> Species and Relationship of the Species Based on Anthocyanin Composition	453
Masaji Koshioka, Naoko Umegaki, Kriangsuk Boontiang, Witayaporn Pornchuti, Kanchit Thammasiri, Satoshi Yamaguchi, Fumi Tatsuzawa, Masayoshi Nakayama, Akira Tateishi and Satoshi Kubota	
Acylated Cyanidin 3-sophoroside-5-glucoside in Purple-violet Flowers of <i>Moricandia arvensis</i> (Brassicaceae)	457
Fumi Tatsuzawa, Kazuhisa Kato, Motoki Sato, Shun Ito, Hiroki Muraoka, Yoshihito Takahata and Satoshi Ogawa	
Molecular Structures of the Stem Tuber Anthocyanins of Colored Potatoes and Their Coloring Effects on the Tubers	461
Chang Ling Zhao, Guo Song Wen, Zi Chao Mao, Shao Zhong Xu, Zheng Jie Liu, Ming Fu Zhao and Chun Lin	
Biological Activity of the Methanol and Water Extracts of the Fruits of Anthocyanin-Rich Plants Grown in South-West Poland	467
Paulina Strugała, Anna Dudra, Alicja Z. Kucharska, Anna Sokół-Lętowska, Dorota Wojnicz, Agnieszka Cisowska, Stefan Walkowski, Zbigniew Sroka, Janina Gabrelska and Andrzej B. Hendrich	
Investigation into the Antioxidant and Antidiabetic Potential of <i>Moringa stenopetala</i>: Identification of the Active Principles	475
Solomon Habtemariam	
Polyphenolic Compounds and Antioxidant Activities of the Leaves of <i>Glochidion hypoleucum</i>	479
Nathhinee Anantachoke, Worawan Kitphati, Supachoke Mangmool and Nuntavan Bunyaphraphatsara	
Evaluation of Antioxidant Activity, and Quantitative Estimation of Flavonoids, Saponins and Phenols in Crude Extract and Dry Fractions of <i>Medicago lupulina</i> Aerial Parts	483
Agnieszka Kicel and Monika Anna Olszewska	
Dual Excitatory and Smooth Muscle-relaxing Effect of <i>Sideritis montana</i> Extract on Guinea-pig Ileum	487
Barbara Tóth, Loránd Barthó, Andrea Vasas, Zsolt Sándor, Nikoletta Jedlinszki, Gyula Pink and Judit Hohmann	
Phenolic Constituents of <i>Carex vulpinoidea</i> Seeds and their Tyrosinase Inhibitory Activities	491
Daniel B. Niesen, Hang Ma, Tao Yuan, Alvin C. Bach II, Geneive E. Henry and Navindra P. Seeram	
Analysis of Active Compounds and Antioxidant Activity Assessment of Six Popular Chinese <i>Juhua</i> Teas	495
Hui Du, Shan-Shan Li, Qian Wu, Kui-Xian Ji, Jie Wu, Yang Liu and Liang-Sheng Wang	
Two New Isoflavanones from the Roots of <i>Erythrina variegata</i>	499
Hitoshi Tanaka, Ikunori Atsumi, Motori Hasegawa, Miyuki Hirata, Tatsuko Sakai, Masaru Sato, Ryozo Yamaguchi, Yoichi Tateishi, Toshiyuki Tanaka and Toshio Fukai	
Croceteneone, a New Rotenoid with an Unusual trans-fused Ring System from <i>Iris crocea</i>	503
Gulzar A. Bhat, Fauzia Mir, Abdul S. Shawl, Bashir A. Ganai, Azra N. Kamili, Akbar Masood and Mudasir A. Tantry	

Accounts/Reviews

Wood Colors and their Coloring Matters: A Review	505
Yoshikazu Yazaki	
Utilization of Flavonoid Compounds from Bark and Wood: A Review	513
Yoshikazu Yazaki	
Flavonoids in Foods: A Review	521
Norihiro Terahara	
Contribution to Flower Colors of Flavonoids Including Anthocyanins: A Review	529
Tsukasa Iwashina	

Number 4

Antiproliferative Effect of Linalool on RPMI 7932 Human Melanoma Cell Line: Ultrastructural Studies	547
Teresa Cerchiara, Serafina Vittoria Straface, Elvira Brunelli, Sandro Tripepi, Maria Caterina Gallucci and Giuseppe Chidichimo	
Synthesis of Chiral Hexasubstituted Cyclohexanediol, a Key Intermediate for the Synthesis of Verticillol, from (+)-Dihydrocarvone; Attempted Cyclization to 12-Membered Carbocycle in Verticillol using RCM Reaction	551
Katsuyuki Nakashima, Yuzuru Kondo, Kosei Yoshimasu, Masakazu Sono and Motoo Tori	
Diterpenoid Derivatives of Kenyan <i>Croton sylvaticus</i>	557
Beth Ndunda, Moses K. Langat, Jacob O. Midiwo and Leonidah K. Omosa	
Degradation Products of Rubusoside under Acidic Conditions	559
Indra Prakash, Cynthia Bunders, Krishna P. Devkota, Romila D. Charan, Rachael M. Hartz, Tracy L. Sears, Tara M. Snyder and Catherine Ramirez	
A Novel Triterpene from the Roots of <i>Paullinia pinnata</i>: 6α-(3'-methoxy-4'-hydroxybenzoyl)-lup-20(29)-ene-3-one	563
Nora Jackson, Kofi Annan, Abraham Y. Mensah, Edmund Ekuadzi, Merlin L. K. Mensah and Solomon Habtemariam	

Effects of Ursolic Acid on Contractile Activity of Gastric Smooth Muscles	565
Natalia Prissadova, Petko Bozov, Kiril Marinkov, Hristo Badakov and Atanas Kristev	
Bioactive Oleanane Glycosides from <i>Polyscias duplicata</i> from the Madagascar Dry Forest	567
Alexander L. Eaton, Peggy J. Brodie, Martin W. Callmander, Roland Rakotondrajaona, Etienne Rakotobe, Vincent E. Rasamison and David G. I. Kingston	
Design, Synthesis and Biological Evaluation of Caudatin and its Ester Derivatives as Novel Antitumor Agents	571
Xuefen Tao, Yongmin Ma, Jing Chen and Huajun Zhao	
Elucidation of the Mass Fragmentation Pathways of Tomatidine and β_1-Hydroxytomatine using Orbitrap Mass Spectrometry	575
Giovanni Caprioli, Michael Cahill, Serena Logrippo and Kevin James	
Alkaloids from <i>Peumus boldus</i> and their Acetylcholinesterase, Butyrylcholinesterase and Prolyl Oligopeptidase Inhibition Activity	577
Anna Hošťáková, Lubomír Opletal, Jiří Kuneš, Zdeněk Novák, Martina Hrabinová, Jakub Chlebek, Lukáš Čegan and Lucie Cahlíková	
Concise Synthesis of N,N-Dimethyltryptamine and 5-Methoxy-N,N-dimethyltryptamine Starting with Bufotenine from Brazilian <i>Anadenanthera</i> ssp.	581
Leandro A. Moreira, Maria M. Murta, Claudia C. Gatto, Christopher W. Fagg and Maria L. dos Santos	
A New Cytotoxic Cytochalasin from the Endophytic Fungus <i>Trichoderma harzianum</i>	585
Huiqin Chen, Georgios Daletos, Festus Okoye, Daowan Lai, Haofu Dai and Peter Proksch	
Inhibition of Soybean 15-Lipoxygenase by Naturally Occurring Acetophenones and Derricidin	589
Vito Alessandro Taddeo, Francesco Epifano*, Salvatore Genovese and Serena Fiorito	
Synthesis of Auronol Derivatives and Their Immunostimulating Activity	591
Phuong Diep Thi Lan, Quoc Vuong Nguyen, Van Chien Vu, Tuan Nguyen Le, Thi Hue Nguyen, Thi Hang Pham, Van Minh Chau and Van Cuong Pham	
Cytotoxic Compounds from Endemic <i>Arnebia purpurea</i>	595
Merve Yuzbasioglu, Ayse Kuruuzum-Uz, Zuhal Guvenalp, András Simon, Gábor Tóth, U. Sebnem Harput, Cavit Kazaz, Bilgehan Bilgili, Hayri Duman, Iclal Saracoglu and L. Omur Demirezer	
Evaluation of the Anti-inflammatory and Antioxidative Potential of Four Fern Species from China Intended for Use as Food Supplements	597
Carine Dion, Christian Haug, Haifeng Guan, Christophe Ripoll, Peter Spitteler, Aurelie Coussaert, Elodie Boulet, Daniel Schmidt, Jianbing Wei, Yijun Zhou and Kai Lamottke	
The Search for Antifungals from Amazonian Trees: A Bio-Inspired Screening	605
Charlie Basset, Véronique Eparvier and Laila S. Espindola	
Structure Elucidation and Antioxidant Activity of the Phenolic Compounds from <i>Rhynchosia suaveolens</i>	609
Aluru Rammohan, Duvvuru Gunasekar, Netala Vasudeva Reddy, Tarte Vijaya, Alexandre Deville and Bernard Bodo	
Anti-Vancomycin-resistant <i>Enterococcus faecium</i> and <i>E. faecalis</i> Activities of (-)-Gossypol and Derivatives from <i>Thespesia garckeana</i>	613
Veronica M. Masila, Jacob O. Midwo, Jin Zhang, Bonface M. Gisacho, Renee Munayi, Leonidah K. Omosa, Frank T. Wiggers, Melissa R. Jacob, Larry A. Walker and Ilias Muhammad	
Coumarins from <i>Murraya exotica</i> Collected in Egypt	617
Naoko Negi, Ahmad Muhamad Abou-Dough, Masumi Kurosawa, Yukako Kitaji, Keiko Saito, Asae Ochi, Kaori Ushijima, Eri Kusakabe, Yoshimi Kitaguchi, Yu Jinguiji, Naoko Teshima, Motoharu Ju-ichi and Chihiro Ito	
Two Chlorinated Benzofuran Derivatives from the Marine Fungus <i>Pseudallescheria boydii</i>	621
Dan-Feng Yan, Wen-Jian Lan, Kun-Teng Wang, Lei Huang, Cai-Wu Jiang and Hou-Jin Li	
A New Citrinin Dimer Isolated from <i>Aspergillus terreus</i> Strain ZDF21	623
Zerihun T. Dame, Nakarin Suwannarach, Saisamorn Lumyong and Hartmut Laatsch	
A New Naphthoquinone from <i>Sinningia leucotricha</i> (Gesneriaceae)	625
Maria Helena Verdan, Hector H. F. Koolen, Marcos José Salvador, Andersson Barison and Maria Elida A. Stefanello	
Caffeic Acid: Potential Applications in Nanotechnology as a Green Reducing Agent for Sustainable Synthesis of Gold Nanoparticles	627
Yu Seon Seo, Song-Hyun Cha, Seonho Cho, Hye-Ran Yoon, Young-Hwa Kang and Youmie Park	
Anti-allergic Inflammatory Activities of Compounds of <i>Amomi Fructus</i>	631
Hyun Gyu Choi, In-Gyu Je, Geum Jin Kim, Hyukjae Choi, Sang Hyun Kim, Jeong Ah Kim and Seung Ho Lee	
Chemical Constituents and Derivatization of Melodorinol from the Roots of <i>Melodorum fruticosum</i>	633
Siriwat Hongnak, Jongkolnee Jongaramruong, Suttira Khumkratok, Pongpun Siriphong and Santi Tip-pyang	
New Bicyclo-spartinols from the Marine-derived Fungus <i>Phaeosphaeria spartinae</i>	637
Mahmoud Fahmi Elsebai, Fayrouz El Maddah, Stefan Kehraus and Gabriele M. König	
Hydropiperside, a new Sphingoglycolipid from <i>Polygonum hydropiper</i>	641
Rajia Sultana, Rashadul Hossain, Achyut Adhikari, Zulfiqar Ali, Muhammad Iqbal Choudhary and Muhammad Shahed Zaman	
Synthetic Studies of Enacyloxins: A Series of Antibiotics Isolated from <i>Fraterulria</i> sp. W-315: C1'-C8' and C9'-C15' Fragments	645
Aki Saito, Wataru Igarashi, Hiroyuki Furukawa, Hiroki Hoshikawa, Teiko Yamada, Shigefumi Kuwahara and Hiromasa Kiyota	
Chemical Composition of the Essential oil of <i>Laserpitium latifolium</i> from Serbia	649
Violeta Mitić, Vesna Stankov-Jovanović, Aleksandra Djordjević, Marija Ilic, Strahinja Simonovic and Gordana Stojanovic	
Chemical Composition of the Essential Oil of <i>Gynoxys meridana</i> from Mérida, Venezuela	653
Johanna Hernández, Luis B. Rojas-Fernán, Juan Amaro-Luis, Laurent Pouységú, Stéphane Quideau and Alfredo Usobilaga	
Chemical Composition and Antibacterial Activity of the Essential Oil of <i>Ruilepezia bracteosa</i>	655
Libia Alarcón, Alexis Peña, Judith Velasco, José Gregorio Baptista, Luis Rojas, Rosa Aparicio and Alfredo Usobilaga	

Comparison of the Chemical Composition of <i>Valeriana parviflora</i> Essential Oils Collected in the Venezuelan Andes in two Different Seasons	
Sammy Fernández, María Rondón, Janne Rojas, Antonio Morales and Luis Rojas-Fermin	657
Endemic Balkan Parsnip <i>Pastinaca hirsuta</i>: the Chemical Profile of Essential Oils, Headspace Volatiles and Extracts	
Snežana Č. Jovanović, Olga P. Jovanović, Goran M. Petrović and Gordana S. Stojanović	661
Chemical Composition and Anti-mildew Activities of Essential Oils from Different Parts of <i>Michelia compressa</i> var. <i>formosana</i>	
Yu-Chang Su, Kuang-Ping Hsu, Eugene I-Chen Wang and Chen-Lung Ho	665
Analgesic and Antiinflammatory Activities of the Essential Oil of the Unique Plant <i>Zhumeria majdae</i>	
Seyyedeh Ghazal Miraghazadeh, Hamed Shafaroodi and Jinous Asgarpanah	669
Antimicrobial Activity and Chemical Composition of the Essential Oils of Portuguese <i>Foeniculum vulgare</i> Fruits	
Ana S. Mota, M. Rosário Martins, Silvia Arantes, Violeta R. Lopes, Eliseu Bettencourt, Sofia Pombal, Arlindo C. Gomes and Lúcia A. Silva	673
Larvicidal Activity Against <i>Aedes aegypti</i> of <i>Foeniculum vulgare</i> Essential Oils from Portugal and Cape Verde	
Diara Kady Rocha, Olivia Matos, Maria Teresa Novo, Ana Cristina Figueiredo, Manuel Delgado and Cristina Moiteiro	677

Accounts/Reviews

Chemical Constituents of the Genus <i>Polygonatum</i> and their Role in Medicinal Treatment	
Xueying Zhao and Ji Li	683

Number 5

<u>Gerald Blunden Award (2014)</u>	<u>Page</u>
Stereocontrolled Total Synthesis of Tetrodotoxin from myo-Inositol and D-Glucose by Three Routes: Aspects for Constructing Complex Multi-Functionalized Cyclitols with Branched-Chain Structures	
Ken-ichi Sato, Shoji Akai and Juji Yoshimura	691

Metabolism and Biological Function of Natural Products in Plants
(Guest editor: Hiroshi Ashihara)

<i>(a) Biosynthesis</i>	
Occurrence and <i>De novo</i> Biosynthesis of Caffeine and Theanine in Seedlings of Tea (<i>Camellia sinensis</i>)	
Wei-Wei Deng and Hiroshi Ashihara	703
Metabolism of Purine Alkaloids and Xanthine in Leaves of Maté (<i>Ilex paraguariensis</i>)	
Yuling Yin, Riko Katahira and Hiroshi Ashihara	707
Comparative Analysis of Two DOPA Dioxygenases from <i>Phytolacca americana</i>	
Kana Takahashi, Kazuko Yoshida and Masaaki Sakuta	713
Biochemical Analysis of <i>Phytolacca</i> DOPA Dioxygenase	
Kana Takahashi, Kazuko Yoshida, Kei Yura, Hiroshi Ashihara and Masaaki Sakuta	717
Unraveling the Biosynthesis of Pilocarpine in <i>Pilocarpus microphyllus</i>	
Alexandra Christine Helena Frankland Sawaya, Yanna Dias Costa and Paulo Mazzafera	721

<i>(b) Allelopathy</i>	
Transcriptomic Evaluation of Plant Growth Inhibitory Activity of Goniothalamin from the Malaysian Medicinal Plant <i>Goniothalamus andersonii</i>	
Naoya Wasano, Tomoko Takemura, Raihan Ismil, Baki Bakar and Yoshiharu Fujii	725
Momilactone Sensitive Proteins in <i>Arabidopsis thaliana</i>	
Hisashi Kato-Noguchi and Shinya Kitajima	729
Effect of Caffeine on the Expression Pattern of Water-Soluble Proteins in Rice (<i>Oryza sativa</i>) Seedlings	
Wei-Wei Deng, Hamako Sasamoto and Hiroshi Ashihara	733
Short Term Effect of Caffeine on Purine, Pyrimidine and Pyridine Metabolism in Rice (<i>Oryza sativa</i>) Seedlings	
Wei-Wei Deng, Riko Katahira and Hiroshi Ashihara	737
Cyanamide Phytotoxicity in Soybean (<i>Glycine max</i>) Seedlings involves Aldehyde Dehydrogenase Inhibition and Oxidative Stress	
John S. Maninang, Shin Okazaki and Yoshiharu Fujii	743
Allelopathy in a Leguminous Mangrove Plant, <i>Derris indica</i>: Protoplast Co-culture Bioassay and Rotenone Effect	
Aya Inoue, Daisuke Mori, Reiko Minagawa, Yoshiharu Fujii and Hamako Sasamoto	747
Effect of Purine Alkaloids on the Proliferation of Lettuce Cells Derived from Protoplasts	
Hamako Sasamoto, Yoshiharu Fujii and Hiroshi Ashihara	751
A Protocol for Axenic Liquid Cell Cultures of a Woody Leguminous Mangrove, <i>Caesalpinia crista</i>, and their Amino Acids Profiling	
Aya Inoue, Shinjiro Ogita, Shinpei Tsuchiya, Reiko Minagawa and Hamako Sasamoto	755
Phytotoxic Substance with Allelopathic Activity in <i>Brachiaria decumbens</i>	
Ai Kobayashi and Hisashi Kato-Noguchi	761

Isolation and Identification of an Allelopathic Substance from <i>Hibiscus sabdariffa</i> Prapaipit Suwitchayanon, Piyatida Pukclai, Osamu Ohno, Kiyotake Suenaga and Hisashi Kato-Noguchi	765
Angelinic as the Principal Allelochemical in <i>Heracleum sosnowskyi</i> Fruit Maryia Mishyna, Nikolai Laman, Valery Prokhorov and Yoshiharu Fujii	767
Identification of Octanal as Plant Growth Inhibitory Volatile Compound Released from <i>Heracleum sosnowskyi</i> Fruit Maryia Mishyna, Nikolai Laman, Valery Prokhorov, John Solomon Maninang and Yoshiharu Fujii	771
Identification of Safranal as the Main Allelochemical from Saffron (<i>Crocus sativus</i>) Hossein Mardani, Takayuki Sekine, Majid Azizi, Maryia Mishyna and Yoshiharu Fujii	775
 (c) Biotechnology	
The Biosynthetic Activities of Primary and Secondary Metabolites in Suspension Cultures of <i>Aquilaria microcarpa</i> Shinjiro Ogita, Jung-Bum Lee, Fumiya Kuroaki and Yasuo Kato	779
A Stepwise Protocol for Induction and Selection of Prominent Coniferous Cell Cultures for the Production of β-Thujaplicin Shinjiro Ogita, Masahito Shichiken, Chizuru Ito, Toshiyuki Yamashita, Taiji Nomura and Yasuo Kato	783
Low Caffeine Content in Novel Grafted Tea with <i>Camellia sinensis</i> as Scions and <i>Camellia oleifera</i> as Stocks Wei-Wei Deng, Min Li, Chen-Chen Gu, Da-Xiang Li, Lin-Long Ma, Yang Jin and Xiao-Chun Wan	789

Accounts/Reviews

Revisiting Caffeine Biosynthesis – Speculations about the Proximate Source of its Purine Ring Thomas W. Baumann	793
Biosynthesis of Caffeine Underlying the Diversity of Motif B' Methyltransferase Fumiyo Nakayama, Kouichi Mizuno and Misako Kato	799
Occurrence, Biosynthesis and Metabolism of Theanine (γ-Glutamyl-L-ethylamide) in Plants: A Comprehensive Review Hiroshi Ashihara	803
Involvement of Allelopathy in the Formation of Monospecific Colonies of Ferns Hisashi Kato-Noguchi	811
Plant Cell, Tissue and Organ Culture: the Most Flexible Foundations for Plant Metabolic Engineering Applications Shinjiro Ogita	815

Number 6

Chemical and Genetic Diversity of <i>Ligularia hodgsonii</i> in China Chiaki Kuroda, Kou Inagaki, Xun Chao, Kyosuke Inoue, Yasuko Okamoto, Motoo Tori, Xun Gong, and Ryo Hanai	823
Constituents of <i>Ligularia brassicoides</i> Collected in China: A New Diels-Alder Adduct of Eremophilan-10β-ol and Methacrylic Acid Mizuho Taniguchi, Katsuyuki Nakashima, Yasuko Okamoto, Xun Gong, Chiaki Kuroda and Motoo Tori	827
Four New Sesquiterpenoids from <i>Ligularia subspicata</i> Collected in China; Isolation of a Bakkane-type Lactone, an Eremophilane-type Lactone, and Two Ortho Esters Yoshinori Saito, Takanori Otsubo, Yuko Iwamoto, Katsuyuki Nakashima, Yasuko Okamoto, Xun Gong, Chiaki Kuroda and Motoo Tori	831
Natural Caryophyllane Sesquiterpenoids from <i>Rumphella antipathies</i> Hsu-Ming Chung, Wei-Hsien Wang, Tsong-Long Hwang, Yang-Chang Wu and Ping-Jyun Sung	835
Bioactive Compounds in Wild, <i>In vitro</i> Obtained, <i>Ex vitro</i> Adapted, and Acclimated Plants of <i>Centaurea davidovii</i> (Asteraceae) Antoaneta Trendafilova, Milka Jadranin, Rossen Gorgorov and Marina Stanilova	839
New Laurene-type Sesquiterpene from Bornean <i>Laurencia nangii</i> Takashi Kamada and Charles Santhanaraju Vairappan	843
New Furanone and Sesquiterpene from the Pericarp of <i>Calocedrus formosana</i> Tzong-Huei Lee, Ming-Shian Lee, Horng-Huey Ko, Jih-Jung Chen, Hsun-Shuo Chang, Mei-Hwei Tseng, Sheng-Yang Wang, Chien-Chih Chen and Yueh-Hsiung Kuo	845
The Importance of the 5-Alkyl Substituent for the Violet Smell of Ionones: Synthesis of Racemic 5-Demethyl-α-ionone Serena Chierici, Serena Bugoni, Alessio Porta, Giuseppe Zanoni and Giovanni Vidari	847
Antiproliferative Activity of <i>seco</i>-Oxacassanes from <i>Acacia schaffneri</i> J. Martín Torres-Valencia, Virginia Motilva, J. Jesús Manríquez-Torres, Sofía García-Mauriño, Miguel López-Lázaro, Hanaa Zbakh, José M. Calderón-Montaño, Mario A. Gómez-Hurtado, Juan A. Gayoso-De-Lucio, Carlos M. Cerda-García-Rojas and Pedro Joseph-Nathan	853
<i>neo</i>-Clerodane Diterpenoids from <i>Ajuga macrosperma</i> var. <i>breviflora</i> Amaya Castro, Josep Coll, Anil K. Pant and Om Pakrash	857
Three New C₂₀-Diterpenoid Alkaloids from <i>Aconitum tanguticum</i> var. <i>trichocarpum</i> Zhong-Tang Zhang, Xiao-Yu Liu, Dong-Lin Chen, and Feng-Peng Wang	861
Manoalide-related Sesterterpene from the Marine Sponge <i>Luffariella variabilis</i> Toshiyuki Hamada, Daisuke Harada, Mitsunobu Hirata, Keisuke Yamashita, Kishneth Palaniveloo, Hiroaki Okamura, Tetsuo Iwagawa, Naomichi Arima, Toshiyuki Iriguchi, Nicole J. de Voogd and Charles S. Vairappan	863
Oxygenated Terpenes from Indo-Pacific Nudibranchs: Scalarane Sesterterpenes from <i>Glossodoris hikuerensis</i> and 12-Acetoxy Dendrillolide A from <i>Goniobranchus albonares</i> I. Wayan Mudianta, Andrew M. White and Mary J. Garson	865

Germinating Seeds of <i>Citrus aurantium</i> a Good Source of Bioactive Limonoids	869
Marta R. Ariza, M. Mar Herrador del Pino and Alejandro F. Barrero	
Chemical Constituents of <i>Lecythis pisonis</i> (Lecythidaceae) – A New Saponin and Complete ^1H and ^{13}C Chemical Shift Assignments	871
Rennê C. Duarte, Carlos R. R. Matos, Raimundo Braz-Filho and Leda Mathias	
Oleanane-type Triterpene Saponins from <i>Glochidion glomerulatum</i>	875
Vu Kim Thu, Nguyen Van Thang, Nguyen Xuan Nghiem, Hoang Le Tuan Anh, Pham Hai Yen, Chau Van Minh, Phan Van Kiem, Nan Young Kim, Seon Ju Park and Seung Hyun Kim	
Cucumarioside E from the Far Eastern Sea Cucumber <i>Cucumaria japonica</i> (Cucumariidae, Dendrochirotida), New Minor Monosulfated Holostane Triterpene Pentaoside with Glucose as the Second Monosaccharide Residue	877
Alexandra S. Silchenko, Anatoly I. Kalinovsky, Pavel S. Dmitrenok, Vladimir I. Kalinin, Andrey N. Mazeika, Natalia S. Vorobieva, Nina M. Sanina and Edward Y. Kosetsky	
Structure Revision of Two Polyoxygenated Sterols from the Marine Sponge <i>Neofibularia nolitangere</i>	881
Yasunori Yaoita, Masao Kikuchi and Koichi Machida	
Ergosterol of <i>Cordyceps militaris</i> Attenuates LPS Induced Inflammation in BV2 Microglia Cells	885
Neeranjini Nallathamby, Lee Guan-Serm, Sharmili Vidyadarshan, Sri Nurestri Abd Malek, Jegadeesh Raman and Vikineswary Sabaratnam	
Two Novel Spirostene Glycosides from <i>Selaginella chrysocaulos</i> and their Chemotaxonomic Significance	887
Olaf Kunert, Rumalla Chidananda Swamy, Bobbala Ravi Kumar, Achanta Venkata Narasimha Appa Rao, Owi Ivar Nandi and Wolfgang Schuehly	
Anti-Acetylcholinesterase Alkaloids from <i>Annona glabra</i> Leaf	891
Shoei-Sheng Lee, Dong-Yi Wu, Sheng-Fa Tsai, and Chien-Kuang Chen	
Increased Oxidative Stress in Cultured 3T3-L1 Cells was Attenuated by Berberine Treatment	895
Shi-fen Dong, Naomi Yasui, Hiroko Negishi, Aya Kishimoto, Jian-ning Sun and Katsumi Ikeda	
Synthesis and Antimicrobial Activities of 3-Methyl-β-Carboline Derivatives	899
Jiwen Zhang, Longbo Li, Wenjia Dan, Jian Li, Qianliang Zhang, Hongjin Bai and Junru Wang	
A Novel One-step Synthesis of Quinoline-2(1H)-thiones and Selones by Treating 3-Aryl-3-(2-aminophenyl)-1-propyn-3-ols with a Base and Elemental Sulfur or Selenium	903
Kazuaki Shimada, Hironori Izumi, Koki Otashiro, Kensuke Noro, Shigenobu Aoyagi, Yuji Takikawa and Toshinobu Korenaga	
Normonanchocidins A, B and D, New Pentacyclic Guanidine Alkaloids from the Far-Eastern Marine Sponge <i>Monanchora pulchra</i>	913
Ksenya M. Tabakmakher, Tatyana N. Makarieva, Vladimir A. Denisenko, Alla G. Guzii, Pavel S. Dmitrenok, Aleksandra S. Kuzmich and Valentyn A. Stonik	
Computational and Investigative Study of Flavonoids Active Against <i>Trypanosoma cruzi</i> and <i>Leishmania</i> spp	917
Frederico F. Ribeiro, Francisco J.B.M. Junior, Marcelo S. da Silva, Marcus Tullius Scotti and Luciana Scotti	
Two New Secondary Metabolites from <i>Tephrosia purpurea</i>	921
Yin-Ning Chen, Yan Peng, Cheng-Hai Gao, Tao Yan, Zhi-Fang Xu, Samuel X. Qiu, Wen-Hao Cao, Ligao Deng and Ri-Ming Huang	
Regioselective Glycosylation of 3-, 5-, 6-, and 7-Hydroxyflavones by Cultured Plant Cells	923
Kei Shimoda, Naoji Kubota, Daisuke Uesugi, Yuuya Fujitaka, Shouta Okada, Masato Tanigawa and Hiroki Hamada	
Unusual Flavonoid Glycosides from the Hawaiian Tree <i>Metrosideros polymorpha</i>	925
Benjamin R. Clark, Swapan Pramanick, Norman Arancon and Robert P. Borris	
Anti-inflammatory Flavonoids Isolated from <i>Passiflora foetida</i>	929
Thi Yen Nguyen, Dao Cuong To, Manh Hung Tran, Joo Sang Lee, Jeong Hyung Lee, Jeong Ah Kim, Mi Hee Woo and Byung Sun Min	
Clovamide and Flavonoids from Leaves of <i>Trifolium pratense</i> and <i>T. pratense</i> subsp. <i>nivale</i> Grown in Italy	933
Aldo Tava, Łukasz Pecio, Anna Stochmal and Luciano Pecetti	
Water Extract of <i>Mentha × villosa</i>: Phenolic Fingerprint and Effect on Ischemia-Reperfusion Injury	937
Silvia Fialova, Lucia Veizerova, Viera Nosalova, Katarina Drabikova, Daniela Tekelova, Daniel Grancal and Ruzena Sotnikova	
Distribution and Taxonomic Significance of Secondary Metabolites Occurring in the Methanol Extracts of the Stonecrops (<i>Sedum</i> L., Crassulaceae) from the Central Balkan Peninsula	941
Gordana S. Stojanović, Snežana Č. Jovanović and Bojan K. Zlatković	
In vitro Xanthine Oxidase Inhibitory Studies of <i>Lippia nodiflora</i> and Isolated Flavonoids and Phenylethanoid Glycosides as Potential Uric Acid-lowering Agents	945
Lee-Chuen Cheng, Vikneswaran Murugaiyah and Kit-Lam Chan	
Enzymatic Synthesis of Quercetin Monoglucopyranoside and Maltooligosaccharides	949
Ryo Yasukawa, Natsumi Moriwaki, Daisuke Uesugi, Fuya Kaneko, Hiroki Hamada and Shin-ichi Ozaki	
Polyurethane Microstructures-a Good or Bad <i>in vitro</i> Partner for the Isoflavone Genistein?	951
Corina Danciu, Florin Borcan, Codruta Soica, Istvan Zupko, Erzsébet Csányi, Rita Ambrus, Delia Muntean, Camelia Sass, Diana Antal, Claudia Toma and Cristina Dehelean	
Chemical Constituents of the Underground Parts of <i>Iris florentina</i> and their Cytotoxic Activity	955
Akihito Yokosuka, Yoshikazu Koyama and Yoshihiro Mimaki	
Synthesis of Arecatannin A1 from Dimeric Epicatechin Electrophile	959
Manato Suda, Kohki Takanashi, Miyuki Katoh, Kiriko Matsumoto, Koichiro Kawaguchi, Sei-ichi Kawahara, Hiroshi Fujii and Hidefumi Makabe	
Anthocyanin Profile and Antioxidant Activity of Various Berries Cultivated in Korea	963
Hong-Sook Bae, Hyun Ju Kim, Jin Hee Kang, Rika Kudo, Takahiro Hosoya, Shigenori Kumazawa, Mira Jun, Oh-Yoen Kim and Mok-Ryeon Ahn	
Metabolite Fingerprinting of <i>Eugenia jambolana</i> Fruit Pulp Extracts using NMR, HPLC-PDA-MS, GC-MS, MALDI-TOF-MS and ESI-MS/MS Spectrometry	969
Ram Jee Sharma, Ramesh C. Gupta, Arvind Kumar Bansal and Inder Pal Singh	

Flavonoids and Phenolic Acids in Methanolic Extracts, Infusions and Tinctures from Commercial Samples of Lemon Balm	977
Agnieszka Arceusz, Marek Wesolowski and Beata Ulewicz-Magulska	
RP-HPLC-DAD-MS^a Analysis and Butyrylcholinesterase Inhibitory Activity of <i>Barbacenia blanchetii</i> Extracts	983
Jósquia S Barbosa, Verônica M Almeida, Rosilene M Marçal and Alexsandro Branco	
Flavonoids and Other Phenolic Compounds in Needles of <i>Pinus peuce</i> and Other Pine Species from the Macedonian Flora	987
Marija Karapandzova, Gjose Stefkov, Ivana Cvetkovikj, Jasmina Petreska Staneva, Marina Stefova and Svetlana Kulevanova	
Anti-inflammatory, Antioxidant and Antimicrobial Activity Characterization and Toxicity Studies of Flowers of "Jarilla", a Medicinal Shrub from Argentina	991
Alejandra Moreno, Gabriela Nuño, Soledad Cuello, Jorge E. Sayago, María Rosa Alberto, Catiana Zampini and María Inés Isla	
Synthesis of Resveratrol Glycosides by Plant Glucosyltransferase and Cyclodextrin Glucanotransferase and Their Neuroprotective Activity	995
Kei Shimoda, Naoji Kubota, Hatsuyuki Hamada and Hiroki Hamada	
Anti-austeritic Constituents of the Congolese Medicinal Plant <i>Aframomum melegueta</i>	997
Dya Fita Dibwe, Suresh Awale, Hiroyuki Morita and Yasuhiro Tezuka	
The Lignan-containing Extract of <i>Schisandra chinensis</i> Berries Inhibits the Growth of <i>Chlamydia pneumoniae</i>	1001
Elina Hakala, Leena L. Hanski, Teijo Yrjönen, Heikki J. Vuorela and Pia M. Vuorela	
A New Aromatic Compound from the Stem Bark of <i>Terminalia catappa</i>	1005
David Pertuit, Anne-Claire Mitaine-Offter, Tomofumi Miyamoto, Chiaki Tanaka, Stéphanie Delemasure, Patrick Dutartre and Marie-Aleth Lacaille-Dubois	
Effect of Non-psychotropic Plant-derived Cannabinoids on Bladder Contractility: Focus on Cannabigerol	1009
Ester Pagano, Vittorino Montanaro, Antonio di Girolamo, Antonio Pistone, Vincenzo Altieri, Jordan K. Zjawiony, Angelo A. Izzo and Raffaele Capasso	
In Cell Interactome of Oleocanthal, an Extra Virgin Olive Oil Bioactive Component	1013
Chiara Cassiano, Agostino Casapullo, Alessandra Tosco, Maria Chiara Monti and Raffaele Riccio	
Synthesis of ε-Viniferin Glycosides by Glucosyltransferase from <i>Phytolacca americana</i> and their Inhibitory Activity on Histamine Release from Rat Peritoneal Mast Cells	1017
Hiroki Hamada, Hatsuyuki Hamada and Kei Shimoda	
Stability of the Ellagitannin Fraction and Antioxidant Capacity of Varietal Pomegranate Juices	1019
Pedro Mena and Cristina García-Viguera	
Phthalide Anions in Organic Synthesis. A Direct Total Synthesis of Furomollugin	1025
George A. Kraus and Pengfei Dong	
Absolute Configuration Assignment of 3',4'-di-O-acylkellactones Using Vibrational Circular Dichroism Exciton Chirality	1027
Abigail I. Buendía-Trujillo, J. Martín Torres-Valencia, Pedro Joseph-Nathan and Eleuterio Burgueño-Tapia	
Antifouling Compounds from the Marine-Derived Fungus <i>Aspergillus terreus</i> SC5GAF0162	1033
Xu-Hua Nong, Xiao-Yong Zhang, Xin-Ya Xu and Shu-Hua Qi	
Goji Berry: Quality Assessment and Crop Adaptation of Plants Cultivated in Tuscany (Italy) by Combination of Carotenoid and DNA Analyses	1035
Giada Capecci, Emanuele Goti, Elena Nicolai, Maria Camilla Bergonzi, Roberto Monnanni and Anna Rita Bilia	
Activity of <i>Vitis vinifera</i> Tendrils Extract Against Phytopathogenic Fungi	1037
Daniele Fraternale, Donata Ricci, Giancarlo Verardo, Andrea Gorassini, Vilberto Stocchi and Piero Sestili	
Long-chain Glucosinolates from <i>Arabis turrita</i>: Enzymatic and Non-enzymatic Degradations	1043
Ivica Blažević, Sabine Montaut, Gina Rosalinda De Nicola and Patrick Rollin	
Aroma of Turmeric: Dependence on the Combination of Groups of Several Odor Constituents	1047
Toshio Hasegawa, Kenta Nakatani, Takashi Fujihara and Hideo Yamada	
Terpenoids Preserved in Fossils from Miocene-aged Japanese Conifer Wood	1051
Agnieszka Ludwicka and Yoshinori Asakawa	
Can Ozone Alter the Terpenoid Composition and Membrane Integrity of <i>in vitro</i> <i>Melissa officinalis</i> Shoots?	1055
Francesca D'Angiolillo, Mariagrazia Tonelli, Elisa Pellegrini, Cristina Nali, Giacomo Lorenzini, Luisa Pistelli and Laura Pistelli	
Composition and Chemical Variability of Ivoirian <i>Xylopia staudtii</i> Leaf Oil	1059
Thierry Acafou Yapi, Jean Brice Boti, Antoine Coffy Ahibo, Sylvain Sutour, Ange Bighelli, Joseph Casanova and Félix Tomi	
Chemoinformatics Approach to Antibacterial Studies of Essential Oils	1063
Dragoljub L. Miladinović, Budimir S. Ilić and Branislava D. Kocić	
Chemical Composition of <i>Nardostachys grandiflora</i> Rhizome Oil from Nepal – A Contribution to the Chemotaxonomy and Bioactivity of <i>Nardostachys</i>	1067
Prabodh Satyal, Bhuwan K. Chhetri, Noura S. Dosoky, Ambika Poudel and William N. Setzer	
Chemical Composition and Biological Activity of Essential Oils from Wild Growing Aromatic Plant Species of <i>Skimmia laureola</i> and <i>Juniperus macropoda</i> from Western Himalaya	1071
Iris Stappen, Nurhayat Tabanca, Abbas Ali, David E. Wedge, Jürgen Wanner, Vijay K. Kaul, Brij Lal, Vikas Jaitak, Velizar K. Gochev, Erich Schmidt and Leopold Jirovetz	
Comparative Chemical Composition and Antioxidant Properties of the Essential Oils of three <i>Sideritis libanotica</i> Subspecies	1075
Carmen Formisano, Filomena Oliviero, Daniela Rigano, Nelly Apostolidis Arnold and Felice Senatore	
Asplenioideae Species as a Reservoir of Volatile Organic Compounds with Potential Therapeutic Properties	1079
Didier Froissard, Sylvie Rapior, Jean-Marie Bessière, Bruno Buatois, Alain Fruchier, Vincent Sol and Françoise Fons	
Composition and Comprehensive Antioxidant Activity of Ginger (<i>Zingiber officinale</i>) Essential Oil from Ecuador	1085
Martina Höferl, Ivanka Stoilova, Juergen Wanner, Erich Schmidt, Leopold Jirovetz, Dora Trifonova, Veselin Stanchev and Albert Krastanov	

Chemical Components of Four Essential Oils in Aromatherapy Recipe Sarin Tadtong, Narisa Kamkaen, Rith Waithanachaiyingcharoen and Nijsiri Ruangrungsi	1091
---	-------------

Accounts/Reviews

Recent Advances in the Synthesis of <i>Stemona</i> Alkaloids Xiao-Yu Liu and Feng-Peng Wang	1093
Flavonoid Properties in Plant Families Synthesizing Betalain Pigments (Review) Tsukasa Iwashina	1103
Phytochemistry and Pharmacology of the Genus <i>Toxotoma</i> Francesco Epifano, Maria Carmela Specchiulli, Vito Alessandro Taddeo, Serena Fiorito and Salvatore Genovese	1115
Fungal Phytotoxins with Potential Herbicidal Activity to Control <i>Chenopodium album</i> Alessio Cimmino, Marco Masi, Marco Evidente and Antonio Evidente	1119
Essential Oils as "A Cry for Help". A Review Christine Zitzelsberger and Gerhard Buchbauer	1127

Number 7

Two New Compounds from <i>Hedyotis lindleyana</i> Tuyen Pham Nguyen Kim, Tram Phan Thi Mai and Phung Nguyen Kim Phi	1141
New Sesquiterpene Glycosides from the Leaves of <i>Eriobotrya japonica</i> Xiancan Ao, Lei Zhao, Han Lü, Bingru Ren, Hankui Wu, Jian Chen and Weilin Li	1145
Isolation and Fast Selective Determination of Nor-abietanoid Diterpenoids from <i>Perovskia atriplicifolia</i> Roots Using LC-ESI-MS/MS with Multiple Reaction Monitoring Sylwester Ślusarczyk, Jakub Topolski, Krzysztof Domaradzki, Michael Adams, Matthias Hamburger and Adam Matkowski	1149
Preferentially Cytotoxic Constituents of <i>Andrographis paniculata</i> and their Preferential Cytotoxicity against Human Pancreatic Cancer Cell Lines Sullim Lee, Hiroyuki Morita and Yasuhiro Tezuka	1153
A New Diterpene Glycoside: 15α-Hydroxy-Rebaudioside M Isolated from <i>Stevia rebaudiana</i> Indra Prakash, Gil Ma, Cynthia Bunders, Krishna P. Devkota, Romila D. Charan, Catherine Ramirez, Tara M. Snyder and Christopher Friedemann	1159
Trocheliolide A, a Hydroperoxycembranoidal Diterpene from the Octocoral <i>Sarcophyton trocheliophorum</i> Kuan-Ming Liu, Ching-Hsiao Cheng, Wu-Fu Chen, Mei-Chin Lu, Lee-Shing Fang, Zhi-Hong Wen, Jui-Hsin Su, Yang-Chang Wu and Ping-Jyun Sung	1163
The Assignment of the Absolute Configuration of C-22 Chiral Center in the Aglycones of Triterpene Glycosides from the Sea Cucumber <i>Cladolabes schmettii</i> and Chemical Transformations of Cladoloside C Anatoly I. Kalinovsky, Alexandra S. Silchenko, Sergey A. Avilov and Vladimir I. Kalinin	1167
New Derivatives of Natural Acyclic Guanidine Alkaloids with TRPV Receptor-Regulating Properties Ekaterina K. Ogurtsova, Tatyana N. Makarieva, Yuliya V. Korolkova, Yaroslav A. Andreev, Irina V. Mosharova, Vladimir A. Denisenko, Pavel S. Dmitrenok, Yeon-Ju Lee, Eugene V. Grishin and Valentin A. Stonik	1171
Cytotoxic and Antimalarial Alkaloids from the Twigs of <i>Dasyaschalon obtusipetalum</i> Atchara Jaidee, Thanika Promchai, Kongkiat Trisuwan, Surat Laphookhieo, Roonglawan Rattanajak, Sumalee Kamchonwongpaisan, Stephen G. Pyne and Thunwadee Ritthiwigrom	1175
Pyrrolizidine Alkaloids in <i>Adenostyles alliariae</i> and <i>A. glabra</i> from the Austrian Alps Remigius Chizzola	1179
A Validated, Rapid HPLC-ESI-MS/MS Method for the Determination of Lycopsamine Nikoletta Jedlinszki and Dezső Csupor	1181
6-Methoxyflavonoids and Other Constituents from <i>Microliabum polymnoides</i> (Asteraceae) Oscar Díaz, Rosana Alarcón, Diego Gutiérrez, Adriana Pacciaroni, Fany Cayo and Virginia Sosa	1183
Phytochemical and Antimicrobial Screening of Flavanones and Chalcones from <i>Galenia africana</i> and <i>Dicerothamnus rhinocerotis</i> Lawrence A. Ticha, Jeremy A. Klaasen, Ivan R. Green, Sivapregasen Naidoo, Bienyameen Baker and Ray-Dean Pietersen	1185
Chemical Constituents of <i>Pyrrosia calvata</i> Yu-Jie Chen, Guo-Yong Xie, Guang-Kai Xu, Yi-Qun Dai, Lu Shi and Min-Jian Qin	1191
Toxicity of <i>Cephalaria</i> Species and their Individual Constituents against <i>Aedes aegypti</i> Nazli Boke Sarikahya, Peyker Kayce, Nurhayat Tabanca, Alden S. Estep, James J. Becnel, Ikhlas A. Khan and Suheyla Kirmizigül	1195
In vitro Toxicity and in vivo Immunomodulatory Effects of Flavokawain A and Flavokawain B in Balb/C Mice Nadiyah Abu, Nurul Elyani Mohamed, Nirosha Tangarajoo, Swee Keong Yeap, M Nadeem Akhtar, Mohd Puad Abdullah, Abdul Rahman Omar and Noorjahan Banu Aliteneen	1199
Chemoreversal Metabolites from the Endophytic Fungus <i>Penicillium citrinum</i> Isolated from a Mangrove <i>Avicennia marina</i> Jin Liu, Meng Xu, Ming-yi Zhu and Yun Feng	1203
Constituents of Bulbs of three Species of the Hyacinthaceae (Hyacinthoideae): <i>Eucomis vandermerwei</i>, <i>E. zambesiaca</i> and <i>Resnova humifusa</i> Jaspreet K. Sihra, Alfred E. Thumser, Moses K. Langat, Neil R. Crouch and Dulcie A. Mulholland	1207
Methyl Jasmonate- and Light-Induced Glucosinolate and Anthocyanin Biosynthesis in Radish Seedlings Naif Abdullah Al-Dhabi, Mariadhas Valan Arasu, Sun Ju Kim, Md. RomijUddin, Woo Tae Park, Sook Young Lee and Sang Un Park	1211

Comparison of the Anti-Adhesion Activity of Three Different Cranberry Extracts on Uropathogenic P-fimbriated <i>Escherichia coli</i>: a Randomized, Double-blind, Placebo Controlled, <i>Ex Vivo</i>, Acute Study	1215
Amy Howell, Dan Souza, Marc Roller and Emilie Fromentin	
Fig (<i>Ficus carica</i>) Liquid Co-Products as New Potential Functional Ingredient: Physico-Chemical and <i>In Vitro</i> Antioxidant Properties	1219
Manuel Viuda-Martos, Esther Sendra, Estrella Sayas, José A. Pérez-Alvarez and Juana Fernández-López	
Methyl Jasmonate Induces Enhanced Podophyllotoxin Production in Cell Cultures of Thracian Flax (<i>Linum thraicum</i> ssp. <i>thraicum</i>)	1225
Pavlina Sasheva, Iliana Ionkova and Nadezhda Stoilova	
Antileishmanial Activity of Compounds Isolated from <i>Sassafras albidum</i>	1229
Divya Pulivarthy, Kelly Marie Steinberg, Lianet Monzote, Abel Piñón and William N. Setzer	
Polyprenylated Phloroglucinols from <i>Hypericum maculatum</i>	1231
Paraskev T. Nedialkov, Georgi Momekov, Zlatina K. Kokanova-Nedialkova and Jörg Heilmann	
First Synthesis of 1,4-Dimethoxy-2-Naphthoxyacetic acid	1237
Kimberly Chinea and Ajoy K. Banerjee	
Determination of the Juglone Content of <i>Juglans regia</i> Leaves by GC/MS	1239
Irena Matlawska, Wiesława Bylka, Ewa Widły-Tyszkiewicz and Beata Stanisz	
Synthesis, Cytotoxic and Contraceptive Activity of 6,8,9-Trihydroxy-2-methyl-2H-naphtho[2,3-<i>b</i>]pyran-5,10-dione, a Pigment of <i>Echinothrix diadema</i>, and its Analogs	1243
Natalia D. Pokhilo, Galina I. Melman, Marina I. Kiseleva, Vladimir A. Denisenko and Victor Ph. Anufriev	
New Metabolites from a Marine Sediment-Derived Fungus, <i>Aspergillus carneus</i>	1247
Anton A. Yurchenko, Olga F. Smetanina, Anatoly I. Kalinovsky, Natalya N. Kirichuk, Mikhail V. Pivkin, Elena V. Ivanets, Ekaterina A. Yurchenko and Shamil Sh. Afiyatullov	
A New Phenyl Ethyl Glycoside from the Twigs of <i>Acer tegmentosum</i>	1251
Seon Ju Park, Hwa Young Lee, Nguyen Xuan Nhieu, Taek Hwan Lee, Nanyoung Kim, Seung Hun Cho and Seung Hyun Kim	
Enhanced Mulberroside A Production from Cell Suspension and Root Cultures of <i>Morus alba</i> Using Elicitation	1253
Jukrapun Komaikul, Tharita Kitisripanya, Hiroyuki Tanaka, Boonchoo Sritularak and Waraporn Putalun	
Synthesis of Stilbene Derivatives: A Comparative Study of their Antioxidant Activities	1257
Miguel A. Romero, José A. González-Delgado and Jesús F. Arteaga	
Soluble Phenolic Compounds in Different Cultivars of Red Clover and Alfalfa, and their Implication for Protection against Proteolysis and Ammonia Production in Ruminants	1263
Isabelle A. Kagan, Ben M. Goff and Michael D. Flythe	
Effects of Increasing Doses of UV-B on Main Phenolic Acids Content, Antioxidant Activity and Estimated Biomass in Lavandin (<i>Lavandula x intermedia</i>)	1269
Jaime Usano-Alemany and Lachinée Panjai	
Bergenin Content and Free Radical Scavenging Activity of <i>Bergenia</i> Extracts	1273
Helena Hendrychová, Jan Martin, Lenka Tůmová and Nina Kočevá-Rába	
Biotransformation of (-)-(10E,15S)-10,11-Dehydrocurvularin	1277
Zhangshuang Deng, Aiping Deng, Dan Luo, Dachun Gong, Kun Zou, Yan Peng and Zhiyong Guo	
Chemical Composition of the Same Brazilian Propolis Sample Analyzed in 1997 and in 2012: No Freezing Effect	1279
Bruno José Conti, Vassyá Bankova and José Maurício Sforcin	
The Use of <i>Cissus quadrangularis</i> (CQR-300) in the Management of Components of Metabolic Syndrome in Overweight and Obese Participants	1281
Dieudonne Kuate, Robert J. Nash, Barbara Bartholomew and Yana Penkova	
Screening of Microbial Extracts for Anticancer Compounds Using <i>Streptomyces</i> Kinase Inhibitor Assay	1287
Prashant Shanbhag, Sarita Bhave, Ashwini Vartak, Asha Kulkarni-Almeida, Girish Mahajan, Ivan Villanueva and Julian Davies	
Characterization of Essential Oil Components from Aromatic Plants that Grow Wild in the "Piana del Sele" (Salerno, Southern Italy) using Gas Chromatography-Mass Spectrometry	1293
Daniele Naviglio, Laura Le Grottagli, Manuela Vitulano, Marco Trifoggi and Monica Gallo	
Chemical Compositions and Biological Activities of Essential Oils of <i>Beilschmiedia glabra</i>	1297
Wan Mohd Nuzul Hakimi Wan Salleh, Farediah Ahmad, Khong Heng Yen and Razauden Mohamed Zulkifli	
Chemotype of <i>Litsea cubeba</i> Essential Oil and Its Bioactivity	1301
Syaliza Abdul Hammad and Fasihuddin Ahmad	
Effect of Hinoki and Meniki Essential Oils on Human Autonomic Nervous System Activity and Mood States	1305
Chi-Jung Chen, K. J. Senthil Kumar, Yu-Ting Chen, Nai-Wen Tsao, Shih-Chang Chien, Shang-Tzen Chang, Fang-Hua Chu and Sheng-Yang Wang	
Chemical Composition and <i>in vitro</i> Antibacterial Activity of the Essential Oil of <i>Verbesina negrensis</i> from the Venezuelan Andes	1309
Flor D. Mora, Yesenia L. Rojas, Viviana González, Judith Velasco, Tulia Díaz, Nurby Ríos, Luis B. Rojas-Fermin, Juan Carmona, Bladimiro Silva and Marcelo Nieto	
Composition, <i>in vitro</i> Cytotoxic, and Antimicrobial Activities of the Flower Essential Oil of <i>Diospyros discolor</i> from Taiwan	1311
Yu-Chang Su, Kuan-Ping Hsu, Eugene I-Chen Wang and Chen-Lung Ho	
GC-FID/MS Profiling of Supercritical CO₂ Extracts of Peels from <i>Citrus aurantium</i>, <i>C. sinensis</i> cv. Washington navel, <i>C. sinensis</i> cv. Tarocco and <i>C. sinensis</i> cv. Doppio Sanguigno from Dubrovnik Area (Croatia)	1315
Igor Jerković, Jasmina Družić, Zvonimir Marijanović, Mirko Gugić, Stela Jokić and Marin Roje	
GC/MS Analysis of the Essential Oil of <i>Vernonia cinerea</i>	1319
Rajesh K. Joshi	

Volatile Constituents of the Leaves of <i>Aniba hostmanniana</i> (Lauraceae) and their Antibacterial Activities	1321
Wilberto De Lima, Luis B. Rojas-Fermín, Sonia Koteich-Khatib, María Eugenia Lucena and Juan Carmona Arzola	
Essential Oil Composition of Summer and Winter Foliage of <i>Chiliadenus bocconei</i>	1323
Joseph A. Buhagiar, Maria T. Camilleri-Podestà, Pierluigi Cioni, Guido Flamini and Luisa Pistelli	

Accounts/Reviews

<i>Eriosema</i> (Fabaceae) Species Represent a Rich Source of Flavonoids with Interesting Pharmacological Activities	1325
Maurice Ducret Awouafack, Pierre Tane, Michael Spiteller and Jacobus Nicolaas Eloff	

Additions/Corrections

<i>Chrysanthemum indicum</i> Attenuates Cisplatin-induced Nephrotoxicity both <i>in vivo</i> and <i>in vitro</i>	1331
Tae-Won Kim, Young-Jung Kim, So-Ra Park, Chang-Seob Seo, Hyekyung Ha, Hyeun-Kyoo Shin and Ju-Young Jung	
<i>Natural Product Communications</i> , 10, 397-402 (2015)	

Number 8

Isolation of Monovalerenester A, an Inhibitor of Fat Accumulation, from <i>Valeriana fauriei</i>	1333
Keiji Yuki, Mariko Ikeda, Shosuke Yoshida, Osamu Ohno, Kiyotake Suenaga, Kaoru Yamada, Daisuke Uemura and Kenji Miyamoto	
Arthropod Deterrents from <i>Artemisia pallens</i> (Davana Oil) Components	1335
Ganga V. Bhagavathy, Glory M Velazquez Nieves, Meiling Z. Webb and Kamlesh R. Chauhan	
Stereoselective Synthesis of 2,15-Dihydroxycalamenene and 2-Methoxycalamenene. Determination of the Configuration of Natural 2,15-Dihydroxycalamenene	1337
Stefano Serra	
Sesquiterpenes from the Vietnamese Marine Sponge <i>Dysidea fragilis</i>	1341
Nguyen Thi Cuc, Hoang Le Tuan Anh, Dan Thi Thuy Hang, Nguyen Xuan Nghiem, Nguyen Hai Dang, Nguyen Hoai Nam, Pham Hai Yen, Do Cong Thung, Vu Kim Thu, Chau Van Minh and Phan Van Kiem	
Vibrational Circular Dichroism Absolute Configuration of 9,12-Cyclomulin-13-ol, a Diterpene from <i>Azorella</i> and <i>Laretia</i> Species	1343
Marcelo A. Muñoz, Aurelio San-Martín and Pedro Joseph-Nathan	
Ultrafine Betulin Formulation with Biocompatible Carriers Exhibiting Improved Dissolution Rate	1345
Svetlana A. Myz, Tatyana P. Shakhtshneider, Mikhail A. Mikhailenko, Andrey G. Ogienko, Ekaterina G. Bogdanova, Anna A. Ogienko, Svetlana A. Kuznetsova, Elena V. Boldyreva and Vladimir V. Boldyrev	
Bio-assay Guided Isolation of Anti-cancer Compounds from <i>Anthocephalus cadamba</i> Bark	1349
Deepak Kumar, Chilukuri Tejaswi, Saiprasanna Rasamalla, Sumana Mallick and Bikas C Pal	
Damarane-type Saponins from <i>Gynostemma longipes</i> and their Cytotoxic Activity	1351
Pham Tuan Anh, Pham Thanh Ky, Nguyen Thi Cuc, Nguyen Xuan Nghiem, Pham Hai Yen, Tran Minh Ngoc, Hoang Le Tuan Anh, Bui Huu Tai, Do Thi Trang, Chau Van Minh and Phan Van Kiem	
A New C₂₃ Steroid from the Venom of <i>Bufo bufo gargarizans</i>	1353
Shi-Lin Luo, Hai-Yan Tian, Jun-Shan Liu, Ying Wang and Wen-Cai Ye	
(-)-Pentylsedinine, a New Alkaloid from the Leaves of <i>Lobelia tupa</i> with Agonist Activity at Nicotinic Acetylcholine Receptor	1355
Cristian Paz, José Becerra, Mario Silva, Viviana Burgos, Matthias Heydenreich, Bernd Schmidt, Thu Tran and Irina Vetter	
Furoquinoline Alkaloids from the Leaves of <i>Evodia lepta</i> as Potential Cholinesterase Inhibitors and their Molecular Docking	1359
Jirapast Sichaem, Thanawan Rojpitkul, Pattara Sawasdee, Kiattisak Lugsanangarm and Santi Tip-pyang	
Asperginine, an Unprecedented Alkaloid from the Marine-derived Fungus <i>Aspergillus</i> sp.	1363
Pinmei Wang, Shizhe Zhao, Ying Liu, Wanjing Ding, Feng Qiu and Jinzhong Xu	
Effect of Quercetin on Cell Cycle and Cyclin Expression in Ovarian Carcinoma and Osteosarcoma Cell Lines	1365
Daniela Catanzaro, Eugenio Ragazzi, Caterina Vianello, Laura Caparrotta and Monica Montopoli	
Anti-<i>Helicobacter pylori</i> Activity of Four <i>Alchemilla</i> Species (Rosaceae)	1369
Marija Krivokuća, Marijan Niketić, Marina Milenković, Nataša Golić, Carla Masia, Maria Maddalena Scaltrito, Francesca Sisto and Tatjana Kundaković	
Peracylated Glucosyl Kaempferols from <i>Pasania dodoniifolia</i> Leaf	1373
Chi-Chih Chang and Shuei-Sheng Lee	
6-Methoxyflavonol Glycosides with <i>In Vitro</i> Hepatoprotective Activity from <i>Chenopodium bonus-henricus</i> Roots	1377
Zlatina Kokanova-Nedialkova, Magdalena Kondeva-Burdina, Dimitrina Zheleva-Dimitrova, Virginia Tzankova, Stefan Nikolov, Jörg Heilmann and Paraskev T. Nedialkov	
Flavonol Glycosides from the Leaves of <i>Allium macrostemon</i>	1381
Risa Nakane and Tsukasa Iwashina	
HPLC Plasma Assay of a Novel Anti-MRSA Compound, Kaempferol-3-O-Alpha-L-(2",3"-di-p-coumaroyl)rhamnoside, from Sycamore Leaves	1383
Yiguan Zhang, Frederick Valeriote, Kenneth Swartz, Ben Chen, Mark T. Hamann, Douglas L. Rodenburg, James D. McChesney and Jiajiu Shaw	
Biological Activity of <i>Dolichandrone serrulata</i> Flowers and Their Active Components	1387
Phanida Phanthong, Noppawan Phumala Morales, Sirirat Chancharunee, Supachoke Mangmool, Natthinee Anantachoke and Nuntavan Bunyaphrathsara	
Prenylhydroquinone-Derived Secondary Metabolites from Cultures of the Basidiomycete <i>Lentinus similis</i> BCC 52578	1391
Masahiko Isaka, Somporn Palasarn, Malipan Sappan, Kitlada Srichomthong, Samantha C. Karunarathna and Kevin D. Hyde	
Effects of Thymoquinone on the Pharmacokinetics and Pharmacodynamics of Glibenclamide in a Rat Model	1395
Ajaz Ahmad, Rao Muzaffar A. Khan, Khalid M. Alkharfy, Mohammad Raish, Fahad I. Al-Jenoobi, and Abdullah M. Al-Mohizea	

Antioxidant and Antiinflammatory Compounds in Nutmeg (<i>Myristica fragrans</i>) Pericarp as Determined by <i>in vitro</i> Assays	1399
Chuan-Rui Zhang, Ettannil Jayashree, Paramasivam Suresh Kumar and Muralleedharan G. Nair	
In Vitro Safety/Protection Assessment of Resveratrol and Pterostilbene in a Human Hepatoma Cell Line (HepG2)	1403
Germana Lombardi, Samuele Vannini, Francesca Blasi, Maria Carla Marcotullio, Luca Dominici, Milena Villarini, Lina Cossignani and Massimo Moretti	
Red Maple (<i>Acer rubrum</i>) Aerial Parts as a Source of Bioactive Phenolics	1409
Yan Zhang, Hang Ma, Tao Yuan and Navindra P. Seeram	
Changes in the Content of the Glycosides, Aglycons and their Possible Precursors of <i>Rhodiola rosea</i> during the Vegetation Period	1413
Iman Mirmazloum, Márta Ladányi and Zsuzsanna György	
Biocompounds Attenuating the Development of Obesity and Insulin Resistance Produced by a High-fat Sucrose Diet	1417
Usune Etxeberria, Ana Laura de la Garza, J. Alfredo Martínez and Fermín I. Milagro	
A Novel C21 Cyclopentenone Derivative from <i>Cipadessa baccata</i>	1421
Jing Zhang, Yao-Wen Chang, Chun-Mao Yuan, Fan Zhang, Ying-Tong Di and Xiao-Jiang Hao	
Effects on MC3T3-E1 Cells and <i>In silico</i> Toxicological Study of Two 6-(Propan-2-yl)-4-methyl-morpholine-2,5-diones	1423
Marija Vukelić-Nikolić, Ana Kolarević, Katarina Tomović, Denitsa Yancheva, Emiliya Cherneva, Stevo Najman, and Andrija Šmelcerović	
Release of Antioxidant Peptides from the Body Wall Proteins of the Sea Cucumber <i>Isostichopus fuscus</i>	1427
Arisai C. Hernández-Sámano and Blanca Hernández-Ledesma	
Bioactivity-guided Separation of the Active Compounds in <i>Acacia pennata</i> Responsible for the Prevention of Alzheimer's Disease	1431
Pattamapan Lomarat, Sirirat Chancharunee, Naththinee Anantachoke, Worawan Kitphati, Kittisak Sripha and Nuntavan Bunyaphraphatsara	
Development and Validation of LC-MS/MS Method for Quantitative Determination of Adenosine, Guanosine, Xanthine and Uric acid in Widely Consumed Vegetables in Thailand	1435
Narisa Rukdee, Piyanuch Rojsanga and Chutima Matayatsuk Phechkrajang	
Chemical Composition of the Essential Oil from <i>Chaerophyllum temulum</i> (Apiaceae)	1439
Jelena G. Stamenković, Gordana S. Stojanović, Ivana R. Radoković, Goran M. Petrović and Bojan K. Zlatković	
Comparison of Essential Oils Obtained from Different Extraction Techniques as an Aid in Identifying Aroma Significant Compounds of Nutmeg (<i>Myristica fragrans</i>)	1443
Suchandra Chatterjee, Sumit Gupta and Prasad. S. Variyar	
Chemical Variability of the Essential Oil Isolated from Aerial Parts of <i>Tetragonia articulata</i> from North-Western Algeria	1447
Maghnia Boussaïd, Chahrazed Bekhechi, Fawzia Beddou, Daoudi Chabane Sari, Ange Bighelli, Joseph Casanova and Félix Tomi	
Composition and Bioactivities of an (E)-β-Farnesene Chemotype of Chamomile (<i>Matricaria chamomilla</i>) Essential Oil from Nepal	1453
Prabodh Satyal, Samon Shrestha and William N. Setzer	
Chemical Composition of the Essential Oil from <i>Croton oblongifolius</i> and its Antibacterial Activity against <i>Propionibacterium acnes</i>	1459
Sirivan Athikomkulchai, Sarin Tadtong, Nijisiri Ruangrungsi and Tapanee Hongratanaworakit	
Composition, <i>in vitro</i> Anti-inflammatory, Antioxidant and Antimicrobial Activities of Essential Oils from Leaf and Twig Parts of <i>Cupressus cashmeriana</i>	1461
Yu-Chang Su, Kuan-Ping Hsu, Kuo-Feng Hua and Chen-Lung Ho	
Antioxidant and Anticholinesterase Activities of Essential Oils of <i>Cinnamomum griffithii</i> and <i>C. macrocarpum</i>	1465
Wan Mohd Nuzul Hakimi Wan Salleh, Farediah Ahmad and Khong Heng Yen	
Essential Oil Composition and Antigermination Activity of <i>Artemisia dracunculus</i> (Tarragon)	1469
Daniele Fraternale, Guido Flamini and Donata Ricci	
In Vitro Activity of Twenty Commercially Available, Plant-Derived Essential Oils against Selected Dermatophyte Species	1473
Simona Nardoni, Silvia Giovanelli, Luisa Pistelli, Linda Mugnaini, Greta Profili, Francesca Pisseri and Francesca Mancianti	
Intracerebral Distribution of α-Pinene and the Anxiolytic-like Effect in Mice Following Inhaled Administration of Essential Oil from <i>Chamaecyparis obtusa</i>	1479
Hikaru Kasuya, Sayuka Iida, Kurumi Ono, Tadaaki Satou and Kazuo Koike	
Accounts/Reviews	
A Comprehensive Review of the Cosmeceutical Benefits of <i>Vanda</i> Species (Orchidaceae)	1483
Hazrina Hadi, Syarifah Nazira Said Razali and Ammar Ihsan Awadh	
Genotoxicity and Antigenotoxicity Studies of Traditional Medicinal Plants: How Informative and Accurate are the Results?	1489
Luc Verschaeve	

Number 9

Alarm Pheromone Activity of Nymph-specific Geraniol in Chrysanthemum Lace Bug <i>Corythucha marmorata</i> against Adults and Nymphs	1495
Kisaki Watanabe and Nobuhiro Shimizu	
One New Conjugate of a Secoiridoid Glucoside with a Sesquiterpene Glucoside from the Flower Buds of <i>Lonicera japonica</i>	1499
Biao Yang, Zhaoqing Meng, Yimin Ma, Zhenzhong Wang, Gang Ding, Wenzhe Huang, Lin Sun, Yumei Hu, Wenjun Liu, Chunxiao Zhang, Zeyu Cao, Jiachun Li, Yan Zhong and Wei Xiao	
Chemical Originalities of New Caledonian Liverworts from Lejeuneaceae Family	1501
Paul Coulombe, Louis Thouvenot, Mohammed Nour and Yoshinori Asakawa	

A Synthetic Butenolide Diterpene is now a Natural Product Isolated from <i>Metaporana sericosepala</i>, a Plant from the Madagascar Dry Forest	1505
Christopher C. Presley, L. Harinantenaina Rakotondraibe, Peggy J. Brodie, Martin W. Callmander, Richard Randrianaivo, Vincent E. Rasamison, Etienne Rakotobe and David G. I. Kingston	1505
Antiproliferative Diterpenes from a <i>Malleastrum</i> sp. from the Madagascar dry forest	1509
Yixi Liu, C. Houston Wiedle Jr., Peggy J. Brodie, Martin W. Callmander, R. Rakotondrajaona, Etienne Rakotobe, Vincent E. Rasamison, and David G. I. Kingston	1509
Bio-guided Isolation of a New Sesterterpene from <i>Serjania goniocarpa</i>	1513
Carlos Quintal-Noveló, Luis W. Torres-Tapia, Rosa Moo-Puc and Sergio R. Peraza-Sánchez	1513
Inhibitory Effects of seco-Tritylpenoids from <i>Acanthopanax sessiliflorus</i> Fruits on HUVEC Invasion and ACE Activity	1517
Jin-Won Lee, Nam-In Baek and Dae-Young Lee	1517
A New Cucurbitane Glycoside from <i>Siraitia grosvenorii</i>	1521
Venkata Sai Prakash Chaturvedula and Srinivasa Rao Meneni	1521
Triterpenoid Saponins from <i>Clematis graveolens</i> and Evaluation of their Insecticidal Activities	1525
Rajeev Rattan, S. G. Eswara Reddy, Shudh Kirti Dolma, Bharat Inder Fozdar, Veena Gautam, Ritika Sharma and Upendra Sharma	1525
Rapid Determination of α-Hederin and Hederacoside C in Extracts of <i>Hedera helix</i> Leaves Available in the Czech Republic and Poland	1529
Lucie Havlíková, Kateřina Macáková, Lubomír Opletal and Petr Solich	1529
Antiinflammatory Steroidal Alkaloids from <i>Sarcococca wallichii</i> of Nepalese Origin	1533
Achyut Adhikari, M. Ismail Vohra, Almas Jabeen, Nida Dastagir and M. Iqbal Choudhary	1533
Antifungal and Antibacterial Activity of Extracts and Alkaloids of Selected Amaryllidaceae Species	1537
Miroslav Ločárek, Jitka Nováková, Pavel Klouček, Anna Hošťálková, Ladislav Kokoška, Lucie Gábrlová, Marcela Šafratová, Lubomír Opletal and Lucie Cahliková	1537
Anti-malarial Activity of Isoquinoline Alkaloids from the Stem Bark of <i>Actinodaphne macrophylla</i>	1541
Mehran Fadaeinab, Hairin Taha, Putri Narrima Mohd Fauzi, Hapipah Mohd Ali and Aty Widyawaruyanti	1541
Effects of Berberine on Adipose Tissues and Kidney Function in 3T3-L1 Cells and Spontaneously Hypertensive Rats	1543
Aya Kishimoto, Shi-fen Dong, Hiroko Negishi, Naomi Yasui, Jian-ning Sun and Katsumi Ikeda	1543
Sagitol D, a New Thiazole Containing Pyridoacridine Alkaloid from a Vietnamese Ascidian	1547
Natalia K. Utkina	1547
A New Terminal Cyano Group-containing Benzodiazepine Alkaloid from the Mangrove Endophytic Fungus <i>Penicillium</i> sp.	1549
Jing Li, Yi-sheng Zhong, Jie Yuan, Xun Zhu, Yong-jun Lu, Yong-cheng Lin and Lan Liu	1549
Tetramethylpyrazine from <i>Pleurotus geesteranus</i>	1553
Hengsheng Shen, Huaizhi Liu, Junchen Chen, Suqin Shao, Honghui Zhu, Rong Tsao and Ting Zhou	1553
A New Flavanone from the Leaves of <i>Chromolaena odorata</i>	1555
Lakshmareddy Emani, Suryachandrarao Ravada, Bharani Meka, Machiraju Garaga and Trimurtulu Golakoti	1555
Antioxidant and α-Glucosidase Inhibitory Constituents from <i>Hornstedtia</i> Species of Malaysia	1561
Siti Ernileyanti Hashim, Hasnah Mohd Sirat, Khong Heng Yen, Intan Safinar Ismail and Siti Nurulhuda Matsuki	1561
Synthesis and Antiviral Activity of Quercetin Brominated Derivatives	1565
Elza Karimova, Lidia Baltina, Leonid Spirikhin, Tagir Gabbasov, Yana Orshanskaya and Vladimir Zarubaev	1565
Pharmacokinetic Profile of μSMIN PlusTM, a new Micronized Diosmin Formulation, after Oral Administration in Rats	1569
Rosario Russo, Angelo Mancinelli, Michele Ciccone, Fabio Terruzzi, Claudio Pisano and Lorella Severino	1569
The Combinatory Effects of Glabridin and Tamoxifen on Ishikawa and MCF-7 Cell Lines	1573
Soe Hui Jen, Melissa Poh Su Wei and Adeline Chia Yoke Yin	1573
Potential of Horse Apple Isoflavones in Targeting Inflammation and Tau Protein Fibrillization	1577
Ehab A. Abourashed, Aida Abraha, Shabana I. Khan, Tanika McCants and Saad Awan	1577
Inhibitory Effect of Isoflavones from <i>Erythrina poeppigiana</i> on the Growth of HL-60 Human Leukemia Cells through Inhibition of Glyoxalase I	1581
Kiyomi Hikita, Saori Yamada, Rina Shibata, Miyako Katoh, Tomiyasu Murata, Kuniki Kato, Hitoshi Tanaka and Norio Kaneda	1581
α-Glucosidase and 15-Lipoxygenase Inhibitory Activities of Phytochemicals from <i>Calophyllum syringontianum</i>	1585
Nurul Iman Aminudin, Farediah Ahmad, Muhammad Taher and Razauden Mohamed Zulkifli	1585
Antifungal Activity of Pyranonaphthoquinones Obtained from <i>Cipura paludosa</i> Bulbs	1589
Adriana Campos, Greice Maria Rodrigues Souza, Franco Delle Monache, Estefânia Butassi, Susana Zacchino and Valdir Cechinel Filho	1589
Plant Extract (<i>Bupleurum falcatum</i>) as a Green Factory for Biofabrication of Gold Nanoparticles	1593
You Jeong Lee, Song-Hyun Cha, Kyoung Jin Lee, Yeong Shik Kim, Seonho Cho and Youmie Park	1593
OM-X[®], Fermented Vegetables Extract Suppresses Antigen-Stimulated Degranulation in Rat Basophilic Leukemia RBL-2H3 Cells and Passive Cutaneous Anaphylaxis Reaction in Mice	1597
Tomohiro Itoh, Yasuyoshi Miyake, Takuya Kasashima, Yoshie Shimomiya, Yuki Nakamura, Masashi Ando, Yasuyuki Tsukamasa and Muneaki Takahata	1597
Siomycin A Induces Apoptosis in Human Lung Adenocarcinoma A549 Cells by Suppressing the Expression of FoxM1	1603
Xuedan Guo, Aiping Liu, Hongxia Hua, Huifen Lu, Dandan Zhang, Yina Lin, Qing Sun, Xue Zhu, Guoxin Yan and Fan Zhao	1603
Novel Pharmacological Properties of <i>Dinoponera quadriceps</i> Giant Ant Venom	1607
Juliana da Costa Madeira, Yves Patric Quinet, Dayanne Terra Tenório Nonato, Paloma Leão Sousa, Edna Maria Camelo Chaves, José Eduardo Ribeiro Honório Júnior, Maria Gonçalves Pereira and Ana Maria Sampaio Assreuy	1607
The Leaf Essential Oil of <i>Eugenia reinwardtiana</i> Growing in Australia	1611
Joseph J. Brophy, John R. Clarkson, Myrna A. Deseo, Andrew J. Ford, Douglas J. Lawes and David N. Leach	1611

Relationship Between Soil and Essential Oil Profiles in <i>Salvia desoleana</i> Populations: Preliminary Results	1615
Emma Rapposelli, Sara Melito, Giovanni Gabriele Barmina, Marzia Foddai, Emanuela Azara and Grazia Maria Scarpa	
Simultaneous Determination of Essential Oil Components and Fatty Acids in Fennel using Gas Chromatography with a Polar Capillary Column	1619
Menča Najdoska-Bogdanov, Jane B. Bogdanov and Marina Stefova	
Antischistosomal and Cytotoxic Effects of the Essential Oil of <i>Tetradenia riparia</i> (Lamiaceae)	1627
Nathalya I. de Melo, André L. L. Mantovani, Pollyanna F. de Oliveira, Milton Gropo, Ademar A. da Silva Filho, Vanderlei Rodrigues, Wilson R. Cunha, Denise C. Tavares, Lizandra G. Magalhães and Antônio E. M. Crotti	
Biological Activity and Chemical Constituents of Essential Oil and Extracts of <i>Murraya microphylla</i>	1631
Hai-Ning Lv, Ke-Wu Zeng, Bing-Yu Liu, Yun Zhang, Peng-Fei Tu and Yong Jiang	
Chemical Constituents and Activity of <i>Murraya microphylla</i> Essential Oil against <i>Lasioderma serricorne</i>	1635
Chun-Xue You, Shan-Shan Guo, Wen-Juan Zhang, Kai Yang, Cheng-Fang Wang, Zhu-Feng Geng, Shu-Shan Du, Zhi-Wei Deng and Yong-Yan Wang	

Number 10

Natural Products from Endophytes (Guest Editors: John A. Johnson and Christopher A. Gray)

Original Paper

Antimycobacterial Natural Products from Endophytes of the Medicinal Plant <i>Aralia nudicaulis</i>	
Haoxin Li, Brandon Doucet, Andrew J. Flewelling, Stéphanie Jean, Duncan Webster, Gilles A. Robichaud, John A. Johnson and Christopher A. Gray	1641
Microsporols A-C from the Plant Endophytic Fungus <i>Pestalotiopsis microspora</i>	1643
Xianfu Wu, Yadan Wang, Shuchun Liu, Xinzong Liu and Liangdong Guo	
Isolation of Phomopsolide A and 6(E)-Phomopsolide A as Antimycobacterial Products from an Unidentified Endophyte of the Canadian Medicinal Plant <i>Heracleum maximum</i>	1647
Trevor N. Clark, Katelyn T. Ellsworth, Stéphanie Jean, Duncan Webster, Gilles A. Robichaud, John A. Johnson and Christopher A. Gray	
Pyrroloclin A, a 3-Decalinyltetramic Acid with Selective Biological Activity, Isolated from Amazonian Cultures of the Novel Endophyte <i>Diaporthales</i> sp. E6927E	1649
Eric V. Partridge, Alicia Darnell, Kaury Kucera, Gillian M. Phillips, Heidi R. Bokesch, Kirk R. Gustafson, Daniel J. Spakowicz, Linda Zhou, William M. Hungerford, Mark Plummer, Denton Hoyer, Alexandra Narváez-Trujillo, Andrew J. Phillips and Scott A. Strobel	
Cytotoxic Cytochalasins and Other Metabolites from Xylariaceae sp. FL0390, a Fungal Endophyte of Spanish Moss	1655
Ya-ming Xu, Bharat P. Bashyal, Mangping X. Liu, Patricia Espinosa-Artiles, Jana M. U'Ren, A. Elizabeth Arnold and A. A. Leslie Gunatilaka	
Endophytic Fungus <i>Nigrospora oryzae</i> from a Medicinal plant <i>Coccinia grandis</i>, a High Yielding New Source of Phenazine-1-carboxamide	1659
Dharushana Thanabalasingam, N. Savitri Kumar, Lalith Jayasinghe and Yoshinori Fujimoto	
Polyketides from an Endophytic <i>Aspergillus fumigatus</i> Isolate Inhibit the Growth of <i>Mycobacterium tuberculosis</i> and MRSA	1661
Andrew J. Flewelling, Amanda I. Bishop, John A. Johnson and Christopher A. Gray	
A 3-Vinyl Cephem Derivative, a Useful Intermediate in the Synthesis of Cepham Antibiotics, from <i>Aspergillus awamori</i> Associated with Banana Fruit	1663
H.M.S.K.H. Bandara, N. Savitri Kumar, Lalith Jayasinghe, Hironori Masubuti and Yoshinori Fujimoto	
Two New Cyclic Depsipeptides from the Endophytic Fungus <i>Fusarium</i> sp.	1667
Fang Lv, Georgios Daletos, Wenhua Lin and Peter Proksch	

Accounts/Reviews

Bioactive Secondary Metabolites Produced by the Fungal Endophytes of Conifers	1671
Andrea A. Stierle and Donald B. Stierle	
<hr/>	
Anti-diabetic Effect of Friedelan Triterpenoids in Streptozotocin Induced Diabetic Rat	1683
Amitava Mandal, Vaskar Das, Pranab Ghosh and Shilpi Ghosh	
Colochirosides B₁, B₂, B₃ and C, Novel Sulfated Triterpene Glycosides from the Sea Cucumber <i>Colochirus robustus</i> (Cucumariidae, Dendrochirotida)	1687
Alexandra S. Silchenko, Anatoly I. Kalinovsky, Sergey A. Avilov, Pelageya V. Andryjaschenko, Pavel S. Dmitrenok, Vladimir I. Kalinin, Ekaterina A. Yurchenko and Igor Yu. Dolmatov	
(+)-Chenabinol (Revised NMR Data) and Two New Alkaloids from <i>Berberis vulgaris</i> and their Biological Activity	1695
Zdeněk Novák, Anna Hošťálková, Lubomír Opletal, Lucie Nováková, Martina Hrabinová, Jiří Kuneš and Lucie Cahliková	
The Influence of Cultivars and Phenological Phases on the Accumulation of Nevadensin and Salvigenin in Basil (<i>Ocimum basilicum</i>)	1699
Botond Bernhardt, Jenő Bernáth, Attila Gere, Zoltán Kókai, Bonifác Komáromi, Szilvia Tavaszi-Sárosi, László Sipos and Krisztina Szabó	

Isoorientin, a Selective Inhibitor of Cyclooxygenase-2 (COX-2) from the Tubers of <i>Pueraria tuberosa</i> Manne Sumalatha, Rachakunta Munikishore, Aluru Rammohan, Duvvuru Gunasekar, Kotha Anil Kumar, Kakularam Kumar Reddy, Rajaram Azad, Pallu Reddanna and Bernard Bodo	1703
Secondary Metabolites of <i>Alchemilla persica</i> Growing in Iran (East Azarbaijan) Fariba Heshmati Afshar, Filippo Maggi, Sara Ferrari, Gregorio Peron and Stefano Dall'Acqua	1705
A Novel Ellagic Acid Derivative from <i>Desbordesia glaucescens</i> Faustine L. DongmoMafodong, Apollinaire Tsopmo, Maurice D. Awouafack, Tchuenguem T. Roland, Jean P. Dzoyem and Pierre Tane	1709
Proliferative Constituents from the Leaves of <i>Micromelum integrerrimum</i> Yuan-bin Hu, Jun-ying Sun, Tang-yun Yu, Jing-cheng Wang, Jin-shan He, Yue-lai Zhou and Xian-wen Li	1711
Xylactam B, A New Isobenzofuranone from an Endophytic <i>Xylaria</i> sp. Nelum P. K. G. Piyasena, Anja Schüffler and Hartmut Laatsch	1715
Separation of Aeruginosin-865 from Cultivated Soil Cyanobacterium (<i>Nostoc</i> sp.) by Centrifugal Partition Chromatography \combined with Gel Permeation Chromatography José Cheel, Mirjana Minceva, Petra Urajová, Rabya Aslam, Pavel Hrouzek and Jiří Kopecký	1719
Effect of Maturation Degree on Composition of Fatty Acids and Tocopherols of Fruit Oil from <i>Pistacia atlantica</i> Growing Wild in Algeria Hamid Guenane, Isabelle Bombarda, Mohamed Didi OuldElhadj and Mohamed Yousfi	1723
Chemoenzymatic Total Synthesis of (<i>R</i>)-4-Dodecanolide and (<i>R</i>)-4-Octanolide Chittamuru Sreelakshmi, Adari Bhaskar Rao, Mangamoori Lakshmi Narasu, Anugu Srinivas Reddy, Palakondu Janardhan Reddy and Basi V. SubbaReddy	1729
Inspired by Nature: The Use of Plant-derived Substrate/Enzyme Combinations to Generate Antimicrobial Activity <i>in situ</i> Ethiene Castellucci Estevam, Sharoon Griffin, Muhammad Jawad Nasim, Dariusz Zieliński, Justyna Aszyk, Magdalena Osowicka, Natalia Dawidowska, Rinaldi Idroes, Agnieszka Bartoszek and Claus Jacob	1733
Effect of Supplementation with Wheat Bran Aqueous Extracts Obtained by Ultrasound-Assisted Technologies on the Sensory Properties and the Antioxidant Activity of Dry Pasta Antonella Pasqualone, Laura Nunzia Delvecchio, Giuseppe Gambacorta, Barbara Laddomada, Valeria Urso, Agata Mazzaglia, Paolo Ruisi and Giuseppe Di Miceli	1739
Development of SCAR Markers Based on Improved RAPD Amplification Fragments and Molecular Cloning for Authentication of Herbal Medicines <i>Angelica sinensis</i>, <i>Angelica acutiloba</i> and <i>Levisticum officinale</i> Chun Zhang, Zhiqiang Mei, Jingliang Cheng, Yin He, Md. Asaduzzaman Khan, Peiyi Luo, Saber Imani and Junjiang Fu	1743
Chemical Composition of <i>Blumea lacera</i> Essential Oil from Nepal. Biological Activities of the Essential Oil and (Z)-Lachnophyllum Ester Prabodh Satyal, Bhawan K. Chhetri, Noura S. Dosoky, Samon Shrestha, Ambika Poudel and William N. Setzer	1749
Essential Oil Composition and Antibacterial Activity of <i>Hyptis colombiana</i> from the Venezuelan Andes Mayalin Flores, Luis Rojas, Rosa Aparicio, María Eugenia Lucena and Alfredo Usobilaga	1751
Repellent and Anti-quorum Sensing Activity of Six Aromatic Plants Occurring in Colombia Leonor Cervantes-Ceballos, Karina Caballero-Gallardo and Jesus Olivero-Verbel	1753
Chemical Composition and Larvicidal Activity of Greek Myrtle Essential Oils against <i>Culex pipiens</i> biotype <i>molestus</i> Aikaterini Koutsaviti, Irene Lignou, Ioannis Bazos, George Kolopoulos, Antonios Michaelakis, Athanassios Giatropoulos and Olga Tzakou	1759
Chemical Composition Variability of the Herb Essential Oil in the Ontogenesis of <i>Artemisia campestris</i> subsp. <i>campestris</i> Anna Lis, Martyna Kowal and Joanna Kończak	1763

Accounts/Reviews

Sesquiterpenes from Essential Oils and Anti-Inflammatory Activity Rita de Cássia da Silveira e Sá, Luciana Nalone Andrade and Damião Pergentino de Sousa	1767
The Interaction of Alpha-synuclein with Membranes and its Implication in Parkinson's Disease: A Literature Review Azucena Gonzalez-Horta	1775
Herbal Supplements and Hepatotoxicity: A Short Review Haszianaliza Haslan, Fariyah Haji Suhaimi and Srijiit Das	1779
Vibrational Circular Dichroism: Recent Advances for the Assignment of the Absolute Configuration of Natural Products Eleuterio Burgueño-Tapia and Pedro Joseph-Nathan	1785

Number 11

Re-Discovery of the Plant Kingdom as a Valuable Source of Novel Drugs (Guest Editor: Francesco Epifano)

Antimicrobial Activity of neo-Clerodane Diterpenoids isolated from <i>Lamiaceae</i> Species against Pathogenic and Food Spoilage Microorganisms Petko Bozov, Tania Girova, Natalia Prisadova, Yana Hristova and Velizar Gochev	1797
Study of an Acid-Free Technique for the Preparation of Glycyrrhetic Acid from Ammonium Glycyrrhizinate in Subcritical Water Anna V. Lekar, Sergey N. Borisenko, Elena V. Vetrova, Olga V. Filonova, Elena V. Maksimenko, Nikolai I. Borisenko and Vladimir I. Minkin	1801

New Flavonol Glycoside from the Leaves of <i>Ventilago africana</i> Diane Patricia Apie Gossan, Abdulmagid Alabdul Magid, Philomène Akoua Yao-Kouassi, Damien Le Faucheur, Antoine Ahibo Coffy, Dominique Harakat and Laurence Voutquenne-Nazabadioko	1805
Change in the Chemical Profile of <i>Mangifera indica</i> Leaves after their Metabolism in the <i>Tropidacris collaris</i> Grasshopper Rodolfo R. da Silva, Marcílio M. Moraes, Claudio A. G. Camara and Clécio S. Ramos	1809
Complexes of Lapachol and Lawsone with Lanthanides Salvatore Genovese, Vito Alessandro Taddeo, Francesco Epifano and Serena Fiorito	1811
Synthesis of the Furan Nucleus Promoted by Ytterbium Triflate Vito Alessandro Taddeo, Salvatore Genovese, Francesco Epifano and Serena Fiorito	1813
Analysis of Organic Acids, Deacetyl Asperulosidic Acid and Polyphenolic Compounds as a Potential Tool for Characterization of Noni (<i>Morinda citrifolia</i>) Products Miroslava Bittová, Dita Hladůvková, Vendula Roblová, Stanislav Kráčmar, Petr Kubáň and Vlastimil Kubáň	1817
Antioxidant Activity and Polyphenol Content of Some Brazilian Medicinal Plants Exploiting the Formation of the Fe(II)/2,2'-bipyridine Complexes Waila Evelyn Lima Santana, Cecilia Verônica Nunez and Horacio Dorigan Moya	1821
Reactive Nitrogen Species Scavenging Capacity of Aqueous and Ethanolic Extracts from <i>Galinsoga parviflora</i> and <i>G. quadriradiata</i> Herbs Marta Rogowska, Siniša Srećec and Agnieszka Bazylko	1825
Combination of Antioxidants from Different Sources Could Offer Synergistic Benefits: A Case Study of Tea and Ginger Blend Solomon A. Makanjuola, Victor N. Enujiugha, Olufunmilayo S. Omoba and David M. Sanni	1829
Lipid Metabolites from the Mushroom <i>Meripilus giganteus</i> Francesca Cateni, Tiziano Altieri, Marina Zacchigna, Giuseppe Procida, Jelena Zilič, Dušan Žigon and Angelo Cichelli	1833
HPLC Analysis, Antioxidant, Anti-inflammatory and Xanthine Oxidase Inhibitory Activity of <i>Cudrania tricuspidata</i> Shivraj Hariram Nile and Doo Hwan Kim	1839
Renoprotective Effects, Protein Thiols and Liver Glycogen Content of Alloxan-induced Diabetic Rats Treated with Different Fractions of Heartwood of <i>Pterocarpus marsupium</i> Vinutha Bhat and B Shivananda Nayak	1843
Medicinal Plants Used by a Mybyá-Guarani Tribe Against Infections: Activity on KPC-Producing Isolates and Biofilm-Forming Bacteria Clara Lia Costa Brandelli, Vanessa Bley Ribeiro, Karine Rigon Zimmer, Afonso Luís Barth, Tiana Tasca and Alexandre José Macedo	1847

Accounts/Reviews

Chemistry and Pharmacognosy of the Genus <i>Durio</i> Rudiyansyah, Kanda Panthong and Mary J Garson	1853
General Characteristics, Phytochemistry and Pharmacognosy of <i>Lippia sidoides</i> Luiz Gustavo de L. Guimarães, Maria Laura M. da Silva, Paula Campos J. Reis, Maria Tereza R. Costa and Lívia L. Alves	1861
Poplar-type Propolis: Chemical Composition, Botanical Origin and Biological Activity Petar Ristivojević, Jelena Trifković, Filip Andrić and Dušanka Milojković-Opsenica	1869
Activities of Tannins – From <i>In Vitro</i> Studies to Clinical Trials Elwira Sieniawska	1877
Organoselenium Compounds as Phytochemicals from the Natural Kingdom Hanane Achibat, Nohad A AlOmari, Federica Messina, Luca Sancinetto, Mostafa Khouili and Claudio Santi	1885
<hr/>	
Spasmolytic Activity of Carvone and Limonene Enantiomers Damião Pergantino de Sousa, Rafael Ferreira Mesquita, Luciano Augusto de Araújo Ribeiro and Julianeli Tolentino de Lima	1893
New Glycosides and Trypanocidal Metabolites from <i>Vangueria edulis</i> Shaymaa M. M. Mohamed, Khaled M. Elokhely, Enaam Y. Bachkeet, Soad A. L. Bayoumi, Vincenzo Carnevale, Michael L. Klein, Stephen J. Cutler and Samir A. Ross	1897
Constituents of the Stem of <i>Nauclea orientalis</i> Phan Thi Anh Dao, Tran Le Quan and Nguyen Thi Thanh Mai	1901
Deodarone Isomers in <i>Cedrus atlantica</i> Essential Oils and Tar Oils Anne Marie Nam, Ange Bighelli, Mohamed Ghanni, Badr Satrani, Joseph Casanova and Félix Tomi	1905
A New Trinor-guaiane Sesquiterpene from an Indonesian Soft Coral <i>Anthelia</i> sp. Novriyandi Hanif, Anggia Murni, Marie Yamauchi, Masahiro Higashi and Junichi Tanaka	1907
A New Cytotoxic Gymnomitrane Sesquiterpene from <i>Ganoderma lucidum</i> Fruiting Bodies Pham Thanh Binh, Dimitri Descoutures, Nguyen Hai Dang, Nguyen Phuong Dai Nguyen, and Nguyen Tien Dat	1911
A New Isocyanosesquiterpene from the Nudibranch <i>Phyllidiella pustulosa</i> Takahiro Jomori, Takahiro Shibutani, Peni Ahmad, Toshimasa Suzuka and Junichi Tanaka	1913
Antimicrobial Diterpenes from <i>Azorella</i> Species Against Gram-Positive Bacteria Viviana Donoso, Mitchell Bacho, Solange Núñez, Juana Rovirosa, Aurelio San-Martín and Sergio Leiva	1915
A Novel Norellerodane Diterpenoid from the Roots of <i>Croton crassifolius</i> Zhan-Xin Zhang, Hui-Hong Li, Gai-Xia Fan, Zheng-Yu Li, Le-Le Dong, Hong-Yu Li and Dong-Qing Fei	1917
Production of Triterpenoid Sapogenins in Hairy Root Cultures of <i>Silene vulgaris</i> Yeon Bok Kim, Darwin W. Reed and Patrick S. Covello	1919

Extraction and Isolation of Antineoplastic Pristimerin from <i>Mortonia greggii</i> (Celastraceae)	1923
Luis Alberto Mejía-Manzano, Bertha A. Barba-Dávila, Janet A. Gutierrez-Uribe, Edgardo J. Escalante-Vázquez and Sergio O. Serna-Saldívar	1923
Bioassay-guided Isolation of Antiproliferative Triterpenoids from <i>Euonymus alatus</i> Twigs	1929
Hee Rae Kang, Hee Jeong Eom, Seoung Rak Lee, Sang Un Choi, Ki Sung Kang, Kang Ro Lee and Ki Hyun Kim	1929
Two New Triterpenoidal Saponins from Roots of <i>Pachystela msolo</i>	1933
Roland N. Ache, Turibio K. Tabopda, Samuel O. Yeboah and Bonaventure T. Ngadjui	1933
The Influence on LPS-Induced ROS Formation in Macrophages of Capelloside A, a New Steroid Glycoside from the Starfish <i>Ogmaster capella</i>	1937
Natalia V. Ivanchina, Alla A. Kicha, Timofey V. Malyarenko, Anatoly I. Kalinovsky, Ekaterina S. Menchinskaya, Evgeny A. Pislyagin and Pavel S. Dmitrenok	1937
Steroidal Saponins from the Mesocarp of the Fruits of <i>Raphia farinifera</i> (Arecaceae) and their Cytotoxic Activity	1941
Leon A. Tapondjou, Kristina J. Siems, Stefan Böttger and Matthias F. Melzig	1941
Bromotyrosine Alkaloids with Acetylcholinesterase Inhibitory Activity from the Thai Sponge <i>Acanthodendrilla</i> sp.	1945
Natchanun Sirimangkalikit, Opeyemi J. Olatunji, Kanokwan Changwichit, Tonghai Saesong, Supakarn Chamni, Pithi Chanvorachote, Kornkanok Ingkaninan, Anuchit Plubulkarn and Khanit Suwanborirux	1945
Ircinal E, a New Manzamine Derivative from the Indonesian Marine Sponge <i>Acanthostrongylophora ingens</i>	1951
Mousa AlTarabeen, Georgios Daletos, Weaam Ebrahim, Werner E. G. Müller, Rudolf Hartmann, Wenhan Lin and Peter Proksch	1951
Ruta graveolens Extracts and Metabolites against <i>Spodoptera frugiperda</i>	1955
Benjamín A. Ayil-Gutiérrez, Jesús M. Villegas-Mendoza, Zuridai Santes-Hernández, Alma D. Paz-González, Maribel Mireles-Martínez, Ninfa M. Rosas-García and Gildardo Rivera	1955
A New Isoflavone Apiooglucoside from the Roots of <i>Dalbergia spinosa</i>	1959
Raja Radha, Vairathevar Sivasamy Vasantha and Kasi Pitchumani	1959
Antioxidant and α-Glucosidase Inhibitory Properties and Chemical Profiles of Moroccan Propolis	1961
Milena Popova, Badiaa Lyoussi, Smail Aazza, Dulce Antunes, Vassya Bankova and Graça Miguel	1961
A Novel Acylated Anthocyanin with a Linear Trisaccharide from Flowers of <i>Convolvulus althaeoides</i>	1965
Luis Cabrita	1965
Bioactive Xanthones from <i>Cratoxylum cochinchinense</i>	1969
Achara Raksat, Tawanun Sriput and Wisanu Maneerat	1969
A New 3'-Prenyloxyporensin from the Raw Fruits of <i>Aegle marmelos</i> and its Cytotoxic Activity	1973
Widchaya Radchatawedchakoon, Suthep Bamrungsuk, Siriporn Namwijit, Nuttapon Apiratikul, Uthai Sakee and Boon-ek Yingyongnarongkul	1973
New Gallotannin and other Phytochemicals from Sycamore Maple (<i>Acer pseudoplatanus</i>) Leaves	1977
Lu Zhang, Zong-cai Tu, Tao Yuan, Hang Ma, Daniel B. Niesen, Hui Wang and Navindra P. Seeram	1977
Three New Chlorinated Cyclopentenols, Palmaenols A and B and Palmaetriol, from the Discomycete <i>Lachnum palmae</i>	1981
Yuka Tanabe, Takunori Matsumoto, Tsuyoshi Hosoya, Hiroshi Tomoda, Motoo Shiro and Hideyuki Shigemori	1981
Prebiotic Effects of <i>Agave salmiana</i> Fructans in <i>Lactobacillus acidophilus</i> and <i>Bifidobacterium lactis</i> Cultures	1985
Adriana Castro-Zavala, Bertha I. Juárez-Flores, Juan M. Pinos-Rodríguez, Rosa E. Delgado-Portales, Juan R. Aguirre-Rivera and Francisco Alcocer-Gouyonnet	1985
Synergy Effects of Three Plant Extracts on Protection of Gastric Mucosa	1989
Caihu Wang, Wen Su, Xingli Su, Guojun Ni, Tao Liu and Yi Kong	1989
<i>Aloe arborescens</i> Extract Protects IMR-32 Cells against Alzheimer Amyloid Beta Peptide via Inhibition of Radical Peroxide Production	1993
Maria Elisabetta Clementi, Giuseppe Tringali, Doriana Triggiani and Bruno Giardina	1993
Volatile Constituents of Three <i>Piper</i> Species from Vietnam	1997
Le D. Hieu, Tran M. Hoi, Tran D. Thang and Isiaka A. Ogunwande	1997
Volatile Constituents from the Flowers of <i>Spathodea campanulata</i> from the Venezuelan Andes	1999
Silvana Villarreal, Deisy Jaimez, Sindy Moreno, Luis B. Rojas, Alfredo Usobilaga and María Rodríguez	1999
Composition and Variability of the Essential Oil of the Flowers of <i>Lavandula stoechas</i> from Various Geographical Sources	2001
Salvatore La Bella, Teresa Tuttolomondo, Giacomo Dugo, Giuseppe Ruberto, Claudio Leto, Edoardo M. Napoli, Angela Giorgia Potortì, Maria Rita Fede, Giuseppe Virga, Raffaele Leone, Eleonora D'Anna and Mario Licata	2001
Antioxidant and Anti-inflammatory Activities of Essential Oil and Extracts of <i>Piper miniatum</i>	2005
Wan Mohd Nuzul Hakimi Wan Salleh, Mohd Fariz Kammil, Farediah Ahmad and Hasnah Mohd Sirat	2005
Potential Skin Regeneration Activity and Chemical Composition of Absolute from <i>Pueraria thunbergiana</i> Flower	2009
Do-Yoon Kim, Kyung-Jong Won, Dae-Il Hwang, Seok Won Yoon, Su Jin Lee, Joo-Hoon Park, Myeong Sik Yoon, Bokyung Kim and Hwan Myung Lee	2009
Composition, <i>in vitro</i> Cytotoxicity, and Anti-mildew Activities of the Leaf Essential Oil of <i>Machilus thunbergii</i> from Taiwan	2013
Yu-Chang Su, Kuan-Ping Hsu, Shu-Ching Li and Chen-Lung Ho	2013

Additions/Corrections

Isolation of Phomopsolide A and 6(E)-Phomopsolide A as Antimycobacterial Natural Products from an Unidentified Endophyte of the Canadian Medicinal Plant *Heracleum maximum*

Trevor N. Clark, Katelyn T. Ellsworth, Stéphanie Jean, Duncan Webster, Gilles A. Robichaud, John A. Johnson and Christopher A. Gray

Natural Product Communications, 10 (10), 1647-1648 (2015)

2017

Number 12

Petchienes A–E, Meroterpenoids from <i>Ganoderma petchii</i>	2019
Qin-Lei Gao, Ping-Xia Guo, Qi Luo, Hui Yan and Yong-Xian Cheng	
Megastigmane Glycosides from the Leaves of <i>Tripterygium wilfordii</i>	2023
Lin Ni, Xiao-mei Zhang, Xing Zhou, Jie Ma, Chuang-jun Li, Li Li, Tian-tai Zhang and Dong-Ming Zhang	
Cytochalasans and Sesquiterpenes from <i>Eutypella scoparia</i> 1–15	2027
Shuang Qi, Yue Wang, Zhonghui Zheng, Qingyan Xu and Xiamming Deng	
Concise Synthesis of Taiwaniaquinol B and 5-<i>epi</i>-Taiwaniaquinone G	2031
Yonggang Meng, Yizhen Liu, Zhigang Lv, Jinqian Wang, Yanyan Wang, Chuanjun Song and Junbiao Chang	
Effect of Enzyme Inhibitors on Terpene Trilactones Biosynthesis and Gene Expression Profiling in <i>Ginkgo biloba</i> Cultured Cells	2033
Lijia Chen, Hui Tong, Mingxuan Wang, Jianhua Zhu, Jiachen Zi, Liyan Song and Rongmin Yu	
Macrocyclic Diterpenoids from the Latex of <i>Euphorbia helioscopia</i>	2037
Juan Hua, Yan-Chun Liu, Shu-Xi Jing, Shi-Hong Luo and Sheng-Hong Li	
A New Triterpenoid from the Aerial Parts of <i>Agrimonia pilosa</i>	2041
Jiang-Hao Ma, Qing-Hua Jiang, Ying Chen, Xiu-Fang Nie, Tie Yao, Li-Qin Ding, Feng Zhao, Li-Xia Chen and Qiu Feng	
Two New 18-Norschiartane-type Schinortriterpenoids from <i>Schisandra lancifolia</i>	2045
Miao Liu, Yuan-Qing Luo, Wei-Guang Wang, Yi-Ming Shi, Hai-Yan Wu, Xue Du, Jian-Xin Pu and Han-Dong Sun	
Terpenoids and Steroids from <i>Euphorbia hypericifolia</i>	2049
Jin-Xin Zhao, Shan-Shan Shi, Li Sheng, Jia Li and Jian-Min Yue	
A Fragmentation Study of Six C₂₁ Steroidal Aglycones by Electrospray Ionization Ion-Trap Time-of-Flight Tandem Mass Spectrometry	2053
Xing-Long Chen, Chang-An Geng and Ji-Jun Chen	
Three New Cytotoxic Withanolides from the Chinese Folk Medicine <i>Physalis angulata</i>	2059
Cai-Yun Gao, Ting Ma, Jun Luo and Ling-Yi Kong	
Diterpenoid Alkaloids from <i>Aconitum soongaricum</i> var. <i>pubescens</i>	2063
Lin Chen, Lianhai Shan, Jifa Zhang, Wenliang Xu, Mingyu Wu, Shuai Huang and Xianli Zhou	
Two New C₁₈-Diterpenoid Alkaloids from <i>Delphinium anthriscifolium</i>	2067
Lianhai Shan, Jifa Zhang, Lin Chen, Jiaxi Wang, Shuai Huang and Xianli Zhou	
Majusine D: A New C₁₉-diterpenoid Alkaloid from <i>Delphinium majus</i>	2069
Qi Zhao, Xiao-jun Gou, Wei Liu, Gang He, Li Liang and Feng-zheng Chen	
Epoxide Opening of a 7,17-Seco-7,8-Epoxy-C₁₉-Diterpenoid Alkaloid	2071
Hong Ji, Feng-Peng Wang and Qiao-Hong Chen	
Further Studies on Structure-Cardiac Activity Relationships of Diterpenoid Alkaloids	2075
Zhong-Tang Zhang, Xi-Xian Jian, Jia-Yu Ding, Hong-Ying Deng, Ruo-Bing Chao, Qiao-Hong Chen, Dong-Lin Chen and Feng-Peng Wang	
Monoterpene Indole Alkaloids from <i>Catharanthus roseus</i> Cultivated in Yunnan	2085
Bei Wang, Lu Liu, Ying-Ying Chen, Qiong Li, Dan Li, Ya-Ping Liu and Xiao-Dong Luo	
Two New Oxindole Alkaloid Glycosides from the Leaves of <i>Nauclea officinalis</i>	2087
Long Fan, Xiao-Jun Huang, Chun-Lin Fan, Guo-Qiang Li, Zhen-Long Wu, Shuo-Guo Li, Zhen-Dan He, Ying Wang and Wen-Cai Ye	
Lycopodium Alkaloids from <i>Diphasiastrum complanatum</i>	2091
Yu Tang, Juan Xiong and Jin-Feng Hu	
Effects of Adding Vindoline and MeJA on Production of Vincristine and Vinblastine, and Transcription of their Biosynthetic Genes in the Cultured CMCs of <i>Catharanthus roseus</i>	2095
Wenjin Zhang, Jiazeng Yang, Jiachen Zi, Jianhua Zhu, Liyan Song and Rongmin Yu	
Structures and Chemotaxonomic Significance of Stemona Alkaloids from <i>Stemona japonica</i>	2097
Min Yi, Xue Xia, Hoi-Yan Wu, Hai-Yan Tian, Chao Huang, Paul Pui-Hay But, Pang-Chui Shaw and Ren-Wang Jiang	
Chemical Constituents of <i>Euonymus glabra</i>	2101
Jie Ren, Yang-Guo Xie, Xing Wang, Shi-Kai Yan, Hui-Zi Jin and Wei-Dong Zhang	
Isoprenylated Flavonoids with PTP1B Inhibition from <i>Ficus tikoua</i>	2105
Lu-Qin Wu, Chun Lei, Li-Xin Gao, Hai-Bing Liao, Jing-Ya Li, Jia Li and Ai-Jun Hou	
Phenolic Derivatives from <i>Hypericum japonicum</i>	2109
Guoyong Luo, Min Zhou, Qi Ye, Jun Mi, Dongmei Fang, Guolin Zhang and Yinggang Luo	
Synthesis and Anti-Proliferative Effects of Quercetin Derivatives	2113
Sami M.R. Al-Jabban, Xiaojie Zhang, Guanglin Chen, Ermias Addo Mekuria, Liva Harinantaina Rakotondraibe and Qiao-Hong Chen	
Compounds with Antifouling Activities from the Roots of <i>Notopterygium franchetii</i>	2119
Chun Yu, Liqing Cheng, Zhongling Zhang, Yu Zhang, Chunmao Yuan, Weiwei Liu, Xiaojiang Hao, Weiguang Ma and Hongping He	
New Isochromane Derivatives from the Mangrove Fungus <i>Aspergillus ustus</i> 094102	2123
Peipei Liu, Cong Wang, Zhenyu Lu, Tonghan Zhu, Kui Hong and Weiming Zhu	
Pericocins A–D, New Bioactive Compounds from <i>Periconia</i> sp.	2127
Yue-Hua Wu, Gao-Keng Xiao, Guo-Dong Chen, Chuan-Xi Wang, Dan Hu, Yun-Yang Lian, Feng Lin, Liang-Dong Guo, Xin-Sheng Yao and Hao Gao	
New Benzenoids from the Roots of <i>Lindera aggregata</i>	2131
Guo-Hao Ma, Che-Wei Lin, Hsin-Yi Hung, Sheng-Yang Wang, Po-Chuen Shieh and Tian-Shung Wu	

12-Membered Resorcylic Acid Lactones Isolated from <i>Saccharicola bicolor</i>, an Endophytic Fungi from <i>Bergenia purpurascens</i>	2135
Da-Le Guo, Min Zhao, Shi-Ji Xiao, Bing Xia, Bo Wan, Yu-Cheng Gu, Li-Sheng Ding and Yan Zhou	
Phenylpropanoid Glycosides from the Leaves of <i>Ananas comosus</i>	2137
Wen-Hao Chen, Xiao-Juan Huang, Huo-Ming Shu, Yang Hui, Fei-Yan Guo, Xiao-Ping Song, Ming-Hui Ji and Guang-Ying Chen	
Tannins and Antioxidant Activities of the Walnut (<i>Juglans regia</i>) Pellicle	2141
Tian-Peng Yin, Le Cai, Yang Chen, Ying Li, Ya-Rong Wang, Chuan-Shui Liu and Zhong-Tao Ding	
Chemical Constituents of <i>Cordyceps cicadae</i>	2145
Zhi-Bo Chu, Jun Chang, Ying Zhu and Xun Sun	
A New Bithiophene from the Root of <i>Echinops grijsii</i>	2147
Fang-Pin Chang, Chien-Chih Chen, Hui-Chi Huang, Sheng-Yang Wang, Jih-Jung Chen, Chang-Syun Yang, Chung-Yi Ou, Jin-Bin Wu, Guan-Jhong Huang and Yueh-Hsiung Kuo	
Cyclic Lipopeptides with Herbicidal and Insecticidal Activities Produced by <i>Bacillus clausii</i> DTM1	2151
Da-Le Guo, Bo Wan, Shi-Ji Xiao, Sarah Allen, Yu-Cheng Gu, Li-Sheng Ding and Yan Zhou	
Synthesis of (6R,12R)-6,12-Dimethylpentadecan-2-one, the Female-Produced Sex Pheromone from Banded Cucumber Beetle <i>Diabrotica balteata</i>, Based on a Chiron Approach	2155
Wei Shen, Xiang Hao, Yong Shi and Wei-Sheng Tian	
A Rapid Study of Botanical Drug–Drug Interaction with Protein by Re-ligand Fishing using Human Serum Albumin–Functionalized Magnetic Nanoparticles	2161
Lin-Sen Qing, Ying Xue, Li-Sheng Ding, Yi-Ming Liu, Jian Liang and Xun Liao	
Serum Metabolomic Profiling of Rats by Intervention of <i>Aconitum soongaricum</i>	2165
Fan Zhang, Jiao Liu, Jun Lei, Wenjing He and Yun Sun	
Re-evaluation of ABTS^{•+} Assay for Total Antioxidant Capacity of Natural Products	2169
Jian-Wei Dong, Le Cai, Yun Xing, Jing Yu and Zhong-Tao Ding	

Accounts/Reviews

Chemical Synthesis of the Echinopine Sesquiterpenoids	2173
Xiao-Yu Liu and Yong Qin	
Synergistic Effects of Dietary Natural Products as Anti-Prostate Cancer Agents	2179
Bao Vue, Sheng Zhang and Qiao-Hong Chen	
<i>Ligustrum lucidum</i> and its Constituents : A Mini-Review on the Anti-Osteoporosis Potential	2189
Chun-Tao Che and Man-Sau Wong	
Alice, Benzene, and Coffee: The ABCs of Ecopharmacognosy	2195
Geoffrey A. Cordell	

Additions/Corrections

Cytotoxic and Antimalarial Alkaloids from the Twigs of <i>Dasymaschalon obtusipetalum</i>	2203
Atchara Jaidee, Thanika Promchai, Kongkiat Trisawan, Surat Laphookhieo, Roonglawan Rattanajak, Sumalee Kamchonwongpaisan, Stephen G. Pyne and Thunwadee Ritthiwigrom	
<i>Natural Product Communications, 10 (7), 1175-1177 (2015)</i>	

Natural Product Communications

Volume 10 (1-12)

2015

Author Index

Aazza, S.....	1961	Anh, PT	1351	Bao, HY	315	Borjihan, G.....	289
Abdullah, MP	1199	Annan, K	563	Bao, N	289	Borris, RP.....	925
Abdullah, SA.....	393	Antal, D.....	951	Baptista, JG	655	Boti, JB.....	1059
Abou-Dough, AM	617	Antunes, D.....	1961	Barba-Dávila, BA	1923	Böttger, S	1941
Abourashed, EA	1577	Anufriev, VP	1243	Barbosa, JS.....	983	Boudermine, S.....	319
Abraha, A	1577	Anyanwu, CS	39	Barison, A	625	Boulet, E.....	597
Abu, N	1199	Ao, W	323	Barmina, GG	1615	Boussaïd, M	1447
Ache, RN.....	1933	Ao, X	1145	Barrero, AF	1,869	Bozov, P	565,1797
Achibat, H	1885	Aoyagi, S.....	903	Barth, AL	1847	Bozov, PI.....	13
Adams, A.....	187	Aparicio, R	655,1751	Bartho, L	487	Branco, A	983
Adams, M	1149	Apiratikul, N	1973	Bartholomew, B	1281	Brandelli, CC	1847
Adhikari, A	641,1533	Aquino, RP.....	319	Bartoszek, A	1733	Braz-Filho, R.....	871
Afiyatullov, SS.....	1247	Arancon, N	925	Bashyal, BP	1655	Brklijača, R	95
Afshar, FH.....	1705	Arantes, S	673	Basset, C	605	Brodie, PJ.....	567,1505,1509
Aguirre-Rivera, JR	1985	Arasu, MV	1211	Bastida, J	171	Brophy, JJ.....	1611
Ahibo, AC	1059	Arceusz, A	977	Bau, T	315	Brunelli, E	547
Ahmad, A	1395	Arima, N	863	Baumann, TW	793	Buatois, B	1079
Ahmad, F.....	1297,1301,1465	Arita, M	329	Bayoumi, SAL	1897	Buchbauer, G	1127
Ahmad, F.....	1585,2005	Ariza, MR	869	Bazos, I	1759	Buendía-Trujillo, AI	1027
Ahmadi, P	1913	Arnold, AE	107,1655	Bazylko, A	1825	Bugoni, S	847
Ahn, MR.....	963	Arnold, NA.....	1075	Becerra, J	1355	Buhagiar, JA	1323
Akai, S	691	Arteaga, JF	1257	Beclen, JJ	1195	Buitrago, A	375
Akhtar, MN	1199	Arzola, JC	1321	Beddou, F	1447	Bunders, C	1159
Akiyama, S	403	Asakawa, Y	5,1051,1501	Beghida, N	319	Bunders, C	559
Alarcón, L.....	655	Asgarpanah, J	369,669	Bekhechi, C	1447	Bunyaphraphatsara, N.....	479,1387
Alarcón, R	1183	Ashihara, H	703,707,717,733	Belaaouaj, A	167	Bunyaphraphatsara, N.....	1431
Alberto, MR	991	Ashihara, H	737,751,803	Bella, SL	2001	Burgos, V	1355
Alcocer-Gouyonnet, F	1985	Aslam, R	1719	Benayache, S	319	Burgueño-Tapia, E	1027,1785
Al-Dhabi, NA	1211	Assreuy, AMS	1607	Bergonzi, MC	1035	But, PPH	2097
Ali, A	133,1071	Aszyk, J	1733	Bernáth, J	1699	Butassi, E	1589
Ali, BH	77	Athikomkulchai, S	1459	Bernhardt, B	1699	Bylka, W	1239
Ali, HM	1541	Atsumi, I	499	Bessière, JM	1079	Caballero-Gallardo, K	1753
Ali, Z	641	Auw, L	57	Bettencourt, E	673	Cabrita, L	1965
Aligiannis, N	83	Avilov, SA	21,1167,1687	Bhagavathy, GV	1335	Cahill, M	575
Alitheen, NB	1199	Awadh, AI	1483	Bhat, GA	503	Cahliková, L	77,577,1537,1695
Al-Jabban, SMR	2113	Awale, S	997	Bhat, V	1843	Cai, L	2141,2169
Al-Jenoobi, FI	1395	Awani, S	1577	Bhatt, V	313	Calderón-Montaño, JM	853
Alkharfy, KM	1395	Awasthi, S	43	Bhatta, RS	293	Callmander, MW	567,1505,1509
Allen, S	2151	Awouafack, MD	1325,1709	Bhave, S	1287	Camara, CAG	1809
Almeida, VM	983	Ayil-Gutiérrez, BA	1955	Bighelli, A	1059,1447,1905	Camilleri-Podestà, MT	1323
Al-Mohizea, AM	1395	Azad, R	1703	Bilgili, B	595	Campos, A	1589
AlOmari, NA	1885	Azara, E	1615	Bilia, AR	125,1035	Cao, WH	921
AlTarabeen, M	1951	Azizi, M	775	Bina, E	369	Cao, Z	1499
Altieri, T	1833	Bach II, AC	491	Binh, PT	1911	Caparrotta, L	1365
Altieri, V	1009	Bachkeet, EY	1897	Bishop, AI	1661	Capasso, R	1009
Alvarado-Castillo, CP	281	Bacho, M	1915	Bittová, M	1817	Capecci, G	1035
Alves, LL.....	1861	Badakov, H	565	Blasi, F	1403	Capellari, SC	99
Amaro-Luis, J	653	Bae, HS	963	Blažević, I	1043	Capello, TM	285
Ambrus, R	951	Baek, NI	1517	Blunden, G	77	Caprioli, G	575
Aminudin, NI	1585	Bahrani, S	369	Bodo, B	609,1703	Cardozo, A	281
An, HJ	389	Bai, H	899	Bogdanov, JB	1619	Carmona, J	1309
An, L	243	Bakar, B	725,1185	Bogdanova, EG	1345	Carnevale, V	1897
Anantachoke, N ...	479,1387,1431	Bala, M	43	Bokesch, HR	1649	Casanova, J	1059,1447,1905
Ancheeva, E	437	Baltina, L	1565	Boldyrev, VV	1345	Casanova, LM	433
Ando, M	1597	Bamrungsuk, S	1973	Boldyрева, EV	1345	Casapullo, A	1013
Andrade, LN.....	1767	Bandara, HMSKH	1663	Bombarda, I	1723	Cassiano, C	1013
Andreev, YA	1171	Banerjee, AK	1237	Bonikowski, R	371	Castro, A	857
Andrić, F	1869	Bankova, V	1279,1961	Boontiang, K	453	Castro-Zavalá, A	1985
Andrijaschenko, PV	1687	Banovac, D	143	Borcan, F	951	Catanzaro, D	1365
Angelis, A	83	Bansal, AK	969	Borisenko, NI	1801	Cateni, F	1833
Anh, HLT	875,1341,1351			Borisenko, SN	1801		

- Cayo, F 1183
 Cazal, CM 17
 Ćegan, L 577
 Celiński, K 371
 Cerchiara, T 547
 Cerdá-García-Rojas, CM 853
 Cervantes-Ceballos, L 1753
 Cha, SH 627,1593
 Chakrabarti, T 297
 Chamni, S 1945
 Chan, KL 945
 Chancharunee, S 1387,1431
 Chang, CC 1373
 Chang, FP 2147
 Chang, HS 845
 Chang, J 2145
 Chang, JU 2031
 Chang, ST 1305
 Chang, WY 345
 Chang, YW 1421
 Changwichit, K 1945
 Chanvorachote, P 1945
 Chao, RB 2075
 Chao, X 823
 Charan, RD 559,1159
 Chatterjee, S 1443
 Chaturvedula, VSP 1521
 Chau, DTM 365
 Chau, VM 591
 Chauhan, KR 1335
 Chaves, EMC 1607
 Che, CT 2189
 Cheel, J 1719
 Chen, JJ 2147
 Chen, L 2063
 Chen, B 1383
 Chen, CC 845,2147
 Chen, CJ 345,1305
 Chen, CK 891
 Chen, DL 861,2075
 Chen, F 2069
 Chen, G 2113
 Chen, GD 2127
 Chen, GY 2137
 Chen, H 585
 Chen, J 187,571,1145,1553
 Chen, JJ 845,2053
 Chen, L 2033,2067
 Chen, LX 2041,2071,2075
 Chen, QH 2113,2179
 Chen, S 341
 Chen, WF 1163
 Chen, WH 2137
 Chen, XL 2053
 Chen, Y 2041,2141
 Chen, YJ 1191
 Chen, YN 921
 Chen, YT 1305
 Chen, YY 2085
 Chen, Z 237
 Cheng, CH 1163
 Cheng, J 1743
 Cheng, L 2119
 Cheng, LC 945
 Cheng, YX 2019
 Cherneva, E 1423
 Chhetri, B 1749
 Chhetri, BK 1067
 Chiang, MY 317
 Chidichimo, G 547
 Chien, SC 1305
 Chierici, S 847
 Chinea, K 1237
 Chinou, I 67
 Chizzola, R 1179
 Chlebek, J 577
 Cho, S 627,1593
 Cho, SH 1251
 Choi, H 631
 Choi, HG 631
 Choi, JS 383
 Choi, SU 1929
 Choi, YH 389
 Chokchaisiri, R 89
 Choudhary, A 379
 Choudhary, MI 641,1533
 Chowdhury, SR 297
 Chu, FH 1305
 Chu, ZB 2145
 Chung, HM 835
 Ciccone, M 1569
 Cichelli, A 1833
 Cimmino, A 1119
 Cioni, P 1323
 Cisowska, A 467
 Clark, BR 925
 Clark, TN 1647
 Clarkson, JR 1611
 Clementi, ME 1993
 Coffy, AA 1805
 Coll, J 13,857
 Conti, BJ 1279
 Cordell, GA 2195
 Corrêa, MFP 433
 Cossignani, L 1403
 Costa, MTR 1861
 Costa, SS 433
 Costa, YD 721
 Coulierie, P 1501
 Coussaert, A 597
 Covello, PS 1919
 Crosby, DC 117
 Crotti, AEM 1627
 Crouch, NR 1207
 Csányi, E 951
 Csupor, D 1181
 Cuc, NT 353,1341,1351
 Cuello, S 991
 Cui, Y 71
 Cunha, WR 1627
 Cuong, NX 353
 Cuong, TD 383
 Cutler, SJ 1897
 Cvetkovikj, I 987
 D'Ambola, M 319
 D'Angiolillo, F 1055
 D'Anna, E 2001
 da Silva, MD 917
 da Silva, MLM 1861
 da Silva, RR 1809
 Dai, DN 365
 Dai, H 585
 Dai, N 323
 Dai, YQ 1191
 Daletos, G 437,585,1667,1951
 Dall'Acqua, S 1705
 Damdimsuren, O 417
 Dame, ZT 623
 Damianakos, H 67
 Dan, W 899
 Danciu, C 951
 Dandi, K 379
 Dang, NH 1341,1911
 Dao, PTA 1901
 Darnell, A 1649
 Das, S 1779
 Das, V 1683
 Dastagir, N 1533
 Dat, NT 1911
 Davies, J 1287
 Dawidowska, NB 1733
 de Farias, CF 285
 de Lima, JT 1893
 De Nicola, GR 1043
 de Sousa, DP 1893
 de Voogd, NJ 863
 Deguchi, J 291
 Dehelean, C 951
 Delemasure, S 1005
 Delgado, M 677
 Delgado-Portales, RE 1985
 Delvecchio, LN 1739
 Demirezer, LO 595
 Deng, A 1277
 Deng, HY 2075
 Deng, J 339
 Deng, L 921
 Deng, W 71
 Deng, WW 703,733,737,787
 Deng, X 2027
 Deng, Z 1277
 Deng, ZW 1635
 Denhez, C 167
 Denisenko, VA 913,1171,1243
 Descoutures, D 1911
 Deseo, MA 1611
 Deville, A 609
 Devkota, KP 559,1159
 Di, YT 1421
 Díaz, C 375
 Díaz, O 1183
 Díaz, T 1309
 Dibwe, DF 997
 Ding, G 1499
 Ding, JY 2075
 Ding, LQ 2041
 Ding, LS 2135,2161
 Ding, W 1363
 Ding, ZT 2141,2169
 Ding, LS 2151
 Dion, C 597
 Djordjevic, A 649
 Dmitrenok, PS 877,913,1171
 Dmitrenok, PS 1687,1937
 Dolma, SK 1525
 Dolmatov, IY 1687
 Domaradzki, K 1149
 Dominici, L 1403
 Dong, JW 2169
 Dong, LL 1917
 Dong, P 1025
 Dong, S 895,1543
 DongmoMafodong, FL 1709
 Donoso, V 1915
 dos Santos, ML 581
 Dosoky, NS 1067
 Dosoky, NS 1749
 Doucet, B 1641
 Drabikova, K 937
 Družić, J 1315
 Du, G 305
 Du, H 495
 Du, P 243
 Du, SS 1635
 Du, X 2045
 Du, Y 233
 Duarte, RC 871
 Dudra, A 467
 Dugo, G 2001
 Duman, H 595
 Dutartre, P 1005
 Dzoyem, JP 1709
 Eaton, AL 567
 Ebrahim, W 1951
 Ekuadzi, E 563
 Ellsworth, KT 1647
 Eloff, JN 1325
 Elokey, KM 1897
 Elsebai, MF 637
 Emani, L 1555
 Enuijuigha, VN 1829
 Eom, HJ 1929
 Eparvier, V 605
 Epifano, F 589,1115,1811,1813
 Escalante-Vázquez, EJ 1923
 Espindola, LS 605
 Espinosa-Artiles, P 1655
 Esposito, T 319
 Estep, AS 1195
 Estevam, EC 1733
 Estrada, O 281
 Etxeberria, U 1417
 Evidente, A 1119
 Evidente, M 1119
 Fadaeinabab, M 1541
 Fagg, CW 581
 Fan, CL 2087
 Fan, GX 1917
 Fan, L 2087
 Fan, PC 387
 Fan, XF 387
 Fang, D 2109
 Fang, LS 1163
 Fang, SR 257
 Faucheur, DL 1805
 Fauzi, PNM 1541
 Fede, MR 2001
 Fei, DQ 1917
 Feng, Q 2041
 Feng, Y 1203
 Fernandes, JB 17
 Fernandes, MFG 17
 Fernández, S 657
 Fernández-López, J 1219
 Ferrari, S 1705
 Fialova, S 937
 Figueiredo, AC 677
 Figueiredo, CR 285
 Filho, AAS 1627
 Filho, VC 1589
 Filonova, OV 1801
 Fiorito, S 1115
 Fiorito, S 589,1115,1811,1813
 Flamini, G 1323,1469
 Flewelling, AJ 1641,1661
 Flores, M 1751
 Flythe, MD 1263
 Foddai, M 1615
 Foley, WJ 379
 Fons, F 1079
 Ford, AJ 1611
 Formisano, C 1075
 Fozdar, BI 1525
 Fraternale, D 1037,1469
 Froissard, D 1079
 Fromentin, E 1215
 Fruchier, A 1079
 Fu, J 1743
 Fujihara, T 1047
 Fujii, H 959
 Fujii, Y 725,743,747,751
 Fujii, Y 767,771,775
 Fujimoto, Y 1659,1663

- Fujitaka, Y 923
 Fukai, T 499
 Furukawa, H 645
 Gabbasov, T 1565
 Gabrielska, J 467
 Gábrlová, L 1537
 Gallo, M 1293
 Gallucci, MC 547
 Gambacorta, G 1739
 Ganai, BA 503
 Gao, CH 921
 Gao, CY 2059
 Gao, G 273
 Gao, H 2127
 Gao, LX 2105
 Gao, P 263
 Gao, QL 2019
 Gao, WY 339
 Gao, X 305
 Gao, Y 239
 Garaga, M 1555
 García-Mauriño, S 853
 García-Viguera, C 81,1019
 Garson, MJ 865,1853
 Garza, AL 1417
 Gatto, CC 581
 Gautam, V 1525
 Gayoso-De-Lucio, JA 853
 Geng, CA 2053
 Geng, ZF 1635
 Genovese, S 589,1115
 Genovese, S 1811,1813
 Gere, A 1699
 Ghanmi, M 1905
 Ghosh, P 1683
 Ghosh, S 1683
 Giardina, B 1993
 Giatropoulos, A 1759
 Gibbs, CG 117
 Giovanelli, S 1473
 Giovanni, V 847
 Girolamo, A 1009
 Gironés-Vilaplana, A 81
 Girova, T 1797
 Gisacho, BM 613
 Gochev, V 1797
 Gochev, VK 133,143,1071
 Goff, BF 1263
 Golakoti, T 1555
 Golić, N 1369
 Gomes, AC 673
 Gómez-Hurtado, MA 853
 Gong, D 1277
 Gong, X 9,53,823,827,831
 González, V 1309
 González-Andrade, M 113
 González-Delgado, JA 1257
 González-Guzmán, JM 281
 Gonzalez-Horta, A 1775
 Gorassini, A 1037
 Gorgorov, R 839
 Gossan, DPA 1805
 Goti, E 1035
 Gou, X 2069
 Graikou, K 67
 Grancai, D 937
 Gray, CA 1641,1647,1661
 Green, IR 1185
 Griffin, S 1733
 Grishin, EV 1171
 Groppo, M 1627
 Grottaglié, LL 1293
 Gu, CC 787
 Gu, W 257
 Gu, YC 2135,2151
 Guan, H 597
 Guan, Y 237
 Guan-Serm, L 885
 Guenane, H 1723
 Gugicé, M 1315
 Guillaume, D 167
 Guimaraes, LGL 1861
 Gunasekar, D 609,1703
 Gunatilaka, AAL 107,1655
 Guo, D 71
 Guo, DL 2135,2151
 Guo, FY 2137
 Guo, L 1643
 Guo, LD 2127
 Guo, PX 2019
 Guo, SS 1635
 Guo, X 1603
 Guo, Z 1277
 Gupta, RC 969
 Gupta, S 1443
 Guragain, YN 201
 Gustafson, KR 1649
 Gutiérrez, D 1183
 Gutierrez-Uribe, JA 1923
 Guvenalp, Z 595
 Guzii, AG 913
 György, Z 1413
 Ha, H 397
 Habtemariam, S 475,563
 Hadi, H 1483
 Hakala, E 1001
 Haleem, MA 99
 Hamada, H 923,949,995,1017
 Hamada, T 863
 Hamann, MT 1383
 Hamburger, M 1149
 Hammid, SA 1301
 Han, AR 445
 Han, G 263
 Han, N 323
 Hanai, R 9,823
 Hang, DTT 1341
 Hanif, N 1907
 Hanski, L 1001
 Hao, X 2119,2155
 Hao, XJ 1421
 Harada, D 863
 Harakat, D 1805
 Harizon 277
 Harput, US 595
 Hartmann, R 1951
 Hartz, RM 559
 Hasegawa, M 499
 Hasegawa, T 1047
 Hashim, SE 1561
 Hashimoto, A 291
 Hashimoto, N 421
 Haslan, H 1779
 Haug, C 597
 Havlíková, L 77,1529
 He, G 2069
 He, H 2119
 He, J 1711
 He, W 2165
 He, Y 1743
 He, ZD 2087
 Heilmann, J 1231,1377
 Hendrich, AB 467
 Hendrychová, H 1273
 Henry, GE 491
 Hernández, J 653
 Hernández-Ledesma, B 1427
 Hernández-Sámano, AC 1427
 Herrador del Pino, MM 869
 Herrador, MM 1
 Herrera, AI 201
 Heydenreich, M 1355
 Hieu, LD 1997
 Higashi, M 1907
 Higuchi, M 5
 Hikita, K 1581
 Hirasa, Y 291
 Hirata, M 499,863
 Hladívková, D 1817
 Ho, CL 665,1311,1461,2013
 Ho, R 33
 Höferl, M 149,1085
 Hohmann, J 487
 Hoi, TM 365,1997
 Hong, K 2123
 Hongnak, S 633
 Hongratanaorakit, T 1459
 Hoshikawa, H 645
 Hosoya, T 963,1981
 Hossain, R 641
 Hošťálková, A 577,1537,1695
 Hou, AJ 2105
 Howell, A 1215
 Hoyer, D 1649
 Hrabinová, M 577,1695
 Hristova, Y 1797
 Hrouzek, P 1719
 Hsu, KP 665,1311,1461,2013
 Hu, D 2127
 Hu, JF 2091
 Hu, Q 305
 Hu, Y 1499,1711
 Hua, H 1603
 Hua, J 2037
 Hua, KIF 1461
 Huang, C 2097
 Huang, CY 353
 Huang, GJ 2147
 Huang, HC 2147
 Huang, L 621
 Huang, RM 921
 Huang, S 2063,2067
 Huang, W 1499
 Huang, XJ 2087,2137
 Hui, Y 2137
 Hung, HY 2131
 Hung, TM 383
 Hungerford, WM 1649
 Huong, LT 367
 Huynh, TNT 167
 Hwang, DI 2009
 Hwang, TL 345,835
 Hyde, KD 1391
 Hyun, CG 389
 Ichihara, M 9
 Idroes, R 1733
 Igarashi, W 645
 Iida, S 1479
 Ikeda, K 1543
 Ikeda, K 895
 Ikeda, M 1333
 Ilić, BS 1063
 Ilic, M 649
 Imani, S 1743
 Imizu, K 425
 Inagaki, K 823
 Ingkaninan, K 301,1945
 Ingram, V 67
 Inoue, A 747,755
 Inoue, K 823
 Inoue, K 9
 Ionkova, I 1225
 Iriguchi, T 863
 Isaka, M 1391
 Isla, MI 991
 Ismail, IS 1561
 Ismil, R 725
 Ito, C 309,617,783
 Ito, S 457
 Itoh, T 1597
 Ivanchina, NV 1937
 Ivanets, EV 1247
 Iwagawa, T 863
 Iwamoto, Y 831
 Iwashina, T 403,407,413,417,421
 Iwashina, T 429,441,447,451,529
 Iwashina, T 1103,1381
 Izumi, H 903
 Izzo, AA 1009
 Jabeen, A 1533
 Jackson, N 563
 Jacob, C 1733
 Jacob, MR 613
 Jadranin, M 839
 Jäger, W 139
 Jaidee, A 1175
 Jaimez, D 1999
 Jaitak, V 133,1071
 James, K 575
 Jamil, S 393
 Jatte, KK 297
 Jayashree, E 1399
 Jayasinghe, L 1659,1663
 Je, IG 631
 Jean, S 1641,1647
 Jedlinski, N 487,1181
 Jemaon, N 393
 Jen, SH 1573
 Jenis, J 291
 Jerković, I 357,1315
 Jha, T 297
 Ji, H 2071
 Ji, KX 495
 Ji, MH 2137
 Jia, ZP 387
 Jian, XX 2075
 Jiang, CL 63
 Jiang, CW 621
 Jiang, QH 2041
 Jiang, RW 2097
 Jiang, Y 1631
 Jin, HZ 2101
 Jin, Y 787
 Jin, Z 289
 Jing Li, J 1549
 Jing, LL 387
 Jing, SX 2037
 Jinguji, Y 617
 Jirovetz, L 133,139,143,149
 Jirovetz, L 1071,1085
 Johnson, JA 1641,1647,1661
 Jokić, S 1315
 Jomori, T 1913
 Jongaramruong, J 633
 Joseph-Nathan, P 853,1027
 Joseph-Nathan, P 1343,1785
 Joshi, RK 1319
 Joshi, T 293
 Jovanović, OP 661
 Jovanović, SC 661,941
 Juárez-Flores, BI 1985
 Ju-ichi, M 309,617
 Jun, M 963
 Jung, JY 397
 Junior, FJBM 917
 Junior, JERH 1607
 Kadota, S 57

- Kagan, IA 1263
 Kalinin, VI 21,877,1167,1687
 Kalinovsky, A 1687
 Kalinovsky, AI 877,1167,1247
 Kalinovsky, AI 1937
 Kamada, T 843
 Kamchonwongpaisan, S 1175
 Kamili, AN 503
 Kamkaen, N 1091
 Kammil, MF 2005
 Kamo, T 441
 Kanaya, S 329
 Kaneda, N 1581
 Kaneda, T 291
 Kaneko, F 949
 Kang, HR 1929
 Kang, JH 963
 Kang, KS 1929
 Kang, SC 349
 Kang, YH 627
 Kanojiya, S 293
 Karapandzova, M 987
 Karimova, E 1565
 Karunarathna, SC 1391
 Kasashima, T 1597
 Kasuya, H 1479
 Katahira, R 707,737
 Kato, K 457,1581
 Kato, M 799
 Kato, Y 777,783
 Katoh, M 959,1581
 Kato-Noguchi, H729,761,765,811
 Kaul, VK 133,1071
 Kawaguchi, K 959
 Kawahara, S 959
 Kawahara, T 53
 Kayce, P 1195
 Kazaz, C 595
 Ke, L 273
 Kehraus, S 637
 Khan, IA 1195
 Khan, MA 1743
 Khan, RMA 1395
 Khan, SI 1577
 Khouili, M 1885
 Khumkratok, S 633
 Kicel, A 483
 Kicha, AA 1937
 Kiem, PV 875,1341,1351
 Kikuchi, M 881
 Kim, B 2009
 Kim, DH 1839
 Kim, DY 2009
 Kim, GJ 631
 Kim, HJ 963
 Kim, JA 383,631
 Kim, JA 929
 Kim, KH 1929
 Kim, N 1251
 Kim, NY 875
 Kim, OY 963
 Kim, SH 631,875,1251
 Kim, SJ 389,1211
 Kim, SS 389
 Kim, TPN 1141
 Kim, TW 397
 Kim, YB 1919
 Kim, YJ 397
 Kim, YS 1593
 Kimpe, ND 187
 Kingston, DGI 567,1505,1509
 Kinoshita, T 309
 Kirichuk, NN 1247
 Kirmizigul, S 1195
 Kiseleva, MI 1243
 Kishimoto, A 895,1543
 Kitaguchi, Y 617
 Kitaji, Y 617
 Kitajima, J 407,417,421
 Kitajima, M 49
 Kitajima, S 729
 Kitisripanya, T 1253
 Kitphati, W 479,1431
 Kiyota, H 645
 Klaasen, JA 1185
 Klein, ML 1897
 Klouček, P 1537
 Ko, HC 389
 Ko, HH 845
 Kobayashi, A 761
 Kočevar-Glavač, N 1273
 Kocić, BD 1063
 Kogure, N 49
 Koike, K 1479
 Kókai, Z 1699
 Kokanova-Nedialkova, Z 1377
 Kokanova-Nedialkova, ZK 1231
 Kokoška, L 1537
 Kolarević, A 1423
 Kolliopoulos, G 1759
 Komaikul, J 1253
 Komáromi, B 1699
 Kończak, J 1763
 Kondeva-Burdina, M 1377
 Kondo, K 417
 Kondo, T 425
 Kondo, Y 551
 Kong, LY 2059
 Kong, Y 1989
 König, GM 637
 König, S 83
 Koolen, HHF 625
 Koordanaly, NA 103
 Kopecký, J 1719
 Korenaga, T 903
 Korolkova, YV 1171
 Kosalec, I 67
 Koshioka, M 425,453
 Kostetsky, EY 877
 Koteich-Khatib, S 1321
 Koutsaviti, A 1759
 Kowal, M 1763
 Koyama, T 49
 Koyama, Y 955
 Kráčmar, S 1817
 Kranjac, M 357
 Krastanov, A 1085
 Kraus, GA 1025
 Krist, S 143
 Kristev, A 565
 Kim, JA 1369
 Kuata, D 1281
 Kubáň, P 1817
 Kubáň, V 1817
 Kubo, S 27
 Kubota, N 923,995
 Kubota, S 453
 Kucera, K 1649
 Kucharska, AZ 467
 Kudo, R 963
 Kulevanova, S 987
 Kulkarni-Almeida, A 1287
 Kumar, A 297
 Kumar, BR 887
 Kumar, D 1349
 Kumar, KA 1703
 Kumar, N 43,313
 Kumar, NS 1659,1663
 Kumar, PS 1399
 Kumar, V 313
 Kumazawa, S 963
 Kundaković, T 1369
 Kunert, O 887
 Kuneš, J 577,1695
 Kuo, CL 345
 Kuo, YH 2147
 Kuo, YH 845
 Kurnia, D 277
 Kuroda, C 9,53,823,827,831
 Kuroda, M 27
 Kurosaki, F 777
 Kurosawa, M 617
 Kuruzum-Uz, A 595
 Kusakabe, E 617
 Kuwahara, S 645
 Kuzmich, AS 913
 Kuznetsova, SA 1345
 Kwon, JE 349
 Ky, PT 1351
 Laatsch, H 623,1715
 Lacaille-Dubois, MA 37,1005
 Ladányi, M 1413
 Laddomada, B 1739
 Lago, JHG 285
 Lai, D 585
 Lal, B 133,143,1071
 Laman, N 767,771
 Lamottke, K 597
 Lan, PDT 591
 Lan, WJ 621
 Langat, MK 557,1207
 Laphookhieo, S 1175
 Larbi, LB 149
 Lathiff, SMA 393
 Lawes, DJ 1611
 Layne, TH 183
 Lazouni, HA 149
 Le, TN 591
 Leach, DN 1611
 Lee, YJ 1171
 Lee, CL 345
 Lee, DY 1517
 Lee, HM 2009
 Lee, HY 1251
 Lee, JB 777
 Lee, JH 383,929
 Lee, JS 929
 Lee, JW 1517
 Lee, KJ 1593
 Lee, KR 1929
 Lee, MS 845
 Lee, NH 389
 Lee, S 1153
 Lee, SH 631
 Lee, SJ 2009
 Lee, SR 1929
 Lee, SS 63,891,1373
 Lee, SY 1211
 Lee, TH 845,1251
 Lee, YJ 1593
 Lei, C 2105
 Lei, J 2165
 Lei, X 117
 Leiva, S 1915
 Lekar, AV 1801
 Leng, B 263
 Leone, R 2001
 Leto, C 2001
 Li, C 2023
 Li, D 329,2085
 Li, DX 787
 Li, GQ 2087
 Li, H 339,1641
 Li, HH 1917
 Li, HJ 621
 Li, HY 1917
 Li, J 683,899,1499,2049,2105
 Li, JY 2105
 Li, L 341,899,2023
 Li, M 787
 Li, N 243
 Li, Q 2085
 Li, SC 2013
 Li, SG 2087
 Li, SH 2037
 Li, SS 495
 Li, W 1145
 Li, X 1711
 Li, Y 2141
 Li, Y 315
 Li, ZY 1917
 Li, W 187
 Lian, YY 2127
 Liang, C 263
 Liang, J 2161
 Liang, L 2069
 Liang, XQ 269
 Liao, HB 2105
 Liao, X 2161
 Licata, M 2001
 Lignou, I 1759
 Lima, WD 1321
 Lin Ni, L 2023
 Lin, C 461
 Lin, CW 2131
 Lin, F 2127
 Lin, KT 353
 Lin, S 239
 Lin, W 219,1667,1951
 Lin, WH 437
 Lin, Y 89,1549,1603
 Lin, YY 317
 Lis, A 1763
 Liu, A 1603
 Liu, BY 1631
 Liu, CS 2141
 Liu, H 1553
 Liu, H 237,1553
 Liu, J 233,2165
 Liu, JS 1353
 Liu, KM 1163
 Liu, L 1549,2085
 Liu, M 2045
 Liu, MX 1655
 Liu, P 2123
 Liu, S 1643
 Liu, T 1989
 Liu, W 341,1499,1643,2069,2119
 Liu, XY 861,1093,2173
 Liu, Y 495,1363,1509,2031
 Liu, YC 2037
 Liu, YM 2161
 Liu, YP 2085
 Liu, ZJ 461
 Ločárek, M 77,1537
 Logrippo, S 575
 Lomarat, P 1431
 Lombardi, G 1403
 Lopes, VR 673
 López-Lázaro, M 853
 Lorenzini, G 1055
 Lü, H 1145
 Lu, H 1603
 Lu, MC 1163
 Lu, Y 1549

- Lu, Z 2123
 Lu, Z 253
 Lucena, E 281
 Lucena, ME 1321
 Lucena, ME 1751
 Ludwiczuk, A 1051
 Lugsanangarm, K 1359
 Lumyong, N S 623
 Luo, D 1277
 Luo, G 2109
 Luo, J 2059
 Luo, P 1743
 Luo, Q 2019
 Luo, SH 2037
 Luo, SL 1353
 Luo, XD 2085
 Luo, Y 2109
 Luo, YQ 2045
 Luo, Z 253
 Luong, HV 383
 Lv, F 1667
 Lv, HN 1631
 Lv, Z 2031
 Lyoussi, B 1961

 Ma, F 269
 Ma, G 1159
 Ma, GH 2131
 Ma, H 491,1409,1977
 Ma, HP 387
 Ma, J 2023
 Ma, JH 2041
 Ma, LL 787
 Ma, T 2059
 Ma, W 2119
 Ma, Y 571,1499
 Macáková, K 1529
 Macedo, AJ 1847
 Machida, K 881
 Macías, FA 17
 Madariaga-Mazón, A 113
 Maddah, FE 637
 Madeira, JC 1607
 Magalhães, LG 1627
 Maggi, F 1705
 Magid, AA 1805
 Mahajan, G 1287
 Maher, R 293
 Maherjan, S 361
 Mai, NTT 1901
 Mai, TPT 1141
 Majumder, HK 297
 Makabe, H 959
 Makانjuola, SA 1829
 Makarieva, TN 913,1171
 Makhlof, A 149
 Maksimenko, EV 1801
 Malafronte, N 319
 Malek, SNA 885
 Malínski, T 371
 Mallick, S 1349
 Malyarenko, TV 1937
 Mancanti, F 1473
 Mancinelli, A 1569
 Mandal, A 1683
 Maneerat, W 1969
 Mangelinckx, S 187
 Mangmool, S 479,1387
 Maninang, JS 743,771
 Manríquez-Torres, JJ 853
 Mantovani, ALL 1627
 Mao, ZC 461
 Marçal, RM 983
 Marcotullio, MC 1403
 Mardani, H 775

 Marijanović, Z 357,1315
 Marinkov, K 565
 Marmann, A 219
 Marsaioli, AJ 99
 Marsh, KJ 379
 Martin, J 1273
 Martínez, JA 1417
 Martins, EGA 285
 Martins, MR 673
 Mashghoozeh, E 335
 Masi, M 1119
 Masia, C 1369
 Masila, VM 613
 Masood, A 503
 Masubuti, H 1663
 Mata, R 113
 Mathias, L 871
 Matkowski, A 1149
 Matławska, I 1239
 Matos, CRR 871
 Matos, O 677
 Matsuki, SN 1561
 Matsumoto, K 959
 Matsumoto, T 1981
 Matsuo, AL 285
 Mazeika, AN 877
 Mazzafra, P 721
 Mazzaglia, A 1739
 McCants, T 1577
 McChesney, JD 1383
 Mei, Z 1743
 Mejía-Manzano, LA 1923
 Meka, B 1555
 Mekuria, EA 2113
 Melito, S 1615
 Melman, GI 1243
 Melo, NI 1627
 Melzig, MF 1941
 Mena, P 1019
 Mencherini, T 319
 Menchinskaya, ES 1937
 Meneni, SR 1521
 Meng, Y 305,2031
 Meng, Z 1499
 Mensah, AY 563
 Mensah, MLK 563
 Mesquita, RF 1893
 Messina, F 1885
 Meybeck, A 33
 Mi, J 2109
 Miceli, GD 1739
 Majumder, HK 297
 Michaelakis, A 1759
 Midiwo, JO 557
 Midiwo, JO 613
 Miguel, G 1961
 Mikhaileenko, MA 1345
 Miladinović, DL 1063
 Milagro, FI 1417
 Milenović, M 1369
 Milojković-Opsenica, D 1869
 Mimaki, Y 27,955
 Min, BS 383,929
 Minagawa, R 747,755
 Minceva, M 1719
 Minh, CV 353,875,1341,1351
 Minkin, VI 1801
 Mir, F 503
 Miraghazadeh, SG 669
 Mireles-Martínez, M 1955
 Mirmazloum, I 1413
 Mishio, T 447
 Mishra, DK 293
 Mishyna, M 767,771,775
 Mitaïne-Offer, AC 37,1005
 Mitić, V 649

 Miyake, Y 1597
 Miyamoto, K 1333
 Miyamoto, T 37,1005
 Mizuno, K 799
 Mizuno, T 417,441
 Mohamed, NE 1199
 Mohamed, SMM 1897
 Moiteiro, C 677
 Molinillo, JMG 17
 Momekov, G 1231
 Monache, FD 1589
 Monnanni, R 1035
 Montanaro, V 1009
 Montaut, S 1043
 Monti, MC 1013
 Montopoli, M 1365
 Monzote, L 1229
 Moo-Puc, R 1513
 Mora, FD 1309
 Moraes, MM 1809
 Morales, A 375,657
 Morales, CP 1
 Morales, NP 1387
 Moreira, LA 581
 Moreno, A 991
 Moreno, DA 81
 Moreno, S 1999
 Moretti, M 1403
 Mori, D 747
 Morita, H 291,997,1153
 Moriwaki, N 949
 Mosharova, IV 1171
 Mota, AS 673
 Motilva, V 853
 Moussaoui, A 149
 Moya, HD 1821
 Mozafari, M 335
 Mudianta, IW 865
 Mugnaini, L 1473
 Muhammad, I 613
 Muharimi, R 437
 Mukhopadhyay, S 297
 Mulholland, DA 1207
 Müller, WEG 1951
 Munayi, R 613
 Munikishore, R 1703
 Muñoz, MA 1343
 Muntean, D 951
 Murai, Y 407,429,441
 Murakami, N 451
 Muraoka, H 457
 Murata, T 1581
 Murni, A 1907
 Murta, MM 581
 Murugaiyah, V 945
 Myz, SA 1345

 Naidoo, S 1185
 Nair, JJ 171
 Nair, MG 1399
 Najdoska-Bogdanov, M 1619
 Najman, S 1423
 Nakamura, Y 1597
 Nakane, R 1381
 Nakashima, K 551,827,831
 Nakatani, K 1047
 Nakayama, F 799
 Nakayama, M 425,453
 Nali, C 1055
 Nallathamby, N 885
 Nam, AM 1905
 Nam, NH 353,1341
 Namwijit, S 1973
 Nandi, OI 887
 Napoli, EM 2001

 Narasu, ML 1729
 Nardoni, S 1473
 Narváez-Trujillo, A 1649
 Nash, RJ 1281
 Nasim, MJ 1733
 Navarro-Barranco, H 113
 Naviglio, D 1293
 Nayak, BS 1843
 Ndunda, B 557
 Nebo, L 17
 Nedalkov, PT 1231,1377
 Negi, N 617
 Negishi, H 895,1543
 Nekooeian, AA 335
 Ngadjui, BT 1933
 Ngoc, TM 1351
 Nguyen, KPP 167
 Nguyen, NPD 1911
 Nguyen, QV 591
 Nguyen, TH 591
 Nguyen, TY 929
 Nhien, NX 875,1251,1341,1351
 Ni, G 1989
 Nicolai, E 1035
 Nie, XF 2041
 Niemann, H 219
 Niesen, DB 491,1977
 Nieto, M 1309
 Nieves, GMV 1335
 Nii, K 5
 Niketić, M 1369
 Nikolov, S 1377
 Nile, SH 1839
 Nomura, T 783
 Nonato, DTT 1607
 Nong, XH 1033
 Noro, K 903
 Nosalova, V 937
 Nour, M 1501
 Novák, Z 577,1695
 Nováková, J 1537,1695
 Novo, MT 677
 Noyama, T 53
 Nugroho, AE 291
 Nunez, CV 1821
 Núñez, S 1915
 Nuño, G 991

 Ochi, A 617
 Ogawa, S 457
 Ogienko, AA 1345
 Ogienko, AG 1345
 Ogita, S 755,777,783,815
 Ogunwande, IA 365,367,1997
 Ogurtsova, EK 1171
 Ohno, O 765,1333
 Ohsawa, R 421
 Okada, S 923
 Okamoto, Y 9,53,823,827,831
 Okamura, H 863
 Okazaki, S 743
 Okoth, DA 103
 Okoye, F 585
 Olatunji, OJ 1945
 Oliveira, PF 1627
 Oliveira-Silva, D 285
 Olivero-Verbel, J 1753
 Oliviero, F 1075
 Olszewska, MA 483
 Omar, AR 1199
 Omoba, OS 1829
 Omosa, LK 557,613
 Ono, E 429
 Ono, K 1479
 Ono, M 413

- Ono, N 329
 Opletal, L77,577,1529,1537,1695
 Orshanskaya, Y 1565
 Osowicka, M 1733
 Otashiro, K 903
 Otsubo, T 831
 Ou, CY 2147
 OuldElhadj, MD 1723
 Ozaki, S 949
 Pacciaroni, A 1183
 Pagano, E 1009
 Pakrash, O 857
 Pal, BC 1349
 Palaniveloo, K 863
 Palasarn, S 1391
 Panjai, L 1269
 Panjeshahin, MR 335
 Pant, AK 857
 Panthong, K 1853
 Papachroni, D 67
 Park, JH 2009
 Park, KJ 389
 Park, SJ 875,1251
 Park, SR 397
 Park, SU 1211
 Park, TS 349
 Park, WT 1211
 Park, Y 627,1593
 Pasqualone, A 1739
 Passero, LFD 285
 Patridge, EV 1649
 Paz, C 1355
 Paz-González, AD 1955
 Pecetti, L 933
 Pecio, L 933
 Pedras, MSC 209
 Pellegrini, E 1055
 Peña, A 655
 Peñaloza, Y 375
 Peng, CY 345
 Peng, Y 921,1277
 Penkova, Y 1281
 Peraza-Sánchez, SR 1513
 Pereira, MG 1607
 Pérez-Alvarez, JA 1219
 Peron, G 1705
 Pertuit, D 1005
 Petrović, GM 661
 Petrović, GTM 1439
 Pham, TH 591
 Pham, VC 591
 Phanthong, P 1387
 Phechkrajang, CM 1435
 Phi, PNK 1141
 Phillips, AJ 1649
 Phillips, GM 1649
 Phuong, DT 353
 Phuwapraisirisan, P 325
 Pietersen, RD 1185
 Pinke, G 487
 Piñón, A 1229
 Pinos-Rodríguez, JM 1985
 Pisano, C 1569
 Pislyagin, EA 1937
 Pisseri, F 1473
 Pistelli, L 1055,1323,1473
 Pistone, A 1009
 Pitchumani, K 1959
 Pivkin, MV 1247
 Piyachaturawat, P 89
 Piyasena, NPG 1711
 Plubrukarn, A 1945
 Plummer, M 1649
 Pokhilo, ND 1243
 Pombal, S 673
 Popova, M 1961
 Pornchuti, W 453
 Porta, A 847
 Potorti, AG 2001
 Poudel, A 1067,1749
 Pouységú, L 653
 Prakash, I 559,1159
 Prakash, O 201
 Pramanick, S 925
 Presley, CC 1505
 Priedemann, C 1159
 Prisadova, N 1797
 Prissadova, N 565
 Procida, G 1833
 Profili, G 1473
 Prokhorov, V 767,771
 Proksch, P219,437,585,1667,1951
 Promchai, T 1175
 Pu, JX 2045
 Pujiastuti, B 277
 Pukclai, P 765
 Pulivarthy, D 1229
 Putalan, W 1253
 Pyne, SG 1175
 Qi, S 2027
 Qi, SH 1033
 Qiao, K 263
 Qiao, Y 289
 Qin, MJ 1191
 Qin, Y 305,2173
 Qing, LS 2161
 Qiu, F 1363
 Qiu, SX 921
 Quan, TL 1901
 Quideau, S 653
 Quílez del Moral, JF 1
 Quinet, YP 1607
 Quintal-Novelo, C 1513
 Radchatawedchakoon, W 1973
 Radha, R 1959
 Radojković, IR 1439
 Radonić, A 357
 Ragazzi, E 1365
 Raharivelomanana, P 33
 Raish, M 1395
 Rakotobe, E 567,1505,1509
 Rakotondraibe, LH 1505,2113
 Rakotondrajaona, R 567,1509
 Raksat, A 1969
 Ramadhan, R 325
 Raman, J 885
 Ramirez, C 559,1159
 Rammohan, A 609,1703
 Ramos, CS 1809
 Randrianaivo, R 1505
 Rao, AB 1729
 Rao, AVNA 887
 Rao, P 273
 Rapior, S 1079
 Rapposelli, E 1615
 Rárová, L 171
 Rasamalla, S 1349
 Rasamison, VE 567,1505,1509
 Rattan, R 1525
 Rattanajak, R 1175
 Ravada, S 1555
 Razali, SNS 1483
 Reddanna, P 1703
 Reddy, AS 1729
 Reddy, KK 1703
 Reddy, NV 609
 Reddy, PJ 1729
 Reddy, SGE 1525
 Reed, DW 1919
 Reinecke, MG 117
 Reis, PCJ 1861
 Ren, B 1145
 Ren, F 341
 Ren, J 2101
 Ren, Y 263
 Rezgui, A 37
 Ribeiro, FF 917
 Ribeiro, LAA 1893
 Ribeiro, VB 1847
 Ricci, D 1037,1469
 Riccio, R 1013
 Rigano, D 1075
 Ríos, N 1309
 Ripoll, C 597
 Ristivojević, P 1869
 Ritthiwigrom, T 1175
 Rivera, G 1955
 Roach, JS 183
 Robichaud, GA 1641,1647
 Robinson, Jr., WE 117
 Roblová, V 1817
 Rocha, DK 677
 Rodenburg, DL 1383
 Rodrigues, V 1627
 Rodríguez, M 1999
 Rogowska, M 1825
 Roh, MS 445
 Rojas, J 375,657
 Rojas, L 375,655,1751
 Rojas, LB 1999
 Rojas, YL 1309
 Rojas-Fermin, L 657
 Rojas-Fermin, LB 653,1309,1321
 Roje, M 1315
 Rojipitkul, T 1359
 Rojsanga, P 1435
 Roland, TT 1709
 Roller, M 1215
 Rollin, P 1043
 Romane, A 149
 Romero, MA 1257
 Rondón, M 657
 Rong A 289
 Rosas-García, NM 1955
 Ross, SA 1897
 Rovirosa, J 1915
 Ruangrungsi, N 1091
 Ruangrungsi, NJ 1459
 Ruberto, G 2001
 Rudiyansyah 1853
 Ruisi,P 1739
 Rukdee, N 1435
 Russo, R 1569
 Ryabchenko, B 139
 Sabaratnam, V 885
 Sabphon, C 301
 Saesong, T 1945
 Šafratová, M 1537
 Saito, A 645
 Saito, K 617
 Saito, Y 9,831
 Sakagami, H 27
 Sakai, T 499
 Sakee, U 1973
 Sakuta, M 713,717
 Salazar-Bookman, MM 281
 Salleh, EHNHW 1465
 Salleh, WHNHW 1297,2005
 Salvador, MJ 625
 Sancinetto, L 1885
 Sándor, Z 487
 Sanina, NM 877
 San-Martín, A 1343,1915
 Sanni, DM 1829
 Santana, WEL 1821
 Santes-Hernández, Z 1955
 Santi, C 1885
 Sappan, M 1391
 Saracoglu, I 595
 Saraf, I 379
 Sari, DC 1447
 Sarikahya, NB 1195
 Sarria, ALF 17
 Sartorelli, P 285
 Sasaki, N 441
 Sasamoto, H 733,747,751,755
 Sasheva, P 1225
 Sass, C 951
 Sato, M 457,499
 Sato,K 691
 Satou, T 1479
 Satrani, B 1905
 Satyal, P 361,1067,1453,1749
 Sawasdee, P 301,1359
 Sayawa, ACHF 721
 Sayago, JE 991
 Sayas, E 1219
 Scaltrito, MM 1369
 Scarpa, GM 1615
 Schmidt, B 1355
 Schmidt, D 597
 Schmidt, E 1071,1085
 Schmidt, E 133,139,143,149
 Schuehly, W 887
 Schüffler, A 1715
 Schwaiger, S 83
 Scotti, L 917
 Scotti, MT 917
 Seeram, NP 491,1409,1977
 Sekine, T 775
 Senatore, F 1075
 Sendra, E 1219
 Senthil Kumar, KJ 1305
 Seo, CS 397
 Seo, EK 445
 Seo, YS 627
 Serna-Saldivar, SO 1923
 Serra, S 157,1337
 Sestili, P 1037
 Setoguchi, H 407,429
 Setzer, WN 153,369,1067,1229
 Setzer, WN 1453,1749
 Severino, L 1569
 Severino, VGP 17
 Sforcin, JM 1279
 Shafaroodi, H 669
 Shakhtsheider, TP 1345
 Shan, L 2063,2067
 Shanbhag, P 1287
 Shao, S 1553
 Shao, X 243
 Sharma, R 1525
 Sharma, RJ 379,969
 Sharma, U 1525
 Sharopov, FS 153
 Shaw, J 1383
 Shaw, PC 2097
 Shawl, AS 503
 Shen, H 1553
 Shen, W 2155
 Sheng, L 2049
 Salleh, L 1191

- Shi, SS 2049
 Shi, Y 2155
 Shi, YM 2045
 Shibata, R 1581
 Shibusuani, T 1913
 Shichiken, M 783
 Shieh, PC 2131
 Shigemori, H 1981
 Shim, SM 349
 Shimada, K 903,923,995,1017
 Shimizu, A 9
 Shimizu, N 1495
 Shimokawa, S 451
 Shimomiya, Y 1597
 Shin, HK 397
 Shiono, Y 277
 Shirai, K 53
 Shiro, M 1981
 Shirota, O 291
 Shrestha, S 1453
 Shrestha, S 1749
 Shu, HM 2137
 Shukla, SK 293
 Siatka, T 77
 Sichaem, J 1359
 Siems, KJ 1941
 Sieniawska, E 1877
 Sihra, JK 1207
 Silchenko, AS. 21,877,1167,1687
 Silva, B 1309
 Silva, LA 673
 Silva, M 1355
 Silveira e Sá, RC 1767
 Simon, A 595
 Simonovic, S 649
 Singh, B 43,313
 Singh, IP 379,969
 Singh, SK 293
 Sipos, L 1699
 Sirat, HM 1561,2005
 Sirimangkalakitti, N 1945
 Siriphong, P 633
 Sisto, F 1369
 Skaltsounis, AL 83
 Ślusarczyk, S 1149
 Šmelcerović, A 1423
 Smetanin, OF 1247
 Smirnov, SV 417
 Snyder, TM 1159
 Snyder, TM 559
 Soica, C 951
 Sokól-Lętowska, A 467
 Sol, V 1079
 Solich, P 1529
 Song, C 2031
 Song, D 253
 Song, G 239
 Song, L 2033,2095
 Song, XP 2137
 Sono, M 551
 Sorensen, JL 39
 Sornkaew, N 89
 Sosa, V 1183
 Sotnikova, R 937
 Sousa, DP 1767
 Sousa, PL 1607
 Souza, D 1215
 Souza, GM 1589
 Spakowicz, DJ 1649
 Specchiulli, MC 1115
 Spirikhin, L 1565
 Spiteller, M 1325
 Spiteller, P 597
 Srećec, S 1825
 Sreelakshmi, C 1729
 Srichomthong, K 1391
 Sripha, K 1431
 Sripisut, T 1969
 Sritularak, B 1253
 Srivastava, P 293
 Sroka, Z 467
 Staden, JV 171
 Stamenković, JG 1439
 Stanchev, V 1085
 Stanilova, M 839
 Stanisz, B 1239
 Stankov-Jovanović, V 649
 Stanoeva, JP 987
 Stappen, I 133,1071
 Stefanello, MEA 625
 Stefkov, G 987
 Stefova, M 987,1619
 Steinberg, KM 1229
 Stierle, AA 1671
 Stierle, DB 1671
 Stocchi, V 1037
 Stochmal, A 933
 Stoilova, I 1085
 Stoilova, N 1225
 Stojanovic, G 649
 Stojanović, GS 661,941,1439
 Stonik, VA 21,913,1171
 Straface, SV 547
 Strnad, M 171
 Strobel, SA 1649
 Strugala, P 467
 Stuppner, H 83
 Su, JH 317,1163
 Su, W 1989
 Su, X 1989
 Su, YC 665,1311,1461,2013
 SubbaReddy, BV 1729
 Subehan 57
 Suda, M 959
 Suebsakwong, P 89
 Suenaga, K 765,1333
 Suhaimi, FH 1779
 Sukrasno 57
 Suksamrarn, A 89
 Sultana, R 641
 Sumalatha, M 1703
 Sumiarsa, D 277
 Sun, H 243
 Sun, HD 2045
 Sun, J 895,1543,1711
 Sun, L 1499
 Sun, Q 1603
 Sun, X 2145
 Sun, Y 2165
 Sun, Z 289
 Sung, PJ 835,1163
 Supratman, U 277
 Sutour, S 1059
 Suwanborirux, K 1945
 Suwannarach, N 623
 Suwitchayanon, P 765
 Suzuka, T 1913
 Swamy, RC 887
 Swartz, K 1383
 Sympson, BB 99
 Szabó, K 1699
 Tabakmakher, KM 913
 Tabanca, N 133,143,1071,1195
 Tabopda, TK 1933
 Taddeo, VA 1115,1811,1813
 Taddeo, VA 589
 Tadtong, S 1091,1459
 Taha, H 1541
 Taher, M 1585
 Tai, BH 1351
 Takahashi, K 713,717
 Takahata, M 1597
 Takahata, Y 457
 Takanashi, K 959
 Takayama, H 49
 Takeda, K 447
 Takemura, T 725
 Takikawa, Y 903
 Tanabe, Y 1981
 Tanaka, C 37,1005
 Tanaka, H 499,1253,1581
 Tanaka, J 1907,1913
 Tanaka, K 329
 Tanaka, T 499
 Tane, P 1325,1709
 Tang, Y 2091
 Tangarajoo, N 1199
 Tanigawa, M 923
 Taniguchi, M 827
 Tantry, MA 503
 Tao, X 571
 Tapondjou, LA 1941
 Tasca, T 1847
 Tateishi, A 453
 Tateishi, Y 499
 Tatsuzawa, F 453,457
 Tava, A 933
 Tavares, DC 1627
 Tavasz-Sárosi, S 1699
 Tchoumtchoua, J 83
 Teai, T 33
 Tejaswi, C 1349
 Tekelova, D 937
 Temkitthawon, P 301
 Terahara, N 521
 Terruzzi, F 1569
 Teshima, N 309
 Teshima, N 617
 Teslov, L 437
 Tezuka, Y 1153
 Tezuka, Y 329
 Tezuka, Y 57
 Tezuka, Y 997
 Thai, TH 365
 Thammasiri, K 453
 Thanabalasingam, D 1659
 Thang, NV 875
 Thang, TD 365,367,1997
 Thao, DT 353
 Thi Nga, NT 353
 Thouvenot, L 1501
 Thu, NV 383
 Thu, VK 875,1341
 Thumser, AE 1207
 Thung, DC 1341
 Tian, HY 1353,2097
 Tian, WS 2155
 Ticha, LA 1185
 Tinto, WF 183
 Tip-pyang, S 1359
 Tip-pyang, S 633
 To, DC 929
 Toma, C 951
 Tomi, F 1059,1447,1905
 Tomoda, H 1981
 Tomović, K 1423
 Tonelli, M 1055
 Tong, H 2033
 Topolski, J 1149
 Tori, M 9,53,551,823,827,831
 Toriello, C 113
 Torres-Tapia, LW 1513
 Torres-Valencia, JM 853,1027
 Tosco, A 1013
 Tóth, B 487
 Tóth, G 595
 Tracy L. Sears, TL 559
 Tran, MH 929
 Tran, NKS 349
 Tran, T 1355
 Trang, DT 1351
 Trang, NT 353
 Trendafilova, A 839
 Trifković, J 1869
 Trifonova, D 1085
 Trifoggi, M 1293
 Triggiani, D 1993
 Tringali, G 1993
 Tripepi, S 547
 Trisawan, K 1175
 Tsai, SF 891
 Tsai, SJ 317
 Tsai, SF 63
 Tsao, NW 1305
 Tsao, R 1553
 Tseng, MH 845
 Tsopmo, A 1709
 Tsuchiya, S 755
 Tsukamasa, Y 1597
 Tu, PF 1631
 Tu, Z 1977
 Tůmová, L 1273
 Tuttolomondo, T 2001
 Tzakou, O 1759
 Tzankova, V 1377
 Uddin, MR 1211
 Uehara, A 403
 Uemura, D 1333
 Uesugi, D 923,949
 Uji, T 309
 Ulewicz-Magulska, B 977
 Umegaki, N 453
 Urajová, P 1719
 Urban, S 95
 U'Ren, JM 1655
 Urso, V 1739
 Usano-Alemany, J 1269
 Ushijima, K 617
 Usubillaga, A 653,655,1751,1999
 Utkina, NK 1547
 Vadlani, PV 201
 Vairappan, CS 843,863
 Valeriote, F 1383
 Vannini, S 1403
 Varela, RM 17
 Varga, L 1699
 Variyar, PS 1443
 Vartak, A 1287
 Vasantha, VS 1959
 Vasas, A 487
 Vassallo, A 319
 Veizerova, L 937
 Velasco, J 375,655,1309
 Verardo, G 1037
 Verdan, MH 625
 Verma, PK 43
 Verschaev, L 1489
 Vetrova, EV 1801
 Vetter, I 1355
 Vianello, C 1365
 Vidyadarshan, S 885
 Vijaya, T 609
 Villanueva, I 1287
 Villarini, M 1403
 Villarreal, S 1999
 Villegas-Mendoza, JM 1955
 Virga, G 2001

- Vitulano, M 1293
 Viuda-Martos, M 1219
 Vohra, MI 1533
 Vorobieva, NS 877
 Voutquenne-Nazabadioko, L 1805
 Vu, VC 591
 Vue, B 2179
 Vukelić-Nikolić, M 1423
 Vuorela, HJ 1001
 Vuorela, PM 1001
 Walker, LA 613
 Walkowski, S 467
 Waltenberger, B 83
 Wan, B 2135, 2151
 Wan, XC 787
 Wang, B 2085
 Wang, C 1989, 2123
 Wang, CF 1635
 Wang, CX 2127
 Wang, EIC 665, 1311
 Wang, F 89
 Wang, FP 861, 1093, 2071, 2075
 Wang, H 273, 1977
 Wang, J 899, 1711, 2031, 2067
 Wang, KT 621
 Wang, LS 495
 Wang, M 2033
 Wang, P 1363
 Wang, Q 273
 Wang, QH 323
 Wang, R 233
 Wang, SY 845, 1305, 2131, 2147
 Wang, W 253
 Wang, WG 2045
 Wang, WH 835
 Wang, X 2101
 Wang, Y 1353, 1643
 Wang, Y 2027, 2031, 2087
 Wang, YR 2141
 Wang, YY 1635
 Wang, Z 1499
 Wang, Z 187
 Wanner, J 1071, 1085
 Wanner, J 133, 139, 143, 149
 Wasano, N 725
 Watanabe, E 53
 Watanabe, K 1495
 Watthanachaiyingcharoen, R 1091
 Webb, MZ 1335
 Webster, D 1641, 1647
 Wedge, DE 133, 143, 1071
 Wei, J 597
 Wei, MPS 1573
 Wen, GS 461
 Wen, ZH 317, 1163
 Werz, O 83
 Wesolowski, M 977
 White, AM 865
 Widayawaruyanti, A 1541
 Widj-Tyszkiewicz, E 1239
 Wiedle Jr., CH 1509
 Wiggers, FT 613
 Wijeratne, EMK 107
 Winekenstädde, D 83
 Wink, M 153
 Wojnicka-Póltorak, A 371
 Wojnicz, D 467
 Won, KJ 2009
 Wong, CP 291
 Wong, MS 2189
 Wongkrajang, K 89
 Woo, MH 383, 929
 Wu, DY 891
 Wu, H 1145
 Wu, HY 2045, 2097
 Wu, J 247, 495
 Wu, JB 2147
 Wu, LQ 2105
 Wu, M 2063
 Wu, Q 495
 Wu, QQ 339
 Wu, TS 2131
 Wu, X 1643
 Wu, Y 49, 253
 Wu, YC 345, 835, 1163
 Wu, YH 2127
 Wu, Z 263
 Wu, ZLK 2087
 Xia, B 2135
 Xia, C 305
 Xia, D 249
 Xia, X 2097
 Xiao, GK 2127
 Xiao, SJ 2135, 2151
 Xiao, W 1499
 Xie, GY 1191
 Xie, YG 2101
 Xing, Y 2169
 Xiong, J 2091
 Xu, GK 1191
 Xu, J 1363
 Xu, M 1203
 Xu, Q 2027
 Xu, SZ 461
 Xu, T 71
 Xu, W 2063
 Xu, XY 1033
 Xu, Y 107, 237, 1655
 Xu, ZF 921
 Xue, Y 2161
 Yada, H 441
 Yamada, H 309, 1047
 Yamada, K 1333
 Yamada, S 1581
 Yamada, T 645
 Yamaguchi, R 499
 Yamaguchi, S 453
 Yamashita, K 863
 Yamashita, T 783
 Yamauchi, M 1907
 Yan, DF 621
 Yan, G 1603
 Yan, H 2019
 Yan, SK 2101
 Yan, T 921
 Yancheva, D 1423
 Yang, B 1499
 Yang, CS 2147
 Yang, J 2095
 Yang, K 1635
 Yang, M 71, 237
 Yang, SQ 339
 Yang, Y 305
 Yao, T 2041
 Yao, XS 2127
 Yaoita, Y 881
 Yao-Kouassi, PA 1805
 Yapi, TA 1059
 Yasui, N 895, 1543
 Yasukawa, R 949
 Yaya, EE 209
 Yazaki, Y 505, 513
 Ye, Q 2109
 Ye, WC 1353
 Ye, WC 2087
 Yeap, SK 1199
 Yeboah, SO 1933
 Yen, KH 1297, 1465, 1561
 Yen, PH 875, 1341, 1351
 Yi, M 2097
 Yin, ACY 1573
 Yin, TP 2141
 Yin, Y 707
 Yingyongnarongkul, B 1973
 Yokosuka, A 27, 955
 Yoon, HS 389
 Yoon, HY 627
 Yoon, MS 2009
 Yoon, SW 2009
 Yoshida, K 713, 717
 Yoshida, S 1333
 Yoshimasu, K 551
 Yoshimura, J 691
 You, CX 1635
 Youn, IS 445
 Yousfi, M 1723
 Yrjönen, T 1001
 Yu, C 2119
 Yu, J 2169
 Yu, R 2033, 2095
 Yu, T 1711
 Yuan, C 2119
 Yuan, CM 1421
 Yuan, J 1549
 Yuan, T 491, 1409, 1977
 Yuan, Y 239
 Yue, JM 2049
 Yuki, K 1333
 Yura, K 717
 Yurchenko, AA 1247
 Yurchenko, EA 1247
 Yurchenko, EA 1687
 Yuzbasioglu, M 595
 Zacchigna, M 1833
 Zacchino, S 1589
 Zaman, MS 641
 Zampini, C 991
 Zan, LF 315
 Zanoni, G 847
 Zarubaev, V 1565
 Zbak, H 853
 Zeng, KW 1631
 Zhan, J 243
 Zhang, A 89
 Zhang, C 1499, 1743
 Zhang, CR 1399
 Zhang, D 1603
 Zhang, DM 2023
 Zhang, F 1421, 2165
 Zhang, G 89, 2109

Natural Product Communications

Volume 10 (1-12)

2015

Keywords Index

A2780	1505	<i>Ajuga macroperma</i> var. <i>breviflora</i>	857	<i>Anthelia</i> sp.....	1907	Antimycobacterial activity...1647	
A549 cells	239	<i>Ajugaflorins</i>	857	<i>Anthocephaline</i>	297	Antimycotic activity	1473
<i>Aaronsohnia pubescens</i>	149	Alarm pheromone	1495	<i>Anthocephalus cadamba</i>	1349	Anti-obesity.....	1417
Absolute configuration.....	1027,1167	<i>Alchemilla persica</i>	1705	<i>Anthocyanin</i> 451,453,457,963		Anti-osteoporotic activity ...	2189
Absolute configuration.....	1337,1343	<i>Alchemilla</i> sp.....	1369	<i>Anthocyanin</i>	1211	Antioxidant	1387,1399,1465
Absolute configuration.....	1785	Aldehyde dehydrogenase	743	<i>Anthocyanins</i> 77,81,447,529,969		Antioxidant activities	503
Absolute configuration.....	2045,2091	Aldose enantiomers.....	1965	<i>Anthraquinone</i>	317	Antioxidant activity ...	1075,1257
Absolute	2009	Alecrim-pimenta	1861	<i>Anthriscifoline</i>	2067	Antioxidant activity ...	1377,1461
Absorption.....	521	Alice in Wonderland	2195	Anti-acetylcholinesterase	891	Antioxidant activity	1547
ABTS.....	153,2169	Alkaloid.....	49,171,1363,2195	Anti-aging	1079,1483	Antioxidant activity ...	1821,1829
<i>Acacia pennata</i>	1431	Alkaloids	291,577,1547	Anti-allergic inflammatory	631	Antioxidant activity ...	1901,1961
<i>Acanthodendrilla</i>	1945	Alkenyl cyclohexenols.....	103	Antibacterial activities	1321,2137	Antioxidant activity....	483,495,937
<i>Acanthopanax sessiliflorus</i> 1517		Alkenyl cyclohexenones	103	Antibacterial activity	133,277,375	Antioxidant activity	963
<i>Acanthostryngylophora ingens</i> 1951		Alkynoates.....	1813	Antibacterial activity.....	655,899	Antioxidant capacity	1019
Acapolia	513	Allelopathic substance	765	Antibacterial activity	1071,1309	Antioxidant enzymes	1085
Accelerated solvent extraction379		Allelopathy	17,729,733,737	Antibacterial activity...	1489,1751	Antioxidant peptides	1427
ACE	1517	Allelopathy	747,751,761,767	Antibacterial.	467,503,1915,1969	Antioxidant potential	1817
<i>Acer pseudoplatanus</i>	1977	Allelopathy	771,775,811	Antibiotics	645	Antioxidant	1219,1297
<i>Acer rubrum</i>	1409	Allenamides.....	267	Anticancer activity	1311	Antioxidant	1561,1577
<i>Acer tegmentosum</i>	1251	Allergy.....	1'767	Anti-cancer.....	1349	Antioxidant	1839,1977,2005
Acereaceae	1251	Alliin.....	1733	Anti- <i>Candida</i> activity	375	Antioxidant	214,243,315,325,
Acetophenones	589	Alliinase	1733	Antichlamydial.....	1001	Antioxidant	393,467,479,597
Acetylcholinesterase inhibitor1945		<i>Allium macrostemon</i>	1381	Anticholinesterase	1465	Antioxidants	1085,1683
Acetylcholinesterase inhibitor1969		<i>Aloe arborescens</i>	1993	Anti-diabetic.....	1683	Anti-oxidation	2123
Acetylcholinesterase ... 577,1297		Alpha-synuclein	1775	Antifeedant activity	2063	Antioxidatnt activity	521
Acetylcholinesterase	1431	Alphitomin-glucopyranoside ..	591	Antifouling	1033	Antiparasitic	285
AChE activity	1359	<i>Alpinia polyantha</i>	367	Antifouling	2119	Antiplasmodial activity	1541
Acne	1459	<i>Alternaria tenuissima</i>	39	Antifungal activity	133,1037,1071	Antiproliferation	1929
<i>Aconitum soongaricum</i> var. <i>pubescens</i>	2063	Alternative medicine	1779	Antifungal activity	1589,1649	Antiproliferative	567
<i>Aconitum soongaricum</i>	2165	Alzheimer's disease	1431	Antifungal	143,149	Antiproliferative activity1509,1513	
<i>Aconitum tanguticum</i>	861	Amaranthaceae	1377	Antifungals	605	Antiproliferative effect	547
<i>Actinodaphne macrophylla</i> 1541		Amaryllidaceae	171,1537	Antigenotoxicity	1403	Antiproliferative.....	1505,1581
Actinodaphnne,	891	Ambuic acid,	1643	Antigermination activity	1469	Antiproliferative	951
Acyclic guanidine alkaloids 1171		American sycamore extract..	1383	Anti-hepatotoxic activity	1377	Antitumor activity	247
Acylated anthocyanins	1965	Ames test	1489	Antihyperlipidemic activity	289	Antitumor constituents	233
Acylated polyphenols	521	Amino acid	2145	Anti-inflammation	345,669	Antityrosinase	1297
Adenostyles	1179	Amino acids	755,969	Anti-inflammatory	597,1399	Anti-viability activities	571
Adipose tissues	1543	Ammonium glycyrrhizinate.	1801	Anti-inflammatory activity	1461	Antiviral activity	1565
<i>Adonis amurensis</i>	27	<i>Amomum villosum</i>	1989	Anti-inflammatory activity	1767	Anti-yeast activity	1537
Adult topical activity	1195	<i>Amomum xanthiodes</i>	631	Anti-inflammatory activity	2037	Aorta	1893
<i>Aedes aegypti</i>	677,1195	<i>Ampelopsis cantoniensis</i>	383	Anti-inflammatory activity	383	<i>Aphis craccivora</i>	1525
<i>Aegle marmelos</i>	1973	Amylase inhibition	1961	Anti-inflammatory activity	929	Apigenin glycosides	441
Aeroplysin-1	219	Amyloid aggregation	1431	Anti-inflammatory	83,317	Apocynaceae	49,281,2085
Aerothionin	219	Analgesic	669	Anti-inflammatory	1297	Apoptosis ..	171,239,249,253,263
Aeruginosin-865	1719	<i>Ananas comosus</i>	2137	Anti-inflammatory	1499,1577	Apoptosis	397,1403
<i>Aflamomum melegueta</i>	997	<i>Anandananthera</i>	581	Anti-inflammatory	1839,2005	<i>Aquilaria microcarpa</i>	777
African propolis	67	<i>Anaxagorea luzonensis</i>	301	Anti-inflammatory	2041,2147	<i>Arabis turrita</i>	1043
<i>Agaricales</i>	1391	<i>Andrographis paniculata</i>	1153	Antimalarial activity	1175	<i>Aralia nudicaulis</i>	1641
<i>Agave salmiana</i>	1985	<i>Angelica acutiloba</i> ,	1743	Antimicrobial activity67,557,673		<i>Arecaceae</i>	1941
Agavins	1985	<i>Angelica sinensis</i> ,	1743	Antimicrobial activity1311,1461		<i>Aristolenol</i>	1067
Aglycone	403	Angelicin	767	Antimicrobial activity1537,1733		<i>Arnebia purpurea</i>	595
<i>Agrimonia pilosa</i>	2041	Angiogenesis	263	Antimicrobial activity1797,1981		Aroma	1443
<i>Agrobacterium rhizogenes</i> ..	1919	Anhydriopilosine	721	Antimicrobial activity	2127	Aromatherapy recipe	1091
AHC analysis	941	<i>Aniba hostmanniana</i>	1321	Antimicrobial . 143,613,951,1001		Aromatherapy	1479
Airborne microbes	143	<i>Annona glabra</i>	891	Antimicrobial ... 1067,1079,1297		Aromatic compound	1005
Airway remodeling	257	<i>Annonaceae</i>	301,891,1059	Antimicrobial 1301,1661,1749		Aromatic esters	1997
		Annulation.....	1025	Anti-mildew activity 665,2013		Aromatic plants	677,1893
				Antimutagenicity	1489	Aromatization	1237

- Artemesia pallens* 1335
Artemisia campestris 1763
Artemisia dracunculus 1469
Artocarpus anisophyllus 393
Arylalkanone 325
Ascidians 1547
Ascochyta caulina 1119
Asparagaceae 37
Aspergillus awamori 1663
Aspergillus carneus, 1247
Aspergillus fumigatus 1661
Aspergillus terreus 1033
Aspergillus ustus 2123
Asperginine 1363
Aspidosperma fendleri 281
Aspidosperma 183
Aspleniaceae 417
Asplenium altajense 417
Asplenium ruta-muraria 417
Asplenium 1079
Asteraceae 403,823,827,831
Asteraceae 653,1309,1319
Asthma 257,1767,1893
Atropoisomerism 433
AURKA 353
Auronates 529
Auronol 591
Averrhoa bilimbi 57
Avicennia marina 1203
Azido-s-triazine 269
Azido-tetrazole isomerism 269
Azorella 1343,1915
Bacillus clausii 2151
Bacterial anti-adhesion 1215
Bacterial biofilm 1847
Bael 1973
Baker's yeast 157
Bakkane 831
BalA 353
Bali 865
Ball-milling 1345
Barbacenia blanchetii 983
Barton reaction 847
Basal media 755
Basidiomycete 1391
Basidiomycetes 1833
Bastadin 219
BChE activity 1359
Beauverolides 113
Beeta-Thujaplicin 783
Beilschmiedia 1297
Benzene 2195
Benzenoids 2131
Benzodiazepine alkaloid 1549
Benzofuran derivatives 621
Benzophenone 609
Benzophenones 1115
Benzoxazinoids 209
Benzyl benzoate 361,1999
Berberine 895,1543
Berberis vulgaris 1695
Bergapten 1315
Bergenia purpurascens 2135
Bergenia 1273
Bergenin 1273
Berkristine 1695
Berry 963
Beta amyloid peptide 1993
Betalain-containing families 1103
Betalains 713,717
Betalamic acid 713,717
Betulin 1345
Biflavonones 53
Bifuran derivative 2145
Bignoniaceae 1999
Binary system 1733
Bioactive chalcones 991
Bioactive Compounds 1,815
Bioactive limonoids 869
Bioactivity 683,1671,1753
Bioactivity *in vitro* 1877
Bioassay method 747
Bioassay 1335
Bioavailability 521
Biodiversity 1753,1913
Bioenergy crops 201
Biofabrication 1593
Biogenetic pathway 2041
Bio-inspired screening, 605
Biological activities 1631
Biological activity 1453
Biological activity 811
Biological Activity 95
Biomarkers 1051,2165
Biomass 1269
Biosynthesis 703,793,803,815,2033
Biotransformation 157,1277
Biphenyl aldehyde 323
Bipyridine 1821
Bisabolane sesquiterpenoid 1247
Bisabolane 823
Bisabolene 375
Bisabolol 143,375
Bithiophene 2147
Biting deterrent activity 1071
Biting deterrent activity 133
Bladder 1009
Blimbing wuluh 57
Blood flow 1517
Blood lipids 1281
Blumea lacera 1749
Bone health 2189
Boraginaceae 595
Borneol esters 371
Botanical ingredients 125
Botanical origin 1869
Brachiaria decumbens 761
Bran 1739
Branched-chain sugar 691
Brassicaceae 457
Brazilian medicinal plants 1821
Bromeliaceae 2137
Bromine 1565
Bromotyrosine alkaloids 1945
Bromotyrosine 219
Broncho-pathology 167
Bryophytes 5
Bufo bufo gargarizans 1353
Bufotenidine 581
Bufotenine 581
Bufotenine-aminoborane complex 581
Buplerol 997
Bupleurum falcatum 1593
Butenolide 1505
Butynyl-bithiophene 2147
Bergenia 1273
Bergenin 1273
Berkristine 1695
Berry 963
Beta amyloid peptide 1993
Betalain-containing families 1103
Betalains 713,717
Betalamic acid 713,717
Betulin 1345
Caffeic acid 627
Caffeine synthase 799
Caffeine 703,707,737,751,793
Caffeoyl 1853
Callus culture 755
Callus 783
Calmodulin 113
Calocedrus formosana, 845
Calolactone 845
Calophyllum symingtonianum 1585
Caloterpene 845
Calyces 77
Calystegia soldanella 429
Camellia sinensis 703
Cancer 1287
Candida albicans 1649
Cannabichromene 1009
Cannabidiol 1009
Cannabidivarin 1009
Cannabigerol 1009
Cannabinoid receptors 1009
Capelloside A 1937
Carboline alkaloids 183,293,1631
Carboline derivatives 899
Carbon-13 NMR 1447,1905
Cardanols 103
Cardenolide glycosides 27
Cardioactive evatuation 2075
Cardiovascular drug screening 281
Carex vulpinoidea 491
Carotenoids 413
Carvacrol 1461,1861
Caryophyllaceae 437
Caryophyllales 713,717,1103
Caryophyllane 835,1319,1611,1751
Caspases 249
Catalytic activity 627,1593
Caterpillars 1127
Catharanthus roseus 2085,2095
Caudatin ester derivatives 571
CDC25A 353
Cedrus atlantica 1905
Celastraceae 1929
Cell cycle analysis 853
Cell cycle 1365
Cell morphology 547
Cell proliferation 2113
Cell suspension cultures 1253
Cellular senescence 33
Cembrane 1163
Centaurea 447,839
Centella asiatica 1989
Central Balkan 941
Centrifugal chromatography 1719
Cephalaria species, 1195
Cephaph antibiotics 1663
Cerin 1683
Ceterach 1079
C-glycosides 437
C-glycosyl flavone 433
C-Glycosylflavones 441
Chaerophyllum temulum 1439
Chalcone 1199
Chalcone 495
Chalcones 1185
Chalcones 1555
Chalcones 529
Chalcones 589
Chamaecyparis formosensis 1305
Chamaecyparis obtusa 1305
Chamomile oil 1453
Checkerboard assay 1063
Chemical altitudinal variation 407
- Chemical composition 1439,1453
Chemical composition 649,673
Chemical constituent 2119
Chemical constituents 683
Chemical defense 751
Chemical degradation 1043
Chemical proteomics 1013
Chemical structure revision 1337
Chemical transformation 2091
Chemical variability 1447
Chemistry 1325
Chemoreversal activity 1203
Chemosystematics 5
Chemotaxonomic significance 2097
Chemotaxonomy 21,309,505
Chemotaxonomy 1323,1965
Chemotype 1301,2001
Chemotypes 673
Chenabinol 1695
Chenopodium album 1119
Chenopodium bonus-henricus 1377
Chiliadenus bocconeи 1323
Chiral center 1167
Chiral resolution 1729
Chlorinated cyclopentenol 1981
Chlorogenic acid 81,495,1417
Chromene 1917
Chromolaena odorata 1555
Chronic venous insufficiency 1569
Chrysanthemum indicum 397
Chrysanthemum lace bug 1495
Chrysanthemum 495
Chrysin 387
Chrysocauloside 887
Cineole 1063
Cinnamomum griffithi 1465
Cinnamomum macrocarpum 1465
Cinnamyl alcohol 1413
Cipacyclonone 1421
Cipadessa cinerascens 1421
Cipura paludosa 1589
Cisplatin 1365
Cissus quadrangularis, 1281
Citrinin 623
Citrus aurantium 1315
Citrus aurantium 869
Citrus sinensis cultivars 1315
Cladolabes schmelztii 1167
Clematis graveolens 1525
Clerodane diterpene 1509
Clerodane 557
Click-chemistry 1013
Clinical trials 1877
Clovamide 933
Clusiaceae 1115,1969
Cluster analysis 453,1453
CMCs 2095
C-Methyl-flavonoids 925
Coagulation 1607
Coastal population 429
Coccinia grandis 1659
Coffee 2195
Colochirosides 1687
Colochirus robustus 1687
Colon-targeted particles 237
Colored potatoes 461
Coloring effects 461
Combination therapy 2179
Combinatory effect 1573
Combretaceae 1005
Comet assay 1403
Comfrey 1181
Common ivy 1529

- Complementary medicine .. 1779
 Compound K 243
 Computer modeling..... 117
 Condensed tannin..... 513
 Congolese medicinal plant... 997
 Conifer..... 783,1671
Coniothyrium sp. 1641
 Connective tissue growth factor1711
 Constructed wetland..... 233
 Contact activity 1635
 Contraceptive activity 1243
Convolutaceae 1965
Convolvulaceae 1505
Convolvulus althaeoides 1965
 COPD 167
 Copigmentation 529
 Co-product..... 1219
Coptotermis homii 1525
 Coral. 835
Cordyceps cicadae 2145
Cordyceps militaris 885
Corythucha marmorata 1495
 Cosmetics 1483
 Cotton swab method..... 771
 Coumaric acid 1417
 Coumarin..... 5
 Coumarins 309,617,1585
 COX-2 353
 CQR-300 1281
 Cranberry extract..... 1215
Crassulaceae 433
Crassulaceae 941
Cratoxylum cochinchinense 1969
 Crinoid..... 317
 Crocetene..... 503
 Crocin..... 249
Croton crassifolius 1917
Croton oblongifolius 1459
Croton sylvaticus..... 557
 Cryptotanshinone 1149
 Cs_2CO_3 267
Cucumaria japonica..... 877
 Cucumarioside E. 877
Cucurbitaceae 1351
Cucurbitaceae 1521
 Cucurbitane glycoside..... 1521
Cudrania tricuspidata 1839
Culex pipiens biotype *molestus*1759
 Cultured plant cells 923
Cupressaceae 1447
Cupressus arizonica 107
Cupressus cashmeriana 1461
Curcuma comosa 89
Curcuma longa..... 329
Curcuma longa..... 63,139
Curcuma zanthorrhiza 139
Curcuma..... 453
 Curcumin..... 1417
Curvularin..... 1277
 Cyanamide..... 743
 Cyanidin 1965
 Cyanidin-3-sambubioside 77
 Cyano group 1549
 Cyanobacteria..... 1719
 Cyanogenic glycosides..... 209
 Cyclases..... 157
 Cyclic depsipeptides..... 1667
Cyclin D1 1365
 Cyclization mechanism 269
 Cycloadditions..... 1813
*Cyclodextrin glucanotransferase*995
 Cyclodepsipeptides 1423
 Cyclopentanic Structures 1
- Cyclopentenone..... 1421
Cyclotetrapsiipeptides 113
Cymbopogon olivieri..... 369
 CYP2D6 57
 CYP3A4 57
 Cypress..... 1671
Cytochalasan 2027
Cytochalasin 585
Cytochalasins 1655
Cytochrome P450 2D6 57
Cytochrome P450 3A4 57
*Cytotoxic activity*27,853,913,955
*Cytotoxic activity*1175,1243,1301
Cytotoxic activity 1513,1655
Cytotoxic activity 1973,2013
Cytotoxic activity 2027,2059
Cytotoxic compound 863
Cytotoxic 285,1067,1687,
Cytotoxicities 1353
*Cytotoxicity*103,139,171,305,341
Cytotoxicity.... 345,585,595,631
*Cytotoxicity*1231,1277,1363,1391
*Cytotoxicity*1627,1749,1907,1941
Dalbergia spinosa 1959
Dandelion honey 357
*Dasymaschalon obtusipetalum*1175
Davana oil 1335
Davanone 1335
De novo synthesis..... 157
*Deacetyl asperulosidic acid.*1817
Decaline derivative 1247
Degradation Product 559
Degradation 803
Degranulation 1597
Dehydrocoronaridine 2085
Dehydrocurvularin 1277
Dehydrovomifolio 357
Delphinidin-3-sambubioside....77
Delphinium anthriscifolium var.
majus 2067
Delphinium majus 2069
Densitometry 379
*Deodorane diastereoisomers*1905
Deoxyphomalone 39
Dereplication 95,1509
Derivatives 2113
Dermal fibroblasts..... 33
Dermatophytes 1473
Derricidin 589
Derris indica 747
Desbordesia glaucescens 1709
Desglauaside 1709
Deterrents 1335
DFT 153
Diabetes mellitus 1843
Diabetes 187,335,475,1395
Diabetic complications..... 187
Diabetic nephropathy 243
Diagnostic ions 2053
Diaporthales 1649
Diarylheptanoids 1711
*Dicerothamnus rhinocerotis*1185
Dicitrinin A 623
Dicitrinin E 623
Didehydroandrographolide ..1153
Diels-Alder adduct 827
Dienone 219
*Dietary natural product*2113,2179
Dihydrocarvone 551
Dihydrodemethoxycurcumin .329
Dihydropyranopyran 323
Dihydroxybenzaldehyde 1079
Dihydroxycalamenene 1337
Di-isobutylpyrimidinone..... 1655
Dimethylpentadecan-2-one..2155
Dimethytryptamine 581
Dinoponera quadriceps, 1607
Diorcinol 1247
Dioscin 2161
Diospyros discolor 1311
*Diphasiastrum complanatum*2091
Diprenylflavonoids 67
Discomycete 1981
Dish Pack Method 775
Distribution pattern 403
Diterpene glycosides 1159
Diterpene 865,1505
Diterpenes 1075,1149,1915,1961
Diterpenoid alkaloid....861,2069
Diterpenoid alkaloid..2071,2075
Diterpenoid alkaloids..2063,2067
Diversity 53
DNA barcoding 1035
DNA microarray 725
DNA phylogenetics 2097
DNA repair pathways 853
DNA topoisomerase IB 297
Docking studies 1703
Docking 917
Dodecanolide 1729
Dolichandrone serrulata 1387
Domination 811
DOPA dioxygenase 713,717
Dopamine analogue 2145
Dosmin 1569
DPBA 777
DPPH.... 153,4831805,1833,1901
Dracaena fragrans 37
*Dracocephalum heterophyllum*133
Drug resistance 117
Drug-drug interaction 2161
Drug-herb interaction 57
Durio 1853
Dysidea fragilis 1341
Dysideidae 1341
Dysinidin A 1341
Dysinidin B 1341
ECD spectra 1897
ECD 2091,2131
Ecdysteroids 33
Echinopine 2173
Echinops grijsii 2147
Echinothrix diadema 1243
Ecopharmacognosy 2195
Edgeworthia chrysanthia 413
Effect of caffeine 733
EGFR-TKI 1911
Elastase 167
Electrochemical assays 1257
Electron spin resonance 1387
Elicitation 1253
Ellagic acid derivative 1709
Ellagic acid 1369
Ellagitannins 1019
Elongation factor Tu 645
Enacyloxins 645
Enantiospecific Synthesis 1
Endolicchenic fungus..... 2127
Endophyte 107
Endophyte 1641,1661,1667,1671
Endophytic fungi.....1659,1751
Endophytic fungus 585,1203
Endophytic fungus1655,1671
Endothelial progenitor cells ..263
ent-Clerodadiene-15-formate.557
Enterococcus faecalis 613
Entomogenous fungus 341
Enzogenol 513
Enzymatic cascade 339
Enzymatic degradation 1043
Enzyme inhibition 1703
Enzyme inhibitors 2033
Enzyme specific activity 117
Enzyme 157
Epi-taiwaniaquinone G 2031
Epoxide-opening 2071
Erectquione 1231
Eremophilane 827,831
Ergosterol 885
Eriobotrya japonica 1145
Eriosema 1325
Erythrina poeppigiana 1581
Erythrina variegata 499
Eryvarin Y 499
Eryvarin Z 499
Escherichia coli 1215
ESI MS 1687
ESI-IT-TOF-MSⁿ 2053
ESI-MS 1801
Essential oil composition....1059
Essential oil composition....1067
Essential oil composition....1319
Essential oil composition....1447
Essential oil composition....1635
*Essential oil composition*1905,1997
*Essential oil composition*361,367
Essential oil.....1063,1071,1075
Essential oil.....1297,1301,1305
Essential oil.....1309,1311,1321
Essential oil.....133,139,149
Essential oil.....1439,1443,1459
Essential oil.....1461,1465,1469
Essential oil.....1619,1627,1631
*Essential oil*1705,1749,1751,1763
Essential oil.....1861,1999,2001
Essential oil.....2001,2005,2013
Essential oil.....285,369,371,375
Essential oil.....649,653,655,657
Essential oil.....661,665,669
Essential oils673,677,1055
Essential oils1293,1473,1611
Essential oils1753,1759,1767
Essential oils1893
Estrogen replacement 1573
Ethnopharmacology 1847
Etingera yunnanensis 365
Eucalyptus oil 1091
Eucalyptus perriniana 923
Eucalyptus sieberi 379
Eucomis vandermerwei 1207
Eucomis zambesiaca 1207
Eudesmol 2013
Eugenia jambolana 969
Eugenia reinwardtiana, 1611
Eugenol 657
Euonymus alatus 1929
Euonymus glabra 2101
Euonymphenylpropane A 2101
Euphorbia helioscopia 2037
Euphorbia hypericifolia 2049
Euphorbiaceae 557,875,149,1917
European Union legislation ...125
Evodia lepta 1359
Ex vivo 1215
Exclusion chromatography ..1923
Expansins 725
External flavonoids1699

- Extract 661
 Extraction solvent 1829

Fabaceae 609,1703,1959
Fallopia japonica 407
Farnesol 143,1311
Fas/Fas ligands 253
Fat accumulation 1333
Fatty acid profile 1619
Fatty Acids 95,1723
Fern 811
Ferns 597
Ferrier(II) reaction 691
Ficus tikoua 2105
Fig 1219
Fingerprint 71
Flavan 3-ols 513
Flavan 2101
Flavanone 403,1555
Flavanones 1185
Flavokawain 1199
Flavone C-glucoside 425
Flavone synthesis 387
Flavone 403,495,923
Flavonoid glycosides 945,1195
Flavonoid 53,63,83,187,209,929
Flavonoids 393,407,413,433,437
Flavonoids 445,447,483,505
Flavonoids 529,521,595,609,631
Flavonoids 839,917,969,977
Flavonoids 983,987,1103,1325
Flavonoids 1365,1381,1585
Flavonoids 1805,1961
Flavonol glycosides 421,429
Flavonol 403,417,925
Flavonols 451,529,933,1381
Floral rewards 99
Flower color change 413,451
Flower colors 447,529
Flower tea 495
Flowers 991,1409,1965
Fluorescence spectroscopy 1775
Foeniculum vulgare 1619
Foeniculum vulgare 673,677
Folin-Ciocalteu 1263
Fomitiporia ellipoidea 315
Food processing analysis 1517
Formal synthesis 1093
Fossil conifer wood 1051
FoxM1 1603
Fragmentation pathways 2053
FRAP 1273
FRAP 153
FRAP 483
Freeze-drying 1345
Fructans 1985
Fruit extracts 467
Fruit oil 1723
Fruit 1517
Fruits 369
Fruits 673
Fucus vesiculosus 1661
Functional drinks 1019
Functional food 991,1399
Functional foods 1739
Functionality 521
Functionalized cyclitol 691
Fungal endophyte 1647,1649
Fungal metabolites 1663
Fungus 95
Furan 1813
Furanocoumarin 1973
Furanocoumophilane 9,823

Furanoguaia-1,3-diene 1059
Furanoguaia-1,4-diene 1059
Furanone 845
Furanones 107
Furocoumarin 767
Furomollugin 1025
Furoquinoline alkaloids 1359
Fusarium sp. 1667
Galenia africana 1185
Galinsoga parviflora 1825
Galinsoga quadriradiata 1825
Gallic acid 479
Gallotannins 1977
gamma-Glutamylethylamide 803
gamma-Glutamylmethyamide 803
Ganoderma lucidum 1911
Ganoderma petchii 2019
Ganodermataceae 2019
Gastric ulcer 1989
GC/EIMS analysis 1469
GC/FID 1085
GC/MS1085,1239,1319,1537,1619
GC/MS analysis 1051
GC-FID 1619
GC-MS 649,777
GC-MS 1043,1279,1283,1315
GC-MS 1323,1553,1619,1705
GC-MS-FID 133
GC-olfactometry 1443
Gene bank 1699
Gene expression profiling 2095
Gene expression 2033
Genetic authentication 1743
Genistein 951
Genotoxicity 1403
Geoterenoids 1051
Geranial 657
Geraniol 1495
Geranylbenzofuranone 313
*Germacrene D*375,1059,1751,1763
Germinating seeds 869
Gesneriaceae 625
Ginger essential oil 1085
Ginger 1829
Ginkgo biloba 2033
Glabridin 1573
Glibenclamide 1395
Global health care 2195
Glochidion glomerulatum 875
Glochidion hypoleucum 479
Glomeruloside I 875
Glomeruloside II 875
Glossodoris 865
Glucopyranosylflavanone 1191
Glucosidase inhibition 1961,2123
Glucosidase inhibitor 325
Glucosidase1409,1561,1585,1977
Glucoside 923,1017
Glucosinolate 1733
Glucosinolates 1043
Glucosinolates 209,1211
Glucosyl kaempferols 1373
Glucosyltransferase 949,1017
Glycine 1345
Glycoside 567,925
Glycosides 1253
Glycosides 1937
Glycyrrhetic acid 1801
Glyoxalase I 1581
Goji berry 1035
Gold nanoparticles 627,1593
Goniobranchus 865
Goniocarpic acid 1513

Goniothalamin 725
Gossypol 613
Gout 1435
Grafted tea 789
Graminin C 107
Grape seed extract 257
Gregatin B 107
Grossulariaceae 467
Growth inhibition 729
Growth inhibitor 761
Growth stage 661
Guanidine alkaloids 913
Gut fungus 1363
Gylongiposide II 1351
Gylongiposide III 1351
Gymnomitrane 1911
Gynostemma longipes 1351
Gynoxys meridana 653
Gynoxys 653

HAB 1263
Habituation 783
Hairy root culture 1919
Hauser-Kraus reaction 1025
hCaM M124C-AF₃₅₀ Biosensor113
HCT116 1349
Headspace microextraction 357
Health-benefit 1399
Heat shock proteins 725,1013
Hedera helix leaves 1529
Hederin 1529
Hederoside C 1529
Hedyotis lindleyana 1141
HeLa cell line 139
Helicobacter pylori 1369
Hemeoxygenase 33
Hemiptera 1495
Hemolytic activity 1687
Henry reaction 691
HepG2 1349
Heptacosane 361
Heptene 631
Heracleum sosnowskyi 767,771
Herbal Medicinal Products 125
Herbicidal 2151
Herbicides 1119
Herbivores 1127
Herbivory 1809
Herbs 1779
Hericium erinaceus 1989
Heterocyclic compound 1141
Heterogeneous catalysis 1813
Hibiscus glaber 451
Hibiscus hamabo 451
Hibiscus sabdariffa 765
Hibiscus sabdiffera 77
Hibiscus tiliaceus 451
Himerometra magnipinna 317
Hinokitiol 783
Histidine 1489
HL-60 cells 27,955
HL-60 1581
HMPS 125
HO-8910 cell 249
Holothuria nobilis 247
Homoisoflavonoids 1207
Hopane 5
Hornstedtia sanhan 365
Hornstedtia 1561
Horsfieldia macrobotrys 325
Host plants 43
HPLC analysis of carotenoids 1035
HPLC method validation 1383

HPLC 789,941,963,1263,1699
HPLC 1413,1529,1553,1699
HPLC-ESI-MS 83
HPLC-MS 1043
HPLC-MS 1705
HPLC-NMR 95
HRMS 1521
HS volatiles 661
HSC-2 cells 27
HS-GC-MS 771
HS-SPME 357
hTRPV3, 1171
Human cancer cells 853
Human serum albumin-functionalized magnetic nanoparticles 2161
Humulene 1611
Humulene 1763
HUVECs 1517
Hyacinthaceae 1207
Hybrid 9
Hydro-distillation 1293
Hydrolysis studies 1521
Hydrolysis 1801
Hydrophobicity 917
Hydropiperide 641
Hydroxyactinodaphnine 891
Hydroxy-lup-diene-oic acid 277
HydroxyRebaudioside M 1159
Hydroxytomatine 575
Hyperibine J 1231
Hypericaceae 375
Hypericum maculatum 1231
Hyperpolyphyllirin 1231
Hyperuricemia 1435
Hypolipidemia 349
Hyptis colombiana 1751
Hyssopus officinalis 133

IL-6 631
Ilex paraguariensis (maté), 707
Imidazole alkaloids 721
Immunomodulatory activity 1767
Immunomodulatory 1199,1533
Immunostimulating 591
In silico toxicological study 1423
In vitro Cultivation 1225
In vitro Cultures 839
In vitro sensitivity 1473
Indole alkaloids 297
Indole 49
Indonesia 1907
Induced-Defense 1127
Inflammation 1607
Influenza virus A/H1N1 1565
Infusions 977
Inhalation 1479
Inhibitor 1333
Inland population 429
Insecticidal activity 1525
Insecticidal 2151
Interaction 1395
Inter-unit linkages 201
Intracellular ROS inhibition 1533
Invasive plant 761
Invasive 767
Ionization energy 153
Ionones 847
Iridaceae 441,955
Iridoid glucosides 1897
Iridoid glycosides 445,1195
Iridoid 1141
Iris crocea 503

- Iris florentina* 955
Iris gracilipes 441
Irvingiaceae 1709
Isaria fumosorosea 113
Isatis indigotica 273
 Ischemia/reperfusion *in vivo* 937
 Ischemia-Reperfusion injury 253
 Isochromane derivatives 2123
 Isoflavanones 499
 Isoflavone apiooglucoside 1959
 Isoflavone 1577,1581
 Isoflavones 933
 Isoflavonoid glycoside 955
 Isogeijerin 1315
 Isoglabratephrin B 921
 Isolation 1923
 Isomurralonginoic acid 617
 Isomurralonginol senecioate 617
 Isoorientin 1703
 Isoorientin 479
 Isoprenoids 209
 Isoprenylated flavonoids 2105
 Isoquinoline alkaloids 1541
Isostichopus fuscus 1427
 Isowogonin 387
 IT 815
 ITS 9,823
- Jaborandi 721
 JA-ILE 1127
 Jasmonates 1127
 Jatrophane diterpenoid 2037
Juglans regia 1239,2141
 Juglone content 1239
 Juice 1817
Juniperus macropoda 1071
- Kaempferol glycoside 417
 Kaempferol glycosides 1381
 Kaempferol 421
Kalanchoe gastonis-bonnieri 433
 Keratinocyte 2009
 Khellactone derivatives 1027
 Kinase 1287
Kopsia 49
 Korea 963
 KPC-producing isolates 1847
 Labdane diterpenes 1509
 Labdane-type diterpenes 1153
 Labiate 13,565,857
 Lachnophyllum ester 1749
Lachnum palmae 1981
 Lactic cultures 1985
 Lamiaceae 487,1751
Lannea schimperi 103
 Lanthanides 1811,1813
 Lapachol 1811
Laretia 1343
Larix kaempferi 407
 Larvical activity 133,677,10171
 Larvidical activity 1195,1759
Laserpitium latifolium 649
Lasioderma serricorne 1635
 Latex 2037
 Lathyrene diterpenoid 2037
 Lauraceae 1321,1541,2131
Laurencia nangii 843
 Laurene-type sesquiterpene 843
 Lavandin 1269
Lavandula spica 565
Lavandula stoechas 2001
 Lawsone 1811
 LC-DAD/ESI-MS^a 987
- LC-DAD-MS/MS 937
 LC-ESI-MS 933
 Leaf extracts 1239
 Leaf pigments 1055
 Leaf 63,1373
 Leaves 1409
Lecythidaceae 871
Lecythis pisonis 871
 Leguminosae 499,747
Leishmania spp. 917
Leishmaniasis 1229
Lejeuneaceae 1501
 Lemon balm 1055
 Lemon balm 977
Lentinus similis 1391
Leontice altaica 291
 Leucine 1417
Leucocoprinus birnbaumii 95
Levisticum officinale, 1743
 Lewis acid 959
Liabeae 1183
 Light, Dark 1211
 Lignan 1229
 Lignan 997
 Lignans 1853
 Lignin isolation 201
 Lignin 201
Ligularia brassicoides, 827
Ligularia hodgsonii 823
Ligularia kanaitzensis 9
Ligularia melanothysra 9
Ligularia subspicata 831
Ligularia velutera 9
Ligustrum Lucidi Fructus 2189
Ligustrum lucidum 2189
 Lime oil 1091
 Limonene 1315,1611
Limonium pruinosum 319
 Limonoids 17
 Linalool 547,657,1315
 Linalyl acetate 1315
Lindera aggregata 2131
 Linear trisaccharide 1965
Linum thraicum 1225
 Lipases 157
 Lipid peroxidation 1055,1901
 Lipogenesis 349
 Lipoxygenae inhibitory activity 1643
 Lipoxygenase 83,1585
Lippia nodiflora 945
 Liquid 1219
Litsea cubeba 1301
 Liver glycogen 1843
 Liver 1779
 Liverworts 5,1501
 Living-body modulating activity 521
Lobelia tupa 1355
 Long chain fatty acids 99
Lonicera japonica 1499
 Low caffeine 789
 LSM 777
Luffariella variabilis 863
 Lung adenocarcinoma 1603
 Lung 253
 Luo Han Guo 1521
 Lupane-type triterpenoid 277
 Lupine 563
Lycium species 1035
Lycopodium alkaloids 2091
 Lycopsamine 1181
 Lycorine 1537
 Lythraceae 277
- Macedonian pine 987
Machilus thunbergii 2013
Maclura pomifera 1577
 Macrophages 1937
 Maculatoquiones A-D 1231
 Maesopsis-glucopyranoside 591
 Mahanimbine 293
 Majusine D 2069
 MALDI-TOF-MS 969
Malleastrum sp. 1509
 Malpighiaceae 99
 Maltese Fleabane 1323
 Maltopentaoside 995
 Maltotetraoside 995
 Maltotrioside 995
 Malvaceae 77
Mangifera indica 1809
 Mangrove Endophytic fungus 1549
 Mangrove plant 747,755
 Manoalide-related sesterterpene 863
 Manzamine 1951
 Maqui 81
 Marine fungus 621
 Marine sponge 913
 Marine sponge 863
 Marine-derived fungi 637
 Marine-derived fungus 1247
Matteuccia struthiopteris 597
 Maturity 1723
 Mbyá-Guarani ethnic group 1847
 MC3T3-E1 cells 1423
 Mechanism 171
 Mechanism-based inactivation 57
 Mechanochemical process 237
Medicago lupulina 483
Medicago sativa 1263
 Medicinal plants 1647,1767
 Medicinal plants 1847
 Megastigmane glycosides 2023
 Melanoidin 1597
 Melanoma 389
 Meliaceae 17,1421
Melissa officinalis 1293
 Melodoinol analogue 631
Melodorum fruticosum 631
Mentha × villosa 937
Mentha spicata 1293
 Meranzin hydrate-palmitate 617
Meripilus giganteus 1833
 Meroterpenoids 2019
 Metabolic channeling 793
 Metabolic engineering 815
 Metabolic inhibition 729
 Metabolism 703,737,1489
 Metabolism 1809,1885
 Metabolites 1955
 Metabolomic Profiling 2165
Metapora 1505
 Methanol extract 941
 Methanolic extracts 977
 Methanolysis protocol 387
 Method validation 71
 Methoxycalamenene 1337
 Methoxydimethyltryptamine 581
 Methoxyflavonoids 1183
 Methoxyflavonol glycosides 1377
 Methoxygossypol 613
 Methoxypanial 309
 Methyl gallate 479
 Methyl isovaleric acid 67
 Methyl jasmonate 1211,1225,1919
 Methyl pyrrolidinone 39
 Methylation 1237
- Methyl-branched chiron 2155
 Methyerythritol phosphate 339
 Methylglyoxal 1581
 Methyl-valerolactone 2155
 Methylxanthine 707,751
Metrosideros polymorpha 925
 Mexioticin-2'-senecioate 309
Michelia compressa var. *formosana* 665
 Microarray 353
 Microbial extract 1287
Microliabum polymnioides 1183
Micromelum integrerrimum 1711
 Microphthalmia transcription factor 389
 Micropropagation 1055
Microsorum grossum 33
 Microsporol 1643
 Migration 263,853,2009
 Miocene 1051
 Mixtures 1019
 Moisturizer 1483
 Molecular Cloning 1743
 Molecular docking 1063
 Molecular structures 461
 Momilactone 729
Monanchora pulchra 1171
Monanchora pulchra 913
 Monimiaceae 577
 Monospecific colony 811
 Monoterpene glycosides 1897
 Monoterpens 367,1893
 Monoterpenoid glucoside 1901
 Monoterpenoid indole alkaloids 2085
 Monovalerianester A 1333
 Mood states 1305
 Mopanol 605
 Moraceae 1577,2105
Moricandia arvensis 457
Morinda citrifolia 1817
Moringa stenopetala 475
Mortonia greggii 1923
Morus alba 1253
 Moslooflavone 387
 Mosquito control 1195
 Mosses 5
 Motif B' methyltransferase 799
 Mountain pine 371
 MRSA 499,1383,1661
 MS 1965
 Mt. Fuji 407
 Mulberroside A 1253
 Mulberry 1253
 Murine adipocytes 1333
 Murrallongic acid 309
 Murrangatin-1'-senecioate 309
 Murrangatin-formate 617
Murraya exotica 617
Murraya microphylla 1631,1635
Murraya paniculata 309
Murraya koenigii 293
Musa acuminata 1663
 Muscarinic receptors 487
 Mushroom 1553,1833
 Mutagenesis 117
 Mutagenicity 1489
 Muurolene 1319
 MYC 1127
Mycobacterium tuberculosis 1641
Mycobacterium tuberculosis 1661
 Myrcene, 655
 Myricitrin 83
 Myristicaceae 325

- Myrosinase 1733
Myrtaceae 1611
Myrtus taxa 1759
 NACr 1355
 NAD 793
 NADH 1273
 Naphthoquinones 595,625,1811
 Naringin 1417
 Nasal cavity 1479
 Natural product 1729,2173
 Natural products 83,959,1671
 Natural products 1767,1785,1893
 Natural *seco*-oxacassanes 853
 Natural Sweetener 559
 Natural wood durability 605
Nauclea orientalis 1901,2087
 Nazarov cyclization 2031
 Needles 371
 Neochlorogenic acid 475
neo-Clerodane diterpenes 13,857
neo-Clerodane diterpenes, 1797
 Neo-clerodane 353
Neofibularia nolitangere 881
Nepeta nuda 1063
 Nephrotoxicity 397
Nerolidol glycoside 1145
Nerolidol 143
 Nervous system activity 1305
 New Caledonia 1501
 NF- κ B 353
Nigrospora oryzae 1659
 Nile red 777
 Nitric oxide (NO) 1533
 Nitric oxide 885,1825
 Nitrile 591
 Nitriles 357
 Nitrophenol reduction 627
 NMR and MS 871
 NMR assignment 63,1373
 NMR fingerprinting 43
 NMR metabolomic screening 1647
 NMR spectroscopy 559,2131
 NMR 297,319,913,969
 NMR 1059,1159,1167,1521
 NMR 1687,1801,1933,1965
 NMR 2067,2165
 NO inhibitory activity 89
 NO production 929,2101
Nobiliside E 247
Noni 1817
 Non-parametric statistics 1699
Norcлеродане 1917
Normonanchocidins 913
Norwogonin 387
Notopterygium franchetii 2119
 Novel triterpene 563
 Nuclear Magnetic Resonance 201
 Nucleoside 2145
Nudibranch 1913
 Nutmeg 1443
 Nutraceuticals 1569
 Nutritional supplements 513
Nu-Zhen-Zi 2189
Nymphoides peltata, 233
 Obese 1281
 Occurrence 703,803
 Octanal 771
 Octanolide 1729
 Odor dependency, 1047
 Odor recognition 1047
 Odor-structure relationship 847
Ogmaster capella 1937
 Oil collecting bees 99
Oleanane 567
Oleanolic acid 239
 Oligomerization 959
 Olive oil 1013
OM-X® 1597
 Optimal harvesting time 1699
 Orbitrap MS 575
 Orchids 1483
 Organic acids 1817
 Ortho ester 831
Oryza sativa 737
Osmunda japonica 597
 Osteoporosis 2189
 Osteosarcoma 1365
 Osthol 1315
 Ovarian carcinoma 1365
 Overweight 1281
 Oxidation 1237
 Oxidative damage 475
 Oxidative stress 335,397,743,895
 Oxidative stress, 1055,1607
 Oxidoreductases 157
 Oxindole alkaloid 2087
 Oxo-12-noryctochalasin D 1655
 Oxononanoic acid 1079
 Oxyperynlated metabolites 589
 Oxyperynlated metabolites 1115
 Oyster shell extract 349
 Pacharán 81
Pachystela msolo 1933
 Pachystelanoside A 1933
 Pachystelanoside B 1933
Paeonia lactiflora 323
 Palmaenols A and B 1981
 Palmaetriol 1981
 Palmitic acid 361
 Pancreatic β -cells 475
 Parasitoids 1127
 Paraxanthine 751
 Parkinson's disease 1775
 Parsnip 661
 Partial least square regression 1829
 Particle design 237
Pasania dodoniifolia 1373
Passiflora foetida 929
 Passifloraceae 929
 Pasta 1739
Pastinaca hirsuta Pančić 661
Paullinia pinnata 563
 PCA 71,2001
 PCTOC 815
 PDCA-cycle 815
 Peat-bog pine 371
 Pedunculagin 2141
 Pellicle 2141
Peltogyne sp. 605
Penicillium citrinum 1203
Penicillium sp. 1641
Penthorum chinense 71
 Pentylsedimine 1355
 Peptide 1719
 Pericocin 2127
Periconia sp. 2127
Perovskia atriplicifolia 1149
 Peroxynitrite 1825
Pestalotiopsis microspore 1643
Peumus boldus 577
Phaeosphaeria spartinae 637
 Pharmacobiology 1001
 Pharmacodynamic 1395
 Pharmacokinetic 1395
 Pharmacokinetics 1569
 Pharmacological features 1869
 Pharmacology 1325
 Phelligrinidin 315
 Phenazine-1-carboxamide 1659
 Phenazine-1-carboxylic acid 1659
 Phenolic acids 977
 Phenolic compound 2169
 Phenolic compounds 83,319,631
 Phenolic compounds 487,1019
 Phenolic compounds 1037,1705
 Phenolic extracts 1739
 Phenolic 1263,2141
 Phenolics Compounds 1279
Phenolics 467,963,1399,1409,1853
 Phenols 483,959
 Phenylacetic acid 357
 Phenylethanoid glycosides 945
 Phenylethyl glycoside 1251
 Phenylpropanoid derivatives 285
 Phenylpropanoid glycosides 2137
 Phenylpropanoids 209,365,2119
 Pheromone 1729
Phoma chenopodiicola 1119
Phomopsis sp. 305
Phomopsis 1647
 Phosphodiesterase 301
Phyllitis 1079
Physalis angulata 2059
 Phytic acid 329
 Phytoalexins 209
 Phytoanticipins 209
 Phytocannabinoids 1009
 Phytochemical profile 1869
Phytolacca americana 713,717
Phytolacca americana 923,949
Phytolacca americana 1017
 Phytopathogenic fungi 1037
 Phytoremediation 1885
 Phytotherapeutic product 991
 Phytotherapy 1479
 Phytoxic activity 765
 Phytoxicity 17
 Phytotoxin 761
 Phytotoxins 1119
 Pigments 505
 Pilosine 721
 Pine oil 1091
 Pine 987,1671
 Pinene 655,1309,1611,1763
 Pinocembrin 379
Pinus peuce 987
Pinus uliginosa 371
Pinus uncinata 371
Piper brevicaule 1997
Piper cernuum 285
Piper harmandii 1997
Piper majusculum 1997
Piper miniatum 2005
 Piperaceae 2005
 Piperic acid derivatives 289
 Piperidine alkaloid 1355
Pistacia atlantica 1723
Pittosporum tobira 413
 PK15 cell 397
 Plant cell biology 815
 Plant extract 597
 Plant glucosyltransferase, 995
 Plant growth inhibitory 725
 Plant growth regulators 755
 Plant innate immunity 273
 Plant organ 661
 Plant resources 233
 Plant-Volatiles 1127
 Plasmid relaxation 297
Plasmodium falciparum 3D7 1541
 Platelet aggregation 1607
Pleurotus geesteranus 1553
 Plumbaginaceae 319
 Poaceae 369
 Podophyllotoxin 1225
 Poisonous plants 1179
 Polar capillary column 1619
 Polar constituents 1705
 Polyethylene glycol 1345
 Polygalacturonase inhibiting protein 273
 Polygonaceae 641
Polygonatum 683
Polygonum hydropiper 641
 Polyketide 1661
 Polyketides 637,1247
 Polyoxxygenated sterol 881
 Polyphenolic compound 479
 Polyphenolic profile 1219
 Polyphenolics 1817
 Polyphenols 839,987,1821
 Polypodiaceae 33,1191
Polyscias duplicita 567
 Polyurethane microstructures 951
 Prebiotic 1985
 Precursor feeding 2095
 Preferential cytotoxicity 997,1153
 Prenyloxyprosoralen 1973
Primula sieboldii 421
Prionsciadium thapsoides 1027
 Pristimerin 1923
 Proinflammatory cytokine 1533
 Proliferation 2009
 Proliferation 263
 Proliferative activity 1711
 Proline 1555
 Prolyl oligopeptidase 577
 Propargyl methyl ether 903
 Propargylamides 267
Propionibacterium acnes 1459
 Propolis 1279,1961,1869
 Prostate cancer 2113,2179
 Proteases 1427
 Protection of gastric mucosa 1989
 Protein expression 733
 Protein thiols 1843
 Protein tyrosine phosphatase 1B 2105
 Proteaceous venom 1607
 Protoplast culture 747,755
Psammoplhin A 219
Pseudallescheria boydii 621
Pseudo-protodioscin 2161
Psoralen 1955
Pterandric acid 99
Pteridium aquilinum var. *latiusculum* 597
Pterostilbene 1403
 PTP1B inhibitor 2049
Pueraria thunbergiana 2009
Pueraria tuberosa 1703
Pueraria 253
 Pulp and paper 505
Pulsatilla chinensis 237
Pulvinula sp. 11120 107
Pulvinulin A 107
 Purification 339
 Purine alkaloid 751,799
 Purine 737
Purdione B 921

Purple-violet flower color	457	Root bark	1923	<i>Sedum sediforme</i>	83	Spirostane	37
Pyconogenol	513	Root cultures	1253	Seem	1387	Spirostone Glycoside	887
Pyranonaphthazarins	1243	Roots	369	<i>Selaginella</i>	887	SPME-GC-MS	1055
Pyranonaphthoquinones	1589	ROS	1937,1993	Selective extraction	869	<i>Spodoptera frugiperda</i>	1955
Pyridine	737	Rosaceae	1145	Selenium	1885	Sponge	1171,1945,1951
Pyridinedicarboxylate	39	<i>Rosaceae</i>	467	Semi-synthesis	571	Sponges	219
Pyridoacridines	1547	Rosarin	1413	Senecioneae Tribe	653	Spruce	1671
Pyrimidine	737	Rosemary oil	1091	Seneciphylline	1179	Starfish	1937
Pyrrolizidine alkaloids	1179	Roseroot	1413	Sequence-characterized amplified		STAT1	2023
Pyrrolizidine alkaloids	1181	Rosin	1413	region	1743	Statistical analysis	1447
<i>Pyrrhosia calvata</i> ,	1191	Rosmarinic acid	1269	Serine protease inhibitor	167	<i>Stellaria</i>	437
qNMR	379	<i>Rosmarinus officinalis</i>	1293	<i>Serjania goniocarpa</i>	1513	<i>Stellera chamaejasme</i>	53
qRT-PCR	789	Rotamer	425	Serotonin	1281	Stem tuber anthocyanins	461
Quality control	2195	RP-HPLC	1817	Sesamin	1229	<i>Stemona</i> alkaloid	1093,2097
Quantification	43,1955	RP-HPLC-UV analyses	483	Sesquiterpenoid	827	<i>Stemona japonica</i>	2097
Quantitative analysis	71,293	rTRPA1	1171	Sesquiterpene Glycoside	1145	Stemonaceae	1093
Quantitative change	451	rTRPV1	1171	Sesquiterpene lactone	5	Stemphyperlyenol	39
Quantitative estimation	1529	Rubiaceae	1897,1901,2087	Sesquiterpene lactones	839	Steptozotocin	1683
Quantitative RT-PCR	2095	Rubusoside	559	Sesquiterpene	1341	Stereoselective synthesis	1337
Quercetin Derivatives	1565	<i>Ruilopezia bracteosa</i>	655	Sesquiterpenes	157,365,625,845	Stereoselective synthesis	959
Quercetin glycoside	433	<i>Rumphella antipathies</i>	835	Sesquiterpenes	367,1767	Steroid C ₂₃	1353
Quercetin glycosides	281,1369,1381	<i>Ruta graveolens</i>	1955	Sesquiterpene	1907,1911,1913	Steroid	2049
Quercetin	421,949,1565,2113	Rutaceae	17,313,1955,1973	Sesquiterpenoid	9,831,835	Steroidal aglycones	2053
Quinoline-2(1H)-selone	903	Rutin	475,1955	Sesquiterpenoid	1711,2173	Steroidal alkaloids	1533
Quinoline-2(1H)-thione	903	Sabinene	1315	Sesterterpene	865,1513	Steroidal saponins	1941
Quinonoid aporphine alkaloid	1175	<i>Saccharicola bicolor</i>	2135	Sex pheromone	2155	Steroids	595,871,1937
Quinovic acid glycosides	281	<i>Saccharomyces cerevisiae</i>	1085	Shapiro reaction	847	<i>Stevia rebaudiana</i>	1159
Quorum sensing	1753	Saffron	775	SHR	1543	Stilbene	491,1257
Radical cyclization	1	Safranal	775	SHR	281	Stilbenes	1253
Radical oxygen species	1993	Sage	1615	<i>Sideritis libanotica</i> ssp. <i>Libanotica</i>	1075	Stomach smooth muscle	565
Radical scavenging activity	609,1805	Salicylic acid	1225	<i>Sideritis libanotica</i> ssp. <i>linearis</i>	1075	Stratification	767
Radical scavenging	153	Salidroside	1413	<i>Sideritis libanotica</i> ssp.		<i>Streptomyces</i> 85E	1287
Radish seedling	1211	<i>Salvia officinalis</i>	1293	<i>michroclamys</i>	1075	Stress protein	729
Ramulosin derivatives	341	<i>Salvia</i>	1797	<i>Sideritis montana</i>	487	Structural elucidation	575
Random amplified polymorphic		Sapindaceae	563	<i>Silene vulgaris</i>	1919	Structure Characterization	559
DNA	1743	Saponin	871	Silymarin	263	Structure elucidation	305,1159
Ranunculaceae	27,2165	Saponins	37,237,483	Similarity	71	Structure elucidation	1643,1667
Rapamycin	263	<i>Sarcococca wallichii</i>	1533	<i>Sinningia leucotricha</i>	625	Structure elucidation	1951
<i>Raphia farinifera</i>	1941	<i>Sarcophyton trocheliophorum</i>	1163	Siomycin A	1603	Structure revision	881
Rat	335	Sasmolytic activity	487	<i>Siraitia grosvenorii</i>	1521	Structure-activity relationships	1171
Rats	397	<i>Sassafras albidum</i>	1229	Sitosterol	103	Structure-activity relationships	1929
RAW264.7 cells	383	Sativex®	1009	<i>Skimmia laureola</i>	1071	Structure-activity relationships	2075
RBL-2H3 cells	1597	Scavenging activity	1273	Skin-active natural products	33	Styrylpyrone	315
RCM	551	Scavenging radical	1387	SKOV3 cells	1365	Subcritical water	1801
Reaction time	2169	Schinotriterpenoids	2045	Sloe	81	Substitute	1743
Reactive nitrogen species	1825	<i>Schisandra chinensis</i>	1001	Smoke	1489	Substitution	1237
Reactive oxygen species	1387	<i>Schisandrala</i>	2045	Smooth muscle	1893	Succinic-semialdehyde	
Recommendation	2169	<i>Schisandrala</i>	2045	Snow clover	933	dehydrogenase	743
Red alga	843	<i>Scutellaria altissima</i>	13	Sodium asperulosidate	1141	Sugars	969
Red clover	933	<i>Scutellaria barbata</i>	353	Soft coral	1907	Supercritical CO ₂ extraction	1315
Red Maple	1409	<i>Scutellaria</i>	1797	Soil composition	1615	Superoxide anion	1833
Reducing power	483	Scopararanes	2027	Soil fungi	39	Supplement regulations	125
Regeneration	2009	Scoparasins	2027	Solanaceae	345	Surfactin	2151
Reinwardione	1611	Scoparone	1315	<i>Solanum macaonense</i>	345	Suspension culture	747,777
Relaxation	565	Screening	1287	<i>Solanum xanthocarpum</i>	361	Sustainable synthesis	627
Re-ligand fishing	2161	Scrophulariaceae	445	Solavetivone	361	Sustained extracellular signal-	
Renal hypertension	335	Seutaltisins	13	Solid-liquid extraction	1923	regulated kinase 2	389
Renal injury	1543	Scutebarbalactone VN	353	Solid-phase extraction	357	Sycamore maple	1977
Renal parameters	1843	<i>Scutellaria altissima</i>	13	Solubilization	1345	<i>Symphytum officinale</i>	1181
Repellency	1635	<i>Scutellaria barbata</i>	353	Solvent	2169	Synergism	1829
<i>Resnova humifusa</i>	1207	<i>Scutellaria</i>	1797	<i>Sonnetaria alba</i>	277	Synergy effect	1989
Resolution	157	Sea cucumber	1427	Soybean	743	Synergy	2179
Resorcyclic acid lactone	2135	Sea cucumbers	21,877,1687	Spartiodine	1179	Synthesis	289,551,591,1257,2155
Resveratrol	335,995,1403	Sea urchin	1243	<i>Spathodea campanulata</i>	1999	Synthetic studies	645
Review	1325	Secobisbenzylisoquinoline	1695	SPE	357	Taiwaniaquinol B	2031
Rhamnaceae	1805	Secoiridoid glucoside	1499	Specialty woods	505	<i>Takakia lepidozoides</i>	5
<i>Rhodiola rosea</i>	1413	Secondary metabolites	1247	Spectroscopic analyses	483	Tamoxifen	1573
Rhodomelaceae	843	Secondary metabolites	1671	Spectroscopic methods	323	<i>Tanacetum vulgare</i> var. <i>boreale</i>	403
<i>Rhynchosia suaveolens</i>	609	Secosesquise	1499	Sphingoglycolipid	641	<i>Tanacetum vulgare</i> var. <i>vulgare</i>	403
Rice seedling	733	<i>seco</i> -Triterpenoids	1517	Sphingolipid	349	Tandem reaction	2031
Rice	737	Sederoxyloideae	1933	Spinescin	1229	Tangeretin	389
Ring-closing metathesis	551	<i>Sedum</i>	941	Spiro-compound	2019	Tannin adhesives	505,513
Ringworm	1473						

Tannin resources	505	UHPLC.....	71	Volatile chemicals.....	771
Tannin.....	2141	<i>Ulomooides dermestoides</i>	1753	Volatile compound.....	1479
Tannins	1705,1877	Ultrasonic solvent extraction	357	Volatile organic compounds	1055
Tanshinones.....	1149	Ultrasound	1739	Volatile Organic Compounds	1079
Tar oil composition	1905	Umbelliferae.....	2119	Vulpinoideol	491
<i>Taraxacum officinale</i> honey..	357	Undecanone.....	1955	Water extract	937
Taraxerol	103	Unsaturated carbonyl groups	725	Weeds	1119
Taraxerone.....	103	Unsaturated selenoamide	903	Western blot	789
Tarragon	1469	Unsaturated thioamide	903	Whole plant	1191
Tau protein	1577	UPLC.....	933	Wild edible plants	597
Tea	703,1829	UPLC-DAD	293	Wild loquat	239
Technology integration	2195	UPLC-MS	43	Wild population	2001
Tendrils.....	1037	Uric acid	1435	Wilfordoninol	2023
Tentacles.....	1427	Uric acid-lowering	945	Wilfordoniside	2023
<i>Tephrosia purpurea</i>	921	Urinary tract infection	1215	<i>Wisteria floribunda</i>	413
<i>Terminalia catappa</i>	1005	Ursane 28-nortriterpene	2041	Withanolides	2059
Terpene profiles	1615	Ursolic acid	239	Wood colors	505
Terpene trilactones	2033	Ursolic acid	565		
Terpenes	17,1997	USE	357	Xanthine oxidase Inhibition	1839
Terpenoid	631	UV-B	1269	Xanthine oxidase inhibitory assay	945
Terpenoids.....	1,1051,1501	<i>Valeriana fauriei</i>	1333	Xanthine	707
Terpinen-4-ol.....	1459	<i>Valeriana parviflora</i>	657	Xanthone	609
Terpineol	657,1315	<i>Valerianaceae</i>	657	Xanthones	301,305,115,1969
<i>Tetraclinis articulata</i>	1447	Validation	1181	Xanthorizol	139
Tetracosane	1431	Vancomycin-resistant <i>Enterococcus faecium</i>	613	X-Ray diffraction	1027
<i>Tetradenia riparia</i>	1627	<i>Tripterygium wilfordii</i>	2023	Xylactam B	1715
Tetrahydrocannabivarin	1009	Triterpene glycosides	21,877	<i>Xylaria</i>	1715
Tetrahydrocurcumin	329	Triterpene glycosides	1167,1687	<i>Xylariaceae</i>	1655
Tetrahydro-oxazine ring	2087	Triterpenes	67,167595,625	Xyloc...	657
Tetramethoxygossypol	613	Triterpenoid derivatives	1207	<i>Xylophia staudtii</i>	1059
Tetramethylpyrazine	1553	Triterpenoid saponin	1525	Yeast	1537
Tetramic Acid	1649	Triterpenoid saponins	1919,1933	Yellow Coast	37
Tetrapeptide	1033	Triterpenoid	1683,2049	Yellow flavonols	447
Tetrodotoxin	691	Triterpenoids	565,871,1853,1929	Yellow pigment	425
TGF- β_1	243	Trocheliolide A	1163	Yield variability	1447
Theanine synthetase	803	<i>Tropidacris collaris</i>	1809	Yohimbine	183
Theanine	703,803	<i>Truncatella angustata</i>	341	Ytterbium triflate	1813
Theanine	803	Trypanocidal	1897	<i>Zantedeschia aethiopica</i>	425
Theobromine synthase	799	<i>Trypanosoma cruzi</i>	917	Zantholide	313
Theobromine	707,751	Turmeric	329,1047	<i>Zanthoxylum armatum</i>	313
Theophylline.....	707,751	Turmerone	1391047	<i>Zhumeria majdae</i>	669
Theoretical study	269	Tuscan crops	1035	<i>Zingiber officinale</i>	1085
Therapeutic medicine	683	Type I allergy	1597	Zingiberaceae	63,89,1561
Thermal degradation	1043	Tyrosinase inhibitory activity	393	Zuccagnia punctata	991
<i>Thespisia garckeana</i>	613	Tyrosinase	389,491		
THMPs	125	Tyrosol	1413		
Thymol	1861	U2OS cells	1365		
Thymoquinone	1395				
<i>Thymus vulgaris</i>	1293				
TIAs	2095				

Compounds with Antifouling Activities from the Roots of <i>Notopterygium franchetii</i> Chun Yu, Liqing Cheng, Zhongling Zhang, Yu Zhang, Chunmao Yuan, Weiwei Liu, Xiaojiang Hao, Weiguang Ma and Hongping He	2119
New Isochromane Derivatives from the Mangrove Fungus <i>Aspergillus ustus</i> 094102 Peipei Liu, Cong Wang, Zhenyu Lu, Tonghan Zhu, Kui Hong and Weiming Zhu	2123
Pericocins A-D, New Bioactive Compounds from <i>Periconia</i> sp. Yue-Hua Wu, Gao-Keng Xiao, Guo-Dong Chen, Chuan-Xi Wang, Dan Hu, Yun-Yang Lian, Feng Lin, Liang-Dong Guo, Xin-Sheng Yao and Hao Gao	2127
New Benzenoids from the Roots of <i>Lindera aggregata</i> Guo-Hao Ma, Che-Wei Lin, Hsin-Yi Hung, Sheng-Yang Wang, Po-Chuen Shieh and Tian-Shung Wu	2131
12-Membered Resorecylic Acid Lactones Isolated from <i>Saccharicola bicolor</i>, an Endophytic Fungi from <i>Bergenia purpurascens</i> Da-Le Guo, Min Zhao, Shi-Ji Xiao, Bing Xia, Bo Wan, Yu-Cheng Gu, Li-Sheng Ding and Yan Zhou	2135
Phenylpropanoid Glycosides from the Leaves of <i>Ananas comosus</i> Wen-Hao Chen, Xiao-Juan Huang, Huo-Ming Shu, Yang Hui, Fei-Yan Guo, Xiao-Ping Song, Ming-Hui Ji and Guang-Ying Chen	2137
Tannins and Antioxidant Activities of the Walnut (<i>Juglans regia</i>) Pellicle Tian-Peng Yin, Le Cai, Yang Chen, Ying Li, Ya-Rong Wang, Chuan-Shui Liu and Zhong-Tao Ding	2141
Chemical Constituents of <i>Cordyceps cicadae</i> Zhi-Bo Chu, Jun Chang, Ying Zhu and Xun Sun	2145
A New Bithiophene from the Root of <i>Echinops grijsii</i> Fang-Pin Chang, Chien-Chih Chen, Hui-Chi Huang, Sheng-Yang Wang, Jih-Jung Chen, Chang-Syun Yang, Chung-Yi Ou, Jin-Bin Wu, Guan-Jhong Huang and Yueh-Hsiung Kuo	2147
Cyclic Lipopeptides with Herbicidal and Insecticidal Activities Produced by <i>Bacillus clausii</i> DTM1 Da-Le Guo, Bo Wan, Shi-Ji Xiao, Sarah Allen, Yu-Cheng Gu, Li-Sheng Ding and Yan Zhou	2151
Synthesis of (6R,12R)-6,12-Dimethylpentadecan-2-one, the Female-Produced Sex Pheromone from Banded Cucumber Beetle <i>Diabrotica balteata</i>, Based on a Chiron Approach Wei Shen, Xiang Hao, Yong Shi and Wei-Sheng Tian	2155
A Rapid Study of Botanical Drug–Drug Interaction with Protein by Re-ligand Fishing using Human Serum Albumin–Functionalized Magnetic Nanoparticles Lin-Sen Qing, Ying Xue, Li-Sheng Ding, Yi-Ming Liu, Jian Liang and Xun Liao	2161
Serum Metabolomic Profiling of Rats by Intervention of <i>Aconitum soongaricum</i> Fan Zhang, Jiao Liu, Jun Lei, Wenjing He and Yun Sun	2165
Re-evaluation of ABTS⁺ Assay for Total Antioxidant Capacity of Natural Products Jian-Wei Dong, Le Cai, Yun Xing, Jing Yu and Zhong-Tao Ding	2169

Accounts/Reviews

Chemical Synthesis of the Echinopine Sesquiterpenoids Xiao-Yu Liu and Yong Qin	2173
Synergistic Effects of Dietary Natural Products as Anti-Prostate Cancer Agents Bao Vue, Sheng Zhang and Qiao-Hong Chen	2179
<i>Ligustrum lucidum</i> and its Constituents : A Mini-Review on the Anti-Osteoporosis Potential Chun-Tao Che and Man-Sau Wong	2189
Alice, Benzene, and Coffee: The ABCs of Ecopharmacognosy Geoffrey A. Cordell	2195

Additions/Corrections

Cytotoxic and Antimalarial Alkaloids from the Twigs of <i>Dasymaschalon obtusipetalum</i> Atchara Jaidee, Thanika Promchai, Kongkiat Trisuwann, Surat Laphookhieo, Roonglawan Rattanajak, Sumalee Kamchonwongpaisan, Stephen G. Pyne and Thunwadee Ritthiwigrom <i>Natural Product Communications</i> , 10 (7), 1175-1177 (2015)	2203
---	------

Cummulative Index

Contents	i-xxi
Author Index	i-viii
Keywords Index	i-viii

Natural Product Communications

2015

Volume 10, Number 12

Contents

Original Paper

Petchienes A–E, Meroterpenoids from <i>Ganoderma petchii</i>	2019
Qin-Lei Gao, Ping-Xia Guo, Qi Luo, Hui Yan and Yong-Xian Cheng	
Megastigmane Glycosides from the Leaves of <i>Tripterygium wilfordii</i>	2023
Lin Ni, Xiao-mei Zhang, Xing Zhou, Jie Ma, Chuang-jun Li, Li Li, Tian-tai Zhang and Dong-Ming Zhang	
Cytochalasans and Sesquiterpenes from <i>Eutypella scoparia</i> 1–15	2027
Shuang Qi, Yue Wang, Zhonghui Zheng, Qingyan Xu and Xiamming Deng	
Concise Synthesis of Taiwaniaquinol B and 5- <i>epi</i> -Taiwaniaquinone G	2031
Yonggang Meng, Yizhen Liu, Zhigang Lv, Jinqian Wang, Yanyan Wang, Chuanjun Song and Junbiao Chang	
Effect of Enzyme Inhibitors on Terpene Trilactones Biosynthesis and Gene Expression Profiling in <i>Ginkgo biloba</i> Cultured Cells	2033
Lijia Chen, Hui Tong, Mingxuan Wang, Jianhua Zhu, Jiachen Zi, Liyan Song and Rongmin Yu	
Macrocyclic Diterpenoids from the Latex of <i>Euphorbia helioscopia</i>	2037
Juan Hua, Yan-Chun Liu, Shu-Xi Jing, Shi-Hong Luo and Sheng-Hong Li	
A New Triterpenoid from the Aerial Parts of <i>Agrimonia pilosa</i>	2041
Jiang-Hao Ma, Qing-Hua Jiang, Ying Chen, Xiu-Fang Nie, Tie Yao, Li-Qin Ding, Feng Zhao, Li-Xia Chen and Qiu Feng	
Two New 18-Norschiartane-type Schinortriterpenoids from <i>Schisandra lancifolia</i>	2045
Miao Liu, Yuan-Qing Luo, Wei-Guang Wang, Yi-Ming Shi, Hai-Yan Wu, Xue Du, Jian-Xin Pu and Han-Dong Sun	
Terpenoids and Steroids from <i>Euphorbia hypericifolia</i>	2049
Jin-Xin Zhao, Shan-Shan Shi, Li Sheng, Jia Li and Jian-Min Yue	
A Fragmentation Study of Six C ₂₁ Steroidal Aglycones by Electrospray Ionization Ion-Trap Time-of-Flight Tandem Mass Spectrometry	2053
Xing-Long Chen, Chang-An Geng and Ji-Jun Chen	
Three New Cytotoxic Withanolides from the Chinese Folk Medicine <i>Physalis angulata</i>	2059
Cai-Yun Gao, Ting Ma, Jun Luo and Ling-Yi Kong	
Diterpenoid Alkaloids from <i>Aconitum soongaricum</i> var. <i>pubescens</i>	2063
Lin Chen, Lianhai Shan, Jifa Zhang, Wenliang Xu, Mingyu Wu, Shuai Huang and Xianli Zhou	
Two New C ₁₈ -Diterpenoid Alkaloids from <i>Delphinium anthriscifolium</i>	2067
Lianhai Shan, Jifa Zhang, Lin Chen, Jiaxi Wang, Shuai Huang and Xianli Zhou	
Majusine D: A New C ₁₉ -diterpenoid Alkaloid from <i>Delphinium majus</i>	2069
Qi Zhao, Xiao-jun Gou, Wei Liu, Gang He, Li Liang and Feng-zheng Chen	
Epoxide Opening of a 7,17-Seco-7,8-Epoxy-C ₁₉ -Diterpenoid Alkaloid	2071
Hong Ji, Feng-Peng Wang and Qiao-Hong Chen	
Further Studies on Structure-Cardiac Activity Relationships of Diterpenoid Alkaloids	
Zhong-Tang Zhang, Xi-Xian Jian, Jia-Yu Ding, Hong-Ying Deng, Ruo-Bing Chao, Qiao-Hong Chen, Dong-Lin Chen and Feng-Peng Wang	2075
Monoterpene Indole Alkaloids from <i>Catharanthus roseus</i> Cultivated in Yunnan	2085
Bei Wang, Lu Liu, Ying-Ying Chen, Qiong Li, Dan Li, Ya-Ping Liu and Xiao-Dong Luo	
Two New Oxindole Alkaloid Glycosides from the Leaves of <i>Nauclea officinalis</i>	2087
Long Fan, Xiao-Jun Huang, Chun-Lin Fan, Guo-Qiang Li, Zhen-Long Wu, Shuo-Guo Li, Zhen-Dan He, Ying Wang and Wen-Cai Ye	
Lycopodium Alkaloids from <i>Diphasiastrum complanatum</i>	2091
Yu Tang, Juan Xiong and Jin-Feng Hu	
Effects of Adding Vindoline and MeJA on Production of Vincristine and Vinblastine, and Transcription of their Biosynthetic Genes in the Cultured CMCs of <i>Catharanthus roseus</i>	2095
Wenjin Zhang, Jiazeng Yang, Jiachen Zi, Jianhua Zhu, Liyan Song and Rongmin Yu	
Structures and Chemotaxonomic Significance of Stemona Alkaloids from <i>Stemona japonica</i>	2097
Min Yi, Xue Xia, Hoi-Yan Wu, Hai-Yan Tian, Chao Huang, Paul Pui-Hay But, Pang-Chui Shaw and Ren-Wang Jiang	
Chemical Constituents of <i>Euonymus glabra</i>	2101
Jie Ren, Yang-Guo Xie, Xing Wang, Shi-Kai Yan, Hui-Zi Jin and Wei-Dong Zhang	
Isoprenylated Flavonoids with PTP1B Inhibition from <i>Ficus tikoua</i>	2105
Lu-Qin Wu, Chun Lei, Li-Xin Gao, Hai-Bing Liao, Jing-Ya Li, Jia Li and Ai-Jun Hou	
Phenolic Derivatives from <i>Hypericum japonicum</i>	2109
Guoyong Luo, Min Zhou, Qi Ye, Jun Mi, Dongmei Fang, Guolin Zhang and Yinggang Luo	
Synthesis and Anti-Proliferative Effects of Quercetin Derivatives	2113
Sami M.R. Al-Jabban, Xiaojie Zhang, Guanglin Chen, Ermias Addo Mekuria, Liva Harinantaina Rakotondraibe and Qiao-Hong Chen	

Continued inside backcover